Alkyne-Nitrone Cycloadditions for Functionalizing Cell Surface Proteins

by

Craig McKay

Thesis Submitted to the Faculty of Graduate and Postdoctoral Studies
In Partial Fulfillment of the Requirements for the
Degree of Doctor of Philosophy

Candidate	Supervisor
Craig McKay	Dr. John Paul Pezacki

Ottawa-Carleton Chemistry Institute
Faculty of Science
University of Ottawa

Alkyne-Nitrone Cycloadditions for Functionalizing Cell Surface Proteins

by
Craig McKay

Submitted to the Faculty of Graduate and Postdoctoral Studies
On July 31, 2012 in Partial Fulfillment of the
Requirements for the Degree of Doctor of Philosophy
In Organic Chemistry

Abstract

Over the past decade, bioorthogonal chemistry has emerged as powerful tools used for tracking biomolecules within living systems. Despite the vast number of organic transformations in the literature, only select few reactions meet the stringent requirements of bioorthogonality. There is increasing demands to develop biocompatible reactions that display high specificity and exquisitely fast kinetics under physiological conditions. With the goal of increasing reaction rates as a means for reducing the concentrations of labelling reagents used for bioconjugation, we have developed metal-catalyzed and metal-free alkyne-nitrone cycloadditions as alternatives to azide-alkyne cycloadditions and demonstrate their applications for imaging cell surface proteins.

The copper(I)-catalyzed alkyne-nitrone cycloaddition, also known as the Kinugasa reaction, is typically conducted with a Cu(I) catalyst in the absence of air. We have developed highly efficient micelle promoted multicomponent Kinugasa reactions in aqueous media to make the reaction faster and more efficient. Despite good product yields, the slow kinetics, limited substrate scope and competing side-reaction pathways precludes its practical applicability for biological labelling. We have designed and synthesized β-lactam alkyne probes obtained from these reactions for activity-based protein profiling of the activities of membrane proteins. Additionally, we report that alkyne tethered β-lactams serve as surface enhanced Raman spectroscopy (SERS) reporters bound to silver nanoparticles, and demonstrated that alkyne bound silver nanoparticles can be used for SERS imaging cell surface proteins.

The strain-promoted alkyne-nitrone cycloaddition (SPANC) was also explored as a rapid alternative bioorthogonal reaction. We found that the reaction proceeded in high yield within aqueous media, and displayed rate enhancements that were 1-2 orders of magnitude faster than analogous reactions involving azides. The scope and kinetics of SPANC was evaluated in model reactions of various nitrones (acyclic and cyclic) with cyclooctynes, with the purpose of identifying stable nitrones that displayed intrinsically faster kinetics than azides in strain-promoted cycloadditions with cyclooctynes. Cyclic nitrones displayed good stability and exceptionally fast reactivity in these reactions. The SPANC reaction exhibited high selectivity in the presence of biological nucleophilic amino acid side chains and the presence of biological media did not adversely affect the reaction. We have utilized SPANC for highly specific labelling of proteins *in vitro* and for imaging ligand-receptor interactions on the surfaces of live cancer cells. The high selectivity, fast reaction rate, and aqueous compatibility of SPANC makes the reaction suitable for a variety of *in vivo* biological imaging applications.

Acknowledgements

Graduate studies at the University of Ottawa, and particularly research in the Pezacki Lab at the National Research Council of Canada, have been a truly wonderful experience. First and foremost, I would like to express my sincere gratitude to my supervisor, Dr. John Paul Pezacki, for his skilled guidance and mentorship. John, you have maintained the fine balance of promoting independence while providing thoughtful direction. I admire your interest in investigating problems at the interface of chemistry and biology. Thank you for providing me with many opportunities to attend scientific conferences and for your influence on my scientific development. Also, thank you for hosting and always providing excellent food and swimming at the annual "Pezacki Lab Classic." I would also like to acknowledge my committee members for taking time out of their busy schedules to be on my committee and for reading my thesis.

Much of the work presented in this thesis is the result of collaborations with colleagues in the Pezacki lab. To all the lab members that I have had the honour of working with, thank you for your friendship and making the lab a fun place to work. I thank my chemistry lab comrades with whom I worked for the majority of my graduate studies: Mr. Marc Legault, Dr. Joseph Moran, Dr. David Kennedy, Mrs. Mariya Chigrinova, Dr. Robert Faragher and Mr. Yiming Qian. I would also like to thank Dr. Selena Sagan, Mr. Ragunath Singaravelu and Mr. Rodney Lyn for sharing their knowledge of HCV biology and CARS microscopy. I am also thankful to past lab mates, particularly Dr. Bojana Rakic, Dr. Rajmohan Poondra, Dr. Stutti Srivastava and Dr. Jyoti Nandi for helping me with my first experiments in the synthetic chemistry lab. I am thankful to Mr. Donald M. Leek for assistance with NMR, and Mrs. Malgosia Daroszewska for her assistance with MS and RP-HPLC method development. To all the other graduate and undergraduates students, technicians and post-docs I have had the pleasure of working with, thank you for providing an exceptional environment in which to learn and grow.

My family has been tremendously supportive and encouraging throughout the course of my graduate studies and education in general. I thank my parents, Gordon and Lynn McKay, and my sister, Megan, for their support and encouragement, and most importantly for believing in my potential, even at times when I had difficulty believing in myself. I will never be able to thank them for everything that they have done for me and I will always be grateful. I would also like to express acknowledgments to my beautiful and loving wife, Jenny, whom I met at the National Research Council in Ottawa at the beginning of my graduate studies. She has been extremely patient and encouraging throughout. She is an amazing person, an excellent scientist and I am lucky to have her in my life.

Table of Contents

List of Abbreviations

ABPP	activity-based protein profiling
Ac	acetyl
Ag	silver
ALO	aryl-less cyclooctyne
Au	gold
BARAC	biaryl-aza-cyclooctynone
BCN	bicyclononyne
Bipy	bipyridine
Bn	benzyl
Boc	*tert*-butyloxycarbonyl
BODIPY	boron-dipyrromethene
BPS	bathophenanthroline disulfonate disodium salt
BSA	bovine serum albumin
BTTAA	2-[4-{(bis[(1-*tert*-butyl-1H-1,2,3-triazol-4-yl)methyl]amino)methyl}-1H-1,2,3-triazol-1-yl]acetic acid
BTTES	2-[4-{(bis[(1-*tert*-butyl-1H-1,2,3-triazol-4-yl)methyl]amino)-methyl}-1H-1,2,3-triazol-1-yl]ethyl hydrogen sulfate
CMPO	5-carboxy-5-methyl-1-pyrroline *N*-oxide
CuAAC	copper(I)-catalyzed azide-alkyne cycloaddition
Cy	cyclohexyl
DBA	dibenzylidene acetone
DCC	*N,N′*-dicyclohexyl carbodiimide
DCM	dichloromethane
DIBAC	dibenzo-aza-cyclooctyne
DIBO	4-dibenzocyclooctynol
DIFO	difluorinated cyclooctyne
DIMAC	dimethoxy-aza-cyclooctyne
DIPA	diisopropylamine
DMAP	4-dimethylaminopyridine
DMEM	Dulbecco's Modified Eagle Medium
DMF	dimethylformamide
DMMB	d7-mercaptomethylbenzene
DMPO	5,5-dimethyl-1-pyrroline-*N*-Oxide
DMSO	dimethylsulfoxide
dppe	1,2-bis(diphenylphosphino)ethane
dppp	1,2-bis(diphenylphosphino)propane
DSC	*N,N′*-disuccinimidyl carbonate
DTSP	3,3′-dithiodipropionic acid di(*N*-hydroxysuccinimide ester)
EA	ethanolamine
EDCI	1-(3-dimethylaminopropyl)-3-ethylcarbodiimide hydrochloride
EDG	electron donating group
EDTA	ethylenediaminetetraacetic acid
EG_3SH	2-[2-(2-methoxy-ethoxy)-ethoxy]-ethanethiol
EGF	epidermal growth factor

EGFR	epidermal growth factor receptor
EMPO	5-ethoxycarbonyl-5-methyl-1-pyrroline *N*-oxide
EPPS	3-(4-(2-hydroxyethyl)-1-piperazinyl)-propanesulfonic acid
EWG	electron withdrawing group
FA	formic acid
FBS	fetal bovine serum
FITC	fluorescein isothiocyanate
FMO	frontier molecular orbital
FP	fluorophosphonate
GalNAz	*N*-azidogalactosamine
GFP	green fluorescent protein
GlcNAc	*N*-acetylglucosamine
HCV	hepatitis C virus
HEPES	4-(2-hydroxyethyl)-1-piperazineethanesulfonic acid
HOBt	1-hydroxy-benzotriazole
HOMO	highest occupied orbital
HPG	homopropargylglycine
IEDDA	inverse-electron demand Diels-Alder reaction
KHMDS	potassium hexamethyldisilazane
Lev	levulinoyl
LUMO	lowest unoccupied molecular orbital
MALDI-MS	matrix-assisted laser desorption/ionization mass spectrometry
ManNAc	*N*-acetyl-mannosamine
ManNAz	*N*-azidomannosamine
MMBNO	4-mercaptomethyl)nitrobenzene
MMByne	4-(mercaptomethyl)ethynyl benzene
MOBO	monobenzocyclooctyne
MOFO	monofluorinated cyclooctyne
mRNA	messenger RNA
MSA	murine serum albumin
$NaBAr^{F}{}_{4}$	Sodium tetrakis[3,5-bis(trifluoromethyl)phenyl]borate
NeuNAc	*N*-acetylneuraminic acid
NHS	*N*-hydroxy succinimide
NMR	nuclear magnetic resonance
NP	nanoparticle
OCT	cyclooctyne
PBP	penicillin binding protein
PBS	phosphate-buffered saline
PDC	pyridinium dichromate
PEG	polyethyleneglycol
Ph	phenyl
Pic	*p*-iodobenzyl cysteine
RLS	Rayleigh light scattering
RP-HPLC	reversed phase high performance liquid chromatography
SAR	structure-activity relationship
SDS PAGE	sodium dodecyl sulfate polyacrylamide gel electrophoresis
SEM	scanning electron microscopy

SERS	surface enhanced Raman scattering spectroscopy
SPAAC	strain-promoted azide-alkyne cycloaddition
SPADC	strain-promoted alkyne-diazoalkane cycloaddition
SPANC	strain-promoted alkyne-nitrone cycloaddition
SPANOC	strain-promoted alkyne-nitrile oxide cycloaddition
sTCO	strained *trans*-cyclooctene
TAMRA	tetramethylrhodamine
TAPS	*N*-tris(hydroxymethyl)methyl-3-aminopropanesulfonate
TBAF	tetrabutylammonium fluoride
TBDMSCl	*tert*-Butylchlorodimethylsilane
TBDPSCl	*tert*-Butylchlorodiphenylsilane
TBTA	tris[(1-benzyl-1H-1,2,3-triazol-4-yl)methyl]amine
TCEP	tris-(2-carboxyethyl)-phosphine
Tf	triflate
TFA	trifluoroacetic acid
THF	tetrahydrofuran
THPTA	tris-(hydroxypropyltriazolyl)-methylamine
TLC	thin layer chromatography
TMDIBO	tetramethoxydibenzocyclooctynol
TMS	trimethylsilyl
TMTH	thiacycloheptyne
TPF	two photon fluorescence
TPPTS	triphenylphosphine-3,3',3"-trisulfonate
Tris	tris-(hydroxymethyl)-aminomethane
tRNA	transfer ribonucleic acid
UV-vis	ultraviolet-visible

List of Figures

Chapter 1

Chapter 2

Chapter 3

Chapter 4

Chapter 5

Chapter 6

List of Schemes

Chapter 1

Chapter 2

Chapter 3

Chapter 4

Chapter 5

Chapter 6

List of Tables

Chapter 2

Chapter 3

Chapter 5

Chapter 6

Chapter 1 : Click Chemistry and Bioorthogonal Reactions

Introduction

The ability to covalently modify biomolecules and track their involvement in cellular processes within living systems has long presented a significant challenge. This is due to the presence of the vast array of interacting biopolymers (proteins, DNA, RNA etc.), ions and metabolites that drive complex cellular processes using a diverse array of chemistry. Since biomolecules are not naturally endowed with special features that permit their direct detection within the complex milieu of a cell, there is increasing demand to develop selective tagging strategies for studying the dynamic structure, function, and localization of biomolecules within living cells and whole organisms.

The use of genetically-encoded fluorescent proteins (eg. green fluorescent protein, GFP) has been revolutionary in enabling the tracking of proteins through the use of fusion proteins as genetic tags. Research on fluorescent proteins has addressed the issue of residue-specific modifications, and has expanded the range of proteins that can be investigated in cellular systems.[1] Despite these advances, genetic tagging is not without limitations, other classes of biomolecules such as nucleic acids, lipids, and glycans, either on their own or as post-translational modifications, are not yet amenable to conventional genetic tagging. Bioorthogonal chemistry has emerged, based on a few highly specific reactions, enabling the study of the dynamic structure, function, and localization of these biomolecules within living systems.[2]

In 2001, Sharpless, Kolb and Finn introduced the concept of ‘click’ chemistry, defined as an efficient approach to the synthesis of diverse compounds based on a handful of “near perfect” carbon-heteroatom bond forming reactions.[3] The philosophy of ‘click’ chemistry describes essentially any chemical process that is rapid under ambient conditions,

chemoselective, high yielding, wide in scope, and provide structures with desired function. This potent combination requires reactions that have a high thermodynamic driving force and are orthogonal to other functional groups that may be present. Chemical reactions that proceed efficiently and do not cross-react with biological functionality have far reaching applications that span chemistry, biology and materials science.[2,4,5]

Bioorthogonal chemistry was coined in 2003 by Bertozzi, and refers to a subset of 'click' reactions,[6] describing any chemical reaction that can occur inside living systems without interfering with native biochemical processes.[2,7,8] Since its inception, bioorthogonal chemistry has enabled the study of nucleic acids, lipids, and glycans, and post-translational modifications that are not accessible using conventional genetically encoded reporters. Bioorthogonal chemical reporters are non-native, non-perturbative, and can be modified in living systems through highly selective reactions with exogenously delivered probes bearing complementary bioorthogonal functionality (Figure 1-1).[7]

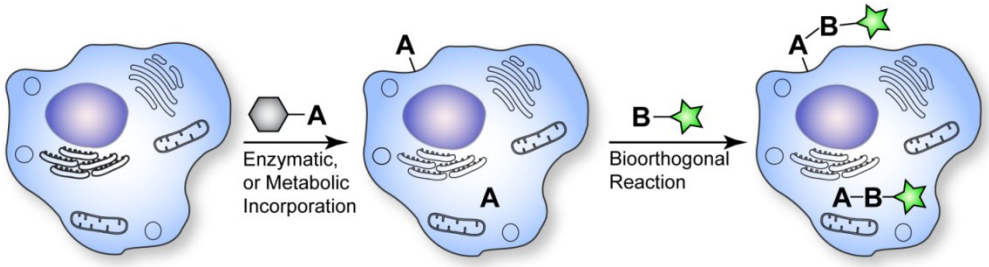

Figure 1-1. Bioorthogonal chemical reporter strategy for probing biological systems pioneered by Bertozzi *et al*.[6,7] Firstly, a non-native functional group is incorporated into a biomolecule of interest either by a enzymatic or metabolic pathway. In the subsequent step, the modified biomolecule is tagged through a bioorthogonal reaction.

The bioorthogonal chemical reporter strategy typically proceeds in two steps. Firstly, a biomolecule precursor of interest (ie. nucleoside, amino acid, glycan or fatty acid) is modified with a bioorthogonal chemical reporter and introduced into the cell either by a

native or engineered biosynthetic pathway. Once incorporated in the target biomolecule, the chemical reporter undergoes reaction with an exogenously delivered chemical probe bearing the complementary functional group. Existing strategies for addressing the first step include, 1) amber codon suppression mutagenesis,[9-11] expressed protein ligation,[12-17] metabolic engineering,[8,18,19] and tagging-*via*-substrate[20-25](substrates include metabolites, enzyme inhibitors *etc.*).[5] The second step can be accomplished by judicious choice of the reaction chemistry based on stringent bioorthogonal criteria.

There are several criteria that must be satisfied when developing bioorthogonal reactions (Figure 1-2). Requirements include: 1) the reaction partners must be mutually reactive and do not cross react with biological functionality (ie. nucleophilic side chains, electrophiles, etc.); 2) the reaction must be high yielding; 3) The reaction must be biocompatible and proceed under physiological settings (aqueous solution and neutral pH); 4) the reaction must display fast kinetics and occur on the time scale of biological processes (ie. minutes) to prevent competition with reactions that may diminish small signals produced by less abundant species; 5) reactants and products are stable and ideally non-toxic; and 6) the chemical reporter must not alter the structure of the substrate to avoid affecting its bioactivity.

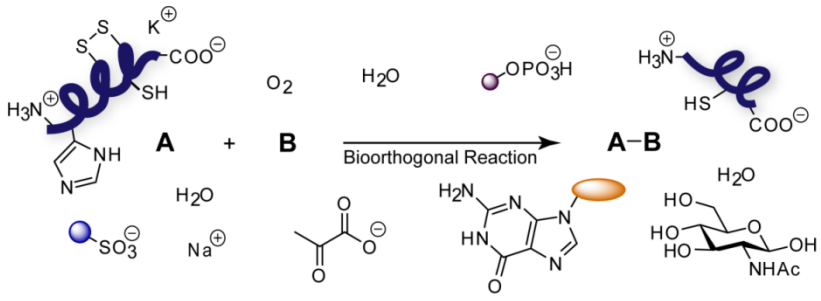

Figure 1-2. Bioorthogonal reactions between reagents **A** and **B** selectively form covalent bonds in the presence of the cellular components of a biological system.[2,6,7]

A major consideration when developing bioorthogonal reactions is that the reaction must proceed with fast enough rates under physiological settings to enable labelling at low reagent concentrations thereby minimizing background signal. Typical metal-free bioorthogonal reactions are bimolecular and bioconjugate formation is proportional to rate.[5] From a practical point of view, reactions with larger k_2 values, and thus faster observed kinetics of bioorthogonal coupling reactions lead to shorter reaction times in biological systems. Also, larger k_2 values enable the reactions to reach completion at lower reagent concentrations as compared to slower reactions over the same reaction times.[26] Larger k_2 values can allow bioorthogonal labelling reactions to take place efficiently in a wider variety of living systems including live animals where the amounts of bioorthogonal reagents required may be limiting.

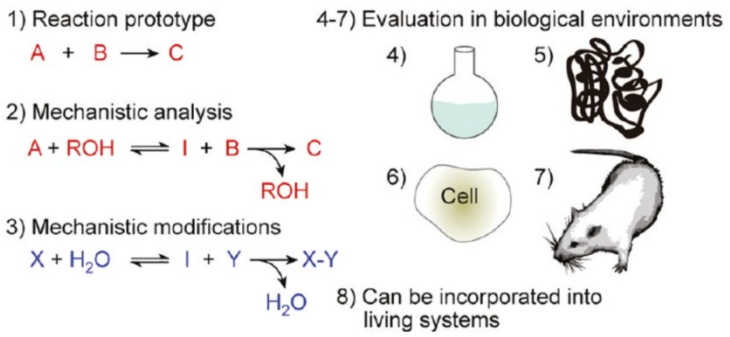

Figure 1-3. Step-by-step guide for developing bona-fide bioorthogonal reactions. Figure was reproduced from the literature.[6]

The process of developing a bioorthogonal reaction requires a multi-disciplinary approach involving mechanistic organic chemistry and biochemistry (Figure 1-3).[6] This endeavour typically begins with analysis of the functionalities and reactions that are present in the cell and selecting reactions and reagents that are abiotic. A prototype reaction is identified, often from early 20th century literature, and functional groups are chosen such that

they are exquisitely stable toward biological moieties, such as nucleophiles, reducing agents, and water (Figure 1-3, step 1).[6]

Once a prototype reaction is selected, analysis of the reaction and anticipation of undesired problems associated with application in biology are assessed to ensure that each step of the mechanism will be biocompatible (Figure 1-3, step 2). At this stage issues related to the stabilities of reactants and products in water, unwanted side reactivity with biological functionalities, and reaction kinetics are addressed. The reaction should be optimized so that the reaction proceeds at the fastest possible rate. Reactions that display second-order rate constants that are less than 10^{-4} $M^{-1}s^{-1}$ are too slow for practical use at low concentrations of reagents required for biological labelling.[6] Mechanistic modifications to reactants and products, and in some cases, the overall mechanism are explored to improve the kinetics of the reaction (Figure 1-3, step 3). Mechanistic modifications may include intercepting a reactive intermediate intramolecularly, addition of sterically encumbered groups to minimize cross-reactivity with biological nucleophiles, exchange of heteroatoms to optimize orbital interactions, or activation of reagents through ring strain or electronic perturbation, amongst other possibilities.[6]

Once a prospective reaction is optimized, it is tested in a variety of biological environments, escalating in complexity from aqueous media to biomolecule solutions to cultured cells and for the most optimized transformations, within living organisms (Figure 1-3, steps 4-7). The reaction must be dependable in aqueous media in the presence of biological functionalities such as amino acid side chains (step 4), the reaction must be examined on biomolecules such as proteins (step 5), live cells (step 6), and ultimately in living organisms (step 7).[6]

A true test of bioorthogonal reactivity requires one of the groups to be incorporated into a living system by native or engineered biosynthetic pathways (Step 8). Not all bioorthogonal reactions that are mentioned in the following section have been successfully employed in living animals or even live cells, albeit applications within living systems is the central goal. Given the stringent requirements listed above, it is not surprising that only select few organic reactions have proven to be bioorthogonal. There is an increasing demand to develop new bioorthogonal reactions that proceed at exceptionally fast rates and do not compromise the function and metabolic processing of biomolecules in living systems.

A number of chemical reactions have been developed that fulfill the requirements of bioorthogonality. This section describes bioorthogonal reactions that have found applications for bioconjugation. Reactions include: oxime/hydrazine condensations, Staudinger ligation, copper(I)-catalyzed azide-alkyne cycloaddition (CuAAC), strain-promoted azide-alkyne cycloaddition (SPAAC), azide-oxabornadiene cycloaddition, strain-promoted cycloadditions of nitrile oxides with strained alkenes and alkynes, tetrazole-alkene photo 'click' reaction, inverse-electron demand Diels-Alder cycloaddition with strained alkenes and alkynes, olefin metathesis, palladium-mediated reactions, and quadricyclane ligation.

Oxime/Hydrazone Ligations

Ketone and aldehyde functionalities are attractive bioorthogonal reporters since they are easily incorporated into biomolecules via biosynthetic machinery,[19,27] and are essentially inert towards endogenous functionalities at neutral pH. The reactivity between aldehydes and hydrazides was first demonstrated in 1986, by Rideout for the *in-situ* drug assembly inside cancer cells.[28] Under physiological conditions, biomolecules bearing ketones (**1.1**) or

aldehydes (**1.2**) react with aminoxy (**1.3**) or hydrazide (**1.4**) probes to form the corresponding oxime (**1.5**) or hydrazone (**1.6**), respectively (Scheme 1-1).

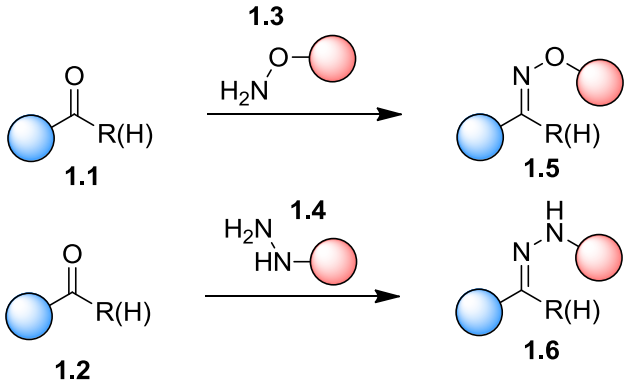

Scheme 1-1. Bioorthogonal reactions of ketones and aldehydes with aminoxy or hydrazide containing probes form oxime or hydrazone products, respectively.

The lack of ketone or aldehydes present on cell surfaces, prompted the use of keto-sugars as metabolic precursors for labelling cell surface sialic acid residues, and capture was accomplished by treatment with a hydrazide-biotin probe following streptavidin chromatography.[19] In this study, it was found that the rate of reaction of *N*-levulinoyl mannosamine modified sialic acids with a hydrazide reagent proceeded with a rate constant of 0.033 $M^{-1}s^{-1}$. Additionally, the oxime-hydrazone ligation was been utilized for modifying biotin ligase,[20] and proteins bearing genetically encoded aldehyde reporters[27] within living systems.

In a different approach, Paulson and co-workers were able to introduce the aldehyde reporter into cell-surface sialic acids by mild periodate oxidation.[29] Interestingly, the bioorthogonal reaction of the corresponding aldehyde with aminooxy-biotin was accelerated in the presence of aniline as a catalyst at neutral pH.[29,30] This is a significant improvement over the typical acidic conditions (pH = 5-6) used for oxime formation.[31] The hydrazone

ligation between 10 μM benzaldehyde and 10 μM 6-hydrazinopyridyl-modified peptide in the presence of 100 mM aniline at neutral pH proceeded with rate constants up to 170 $M^{-1}s^{-1}$.

Staudinger Ligations

A cornerstone reaction of bioorthogonal chemistry is the Staudinger ligation (Scheme 1-2A),[32] developed by the Bertozzi group in 2001, based on the prototypical Staudinger reduction of phenyl azide with triaryl phosphines to yield aniline and phosphine oxide.[33] Through modification of the triaryl phosphine with an *ortho*-methyl ester electrophilic trap (**1.8**), upon reaction with azide modified biomolecules (**1.7**) the ensuing aza-ylide intermediate (**1.10**), can be intercepted through nucleophilic attack of the nitrogen onto the ester moiety. Upon hydrolysis of the intermediate (**1.11**), a stable amide-linked product (**1.12**) is formed (Scheme 1-2A).[32]

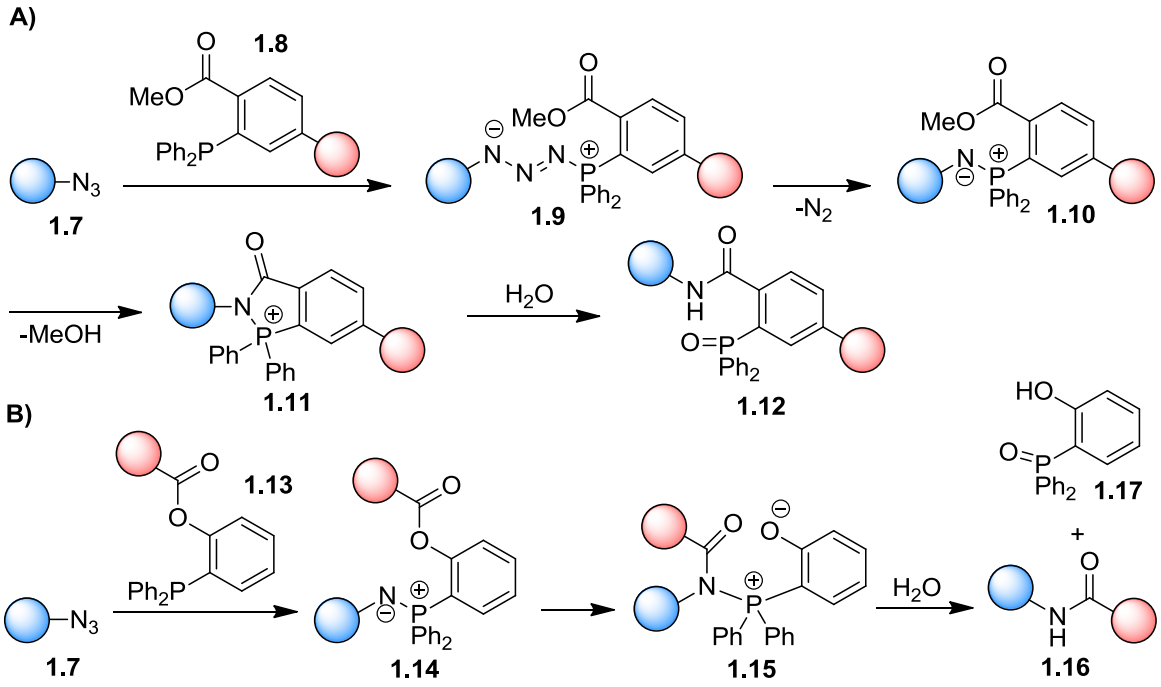

Scheme 1-2. A) Staudinger ligation and B) "traceless" Staudinger ligation.

Although the Staudinger ligation worked well in the presence of biological environments, the groups of Bertozzi and Raines simultaneously recognized. that a further modification to form a native amide bond without leaving the bulky phosphine oxide in the ligated product would be advantageous.[34,35] Modification of the phosphine reagent to create a cleavable linker between the acyl group and the phosphine that is expelled during the reaction resulted in the "traceless" Staudinger ligation (Scheme 1-2B).

The Staudinger reaction is highly specific, as evidenced from seminal studies in the presence of cellular lysates.[36] The Staudinger ligation has been implemented for glycoproteomic studies,[23] and for immobilization of azide-labelled proteins among other applications.[37,38] Recently, the Staudinger ligation has also been used for modification of cell-surface glycans in live mice.[8] The limitations of the Staudinger ligation include the susceptibility of the phosphine reagent to air oxidation catalyzed by cytochrome P_{450}. Additionally, the kinetics of Staudinger ligation are rather slow proceeding with second-order rate constants up to 0.0020 $M^{-1}s^{-1}$. The inherent slow rate necessitates the use of high concentrations of phosphine reagents. This is problematic for *in vivo* imaging applications, since removal of the excess phosphine reagent is difficult and results in background fluorescence signals.

Copper(I)-Catalyzed Azide-Alkyne Cycloadditions

The 1,3-dipolar cyloaddition of linear alkynes with azides to yield triazoles was developed by Huisgen,[39] and required extensive heating to overcome the activation barrier to deform the alkyne bond during the transition state. In 2002, the laboratories of Sharpless[40] and Meldal,[41] independently reported dramatic rate accelerations to the azide-alkyne cycloaddition upon using a copper(I) catalyst (Scheme 1-3). Since these ground breaking

reports, the scope of Cu(I)-catalyzed azide-alkyne cycloaddition (CuAAC) has been thoroughly investigated, including reaction rate acceleration, improved chemo- and regioselectivity, reaction scope and water compatibility, as well as mechanistic investigations.[42-44]

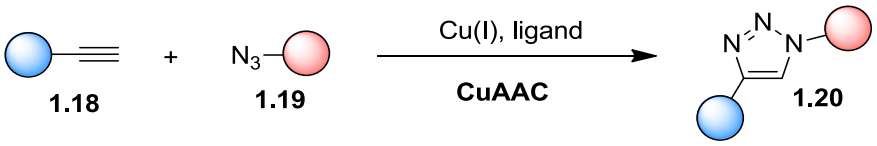

Scheme 1-3. Copper(I)-catalyzed alkyne-azide cycloaddition (CuAAC).

CuAAC has been applied broadly in diverse fields spanning bioconjugation *in vitro*[45-47] and in cell lysates,[48-51] polymer ligation,[52-56] dendrimer synthesis,[57,58] surface science[59-63] and combinatorial organic synthesis.[64,65] Effective labelling of biomolecules via CuAAC requires a ligand coordinated to copper to stabilize the Cu(I) oxidation state, enhance the reaction rate while preventing formation of undesired byproducts, and for sequestration of Cu(I) ions to prevent biomolecule damage and facilitate their removal.

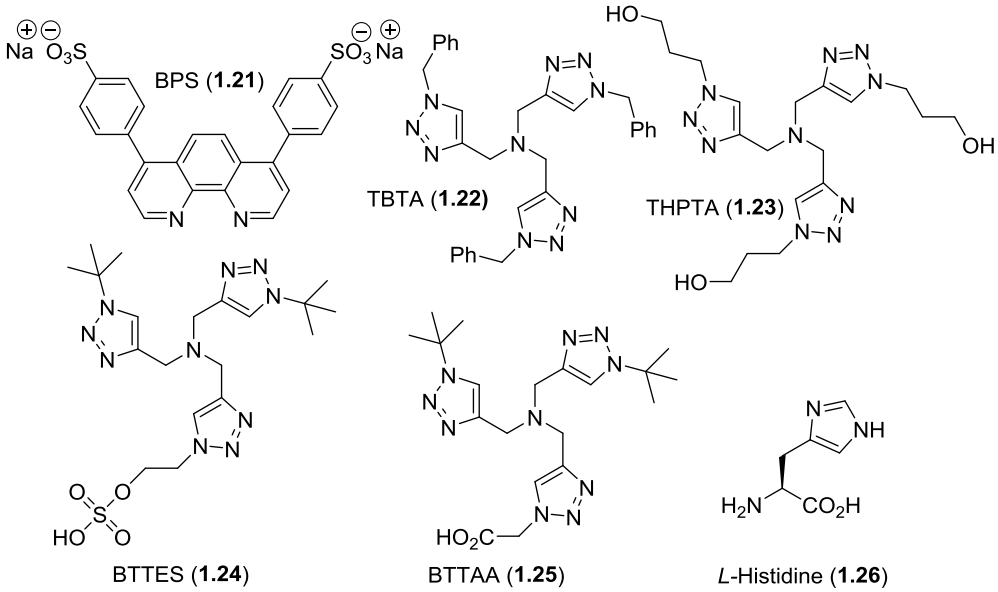

Figure 1-4. Ligands commonly used in Cu(I)-catalyzed azide-alkyne cycloadditions.

Prototypical CuAAC ligands (Figure 1-4) include: bathophenanthroline disulfonate disodium salt (BPS, **1.21**),[46,66] tris((1-benzyl-1H-1,2,3-triazol-4-yl)methyl)amine (TBTA, **1.22**),[67,68] tris-(hydroxypropyltriazolyl)-methylamine (THPTA, **1.23**),[69] 2-[4-{(bis[(1-*tert*-butyl-1H-1,2,3-triazol-4-yl)methyl]amino)-methyl}-1H-1,2,3-triazol-1-yl]ethyl hydrogen sulfate (BTTES, **1.24**),[70,71] 2-[4-{(bis[(1-*tert*-butyl-1H-1,2,3-triazol-4-yl)methyl]amino)methyl}-1H-1,2,3-triazol-1-yl]acetic acid (BTTAA, **1.25**),[72] and *L*-histidine (**1.26**).[73]

With regards to bioorthogonal labelling, CuAAC has primarily been effective for *in vitro* biological labelling and at live cell surfaces, due to its reliance on delivery of the copper catalyst to the reaction site and the toxicity of the copper complexes at concentrations employed for labelling.[51,74] CuAAC has been utilized for live-cell labelling of metabolically incorporated azide-containing[71,75,76] or alkyne-containing[77] *N*-acetylmannosamine derivatives into cell surface sialic acids.[70,73,78] Attempts to move this versatile chemistry from cell culture to more complex physiological settings have proven challenging. Despite improvements to the Cu(I)-catalyst that require shorter labelling times and have thus exhibited fewer toxic effects when administered to cells,[70,73] there is still a lack of options for *in vivo* labelling strategies where prolonged metal catalyst exposures cannot be avoided.

Strain-Promoted Azide-Alkyne Cycloadditions

In 1961, Wittig and Kreb reported that cyclooctyne, a small stable cyclooalkyne reacted "like an explosion" with phenyl azide.[79] The enhanced reactivity of the cyclooctyne is attributed to ~18 kcal/mol of ring strain associated with bond angle deformation in cyclooctyne that is released in the transition state. To improve upon the biocompatibility and kinetics of CuAAC, a copper-free variant, strain-promoted azide-alkyne cycloaddition

(SPAAC) was developed by Bertozzi *et al.*(Scheme 1-4).[80] The cyclooctyne (**1.27**) was functionalized with biological probes (ie. fluorophores or affinity tags) and used to isolate azide (**1.27**) modified glycans on proteins, in cell lysates, and on the surface of live cells.[81]

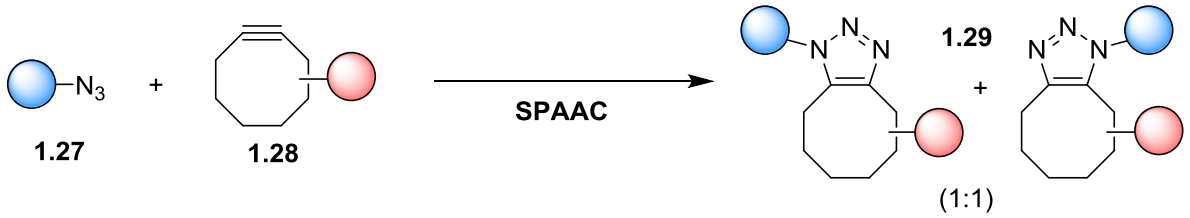

Scheme 1-4. Strain-promoted azide-alkyne cycloaddition (SPAAC).

A number of mechanism-based modifications to the strained alkyne component have been made to increase the kinetics of the reaction and improve bioavailability of SPAAC for applications *in vivo* (Figure 1-5). The first generation cyclooctyne (OCT, **1.30**), displayed a second-order rate constant of 0.0024 $M^{-1}s^{-1}$ in model reaction with benzyl azide. It was found that removal of the aryl side chain, termed aryl-less cyclooctyne (ALO, **1.31**), improved the water solubility however had marginal effect on the kinetics of SPAAC.[80] Since the reaction involved the alkyne lowest unoccupied molecular orbital (LUMO) and the highest occupied orbital (HOMO) of the the azide, lowering the LUMO of the alkyne through incorporation of electron withdrawing fluorine at the propargylic position, monofluorinated cyclooctyne (MOFO, **1.32**), resulted in a 3-fold enhancement in rate (k_2 = 0.0043 $M^{-1}s^{-1}$).[81] Incorporation of a *gem*-difluoro group at the propargylic position, difluorinated cyclooctyne (DIFO, **1.33**), increased the rate of SPAAC by 59-fold (k_2 = 0.0076 $M^{-1}s^{-1}$).[82]

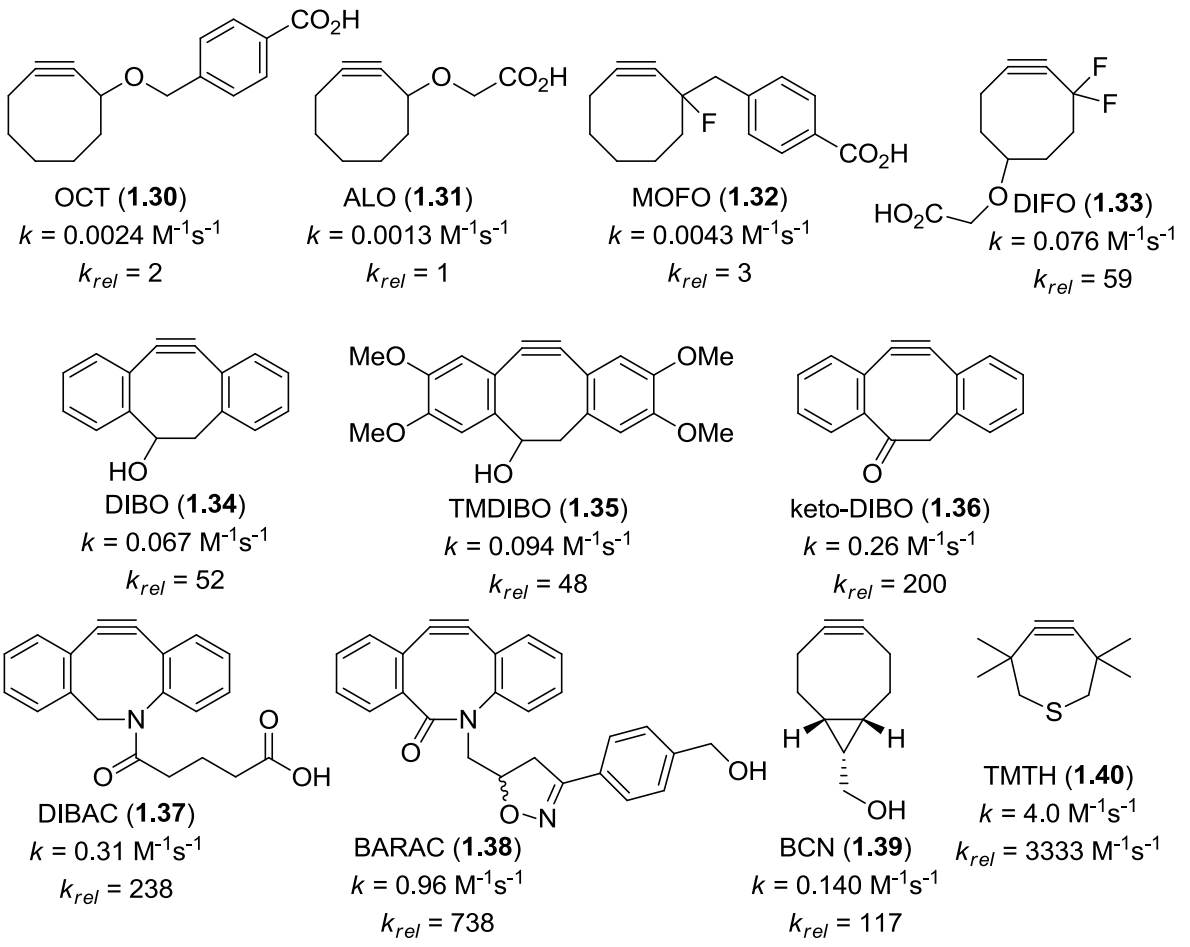

Figure 1-5. Cyclooctynes used in strain-promoted cycloadditions with benzyl azide, and their associated rate constants in MeCN (OCT, ALO, MOFO, BARAC) or MeOH (DIBO, TMDIBO, keto-DIBO, DIBAC).

Subsequently, strain modulation was also investigated. In 2008, the laboratory of Boons demonstrated that 4-dibenzocyclooctynol (DIBO, **1.34**, k_2 = 0.056 $M^{-1}s^{-1}$) displayed kinetics that are similar to the DIFO. Despite the low water solubility of DIBO, the reagent is attractive due to its synthetic tractability. Modifications to employ a photo caged DIBO synthon,[83] tetramethoxydibenzocyclooctynol (TMDIBO, **1.35**, k_2 = 0.094 $M^{-1}s^{-1}$),[84] and keto-DIBO (**1.36**, k_2 = 0.26 $M^{-1}s^{-1}$)[85] were subsequently reported. It was evident that the number of sp^2-hybridized atoms in the ring correlated well with the rate of cycloaddition with benzyl azide.

Through incorporation of an exocyclic amide off of the cyclooctyne, DIBAC (**1.37**) was prepared independently by the labs of Van delft and Popik.[86,87] In model reactions with benzyl azide it was found that DIBAC displayed rate constants of 0.31 $M^{-1}s^{-1}$ and had greater water solubility. The laboratory of Bertozzi returned to the forefront by incorporating an endocyclic amide, biaryl-aza-cyclooctynone (BARAC, **1.38**, k_2 = 0.96 $M^{-1}s^{-1}$),[88] that increased the reaction rate by another order of magnitude. Recent cyclopropane fusion distal to the alkyne reactive site was reported by Rutjes and van Delft.[89] Bicyclononyne (BCN, **1.39**, k_2 = 0.140 $M^{-1}s^{-1}$) shows reactivity that is comparable with DIBAC. Most recently, incorporation of a larger sulfur heteroatom has enabled the preparation of thiacycloheptyne (TMTH, **1.40**, k_2 = 4.0 $M^{-1}s^{-1}$), the smallest cycloalkyne known to date.[90] TMTH displays minimal steric hindrance surrounding the alkyne and exhibits a 4-fold enhancement in rate relative to BARAC.

In addition to captivating the chemical biology community, SPAAC has attracted the attention of physical organic chemists with the challenge of explaining the physical basis of the rate enhancement of cyclooctynes over linear alkynes in reactions with azides (ie. the effect of fluorination, aryl ring fusions, and other modifications to the cyclooctyne ring). Generally, there are two methods for activating alkynes; decrease the energy of the transition state or decrease the reactant stability (Figure 1-6). The decrease in activation energy is typical for reagents that are activated by reactant destabilization (ie. strain modulation), as is the case with DIBO, keto-DIBO, DIBAC, and BARAC. The lower stability of BARAC suggests that this approach is nearing the limit of practical applicability. Alternatively, activation of alkynes toward SPAAC, without sacrificing their stability or compromising functional group tolerance, can be accomplished by decreasing the transition state energy, either by minimizing unfavorable steric interactions (*ortho*-hydrogens in DIBO, DIBAC and

BARAC),[91] or by maximizing stabilizing effects in the transition state (ie incorporation of *gem*-difluoro electron withdrawing groups at the propargylic position in DIFO).

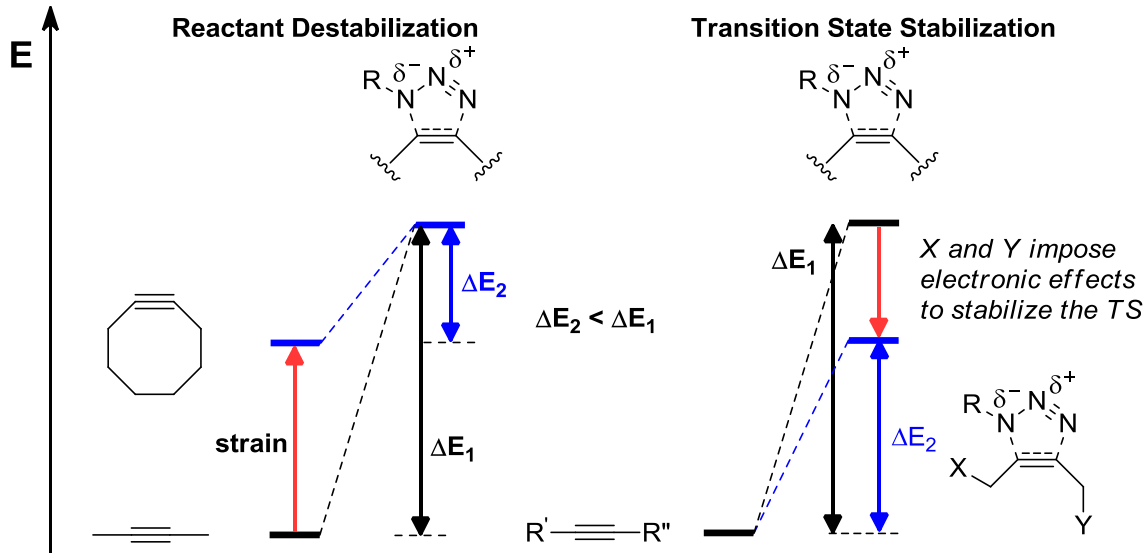

Figure 1-6. Comparison of various strategies for acceleration of SPAAC. Figure was reprinted from the literature.[92]

Houk[93] and Goddard[91] have shown a ~2 kcal/mol decrease in the energy of activation for DIFO relative to cyclooctyne. Houk and co-workers have hypothesized that the rate acceleration of SPAAC can be attributed to minimization of distortion energy during the transition state.[94] Goddard proposed the monobenzocyclooctyne (MOBO, k_2 = 0.0095 $M^{-1}s^{-1}$)[96] yields the optimal balance between stratain-release and minimization of the steric hindrance of the alkyne moiety.[91]

According to the minimization of distortion model of SPAAC (Figure 1-7), the differences in the energy required to distort the azide and alkyne into the transition state geometries controls the activation energy for the reaction.[94] The activation energy (ΔE), is the sum of the destabilizing distortions ($E_d^{\ddagger}$) and stabilizing interactions ($E_i^{\ddagger}$). Despite the azide functional group being the most significant source of distortions in SPAAC, the alkyne

is often the component that can easily be modified for higher reactivity in SPAAC. The calculated activation energy for the reaction of acetylene with phenyl azide is 16.2 kcal/mol, whereas the reaction of cyclooctyne with phenyl azide is 8.0 kcal/mol. This corresponds to a rate increase of 10^6. Additionally, the cyclooctyne requires less distortion energy (1.6 kcal/mol) relative to acetylene (4.6 kcal/mol) resulting in a lower activation energy despite smaller interaction energy.

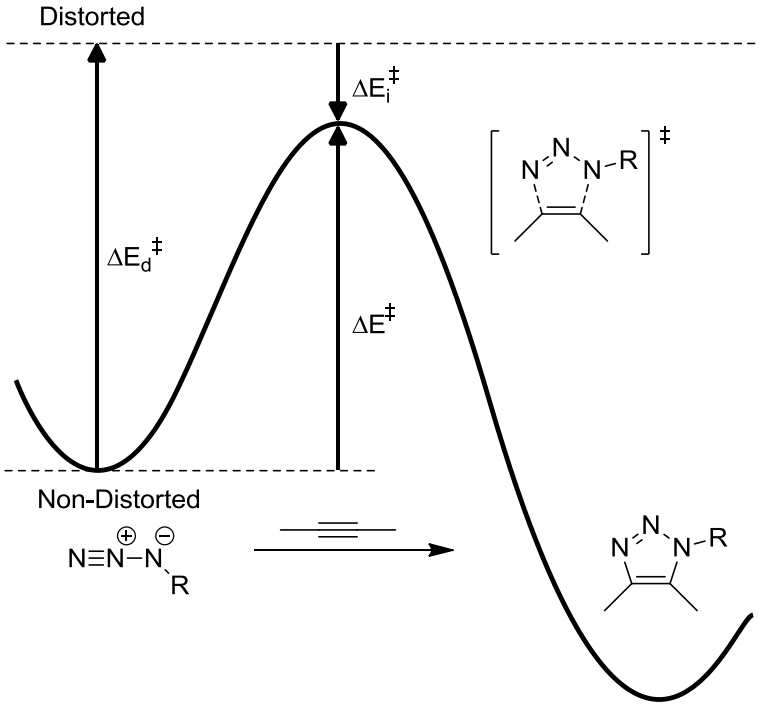

Figure 1-7. Relationships between activation, distortion, and interaction energies in cycloaddition of azides with alkynes. Figure was reproduced from the literature.[96]

Also, it has been postulated that electron withdrawing groups such as fluorine increase the rate by decreasing LUMO energy and the HOMO-LUMO energy gap. This leads to greater charge transfer from the azide to the cyclooctyne during the transition state, increasing interaction energy and decreases the overall activation energy.[96] The lowering of the LUMO, has recently been shown by Alabugin *et al.* to be the result of hyperconjugative

stabilization of the transition state via electron donation from the alkyne in-plane π donor orbital to the C-F σ* acceptor bond in DIFO.[92]

Applications of SPAAC for *in vivo* imaging, has been achieved using the reaction of DIFO probes with cell surface sialosides bearing the azide reporter. Various DIBO-fluorophore conjugates have been used to monitor the spatial and temporal dynamics of cell surface glycosylation during the development of nematode, *Caenorhabditis elegans*.[97] and zebrafish embryos.[98,99] SPAAC has also been used in a mouse model, where it was found that the water solubility of the DIFO caused the alkyne to be sequestered from tissue-resident azides, due to its high affinity for murine serum albumin (MSA).[100] To address this issue of non-specific protein binding, the hydrophilic yet less reactive, dimethoxy-aza-cyclooctyne (DIMAC, k_2 = 0.0030 $M^{-1}s^{-1}$)[101] was employed. Unfortunately, DIMAC's improved solubility did not compensate for its sluggish reactivity.[100] There is need for further optimization of the cyclooctyne probes to find the optimal balance between their reactivity and stability, as well as improved pharmacokinetic properties.

Cycloadditions of Azides with Strained Alkenes

Azides modified biomolecules (**1.41**) have found additional applications in [3+2] cycloadditions with the alkyne surrogates, oxanorbornadiene probes (**1.42**), yielding regioisomeric triazole products (**1.44**) (Scheme 1-5).[102] The initially formed triazoline cycloadduct (**1.43**) undergoes spontaneous retro-Diels-Alder reaction, releasing furan and **1.44**. Preliminary work has established its usefulness in peptide labelling experiments,[102] and it has also been used in the generation of imaging compounds.[104] The ring strain and electron deficiency in the oxanorbornadiene increases reactivity towards the cycloaddition. However, the reaction is limited by slow kinetics on the order of 10^{-4} $M^{-1}s^{-1}$.

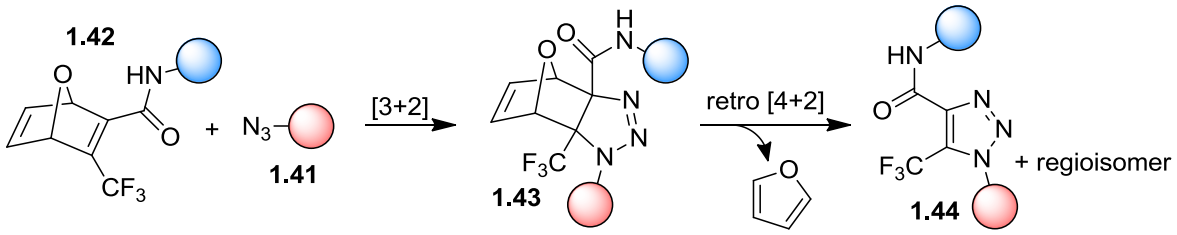

Scheme 1-5. Two step oxanorbornadiene-azide cycloaddition reaction to form triazoles.[104]

Cycloadditions of Nitrile-Oxides with Strained Alkenes

The copper-free cycloaddition of *in-situ* generated nitriles oxide with strained dipolarophiles has been reported (Scheme 1-6). The cycloaddition of nitrile oxide (**1.45**) with norbornene (**1.46**) proceeds effectively in a wide range of solvents, leading to a regioisomeric mixture of 2-isoxazolines (**1.47**), and has been employed for modification of oligonucleotides, yielding fluorescently labelled conjugates.[105,106] Nitrile oxides can be easily and quantitatively generated by oxidation of oximes (**1.48**) with phenyl iodine bis(trifluoroacetate) (PIFA) under aqueous conditions,[107] or by deprotonating the relatively stable arylchlorooximes (**1.49**) using a mild base.[106]

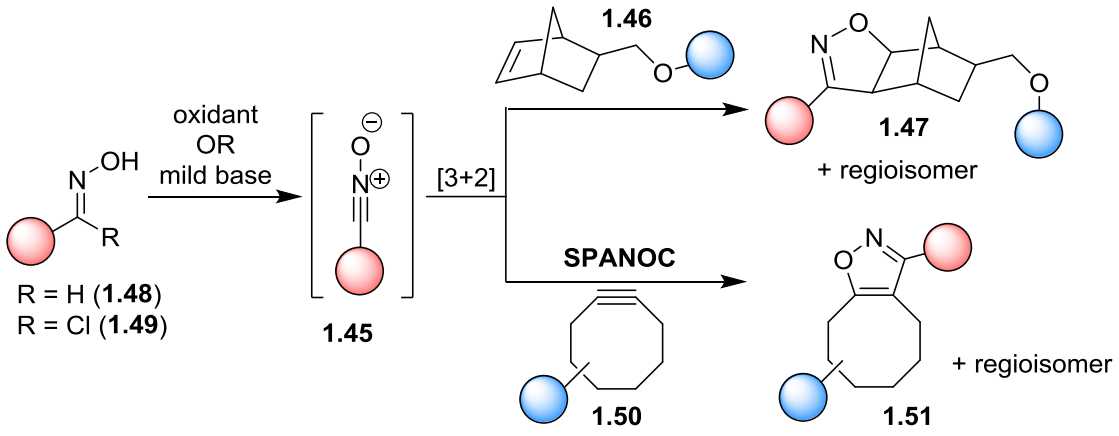

Scheme 1-6. *In situ* generation of nitrile oxide and subsequent 1,3-dipolar cycloaddition with norbornene or cyclooctyne probes.

Nitrile oxides (**1.45**) have also been used in strain-promoted cycloadditions with cyclooctynes (**1.50**), yielding a mixture of isoxazole products (**1.51**), demonstrating rate constants that are approximately 10 times faster SPAAC.[109] The strain-promoted alkyne-nitrile oxide cycloaddition (SPANOC) methodology has been employed for modification of a series of oxime containing nucleotides and peptides,[107] as well as carbohydrates.[108] Aside from the potential cross reactivity problems associated with *in situ* generation of nitrile oxides, the attractiveness of SPANOC includes: 1) the ease of nitrile oxide formation; 2) the cycloaddition of nitrile oxides to alkynes is ~6 kcal/mol lower than that for azides; and 3) the isoxazole product is stable.

Tetrazole-Alkene Cycloaddition Reactions

Photo inducible bioorthogonal reactions provide a time resolved chemical tool that can be used to study the spatial and temporal dynamics of biological processes. The photo triggered reaction between diaryl tetrazoles and alkenes was developed for bioconjugation by Lin *et al.*[109,110] The reaction follows a concerted mechanism whereby the diaryltetrazole (**1.52**) undergoes photo reversion releasing N_2 upon irradiation, thereby generating a nitrile imine dipole (**1.53**) that undergoes rapid 1,3-dipolar cycloaddition alkenes (**1.54**), yielding the corresponding pyrazoline cycloadduct (**1.55**) (Scheme 1-7).[110,111]

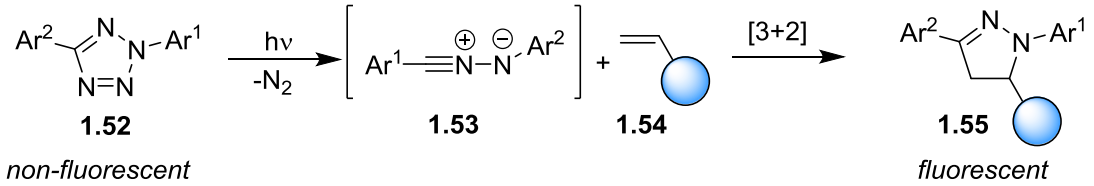

Scheme 1-7. Photo-induced 1,3-dipolar cycloadditions of 2,5-diaryltetrazoles and alkenes.[112]

Studies have shown that tetrazole-alkyne reaction can be utilized for modifying proteins bearing tetrazoles.[109] It was shown that in aqueous media (PBS pH = 7.5), upon photo irradiation at 302 nm, the nitrile imine undergoes facile 1,3-dipolar cycloaddition with alkenes with fast reaction kinetics (rate constants up to 11.0 $M^{-1}s^{-1}$). This rate constant is significantly faster than Staudinger ligation and is an order of magnitude faster than SPAAC. Subsequently, the bioorthogonality of the reaction was tested for residue-specific and site-specific modification of proteins. Fortuitously, the pyrazoline cycloadducts were also fluorescent, allowing direct in-gel fluorescence imaging during pyrazoline formation.

The utility of photo-induced nitrile imine-alkene cycloaddition for *in-vivo* labelling of protein was demonstrated with *E. coli* cells overexpressing an alkene-containing *Z*-domain protein.[113] An important mechanistic modification was uncovered to optimize the orbital energies, where the tetrazole was functionalized with electron donating groups to increase the HOMO of the nitrile-imine leading to an increased reactivity with terminal alkenes.[114] The reaction has been modified further to ensure utilization of longer wavelength light, to minimize biomolecule damage. Through the incorporation of conjugative groups into the diaryltetrazole, irradiation at longer wavelengths has enabled site specific labeling of homo-allyl glycine containing proteins *in vitro* and for spatiotemporally controlled imaging of newly synthesized proteins in *E. coli* and live mammalian cells.[112]

The majority of applications have been labelling of biosynthetically incorporated alkenes, however, recently, this methodology has been extended to genetic site-specific incorporation of tetrazole-amino acids into *E. coli.*,[115] and mammalian cells.[116] The major advantage of the tetrazole-alkene ligation is the photo inducibility of the 1,3-dipole component, enabling spatial-temporal control over reaction initiation.

Tetrazine-Based Inverse-Electron Demand Diels-Alder Reactions

The Diels-Alder reaction is a particularly attractive bioorthogonal reaction, since it is known to proceed faster in water than in organic solvents due to the hydrophobic effect.[117] Not surprisingly, the Diels-Alder reaction has been employed in bioconjugation for more than a decade.[118-121] Recently, an extraordinarily fast inverse-electron demand Diels-Alder reaction (IEDDA) between *trans*-cyclooctene[122,123] (**1.56**) and 1,2,4,5-tetrazines (**1.57**) was reported by Fox *et al.*[124] In this reaction the tetrazine serves as the diene in reaction with *trans*-cyclooctene to yield the dihydropyrazine cycloadduct (**1.59**) upon extrusion of nitrogen and tautomerization (Scheme 1-8). This reaction displays second-order rate constants up to 2000 $M^{-1}s^{-1}$, which are several orders of magnitude greater than the other bioorthogonal reactions mentioned above. The reaction has undergone significant mechanistic modification to improve the kinetics of this reaction by optimizing the reactivity, stability, and cell permeability of the tetrazine[125] and *trans*-cyclooctene[126] derivatives.

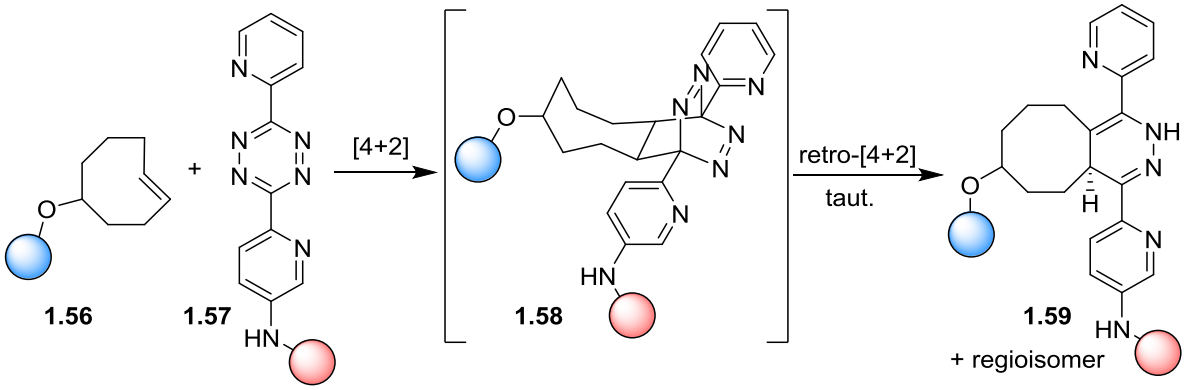

Scheme 1-8. Inverse electron-demand Diels-Alder reactions of tetrazines with *trans*-cyclooctenes.

Applications of tetrazine-*trans*-cyclooctene ligations have included fluorescence labelling of cancer cells,[127,128] *in vivo* cancer imaging with ^{111}In,[129] and ^{18}F radiolabelling,[130-132] cancer

cell detection,[133] fluorescent imaging cytoskeletal proteins within living mammalian cells,[134] and recently the methodology has been used with amino acids modified by tetrazine[135] and *trans*-cyclooctene[136] for genetic incorporation into proteins *in vivo*. The fast kinetics of tetrazine-*trans*-cyclooctene ligation will be particularly useful for tracking fast biological processes and for labelling low-abundance proteins.

Shortly after the inception of the tetrazine-*trans*-cyclooctene ligation, Hilderbrand and co-workers reported the reaction between norbornene (**1.60**) and monoaryltetrazine-tethered fluorophore (**1.61**) modified monoclonal antibody for pre-targeted imaging of live human cancer cells (Scheme 1-9).[137] Subsequently, genetic incorporation of a norbornene amino acid using the pyrrolysyl tRNA synthetase/$tRNA_{CUA}$ pair in *E. coli* and mammalian cells has enabled fluorescence labelling of newly synthesized proteins.[138]

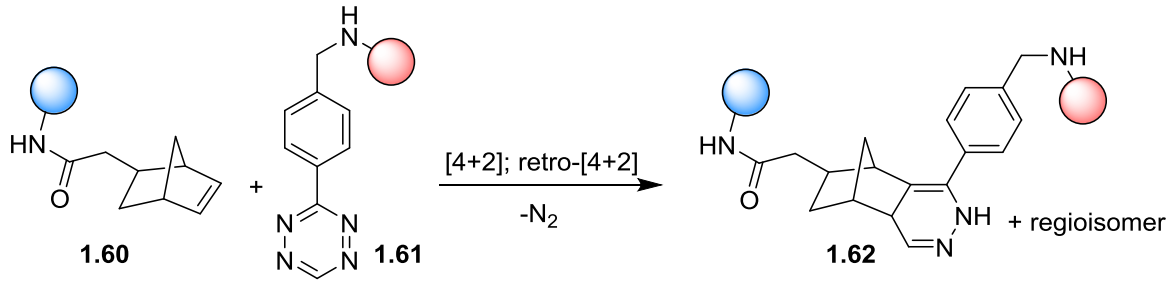

Scheme 1-9. IEDDA reactions of tetrazines with norbornene functionalized biomolecules.

In yet other independent efforts, tetrazines (**1.63**-**1.65**) have been employed for bioconjugation with other dienophiles, including cyclobutene containing peptides (**1.66**),[139] with proteins bearing genetically encoded cyclooctyne amino acids (**1.67**),[140] and most recently with phospholipids containing a cyclopropene motif (**1.68**) (Scheme 1-10).[141] The reactions of tetrazines with cyclooctynes or cyclopropenes provide rate constants up to 45 $M^{-1}s^{-1}$ and 13 $M^{-1}s^{-1}$, respectively. It has been demonstrated that the tetrazine-*trans*-cyclooctene displays superior reaction kinetics that are 3-7 orders of magnitude greater than many other

bioorthogonal reactions. The tetrazine-*trans*-cyclooctene ligation proceeds with rates that are ~10-15 times faster than reactions of tetrazines with cyclooctynes, and ~1000 times faster than the tetrazine-norbornene cycloaddition.[136] As bioorthogonal reagents, tetrazines are only limited by their bulky size. Attempts to improve the kinetics of the tetrazine-*trans*-cyclooctene ligation have involved increasing the strain in the *trans*-cyclooctene reagent through cyclopropyl fusion. The reactions of tetrazine with strained *trans*-cyclooctene (sTCO, **1.65**), were too fast for accurate measurement by stop flow and it was estimated that these reactions were ~ 50 times faster than analogous reactions with *trans*-cyclooctene.[136]

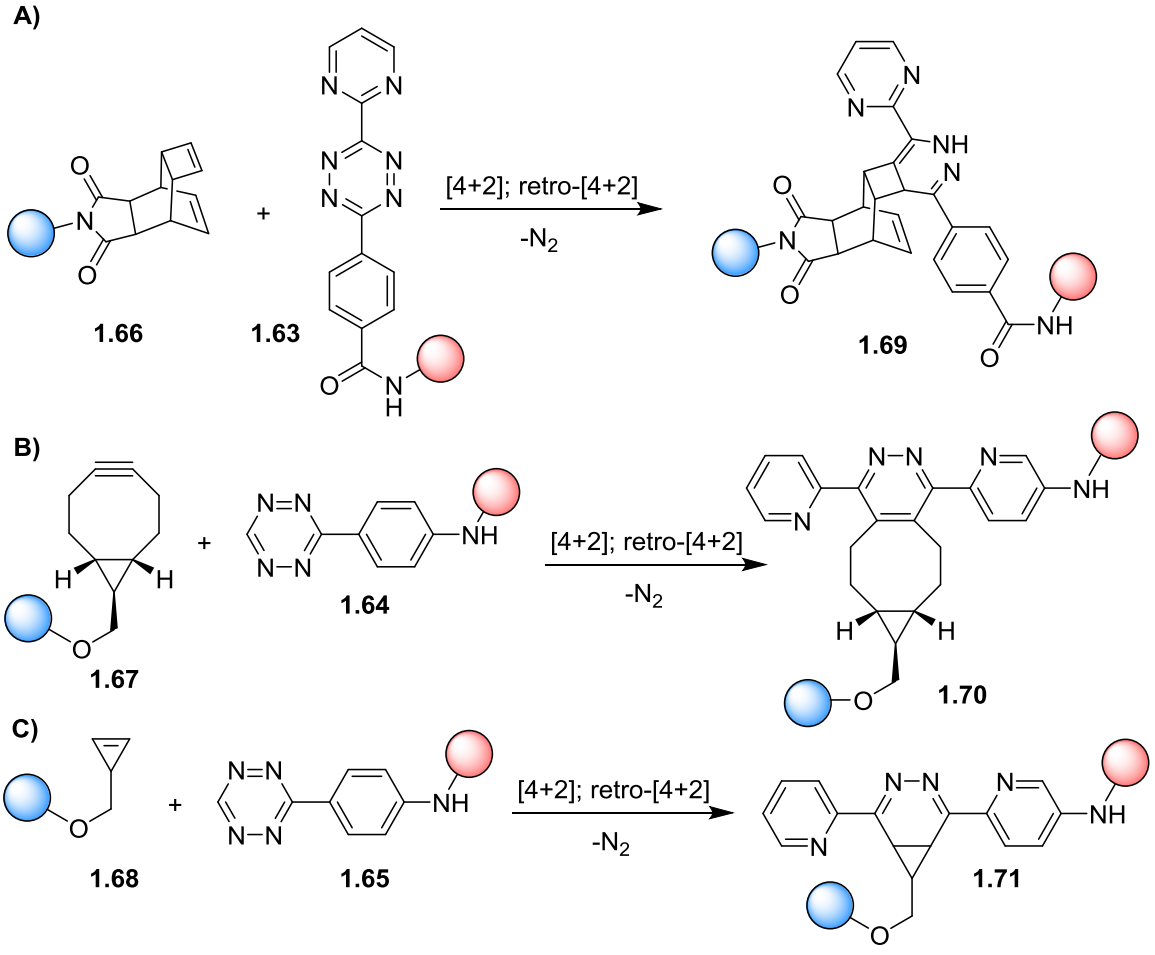

Scheme 1-10. Second generation tetrazine-based IEDDA ligations. A) Tetrazine-Cyclobutene reaction. B) Tetrazine-Cyclooctyne reaction. C) Tetrazine-Cyclopropene reaction.

Olefin Metathesis on Proteins

Another transformation that takes advantage of the alkene as a bioorthogonal reactive group is olefin metathesis, that has emerged as a viable bioorthogonal reaction for selective covalent modification on peptides and proteins, primarily due to its functional group tolerance (Scheme 1-11).[142]

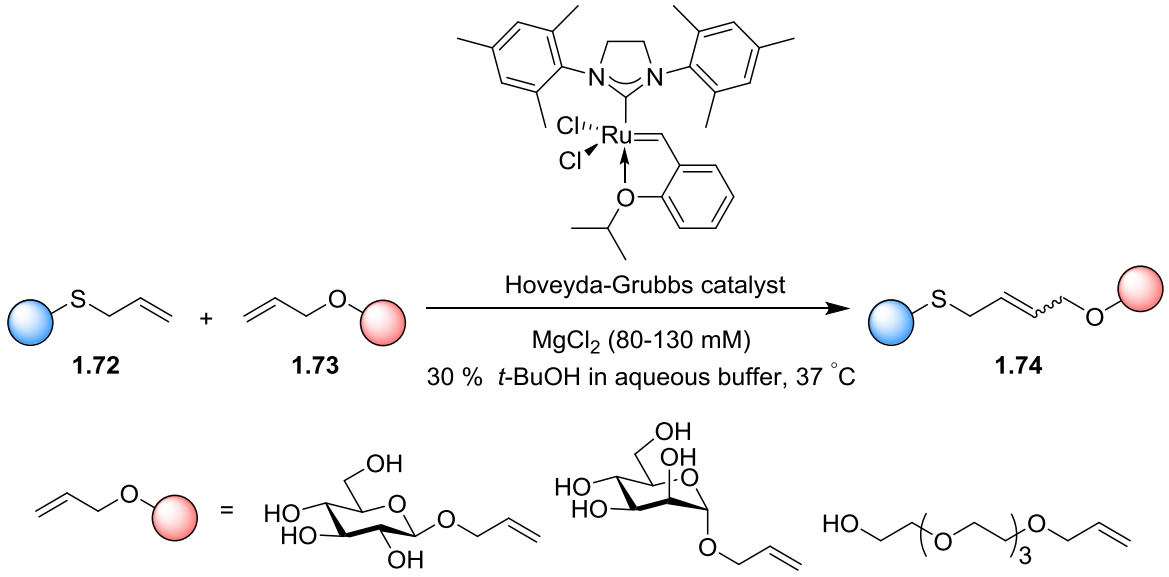

Scheme 1-11. Protein functionalization by olefin cross-metathesis.[5]

Using the Hoveyda-Grubbs second generation catalyst in a screen of several alkene containing amino acids, it was found that *S*-allylcysteine (**1.72**) was an exceptional substrate in cross metathesis on proteins.[143] *S*-allylcysteine can be easily introduced to proteins by conjugate addition of allyl thiol to dehydroalanine, direct allylation of cysteine, or by desulfurization of allyl disulfide. Through incorporation of *S*-allylcysteine on the surface of a single cysteine mutant of serine protease subtilisin *Bacillus lentus* (SBL), olefin metathesis has been used to introduce modifications such as glycosylation and PEGylation (Scheme 1-11).[143]

Encouraged by the fact that *S*-allylcysteine can be metabolically incorporated into proteins, either as a methionine surrogate in methionine auxotrophic *E. coli*,[144] or by reassignment of the amber stop codon,[145] the true potential of allyl sulfides as a bioorthogonal reporter for cross-metathesis *in-vivo* remains to be reported.

Palladium Catalyzed Cross-Coupling Reactions

Palladium catalyzed cross-coupling reactions are amongst the most powerful and versatile organic transformations known today.[146] They are particularly attractive for bioorthogonal reaction development because they display excellent functional group tolerance and compatibility with water.[147]

Mizoruki-Heck reaction

Yokoyama and co-workers have recently used the Mizoruki-Heck reaction for modifying a genetically engineered Ras protein bearing an *p*-iodophenylalanine (**1.75**) with an alkene tethered to biotin (**1.76**) (Scheme 1-12).[148] The reaction was facilitated by the water soluble Pd-TPPTS (triphenylphosphine-3,3',3"-trisulfonate) catalyst in a *N*-tris(hydroxymethyl)methyl-3-aminopropanesulfonate (TAPS) aqueous medium containing $MgCl_2$ and 5 ˚C.

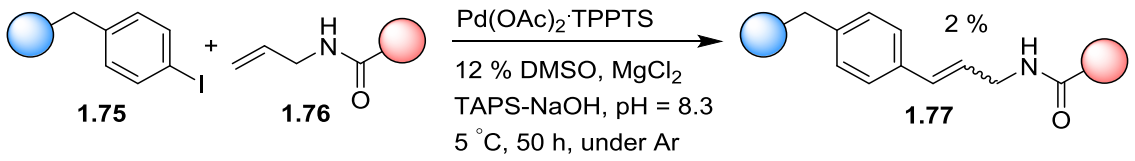

Scheme 1-12. Protein functionalization by the Mizoruki-Heck reaction.[5]

The reaction has come with minimal success for protein modification, due to the requirement of 12 % DMSO to achieve minimal conversion after prolonged reaction time under argon gas.

Sonagashira reaction

The site specific modification of *p*-iodophenylalanine-encoded Ras proteins (**1.78**) with a propargyl-tethered biotin (**1.79**) under aqueous Sonagashira coupling conditions was subsequently reported (Scheme 1-13).[149] The reaction still involved a complex mixture of reagents to achieve 25 % conversion, but in a significantly shorter reaction time than the previously reported Mizoruki-Heck reaction.

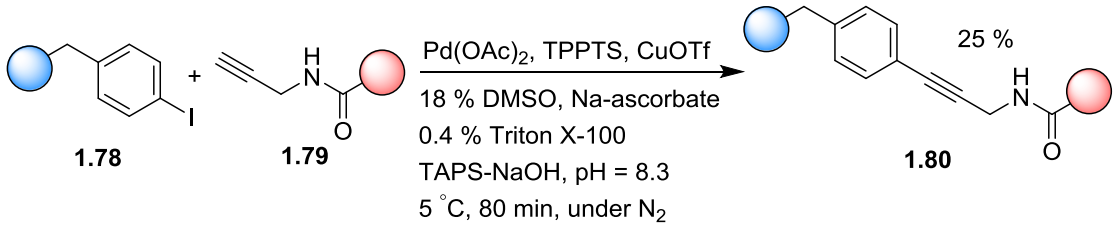

Scheme 1-13. Protein functionalization by Sonagashira cross-coupling.[5]

In 2011, a breakthrough copper-free Sonagashira variant was reported by Lin *et al.* (Scheme 1-14).[150] An aminopyrimidine-palladium(II) complex was used to ligate a genetically encoded homopropargylglycine (HPG) containing ubiquitin peptide (**1.81**) to a range of fluorophores and fluorinated aromatic compounds (**1.82**) in aqueous medium. The reaction can be conducted under much milder conditions than the previously reported Sonagashira coupling and provides good to excellent yields (55-93 %).

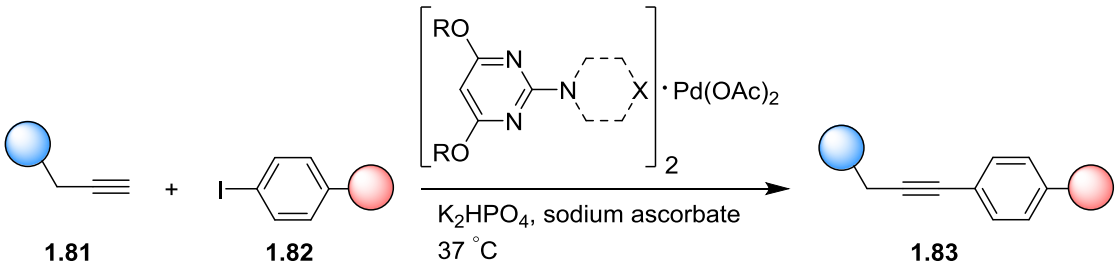

Scheme 1-14. Copper-free Sonagashira cross-coupling.[150]

Suzuki-Miyuara cross-coupling reaction

In 2008, the Suzuki-Miyuara cross-coupling between a *Z*-domain protein bearing a genetically encoded *p*-boronophenylalanine and a BODIPY aryliodide probe in a basic buffered solution (pH=8.5) using a Pd^0-dibenzylidene acetone (Pd-DBA) in 3-(4-(2-hydroxyethyl)-1-piperazinyl)-propanesulfonic acid (EPPS) buffer at 70 ˚C was reported by Schultz *et al*.[5,151] Recently, Davis *et al.* have demonstrated protein modification via Suzuki-Miyaura cross-coupling reaction using a water soluble Pd-catalyst, containing the sodium salt of 2-amino-4,6-dihydroxypyrimidine.[152] In the latter publication, subtilisin *Bacillus lentus* (SBL) bearing the S156C mutation was functionalized with *p*-iodobenzyl cysteine (Pic) (**1.84**) and coupled with various alkenyl and arylboronic acids (**1.85**) at 37 ˚C in aqueous media (Scheme 1-15). The reaction has also been used for modification of genetically encoded iodophenyl alanine[153] on the cell surfaces of *E. coli*.[154]

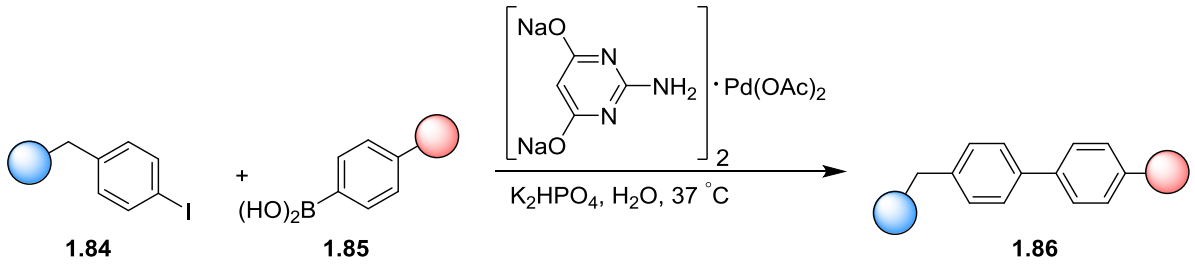

Scheme 1-15. Protein functionalization by Suzuki-Miyuara cross-coupling.

Quadricyclane Ligations

Recently, Bertozzi *et al.* have shown that highly strained quadricyclane (**1.87**) undergoes rapid [2+2+2] cycloaddition with the π-system of Ni-bis(dithiolene) reagents (**1.88**) with a rate constant of 0.25 $M^{-1}s^{-1}$ (Scheme 1-16).[155] Quadricyclane modified bovine serum albumin (BSA) can be efficiently labelled in the presence of cell lysates. The reaction

is orthogonal to SPAAC and oxime ligation. Quadricyclane is abiotic, stable at r.t. in aqueous media at pH 7 and is not known to react with biomolecules.

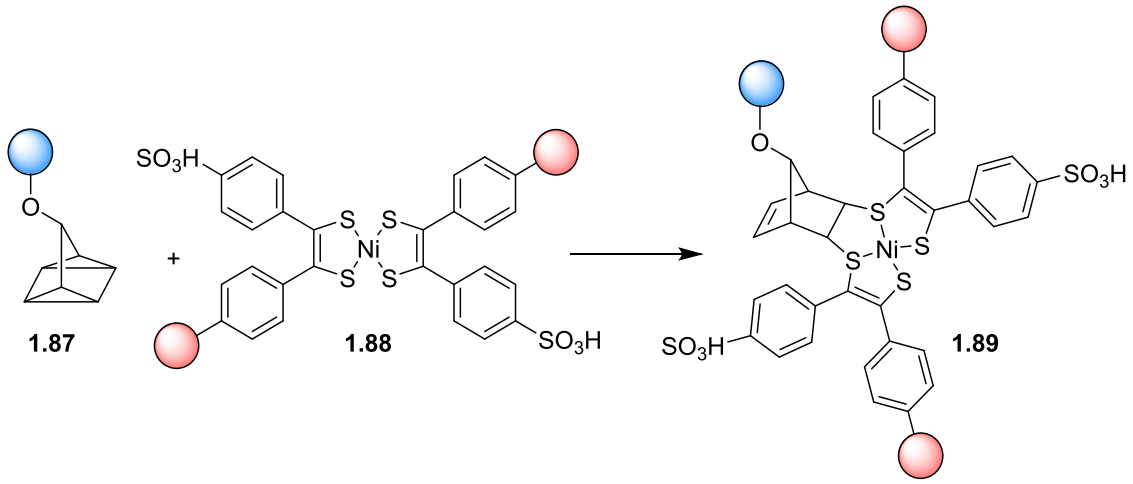

Scheme 1-16. Protein functionalization by quadricyclane ligation.[155]

Conclusions

The repertoire of bioorthogonal reactions has grown significantly in recent years. A number of water-compatible reactions based on nucleophilic additions, 1,3-dipolar cycloadditions, inverse-electron demand Diels-Alder reactions, olefin metathesis, palladium-mediated reactions, and quadricyclane reactions have been optimized for biomolecular substrates and each are at varying stages of bioorthogonal reaction development. As compared to conventional organic transformations, a much greater set of variables needs to be optimized concurrently (ie. bioorthogonality, reaction kinetics, inducibility, reactant encodability, etc.).

Amongst all known bioorthogonal reactions and depending on substrate structure, the tetrazine-*trans*-cyclooctene reaction demonstrates the fastest kinetics (k_2 = 2000 - 6000 $M^{-1}s^{-1}$). While strain-promoted azide-alkyne cycloadditions displays slower kinetics (rate constants up to 4 $M^{-1}s^{-1}$), SPAAC has displays greater biocompatibility due to the small size

of the azide reporter. Transition metal catalyzed reactions are limited by high catalyst loadings and the toxicity of the catalysts. The slowest reactions exhibit rate constants on the order of 10^{-4} $M^{-1}s^{-1}$. The ability to genetically encode or metabolically incorporate bioorthogonal reporter groups is of paramount importance. In this regard, the most successful reagents are small and non-perturbative, usually consisting of 3-4 atoms (eg. azides, alkynes and simple alkenes).

Cycloadditions have been most well developed likely due to the fact that the reactions are typically water-compatible, often display rate enhancements under aqueous conditions, and lack reactive intermediates that can be intercepted by biological nucleophiles and electrophiles. Emerging strategies utilize combinations of these reactions (orthogonal to each other) to functionalize multiple biomolecules *in vivo*. This provides avenues for investigating multiple processes that are not possible using one reaction alone.

Thesis Outlook

The above examples affirm the power of bioorthogonal chemistry and the impact these chemistries have had on advancing biological research. A central theme to the field of bioorthogonal chemistry is the development of highly specific organic reaction methodologies in water that proceed at fast enough rates to permit biological labelling at low reagent concentrations. The goal of the work presented in this thesis is to develop rapid bioorthogonal reaction methodology, and apply the reactants and products as tools for *in vivo* imaging of cell surface proteins. Despite the tremendous effort to develop biocompatible ligands in CuAAC and optimize the strained alkyne component in SPAAC reactions, less attention has been focused on alternative 1,3-dipoles, exhibiting different reactivity. Here we

describe the development of nitrones as 1,3-dipoles in cycloadditions with alkynes, and their applications for biological labelling.

The onset of this dissertation describes the development of a Cu(I)-catalyzed alkyne-nitrone cycloadditions (Kinugasa reaction) as an alternative to CuAAC for biological labelling. The established Kinugasa reaction methodology is then utilized to develop 'clickable' activity-based probes that can be used for studying the function of rhomboid proteases and other non-conventional targets of β-lactams. Alkyne functionalized β-lactams products of the Kinugasa reaction are then exploited as ligands for silver (Ag) nanoparticles and alkyne bound nanoparticles are used for SERS imaging cell surface proteins.

To improve the kinetics and biocompatibility of the developed Kinugasa reaction under 'click' chemistry conditions, we have explored copper-free 1,3-dipolar cycloadditions between nitrones or diazoalkanes and cyclooctynes. A series of acyclic and cyclic nitrones as well as diazoalkanes were synthesized, and tested in model cycloadditions with cyclooctynes. The observed rates were compared with analogous reactions of benzyl azide. Lastly, we describe the kinetics and scope of SPANC reactions involving cyclic nitrones, and applications of SPANC for protein functionalization *in vitro* and for imaging cell surface proteins.

References

(1) Nienhaus, G. U. *Angew. Chem. Int. Ed.* **2008**, *47*, 8992-8994.
(2) Sletten, E. M.; Bertozzi, C. R. *Angew. Chem. Int. Ed.* **2009**, *48*, 6974-6998.
(3) Kolb, H. C.; Finn, M. G.; Sharpless, K. B. *Angew. Chem. Int. Ed.* **2001**, *40*, 2004-2021.
(4) Kalia, J.; Raines, R. T. *Curr. Org. Chem.* **2010**, *14*, 138-147.
(5) Lim, R. K. V.; Lin, Q. *Chem. Commun.* **2010**, *46*, 1589-1600.
(6) Sletten, E. M.; Bertozzi, C. R. *Acc. Chem. Res.* **2011**, *44*, 666-676.
(7) Prescher, J. A.; Bertozzi, C. R. *Nat. Chem. Biol.* **2005**, *1*, 13-21.
(8) Prescher, J. A.; Dube, D. H.; Bertozzi, C. R. *Nature* **2004**, *430*, 873-877.
(9) Chin, J. W.; Cropp, T. A.; Anderson, J. C.; Mukherji, M.; Zhang, Z.; Schultz, P. G. *Science* **2003**, *301*, 964-967.
(10) Wang, L.; Brock, A.; Herberich, B.; Schultz, P. G. *Science* **2001**, *292*, 498-500.
(11) Xie, J.; Schultz, P. G. *Curr. Opin. Chem. Biol.* **2005**, *9*, 548-554.
(12) Arnold, U.; Hinderaker, M. P.; Nilsson, B. L.; Huck, B. R.; Gellman, S. H.; Raines, R. T. *J. Am. Chem. Soc.* **2002**, *124*, 8522-8523.
(13) Cotton, G. J.; Ayers, B.; Xu, R.; Muir, T. W. *J. Am. Chem. Soc.* **1999**, *121*, 1100-1101.
(14) Low, D. W.; Hill, M. G. *J. Am. Chem. Soc.* **1998**, *120*, 11536-11537.
(15) Muir, T. W.; Sondhi, D.; Cole, P. A. *Proc. Natl. Acad. Sci. U.S.A.* **1998**, *95*, 6705-6710.
(16) Pellois, J.-P.; Muir, T. W. *Curr. Opin. Chem. Biol.* **2006**, *10*, 487-491.
(17) Schnolzer, M.; Kent, S. B. H. *Science* **1992**, *256*, 221-225.
(18) Bertozzi, C. R.; Kiessling; Laura, L. *Science* **2001**, *291*, 2357-2364.
(19) Mahal, L. K.; Yarema, K. J.; Bertozzi, C. R. *Science* **1997**, *276*, 1125-1128.
(20) Chen, I.; Howarth, M.; Lin, W.; Ting, A. Y. *Nat. Methods* **2005**, *2*, 99-104.
(21) Keppler, A.; Gendreizig, S.; Gronemeyer, T.; Pick, H.; Vogel, H.; Johnsson, K. *Nat. Biotechnol.* **2003**, *21*, 86-89.
(22) Khidekel, N.; Ficarro, S. B.; Peters, E. C.; Hsieh-Wilson, L. C. *Proc. Natl. Acad. Sci. U.S.A.* **2004**, *101*, 13132-13137.
(23) Kho, Y.; Kim, S. C.; Jiang, C.; Barma, D.; Kwon, S. W.; Cheng, J.; Jaunbergs, J.; Weinbaum, C.; Tamanoi, F.; Falck, J.; Zhao, Y. *Proc. Natl. Acad. Sci. U.S.A.* **2004**, *101*, 12479-12484.
(24) Lin, C.-W.; Ting, A. Y. *J. Am. Chem. Soc.* **2006**, *128*, 4542-4543.
(25) Tai, H.-C.; Khidekel, N.; Ficarro, S. B.; Peters, E. C.; Hsieh-Wilson, L. C. *J. Am. Chem. Soc.* **2004**, *126*, 10500-10501.
(26) McKay, C. S.; Chigrinova, M.; Blake, J. A.; Pezacki, J. P. *Org. Biomol. Chem.* **2012**, *10*, 3066-3070.
(27) Carrico, I. S.; Carlson, B. L.; Bertozzi, C. R. *Nat. Chem. Biol.* **2007**, *3*, 321-322.
(28) Rideout, D. *Science* **1986**, *233*, 561-563.
(29) Zeng, Y.; Ramya, T. N. C.; Dirksen, A.; Dawson, P. E.; Paulson, J. C. *Nat. Methods* **2009**, *6*, 207-209.
(30) Dirksen, A.; Hackeng, T. M.; Dawson, P. E. *Angew. Chem. Int. Ed.* **2006**, *45*, 7581-7584.
(31) Jencks, W. P. *J. Am. Chem. Soc.* **1959**, *81*, 475-481.

(32) Saxon, E.; Bertozzi, C. R. *Science* **2000**, *287*, 2007-2010.
(33) Staudinger, H.; Meyer, J. *Helv. Chim. Acta* **1919**, *2*, 635-646.
(34) Nilsson, B. L.; Kiessling, L. L.; Raines, R. T. *Org. Lett.* **2000**, *2*, 1939-1941.
(35) Saxon, E.; Armstrong, J. I.; Bertozzi, C. R. *Org. Lett.* **2000**, *2*, 2141-2143.
(36) Kiick, K. L.; Saxon, E.; Tirrell, D. A.; Bertozzi, C. R. *Proc. Natl. Acad. Sci. U.S.A.* **2002**, *99*, 19-24.
(37) Chang, P. V.; Prescher, J. A.; Hangauer, M. J.; Bertozzi, C. R. *J. Am. Chem. Soc.* **2007**, *129*, 8400-8401.
(38) Köhn, M. *J. Pept. Sci.* **2009**, *15*, 393-397.
(39) Huisgen, R. *Angew. Chem. Int. Ed.* **1963**, *2*, 565-598.
(40) Rostovtsev, V. V.; Green, L. G.; Fokin, V. V.; Sharpless, K. B. *Angew. Chem. Int. Ed.* **2002**, *41*, 2596-2599.
(41) Tornøe, C. W.; Christensen, C.; Meldal, M. *J. Org. Chem.* **2002**, *67*, 3057-3064.
(42) Himo, F.; Lovell, T.; Hilgraf, R.; Rostovtsev, V. V.; Noodleman, L.; Sharpless, K. B.; Fokin, V. V. *J. Am. Chem. Soc.* **2004**, *127*, 210-216.
(43) Rodionov, V. O.; Presolski, S. I.; Díaz Díaz, D.; Fokin, V. V.; Finn, M. G. *J. Am. Chem. Soc.* **2007**, *129*, 12705-12712.
(44) Wu, P.; Fokin, V. V. *Aldrichimica Acta* **2007**, *40*, 7-17.
(45) Dirks, A. J. T.; Berkel, S. S. v.; Hatzakis, N. S.; Opsteen, J. A.; Delft, F. L. v.; Cornelissen, J. J. L. M.; Rowan, A. E.; Hest, J. C. M. v.; Rutjes, F. P. J. T.; Nolte, R. J. M. *Chem. Commun.* **2005**, *41*, 4172-4174.
(46) Gupta, S. S.; Kuzelka, J.; Singh, P.; Lewis, W. G.; Manchester, M.; Finn, M. G. *Bioconjugate Chem.* **2005**, *16*, 1572-1579.
(47) Salisbury, C. M.; Cravatt, B. F. *QSAR & Comb. Sci.* **2007**, *26*, 1229-1238.
(48) Beatty, K. E.; Fisk, J. D.; Smart, B. P.; Lu, Y. Y.; Szychowski, J.; Hangauer, M. J.; Baskin, J. M.; Bertozzi, C. R.; Tirrell, D. A. *ChemBioChem* **2010**, *11*, 2092-2095.
(49) Link, A. J.; Tirrell, D. A. *J. Am. Chem. Soc.* **2003**, *125*, 11164-11165.
(50) Sieber, S. A.; Niessen, S.; Hoover, H. S.; Cravatt, B. F. *Nat. Chem. Biol.* **2006**, *2*, 274-281.
(51) Speers, A. E.; Cravatt, B. F. *Chem. Biol.* **2004**, *11*, 535-546.
(52) Binder, W. H.; Kluger, C. *Macromolecules* **2004**, *37*, 9321-9330.
(53) Gupta, S. S.; Raja, K. S.; Kaltgrad, E.; Strable, E.; Finn, M. G. *Chem. Commun.* **2005**, *41*, 4315-4317.
(54) Opsteen, J. A.; van Hest, J. C. *Chem. Commun.* **2005**, *41*, 57-59.
(55) Parrish, B.; Breitenkamp, R. B.; Emrick, T. *J. Am. Chem. Soc.* **2005**, *127*, 7404-7410.
(56) Sumerlin, B. S.; Tsarevsky, N. V.; Louche, G.; Lee, R. Y.; Matyjaszewski, K. *Macromolecules* **2005**, *38*, 7540-7545.
(57) Malkoch, M.; Thibault, R. J.; Drockenmuller, E.; Messerschmidt, M.; Voit, B.; Russell, T. P.; Hawker, C. J. *J. Am. Chem. Soc.* **2005**, *127*, 14942-14949.
(58) Wu, P.; Malkoch, M.; Hunt, J. N.; Vestberg, R.; Kaltgrad, E.; Finn, M. G.; Fokin, V. V.; Sharpless, K. B.; Hawker, C. J. *Chem. Commun.* **2005**, *41*, 5775-5777.
(59) Collman, J. P.; Devaraj, N. K.; Chidsey, C. E. D. *Langmuir* **2004**, *20*, 1051-1053.
(60) Devaraj, N. K.; Miller, G. P.; Ebina, W.; Kakaradov, B.; Collman, J. P.; Kool, E. T.; Chidsey, C. E. D. *J. Am. Chem. Soc.* **2005**, *127*, 8600-8601.
(61) Díaz, D. D.; Punna, S.; Holzer, P.; McPherson, A. K.; Sharpless, K. B.; Fokin, V. V.; Finn, M. G. *J. Polym. Sci. Pol. Chem.* **2004**, *42*, 4392-4403.
(62) Lummerstorfer, T.; Hoffmann, H. *J. Phys. Chem. B* **2004**, *108*, 3963-3966.

(63) Meng, J.-C.; Averbuj, C.; Lewis, W. G.; Siuzdak, G.; Finn, M. G. *Angew. Chem. Int. Ed.* **2004**, *43*, 1255-1260.
(64) Fazio, F.; Bryan, M. C.; Blixt, O.; Paulson, J. C.; Wong, C.-H. *J. Am. Chem. Soc.* **2002**, *124*, 14397-14402.
(65) Goess, B. C.; Hannoush, R. N.; Chan, L. K.; Kirchhausen, T.; Shair, M. D. *J. Am.Chem. Soc.* **2006**, *128*, 5391-5403.
(66) Lewis, W. G.; Magallon, F. G.; Fokin, V. V.; Finn, M. G. *J. Am. Chem. Soc.* **2004**, *126*, 9152-9153.
(67) Chan, T. R.; Hilgraf, R.; Sharpless, K. B.; Fokin, V. V. *Org. Lett.* **2004**, *6*, 2853-2855.
(68) Hein, J. E.; Krasnova, L. B.; Iwasaki, M.; Fokin, V. V. *Org. Synth.* **2011**, *88*, 238-246.
(69) Hong, V.; Presolski, S. I.; Ma, C.; Finn, M. G. *Angew. Chem. Int. Ed.* **2009**, *48*, 9879-9883.
(70) Soriano del Amo, D.; Wang, W.; Jiang, H.; Besanceney, C.; Yan, A. C.; Levy, M.; Liu, Y.; Marlow, F. L.; Wu, P. *J. Am. Chem. Soc.* **2010**, *132*, 16893-16899.
(71) Zheng, T.; Jiang, H.; Gros, M.; Soriano del Amo, D.; Sundaram, S.; Lauvau, G.; Marlow, F.; Liu, Y.; Stanley, P.; Wu, P. *Angew. Chem. Int. Ed.* **2011**, *123*, 4199-4204.
(72) Besanceney-Webler, C.; Jiang, H.; Zheng, T.; Feng, L.; Soriano del Amo, D.; Wang, W.; Klivansky, L. M.; Marlow, F. L.; Liu, Y.; Wu, P. *J. Am. Chem. Soc.* **2011**, *50*, 1-7.
(73) Kennedy, D. C.; McKay, C. S.; Legault, M. C. B.; Danielson, D. C.; Blake, J. A.; Pegoraro, A. F.; Stolow, A.; Mester, Z.; Pezacki, J. P. *J. Am. Chem. Soc.* **2011**, *133*, 17993-18001.
(74) Soares, E. V.; Hebbelinck, K.; Soares, H. M. *Can. J. Microbiol.* **2003**, *49*, 336-343.
(75) Dehnert, K. W.; Beahm, B. J.; Huynh, T. T.; Baskin, J. M.; Laughlin, S. T.; Wang, W.; Wu, P.; Amacher, S. L.; Bertozzi, C. R. *ACS Chem. Biol.* **2011**, *6*, 547-552.
(76) Hong, V.; Steinmetz, N. F.; Manchester, M.; Finn, M. G. *Bioconjugate Chem.* **2010**, *21*, 1912-1916.
(77) Hsu, T. L.; Hanson, S. R.; Kishikawa, K.; Wang, S. K.; Sawa, M.; Wong, C. H. *Proc. Natl. Acad. Sci. U.S.A.* **2007**, *104*, 2614-2619.
(78) Besanceney-Webler, C.; Jiang, H.; Zheng, T.; Feng, L.; Soriano del Amo, D.; Wang, W.; Klivansky, L. M.; Marlow, F. L.; Liu, Y.; Wu, P. *Angew. Chem. Int. Ed.* **2011**, *50*, 8051-8056.
(79) Wittig, G.; Krebs, A. *Chem. Ber.* **1961**, *94*, 3260-3275.
(80) Agard, N. J.; Prescher, J. A.; Bertozzi, C. R. *J. Am. Chem. Soc.* **2004**, *126*, 15046-15047.
(81) Agard, N. J.; Baskin, J. M.; Prescher, J. A.; Lo, A.; Bertozzi, C. R. *ACS Chem. Biol.* **2006**, *1*, 644-648.
(82) Baskin, J. M.; Prescher, J. A.; Laughlin, S. T.; Agard, N. J.; Chang, P. V.; Miller, I. A.; Lo, A.; Codelli, J. A.; Bertozzi, C. R. *Proc. Natl. Acad. Sci. U.S.A.* **2007**, *104*, 16793-16797.
(83) Poloukhtine, A. A.; Mbua, N. E.; Wolfert, M. A.; Boons, G.-J.; Popik, V. V. *J. Am. Chem. Soc.* **2009**, *131*, 15769-15776.
(84) Stöckmann, H.; Neves, A. A.; Stairs, S.; Ireland-Zecchini, H.; Brindle, K. M.; Leeper, F. J. *Chem. Sci.* **2011**, *2*, 932-936.

(85) Mbua, N. E.; Guo, J.; Wolfert, M. A.; Steet, R.; Boons, G.-J. *ChemBioChem* **2011**, *12*, 1912-1921.
(86) Debets, M. F.; van Berkel, S. S.; Schoffelen, S.; Rutjes, F. P. J. T.; van Hest, J. C. M.; van Delft, F. L. *Chem. Commun.* **2010**, *46*, 97-99.
(87) Kuzmin, A.; Poloukhtine, A.; Wolfert, M. A.; Popik, V. V. *Bioconjugate Chem.* **2010**, *21*, 2076-2085.
(88) Jewett, J. C.; Sletten, E. M.; Bertozzi, C. R. *J. Am. Chem. Soc.* **2010**, *132*, 3688-3690.
(89) Dommerholt, J.; Schmidt, S.; Temming, R.; Hendriks, L. J. A.; Rutjes, F. P. J. T.; van Hest, J. C. M.; Lefeber, D. J.; Friedl, P.; van Delft, F. L. *Angew. Chem. Int. Ed.* **2010**, *49*, 9422-9425.
(90) de Almeida, G.; Sletten, E. M.; Nakamura, H.; Palaniappan, K. K.; Bertozzi, C. R. *Angew. Chem. Int. Ed.* **2012**, *51*, 2443-2447.
(91) Chenoweth, K.; Chenoweth, D.; Goddard III, W. A. *Org. Biomol. Chem.* **2009**, *7*, 5255-5258.
(92) Gold, B.; Shevchenko, N. E.; Bonus, N.; Dudley, G. B.; Alabugin, I. V. *J. Org. Chem.* **2012**, *77*, 75-89.
(93) Ess, D. H.; Houk, K. N. *J. Am. Chem. Soc.* **2008**, *130*, 10187-10198.
(94) Ess, D. H.; Jones, G. O.; Houk, K. N. *Org. Lett.* **2008**, *10*, 1633-1636.
(95) Sletten, E. M.; Nakamura, H.; Jewett, J. C.; Bertozzi, C. R. *J. Am. Chem. Soc.* **2010**, *132*, 11799-11805.
(96) Schoenebeck, F.; Ess, D. H.; Jones, G. O.; Houk, K. N. *J. Am. Chem. Soc.* **2009**, *131*, 8121-8133.
(97) Laughlin, S. T.; Bertozzi, C. R. *ACS Chem. Biol.* **2009**, *4*, 1068-1072.
(98) Baskin, J. M.; Dehnert, K. W.; Laughlin, S. T.; Amacher, S. L.; Bertozzi, C. R. *Proc. Natl. Acad. Sci. U.S.A.* **2010**, *107*, 10360-10365.
(99) Laughlin, S. T.; Baskin, J. M.; Amacher, S. L.; Bertozzi, C. R. *Science* **2008**, *320*, 664-667.
(100) Chang, P. V.; Prescher, J. A.; Sletten, E. M.; Baskin, J. M.; Miller, I. A.; Agard, N. J.; Lo, A.; Bertozzi, C. R. *Proc. Natl. Acad. Sci. U.S.A.* **2010**, *107*, 1821-1826.
(101) Sletten, E. M.; Bertozzi, C. R. *Org. Lett.* **2008**, *10*, 3097-3099.
(102) van Berkel, S. S.; Dirks, A. J.; Debets, M. F.; van Delft, F. L.; Cornelissen, J. J. L. M.; Nolte, R. J. M.; Rutjes, F. P. J. T. *ChemBioChem* **2007**, *8*, 1504-1508.
(103) van Berkel, S. S.; Dirks, A. J.; Meeuwissen, S. A.; Pingen, D. L. L.; Boerman, O. C.; Laverman, P.; van Delft, F. L.; Cornelissen, J. J. L. M.; Rutjes, F. P. J. T. *ChemBioChem* **2008**, *9*, 1805-1815.
(104) Debets, M. F.; van Berkel, S. S.; Dommerholt, J.; Dirks, A. J.; Rutjes, F. P. J. T.; van Delft, F. L. *Acc. Chem. Res.* **2011**, *44*, 805-815.
(105) Singh, I.; Heaney, F. *Chem. Commun.* **2011**, *47*, 2706-2708.
(106) Gutsmiedl, K.; Wirges, C. T.; Ehmke, V.; Carell, T. *Org. Lett.* **2009**, *11*, 2405-2408.
(107) Jawalekar, A. M.; Reubsaet, E.; Rutjes, F. P. J. T.; van Delft, F. L. *Chem. Commun.* **2011**, *47*, 3198-3200.
(108) Sanders, B. C.; Friscourt, F.; Ledin, P. A.; Mbua, N. E.; Arumugam, S.; Guo, J.; Boltje, T. J.; Popik, V. V.; Boons, G.-J. *J. Am. Chem. Soc.* **2011**, *133*, 949–957.
(109) Song, W.; Wang, Y.; Qu, J.; Madden, M. M.; Lin, Q. *Angew. Chem. Int. Ed.* **2008**, *47*, 2832-2835.
(110) Wang, Y.; Rivera Vera, C. I.; Lin, Q. *Org. Lett.* **2007**, *9*, 4155-4158.

(111) Wang, Y.; Hu, W. J.; Song, W.; Lim, R. K. V.; Lin, Q. *Org. Lett.* **2008**, *10*, 3725-3728.
(112) Lim, R. K. V.; Lin, Q. *Acc. Chem. Res.* **2011**, *44*, 828-839.
(113) Song, W.; Wang, Y.; Qu, J.; Lin, Q. *J. Am. Chem. Soc.* **2008**, *130*, 9654-9655.
(114) Wang, Y.; Song, W.; Hu, W. J.; Lin, Q. *Angew. Chem. Int. Ed.* **2009**, *48*, 5330-5333.
(115) Wang, J.; Zhang, W.; Song, W.; Wang, Y.; Yu, Z.; Li, J.; Wu, M.; Wang, L.; Zang, J.; Lin, Q. *J. Am. Chem. Soc.* **2010**, *132*, 14812-14818.
(116) Song, W.; Wang, Y.; Yu, Z.; Vera, C. I. R.; Qu, J.; Lin, Q. *ACS Chem. Biol.* **2010**, *5*, 875-885.
(117) Rideout, D. C.; Breslow, R. *J. Am. Chem. Soc.* **1980**, *102*, 7816-7817.
(118) de Araújo, A. D.; Palomo, J. M.; Cramer, J.; Köhn, M.; Schröder, H.; Wacker, R.; Niemeyer, C.; Alexandrov, K.; Waldmann, H. *Angew. Chem. Int. Ed.* **2006**, *45*, 296-301.
(119) Latham-Timmons, H. A.; Wolter, A.; Shawn Roach, J.; Giare, R.; Leuck, M. *Nucleosides, Nucleotides Nucleic Acids* **2003**, *22*, 1495-1497.
(120) Seelig, B.; Jäschke, A. *Tetrahedron Lett.* **1997**, *38*, 7729-7732.
(121) Yousaf, M. N.; Mrksich, M. *J. Am. Chem. Soc.* **1999**, *121*, 4286-4287.
(122) Thalhammer, F.; Wallfahrer, U.; Sauer, J. *Tetrahedron Lett.* **1990**, *31*, 6851-6854.
(123) Royzen, M.; Yap, G. P. A.; Fox, J. M. *J. Am. Chem. Soc.* **2008**, *130*, 3760-3761.
(124) Blackman, M. L.; Royzen, M.; Fox, J. M. *J. Am. Chem. Soc.* **2008**, *130*, 13518-13519.
(125) Karver, M. R.; Weissleder, R.; Hilderbrand, S. A. *Bioconjugate Chem.* **2011**, *22*, 2263-2270.
(126) Taylor, M. T.; Blackman, M. L.; Dmitrenko, O.; Fox, J. M. *J. Am. Chem. Soc.* **2011**, *133*, 9646-9649.
(127) Devaraj, N. K.; Hilderbrand, S.; Upadhyay, R.; Mazitschek, R.; Weissleder, R. *Angew. Chem. Int. Ed.* **2010**, *49*, 2869-2872.
(128) Devaraj, N. K.; Upadhyay, R.; Haun, J. B.; Hilderbrand, S. A.; Weissleder, R. *Angew. Chem. Int. Ed.* **2009**, *48*, 7013-7016.
(129) Rossin, R.; Renart Verkerk, P.; van den Bosch, S. M.; Vulders, R. C. M.; Verel, I.; Lub, J.; Robillard, M. S. *Angew. Chem. Int. Ed.* **2010**, *49*, 3375-3378.
(130) Keliher, E. J.; Reiner, T.; Turetsky, A.; Hilderbrand, S. A.; Weissleder, R. *ChemMedChem* **2011**, *6*, 424-427.
(131) Li, Z.; Cai, H.; Hassink, M.; Blackman, M. L.; Brown, R. C. D.; Conti, P. S.; Fox, J. M. *Chem. Commun.* **2010**, *46*, 8043-8045.
(132) Reiner, T.; Keliher, E. J.; Earley, S.; Marinelli, B.; Weissleder, R. *Angew. Chem. Int. Ed.* **2011**, *50*, 1922-1925.
(133) Haun, J. B.; Devaraj, N. K.; Hilderbrand, S. A.; Lee, H.; Weissleder, R. *Nat. Nanotechnol.* **2010**, *5*, 660-665.
(134) Liu, D. S.; Tangpeerachaikul, A.; Selvaraj, R.; Taylor, M. T.; Fox, J. M.; Ting, A. Y. *J. Am. Chem. Soc.* **2012**, *134*, 792-795.
(135) Seitchik, J. L.; Peeler, J. C.; Taylor, M. T.; Blackman, M. L.; Rhoads, T. W.; Cooley, R. B.; Refakis, C.; Fox, J. M.; Mehl, R. A. *J. Am. Chem. Soc.* **2012**, *134*, 2898-2901.
(136) Lang, K.; Davis, L.; Wallace, S.; Mahesh, M.; Cox, D. J.; Blackman, M. L.; Fox, J. M.; Chin, J. W. *J. Am. Chem. Soc.* **2012**, *134*, 10317-10320.
(137) Devaraj, N. K.; Weissleder, R.; Hilderbrand, S. A. *Bioconjugate Chem.* **2008**, *19*, 2297-2299.

(138) Lang, K.; Davis, L.; Torres-Kolbus, J.; Chou, C.; Deiters, A.; Chin, J. W. *Nat. Chem.* **2012**, *4*, 298-304.
(139) Pipkorn, R.; Waldeck, W.; Didinger, B.; Koch, M.; Mueller, G.; Wiessler, M.; Braun, K. *J. Pept. Sci.* **2009**, *15*, 235-241.
(140) Chen, W.; Wang, D.; Dai, C.; Hamelberg, D.; Wang, B. *Chem. Commun.* **2012**, *48*, 1736-1738.
(141) Yang, J.; Šečkutė, J.; Cole, C. M.; Devaraj, N. K. *Angew. Chem. Int. Ed.* **2012**, *51*, 7476–7479.
(142) Lin, Y. A.; Chalker, J. M.; Davis, B. G. *J. Am. Chem. Soc.* **2010**, *132*, 16805-16811.
(143) Lin, Y. A.; Chalker, J. M.; Floyd, N.; Bernardes, G. a. J. L.; Davis, B. G. *J. Am. Chem. Soc.* **2008**, *130*, 9642-9643.
(144) van Hest, J. C. M.; Kiick, K. L.; Tirrell, D. A. *J. Am. Chem. Soc.* **2000**, *122*, 1282-1288.
(145) Ai, H.-W.; Shen, W.; Brustad, E.; Schultz, P. G. *Angew. Chem. Int. Ed.* **2010**, *49*, 935-937.
(146) Nicolaou, K. C.; Bulger, P. G.; Sarlah, D. *Angew. Chem. Int. Ed.* **2005**, *44*, 4442-4489.
(147) Shaughnessy, K. H. *Eur. J. Org. Chem.* **2006**, *2006*, 1827-1835.
(148) Kodama, K.; Fukuzawa, S.; Nakayama, H.; Kigawa, T.; Sakamoto, K.; Yabuki, T.; Matsuda, N.; Shirouzu, M.; Takio, K.; Tachibana, K.; Yokoyama, S. *ChemBioChem* **2006**, *7*, 134-139.
(149) Kodama, K.; Fukuzawa, S.; Nakayama, H.; Sakamoto, K.; Kigawa, T.; Yabuki, T.; Matsuda, N.; Shirouzu, M.; Takio, K.; Yokoyama, S.; Tachibana, K. *ChemBioChem* **2007**, *8*, 232-238.
(150) Li, N.; Lim, R. K. V.; Edwardraja, S.; Lin, Q. *J. Am. Chem. Soc.* **2011**, *133*, 15316-15319.
(151) Brustad, E.; Bushey, M. L.; Lee, J. W.; Groff, D.; Liu, W.; Schultz, P. G. *Angew. Chem. Int. Ed.* **2008**, *47*, 8220-8223.
(152) Chalker, J. M.; Wood, C. S. C.; Davis, B. G. *J. Am. Chem. Soc.* **2009**, *131*, 16346-16347.
(153) Xie, J.; Wang, L.; Wu, N.; Brock, A.; Spraggon, G.; Schultz, P. G. *Nat. Biotechnol.* **2004**, *22*, 1297-1301.
(154) Spicer, C. D.; Triemer, T.; Davis, B. G. *J. Am. Chem. Soc.* **2012**, *134*, 800-803.
(155) Sletten, E. M.; Bertozzi, C. R. *J. Am. Chem. Soc.* **2011**, *133*, 17570-1757.

Chapter 2 : Studies of Micelle-Promoted Kinugasa Reactions in Aqueous Media

A significant portion of the work presented in this chapter was published in:

McKay, C. S.; Kennedy, D. C.; Pezacki, J. P. *Tetrahedron Lett.* **2009**, *50*, 1893-1896.

Introduction

Azide-based cycloadditions have been used successfully in bioorthogonal chemistry for tracking biomolecules in living systems via the Staudinger ligation, Cu(I)-catalyzed azide-alkyne cycloaddition, and copper-free azide-alkyne cycloaddition.[1] The 1,3-dipolar cycloaddition reactions between azides and alkynes has been particularly successful for labelling biomolecules at low reagent concentrations due to the fast kinetics when catalyzed by Cu(I) or by strain-release of the alkyne moiety. Despite significant advances to generate more efficient and biocompatible Cu(I)-catalysts or to optimize strained alkyne structures, less attention has been focused on more common 1,3 dipoles, such as nitrones, as a means for improving the kinetics of bioorthogonal 1,3-dipolar cycloaddition reactions with alkynes.

The general applications of 1,3-dipolar cycloadditions was first established by Huisgen in the 1960s.[2] 1,3-dipolar cycloaddition reactions involve 4 π electrons from the dipole and 2 π electrons from the dipolarophile (Scheme 2-1). It is generally accepted that 1,3-dipolar cycloadditions follow a concerted mechanism, whereby three p_z orbitals from the dipole and two p_z orbitals from the dipolarophile combine suprafacially, with the description $[_{\pi}4_s + _{\pi}2_s]$ according to the Woodward-Hoffman rules.[3]

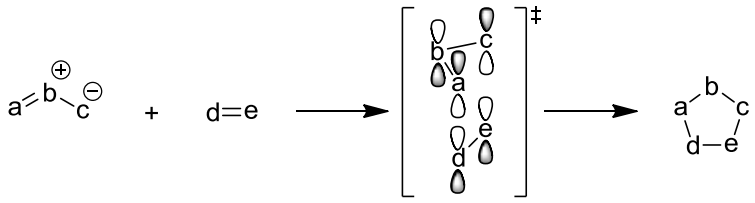

Scheme 2-1. [3+2] cycloadditions of 1,3-dipoles with dipolarophiles.

1,3-dipoles can be classified into two different types: allyl anion type and propargyl/allenyl anion type.[4-6] The allyl anion type 1,3-dipoles are bent and characterized by three p_z orbitals laying perpendicular to the plane of the dipole. The propargyl allenyl

anion type are linear and contain an extra π orbital in the plane orthogonal to the allenyl anion molecular orbital that is not involved in reactions of the dipole. The chemistry of 1,3-dipolar cycloaddition has evolved for more than 100 years and a variety of 1,3-dipoles have been discovered and are classified in Table 2-1.[4]

Table 2-1. Classification of 1,3-dipoles. Table was reprinted from literature.[6]

Allyl anion type			
Nitrogen in the middle		Oxygen in the middle	
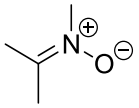	Nitrones	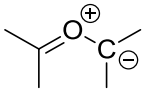	Carbonyl Ylides
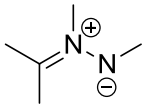	Azomethine Ylides	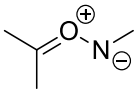	Carbonyl Imines
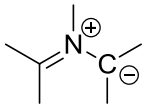	Azomethine Imines	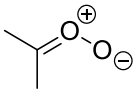	Carbonyl Oxides
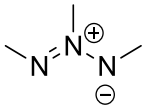	Azimines	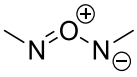	Nitrosimines
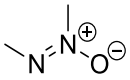	Azoxy Compounds	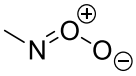	Nitrosoxides
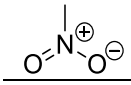	Nitro Compounds	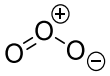	Ozone
Propargyl/allenyl anion type			
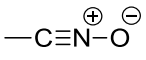	Nitrile Oxides	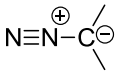	Diazoalkanes
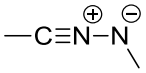	Nitrile Imines	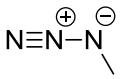	Azides
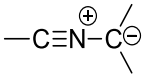	Nitrile Ylides	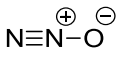	Nitrous Oxide

In the 1960's, the reaction mechanism for 1,3-dipolar cycloadditions attracted a significant amount of attention (Scheme 2-2).[7-9] Rolf Huisgen proposed a detailed rationale for the concerted mechanism based on kinetic measurements, stereochemical results, as well

as solvent and substituent effects.[9] On the other hand, Firestone considered that the reaction proceeded through a diradical intermediate, and presented a variety of challenges to the concerted mechanism.[7] The 1,3-dipolar reaction of benzonitrile oxide with *trans*-dideuterated ethylene gave exclusively the 5-substituted *trans*-isoxazoline.[6] Had a diradical intermediate been formed, 180° rotation of the terminal bond would have scrambled the stereochemistry yielding a mixture of the *cis* and *trans* isomers.[6] On the basis of the stereospecificity of the 1,3-dipolar cycloaddition, the dispute was settled in favour of the concerted mechanism:

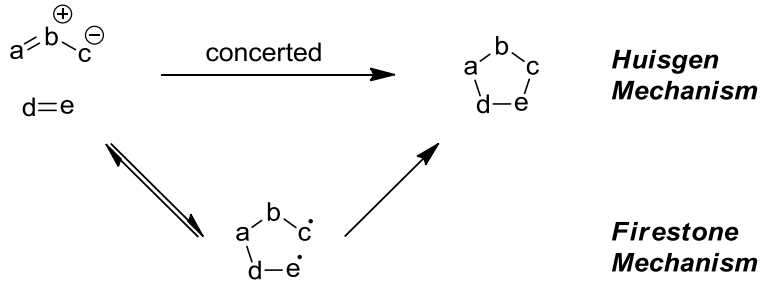

Scheme 2-2. Postulated mechanisms of 1,3-dipolar cycloadditions. Scheme was reprinted from the literature.[9]

The transition state of the concerted 1,3-dipolar cycloadditions is controlled by the frontier molecular orbitals (FMO) of the substrates.[6,10] The $LUMO_{dipole}$ can interact with the $HOMO_{dipolarophile}$, and conversely the $HOMO_{dipole}$ can interact with the $LUMO_{dipolarophile}$. As the HOMO-LUMO energy gap decreases the reactivity increases. Sustman has classified 1,3-dipolar cycloadditions into three types, on the basis of the relative FMO energies between the dipole and dipolarophile (Figure 2-1).[6,11,12] Type I reactions are dominated by $HOMO_{dipole}$-$LUMO_{dipolarophile}$ interactions. For type II, the similarity of the dipole and dipolarophile FMO energies indicate both HOMO-LUMO interactions are important. In type III, interactions between the $LUMO_{dipole}$ and the $HOMO_{dipolarophile}$ predominate.

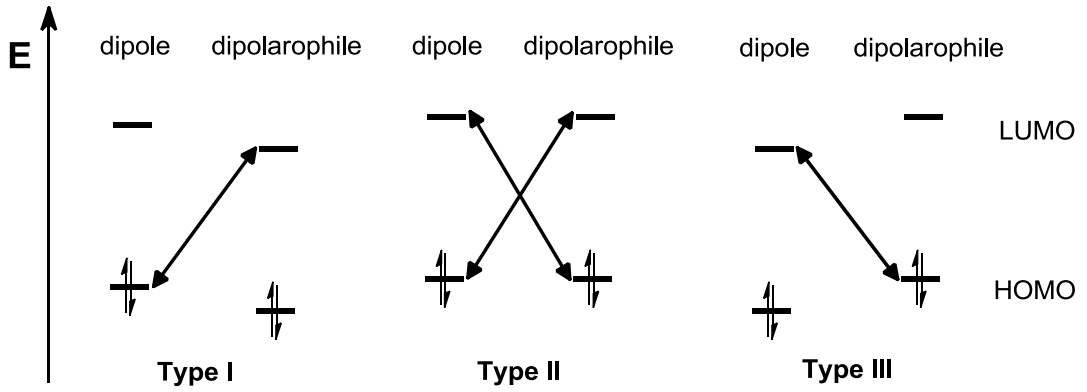

Figure 2-1. Classification of FMOs for 1,3-dipolar cycloadditions. Figure was reprinted from the literature.[6]

The introduction of electron-donating or electron-withdrawing substituents on the dipole or dipolarophile has effects on the relative FMO energies. Additionally, the use of a transition metal catalyst alters both the orbital coefficients of the starting atoms and the energy of the FMOs of both the 1,3-dipole and dipolarophile depending on the electronic properties of the reactants. The catalytic effect of a Lewis acid on 1,3-dipolar cycloadditions can be accounted for by the FMOs of either the dipole, or the dipolarophile when coordinated to the metal (Figure 2-2).

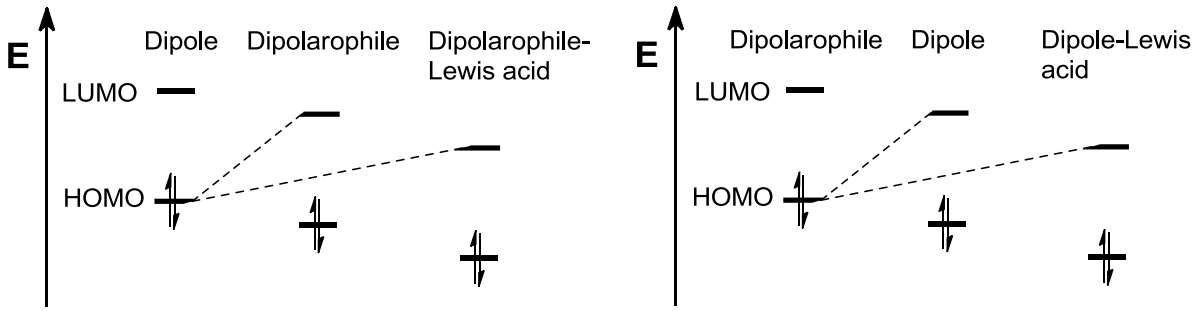

Figure 2-2. Influence of lewis acid coordination to the dipolarophile (left) or to the dipole (right) during 1,3-dipolar cycloadditions. Figure was adapted from the literature.[13]

In the absence of metal catalyst, linear alkynes react very slowly with nitrones. The dramatic rate acceleration of terminal alkyne-nitrone cycloaddition in the presence of copper-

(I) was first reported by Kinugasa and Hashimoto in 1972 (Scheme 2-3).[14] In the seminal account, the reaction of Cu-phenyl acetylide (**2.1**) with *α,N*-diphenyl nitrone (**2.2**), in anhydrous pyridine at r.t. under nitrogen atmosphere provided exclusively *cis*-1,3,4-triphenyl-2-azetidinone (***cis*-2.3**) in 50-60% yield within 30 min.

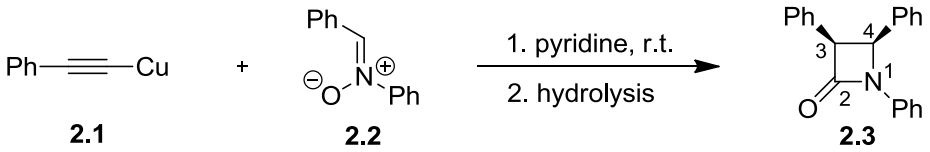

Scheme 2-3. Kinugasa reaction of Cu(I)-phenylacetylide with diaryl nitrones.

Four years later, Ding and Irwin reported a full paper on the scope and limitations of the Kinugasa reaction,[15] and found that under the general reaction conditions, mixtures of ***cis*-2.3** and ***trans*-2.3** were consistently obtained in varying ratios, ranging from 1:1 to 12:1, with the ***cis*-**diastereomer being favored. This finding led them to propose the first mechanism for the Kinugasa reaction (Scheme 2-4). It was suggested that β-lactam formation proceeded through a highly strained bicyclic oxaziridinium intermediate (**2.5**), and that the initially formed ***cis*-2.3** is the kinetic favored product, because the isoxazoline intermediate (**2.4**) preferred to be protonated from the less sterically hindered face of the molecule in the protonation step. The extent of formation of the ***trans*-2.3** likely resulted from the ease of isomerization at C-3 under the basic reaction conditions.

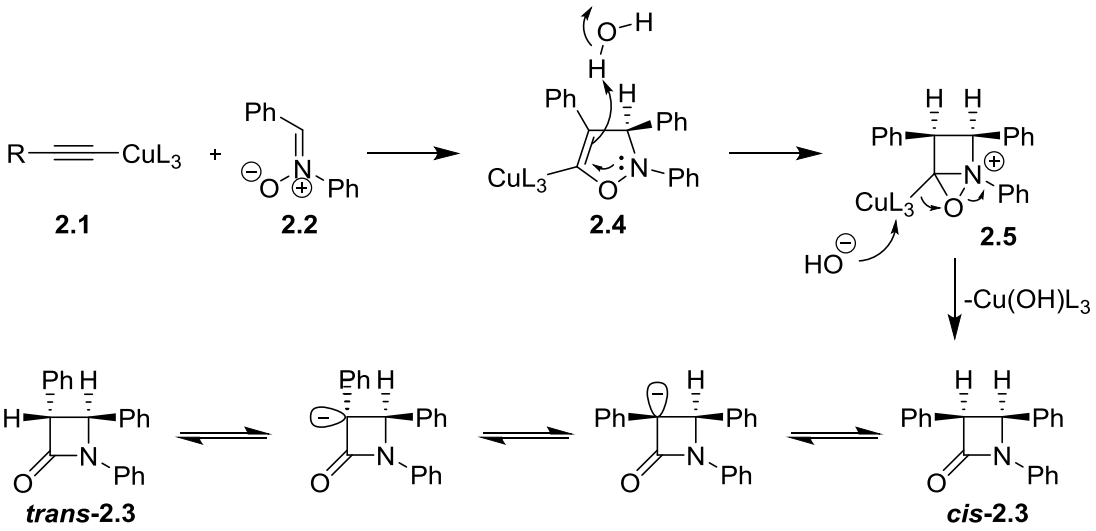

Scheme 2-4. Mechanism of the Kinugasa reaction proposed by Ding and Irwin.[15]

An alternate path II was reported shortly thereafter by Tang *et al.*,[16] whereby the isoxazoline **2.4** supposedly underwent ring opening fragmentation to the ketene (**2.7**),[16-18] as in the Staudinger ligation, followed by intramolecular cyclization to give the enolate (**2.8**), and protonation to yield β-lactams **2.3** (Scheme 2-5). The stereochemical outcome of the Kinugasa reaction is dependent on the initial cycloaddition to form the isoxazoline derivative **2.4** (common for both mechanisms). The initial cycloaddition fixes the configuration at C-4, which in turn, influences the stereochemistry at C-3.

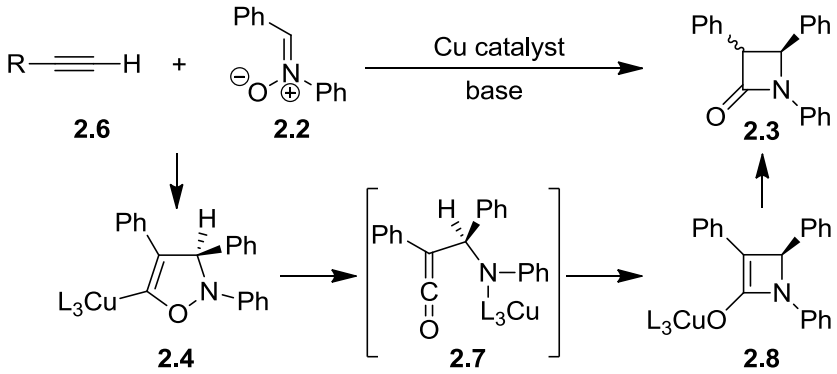

Scheme 2-5. Alternative mechanism for the Kinugasa reaction proposed by Tang.[16]

Although no definitive evidence exists to unambiguously prove or disprove either of the mechanisms, for example by trapping or isolating intermediates, the mechanism involving the ketene intermediate, appears to have gained support on the basis of the work of De Shong *et al.*[17] In their studies, they were able to show formation of β-lactams (**2.9**) via the cycloaddition of nitrones (**2.10**) with trimethylsilylacetylene (**2.11**) followed by desilylation of the corresponding 5-(trimethylsilyl)-isoxazoline (**2.12**) with fluoride (Scheme 2-6).

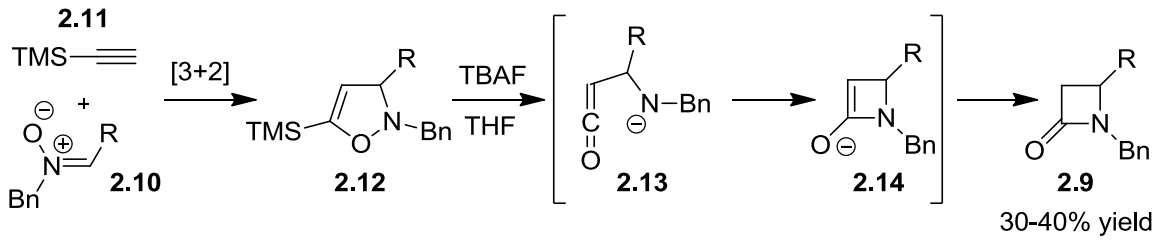

Scheme 2-6. Mechanism of β-lactam formation by fragmentation of 5-(trimethylsilyl)-isoxazolines.

An interesting catalytic modification of the original Kinugasa reaction was reported by Muira *et al.*,[19,20] based on the reaction between phenyl acetylene (**2.6**) and a *α,N*-diphenyl nitrone (**2.2**) in the presence of catalytic CuI and potassium carbonate (Scheme 2-7). The terminal alkyne is converted into copper acetylide in the presence of Cu(I) and a base, and underwent Kinugasa reaction with diaryl nitrones. According to the conditions shown in Scheme 2-7, the ratio of ***cis*-2.3** to ***trans*-2.3** was dependent on the type of phosphorus or nitrogen containing ligands employed. They also noted the formation *N*-(1,3-diphenyl-2-propynylidene)aniline (**2.15)**, *N*-benzylideneaniline (**2.16**), and phenylacetic acid (**2.17**), resulting from competing nitrone deoxygenation and nucleophilic additions of the Cu-acetylide. When the reaction was conducted with phosphines such as Ph_3P, Bu_3P, dppe or dppp, the *trans*-β-lactam was the exclusively formed β-lactam product although in poor yield (6-36 %). In the presence of nitrogen containing ligands such as pyridine or 1,10-

phenanthroline, the yield of β-lactams was significantly increased (55-71 %) and both ***cis*-2.3** and ***trans*-2.3** were obtained, in ratios of 2:1 for pyridine, and 1:1.2 when 1,10-phenanthroline was employed as a ligand.

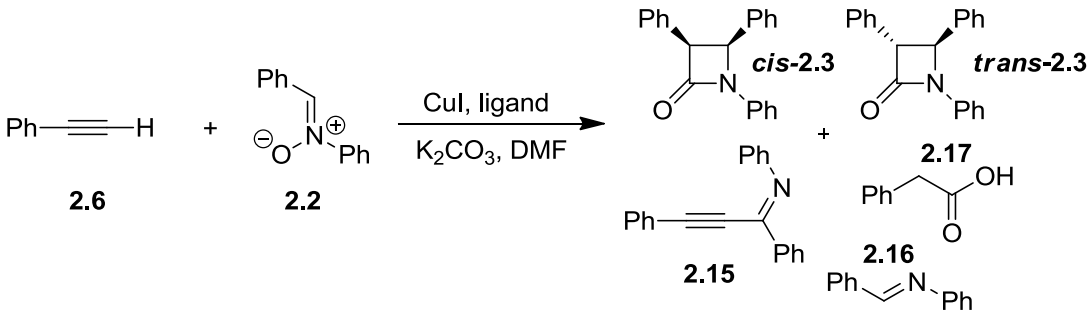

Scheme 2-7. Kinugasa reaction variant reported by Muira.[19]

Since Muira's report there have been several modification to the reaction conditions that include: intramolecular,[18,21] diastereo-[22-26] and enantioselective[16,18,19,27-29] versions that have been achieved by using chiral auxiliary groups and chiral ligands. Asymmetric induction in the Kinugasa reaction has also been accomplished in one of three ways: 1) use of a chiral ligand designed for chelation to Cu(I), 2) use of a chiral nitrone, or 3) use of a chiral acetylene.

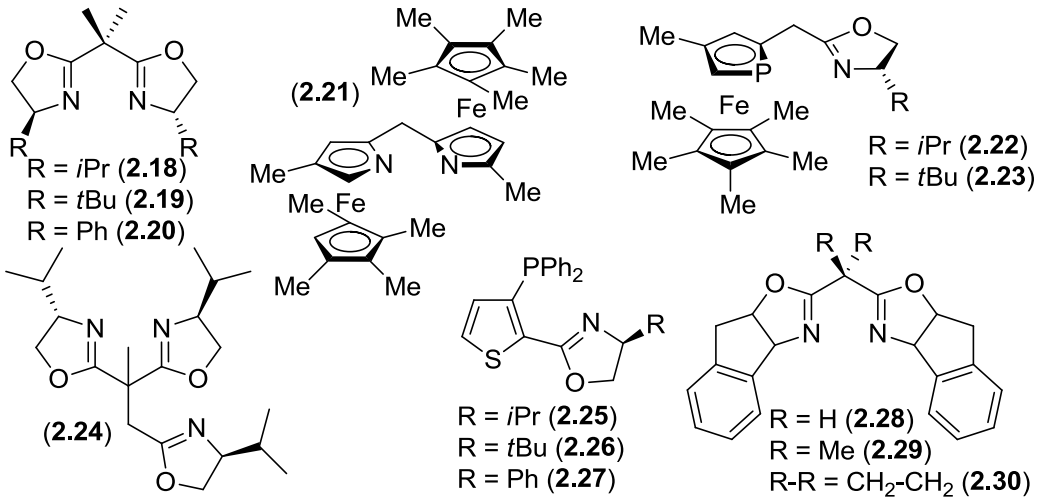

Figure 2-3. Ligands commonly used in Kinugasa reactions.

Muira *et al.* were the first to explore the first strategy by using C_2-symmetric chiral bisoxazoline ligands (**2.18**-**2.20**).[19,20] In the following years, C_2-symmetric bis(azaferrocene) (**2.21**) and mixed *P,N*-complexes (**2.22-2.23**),[18,28] pseudo C_3-symmetric trisoxazoline (**2.24**),[16,30] HETPHOX (**2.25-2.27**),[27] and IndaBox C_2-symmetric chiral bis(oxazoline) ligands (**2.28-2.30**) have been used to coordinate copper catalysts during the Kinugasa reaction (Figure 2-3).[29]

Although the Kinugasa reaction has been applied most exclusively to diarylnitrones,[15,16,18,19,22,26-32] the reaction has also been extended to non-racemic chiral cyclic nitrones to generate the corresponding carbapenams with excellent *cis*-diastereoselectivity.[15,23-25] Asymmetric induction in such systems has also been achieved using terminal acetylenes bearing chiral auxillaries.[26,33]

Towards using nitrones as bioorthogonal chemical reporters in cycloadditions with alkynes, this chapter describes development of multicomponent Kinugasa reactions in aqueous media. The attractive atom economy associated with Cu(I)-catalyzed alkyne-nitrone cycloadditions prompted us to explore the Kinugasa reaction as an alternative to CuAAC. The great potential of the Kinugasa reaction as an alternative bioorthogonal reaction includes: 1) the ease of nitrone preparation; 2) nitrones are typically stable and easily purified; 3) numerous alkynes with widely varying substituents are commercially available; and 4) the Kinugasa reaction is known to be tolerant to a wide range of functional groups (ie. alcohols, amines, halides and esters).

Hypothesis

Micelle-promoted multicomponent Kinugasa reactions proceed efficiently under aqueous conditions.

Results and Discussion

Multicomponent Kinugasa Reactions in Aqueous Media

The Copper-free cycloaddition of nitrones with terminal alkynes normally proceeds under refluxing conditions, but in the presence of Cu(I), the Kinugasa reaction takes place at r.t. or even at 0 ˚C. The notorious instability of Cu(I) in the presence of air has previously limited Kinugasa reactions to being conducted in organic solvents in the absence of air. We envisioned that by using sodium ascorbate to generate a reductive atmosphere thereby reducing Cu(II) to Cu(I), the Kinugasa reaction could be conducted in aqueous solution, and could ultimately be applied as a novel biological labelling reaction.

During the course of this work, Basak and co-workers reported a Kinugasa reaction variant to generate monocyclic β-lactams in aqueous solution using sub-stoichiometric copper catalyst.[34] In their work, it was found that due to reagent solubility, DMF-H_2O solvent combination (2:1) gave the best results in terms of yield (~70 %), and that performing the reaction in water as the sole solvent caused the reaction to work less efficiently. This caused us to re-evaluate our approach, and explore the possibility of using micelle catalysis to conduct multicomponent Kinugasa reactions in aqueous media. We anticipated that a micelle-promoted Kinugasa reaction would not only circumvent the requirement of organic co-solvents and avoid the requirement of pre-formation of nitrones, but would potentially lead to rate accelerations in the Kinugasa reaction.

Previously Chatterjee *et al.* reported a convenient 'single pot' synthesis of isoxazolidines that involved micelle surfactant catalyzed *α*,*N*-diaryl nitrone formation followed by [3+2] cycloaddition with ethyl acrylate in water at r.t., to generate *trans*-isoxazolidines.[35] Additionally, we had recently utilized similar methodology to functionalize

an unnatural amino acid containing a cyclic *α,β*-unsaturated ketone with *in situ* generated *α,N*-diphenyl nitrone in aqueous media.[36] Herein we report our studies of simultaneous micelle-promoted and copper-catalyzed multicomponent Kinugasa reactions in aqueous media (Scheme 2-8).

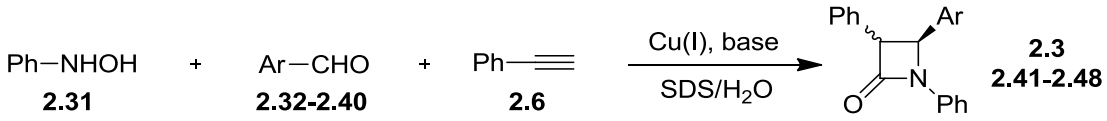

Scheme 2-8. Multicomponent Kinugasa reactions in aqueous media.

The proposed multicomponent Kinugasa reaction proceeds by a two-step reaction sequence involving micelle-promoted *in situ* nitrone formation from an aryl aldehyde (**2.32-2.40**) and *N*-phenyl hydroxyl amine (**2.31**) followed by the Cu(I)-catalyzed Kinugasa reaction with phenylacetylene **2.6** to yield a diastereomeric mixture of *cis*- and *trans*-β-lactams (**2.3**, **2.41**-**2.48**) (Figure 2-4).

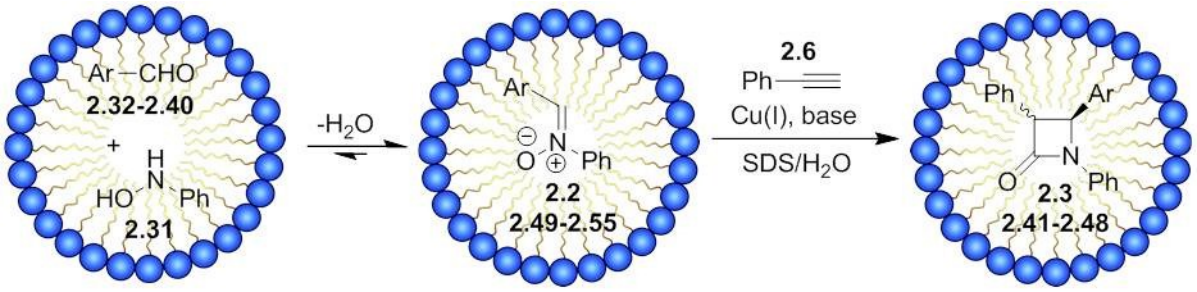

Figure 2-4. Micelle-promoted multicomponent Kinugasa reactions in aqueous media.

Toward establishing optimal reaction conditions for micelle promoted multicomponent Kinugasa reactions, firstly, the *in situ* nitrone formation was optimized. Dehydrative nitrone formation from *N*-phenyl hydroxyl amine (**2.31**) and benzaldehyde (**2.32**) in the presence of aqueous SDS micelle solution in degassed water at r.t. resulted in efficient formation of *α,N*-diphenyl nitrone (**2.2**) within 30 min. It was found that brief

sonication of the reaction mixture decreased the time of nitrone formation, presumably by helping to effectively solubilize the reactants by the surfactant. This method of nitrone formation complements traditional approaches using organic solvents and dehydrating agents.[22]

It was found that cooling the *in situ* generated nitrone to 0 °C prior to addition of the remaining reagents led to increased yields of the corresponding β-lactam**.** The solution of *in situ* generated *α,N*-diphenyl nitrone (**2.2)** was reacted with phenylacetylene (**2.6**), (+)-sodium L-ascorbate, $Cu(SO)_4$, pyridine and ethanolamine (EA) buffered at pH = 10. This mixture was allowed to react for 30 min at 0 °C and was then stirred at r.t. for 10 h. The reaction mixture consisted of three major products, the ***cis*-2.3** and ***trans*-2.3** in 46 % overall yield in a ratio of 1.2:1, respectively, along with an amide-linked product **2.56** in 36 % yield (Table 2-2).

Table 2-2. Effect of Cu-catalyst loading on the multicomponent Kinugasa reaction.

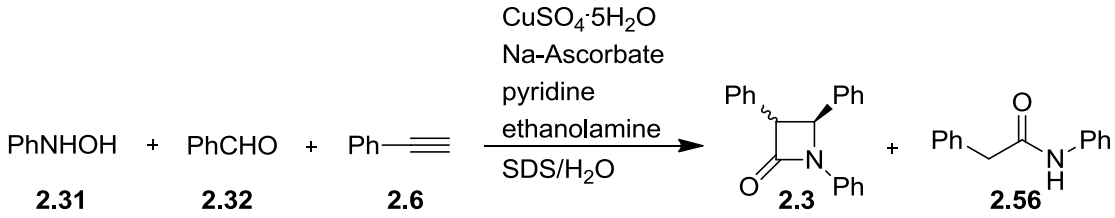

2.31 **2.32** **2.6** **2.3** **2.56**

			Yield %	
Entry	**Cu catalyst (mol %)[a]**	**Time (h)**	**2.3 (*cis*:*trans*)**	**2.56**
1	100	6	46 (1.2:1)	36
2	80	7	46 (1.2:1)	36
3	20	10	46 (1.2:1)	36

Reaction conditions: [PhCHO] : [PhNHOH] : [Ph-≡] : ethanolamine (0.1 M, pH = 10) : pyridine = 2 : 2.4 : 1 : 2 : 8 in degassed SDS/H_2O (0.05 M) in dark from 0 °C to r.t. under Argon. [a]Na-ascorbate : $CuSO_4$ = 2 : 1.

Under the conditions listed in Table 2-2, the reaction was tolerant to sub-stoichiometric Cu-catalyst loadings without compromising the product composition and without sacrificing the yield. However, it was found that catalyst loading below 20 mol % caused the reaction to be sluggish and gave poor yields of **2.3**. Amide **2.56** is not a typical by-product of the Kinugasa reaction or a common decomposition product of β-lactams. The structure **2.56** was confirmed by ^{1}H NMR, ^{13}C NMR, and X-ray crystallography (Figure 2-5).

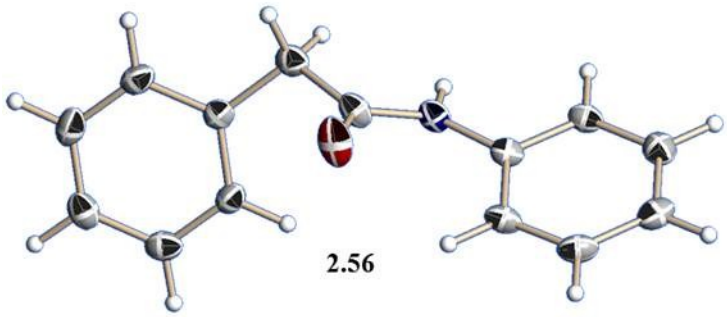

Figure 2-5. ORTEP plot of **2.56** with thermal ellipsoids drawn. The crystal structure is in agreement with that reported previously.[37]

In an effort to improve the yield and efficiency of the multicomponent Kinugasa reaction and minimize the formation of **2.56**, we screened three nitrogen containing ligands: pyridine, 2,2'-bipyridine (bipy), and tris[(1-benzyl-1H-1,2,3-triazol-4-yl)methyl]amine (TBTA)[26] (Table 2-3). In accordance with the previous findings of Muira *et al.*,[19] it was found that conducting the reaction with a 10-fold excess amount of pyridine gave the highest yield of **2.3** (46% overall). Decreasing the amount of pyridine below two equivalents resulted in a slow reaction and **2.3** was obtained in 15 % overall yield. Presumably, excess pyridine facilitated regeneration of the active Cu(I) catalyst. Alternatively, the bidentate ligand, bipy was found to be a more efficient ligand in the reaction and provided ***cis*-2.3** and ***trans*-2.3** and **2.56** in yields of 42 % and 29 %, respectively, with the addition of only one equivalent.

This is attributed to stronger Cu(I) binding of the bidentate ligand in solution. Lastly, we employed TBTA, a ligand commonly used in Cu(I)-catalyzed azide-alkyne cycloadditions.[26] The reaction was slow and provided β-lactams **2.3** and **2.56** in reduced yields (31 % and 22 %, respectively) after extended reaction time. The lower yield may be due to the poor solubility of TBTA under the aqueous conditions of this system.

Table 2-3. Effect of ligand on the micelle catalyzed Kinugasa reaction.

			Yield %	
Entry	**Ligand (eq.)**	**Time (h)**	**2.3 (*cis*:*trans*)**	**2.56**
1	pyridine (10)	9	46 (1.2:1)	36
2	pyridine (8)	10	46 (1.2:1)	36
3	pyridine (2)	20	15(1:1)	18
4	2,2'-bipyridine (1)	10	42 (1.4:1)	29
5	TBTA (0.2)	24	31 (1:1)	22

Reaction conditions: [PhCHO] : [PhNHOH] : [Ph-≡] : sodium ascorbate : $CuSO_4$: ethanolamine (0.1 M, pH = 10) = 2 : 2.4: 1 : 0.4 : 0.2 : 2 in degassed SDS/H_2O (0.05 M) in dark from 0 °C to r.t. under argon.

Utilizing pyridine as a ligand to coordinate to Cu(I), we examined the influence of base on β-lactam yield and diastereoselectivity of the reaction. As shown in Table 2-4, all bases employed effectively promoted the reaction and formed the desired β-lactam **2.3** in 31-46 % yield along with the amide by-product in 26-46 % yield. The choice of the base for the reaction did not have significant effects on minimizing the side reaction. It was found that bulky secondary amines, DIPA and Cy_2NH, afforded the β-lactam products with moderately better *cis*-diastereoselectivity (Table 2-4, Entries 3, 4). This supports the proposed mechanism, suggesting that protonation at C-3 occurs from the less sterically hindered face of the isoxazoline intermediate leading to preferential formation of the ***cis*-2.3** in the presence of bulkier amine bases.[30]

Table 2-4. Effect of base on the multicomponent Kinugasa reaction.

			Yield %	
Entry	**Base**	**Time (h)**	**2.3 (*cis:trans*)**	**2.56**
1	Na_2CO_3	10	38 (1.2:1)	46
2	$NaHCO_3$	8	44 (1.1:1)	43
3	DIPA	11	42 (2.5:1)	45
4	Cy_2NH	12	31 (2.8:1)	39
5	Et_3N	10	45 (1.6:1)	43
6	Tris	12	38 (1:1)	45
7	EA	10	46 (1.2:1)	36

Reaction conditions: [PhCHO] : [PhNHOH] : [Ph-≡] : sodium ascorbate : $CuSO_4$: pyridine : base = 2 : 2.4 : 1 : 0.4 : 0.2 : 8 : 2 in degassed SDS/H_2O (50 mM) in dark from 0 °C to r.t. under argon.

During the course these studies it was found that after prolonged reaction times the reaction pH changed from basic to mildly acidic and gave lower β-lactam yields, presumably by the presence of pyridinium ion in solution. To address this issue, we tested the reaction under buffered conditions to maintain the pH throughout the course of the reaction. Interestingly, the multicomponent Kinugasa reaction proceeded in the presence of tris-(hydroxymethyl)-aminomethane (Tris) buffer at pH = 8, although with lower yield than when ethanolamine (EA) buffer at pH = 10 was employed (Table 2-4). It was found that keeping the pH of solution constant during the course of the Kinugasa reaction was beneficial in terms of minimizing side product formation during the formation of the β-lactam.

To further optimize the yield of the micelle-promoted multicomponent Kinugasa reaction, we varied the stoichiometry of nitrone to alkyne ratio (Table 2-5), since copper-mediated deoxygenation of nitrones[38] and Glaser alkyne couplings[39] are processes that could

have potentially been competing side reactions leading to lower yields of β-lactams. The yield of **2.3** was consistently higher when using an excess of nitrone relative to phenylacetylene. It is noteworthy that GC-MS analysis of the reaction mixture indicated that the *in situ* generated diphenyl nitrone **2.2** underwent Cu(I)-mediated deoxygenation leading to formation of the imine, and that Cu-mediated homo-coupling of phenylacetylene occurred after prolonged reaction times.

Table 2-5. Effect of nitrone to alkyne ratio on the multicomponent Kinugasa reaction.

			Yield %	
Entry	**PhCHO : PhNHOH : Ph-≡**	**Buffer**	**2.3 (*cis*:*trans*)**	**2.56**
1	4 : 4.8 : 1	EA	44 (1.1:1)	35
2	2 : 2.4 : 1	EA	46 (1.2:1)	36
3	2 : 2.4 : 1	Tris	39 (1:1)	41
4	2 : 2.4 : 1	-	40 (2:1)	47
5	1 : 1.2 : 2	EA	24 (1:1)	24
6	1 : 1.2 : 2	Tris	37 (1:1)	39
7	1 : 1.2 : 2	-	33 (1.5:1)	37

Reaction conditions: sodium ascorbate : $CuSO_4$: buffer : pyridine = 0.4 : 0.2 : 2 : 8 in degassed SDS/H_2O (0.05 M) in dark from 0 °C to r.t. under argon.

Next, we varied the ratio of sodium ascorbate to Cu-catalyst in hopes of minimizing side reactions (Table 2-6). It was hypothesized that non-ligated Cu(I) may have been partially oxidized during the course of the multicomponent reaction in water. In the absence of sodium ascorbate, the reaction did not work. This ruled out the involvement of Cu(II) in the Kinugasa reaction. It was found that maintaining an excess of reducing agent was essential to the successful outcome of the reaction. Having a 2-fold excess of sodium ascorbate provided satisfactory yields of the **2.3** and **2.56** in 46 % and 33 %, respectively.

Table 2-6. Effect of reducing agent concentration on multicomponent Kinugasa reaction.

		Yield %	
Entry	**sodium ascorbate : $CuSO_4$**	**2.3 (*cis*:*trans*)**	**2.56**
1	10:1	45 (1.2:1)	33
2	2:1	46 (1.2:1)	36
3	1:1	34 (1.2:1)	31
4	0:1	trace	0

Reaction conditions: sodium ascorbate : $CuSO_4$: ethanolamine (0.1 M, pH = 10) : pyridine = varied : 0.2 : 2 : 8 in degassed SDS/H_2O (0.05 M) in dark from 0 °C to r.t. under argon.

Having optimized the multicomponent reaction conditions, we investigated the generality of the micelle-promoted multicomponent Kinugasa reaction in aqueous media by testing a series of *para*- and *meta*-substituted benzaldehydes bearing electron withdrawing and electron donating groups (Table 2-7). The presence of benzaldehydes bearing EDGs resulted in lower yields of the corresponding *cis*- and *trans*-β-lactams (**2.41** and **2.42**) in slightly shorter reaction times relative to when EWGs were employed (**2.43**-**2.48**). The yield of amide by-product **2.56** was consistently lower when the EWGs were present on the benzaldehyde. There are three competing reactions that affect the product composition: formation of β-lactams, formation of **2.56**, and decomposition of the *in situ* generated nitrone. Reactions of nitrones bearing EWGs (Table 2-7, Entries 4-9) resulted in a higher overall yield of β-lactam (**2.43-2.48**), a lower yield of **2.56**, and less nitrone decomposition relative to reactions containing EDGs. Despite the longer reaction times for nitrones bearing EWGs, competing side reactions were less of a problem and resulted in increased yields of β-lactams.

Table 2-7. Micelle-promoted multicomponent Kinugasa reaction scope.

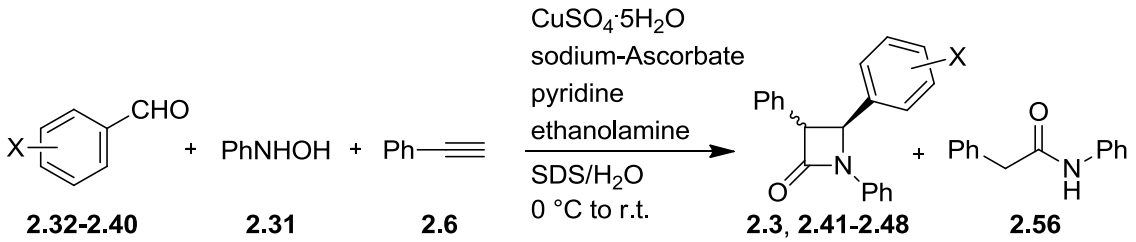

2.32-2.40 **2.31** **2.6** **2.3, 2.41-2.48** **2.56**

			Yield %		
Entry	**X-PhCHO (X=)**	**Time (h)**	**β-lactam**	**(*cis*/*trans*)**	**2.56**
1	H (**2.32**)	10	**2.3**	46 (1.2:1)	36
2	*p*-CH_3 (**2.33**)	13	**2.41**	45 (1.3:1)	24
3	*p*-OCH_3 (**2.34**)	8	**2.42**	62 (1.2:1)	26
4	*m*-OMe (**2.35**)	9	**2.43**	60 (1.2:1)	15
5	*p*-Br (**2.36**)	18	**2.44**	73 (1.6:1)	22
6	*p*-CO_2Me (**2.37**)	18	**2.45**	85 (1:1)	13
7	*p*-CN (**2.38**)	18	**2.46**	67 (1.2:1)	18
8	*m*-NO_2 (**2.39**)	18	**2.47**	79 (1.3:1)	11
9	*p*-NO_2 (**2.40**)	18	**2.48**	82 (1.1:1)	15

Reaction conditions: [X-PhCHO] : [PhNHOH] : [Ph-≡] : Na-ascorbate : $CuSO_4$: pyridine : ethanolamine (0.1 M, pH = 10) = 2 : 2.4 : 1 : 0.4 : 0.2 : 8 : 2 in degassed SDS/H_2O (50 mM) in dark from 0 °C to r.t. under argon.

The longer reaction times likely result from a modest substituent effect on the rate constant for cycloaddition between the *in situ* generated Cu(I) phenylacetylide and the *in situ* generated nitrone. Alternatively, the presence of EWGs stabilized the nitrone, and less decomposition over the first 10 h contributed to the much higher β-lactam yields. The ratio of *cis*:*trans* for all β-lactams prepared by the multicomponent Kinugasa reaction in aqueous media did not change significantly. A representative HPLC trace for reactions involving aldehydes **2.34** and **2.36** (Table 2-7, Entries 3 and 5) is shown in Figure 2-6.

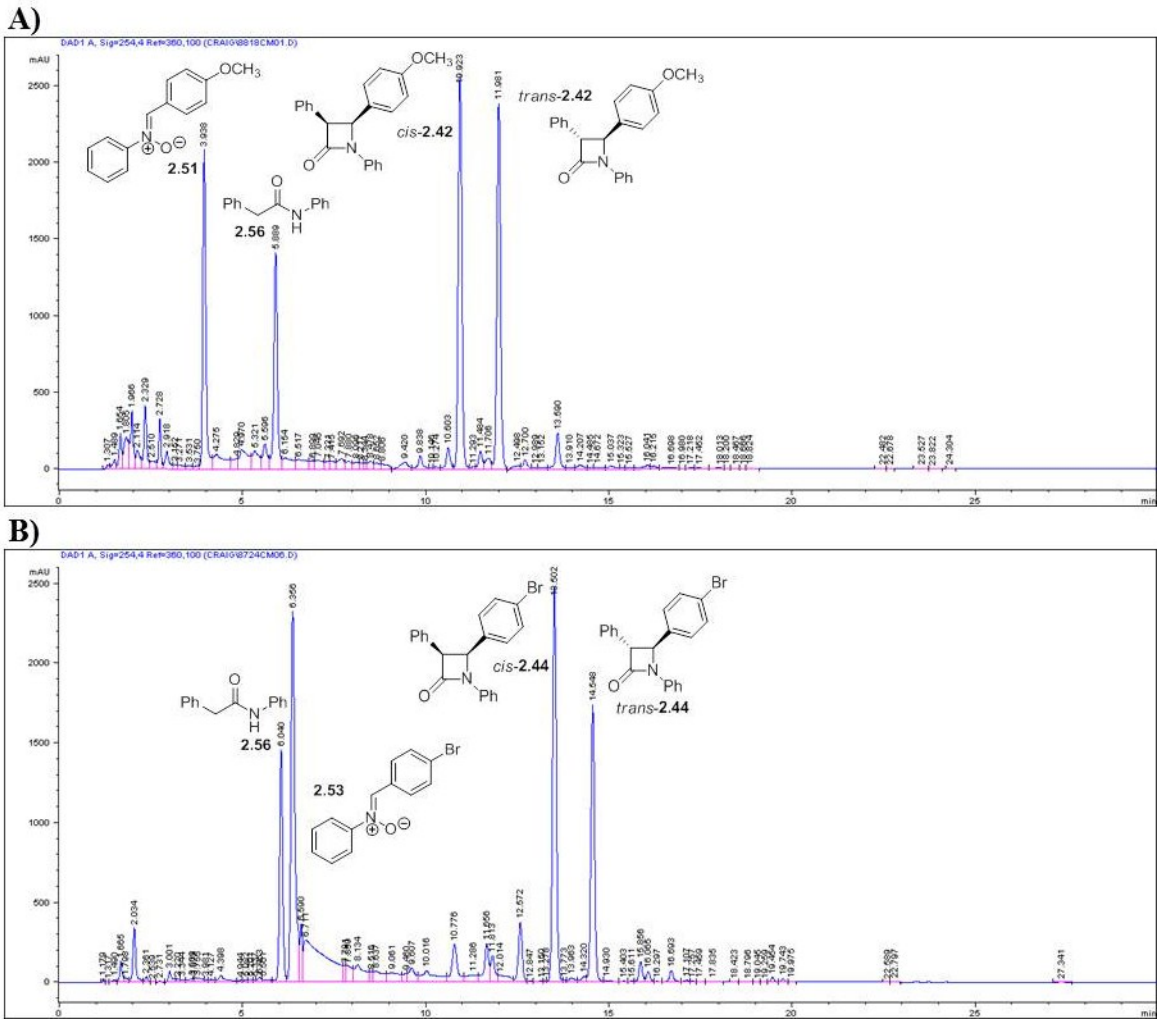

Figure 2-6. Representative HPLC traces for micelle promoted multicomponent Kinugasa reactions in aqueous media.

Mechanism of Micelle-Promoted Multicomponent Kinugasa Reactions

A proposed catalytic cycle for the Cu(I)-catalyzed Kinugasa reaction in aqueous media is shown in Figure 2-7. The process begins with reduction of Cu(II) (**2.57**) to Cu(I) (**2.58**) using sodium-ascorbate, thereby allowing for coordination of the alkyne to Cu(I) species (**2.1**) to form a π-complex (**2.59**) in which the copper ion can be bound to other nucleophilic atoms (oxygen atom, nitrogen ligands, phenyl rings, etc.) and serves to increase the acidity of the terminal alkyne in aqueous media. Deprotonating **2.59** gives rise to the

Cu(I)-acetylide complex **2.1**. In the presence of nitrone **2.2**, the Cu(I)-phenyl acetylide complex undergoes stepwise or concerted [3+2] cycloaddition leading to the isoxazoline **2.4**. The stepwise process is plausible in the case of the metal catalyzed reaction, and it may proceed through intermediates **2.60** and **2.61**, in analogy to the mechanism of Cu(I)-catalyzed azide-alkyne cycloadditions proposed previously.[40] The six membered copper-metallocycle intermediate **2.61** then contracts to the five-membered isoxazoline **2.4**, and the isoxazoline contracts further and rearranges to the β-lactams **2.3**, via the oxaziridinium intermediate **2.5**.

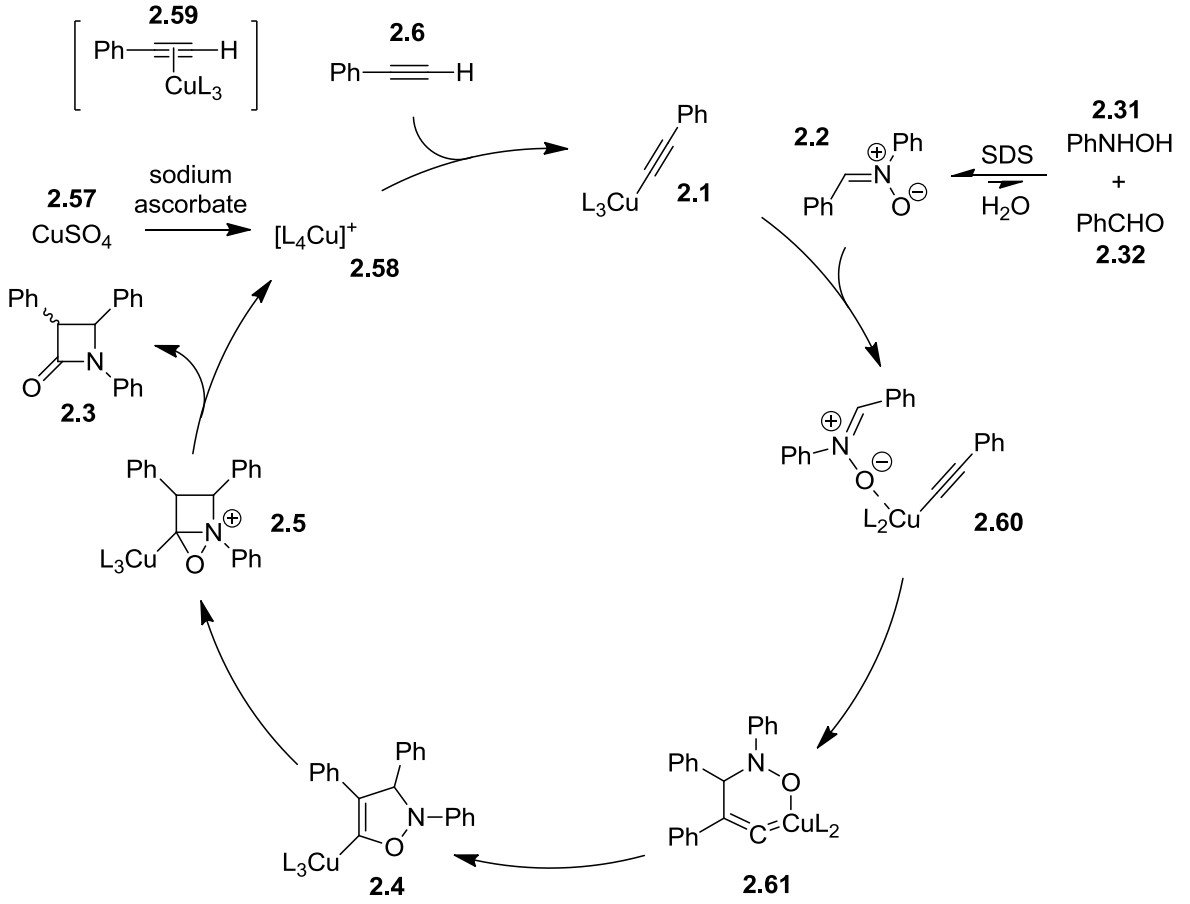

Figure 2-7. Plausible catalytic cycle for multicomponent Kinugasa reactions in aqueous media.

The Origins of Amide By-Product Formation

To investigate the origins of the side product **2.56**, we performed a series of control reactions. We systematically removed *N*-phenyl hydroxyl amine **2.31**, benzaldehyde **2.32**, and phenylacetylene **2.6**, from the multicomponent reaction. None of these experiments led to the formation of **2.56**. Additionally, we tested the reaction of nitroso benzene, a partially oxidized product from *N*-phenyl-hydroxylamine, with phenyl acetylene under our Kinugasa reaction conditions and the amide by-product was not observed. Additionally, to determine if **2.56** was a decomposition product of **2.3**, we subjected ***cis*-2.3** and ***trans*-2.3** to an aqueous SDS solution of $CuSO_4$, sodium ascorbate, pyridine and ethanolamine. We did not observe any reaction of **2.3** under these conditions. Therefore, side product **2.56** clearly does not arise from decomposition of **2.3**. Collectively these experiments supported a unique role of the nitrone in Cu(I)-catalyzed amide formation from phenylacetylene and diaryl nitrones.

Tang and coworkers rationalized the formation of an imine side product (**2.16**) to occur via a ketene intermediate **2.7**.[16] We speculated that a similar mechanism may be operative in formation of **2.56** (Scheme 2-9).

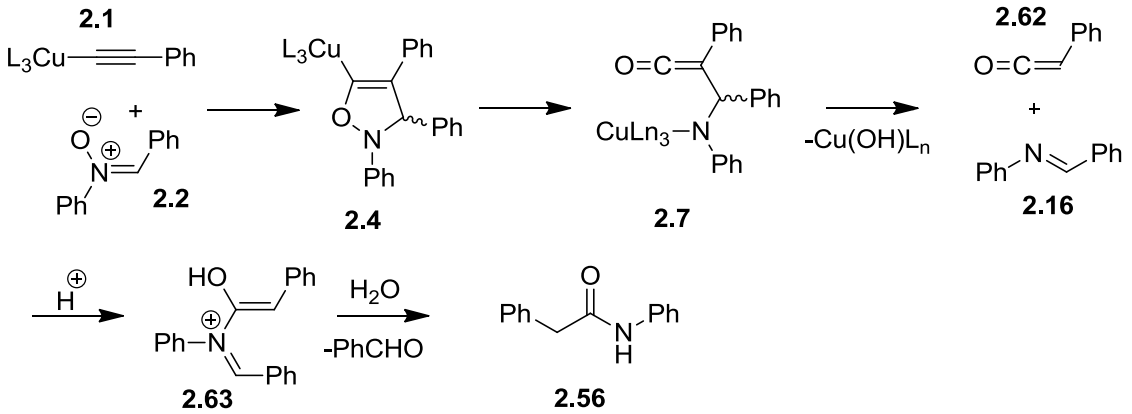

Scheme 2-9. Proposed mechanism for formation of amide by-product **2.56**.

To determine if we could detect ketene intermediate **2.7** over the course of the multicomponent Kinugasa reaction in aqueous media, we performed a trapping experiment. We substituted 2-ethynyl aniline (**2.64**) in place of phenyl acetylene, under our reaction conditions and did not observe formation of the expected γ-lactam (**2.65**) (Scheme 2-10).

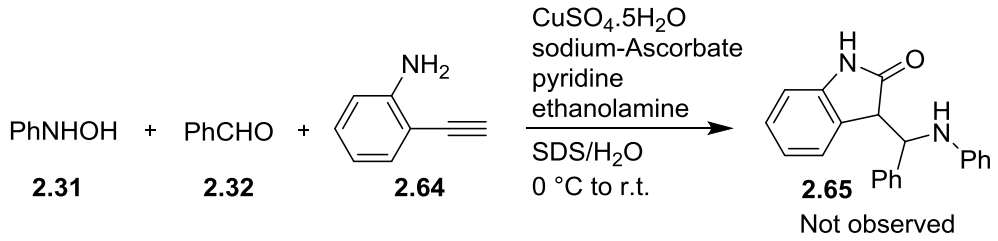

Scheme 2-10. Attempts to trap the ketene intermediate in the multicomponent Kinugasa reaction.

This result is in agreement with previous efforts by Deshong *et al.*, where they had attempted to desilylate the isoxazoline **2.12** in aqueous HF solution (Scheme 2-11).[17] In their case, protonation of the isoxazoline nitrogen and fluoride induced fragmentation did not lead to β-lactam, but rather the amino group initiated intermolecular polymerization. Under acidic conditions, β-elimination resulted in formation of the α,β-unsaturated amide (**2.67**).

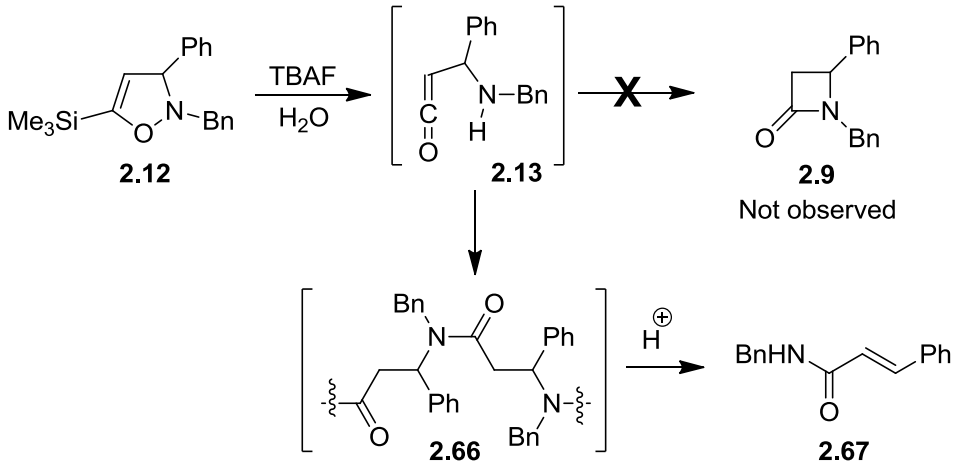

Scheme 2-11. Desilylation of isoxazolines in aqueous HF.

On the basis of our efforts to improve the yield and overall efficiency of the Kinugasa reaction in water we discovered a new amide by-product and more insight into the reaction. A main reason for by-product formation and low yields in the Kinugasa reaction is likely a combination of factors such as its inherent slow rate and the dual character of the copper acetylide, which may react as either a dipolarophile or as a nucleophile. It has been proposed that the 1,3-dipolar cycloaddition is slow and reversible.[19] The second step, rearrangement of the isoxazoline is also slow due to the high energy barrier of contraction of the five membered isoxazoline (**2.4**) to the four membered metal enolate (**2.8**) or oxaziridinium ion (**2.5**). Due to the low rates of these processes, side reactions become operative and involve multiple pathways involving both the nitrone and alkyne. For example, Cu(I)-mediated deoxygenation,[38] as well as copper mediated Glaser alkyne couplings[39] have been also observed in these reactions. While we established a new way for synthesizing β-lactams via a multicomponent Kinugasa reaction in water, this chemistry is not amenable to bioconjugation.

Future Directions

For the Kinugasa reaction to be useful as a bioorthogonal reaction, the reaction rate needs to be increased in order to minimize competing side reaction pathways. In the absence of faster catalytic systems, future work would focus on using different dipolarophiles that display increased reactivity with nitrones. Additionally, the β-lactam products and derivatives thereof from these reactions could find applications as biological probes for activity based protein profiling (ABPP) and as surface enhanced Raman spectroscopy (SERS) imaging contrast agents.

Conclusions

We have studied multicomponent Kinugasa reaction for the simultaneous micelle promoted and Cu(I)-catalyzed coupling of alkynes with *in situ* generated diaryl nitrones to form 1,3,4-triaryl substituted β-lactams and an unprecedented amide-linked product. The reaction is tolerant to substituents at the α-aryl position of the nitrone, and β-lactams were prepared in 46–85 %. The highest yields were obtained when benzaldehydes bearing EWGs were employed. This reaction provides a convenient method for constructing the β-lactam ring in aqueous media. However, the slow kinetics of the developed reaction precludes its practical applicability as a bioorthogonal reaction, since the presence of biological functionality will likely complicate the reaction even further.

Acknowledgements

I would like to thank Kenneth Chan for MALDI-MS analysis of the products, Donald M. Leek for assistance with NMR, Malgosia Daroszewska for assistance with HPLC and mass spectrometry, and Dr. Gary Enright for X-ray analysis of the amide by-product. I would also like to thank Dr. David Kennedy for critical reading of the manuscript and useful discussions.

Materials and Methods

General

All chemical reagents were purchased from commercial suppliers and used without further purification. Water and buffers were degassed thoroughly and stored under argon prior to use. All reactions were carried out in oven dried glassware under an atmosphere of argon with magnetic stirring. Reactions were monitored by thin layer chromatography (TLC) pre-coated silica gel glass plates (60Å F_{254}, layer thickness 250μm), using UV light and potassium permanganate stain to visualize the course of reaction. For Flash column chromatography technical grade solvents were used, and chromatographic purification was performed using silica gel (60 Å, particle size 40–63 μm). HPLC-MS/MS of the reaction mixtures was performed using a WATERS system consisting of a WATERS 996 Photodiode Array Detector, an Alliance HT – WATERS 2795 Separations Module, a WATERS Micromass ZQ 2000 unit equipped with a pneumatically assisted electrospray ionization source. Samples were ran on a WATERS Sunfire C_{18} (100 mm x 2.10 mm x 3.5 μm) column. Standard conditions used, unless otherwise stated, were a gradient of 10-95% acetonitrile/0.1% formic acid in H_2O/0.1% formic acid over 10 min with a flow rate of 0.2 mL/min. Eluent was directed first to the diode array detector and then to the mass spectrometer. The source temperature was set at 80˚C, electrospray capillary set at 3.5 kV with cone voltage set at 10 V. Samples were introduced using loop injection (50:50/MeCN+0.1 % formic acid:H_2O+0.1 % formic acid) operating in positive mode (scan range 150-1000 m/z). Data was collected in unit mass recording mode and processed using Mass lynx software. ^{1}H NMR and ^{13}C NMR spectra were recorded using a Bruker-DRX-400 spectrometer using a frequency of 400.13 MHz for ^{1}H and 100.61 MHz for ^{13}C and

processed using Bruker TOPSPIN 2.1 software. Chemical shifts are reported in parts per million (δ) using residual $CHCl_3$ resonance as an internal reference (7.26 and 77.0 ppm for ^1H and ^{13}C NMR, respectively). The following abbreviations were used to designate chemical shift multiplicities: s = singlet, d = doublet, t = triplet, m = multiplet or unresolved, br = broad signal and *J* = coupling constants in Hz.

Synthetic Procedures and Characterization Data:

***N*-phenylhydroxylamine (2.31):** A mixture of nitrobenzene (10.8 mL, 0.105 mol), NH_4Cl (6.5 g, 0.12 mol) and degassed H_2O (200 mL) under argon at r.t. was stirred vigorously while zinc dust (15.4 g, 0.21 mol) was added portion wise over 20 min. After addition was complete, the reaction mixture was stirred for an additional 20 min. and was filtered while still warm. The resultant filter cake was washed with hot distilled water (50 mL) and the combined filtrate was saturated with NaCl, and cooled to 0°C. The resulting precipitate was collected by filtration and dried thoroughly under reduced pressure. The crude N-phenyl hydroxylamine was re-crystallized from petroleum ether/ethyl acetate (8.2 g, 72 %), dried thoroughly, and stored under an atmosphere of argon at -20°C. ^1H and ^{13}C NMR spectra for **2.31** were identical to those previously reported in the literature.[35] **^1H NMR (400 MHz, $CDCl_3$):** δ 7.29 (t, 2H), 7.02-6.98 (m, 3H), 6.80 (br s, 1H), 5.85 (br s, 1H).

General Procedure for Multicomponent by Kinugasa Reactions in Aqueous Media:

SDS (11.5 mg, 0.04 mmol) was dissolved into degassed H_2O (8 mL) in a 25mL pear shaped flask wrapped with aluminum foil. A substituted benzaldehyde (0.4 mmol) and *N*-phenyl hydroxylamine (55 mg, 0.5 mmol) were added sequentially at r.t. and the reaction mixture stirred vigorously for 5 min. after which it was sonicated for 5 min. and stirred at r.t. for 2 hrs. Nitrone formation was monitored by TLC for the disappearance of aldehyde. The *in situ*

generated nitrone was cooled to 0°C, and was added ethanolamine buffer pH = 10 (0.4 mL, 0.4mmol from a 1 M degassed solution), pyridine (129 μL, 1.6 mmol), (+)-sodium-*L*-ascorbate (16 mg, 0.08 mmol), $CuSO_4{\cdot}5H_2O$ (10 mg, 0.04 mmol) and the mixture was stirred for 10 min. at this temperature. Then phenyl acetylene (22uL, 0.2mmol) was added in one portion and the reaction mixture was allowed to warm to r.t. over 30min, and was stirred for the specified amount of time. Upon completion, the reaction mixture was diluted with brine (8 mL) and extracted with EtOAc (3 x 10 mL). The combined organic layers were washed with brine (30 mL), dried over anhydrous Na_2SO_4, filtered, and concentrated *in vacuo*. The crude reaction mixtures were purified by silica gel flash column chromatography.

***cis*-1,3,4-triphenylazetidin-2-one (*cis*-2.3)** and ***trans*-1,3,4-triphenylazetidin-2-one (*trans*-2.3)**:

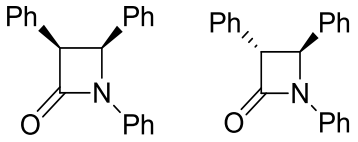

***cis*-2.3** ***trans*-2.3**

(1.2:1)
mixture of diastereomers

Purified by flash column chromatography eluting 95:5/hexanes:EtOAc. Spectral data corresponded to that previously described in the literature.[15] ***cis*-2.3**: Isolated as a white solid (15 mg, 0.05mmol, 25 %). $\mathbf{R_f}$ = 0.29 (90:10/hexanes:EtOAc). **^{1}H NMR (400 MHz, $CDCl_3$)**: δ 7.42 (m, 2H), 7.29 (m, 2H), 7.11-7.04 (m, 11H), 5.47 (d, *J* = 6.1 Hz, 1H), 5.02 (d, *J* = 6.1 Hz, 1H). **^{13}C NMR (100 MHz, $CDCl_3$)**: δ 165.6, 137.7, 134.4, 132.1, 129.1, 128.9, 128.2, 128.1, 127.9, 127.1, 127.1, 124.0, 117.2, 60.3, 60.3. **LRMS**: Calculated for $C_{21}H_{18}NO$ (M^+) 300.1, Found 300.3. ***trans*-2.3**: Isolated as a white solid (13 mg, 0.04 mmol, 21 %). $\mathbf{R_f}$ = 0.39 (90:10/hexanes:EtOAc). **^{1}H NMR (400 MHz, $CDCl_3$)**: δ 7.42-7.05 (m, 15H), 4.96 (d, *J* =

2.6 Hz, 1H), 4.29 (d, *J* = 2.6 Hz, 1H). **^{13}C NMR (100 MHz, $CDCl_3$)**: δ 165.6, 137.7, 134.3, 132.1, 129.1, 128.9, 128.2, 128.1, 127.9, 127.1, 127.1, 124.0, 117.2, 60.3, 60.3. **LRMS**: Calculated for $C_{21}H_{18}NO$ (M^+) 300.1, Found 300.3.

***cis*-1,3-diphenyl-4-p-tolylazetidin-2-one (*cis*-2.41)** and ***trans*-1,3-diphenyl-4-p-tolylazetidin-2-one (*trans*-2.41)**:

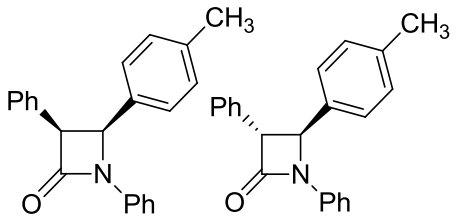

***cis*-2.41** ***trans*-2.41**

(1.3:1)
mixture of diastereomers

Purified by flash column chromatography eluting 95:5/hexanes:EtOAc. Spectral data corresponded to that previously described in the literature.[15] ***cis*-2.41**: Isolated as a white solid (15 mg, 0.05 mmol, 25 %). **R_f** = 0.31 (85:15/hexanes:EtOAc). **^{1}H NMR (400 MHz, $CDCl_3$)**: δ 7.41 (m, 2H), 7.28 (m, 2H), 7.10-7.06 (m, 6H), 6.96 (d, *J* = 8.2 Hz, 2H), 6.91 (d, *J* = 8.1 Hz, 2H), 5.43 (d, *J* = 6.1 Hz,1H), 4.99 (d, *J* = 6.1 Hz, 1H), 2.19 (s, 3H). **^{13}C NMR (100 MHz, $CDCl_3$)**: δ 165.8, 137.8, 137.6, 132.2, 131.2, 129.0, 128.9, 128.9, 128.1, 127.1, 124.0, 117.2, 60.2, 60.2, 21.2. **LRMS**: Calculated for $C_{22}H_{20}NO$ (M^+) 314.2, Found m/z=314.2. ***trans*-2.41**: Isolated as a white solid (12 mg, 0.04 mmol, 20 %). **R_f** = 0.55 (90:10/hexanes:EtOAc). **^{1}H NMR (400 MHz, $CDCl_3$)**: δ 7.40-7.20 (m, 13H), 7.06 (m, 1H), 4.92 (d, *J* = 2.2 Hz, 1H), 4.26 (d, *J* = 2.1 Hz, 1H), 2.37 (s, 3H). **^{13}C NMR (100 MHz, $CDCl_3$)**: δ 165.7, 138.6, 137.5, 134.8, 134.5, 130.0, 129.1, 129.0, 127.8, 127.5, 125.9, 124.0, 117.2, 65.2, 63.6, 21.2. **LRMS**: Calculated for $C_{22}H_{20}NO$ (M^+) 314.2, Found m/z=314.2.

***cis*-4-(4-methoxyphenyl)-1,3-diphenylazetidin-2-one (*cis*-2.42)** and ***trans*-4-(4-methoxyphenyl)-1,3-diphenylazetidin-2-one (*trans*-2.42)**:

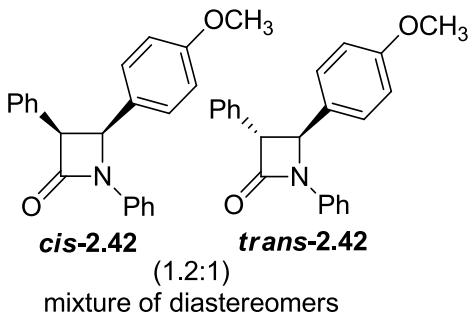

***cis*-2.42** ***trans*-2.42**

(1.2:1)

mixture of diastereomers

Purified by flash column chromatography eluting 85:15/hexanes:EtOAc. Spectral data corresponded to that previously described in the literature.[19] ***cis*-2.42**: Isolated as a white solid (20 mg, 0.06 mmol, 30 %). $\mathbf{R_f}$ = 0.26 (85:15/hexanes:EtOAc. **^{1}H NMR (400 MHz, $CDCl_3$)**: δ = 7.42 (m, 2H), 7.28 (m, 2H), 7.13-7.06 (m, 6H), 6.99 (m, 2H), 6.64 (m, 2H), 5.42 (d, *J* = 6.0 Hz, 1H), 4.98 (d, *J* = 6.0Hz, 1H), 3.67 (s, 3H). **^{13}C NMR (100 MHz, $CDCl_3$)**: δ 165.7, 159.1, 137.7, 132.3, 129.0, 128.8, 128.3, 128.1, 127.1, 126.2, 123.9, 117.2, 113.6, 60.2, 59.9, 55.0. **LRMS**: Calculated for $C_{22}H_{20}NO_2$ (M^+) 330.2, Found 330.4. ***trans*-2.42**: Isolated as a white solid (17 mg, 0.05 mmol, 26 %). $\mathbf{R_f}$ = 0.31 (85:15/hexanes:EtOAc). **^{1}H NMR (400 MHz, $CDCl_3$)**: δ 7.40-7.25 (m, 11H), 7.06 (m, 1H) 6.93 (m, 2H), 4.91 (d, *J* = 2.4 Hz, 1H), 4.26 (d, *J* = 2.4 Hz, 1H), 3.82 (s, 3H). **^{13}C NMR (100 MHz, $CDCl_3$)**: δ 165.8, 159.9, 137.5, 134.8, 129.4, 129.1, 129.0, 127.8, 127.4, 127.2, 124.0, 117.2, 114.7, 65.2, 63.4, 55.3. **LRMS**: Calculated for $C_{22}H_{20}NO_2$ (M^+) 330.2, Found 330.4.

***cis*-4-(3-methoxyphenyl)-1,3-diphenylazetidin-2-one (*cis*-2.43)** and ***trans*-4-(3-methoxyphenyl)-1,3-diphenylazetidin-2-one (*trans*-2.43)**:

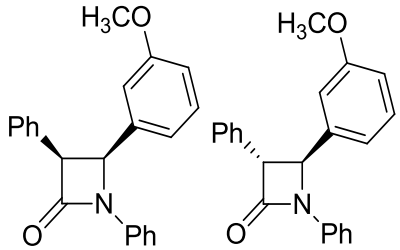

***cis*-2.43** ***trans*-2.43**

(1.2:1)
mixture of diastereomers

Purified by flash column chromatography eluting 90:10/hexanes:EtOAc. Spectral data corresponded to that previously described in the literature.[41] ***cis*-2.43**: Isolated as a white solid (19 mg, 0.06 mmol, 29 %). $\mathbf{R_f}$ = 0.26 (9:1/hexanes:EtOAc). **^{1}H NMR (400 MHz, $CDCl_3$)**: δ 7.43 (m, 2H), 7.29 (m, 2H), 7.13-7.02 (m, 7H), 6.71-6.57 (m, 3H), 5.42 (d, *J* = 6.1 Hz, 1H), 5.00 (d, *J* = 6.1 Hz, 1H), 3.60 (s, 3H). **^{13}C NMR (100 MHz, $CDCl_3$)**: δ 165.6, 159.4, 137.7, 136.0, 132.1, 129.3, 129.0, 128.8, 128.1, 127.2, 124.0, 119.6, 117.2, 113.5, 112.7, 60.2, 60.2, 55.1. **HRMS**: Calculated for $C_{22}H_{20}NO_2$ (M^+) 330.1494, Found 330.1479. ***trans*-2.43**: Isolated as a white solid (16 mg, 0.05 mmol, 24 %). $\mathbf{R_f}$ = 0.32 (85:15/hexanes:EtOAc). **^{1}H NMR (400MHz, $CDCl_3$)**: δ 7.40-7.28 (m, 10H), 7.09-6.88 (m, 4H), 4.91 (d, *J* = 2.5Hz, 1H), 4.29 (d, *J* = 2.5 Hz, 1H), 3.79 (s, 3H). **^{13}C NMR (100 MHz, $CDCl_3$)**: δ 165.6, 160.3, 139.2, 137.5, 134.7, 130.4, 129.1, 129.0, 127.9, 127.5, 124.1, 118.1, 117.2, 113.9, 111.5, 65.0, 63.6, 55.3. **HRMS**: Calculated for $C_{22}H_{20}NO_2$ (M^+) 330.1494, Found 330.1469.

***cis*-4-(4-bromophenyl)-1,3-diphenylazetidin-2-one (*cis*-2.44)** and ***trans*-4-(4-bromophenyl)-1,3-diphenylazetidin-2-one (*trans*-2.44)**:

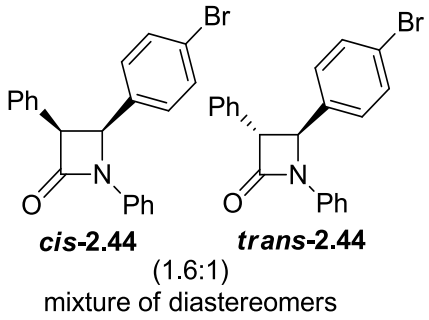

***cis*-2.44** ***trans*-2.44**

(1.6:1)

mixture of diastereomers

Purified by flash column chromatography eluting 90:10/hexanes:EtOAc. Spectral data corresponded to that previously described in the literature.[42] ***cis*-2.44**: Isolated as a white solid (31 mg, 0.08 mmol, 41 %). $\mathbf{R_f}$ = 0.21 (9:1/hexanes:EtOAc,). **^{1}H NMR (400 MHz, $CDCl_3$)**: δ 7.38 (d, 2H), 7.31-7.23 (m, 4H), 7.15-7.04 (m, 6H), 6.95 (d, 2H), 5.42 (d, *J* = 6.1 Hz, 1H), 5.01 (d, *J* = 6.1 Hz, 1H). **^{13}C NMR (101 MHz, $CDCl_3$)**: δ 165.3, 137.4, 133.6, 131.7, 131.4, 129.1, 128.8, 128.3, 127.5, 124.2, 121.9, 117.1, 60.3, 59.7. **HRMS** Calculated for $C_{21}H_{17}BrNO$ (M^+) 378.0493, Found 378.0467 and 380.0456. ***trans*-2.44**: Isolated as an off white solid (20 mg, 0.05 mmol, 27 %). $\mathbf{R_f}$ = 0.32 (9:1/hexanes:EtOAc). **^{1}H NMR (400 MHz, $CDCl_3$)**: δ 7.54 (m, 2H), 7.41-7.26 (m, 11H), 7.09 (m,1H), 4.92 (d, *J* = 2.5 Hz, 1H), 4.25-4.24 (d, *J* = 2.5 Hz, 1H). **^{13}C-NMR (100 MHz, $CDCl_3$)**: δ 165.2, 137.2, 136.5, 134.3, 132.5, 129.2, 129.1, 128.0, 127.5, 127.4, 124.2, 122.6, 117.1, 65.1, 63.1. **HRMS** Calculated for $C_{21}H_{17}BrNO$: 378.0493, Found 378.0453 and 380.0430.

methyl-4-((*cis*)-4-oxo-1,3-diphenylazetidin-2-yl)benzoate (*cis*-2.45) and **methyl-4-((*trans*)-4-oxo-1,3-diphenylazetidin-2-yl)benzoate (*trans*-2.45)**:

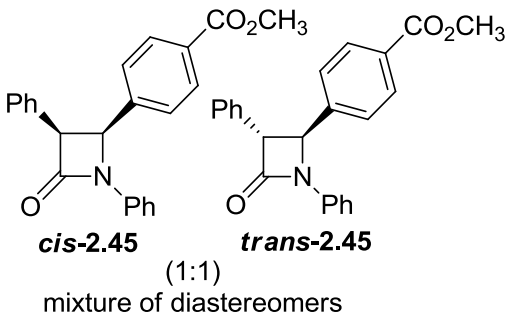

Purified by flash column chromatography eluting 85:15/hexanes:EtOAc. Spectral data corresponded to that previously described in the literature.[19] ***cis*-2.45**: Isolated as a white solid (29 mg, 0.08 mmol, 41 %). $\mathbf{R_f}$ = 0.27 (85:15/hexanes:EtOAc). **^{1}H NMR (400 MHz, $CDCl_3$)**: δ 7.78 (d, *J* = 8.2 Hz, 2H), 7.38 (m, 2H), 7.29 (m, 2H), 7.15 (d, *J* = 8.2 Hz, 2H), 7.11-7.04 (m, 6H) 5.50 (d, *J* = 6.2 Hz, 1H), 5.05 (d, *J* = 6.2Hz, 1H), 3.83 (s, 3H). **^{13}C NMR (100 MHz, $CDCl_3$)**: δ 166.5, 165.2, 139.8, 137.4, 131.6, 129.7, 129.5, 129.2, 128.8, 128.3, 128.2, 127.5, 127.1, 124.3, 117.1, 60.5, 60.0, 52.1. **LRMS**: Calculated for $C_{23}H_{20}NO_3$ (M^+) 358.1, Found 358.4. ***trans*-2.45**: Isolated as a white solid (28 mg, 0.08 mmol, 40 %). $\mathbf{R_f}$ = 0.41 (85:15/hexanes:EtOAc). **^{1}H NMR (400 MHz, $CDCl_3$,)**: δ 8.10 (d, *J* = 8.3 Hz, 2H), 7.50 (d, *J* = 8.3 Hz, 2H), 7.41-7.28 (m, 9H), 7.09 (m, 1H), 5.01 (d, *J* = 2.5Hz. 1H), 4.27 (d, *J* = 2.5 Hz, 1H), 3.92 (s, 3H). **^{13}C NMR (100 MHz, $CDCl_3$)**: δ 166.5, 165.2, 142.6, 137.2, 134.3, 130.6, 130.6, 129.2, 129.1, 128.1, 127.4, 125.9, 124.3, 117.1, 104.6, 65.1, 63.3, 52.3. **LRMS**: Calculated for $C_{23}H_{20}NO_3$ (M^+) 358.1, Found 358.4.

4-((*cis*)-4-oxo-1,3-diphenylazetidin-2-yl)benzonitrile (*cis*-2.46) and **4-((*trans*)-4-oxo-1,3-diphenylazetidin-2-yl)benzonitrile (*trans*-2.46)**:

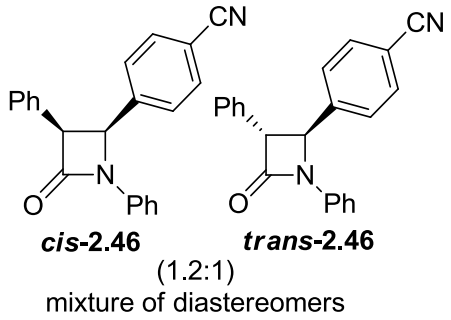

***cis*-2.46** ***trans*-2.46**

(1.2:1)

mixture of diastereomers

Purified by flash column chromatography eluting 80:20/hexanes:EtOAc. ***cis*-2.46**: Isolated as a white solid (23 mg, 0.07 mmol, 34 %). $\mathbf{R_f}$ = 0.23 (8:2/hexanes:EtOAc). **^{1}H NMR (400 MHz, $CDCl_3$)**: δ 7.41-7.01 (m, 14H), 5.50 (d, *J* = 6.2 Hz, 1H), 5.07 (d, *J* = 6.2 Hz, 1H). **^{13}C NMR (100 MHz, $CDCl_3$)**: δ 164.9, 140.2, 137.2, 132.0, 131.2, 129.3, 128.7, 128.4, 127.8, 124.5, 118.3, 117.0, 111.8, 60.6, 59.7. **HRMS**: Calculated for $C_{22}H_{17}N_2O$ (M^+) 325.1340, Found 325.1335. ***trans*-2.46**: Isolated as a white solid (19 mg, 0.06 mmol, 29 %). $\mathbf{R_f}$ = 0.29 (8:2/hexanes:EtOAc). **^{1}H NMR (400 MHz, $CDCl_3$)**: δ 7.71 (d, *J* = 8.0 Hz, 2H), 7.51 (d, *J* = 8.0 Hz, 2H), 7.42-7.26 (m, 9H), 7.11 (m, 1H), 5.01 (d, *J* = 2.5 Hz, 1H), 4.25 (d, *J* = 2.5 Hz, 1H). **^{13}C NMR (100 MHz, $CDCl_3$)**: δ 164.8, 142.9, 137.0, 133.9, 133.2, 129.3, 129.2, 128.3, 127.4, 126.6, 124.5, 118.2, 117.0, 112.7, 65.2, 63.0. **HRMS**: Calculated for $C_{22}H_{17}N_2O$ (M^+) 325.1340, Found 325.1335.

(*cis*)-4-(3-nitrophenyl)-1,3-diphenylazetidin-2-one (*cis*-2.47) and **(*trans*)-4-(3-nitrophenyl)-1,3-diphenylazetidin-2-one (*trans*-2.47)**:

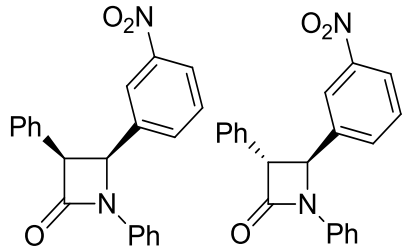

***cis*-2.47** ***trans*-2.47**

(1.3:1)
mixture of diastereomers

Purified by flash column chromatography eluting 85:15/hexanes:EtOAc. Spectral data corresponded to that previously described in the literature.[43] ***cis*-2.47**: Isolated as a white solid (28 mg, 0.08 mmol, 41 %). $\mathbf{R_f}$ = 0.29 (85:15/hexanes:EtOAc). **^{1}H NMR (400 MHz, $CDCl_3$)**: δ 7.95 (m, 2H), 7.39-7.28 (m, 6H), 7.14-7.03 (m, 6H), 5.56 (d, *J* = 6.1 Hz, 1H), 4.11 (d, *J* = 6.1 Hz, 1H). **^{13}C NMR (100 MHz, $CDCl_3$)**: δ 164.8, 148.0, 137.1, 132.8, 131.3, 129.3, 128.7, 128.5, 127.7, 124.6, 123.0, 122.2, 117.0, 60.6, 59.4. **HRMS**: Calculated for $C_{21}H_{17}N_2O_3$ (M^+) 345.1239, Found 345.1226. ***trans*-2.47**: Isolated as a white solid (22 mg, 0.06 mmol, 32 %). $\mathbf{R_f}$ = 0.38 (7:3/hexanes:EtOAc). **^{1}H NMR (400 MHz, $CDCl_3$)**: δ 8.27-8.23 (m, 2H), 7.75 (m, 1H), 7.62 (m, 1H), 7.43-7.28 (m, 9H), 7.11 (m, 1H), 5.07 (d, *J* = 2.5 Hz, 1H), 4.30 (d, *J* = 2.5 Hz, 1H). **^{13}C NMR (100 MHz, $CDCl_3$)**: δ 164.9, 148.9, 139.9, 136.9, 133.8, 131.6, 130.6, 129.4, 129.3, 128.3, 127.4, 124.6, 123.8, 121.2, 117.1, 65.3, 62.7. **HRMS** Calculated for $C_{21}H_{17}N_2O_3$ (M^+) 345.1239, Found 345.1221.

(*cis*)-4-(4-nitrophenyl)-1,3-diphenylazetidin-2-one (*cis*-4.28) and **(*trans*)-4-(4-nitrophenyl)-1,3-diphenylazetidin-2-one (*trans*-2.48)**:

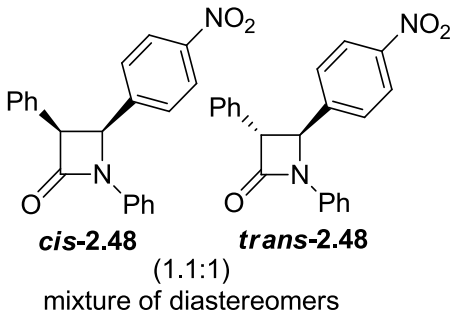

Purified by flash column chromatography eluting 85:15/hexanes:EtOAc. Spectral data corresponded to that previously described in the literature.[42] ***cis*-2.48**: Isolated as an off-white solid (27 mg, 0.08 mmol, 39 %). $\mathbf{R_f}$ = 0.33 (85:15/hexanes:EtOAc). **^{1}H NMR (400 MHz, $CDCl_3$)**: δ 7.98 (d, J = 8.6 Hz, 2H), 7.37-7.03 (m, 12H), 5.55 (d, *J* = 6.2 Hz, 1H), 5.10(d, *J* = 6.2 Hz, 1H). **^{13}C NMR (100 MHz, $CDCl_3$)**: δ 164.8, 147.4, 142.2, 137.2, 131.1, 129.3, 128.7, 128.5, 128.0, 127.8, 124.6, 123.5, 117.0, 60.7, 59.5. **LRMS**: Calculated for $C_{21}H_{17}N_2O_3$ (M^+) 345.1, Found 345.1. ***trans*-2.48**: Isolated as an off-white solid (24 mg, 0.07 mmol, 35 %). $\mathbf{R_f}$ = 0.37 (85:15/hexanes:EtOAc). **^{1}H NMR (400 MHz, $CDCl_3$)**: δ 8.28 (d, J = 8.7 Hz, 2H), 7.58 (d, J = 8.7 Hz, 2H), 7.43-7.30 (m, 9H), 7.12 (m, 1H), 5.07(d, *J* = 2.5 Hz, 1H), 4.27 (d, *J* = 2.5 Hz, 1H). **^{13}C NMR (100 MHz, $CDCl_3$)**: δ 164.7, 148.1, 144.8, 136.9, 133.8, 129.4, 129.3, 128.4, 127.4, 126.8, 124.7, 124.6, 117.0, 65.3, 62.8. **LRMS**: Calculated for $C_{21}H_{17}N_2O_3$ (M^+) 345.1, Found 345.4.

***N*,2-diphenylacetamide (2.56)**:

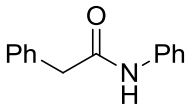

2.56

Purified by flash column chromatography eluting 70:30/hexanes:EtOAc. The title compound **2.56** was obtained as a brown solid. The spectral data corresponded to that previously described in the literature.[44] $\mathbf{R_f}$ = 0.31 (7:3/hexanes:EtOAc). **^{1}H NMR (400 MHz, $CDCl_3$)**: δ 7.42-7.08 (m, 10H), 7.13 (br s, 1H), 3.74 (s, 2H). **^{13}C NMR (100 MHz, $CDCl_3$)**: δ 169.5, 138.0, 134.8, 130.0, 129.7, 129.4, 128.1, 124.9, 120.2, 45.3. **LRMS**: Calculated for $C_{14}H_{14}NO$ (M^+) 212.1; found 212.3.

References

(1) Sletten, E. M.; Bertozzi, C. R. *Angew. Chem. Int. Ed.* **2009**, *48*, 6974-6998.
(2) Huisgen, R. *Angew. Chem. Int. Ed.* **1963**, *2*, 565-598.
(3) Woodward, R. B.; Hoffmann, R. *The Conservation of Orbital Symmetry*; Verlag Chemie: Weinheim, 1970.
(4) Huisgen, R. *1,3-Dipolar Cycloaddition Chemistry* Padwa, A. Ed.; Wiley: New York, 1984; Vol. 1.
(5) Padwa, A. *Comprehensive Organic Synthesis*; Trost, B. M., Flemming, I., Eds.; Pergamon Press: Oxford, 1991; Vol. 4, pp 1069.
(6) Gothelf, K. V.; Jørgensen, K. A. *Chem. Rev.* **1998**, *98*, 863-910.
(7) Firestone, R. A. *J. Org. Chem.* **1968**, *33*, 2285-2290.
(8) Houk, K. N.; Gonzalez, J.; Li, Y. *Acc. Chem. Res.* **1995**, *28*, 81-90.
(9) Huisgen, R. *J. Org. Chem.* **1968**, *33*, 2291-2297.
(10) Gothelf, K. V.; Jørgensen, K. A. *Chem. Commun.* **2000**, 1449-1458.
(11) Sustmann, R. *Tetrahedron Lett.* **1971**, *12*, 2717-2720.
(12) Sustmann, R. *Pure Appl. Chem.* **1974**, *40*, 569-593.
(13) Stanley, L. M.; Sibi, M. P. *Chem. Rev.* **2008**, *108*, 2887-2902.
(14) Kinugasa, M.; Hashimoto, S. *Chem. Commun.* **1972**, 466-467.
(15) Ding, L. K.; Irwin, W. J. *J. Chem. Soc., Perkin Trans. 1* **1976**, *22*, 2382-2386.
(16) Ye, M.-C.; Zhou, J.; Tang, Y. *J. Org. Chem.* **2006**, *71*, 3576-3582.
(17) Ahn, C.; Kennington, J. W.; DeShong, P. *J. Org. Chem.* **1994**, *59*, 6282-6286.
(18) Shintani, R.; Fu, G. C. *Angew. Chem. Int. Ed.* **2003**, *42*, 4082-4085.
(19) Miura, M.; Enna, M.; Okuro, K.; Nomura, M. *J. Org. Chem.* **1995**, *60*, 4999-5004.
(20) Okuro, K.; Enna, M.; Miura, M.; Nomura, M. *J. Chem. Soc. Chem. Commun.* **1993**, 1107-1108.
(21) Pan, S. C.; List, B. *Angew. Chem. Int. Ed.* **2008**, *47*, 3622-3625.
(22) Basak, A.; Ghosh, S. C.; Bhowmich, T.; Das, A. K.; Bertolasi, V. *Tetrahedron Lett.* **2002**, *43*, 5499-5501.
(23) Mames, A.; Stecko, S.; Mikołajczyk, P.; Soluch, M.; Furman, B.; Chmielewski, M. *J. Org. Chem.* **2010**, *75*, 7580-7587.
(24) Stecko, S.; Mames, A.; Furman, B.; Chmielewski, M. *J. Org. Chem.* **2009**, *74*, 3094-3100.
(25) Stecko, S.; Mames, A.; Furman, B.; Chmielewski, M. *J. Org. Chem.* **2008**, *73*, 7402-7404.
(26) Zhang, X.; Hsung, R. P.; Li, H.; Zhang, Y.; Johnson, W. L.; Figueroa, R. *Org. Lett.* **2008**, *10*, 3477-3479.
(27) Coyne, A. G.; Mueller-Bunz, H.; Guiry, P. J. *Tetrahedron Asymm.* **2007**, *18*, 199-207.
(28) Lo, M. M. C.; Fu, G. C. *J. Am. Chem. Soc.* **2002**, *124*, 4572-4573.
(29) Saito, T.; Kikuchi, T.; Tanabe, H.; Yahiro, J.; Otani, T. *Tetrahedron Lett.* **2009**, *50*, 4969-4972.
(30) Ye, M.-C.; Zhou, J.; Huang, Z.-Z.; Tang, Y. *Chem. Commun.* **2003**, *39*, 2554-2555.
(31) Basak, A.; Bhattacharya, G.; Bdour, H. M. M. *Tetrahedron* **1998**, *54*, 6529-6538.
(32) Basak, A.; Pal, R. *Bioorg. Med. Chem. Lett.* **2005**, *15*, 2015-2018.
(33) Basak, A.; Ghosh, S. C.; Das, A. K.; Bertolasi, V. *Org. Biomol. Chem.* **2005**, *3*, 4050-4052.

(34) Basak, A.; Chandra, K.; Pal, R.; Ghosh, S. C. *Synlett* **2007**, *2007*, 1585-1588.
(35) Chatterjee, A.; Maiti, D. K.; Bhattacharya, P. K. *Org. Lett.* **2003**, *5*, 3967-3969.
(36) Lorello, G. R.; Legault, M. C. B.; Rakić, B.; Bisgaard, K.; Pezacki, J. P. *Bioorg. Chem.* **2008**, *36*, 105-111.
(37) Lewis, R. J.; Camilleri, P.; Kirby, A. J.; Marby, C. A.; Slawin, A. A.; Williams, D. J. *J. Chem. Soc., Perkin Trans. 2* **1991**, 1625-1630.
(38) Singh, S. K.; Srinivasa Reddy, M.; Mangle, M.; Ravi Ganesh, K. *Tetrahedron* **2007**, *63*, 126-130.
(39) Siemsen, P.; Livingston, R. C.; Diederich, F. *Angew. Chem. Int. Ed.* **2000**, *39*, 2632-2657.
(40) Himo, F.; Lovell, T.; Hilgraf, R.; Rostovtsev, V. V.; Noodleman, L.; Sharpless, K. B.; Fokin, V. V. *J. Am. Chem. Soc.* **2004**, *127*, 210-216.
(41) Pfleger, R.; Jäger, A. *Chem. Ber.* **1957**, *90*, 2460-2470.
(42) Bolognese, A.; Diurno, M. V.; Mazzoni, O.; Giordano, F. *Tetrahedron* **1991**, *47*, 7417-7428.
(43) Chen, R.; Bingjian, Y.; Weike, S. *Synth. Commun.* **2006**, *36*, 3167-3174.
(44) Nordstrøm, L. U.; Vogt, H.; Madsen, R. *J. Am. Chem. Soc.* **2008**, *130*, 17672-17673.

Chapter 3 : Synthesis of β-Lactam Probes for Activity-Based Protein Profiling of Rhomboid Proteases

The cellular studies described herein were performed in collaboration with Dr. Allison Sherratt at the National Research Council of Canada in Ottawa.

Introduction

Having developed a multicomponent Kinugasa in aqueous media in the last chapter, the slow kinetics associated with β-lactam formation via the Kinugasa reaction precluded its application as a bioorthogonal reaction. However, the β-lactams themselves are useful biomolecular substrates. This chapter describes the synthesis of β-lactam activity-based probes using the Kinugasa reaction and applications of the probes for studying the structure and functions of rhomboid proteases.

β-lactams represent one of the best known and extensively studied classes of antibiotics, due to both their biological activity and utility as synthetic intermediates.[1,2] Since the discovery of penicillin (**3.1**), antibacterial agents such as cephalosporins (**3.2**), carbapenams (**3.3**), monobactams (**3.4**), and nocardicins (**3.5**) have been developed. Their use worldwide continues to be a first line of defense against infectious bacterial pathogens (Figure 3-1).

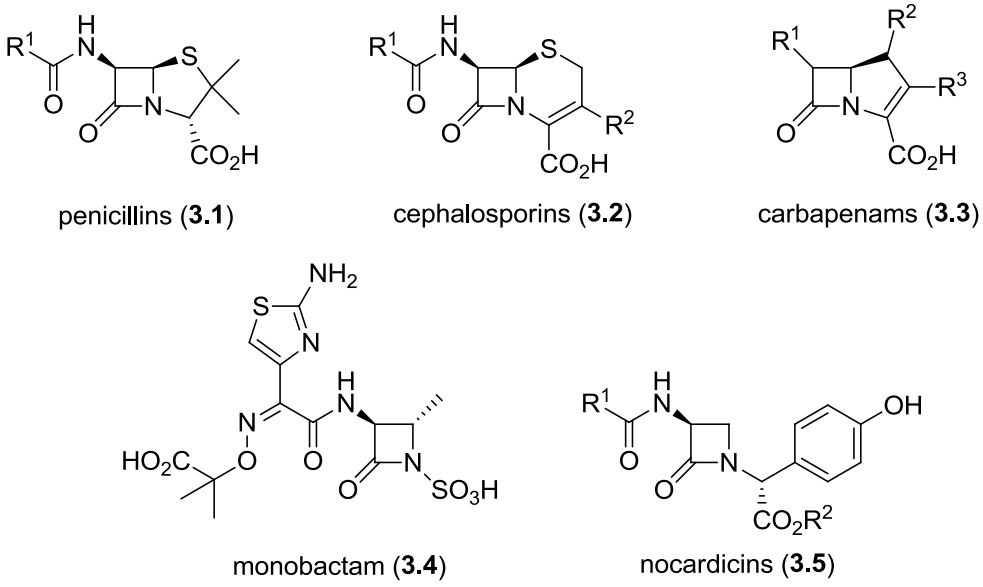

Figure 3-1. Important classes of antibacterial agents that contain the β-lactam moiety.

β-lactams halt bacterial growth by inhibiting penicillin binding proteins (PBPs) that are required for cross-linking during cell-wall biosynthesis.[3,4] The powerful antibiotic activities of β-lactams stem from their reaction with a catalytically active serine residue in bacterial trans peptidases and carboxy-peptidases via a nucleophilic ring opening reaction of the β-lactam (Scheme 3-1).[5] Ring opening of the β-lactam forms a stable covalently bound acyl-enzyme adduct, which effectively inhibits these enzymes. Only clavulanic acid and some of the cephalosporins deviate in their mechanism from the common scheme as they involve secondary chemical transformations following the initial cleavage of the lactam ring.[6,7]

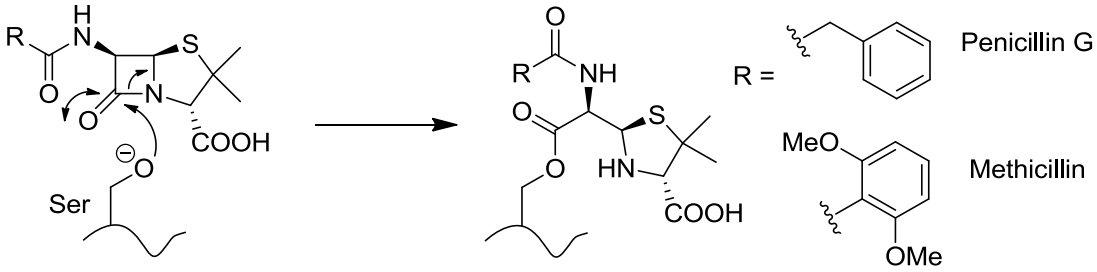

Scheme 3-1. Covalent enzyme inhibition of an active-site serine residue by penicillin β-lactams.[5]

In recent years the effectiveness of the β-lactam antibiotics has slowed since bacteria often develop resistance to antibiotics, resulting from evolution of β-lactamase enzymes which effectively hydrolyze β-lactams without being inhibited.[8] While the synthesis of new classes of β-lactam antibiotics and the development of β-lactamase inhibitors will likely extend the lifetime of β-lactams as effective antibiotics, many scientists have begun investigations of β-lactams for inhibition of other hydrolytic enzymes.

Recently, β-lactams have found other important therapeutic uses, such as inhibition of cholesterol absorption, serine proteases such as β-lactamases,[9] cysteine proteases, human

cytomegalovirus protease,[10] prostate-specific antigen,[11] thrombin,[12] chymases and elastases,[13] and fatty acid synthase.[14] Relevant to our recent studies of multicomponent Kinugasa reactions, the 3-alkyl-1,4-diaryl-2-azetidinones represent a class of compounds that exhibit interesting biological properties and share homology with structures that could be accessed by the Kinugasa reaction (Figure 3-2). *N*,4-diaryl substituted β-lactams have been shown to be potent cholesterol absorption inhibitors[15-21] (**3.6**-**3.9**), whereas others exhibit antifungal[22] (**3.10**), analgesic (**3.11**),[23] and anticancer[24,25] (**3.12** and **3.13**) activities. Recently, the Kinugasa reaction was employed in the formal synthesis of Ezitimibe (**3.6**).[26]

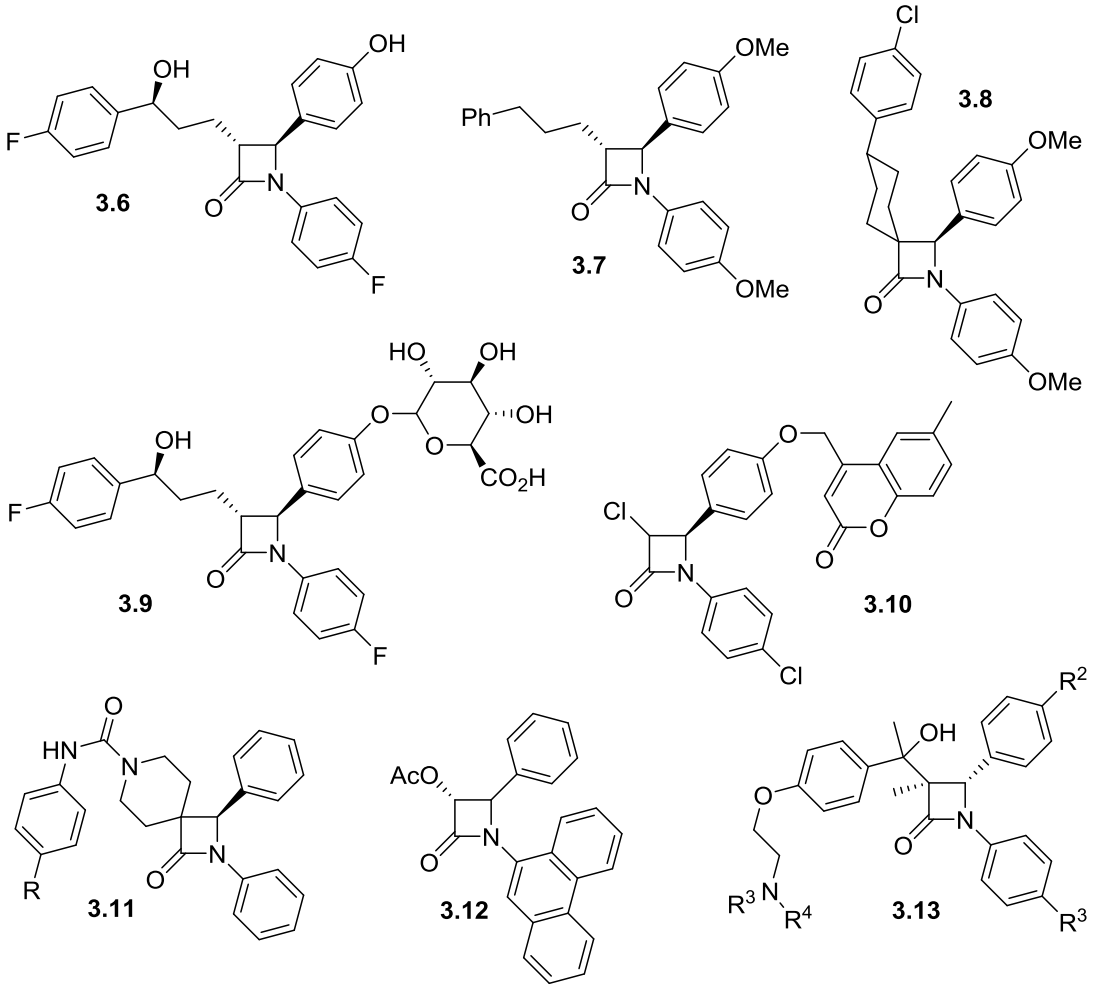

Figure 3-2. 1,4-diaryl β-lactams possess an increasingly wide range of biological activities. Figure was adapted from the literature.[27]

Several strategies have been developed to study the targets and off-targets of β-lactams, and for identifying mechanisms of antibiotic resistance. Early efforts utilized ^{125}I radio-labelled β-lactams to profile penicillin binding proteins (PBPs), the main targets of many β-lactams.[28,29] While radioisotope labelled β-lactams provide valuable insights into the cellular targets of these antibiotics, there are numerous limitations associated with radioisotope labelling (handling of radioactive material, instability, labour and expensive cost).[29] Emerging strategies rely on fluorophore labelled β-lactam probes, that allowed for electrophoretic separation of the active enzymes that were targeted.[30,31] Activity-based protein profiling (ABPP), utilizes β-lactam activity-based probes originating from several known antibiotics as well as synthetic analogs, to provide insight into the target preferences of these privileged scaffolds.[32]

Protein expression and activity regulates complex processes in living organisms. A formidable challenge is to understand how protein activity regulates protein function.[33] While classical genetic[34,35] and proteomic[36,37] strategies have provided valuable information for quantifying protein expression based on quantities of mRNA and protein present, the abundance of a given protein does not necessarily correlate with its activity. Post translational modifications are often responsible for spatial and temporal control of *in situ* enzyme activities. [38] To overcome limitations associated with abundance based methods, activity-based protein profiling (ABPP) has emerged as a modern proteomic strategy that utilizes molecular probes to characterize and assign function to active enzyme families within complex proteomes and to discover novel customized enzyme inhibitors.[39-43] The approach has been applied successfully to important problems related to human health, such as cancer, neurobiology, parasitology and virology.[43,44] A variety of enzyme classes have

also been studied using this technique, including serine proteases, metalloproteases, kinases, phosphatases, lipid transferases, and histone deacetylases.[40,42-45]

The ABPP technology relies on active-site directed molecular probes with tailored specificity toward enzymes. The probes become covalently bound to the target, via diversion of the enzyme mechanism, enzyme inhibition mechanism, or by reversible inhibition followed by subsequent photo-cross-linking. The probes are equipped with a reporter tag for visualization or enrichment using fluorophores or biotin, respectively (Figure 3-3).[40,42-45] Gel electrophoresis (SDS-PAGE) and fluorescence analysis allow visualization of the active enzymes that are bound to the probe. Selective enrichment of labelling events for target identification by MS/MS is achieved using the strong affinity of biotin for streptavidin. Inactive enzymes or those with blocked active sites are not labelled by the probe and thus are not visualized or enriched. A limitation of the single-step ABPP is that the bulky reporter (fluorescent dye or biotin) has an influence on target selectivity. This can be overcome by using bioorthogonal chemistry, in which the reporter tag is appended in a subsequent step using click chemistries (eg. Cu(I)-catalyzed azide-alkyne cycloaddition).[46-48]

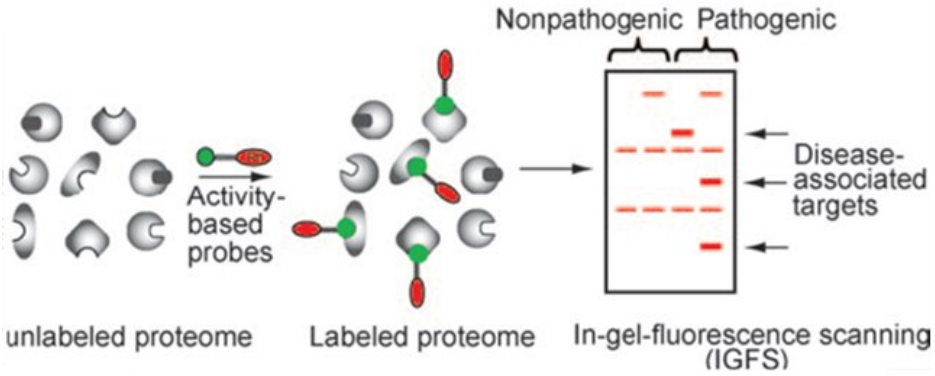

Figure 3-3. Typical activity-based protein profiling experimental design. Activity based probes containing a reactive group (green circle) and reporter tag (red oval) react with their biological target in the proteome. Protein targets are visualized by fluorescence scanning. Figure was reprinted from the literature.[5,39]

The tag-free ABPP approach has recently been employed by Staub and Sieber, where they employed a series of alkyne tagged β-lactam probes.[32] These probes comprised penam (ampicillin), cephem (cephalosporin), and monobactam (astreonam) drug scaffolds as wells as a structurally diverse library of synthetic monocyclic β-lactam probes (Figure 3-4). Several high and low molecular weight PBPs were targeted by the penam and cephem probes. Interestingly, the targets of the synthetic β-lactam probes based around the monocyclic aztreonam (Azt) structure did not include any PBPs, but rather these probes had preference for other enzymes such as β-ketoacyl acyl carrier protein III (KAS III), β-lactamase, lipase acylhydrolase, alkyl hydroperoxide reductase subunit C (AhpC), and the virulence-associated protein ClpP.[32]

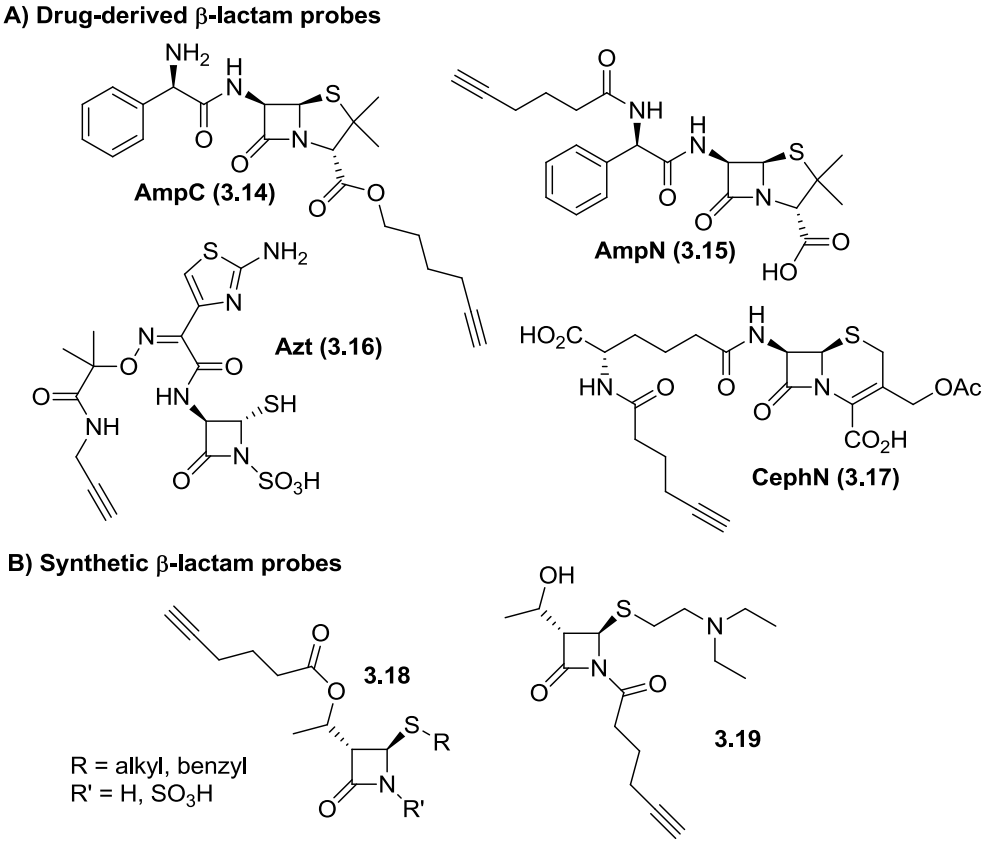

Figure 3-4. Structures of alkyne tethered β-lactam activity-based probes for ABPP of bacterial enzymes *in-vivo*. Figure was reproduced from the literature.[32]

In a following publication, Staub and Sieber utilized the monocyclic β-lactam probes for the *in situ* comparative profiling of antibiotic-sensitive and multi-resistant *Staphylococcus aureus* strain (MSRA).[49] With these probes, they were able to identify five unique resistance associated enzymes for the MRSA strain. MS analysis revealed enzyme targets as PBP2',[50] antibiotic sensing protein MCR1,[51] and a previously uncharacterized serine protease SPD_0, esterase E28, dipeptidase which displayed significant β-lactamase activity. The synthetic β-lactam probes provided useful tools to not only monitor these enzymes, but also to unravel the functions of yet uncharacterized MRSA specific enzymes with a potential for therapeutic intervention.[49]

The application of ABPP for the characterization of membrane-embedded enzymes has not yet been exploited to its full potential. Rhomboids are a relatively recently discovered integral membrane serine proteases that are conserved throughout evolution,[52,53] and utilize a serine protease mechanism within the lipid bilayer to cleave transmembrane substrates giving rise to a wide range of biological functions of which many are unknown. Rhomboids have been shown to play roles in diverse processes such as cell signaling,[54-56] mitochondrial function,[57-59] invasion of host cells by apicomplexan parasite,[60-62] and activations of bacterial protein export.[63] The active site of rhomboids is quite different from other serine proteases being formed by residues contributed by transmembrane helices buried within the hydrophobic lipid bilayer of cell membranes.[55,64]

This hydrophobic environment places certain biophysical constraints on potential inhibitors and raises questions about the potential *in vivo* availability of inhibitors that may work *in-vitro* in a detergent micelle system where rhomboid are typically studied.[65] Rhomboids have only been weakly inhibited by serine protease inhibitors such as isocourmarins and a few others.[55,66] Recently, a series of monocyclic β-lactams were

identified as selective and potent inhibitors of rhomboid proteases.[65] On the basis of a 58, 000 small molecule screen, β-lactam structure **3.20** was identified as a potent inhibitor of rhomboids (Figure 3-5).

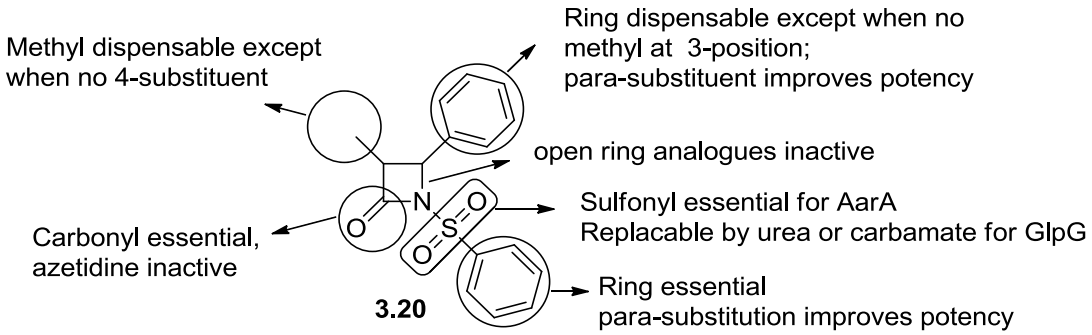

Figure 3-5. Summary of structure-activity relationship results from a library of structurally modified β-lactam inhibitory effects on rhomboid proteases. Positions of structural modifications are circled. Figure was reproduced from the literature.[65]

Based on the structure-activity relationship (SAR) previously determined by Pierrat *et al.*,[65] structural changes were introduced at all four positions of the β-lactam and their effects are summarized: 1) the azetidinone C-2 carbonyl group was essential for activity, which supports the mechanism-based inhibition in accordance with other β-lactam serine protease inhibitors; 2) the *N*-phenyl-sulfonyl group greatly enhanced the reactivity of the β-lactam group and the ring opened form was inactive, suggesting that electron withdrawing groups present at *N*-1 are responsible for inhibitory activity; 3) an aryl group at C-4 was not required for activity, although *para*-substitution increased its potency; and 4) The C-3 methyl group was not essential, but the C-3 unsubstituted β-lactam was inactive.

On the basis of these SARs and our previously developed Kinugasa reaction methodology, we set out to design hydrophobic β-lactams that could be easily accessed with potentially even greater inhibitory effects. Furthermore, by appending a bioorthogonal alkyne reporter group, *in situ* ABPP via CuAAC reactions may shed light on the mechanism

of action of β-lactam rhomboid inhibitors and establish if the inhibitors form covalent complexes with the rhomboid. Furthermore, such probes could provide valuable information regarding other targets of the inhibitors *in vivo*. The designed probes therefore could be useful tools to correlate enzyme activity with function.

Hypothesis

Novel monocyclic β-lactams activity-based probes can be prepared via the Kinugasa reaction in aqueous media and can be used to study the function of rhomboid proteases.

Results and Discussion

Design of β-lactam Activity-Based Probes

With the goal of designing a hydrophobic β-lactam activity-based probe, we sought to replace the electron withdrawing *N*-sulfonyl-aryl group in β-lactam **3.20** with an aryl group. We anticipated that this modification could be accomplished without compromising the reactivity of the β-lactam toward ring opening by active site nucleophiles. We decided to append the alkyne reporter at the *para*-position of the C-4 aryl substituent of the β-lactam. This is supported by the structure-activity relationships done previously by Pierratt *et al.*, where they found that increased inhibitory effects were observed for β-lactams bearing C-4 aryl substitution.[65] Our initially designed probes contain a bulky phenyl ring at the C-3 position, but could be further modified to remove the aryl ring. It has been shown previously, that the Kinugasa reaction is amenable to aliphatic alkynes.[26] The structures of the designed β-lactam activity-based probes are shown in Figure 3-6.

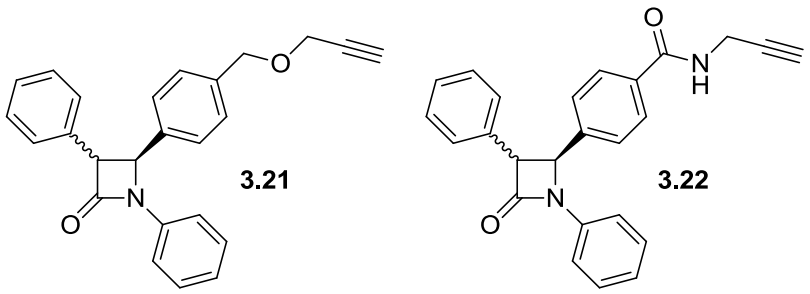

Figure 3-6. Structures of the designed β-lactam activity-based probes **3.21** and **3.22**.

Synthesis of β-lactam Activity-Based Probes

Having optimized simple conditions for performing multicomponent Kinugasa reactions in aqueous media in Chapter 2, we sought to utilize the aforementioned methodology for the preparation of β-lactam activity based probes described here. We decided to append the alkyne bioorthogonal chemical reporter group to the β-lactam core by a late stage *O*-alkylation or by an amide forming reaction for the synthesis **3.21** and **3.22**, respectively (Scheme 3-2).

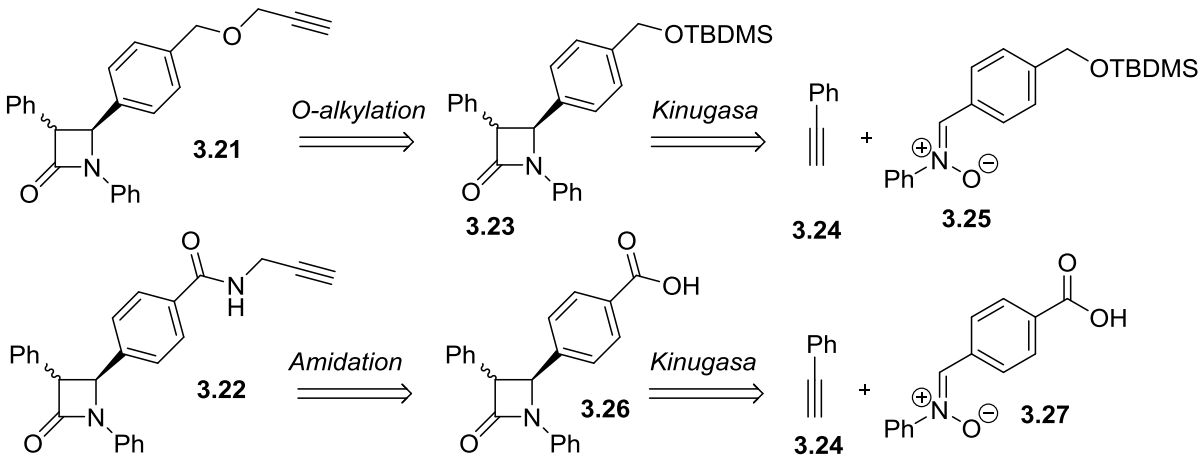

Scheme 3-2. Retrosynthetic analysis for β-lactam activity-based probes **3.21** and **3.22**.

Our initial efforts focused on synthesis of β-lactam **3.21**. We hypothesized that the efficiency of the Kinugasa reaction could be improved by protecting the benzyl alcohol as a

TBDMS ether prior to β-lactam formation. Nitrone **3.25** was synthesized in 90 % over four steps, starting from commercially available (diethoxymethyl)benzaldehyde, **3.28** (Scheme 3-3). Reduction of the **3.28** with $NaBH_4$ provided 4-(diethoxymethyl)-benzenemethanol[67] (**3.29**) which was subsequently protected using TBDMSCl, in the presence of DMAP and triethylamine at r.t. for 4 hrs, affording the silylated product **3.30** in 70 % yield.[68] Selective deprotection of the acetal was accomplished using the catalytic action of $NaBAr^F_4$ in excellent yield (95 %). The corresponding aldehyde **3.31** was reacted with *N*-phenyl hydroxyl amine in the presence of SDS micelles, affording the silylated nitrone **3.25** in 95 %.

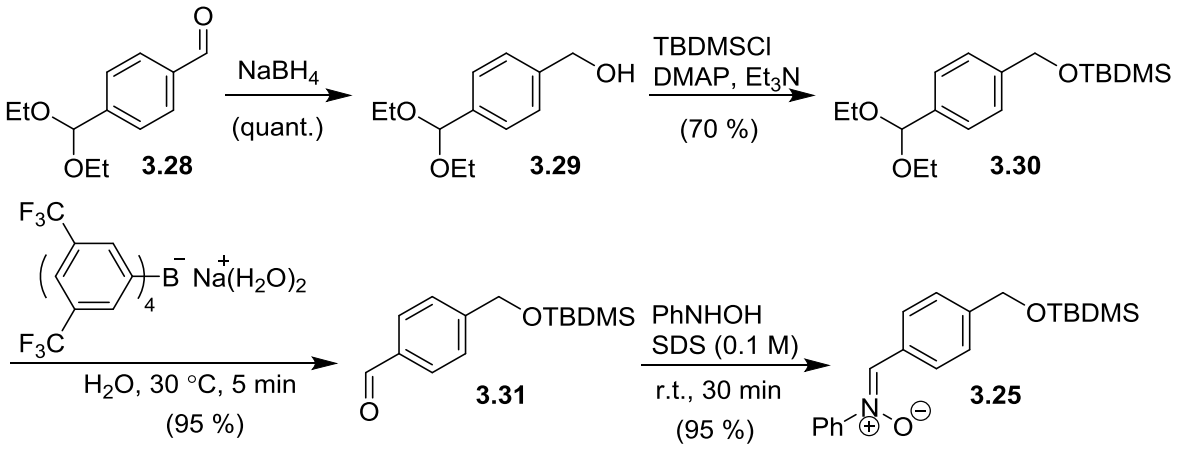

Scheme 3-3. Synthesis of nitrone intermediate **3.25**.

The silylated nitrone **3.25** was reacted with phenylacetylene (**3.24**) under our previously developed aqueous Kinugasa reaction conditions, the β-lactam intermediates, ***cis*-3.23** and ***trans*-3.23**, were obtained as a diastereomeric mixture (1.4 : 1) in a combined 60 % yield (Scheme 3-4).

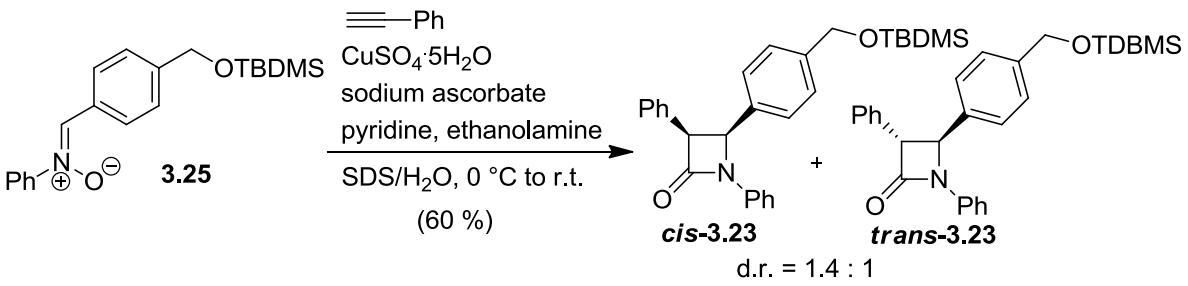

Scheme 3-4. Micelle-promoted Kinugasa reaction synthesis of β-lactam intermediate **3.23**.

Interestingly, upon desilylation of ***cis*-3.23** using TBAF, a mixture of ***cis*-3.32** and ***trans*-3.32** in a ratio of 1 to 11.4 was obtained in a combined yield of 69 % (Scheme 3-5). This result suggests that under the basic reaction conditions, the substituent at C-3 was epimerized to the thermodynamically stable *trans*-β-lactam product via a carbanion intermediate. This is corroborated by desilylation of the ***trans*-3.23**, which similarly yielded a diastereomeric mixture of ***cis*-3.32** and ***trans*-3.32** in a ratio of 1 to 11.8, respectively, in a combined yield of 63 %.

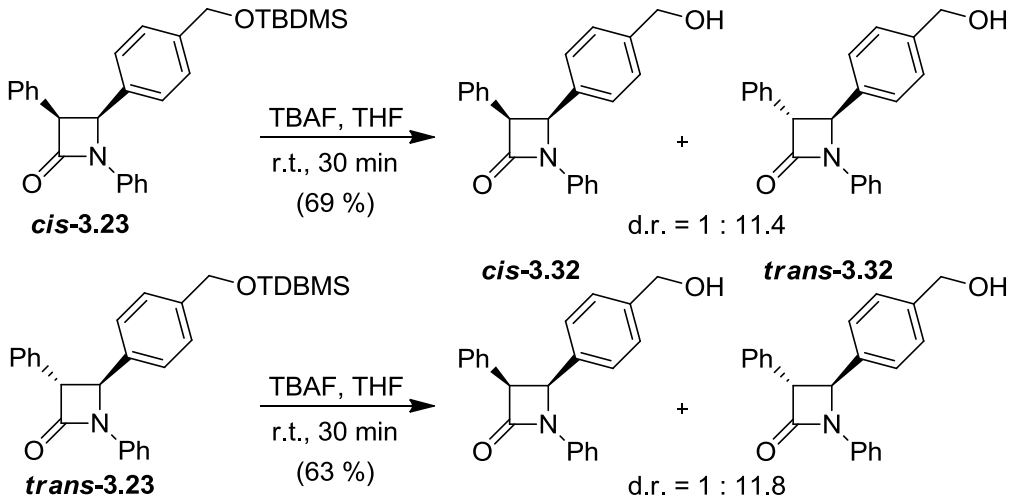

Scheme 3-5. Desilylation of β-lactam intermediates ***cis*-3.23** and ***trans*-3.23**.

To avoid issues with epimerization of the β-lactam during desilylation en route to **3.21**, we attempted to avoid the use of protecting groups for the synthesis of the penultimate

β-lactam intermediate **3.32**. Accordingly to Scheme 3-6, deprotection of **3.29** using aqueous HCl yielded the aldehyde **3.33** in quantitative yield,[69] and micelle promoted nitrone formation proceeded smoothly furnishing **3.34** in 89 % yield. The Kinugasa reaction of nitrone **3.34** with phenylacetylene **3.24** yielded the corresponding β-lactams, ***cis*-3.32** and ***trans*-3.32**, in a combined yield of 83 % and diastereomeric ratio of 1.3 to 1. The improved yield for the Kinugasa reaction involving **3.34** may be partially attributed to coordination of the hydroxyl group to the copper catalyst.

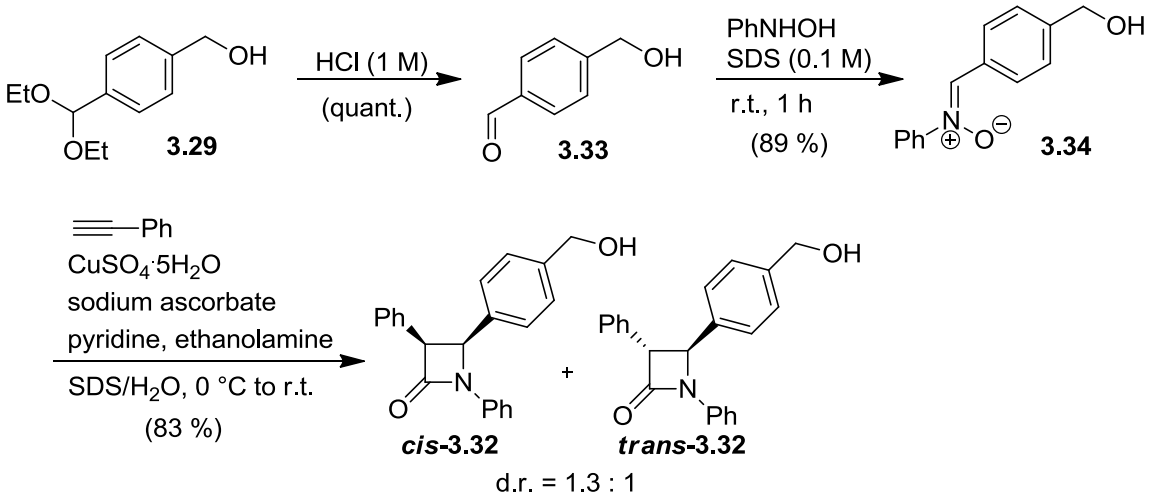

Scheme 3-6. Synthesis of β-lactams **3.26** by the Kinugasa reaction.

Next, we examined conditions for *O*-alkylation of the **3.32** with propargyl tosylate[70] (**3.35**) (Table 3-1). We tested two bases, K_2CO_3 and NaH, neither of which yielded the *O*-alkylated β-lactam product **3.21**. Instead, efficient ring opening yielded β-amino acid **3.36**. Due to ring opening and possibility for epimerization of the stereochemistry at C-3 under the basic conditions required for *O*-alkylation, we decided that this approach was not compatible with the β-lactam ring system and that we would explore the possibility of installing the alkyne moiety through an amide forming reaction using β-lactam **3.26** bearing a carboxylic acid handle.

Table 3-1. Attempted *O*-alkylation of β-lactam **3.32**.

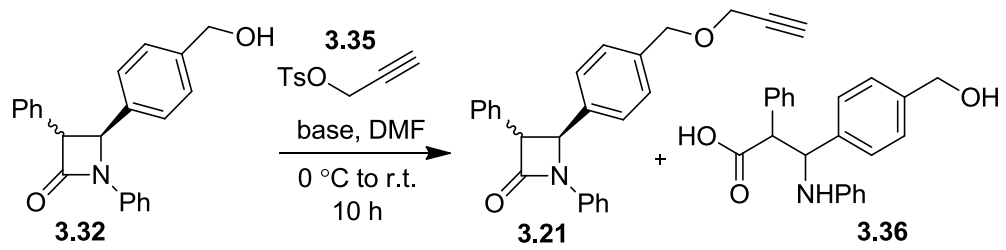

		% Yield	
Entry	**Base**	**3.21**	**3.36**
1	K_2CO_3	trace	83
2	NaH	trace	76

With the given success of our prior Kinugasa reaction involving nitrone **3.34**, bearing an unprotected benzyl alcohol, we reasoned that the presence of a carboxylic acid in **3.27** in place of the alcohol (**3.34**) may be compatible with the micelle promoted Kinugasa reaction conditions. Furthermore, the presence of the carboxylic acid in β-lactam **3.26** would enable facile coupling with alkyne terminated amines and would simplify the overall sequence.

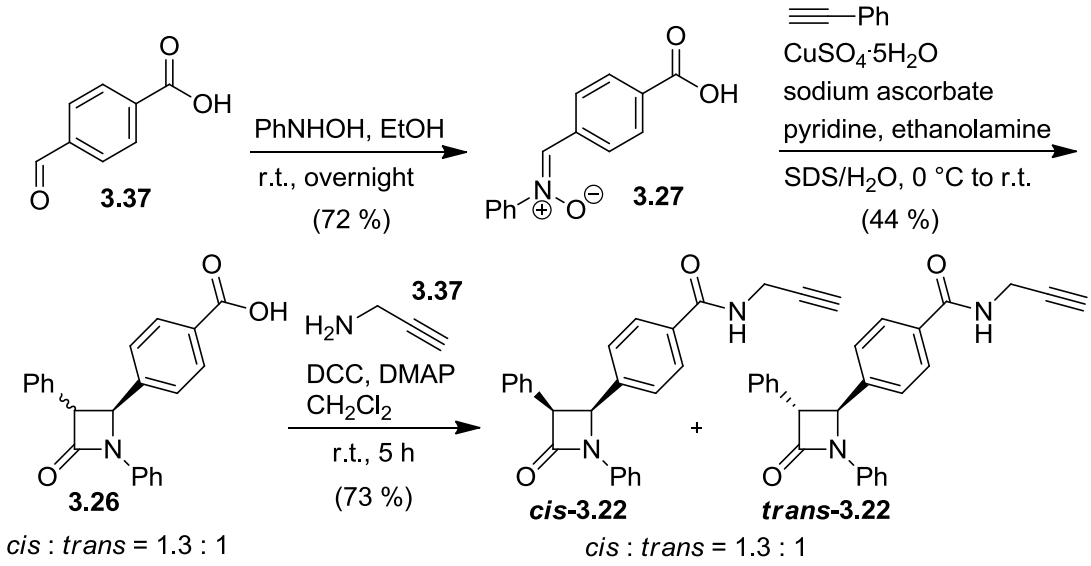

Scheme 3-7. Synthesis of β-lactam activity-based probes ***cis*-3.22** and ***trans*-3.22**.

According to Scheme 3-7, 4-carboxybenzaldehyde (**3.37**) was condensed with *N*-phenyl hydroxyl amine in ethanol, providing the corresponding nitrone intermediate **3.27** in 72 % yield. The reaction of nitrone **3.27** with phenylacetylene **3.24** under standard micelle-promoted Kinugasa reaction in aqueous media provided β-lactams, ***cis*-3.26** and ***trans*-3.26**, in a ratio of 1.3 to 1 and a combined yield of 44 %. The end game involved amide coupling of the carboxylic acid of lactam **3.26** with propargylamine (**3.37**) using carbodiimide coupling conditions. The β-lactams ***cis*-3.22** and ***trans*-3.22** were obtained in 73 % and the configuration at C-3 remained unchanged.

Activity-Based Protein Profiling of Rhomboid Protease Activity

The laboratories of Goto and Pezacki have recently utilized a fluorophosphonate activity based probe (**3.38**) for highly specific labelling of GlpG rhomboid protein, and for screening its protease function in crude lipid extracts isolated from *E. coli*.[71] The ABPP approach has enabled high throughput screening of the functional state of various rhomboid mutants in proteomic samples, relative to the purified GlpG.[71] To assess the utility of the aforementioned β-lactam probes ***cis*-3.22** and ***trans*-3.22** to study rhomboid function, we performed preliminary *in-vitro* ABPP with the crude membrane fractions isolated from bacteria expressing wild-type GlpG. Crude membrane fractions were incubated with various concentrations of β-lactam probes, and were subsequently reacted with rhodamine azide[72] (**3.39**) under CuAAC bioconjugation conditions. Fluorescence labelling was detected by in-gel fluorescence scanning and is shown in Figure 3-7.

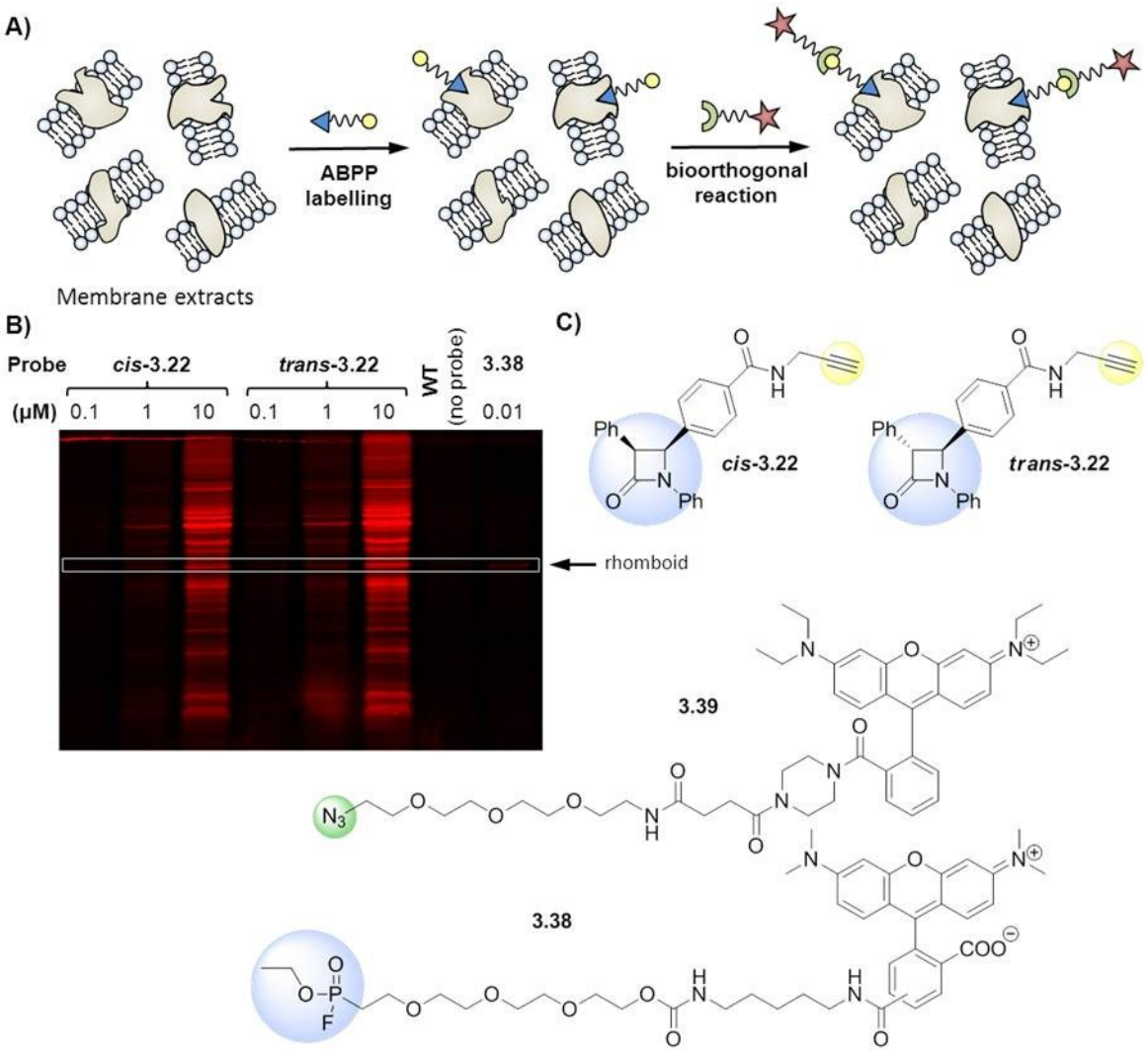

Figure 3-7. Rhomboid active-site labelling using β-lactam probes and fluorescent labelling via bioorthogonal CuAAC reaction. A) ABPP of rhomboid protease activity. B) Fluorescent probe labelling of wild-type GlpG rhomboid protease in crude membrane proteome. β-lactam probes ***cis*-3.22** (0.1, 1, 10 μM), ***trans*-3.22** (0.1, 1, 10 μM), or **3.38** (0.01 μM), was incubated with crude membrane extracts in 50 mM HEPES pH 7.3, 0.1 % dodecyl maltoside (DDM), 200 mM NaCl, 10% glycerol and 100 μM EDTA for 1 h at 37 ˚C. The alkyne labelled proteome was reacted with **3.39** (100 μM) in the presence of $CuSO_4$ (0.5 mM), TCEP (0.5 mM) and TBTA (0.05 mM) for 2 h at r.t. The protein was acetone precipitated to isolate the protein fraction from unreacted probe, and the resultant sample separated on 15 % SDS-PAGE. Visualization of protein activities was accomplished by rhodamine fluorescence scan. WT refers to crude wild-type treated as above in the absence of **3.22** or **3.38**. The expected position for full-length GlpG is indicated by the arrow. C) Chemical structures of β-lactam probes (***cis*-3.22** and ***trans*-3.22**), fluorophosphonate probe (**3.38**), and rhodamine azide probe (**3.39**).

Our preliminary results demonstrate concentration dependent increases in fluorescence signal for samples treated with ***cis*-3.22** and ***trans*-3.22** (Figure 3-7, lane 1-6), and we observe no fluorescence labelling in the absence of the β-lactam probes. We utilized FP-PEG-rhodamine,[73] **3.38** as a control to verify labelling and position of GlpG on the gel (Lane 8).[71] Fluorescence labelling of GlpG was detected at as low as 10 μM concentration of β-lactam probes as compared with **3.38** (0.01 μM). Despite concentration dependent inhibition of the rhomboid protease by the β-lactam probes, we observe a number of additional enzymes that were potentially targeted. The designed β-lactam probes appear to display broad specificity for other proteases in the crude membrane fraction.

To show that the β-lactam probes were specific active-site inhibitors of GlpG, we performed a heat denatured negative control for the probe treat samples (Figure 3-8). For the ***cis*-3.22** (10 μM) treated heat denatured sample, non-specific labelling is evident (lane 1 relative to 2). Alternatively, the ***trans*-3.22** (10 μM) displayed highly specific reactivity with the crude membrane extracts at the concentration employed, and was not targeted by the non-active heat denatured proteome (lane 5 relative to 6). The specificity of the β-lactams for GlpG was evaluated by comparing the labelling efficiency obtained using the wild type with that of an active-site serine knockout S201A mutant[71] (Figure 3-8, lanes 2 versus 3 and 7 versus 8). We observed labelling of both the wild type and S201A mutant, this demonstrates that ***cis*-3.22** and ***trans*-3.22** are non-specific inhibitors of residue S201 of GlpG. Had these β-lactam probes been specific for this GlpG residue, the S201A mutant would not have been labelled. However, it appears that ***trans*-3.22** did target the active site of several other active enzymes in the crude membrane extract. The fluorescently tagged proteins will be separated by two-dimensional gel electrophoresis and will be identified by LC-MS/MS.

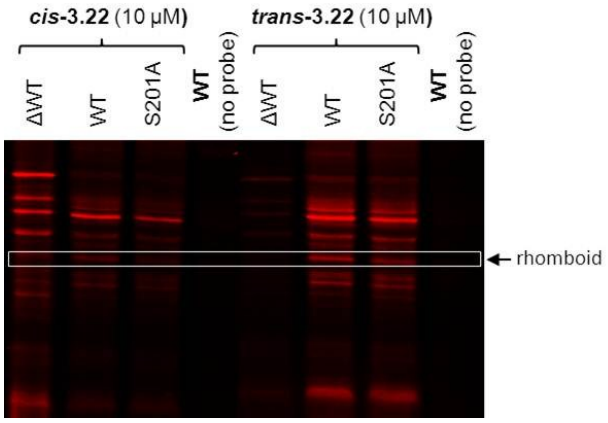

Figure 3-8. Activity-based protein profiling of wild type and mutant GlpG rhomboid protease from crude membrane extracts using β-lactam probes and fluorescent labelling via bioorthogonal CuAAC reaction. ΔWT refers to a crude wild-type that was heat-denatured at 100 °C for 10 min.

The FP-PEG-rhodamine probe will be used in competitive ABPP assays to screen for more potent/selective β-lactam inhibitors that are proposed in the future directions. Identification of new and more selective rhomboid inhibitors not only has a medical relevance in drug development against pathogens, but could also be used to speed progress in uncovering the biological roles of these intramembrane proteases.

Future Directions

Modifications to the β-lactam probes to increase their affinity for the GlpG rhomboid protease will be pursued. The first modification would be to remove the aryl ring at C-3, in accord with the SAR done previously by Pierrat *et al.*[65] According to Scheme 3-8, β-lactam (**3.40**) can be prepared by 1,3-dipolar cycloaddition of **3.27** with ethynyltrimethylsilane (**3.41**), and subsequent desilylative fragmentation of TMS-isoxazoline (**3.42**) with TBAF yields the C-3 non-substituted β-lactam (**3.43**). The alkyne reporter tag in **3.40** can be installed through amide coupling between **3.43** with **3.37**, similar to that done previously during the synthesis of **3.22**.

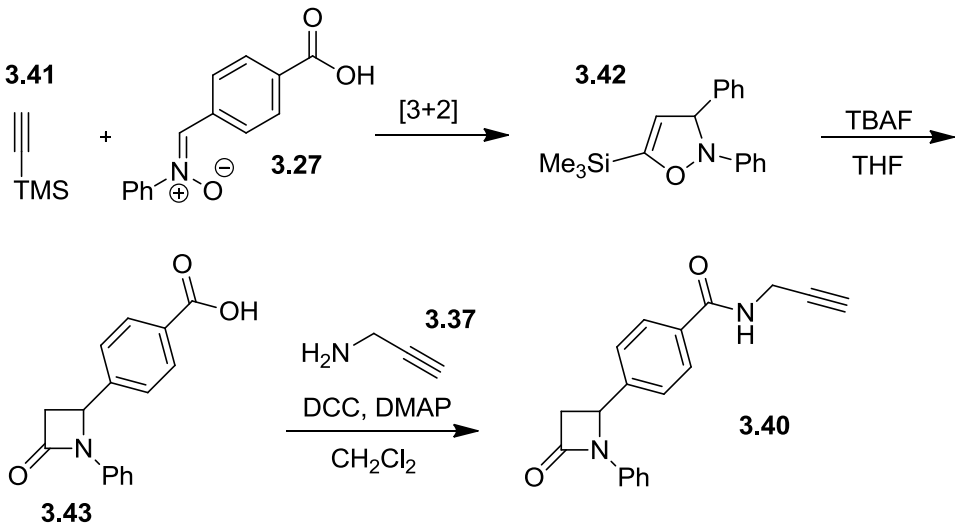

Scheme 3-8. Synthesis of β-lactams probes containing no substitution at C-3.

We also intend to apply probes ***cis*-3.22** and ***trans*-3.22** for *in vivo* ABPP of other systems such as Hepatitis C virus (HCV). Since HCV relies on many interactions with host cell proteins for propagation, and successful HCV infection requires enzymatic activity of host cell enzymes for key posttranslational modifications. These β-lactam activity-based probes will be used in comparative ABPP experiments to identify previously unidentified active-enzymes that are differentially regulated in HCV-infected relative to non-infected liver proteomes.

Conclusions

The synthesis of β-lactam activity-based probes via the Kinugasa reaction has been described. The Kinugasa reaction offered an efficient, and atom economical method for constructing the β-lactam core structure. It was found that the conditions required for installing an ether linkage between the β-lactam and alkyne tag proved problematic and resulted in ring opening of the β-lactam **3.21**. An amide bond forming reaction proved to be a simple and efficient approach for installing the alkyne handle in **3.22**. Preliminary ABPP

experiments on crude membrane fractions containing the GlpG rhomboid demonstrate concentration dependent inhibition of rhomboid proteases *in vitro*. However, β-lactam **3.22** shows low specificity for GlpG. Future efforts are directed toward designing β-lactam probes that display greater affinity for GlpG, and we intend to apply these probes to other systems of interest aswell.

Acknowledgements

Kathrine Bisgaard and Dr. Robert Faragher are acknowledged for fruitful discussions regarding probe synthesis. Dr. Allison Sherratt is thanked for offering background knowledge and expertise related to rhomboid proteases and performing the preliminary ABPP experiments.

Materials and Methods

General

All chemical reagents were purchased from commercial suppliers and used without further purification. Reactions were monitored by thin layer chromatography (TLC) pre-coated silica gel glass plates (60 Å, F_{254}, layer thickness 250μm), using UV light and potassium permanganate stain to visualize the course of reaction. For flash column chromatography technical grade solvents were used, and chromatographic purification was performed using silica gel (60 Å, particle size 40–63 μm). ^{1}H NMR and ^{13}C NMR spectra were recorded using a Bruker-DRX-400 spectrometer using a frequency of 400.13 MHz for ^{1}H and 100.61 MHz for ^{13}C and processed using Bruker TOPSPIN 2.1 software. Chemical shifts are reported in parts per million (δ) using residual $CHCl_3$ resonance as an internal reference (7.26 and 77.0 ppm for ^{1}H and ^{13}C NMR, respectively). The following abbreviations were used to designate chemical shift multiplicities: s = singlet, d = doublet, t = triplet, m = multiplet or unresolved, br = broad signal and J = coupling constants in Hz.

Synthetic Procedures and Characterization Data:

***tert*-butyl-(4-diethoxymethyl-benzyloxy)-dimethyl-silane (3.30):**

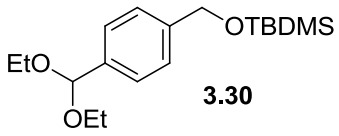

3.30

Triethylamine (1.2 mL, 12.2 mmol), DMAP (0.68g, 5.6 mmol) and tert-butyldimethylsilyl chloride (1.84 g, 12.2 mmol) were added to a stirred solution of 4-(diethoxymethyl)-benzenemethanol,[67] (2.0 g, 9.5 mmol) dissolved in CH_2Cl_2 (40 mL). The reaction mixture was stirred at r.t. for 4 h. Upon completion, the reaction mixture was diluted with CH_2Cl_2 (20

mL), washed with water (4 x 25 mL), and brine (50 mL). The organic phase was dried over anhydrous Na_2SO_4, filtered, and the solvent evaporated by rotary evaporation to a yellow oil. The crude product was purified by flash column chromatography (95:5/hexanes:EtOAc), affording the title compound as a colourless oil (2.2 g, 6.6 mmol, 69 %). Spectral data corresponded to that previously described in the literature.[68] **R_f** = 0.88 (70:30/hexanes:EtOAc). **^{1}H NMR ($CDCl_3$, 400 MHz)**: δ 7.44 (d, *J* = 8.2 Hz, 2H), 7.32 (d, 2H) 5.51 (s, 1H), 4.75 (s, 2H), 3.65-3.49 (m, 4H), 1.24 (t, *J* = 7.0 Hz, 6H), 0.95 (s, 9H), 0.10 (s, 6H). **^{13}C NMR ($CDCl_3$, 100 MHz)**: δ 141.5, 137.7, 126.5, 125.8, 101.4, 64.7, 60.9, 25.9, 18.4, 15.2, -5.3.

4-(*tert*-butyl-dimethyl-silanyloxymethyl)-benzaldehyde (3.31):

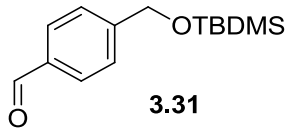

3.31

Sodium tetrakis[3,5-bis(trifluoromethyl)phenyl]borate (2.7 mg, 0.003 mmol, 0.001 equiv.) was added to a stirred suspension of **3.30** (990 mg, 3 mmol, 1 equiv.) in H_2O (6 mL). The reaction was stirred at r.t. for 5 min. Upon completion, the mixture was extracted with DCM (3 x 5 mL), the combined organic phases were dried over anhydrous $MgSO_4$, filtered, and concentrated *in vacuo*. The crude oil was purified by silica gel chromatography (95:5/hexanes:EtOAc). **3.31** was obtained as a colourless oil (716 mg, 2.86 mmol, 95 %). Spectral data corresponded to that previously described in the literature.[74] **R_f** = 0.50 (90:10/hexanes:EtOAc). **^{1}H NMR ($CDCl_3$, 400 MHz)**: δ 9.99 (s, 1H), 7.85 (d, *J* = 8.2 Hz, 2H), 7.48 (d, *J* = 8.0 Hz, 2H), 4.81 (s, 2H), 0.95 (s, 9H), 0.11 (s, 6H). **^{13}C NMR ($CDCl_3$, 100 MHz)**: δ 192.0 (CH), 148.6 (C), 135.3 (C), 129.8 (CH), 126.2 (CH), 64.4 (CH_2), 25.9 (CH_3), 18.3 (C), –5.4 (CH_3).

***N*-(4-((*tert*-butyldiphenylsilyloxy)methyl)benzylidene)benzenamine oxide (3.25):**

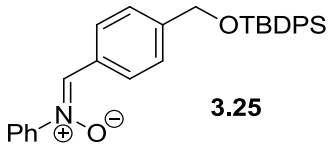

3.25

To a solution of SDS (0.288 g, 1 mmol) in H_2O (10 mL) was added aldehyde **3.25** (600 mg, 2.4 mmol, 1.0 equiv.) and *N*-phenyl hydroxyl amine[75] (314 mg, 2.9 mmol, 1.2 equiv.). The reaction was stirred for 30 min. The reaction mixture was diluted with brine (10 mL) and extracted with EtOAc (3 x 10 mL). The organic phases were dried over anhydrous $MgSO_4$, filtered, and concentrated *in vacuo*. The crude was purified by silica gel column chromatography (70 : 30 / Hexanes : EtOAc) affording **3.25** as pale brown solid (650 mg, 1.90 mmol, 79 %). $\mathbf{R_f}$ = 0.26 (75 : 25 / Hexanes : EtOAc) **^{1}H NMR ($CDCl_3$, 400 MHz)**: δ.8.37 (d, 2H), 7.90 (s, 1H), 7.76-7.74 (m, 2H), 7.46-7.42 (m, 5H), 4.79 (s, 2H), 0.96 (s, 9H), 0.11 (s, 6H). **^{13}C NMR ($CDCl_3$, 100 MHz)**: δ 148.9 (C), 144.6 (C), 134.6 (CH), 131.5 (CH),129.7 (CH), 129.5 (CH), 129.2 (C), 129.0 (CH), 129.0 (CH), 128.7 (CH), 128.6 (CH), 125.9 (CH), 122.2 (CH), 121.6 (CH), 64.6 (CH_2), 25.8 (CH), 18.3 (C), -5.4 (CH). **LRMS**: calculated for $C_{20}H_{28}NO_2Si$ (M^+) 342.2; Found: 342.2.

***N*-(4-(hydroxymethyl)benzylidene)benzenamine oxide (3.34):**

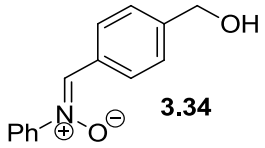

3.34

A solution of 4-(hydroxymethyl)-Benzaldehyde,[69] **3.33** (184 mg, 0.74 mmol) and *N*-phenyl hydroxyl amine (162 mg, 0.89 mmol) dissolved in 0.1M sodium dodecyl sulfate (4 mL), was sonicated for 5 min, then allowed to stir at r.t. for 1 hr. Upon completion, the reaction was diluted with H_2O (5 mL), and extracted with EtOAc (3 x 5 mL). The combined organic

phases were dried over anhydrous $MgSO_4$, filtered, and concentrated *in vacuo*. The crude was purified by silica gel column chromatography eluting 6:4/hexanes:EtOAc to 100 % EtOAc. The title compound was obtained as an off-white solid (150 mg, 0.66 mmol, 89 %). **R_f** = 0.48 (EtOAc). **^{1}H NMR ($CDCl_3$, 400 MHz)**: 8.27 (d, 2H), 7.88 (s, 1H), 7.73 (m, 2H), 7.46-7.37 (m, 5H), 4.67 (s, 2H), 3.28 (br s, 1H). **^{13}C NMR ($CDCl_3$, 100 MHz)**: δ 148.7 (C), 144.8 (C), 135.1 (CH), 129.9 (CH), 129.3 (CH), 129.3 (CH), 129.2 (CH), 126.7 (CH), 121.6 (CH), 64.5 (CH_2). **LRMS**: Calculated for $C_{14}H_{14}NO_2$ (M^+) 228.1, Found 228.2.

***N*-(4-carboxybenzylidene)benzenamine oxide (3.27):**

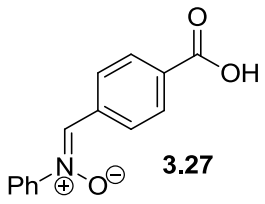

3.27

4-carboxybenzaldehyde (450.4 mg, 3 mmol) and *N*-phenyl hydroxyl amine[75] (360.0 mg, 3.3 mmol) suspended in anhydrous EtOH (4.3 mL). The reaction was heated to reflux for 5 min, then was stirred at r.t. for 30 min. The resultant precipitate was filtered, washed with copious amounts of EtOH, dried under high vacuum. The title compound was obtained as a pale-yellow crystalline solid (517.7 mg, 2.15 mmol, 72 %). Spectral data corresponded to that previously described in the literature.[76] **R_f** = 0.38 (90:10/CH_2Cl_2:CH_3OH). **^{1}H NMR (DMSO-d_6, 400 MHz)**: δ 13.13 (br s, 1H), 8.63 (s, 1H), 5.56 (d, *J* = 8.4 Hz, 2 H), 8.05 (d, *J* = 8.4 Hz, 2H), 7.93 (dd, *J* = 8.1, 2.1 Hz, 2H), 7.60-7.53 (m, 3H). **^{13}C NMR (DMSO-d_6, 100 MHz)**: δ 166.8 (C), 148.5 (C), 134.8 (CH), 133.0 (CH), 131.8 (C), 130.2 (CH), 129.4 (CH), 129.2 (CH), 128.6 (CH), 121.6 (CH). **LRMS**: Calculated for $C_{14}H_{12}NO_3$ (M^+) 225.1; Found 225.2.

General Procedure for Micelle-Promoted Kinugasa Reactions in Aqueous Media:

To a solution of SDS (288 mg, 1 mmol) in H_2O (10 mL), was added (+)-sodium-(*L*)-ascorbate (475 mg, 2.4 mmol), $CuSO_4 \cdot 5H_2O$ (300 mg, 1.2 mmol), pyridine (775 μL, 9.6 mmol), ethanolamine (78 μL, 1.3 mmol) and phenyl acetylene (134 μL, 1.2 mmol). The resultant was allowed to stir at r.t. for 30 min. The mixture was cooled to 0˚C using an ice bath, and nitrone (1.46 mmol) was added. The reaction mixture was allowed to warm slowly to r.t. over 30 min, and was stirred for an additional 6 h at this temperature. Upon completion, the reaction was diluted with brine (10 mL) and extracted with EtOAc (3 x 10 mL). The combined organic phases were washed with brine (30 mL). The combined organic phases were dried over anhydrous $MgSO_4$, filtered, and concentrated *in vacuo*. The crude was pre-absorbed onto silica gel and the *cis*- and *trans*-β-lactams were purified by flash column chromatography.

***cis*-4-(4-((*tert*-butyldiphenylsilyloxy)methyl)phenyl)-1,3-diphenylazetidin-2-one (*cis*-3.23)** and ***trans*-4-(4-((tert-butyldiphenylsilyloxy)methyl)phenyl)-1,3-diphenylazetidin-2-one (*trans*-3.23):**

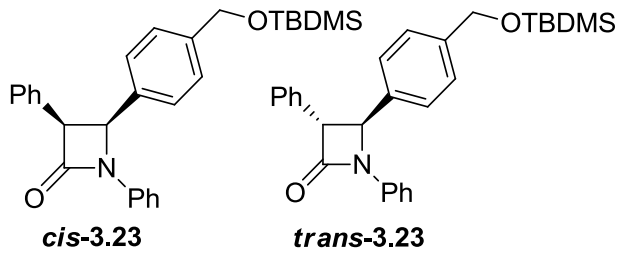

***cis*-3.23** ***trans*-3.23**

(1.4:1)
mixture of diastereomers

These compounds were obtained by following the general Kinugasa reaction procedure. Purified by flash column chromatography eluting 95:5 to 90:10/hexanes:EtOAc, affording the title compounds ***cis*-3.23** (184.1 mg, 0.42 mmol) and ***trans*-3.23** (135.0 mg, 0.30 mmol) as off-white solids in a combined yield of 60 %. ***cis*-3.23**: $\mathbf{R_f}$ = 0.22 (90:10/hexanes:EtOAc).

^{1}H NMR ($CDCl_3$, 400 MHz): δ 7.43 (dd, *J* = 8.6, 1.1 Hz, 2H), 7.28 (t, *J* = 7.5 Hz, 2H), 7.10-7.03 (m 10H), 5.46 (d, *J* = 6.1 Hz, 1H), 5.00 (d, *J* = 6.1 Hz, 1H), 4.60 (s, 2H), 0.90 (s, 9H), 0.01 (s, 6H). **^{13}C NMR ($CDCl_3$, 100 MHz)**: δ 165.6 (C), 141.1 (C), 137.7 (C), 132.9 (C), 132.1 (C), 129.0 (CH), 128.8 (CH), 128.0 (CH), 127.1 (CH), 127.0 (CH), 125.9 (CH), 123.9 (CH), 117.2 (CH), 64.5 (CH_2), 60.2 (CH), 60.1 (CH), 25.8 (CH), 18.3 (C), -5.3 (CH). **LRMS**: calculated for $C_{28}H_{33}NO_2Si$ [M+] 444.2; Found: 444.2. ***trans*-3.23**: **R_f** = 0.43 (90:10/hexanes:EtOAc). **^{1}H NMR ($CDCl_3$, 400 MHz)**: δ 7.40-7.25 (m, 13H), 7.07 (t, *J* = 7.4 Hz, 1H), 4.95 (d, J = 2.6 Hz, 1H), 4.76 (s, 2H), 4.27 (d, *J* = 2.5 Hz, 1H), 0.95 (s, 9H), 0.12 (s, 6H). **^{13}C NMR ($CDCl_3$, 100 MHz)**: δ 165.6 (C), 142.1 (C), 137.5 (C), 136.1 (C), 134.7 (C), 129.1 (CH), 129.0 (CH), 127.9 (CH), 127.4 (CH), 126.9 (CH), 125.8 (CH), 124.0 (CH), 117.2 (CH), 65.2 (CH), 64.5 (CH_2), 63.6 (CH), 25.9 (CH), 18.4 (C), -5.3 (CH). **LRMS**: calculated for $C_{28}H_{33}NO_2Si$ (M^+) 444.2; Found: 444.2.

***cis*-4-(4-(hydroxymethyl)phenyl)-1,3-diphenylazetidin-2-one (*cis*-3.32)** and ***trans*-4-(4-(hydroxymethyl)phenyl)-1,3-diphenylazetidin-2-one (*trans*-3.32):**

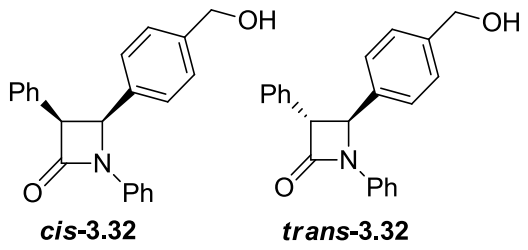

***cis*-3.32** ***trans*-3.32**

(1.3:1)
mixture of diastereomers

These compounds were prepared following the general Kinugasa reaction procedure. The crude was purified by flash column chromatography eluting 60:40/hexanes:EtOAc, affording the title compounds ***cis*-3.32** (186.2 mg, 0.57 mmol) and ***trans*-3.32** (141.0 mg, 0.43 mmol) as white solids in a combined yield of 83 %. ***cis*-3.32**: **R_f** = 0.29 (60 : 40 / Hexanes :

EtOAc).**^{1}H NMR ($CDCl_3$, 400 MHz)**: δ 7.40 (m, 2H), 7.28 (t, *J* = 7.5 Hz, 2H), 7.12-7.03 (m, 10H), 5.47 (d, *J* = 6.1 Hz, 1H), 5.01 (d, *J* = 6.1 Hz, 1H), 4.54 (s, 2H), 1.58 (br s, 1H). **^{13}C NMR ($CDCl_3$, 100 MHz)**: δ 165.6 (C), 140.5 (C), 137.6 (C), 133.8 (C), 132.0 (C), 129.1 (CH), 128.9 (CH), 128.1 (CH), 127.4 (CH), 127.2 (CH), 126.8 (CH), 124.1 (CH), 117.2 (CH), 64.8 (CH_2), 60.3 (CH), 60.1 (CH). **LRMS**: Calculated for $C_{22}H_{20}NO$ (M^+) 330.1, Found 330.1. ***trans*-3.32**: R_f = 0.30 (60:40/hexanes:EtOAc). **^{1}H NMR ($CDCl_3$, 400 MHz)**: δ 7.41-7.24 (m, 13H), 7.07 (t, *J* = 7.4 Hz, 1H), 4.96 (d, *J* = 2.5 Hz, 1H), 4.68 (s, 2H), 4.22 (d, *J* = 2.2 Hz, 1H), 2.28 (br s, 1H). **^{13}C NMR ($CDCl_3$, 100 MHz)**: δ 165.6 (C), 141.6 (C), 137.3 (C), 136.6 (C), 134.5 (C), 129.1 (CH), 129.0 (CH), 127.9 (CH), 127.8 (CH), 127.4 (CH), 126.0 (CH), 124.1 (CH), 117.1 (CH), 65.0 (CH), 64.6 (CH_2), 63.4 (CH). **LRMS**: Calculated for $C_{22}H_{20}NO$ (M^+) 330.1, Found 330.2.

4-((*cis*)-4-oxo-1,3-diphenylazetidin-2-yl)benzoic acid (*cis*-3.26) and **4-((*trans*)-4-oxo-1,3-diphenylazetidin-2-yl)benzoic acid (*trans*-3.26):**

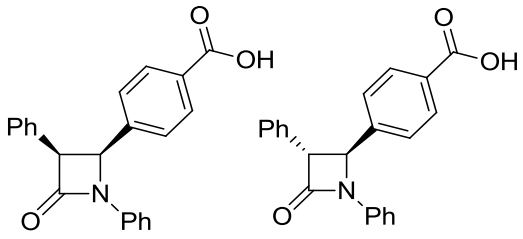

***cis*-3.26** ***trans*-3.26**

(1.3:1)
mixture of diastereomers

These compounds were prepared following the general Kinugasa reaction procedure. The crude was purified by flash column chromatography eluting 99:1/CH_2Cl_2:CH_3OH, affording the title compounds ***cis*-3.26** (102.1 mg, 0.30 mmol) and ***trans*-3.26** (79.0 mg, 0.23 mmol) as white solids in a combined yield of 44 %. ***cis*-3.26**: R_f = 0.24 on silica (98:2/CH_2Cl_2:CH_3OH). **^{1}H NMR ($CDCl_3$, 400 MHz)**: δ 7.83 (d, *J* = 8.1 Hz, 2H), 7.38 (d, *J*

= 7.9 Hz, 2H), 7.30 (t, *J* = 7.6 Hz, 2H), 7.17 (d. *J* = 8.1 Hz, 2H), 7.12-7.03 (m, 6H), 5.52 (d, *J* = 6.1 Hz, 1H), 5.07 (d, *J* = 6.1 Hz, 1H). **^{13}C NMR ($CDCl_3$, 100 MHz)**: δ 171.2 (C), 165.2 (C), 140.8 (C), 137.4 (C), 131.5 (C), 130.1 (CH), 129.2 (CH), 128.8 (CH), 128.7 (C), 128.3 (CH), 127.6 (CH), 127.3 (CH), 124.4 (CH), 117.1 (CH), 60.5 (CH), 60.0 (CH). **LRMS**: Calculated for $C_{22}H_{18}NO_3$ (M^+) 344.1, found 344.2. ***trans*-3.26**: **R_f** = 0.29 on silica (98:2/CH_2Cl_2:CH_3OH). **^{1}H NMR ($CDCl_3$, 400 MHz, 298 K, $CHCl_3$)** : δ 8.16 (d, *J* = 8.2 Hz, 2H), 7.52 (d, *J* = 8.2 Hz, 2H), 7.42-7.27 (m, 9H), 7.10 (t, *J* =7.2 Hz, 1H), 5.04 (d, *J* = 2.4Hz, 1H), 4.30 (d, *J* = 2.4 Hz, 1H). **^{13}C NMR ($CDCl_3$, 100 MHz, 298 K, $CHCl_3$)** : δ 171.2 (C), 165.2 (C), 143.6 (C), 137.1 (C), 134.2 (C), 131.3 (CH), 129.7 (C), 129.2 (CH), 129.2 (CH), 128.2 (CH), 127.5 (CH), 126.0 (CH), 124.4 (CH), 117.1 (CH), 65.1 (CH), 63.2 (CH). **LRMS**: Calculated for $C_{22}H_{18}NO_3$ (M^+) 344.1, found 344.3.

4-((*cis*)-4-oxo-1,3-diphenylazetidin-2-yl)-*N*-(prop-2-ynyl)benzamide (*cis*-3.22) and **4-((*trans*)-4-oxo-1,3-diphenylazetidin-2-yl)-*N*-(prop-2-ynyl)benzamide (*trans*-3.22):**

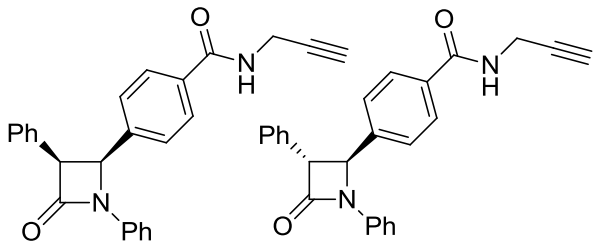

β-lactam intermediates **3.26** (98.1 mg, 0.29 mmol) were dissolved in CH_2Cl_2 (4 mL). Then added DCC (90 mg, 0.435 mmol), DMAP (17.7 mg, 0.145 mmol) and propargyl amine (22.3 μL, 0.348 mmol). The reaction was stirred at r.t. overnight. Upon completion, the reaction was filtered over a bed of celite and the solvent was evaporated. The crude reaction was diluted with CH_2Cl_2 (5 mL), washed with H_2O (5 mL), then extracted with CH_2Cl_2 (2 x 5

mL). The combined organic phases were dried over anhydrous $MgSO_4$, filtered, and concentrated *in vacuo*. The residue was purified by flash column chromatography eluting 65:35/hexanes:EtOAc. The title compounds ***cis*-3.22** (44.8 mg, 0.12 mmol) and ***trans*-3.22** (34.0 mg, 0.09 mmol) as white solids in a combined yield of 73 %. ***cis*-3.22**: $\mathbf{R_f}$ = 0.17 (65:35/hexanes:EtOAc). **^{1}H NMR ($CDCl_3$, 400 MHz)**: δ 7.54 (d, *J* = 8.2 Hz, 2H), 7.36 (d, *J* = 5.6 Hz, 2H), 7.28 (t, *J* = 7.5 Hz, 2H), 7.15 (d, *J* = 8.2 Hz, 2H), 7.11-7.03 (6H, m), 6.18 (br s, 1H), 5.49 (d, *J* = 6.2 Hz, 1H), 5.05 (d, *J* = 6.2 Hz, 1H), 4.16 (dd, *J* = 5.2, 2.5 Hz, 2H), 2.24 (t, *J* = 2.5 Hz, 1H).**^{13}C NMR ($CDCl_3$, 100 MHz)**: δ 166.3 (C), 165.3 (C), 138.6 (C), 137.4 (C), 133.1 (C), 131.6 (C), 129.2 (CH), 128.8 (CH), 128.3 (CH), 127.5 (CH), 127.4 (CH), 127.1 (CH), 124.3 (CH), 117.1 (CH), 79.3 (CH), 71.9 (CH), 60.4 (CH), 59.9 (CH), 29.7 (CH_2). **LRMS**: Calculated for $C_{25}H_{21}N_2O_2$ (M^+) 381.2, Found 381.2. ***trans*-3.12**: $\mathbf{R_f}$ = 0.28 (65:35/hexanes:EtOAc).**^{1}H NMR ($CDCl_3$, 400 MHz)**: δ 7.82 (d, *J* = 8.3 Hz, 2H), 7.47 (d, *J* = 8.2 Hz, 2H), 7.41-7.25 (m, 11H), 7.08 (t, *J* = 7.2 Hz, 1H), 6.36 (t, *J* = 4.8 Hz, 1H), 4.99 (d, *J* = 2.5 Hz, 1H), 4.26-4.25 (m 2H), 4.24 (d, *J* = 2.5 Hz, 1H), 2.28 (t, *J* = 2.5 Hz, 1H).**^{13}C NMR ($CDCl_3$, 100 MHz)**: δ 166.4 (C), 165.2 (C), 141.4 (C), 137.2 (C), 134.2 (C), 134.2 (C), 129.2 (CH), 129.1 (CH), 128.1 (CH), 127.4 (CH), 126.2 (CH), 124.3 (CH), 117.1 (CH), 79.2 (CH), 72.0 (CH), 65.2 (CH), 63.2 (CH), 30.3 (CH_2). **LRMS**: Calculated for $C_{25}H_{21}N_2O_2$ (M^+) 381.2, Found 381.2.

β-lactam Probe Labelling of Active Rhomboid in Crude Membrane Extracts:

Wild type or mutant (S203A) crude membrane extracts in 50 mM HEPES pH 7.3, 1% dodecyl maltoside (DDM, 40 μg total protein at 1 mg/mL), 200 mM NaCl, 10% glycerol and 100 μM EDTA 1% prepared as described previously,[71] was incubated the with β-lactam probes ***cis*-3.22** (0.1, 1, 10 μM), ***trans*-3.22** (0.1, 1, 10 μM), or **3.38** (0.01 μM), for 1 h at 37

˚C. The alkyne labelled proteome was reacted with **3.39** (100 μM) in the presence of $CuSO_4$ (0.5 mM), TCEP (0.5 mM) and TBTA (0.05 mM) for 2 h at r.t. Upon completion, the reaction was quenched by precipitating the proteome with five volumes of ice-cold acetone to remove unreacted probe. The precipitated protein samples were subjected to SDS-PAGE separation on a 15 % gel (1.5 mm thickness) at 100 V. The gels were scanned for fluorescence using the FMBIO III (Hitachi Solutions Ltd, Tsurumi-ku Yokohama, Japan) to visualize the active protein.

References

(1) *Chemistry and Biology of β-Lactam Antibiotics*; Morin, R. B.; Gorman, M., Eds.; Academic Press: New York, 1982.

(2) *Comprehensive Heterocyclic Chemistry II*; Katritzky, A. R., Rees, C. W., Schriven, E. F. V., Eds.; Permagon: New York, 1996; Chapter 1.18-1.20.

(3) Walsh, C. T. *Antibiotics: Actions, Origins, Resistance*; ASM Press: Washington, DC, 2003.

(4) Waxman, D. J.; Strominger, J. L. *Annu. Rev. Biochem.* **1983**, *52*, 825-869.

(5) Böttcher, T.; Sieber, S. A. *Med. Chem. Commun.* **2012**, *3*, 408-417.

(6) Imtiaz, U.; Billings, E.; Knox, J. R.; Manavathu, E. K.; Lerner, S. A.; Mobashery, S. *J. Am. Chem. Soc.* **1993**, *115*, 4435-4442.

(7) Page, M. I.; Proctor, P. *J. Am. Chem. Soc.* **1984**, *106*, 3820-3825.

(8) Fisher, J. F.; Meroueh, S. O.; Mobashery, S. *Chem. Rev.* **2005**, *105*, 395-424.

(9) Danelon, G. O.; Laborde, M.; Mascaretti, O. A.; Boggio, S. B.; Roveri, O. A. *Bioorg. Med. Chem.* **1993**, *1*, 447-455.

(10) Bonneau, P. R.; Hasani, F.; Plouffe, C.; Malenfant, E.; LaPlante, S. R.; Guse, I.; Ogilvie, W. W.; Plante, R.; Davidson, W. C.; Hopkins, J. L.; Morelock, M. M.; Cordingley, M. G.; Déziel, R. *J. Am. Chem. Soc.* **1999**, *121*, 2965-2973.

(11) Singh, P.; Williams, S. A.; Shah, M. H.; Lectka, T.; Pritchard, G. J.; Isaacs, J. T.; Denmeade, S. R. *Proteins Struct. Funct. Bioinf.* **2008**, *70*, 1416-1428.

(12) Han, W. T.; Trehan, A. K.; Kim Wright, J. J.; Federici, M. E.; Seiler, S. M.; Meanwell, N. A. *Bioorg. Med. Chem.* **1995**, *3*, 1123-1143.

(13) Wilmouth, R. C.; Westwood, N. J.; Anderson, K.; Brownlee, W.; Claridge, T. D. W.; Clifton, I. J.; Pritchard, G. J.; Aplin, R. T.; Schofield, C. J. *Biochemistry* **1998**, *37*, 17506-17513.

(14) Zhang, W.; Richardson, R. D.; Chamni, S.; Smith, J. W.; Romo, D. *Bioorg. Med. Chem. Lett.* **2008**, *18*, 2491-2494.

(15) Bays, H. E.; Moore, P. B.; Drehobl, M. A.; Rosenblatt, S.; Toth, P. D.; Dujovne, C. A.; Knopp, R. H.; Lipka, L. J.; LeBeaut, A. P.; Yang, B.; Mellars, L. E.; Cuffie-Jackson, C.; Veltri, E. P. *Clin. Ther.* **2001**, *23*, 1209-1230.

(16) Burnett, D. A.; Caplen, M. A.; Davis, H. R.; Burrier, R. E.; Clader, J. W. *J. Med. Chem.* **1994**, *37*, 1733-1736.

(17) Chen, L.-Y.; Zaks, A.; Chackalamannil, S.; Dugar, S. *J. Org. Chem.* **1996**, *61*, 8341-8343.

(18) Clader, J. W. *J. Med. Chem.* **2003**, *47*, 1-9.

(19) Dugar, S.; Clader, J. W.; Chan, T.-M.; Davis, H. *J. Med. Chem.* **1995**, *38*, 4875-4877.

(20) Ghosal, A.; Zbaida, S.; Chowdhury, S. K.; Iannucci, R. M.; Feng, W.; Alton, K. B.; Patrick, J. E.; Davis, H. R. Pat. Appl. WO 2002/050090A1, 2002.

(21) Knopp, R. H.; Gitter, H.; Truitt, T.; Bays, H.; Manion, C. V.; Lipka, L. J.; LeBeaut, A. P.; Suresh, R.; Yang, B.; Veltri, E. P. *Eur. Heart J.* **2003**, *24*, 729-741.

(22) Keri, R. S.; Hosamani, K. M.; Reddy, H. S.; Shingalapur, R. V. *Arch. Pharm.* **2010**, *343*, 237-247.

(23) Aslanian, R. G.; Bennett, C. E.; Burnett, D. A.; Chan, T.-Y.; Kiselgof, E. Y.; Knutson, C. E.; Harris, J. M.; McKittrick, B. A.; Palani, A.; Smith, E. M.; Vaccaro, H. M.; Xiao, D.; Kim, H. M. Pat. Appl. WO 2008/033464A2, 2008.

(24) Banik, I.; Becker, F. F.; Banik, B. K. *J. Med. Chem.* **2002**, *46*, 12-15.
(25) Meegan, M. J.; Carr, M.; Knox, A. J. S.; Zisterer, D. M.; Lloyd, D. G. *J. Enz. Inhib. Med. Chem.* **2008**, *23*, 668-685.
(26) Michalak, M.; Stodulski, M.; Stecko, S.; Mames, A.; Panfil, I.; Soluch, M.; Furman, B.; Chmielewski, M. *J. Org. Chem.* **2011**, *76*, 6931-6936.
(27) Michalak, M.; Stodulski, M.; Stecko, S.; Woźnica, M.; Staszewska-Krajewska, O.; Kalicki, P.; Furman, B.; Frelek, J.; Chmielewski, M. *Tetrahedron* **2012**, *68*, 10806-10817.
(28) Livermore, D. M. *J. Antimicrob. Chemother.* **1987**, *19*, 733-742.
(29) Preston, D. A.; Wu, C. Y.; Blaszczak, L. C.; Seitz, D. E.; Halligan, N. G. *Antimicrob. Agents Chemother.* **1990**, *34*, 718-721.
(30) Galleni, M.; Lakaye, B.; Lepage, S.; Jamin, M.; Thamm, I.; Joris, B.; Frère, J. M. *Biochem. J.* **1993**, *291*, 19-21.
(31) Zhao, G.; Meier, T. I.; Kahl, S. D.; Gee, K. R.; Blaszczak, L. C. *Antimicrob. Agents Chemother.* **1999**, *43*, 1124-1128.
(32) Staub, I.; Sieber, S. A. *J. Am. Chem. Soc.* **2008**, *130*, 13400-13409.
(33) Pandey, A.; Mann, M. *Nature* **2000**, *405*, 837-846.
(34) Ansorge, W. J. *New Biotechnol.* **2009**, *25*, 195-203.
(35) Harrington, C. A.; Rosenow, C.; Retief, J. *Curr. Opin. Microbiol.* **2000**, *3*, 285-291.
(36) Aebersold, R.; Mann, M. *Nature* **2003**, *422*, 198-207.
(37) Fournier, M. L.; Gilmore, J. M.; Martin-Brown, S. A.; Washburn, M. P. *Chem. Rev.* **2007**, *107*, 3654-3686.
(38) Walsh, C. T.; Garneau-Tsodikova, S.; Gatto, G. J. *Angew. Chem., Int. Ed.* **2005**, *44*, 7342-7372.
(39) Böttcher, T.; Pitscheider, M.; Sieber, S. A. *Angew. Chem., Int. Ed.* **2010**, *49*, 2680-2698.
(40) Cravatt, B. F.; Wright, A. T.; Kozarich, J. W. *Annu. Rev. Biochem.* **2008**, *77*, 383-414.
(41) Evans, M. J.; Cravatt, B. F. *Chem. Rev.* **2006**, *106*, 3279-3301.
(42) Fonovic, M.; Bogyo, M. *Expert Rev. Proteomics* **2008**, *5*, 721-730.
(43) Blais, D. R.; Nasheri, N.; McKay, C. S.; Legault, M. C. B.; Pezacki, J. P. *Trends Biotechnol.* **2012**, *30*, 89-99.
(44) Puri, A. W.; Bogyo, M. *ACS Chem. Biol.* **2009**, *4*, 603-616.
(45) Uttamchandani, M.; Li, J.; Sun, H.; Yao, S. Q. *ChemBioChem* **2008**, *9*, 667-675.
(46) Rostovtsev, V. V.; Green, L. G.; Fokin, V. V.; Sharpless, K. B. *Angew. Chem. Int. Ed.* **2002**, *41*, 2596-2599.
(47) Speers, A. E.; Cravatt, B. F. *Chem. Biol.* **2004**, *11*, 535-546.
(48) Tornøe, C. W.; Christensen, C.; Meldal, M. *J. Org. Chem.* **2002**, *67*, 3057-3064.
(49) Staub, I.; Sieber, S. A. *J. Am. Chem. Soc.* **2009**, *131*, 6271-6276.
(50) Pinho, M. G.; de Lencastre, H.; Tomasz, A. *Proc. Natl. Acad. Sci. U. S. A.* **2001**, *98*, 10886-10891.
(51) Niemeyer, D. M.; Pucci, M. J.; Thanassi, J. A.; Sharma, V. K.; Archer, G. L. *J. Bacteriol.* **1996**, *178*, 5464-71.
(52) Brown, M. S.; Ye, J.; Rawson, R. B.; Goldstein, J. L. *Cell* **2000**, *100*, 391-398.
(53) Koonin, E.; Makarova, K.; Rogozin, I.; Davidovic, L.; Letellier, M.-C.; Pellegrini, L. *Genome Biol.* **2003**, *4*, R19.
(54) Lee, J. R.; Urban, S.; Garvey, C. F.; Freeman, M. *Cell* **2001**, *107*, 161-171.

(55) Urban, S.; Lee, J. R.; Freeman, M. *Cell* **2001**, *107*, 173-182.
(56) Urban, S.; Lee, J. R.; Freeman, M. *EMBO J* **2002**, *21*, 4277-4286.
(57) Herlan, M.; Vogel, F.; Bornhövd, C.; Neupert, W.; Reichert, A. S. *J. Biol. Chem.* **2003**, *278*, 27781-27788.
(58) McQuibban, G. A.; Lee, J. R.; Zheng, L.; Juusola, M.; Freeman, M. *Current Biology* **2006**, *16*, 982-989.
(59) McQuibban, G. A.; Saurya, S.; Freeman, M. *Nature* **2003**, *423*, 537-541.
(60) Baker, R. P.; Wijetilaka, R.; Urban, S. *PLoS Pathog.* **2006**, *2*, e113.
(61) O'Donnell, R. A.; Hackett, F.; Howell, S. A.; Treeck, M.; Struck, N.; Krnajski, Z.; Withers-Martinez, C.; Gilberger, T. W.; Blackman, M. J. *J. Cell Biol.* **2006**, *174*, 1023-1033.
(62) Srinivasan, P.; Coppens, I.; Jacobs-Lorena, M. *PLoS Pathog.* **2009**, *5*, e1000262.
(63) Stevenson, L. G.; Strisovsky, K.; Clemmer, K. M.; Bhatt, S.; Freeman, M.; Rather, P. N. *Proc. Natl. Acad. Sci. U. S. A.* **2007**, *104*, 1003-1008.
(64) Wang, Y.; Zhang, Y.; Ha, Y. *Nature* **2006**, *444*, 179-180.
(65) Pierrat, O. A.; Strisovsky, K.; Christova, Y.; Large, J.; Ansell, K.; Bouloc, N.; Smiljanic, E.; Freeman, M. *ACS Chem. Biol.* **2011**, *6*, 325-335.
(66) Urban, S.; Wolfe, M. S. *Proc. Natl. Acad. Sci. U. S. A.* **2005**, *102*, 1883-1888.
(67) Bartholomew, G. P.; Rumi, M.; Pond, S. J. K.; Perry, J. W.; Tretiak, S.; Bazan, G. C. *J. Am. Chem. Soc.* **2004**, *126*, 11529-11542.
(68) Eash, K. J.; Pulia, M. S.; Wieland, L. C.; Mohan, R. S. *J. Org. Chem.* **2000**, *65*, 8399-8401.
(69) Pettersson, S.; Pérez-Nueno, V. I.; Mena, M. P.; Clotet, B.; Esté, J. A.; Borrell, J. I.; Teixidó, J. *ChemMedChem* **2010**, *5*, 1272-1281.
(70) Mamane, V.; Gress, T.; Krause, H.; Fürstner, A. *J. Am. Chem. Soc.* **2004**, *126*, 8654-8655.
(71) Sherratt, A. R.; Blais, D. R.; Pezacki, J. P.; Goto, N. K. *Biochemistry* **2012**, *51*, 7794-7803.
(72) Yang, P.-Y.; Liu, K.; Ngai, M. H.; Lear, M. J.; Wenk, M. R.; Yao, S. Q. *J. Am. Chem. Soc.* **2009**, *132*, 656-666.
(73) Jessani, N.; Cravatt, B. F. *Curr. Opin. Chem. Biol.* **2004**, *8*, 54-59.
(74) Chang, C.-C.; Liao, B.-S.; Liu, S.-T. *Synlett* **2007**, *2007*, 283-287.
(75) Chatterjee, A.; Maiti, D. K.; Bhattacharya, P. K. *Org. Lett.* **2003**, *5*, 3967-3969.
(76) Dooley, B. M.; Bowles, S. E.; Storr, T.; Frank, N. L. *Org. Lett.* **2007**, *9*, 4781-4783.

Chapter 4 : Alkyne Functionalized Silver Nanoparticles for SERS Imaging of Cell Surface Proteins

A significant portion of the work presented in this chapter was published in:

Kennedy, D. C.; McKay, C. S.; Tay, L.-L.; Rouleau, Y.; Pezacki, J. P. *Chem. Commun.* **2011**, *47*, 3156-3158.

Introduction

Alkynes are well known reporter groups that have been widely used in azide-alkyne cycloadditions for labelling of biomolecules *in vivo*. We have recently developed a highly efficient multicomponent Kinugasa reaction in aqueous media and have utilized this synthetic method for preparing alkyne-tethered β-lactam activity-based probes for proteomics applications. Here we describe the synthesis of alkyne-tethered β-lactam probes that can be used as contrast agents for imaging cell surface proteins using surface enhanced Raman scattering (SERS) spectroscopy.

Thiolate functionalized silver and gold plasmonic nanoparticles (NPs) have been developed for SERS microscopy in biological imaging.[1-4] SERS imaging is also emerging as a promising technique for clinical imaging and a highly sensitive multiplexed detection alternative to fluorescence imaging.[5-8] Functionalized NPs have been used in SERS imaging to detect cancer cells, and are themselves efficient labelling probes for cell surface receptors.[9-13] In parallel with other imaging techniques (e.g. two photon fluorescence (TPF), Rayleigh light scattering (RLS) and scanning electron microscopy (SEM)), SERS microscopy can give highly detailed information about protein localization at the cell surface and report on receptor aggregation.[14] Silver NPs have also been used to design novel SERS probes that can function as both diagnostic and therapeutic tools[13] or markers of enzymatic activity.[15]

One advantage of using SERS microscopy over fluorescence based methods to report on protein localization is the increased enhancement in signal that arises upon NP coupling when protein aggregation drives the targeted NP aggregation at the cell surface to form SERS hotspots.[16,17] We have shown the utility of mercaptomethylbenzyl nitrile

functionalized NPs for SERS imaging of mammalian cells surfaces.[2,14] Additionally we have adapted this same NP design to incorporate carborane molecules as potential therapeutics, transforming the NP contrast agent into a drug delivery particle as well.[13] The carborane and nitrile reporter molecules each contain unique Raman stretches (1700 and 2800 cm^{-1}, respectively) that are in the spectroscopically silent region of the cell.

Silver nanoparticles can be coated with other SERS active labels that display distinct signals. Reporter groups containing C≡N, C-D, C≡C, NO_2 or B-H have been successfully employed.[2,6,13] SERS spectra obtained from NPs coordinated to benzylthiol based ligands provide much stronger and better resolved signals than those of the analogous linear DTSP based ligand set NPs.[6] The proximity of the functional groups to the NP surface plays an important role in the strength of the observed signals.[6,18]

The Raman spectra of four commonly employed benzyl thiol reporter ligands; 4-mercaptomethyl)nitrobenzene (MMBNO, **4.1**), 4-(mercaptomethyl)ethynyl benzene (MMByne, **4.2**), mercaptomethylbenzene-d_7 (DMMB, **4.3**), and 4-(mercaptomethyl)benzonitrile (MMBN, **4.4**) are shown in Figure 4-1.[6] The Raman spectra for MMByne, DMMB, and MMBN show distinct signals in the desired region of the spectrum ranging from 1700 - 2800 cm^{-1} (Figure 4-1B). Although MMBNO lacking signals in this region, the two prominent signals arise at 1352 cm^{-1} (NO_2 symmetric stretching) and 1599 cm^{-1} (NO_2 asymmetric stretching), the former peak at 1352cm^{-1} is unique to this molecule while the latter peak at 1600 cm^{-1} overlaps with the C=C phenyl ring deformations (1570-1620 cm^{-1}) observed for all the reporter molecules.[6] Characteristic signals of the remaining SERS reporter molecules include the C≡C stretching for MMBYNE (2112 cm^{-1}), C≡N stretching for MMBN (2234 cm^{-1}), phenyl C-D bending (1047 cm^{-1}) and two diagnostic

peaks for C-D stretching (2168 and 2287 cm^{-1}) in DMMB. For each probe, the peak occurring at 2550-2580 cm^{-1} results from S-H stretching.

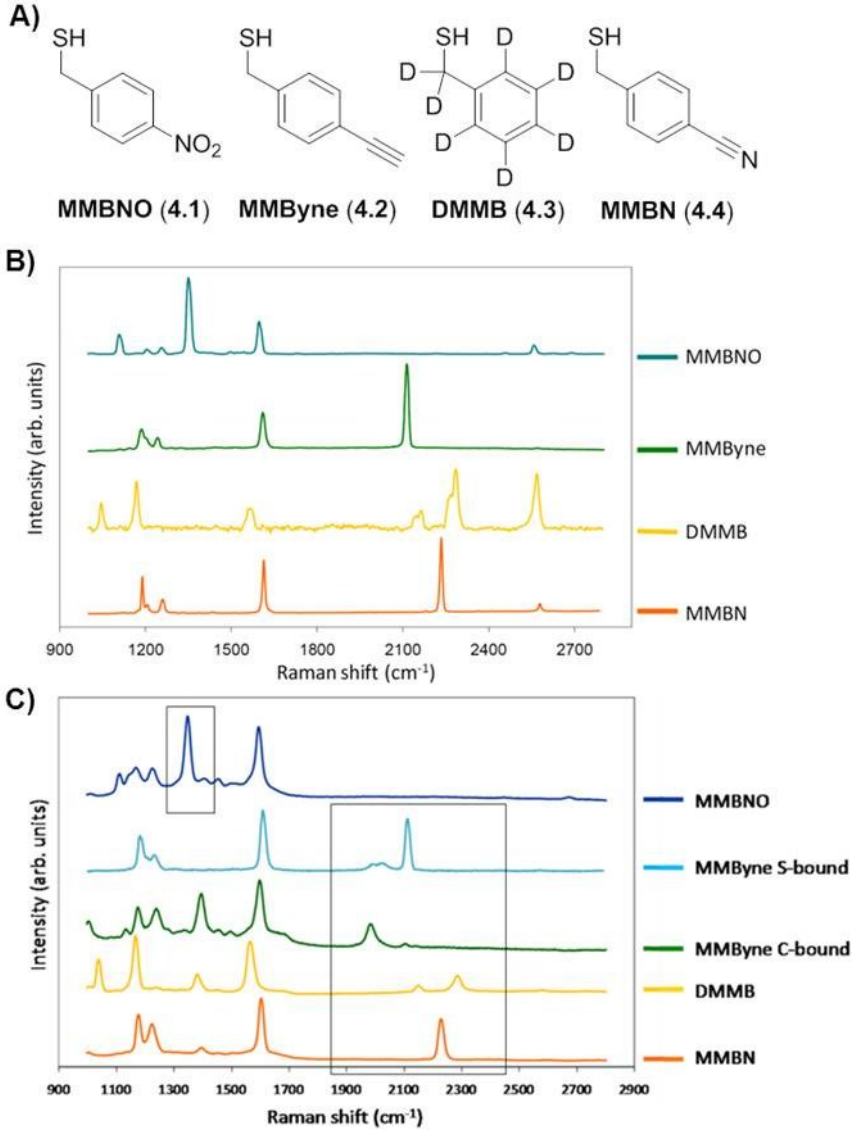

Figure 4-1. Raman reporter ligands and Ag-NPs with benzyl thiol based ligands for use in nanoparticle-based SERS imaging. A) Chemical structures of four benzyl thiol ligands. B) Raman spectra for commonly employed NPs containing C≡N, C-D, C≡C, NO_2 reporter groups. C) SERS spectra of functionalized Ag-NPs using the 4-(mercaptomethyl)benzene-derived reporter molecules. This figure was reprinted from the literature.[6]

All of these ligands (**4.1**-**4.4**) have been utilized to functionalize the surface of Ag NPs and the associated SERS spectra of the resulting NPs upon ligand binding are shown in Figure 4-1C. All benzylthiol based ligand NP SERS spectra exhibit a peak between 1160-

1180 cm^{-1} associated with the phenyl ring (in plane C-H bending), as well as two peaks between 1340-1400 cm^{-1} and 1560-1610 cm^{-1} that are associated with ring deformations. The SERS spectra of MMBNO NPs exhibit representative signals from NO_2 at 1347 cm^{-1} and 1594 cm^{-1}. However, these two peaks overlap with the phenyl ring deformation making them indistinguishable. In the case of MMBN a sharp peak resulting from C≡N stretching is observed at 2226 cm^{-1}. The SERS spectrum of MMByne NP displays a diagnostic C≡C stretch at 1983 cm^{-1} (MMByne C-bound). The shift in the C≡C mode to lower wavenumber is consistent with terminal alkyne coordination. Additionally, a small peak at 2101 cm^{-1} was also observed, suggesting that there was competition between thiol and alkyne binding to the NP.[6] The SERS spectrum of DMMB NPs showed two peaks at 2146 cm^{-1} and 2283 cm^{-1}, C-D stretching with the double peak being characteristic of deuterated compounds,[19] with both spectra resembling their corresponding non-ligated Raman spectra.

Ag NPs are synthesized and assembled using a mixed ligand coating that contains the Raman reporter molecule for imaging, a water solubilizing PEGylated thiol, and a short chain succinimide ester that can be used to bind targeting antibodies to the NP. As shown in Figure 4-2, NPs are coated with a mixture of 3,3′-dithiodipropionic acid di(*N*-hydroxysuccinimide ester) (DTSP, **4.5**), 2-(2-(2-methoxy-ethoxy)-ethoxy)-ethanethiol (EG_3SH, **4.6**), and Raman reporter ligands (**4.1**-**4.4**) in a molar ratio of 2:5:5, respectively. DTSP is readily reduced *in situ* by the NP surface to form to coordinated thiols on the NP, and provides a handle for further functionalization with targeting antibodies.[20] EG_3SH is a simple PEGylated thiol that is used to coordinate NPs to form water soluble particles.[21] The resultant particles are functionalized with antibodies and the remaining sites are blocked with bovine serum albumin (BSA). The NPs are readily used to carryout highly sensitive detection of membrane receptor proteins using SERS microscopy.

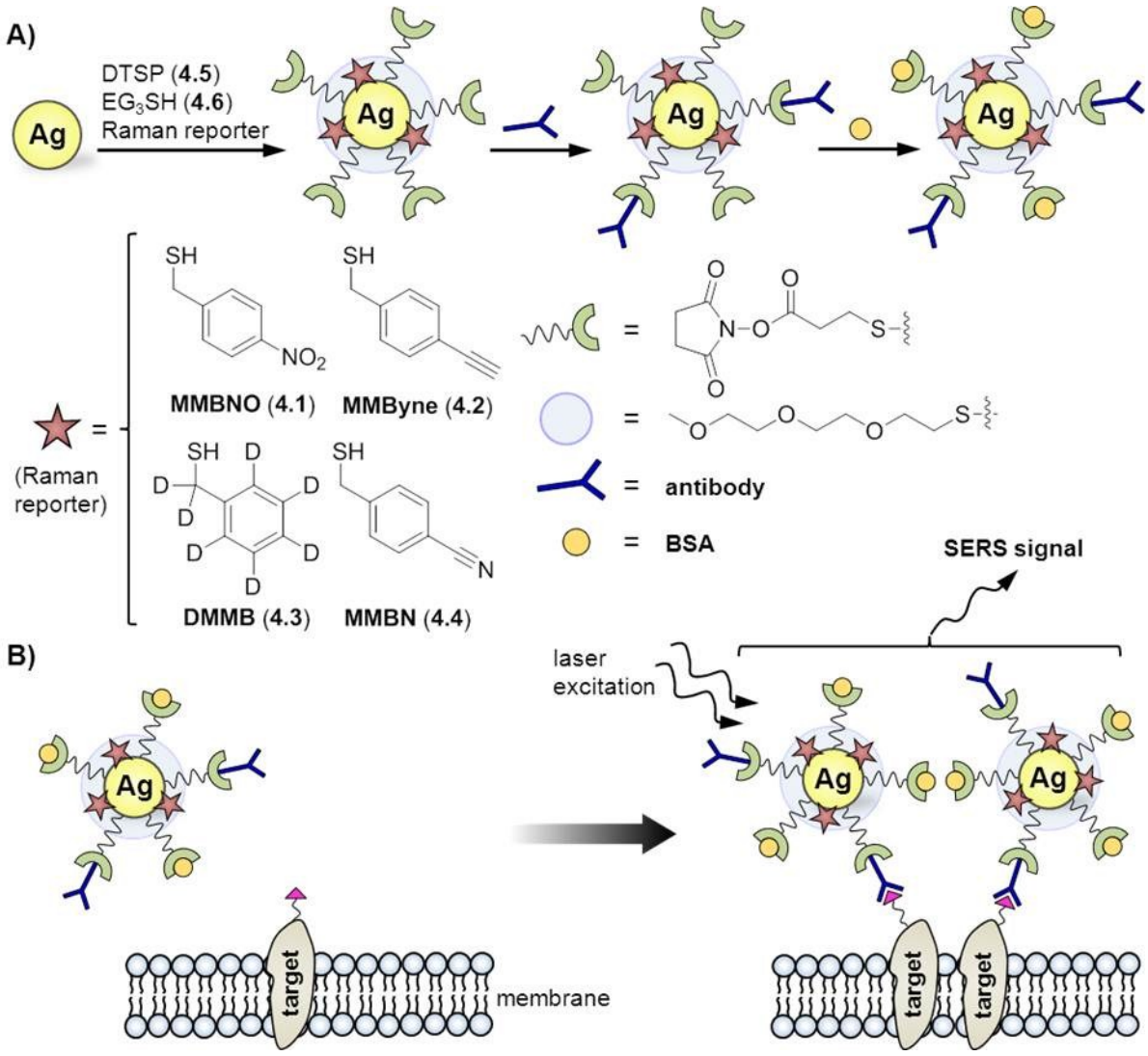

Figure 4-2. Synthesis of functionalized particles and basic premise for SERS imaging of coupled nanoparticles. Molecular structures of the functionalized silver NPs for cell surface labeling. (a) A) Schematic for synthesis of SERS active Ag NPs and structures of the ligands used to coat the nanoparticles. A colloidal Ag solution is first reacted with a mixture of DTSP, EG_3SH and Raman reporter, then is activated with an antibody, followed by blocking on the remainder of the particle with BSA. B) Particles bind to the cell surface receptors via the covalently linked antibody and are then imaged with a Raman microscope. Figure was adapted from the literature.[2]

In order for the Nanotag to be exploited in cellular imaging applications, the specific functional groups that are being studied must meet the stringent requirements of bioorthogonality. For *in vivo* imaging the ligand-NP interaction must be highly specific, non-toxic toward the host, and must not alter the biochemistry of the cell. This chapter describes

applications of micelle-promoted Kinugasa reactions for the synthesis of an alkyne functionalized β-lactam that can be used as a ligand for binding Ag NPs. The ability to display electrophilic moieties such as β-lactams on the surface of NPs presents a distinct advantage over thiolate-based ligands that are not compatible with electrophilic groups. Furthermore we show the utility of alkyne-bonded silver NPs for cell surface imaging, and present the potential for novel diagnostic and therapeutic uses.

Hypothesis

β-lactams bind NPs via alkyne tethers and provide a SERS reporting platform for imaging cell surface proteins.

Results and Discussion

Alkyne-Tethered β-Lactams as Reporter Ligands for SERS Imaging

Recently, linear terminal alkynes have been shown to coordinate Ag or Au NPs as alternatives to thiol-based ligands.[17,22,23] The energy of the Raman band for the C≡C bond shifts approximately 100 cm^{-1} to lower energy from ~2100 cm^{-1} to ~2000 cm^{-1} upon coordination to the NP.[24] Both experiment and theory indicate that the magnitude of the shift is highly dependent on the orientation of the bond.[22] Similarly, functionalization of Ag NPs with 1,4-diethynylbenzene (**4.7**) results in a similar shift in the peak for the coordinated alkyne, while that for the unbound alkyne remains unchanged.[23,25] Interestingly, Yoo and Joo have observed a second peak for the C≡C stretch resulting from coordination of 1,4-diethynylbenzene to both NPs that is shifted to higher energy to ~2200 cm^{-1}.[22,23,25] The latter peak was more prominent when they bound structurally more complex terminal alkynes such as 3-(4-(4-ethynylphenyl)-1H-1,2,3-triazol-1-yl)propan-1-ol at the NP surface.[25]

We have shown that MMByne binds to the surface of Ag NPs either via the alkyne or the thiol depending on the total ligand concentration.[6] To develop probes for biological imaging, we hypothesized that the signature C≡C stretch of phenylacetylene (**4.8**) would be shifted from 2225 cm^{-1} to ~2000 cm^{-1} upon coordination to Ag NPs, and would be unique to background interference that may arise from cellular components. The Raman spectrum of **4.8** coordinated to Ag NPs is shown in Figure 4-3.

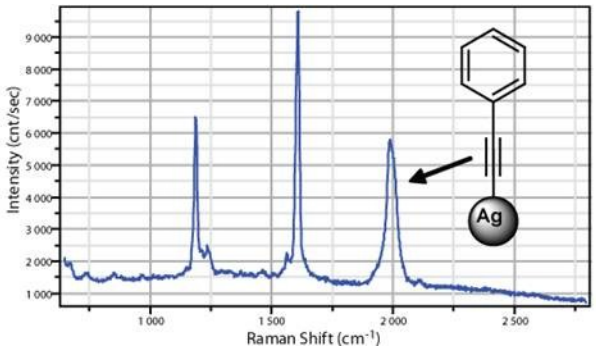

Figure 4-3. Surface enhanced Raman scattering spectrum of phenylacetylene functionalized Ag NPs. The arrow denotes the position of the coordinated alkyne peak.

Silver NPs were synthesized as previously mentioned using a mixture of ligands that included phenylacetylene, DTSP and EG_3SH to increase water solubility of the NPs.[2,3,6] For these particles, we see only a single broad peak for coordinated alkyne at 1986 cm^{-1}. This bond is highly sensitive to the surface chemistry as signal enhancement arises from atoms directly bonded to the metal surface and changes in binding modes due to a rough asymmetric surface (likely due to bridging versus axial binding modes) as is found on NPs could change the energy of the observed Raman peak.

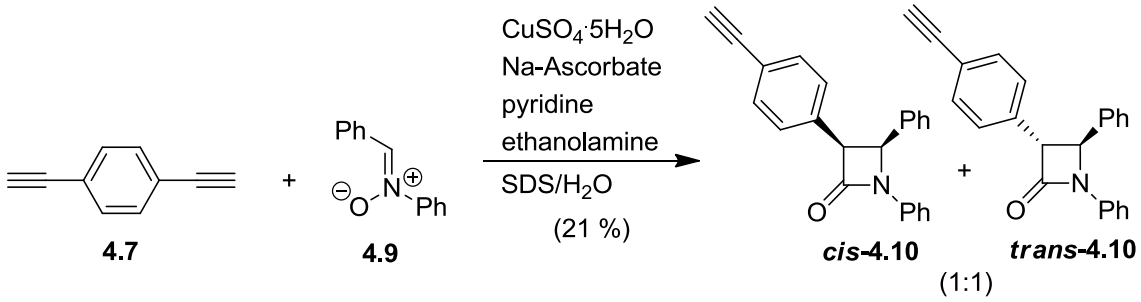

Scheme 4-1. Synthesis of alkyne tethered β-lactam ligand via the Kinugasa reaction.

In order to demonstrate the utility of alkynes as ligands to functionalize NPs, the previously developed micelle-promoted Kinugasa reaction in aqueous media[26] was used to synthesize alkyne tethered β-lactams (**4.10**) (Scheme 4-1). β-lactams are electrophilic and undergo reactions with nucleophiles such as thiols, making them not generally compatible with benzyl thiol reporter molecules. Alternatively, β-lactams are orthogonal to alkyne reporters groups, suggesting that β-lactams containing aryl alkynes would be amenable to SERS imaging. The Kinugasa reaction between 1,4-diethynylbenzene (**4.7**) and *α,N*-diphenyl nitrone (**4.9**) provided a 1:1 diastereomeric mixture of ***cis*-4.10** and ***trans*-4.10** in 21 % yield. Attempts to synthesize the analogous thiol-containing β-lactams by substituting MMByne (**4.2**) as substrate for the Kinugasa reaction with **4.9** did not provide the thiolated β-lactam products.

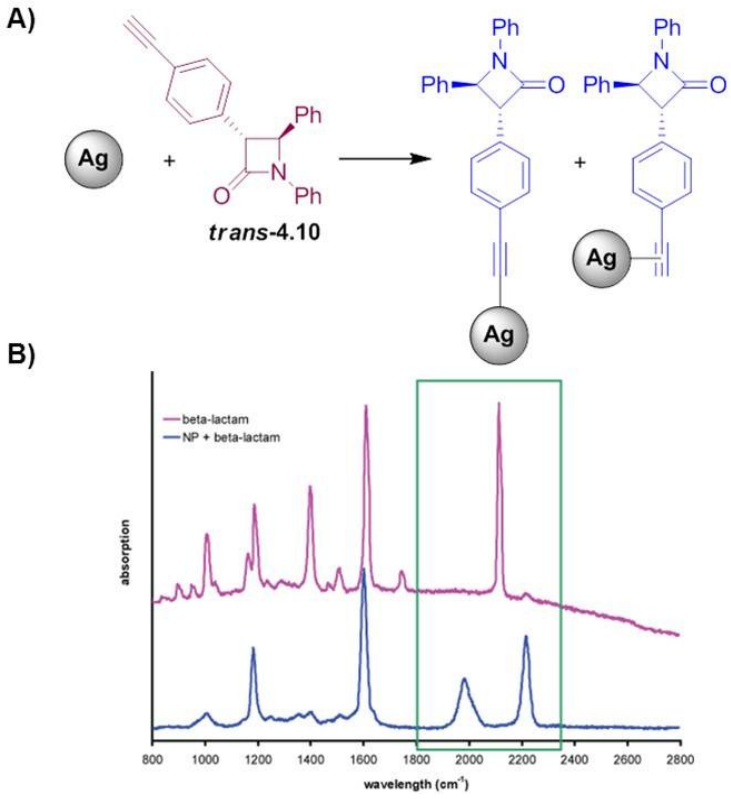

Figure 4-4. A) Functionalization of silver NPs with alkyne-labelled β-lactams. B) Raman spectrum of alkyne functionalized β-lactam and SERS spectrum of that lactam bonded to the surface of a silver NP.

The Raman spectrum for the alkyne tethered β-lactam product exhibits a C≡C stretch at 2112 cm^{-1} that is consistent with a terminal alkyne, and a C=O stretch for the β-lactam visible as a weak peak at 1749 cm^{-1}. We then functionalized silver NPs at pH 8 with the alkyne-labelled β-lactam exclusively in the absence of other ligands (Figure 4-4). The resulting NPs clearly exhibited two peaks for the alkyne at 1983 and 2214 cm^{-1} that may arise from two or more binding motifs for the molecule at the particle surface. A mixture of coordination geometries at the cell surface has been previously postulated to explain these two peaks for other multi-functional alkynes on silver surfaces.[22,23,25] The C=O peak of the β-lactam at 1749 cm^{-1} is not observed in the SERS spectrum; however, this is consistent with the SERS spectra of other β-lactams that have been previously reported.[27]

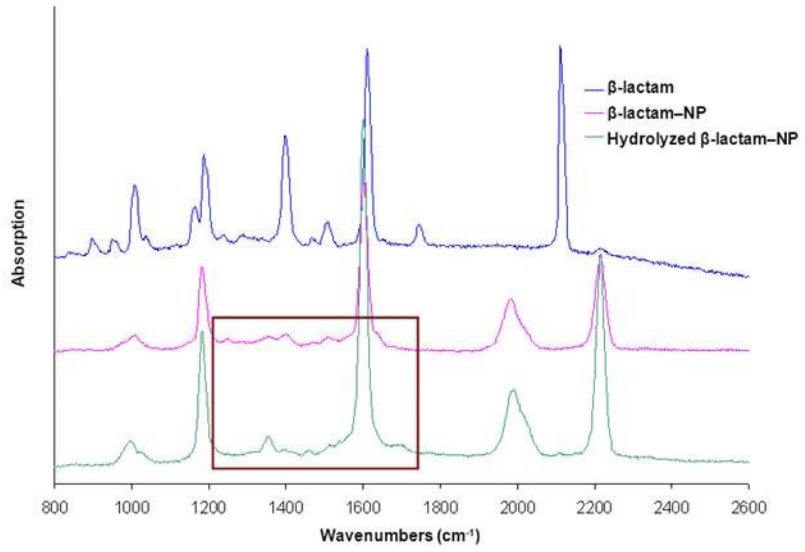

Figure 4-5. Raman spectra for alkyne tethered β-lactam (top), β-lactam bonded to the surface of a Ag NP (middle), and of particles after β-lactam hydrolysis (bottom). The inlay highlights changes that occurred following hydrolysis with NaOH.

The Kinugasa reaction offers a simple approach for developing novel alkyne-functionalized β-lactams that can be explored for biological properties. The affinities of alkynes for gold and silver surfaces make them ideal targeting molecules and probes for SERS imaging. In the absence of enhancement of the C=O peak of the β-lactam to prove that the ring structure was still intact, we hydrolyzed the bound β-lactams with dilute NaOH. The spectrum of the resulting NPs showed a number of changes between 1200 cm^{-1} and 1600 cm^{-1} as well as a small peak at 1694 cm^{-1} that is consistent with the formation of a carboxylic acid (Figure 4-5). The absence of the β-lactam C=O stretch in the β-lactam NP sample and the similarity of the spectrum with that of the hydrolyzed sample indicates that the β-lactam had been hydrolyzed during NP synthesis.

SERS Imaging of Cell Surface Proteins Using Alkyne Tethered Nanoparticles

In order to demonstrate the utility of aryl alkynes as SERS reporter molecules for cell surface labelling we prepared phenylacetylene functionalized NPs that also were

functionalized with targeting antibodies to label cell-surface receptors.[2,6,13] We have previously labelled EGFR with functionalized Ag NPs for SERS and two-photon fluorescence imaging as a possible tool for cancer detection[13] and have labelled β_2-adrenergic receptors as a target in cardiovascular disorders.[2] We have now started to explore the localization of tight junction proteins that are often down-regulated in tumor metastases and may undergo changes in localization and aggregation that accompany these changes in expression.

Occludin is an important protein for proper tight junction formation that is down regulated in a number of tumor cell types.[28,29] Greater decreases in occludin expression correspond to higher levels of metastases. Using phenylacetylene functionalized NPs we have targeted occludin (Figure 4-6) to determine how this protein is aggregated at the cell surface in human hepatoma Huh7.5 cells. In healthy primary cells, occludin is found primarily at cell–cell contacts where it co-localizes with ZO-1 and other tight junction proteins in the formation of tight junctions with neighbouring cells.[29] Using phenylacetylene-functionalized NPs co-functionalized with antibodies that target the extracellular domain for occludin, we successfully identified a subpopulation of aggregated receptors in this cell line that are not localized to tight junctions. Control experiments that lacked the targeting antibody showed no adhesion to the cells confirming that aggregation was being driven by the biological recognition of occludin.

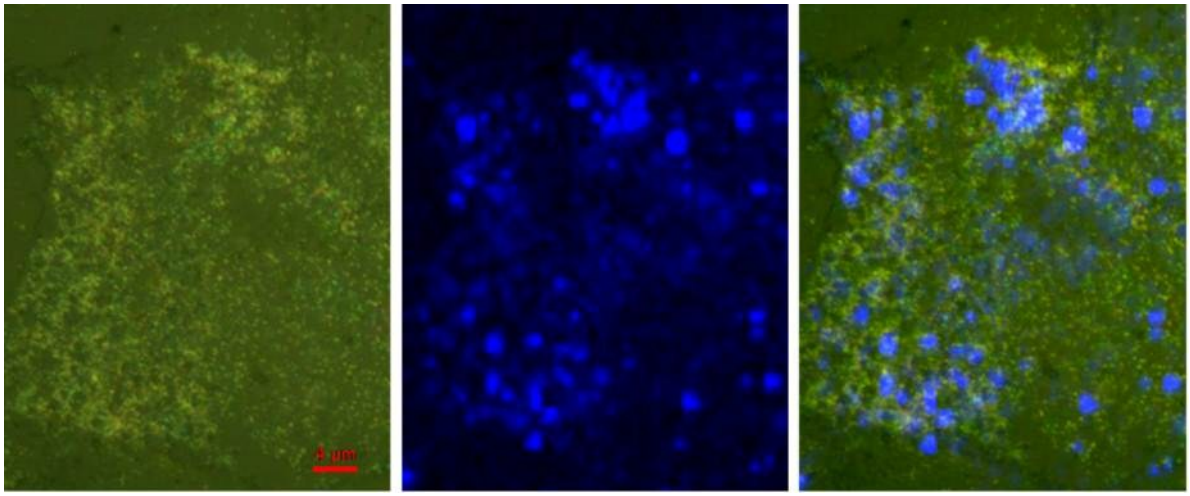

Figure 4-6. Brightfield (left) and SERS image (middle) of a cluster of Huh7.5 liver cells functionalized with phenylacetylene and targeted with anti-occludin antibodies. The overlay (right) clearly shows that hot spots exist where the NPs are clustered and that these clusters are distributed uniformly across the cell surface. Previous studies have shown that the SERS signal only arises from coupled nanoparticles[16,17] indicating that the proteins are at distances of only a few nm at most in these clusters.

Immunofluorescence staining of the intracellular C-terminus of occludin confirms that the protein does still co-localize to tight junctions in Huh7.5 human hepatoma cells.[30,31] Interestingly, the sub-population identified by extra-cellular targeting is uniformly distributed in aggregated clusters across the cell surface. A similar pattern is also observed using immunofluorescence with this antibody targeting the extracellular domain of occludin in this cell line. This suggests that the intracellular interactions of occludin may be different for this subpopulation resulting in the change in localization away from tight junctions and this different state also gives rise to the difference in labelling based on the epitope that is targeted with different antibodies.

SERS imaging reveals that the occludin proteins are clustered at the cell surface at a nano-scale in order to give rise to SERS hotspots.[15,16] The data also demonstrate that the carbon-bonded NPs are stable in mammalian cell culture experiments and are suitable for receptor protein targeting.

Future Directions

We are currently conducting detailed studies of the membrane protein occludin using multiplexed SERS imaging and multimodal imaging to monitor changes in occludin expression in conjunction with other cancer biomarkers in order to understand the importance of nanometer clustering of these proteins as well as local environment. SERS microscopy has several potential advantages over fluorescence imaging including a greater potential for multiplex imaging and a lack of photo-bleaching.

Conclusion

In summary, we have shown that carbon-bonded silver NPs are a convenient way of making NPs that display electrophilic functional groups such as β-lactams that are incompatible with thiolate ligands. Alkyne-based ligands open up new avenues for NP synthesis and allow for more diverse applications to be conducted. We also demonstrate that carbon bonded silver NPs can be used for mammalian cell labelling and give rise to strong signals from SERS of their characteristic vibrational resonances. We have shown that mixed ligand NPs containing carbon-bonded reporter ligands can be used to study the localization of the tight junction protein occludin and may offer new insight into disease progression.

Acknowledgements

Dr. David Kennedy is thanked for providing nanoparticle synthesis and Dr. Li-Lin. Tay is kindly acknowledged for performing SERS spectroscopy and microscopy.

Materials and Methods

General: All chemical reagents were purchased from Sigma-Aldrich and were used without further purification. EG_3SH was prepared according literature procedures.[32] Deuterated solvents were purchased from Cambridge Isotope laboratories. Thin layer chromatography (TLC) was carried out on Analtech Uniplate® silica gel plates (60 Å F254, layer thickness 250μm) using UV light to visualize the course of the reaction. Flash column chromatography was performed using silica gel (60 Å, particle size 40–63 μm). ^1H NMR and ^{13}C NMR spectra were obtained using a 400 MHz Bruker NMR spectrometer. Chemical shifts are reported as δ referenced to solvent and coupling constants (*J*) are reported in Hz. 2 mM solutions of DTSP in DMF and of EG_3SH in MeOH were prepared.

Synthetic Procedures and Characterization Data:

***cis*-3-(4-ethynyl-phenyl)-1,4-diphenyl-azetidin-2-one (*cis*-4.10)** and ***trans*-3-(4-ethynyl-phenyl)-1,4-diphenyl-azetidin-2-one (*trans*-4.10)**:

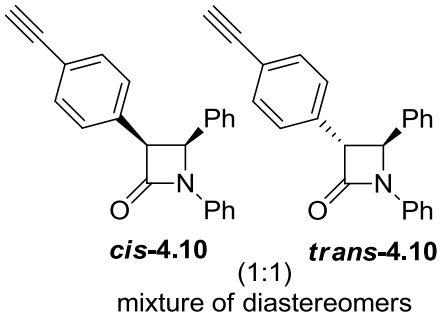

***cis*-4.10** (1:1) ***trans*-4.10**

mixture of diastereomers

A mechanically stirred solution of *α,N*-diphenyl-nitrone[34] (297.2 mg, 1.5 mmol) in SDS/H_2O (15 mL, 0.1M) was cooled to 0 ˚C and was added (+)-sodium L-ascorbate (476 mg, 2.4 mmol), $CuSO_4{\cdot}5H_2O$ (299.6 mg, 1.2 mmol), pyridine (971 μL, 12 mmol), ethanolamine (78 μL, 1.3 mmol) and 1,4-diethynyl benzene (151.4 mg, 1.2 mmol). The reaction mixture was warmed to r.t. over 30 min and was stirred for an additional 8 h. The

reaction progress was monitored by TLC (9:1/Hx:EtOAc). Upon completion, the reaction was diluted with brine (10 mL) and extracted with EtOAC (3 x 10 mL). The combined organic phases were dried over anhydrous $MgSO_4$, filtered, and concentrated *in vacuo*. The resultant residue was purified by silica gel flash column chromatography (95:5 to 90:10/Hx:EtOAc), affording ***cis*-4.10** (38 mg, 0.12 mmol) and ***trans*-4.10** (42 mg, 0.13 mmol) as off-white solids (21 %). ***cis*-4.10**: $\mathbf{R_f}$ = 0.29 (90:10/Hexanes:EtOAc). **^{1}H NMR ($CDCl_3$, 400 MHz)**: δ 7.40 (d, 2H), 7.29 (t, 2H), 7.22 (d, 2H), 7.15-7.01 (m, 8H), 5.47 (d, *J* = 6.2 Hz, 1H), 4.99 (d, *J* = 6.1 Hz, 1H), 3.00 (s, 1H). **^{13}C NMR ($CDCl_3$, 100 MHz)**: δ 165.1 (C), 137.5 (C), 134.0 (C), 133.0 (C), 131.9 (CH), 129.1 (CH), 128.8 (CH), 128.4 (CH), 128.1 (CH), 127.0 (CH), 124.2 (CH), 120.8 (C), 117.2 (CH), 83.3 (C), 60.2 (CH), 60.0 (CH). **LRMS**: Calculated for $C_{23}H_{18}NO$ (M^+) 324.1, Found 324.2. ***trans* 4.10**: $\mathbf{R_f}$ = 0.36 (90:10/Hexanes:EtOAc). **^{1}H NMR ($CDCl_3$, 400 MHz, 298 K, $CHCl_3$)**: δ 7.51 (d, 2H), 7.42-7.25 (m, 11H), 7.08 (t, 1H), 4.94 (d, *J* = 2.6 Hz, 1H), 4.29 (d, *J* = 2.6 Hz, 1H), 3.10 (s, 1H). **^{13}C NMR ($CDCl_3$, 100 MHz)**: δ 165.0 (C), 137.3 (C), 137.2 (C), 135.4 (C), 132.8 (CH), 129.4 (CH), 129.2 (CH), 128.8 (CH), 127.5 (CH), 125.9 (CH), 124.2 (CH), 121.8 (C), 117.2 (CH), 83.2 (C), 64.9 (CH), 63.6 (CH). **LRMS**: Calculated for $C_{23}H_{18}NO$ (M^+) 324.1, Found 324.1.

Synthesis of Ag Nanoparticles:

Ag NPs (~25 nm in diameter) were synthesized according to the Lee and Meisel protocol.[3] Briefly, a solution of $AgNO_3$ (50.0 ml, 1.0 mM) in 18.2 MΩ deionized water was heated to boil under reflex. A 1.0 ml of 51.0 mM sodium citrate solution was added to the boiling $AgNO_3$ solution. The colour of the solution slowly turned into grayish-yellow. The solution was refluxed for another 60 min. The Ag solution was cooled to r.t. before storage at 4 °C.

Functionalization of Nanoparticles:

To 1 mL of Ag nanoparticles (~10^{13}/mL) in a glass vial was added either (a) 1 μL of 2 mM DTSP, 6 μL of 2 mM phenylacetylene and 6 μL of 2mM EG_3SH or (b) 15 μL of 2 mM alkynyl-β-lactam (**4.10**). The resulting solutions were left stirring for 4 h. Solution (b) was transferred to a 1.5 mL Eppendorf micro-centrifuge tube and spun at 13.4 k rpm for 20 min to pellet the particles. The supernatant was then removed and the particles re-suspended in 500 μL of water. To (a): 50 μL of the secondary antibody solution (Affinipure bovine anti-goat IgG (H+L) 2.4 mg/mL (Jackson Immunoresearch)) was added and the resulting solution mixed by pipetting it slowly several times. This solution was left in the fridge at 4 ^{o}C overnight for 16 h. Upon completion, the solution was warmed to r.t. and 30 μL of 30 % bovine serum albumin (BSA) was added. This solution was mixed with a pipette and left to stand at r.t. for 30 min. Next the solution was transferred to a 1.5 mL Eppendorf micro-centrifuge tube and spun at 13.4 k rpm for 20 min to pellet the particles. The supernatant was then removed and the particles were re-suspended in 500 μL of PBS. The resulting solutions were determined to be approximately 1 nM in size as determined by UV-Vis spectroscopy. The particles were stored at 4 ^{o}C.

Cell Culture and Sample Preparation:

Huh7.5 cells (ATCC, Manassas, VA) were grown in Dulbecco's modified Eagle's medium (Invitrogen, Burlington, ON) supplemented with 10 % fetal bovine serum (FBS) (NorthBio, Toronto, ON) under standard culture conditions (37 °C, 5% CO_2) and were plated onto silica wafers in a 12-well plate. After 24 h, cells were fixed and rinsed with PBS. To this, anti-occludin antibody (AB) (Occludin (Y-12)) goat polyclonal IgG (Santa Cruz Biotechnology 0.2 mg/mL, 4 uL used per mL PBS) was added, and the cells stored in the fridge with the AB

for 24 h at 4 ^{o}C. Cells were then rinsed 3 times with PBS and then the 1 mL NP solution in PBS was used to cover the cells after the final wash. This cells were then stored again for 24 hrs at 4 ^{o}C with the NPs. Subsequently, the NP solution was recovered, and cells were again rinsed 3 times with PBS. The cells were then stored at 4 ^{o}C in PBS until imaged.

Raman Imaging and Spectroscopy:

Raman spectroscopy and microscopy were acquired with a commercial microRaman system (LabRAM HR, Horiba Jobin Yvon) equipped with a software controlled XYZ stage and a thermal-electric cooled CCD detector. In typical SERS experiments, samples were excited with 632.8 nm radiation at a power density of ~ 10^4 W/cm^2. Incident radiation was coupled into an Olympus BX51 optical microscope and focused to ~1 μm diameter spot through a 100X objective. The same objective also collects the retro-reflected radiation and guides it to a notch filter which removes the Rayleigh radiation. In the Raman mapping experiments, a fine set of grid points within an area of interest is defined in the software and imaged by raster of the sample under the tightly focused laser beam. At each of the grid points, a full Raman spectrum was acquired. The SERS images were generated with 1 s acquisition time (2 accumulations) with a power density of 10^4 W/cm^2. The multiple accumulations are necessary for the spike removal algorithm to function. Upon completion of the mapping, Raman intensity map of the C≡C vibrational mode is regenerated by fitting and removing the associated background for each spectrum in the predefined spatial grid. The C≡C intensity is displayed as a thermal map. This is achieved by the Labspec 5.25 software (Horiba Jobin Yvon). The solid Raman spectrum was acquired by 632.8 nm irradiation at a power density of ~10^5 W/cm^2.

Additional Imaging Data:

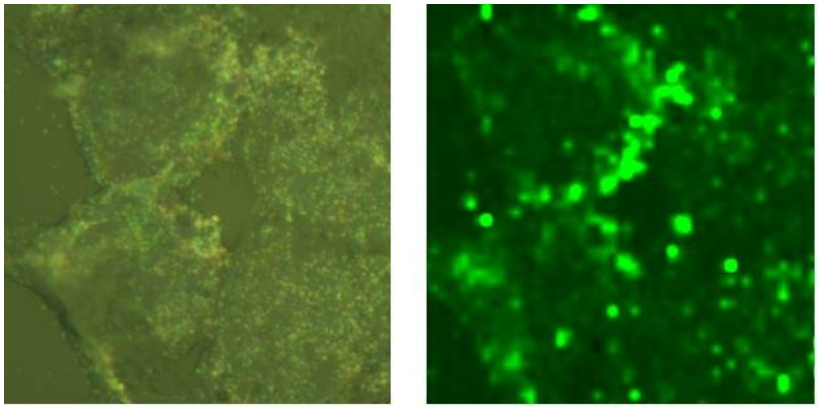

Figure 4-7. Additional bright field and SERS image of Huh 7.5 cells showing a high abundance of occludin localized away from tight junctions.

References

(1) Hudson, S. D.; Chumanov, G. *Anal. Bioanal. Chem.* **2009**, *394*, 679-686.
(2) Kennedy, D. C.; Tay, L.-L.; Lyn, R. K.; Rouleau, Y.; Hulse, J.; Pezacki, J. P. *ACS Nano* **2009**, *3*, 2329-2339.
(3) Kneipp, J.; Kneipp, H.; Kneipp, K. *Chem. Soc. Rev.* **2008**, *37*, 1052-1060.
(4) Stuart, D. A.; Haes, A. J.; Yonzon, C. R.; Hicks, E. M.; Van Duyne, R. P. *IEE Proc.-Nanobiotechnol.* **2005**, *152*, 13-32.
(5) Braun, G. B.; Lee, S. J.; Laurence, T.; Fera, N.; Fabris, L.; Bazan, G. C.; Moskovits, M.; Reich, N. O. *J. Phys. Chem. C* **2009**, *113*, 13622-13629.
(6) Kennedy, D. C.; Hoop, K. A.; Tay, L.-L.; Pezacki, J. P. *Nanoscale* **2010**, *2*, 1413-1416.
(7) Kim, J.-H.; Kim, J.-S.; Choi, H.; Lee, S.-M.; Jun, B.-H.; Yu, K.-N.; Kuk, E.; Kim, Y.-K.; Jeong, D. H.; Cho, M.-H.; Lee, Y.-S. *Anal. Chem.* **2006**, *78*, 6967-6973.
(8) Zavaleta, C. L.; Smith, B. R.; Walton, I.; Doering, W.; Davis, G.; Shojaei, B.; Natan, M. J.; Gambhir, S. S. *Proc. Natl. Acad. Sci. U. S. A.* **2009**, *106*, 13511-13516.
(9) Durr, N. J.; Larson, T.; Smith, D. K.; Korgel, B. A.; Sokolov, K.; Ben-Yakar, A. *Nano Lett.* **2007**, *7*, 941-945.
(10) El-Sayed, I. H.; Huang, X.; El-Sayed, M. A. *Nano Lett.* **2005**, *5*, 829-834.
(11) El-Sayed, I. H.; Huang, X.; El-Sayed, M. A. *Cancer Lett.* **2006**, *239*, 129-135.
(12) Huang, X.; El-Sayed, I. H.; Qian, W.; El-Sayed, M. A. *Nano Lett.* **2007**, *7*, 1591-1597.
(13) Kennedy, D. C.; Duguay, D. R.; Tay, L.-L.; Richeson, D. S.; Pezacki, J. P. *Chem. Commun.* **2009**, *45*, 6750-6752.
(14) Hu, Q.; Tay, L.-L.; Noestheden, M.; Pezacki, J. P. *J. Am. Chem. Soc.* **2006**, *129*, 14-15.
(15) Larmour, I. A.; Faulds, K.; Graham, D. *Chem. Sci.* **2010**, *1*, 151-160.
(16) Tay, L.-L.; Hulse, J.; Kennedy, D.; Pezacki, J. P. *J. Phys. Chem. C* **2010**, *114*, 7356-7363.
(17) Wustholz, K. L.; Henry, A.-I.; McMahon, J. M.; Freeman, R. G.; Valley, N.; Piotti, M. E.; Natan, M. J.; Schatz, G. C.; Duyne, R. P. V. *J. Am. Chem. Soc.* **2010**, *132*, 10903-10910.
(18) Skadtchenko, B. O.; Aroca, R. *Spectrochim. Acta, Part A* **2001**, *57*, 1009-1016.
(19) Jones, R. N.; Ripley, R. A. *Can. J. Chem.* **1964**, *42*, 305-325.
(20) Friedrich, M. G.; Kirste, V. U.; Zhu, J.; Gennis, R. B.; Knoll, W.; Naumann, R. L. C. *J. Phys. Chem. B* **2008**, *112*, 3193-3201.
(21) Zheng, M.; Li, Z.; Huang, X. *Langmuir* **2004**, *20*, 4226-4235.
(22) Jang, Y. H.; Hwang, S.; Oh, J. J.; Joo, S.-W. *Vib. Spectrosc.* **2009**, *51*, 193-198.
(23) Lim, J. K.; Joo, S.-W.; Shin, K. S. *Vib. Spectrosc.* **2007**, *43*, 330-334.
(24) Chui, S. S. Y.; Ng, M. F. Y.; Che, C.-M. *Chem. Eur. J.* **2005**, *11*, 1739-1749.
(25) Yoo, B. K.; Joo, S.-W. *J. Colloid Interface Sci.* **2007**, *311*, 491-496.
(26) McKay, C. S.; Kennedy, D. C.; Pezacki, J. P. *Tetrahedron Lett.* **2009**, *50*, 1893-1896.
(27) Clarke, S. J.; Littleford, R. E.; Smith, W. E.; Goodacre, R. *Analyst* **2005**, *130*.
(28) Lee, N. P.; Luk, J. M. *World J. Gastroenterol.* **2010**, *16*, 289-295.
(29) Orbán, E.; Szabó, E.; Lotz, G.; Kupcsulik, P.; Páska, C.; Schaff, Z.; Kiss, A. *pathol. Oncol. Res.* **2005**, *14*, 299-306.

(30) Benedicto, I.; Molina-Jiménez, F.; Bartosch, B.; Cosset, F.-L.; Lavillette, D.; Prieto, J.; Moreno-Otero, R.; Valenzuela-Fernández, A.; Aldabe, R.; López-Cabrera, M.; Majano, P. L. *J. Virol.* **2009**, *83*, 8012-8020.
(31) Liu, S.; Yang, W.; Shen, L.; Turner, J. R.; Coyne, C. B.; Wang, T. *J. Virol.* **2009**, *83*, 2011-2014.
(32) Zheng, M.; Li, Z.; Huang, X. *Langmuir* **2004**, *20*, 4226-35.
(33) Evans, D. A.; Song, H.-J.; Fandrick, K. R. *Org. Lett.* **2006**, *8*, 3351-3354.

Chapter 5 : Strain-Promoted 1,3-Dipolar Cycloadditions of Cyclooctynes with Nitrones and Diazoalkanes

A significant portion of the work presented in this chapter was published in:

McKay C. S.; Moran, J.; Pezacki, J. P. Nitrones as dipoles for rapid strain-promoted 1,3-dipolar cycloadditions with cyclooctynes. *Chem. Commun.* **2010**, *46*, 931–933.

Moran, J, McKay, C. S.; Pezacki, J. P. Strain-promoted 1,3-dipolar cycloadditions of diazo compounds with cyclooctynes. *Can. J. Chem.* **2011**, *89*, 148-151.

Introduction

Reactions that meet the requirements of bioorthogonality have far reaching applications for monitoring proteins, nucleic acids, glycans and lipids on their own or as post-translational modifications.[1-3] Despite the number of developed organic transformations, there exists only a handful of reactions have been deemed bioorthogonal. Issues arising due to toxicity of reagents, compatibility with water, and competing side reactions have hampered the number of reactions that have been successfully transferred from the round bottom flask to biological systems. Not only must the bioorthogonal reactive groups be mutually reactive, bio-inert and ideally non-toxic, the reaction must proceed with exceptionally fast reaction rates to ensure formation of the product at low concentrations typically required in biological labelling experiments. These limitations present unique challenges for chemists to develop selective reactions that display exceptionally fast kinetics and high yield and can ultimately be used for studying dynamic cellular processes.

A number of bioorthogonal strain-promoted 1,3-dipolar cycloaddition reactions have been developed that show fast kinetics, and high selectivity for functionalizing biomolecules. The quintessential metal-free bioorthogonal reaction, strain-promoted azide-alkyne cycloaddition (SPAAC)[1,3-5] has found wide utility for labelling glycans,[6] proteins,[7] lipids of living cells.[8] Additionally, SPAAC has been employed for glycoprotein enrichment of proteomic samples,[9] proteins,[10] oligonucleotide modification[11] and tissue engineering.[12,13] As mentioned in Chapter 1, density function theory (B3LYP) calculations of the transition state of cycloadditions of phenylazide with acetylene or cyclooctyne indicate that the fast rate of the strain-promoted cycloaddition is due to a lower energy required for distorting the 1,3-dipole and alkyne into the transition state geometry.[13-17]

A tremendous amount of effort has been directed toward improving the kinetics of SPAAC by increasing the reactivity of the alkyne component. Modifications to the cyclooctyne have included fluorination,[18,19] sp^2 hybridization of ring atoms,[20-24] fusion to cyclopropane moieties,[25] or by substituting a heteroatom for ring carbon atoms.[26] Despite these improvements to the kinetics of SPAAC, less attention has been focused on the use of alternative 1,3-dipoles that display increased reactivity in strain promoted cycloadditions with cyclooctynes. Recently, the kinetics of SPAAC have been improved through substituting the azide with a more reactive dipole such as nitrile oxides.[27] Although nitrile oxides display enhanced reactivity relative to azides in 1,3-dipolar cycloadditions, they require *in situ* generation due to their instability under physiological settings and require external oxidants or bases for their generation.[13]

Having recently become interested in using nitrones as dipoles in [3+2] cycloadditions with terminal alkynes via the Kinugasa reaction,[28] we speculated that nitrones may display faster kinetics in reactions with strained alkynes. Strain-promoted alkyne-nitrone cycloaddition (SPANC) would not only circumvent the use of potentially toxic copper catalysts,[29-31] but would also avoid the energetically disfavored ring contraction required for β-lactam formation by the Kinugasa reaction, giving rise to selective formation of isoxazoline products. Given the value of increasing reaction rates of bioorthogonal reactions as a means for reducing the concentration of labelling reagents, we set out to explore the use of nitrones and diazoalkanes as alternative 1,3-dipoles in strain-promoted cycloadditions with cyclooctynes (Scheme 5-1).

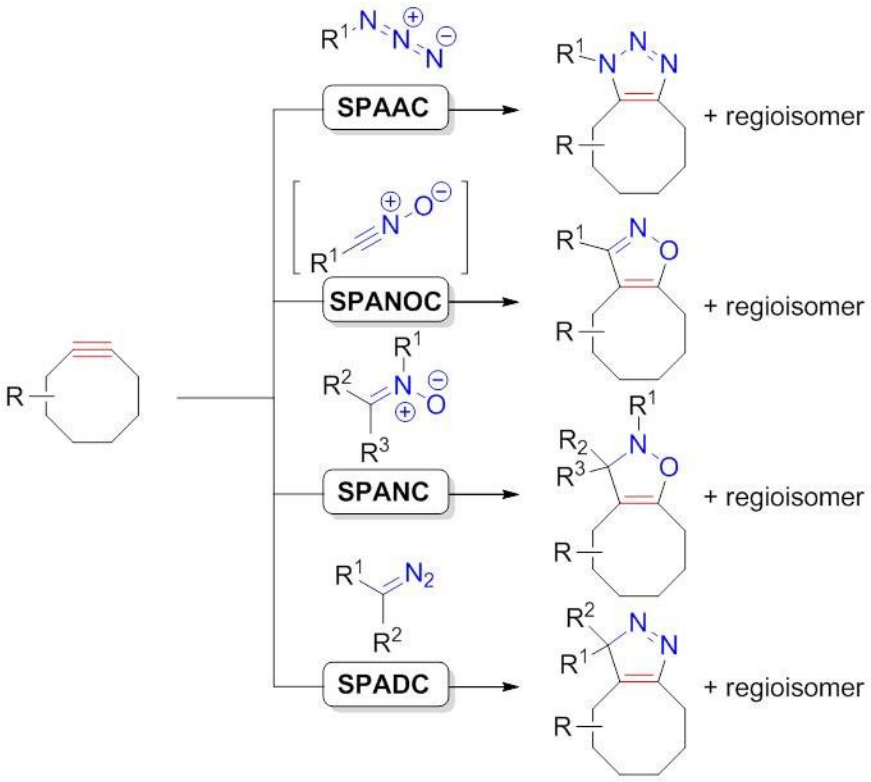

Scheme 5-1. Strain-promoted cycloadditions of cyclooctynes with 1,3-dipoles of different reactivity; strain-promoted azide-alkyne cycloaddition (SPAAC), strain-promoted alkyne-nitrile oxide cycloaddition (SPANOC), strain-promoted alkyne-nitrone cycloaddition (SPANC), and strain-promoted alkyne-diazoalkane cycloaddition (SPADC).

Hypothesis

Nitrones serve as rapid alternatives to azides in strain-promoted 1,3-dipolar cycloadditions with cyclooctynes.

Results and Discussion

This chapter describes the development of strain-promoted alkyne-nitrone cycloaddition (SPANC) and strain-promoted alkyne-diazoalkane cycloaddition (SPADC) for biological labelling. A series of nitrones, diazoalkane compounds, and dibenzocyclooctyne were synthesized and tested in model reactions. The generality of SPANC and SPADC was evaluated with respect to the conformational flexibility and electronics of the respective 1,3-

dipole component. Rate constants were measured for the fastest reacting 1,3-dipoles, and the obtained rate constants were compared with analogous reaction involving benzyl azide.

Kinetics of Strain-Promoted Alkyne-Nitrone Cycloadditions

At the onset of this work, Boons *et al*. had reported 4-dibenzocyclooctynol[24] (DIBO) and demonstrated its fast reactivity for the visualization of metabolically labelled azido glycans on the surface of living cells.[24] The attractive features of DIBO included its synthetic tractability and nontoxicity. Towards establishing the chemistry of SPANC and SPADC, we felt that it would be advantageous to utilize a symmetric cyclooctyne with exquisite reactivity towards 1,3-dipoles. The lack of regioselectivity of strain-promoted 1,3-dipolar cycloadditions in the solution phase, in combination with introducing additional chiral centers in the products would only lead to complicated mixtures of regio- and diastereomeric cycloadducts.

Dibenzocyclooctyne[32] (**5.1**) was chosen due to its ease of preparation and by virtue of its symmetric structure as well as its fast reaction rates in SPAAC. The synthesis of **5.1** was accomplished in 61 % over four steps starting from phenyl acetaldehyde **5.2** (Scheme 5-2). The key step en route to **5.1** involved a double *ortho*-Friedel-Crafts cyclization effected by iodo-trimethylsilane to generate the tetracyclic ether (**5.3**) according to the method of Kagan.[33] Reductive ring opening of Kagan's ether using lithium naphthalenide afforded the alcohol (**5.4**) in 39 % yield.[34] Oxidation of the alcohol with pyridinium dichromate afforded the ketone (**5.5**) in excellent yield. Treatment of **5.5** with KHMDS and *N*-phenyl-bis(trifluorosulfonimide) facilitated formation of the vinyl triflate, and subsequent elimination yielded **5.1** in 60 % over 2 steps.

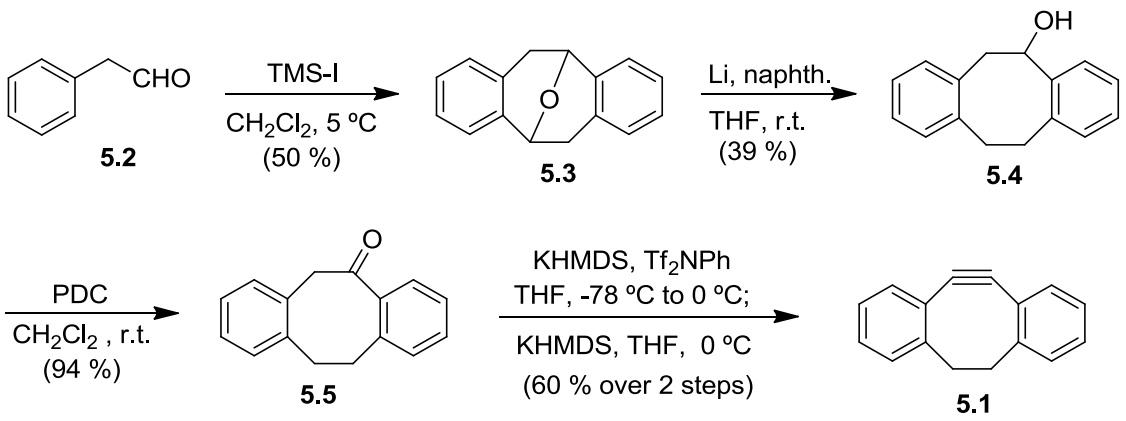

Scheme 5-2. Reagents and conditions for the synthesis of dibenzocyclooctyne **5.1**.

Nitrones are conveniently prepared by several methods that are well documented in the literature (Scheme 5-3).[35] One of the most useful ways for preparing nitrones involves the condensation of *N*-substituted hydroxylamines (**5.6**) with carbonyl compounds (**5.7**) in the presence of a dehydrating agent.[36,37] This method is especially suitable for the preparation of acyclic aldonitrones,[35] but has also been developed for preparing cyclic nitrones via intramolecular cyclization.[38] Methods for preparing nitrones include: 1) oxidizing secondary amines (**5.8**),[39,40] imines (**5.9**),[41] and hydroxylamines (**5.10**);[42-46] 2) *N*-alkylation of oximes (**5.11**) at an electrophilic center (**5.12**) under basic conditions;[47] and 3) intramolecular *N*-alkylation of oximes for the preparation of cyclic nitrones.[48] For our purposes, we elected to utilize micelle-promoted condensations of aldehydes with *N*-hydroxylamine compounds for the generation of a series of acyclic aldonitrones. For the synthesis of cyclic nitrones we decided to employed oxidation of secondary amines and intramolecular *N*-hydroxylamine/aldehyde cyclizations.

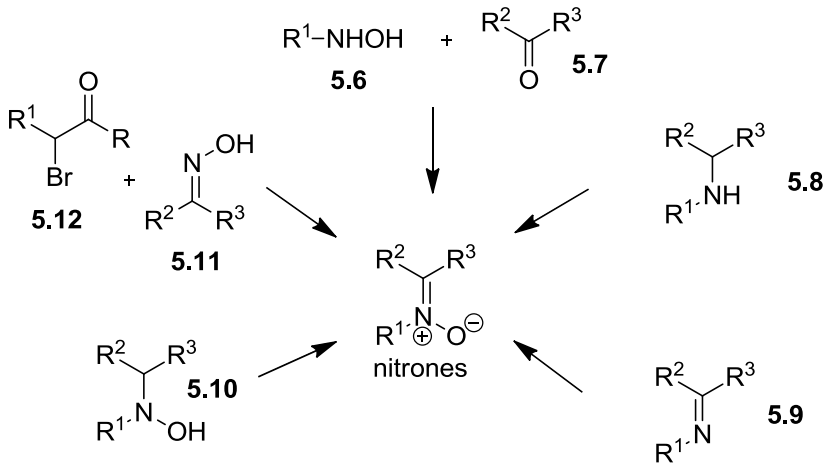

Scheme 5-3. Common strategies for preparation of nitrones.

Toward establishing nitrones as alternative 1,3-dipoles in rapid strain promoted cycloadditions with cyclooctynes, our preliminary investigations involved performing a solvent screen for reaction of *α,N*-diphenyl nitrone (**5.13**) with **5.1** in a series of solvents. Interestingly, the reaction yielded cycloadduct (**5.14**) in excellent yield and in less than 1 h for each of the solvents that were tested, with toluene being optimal (Table 5-1).

Table 5-1. Solvent screen of strain-promoted alkyne-nitrone cycloadditions.

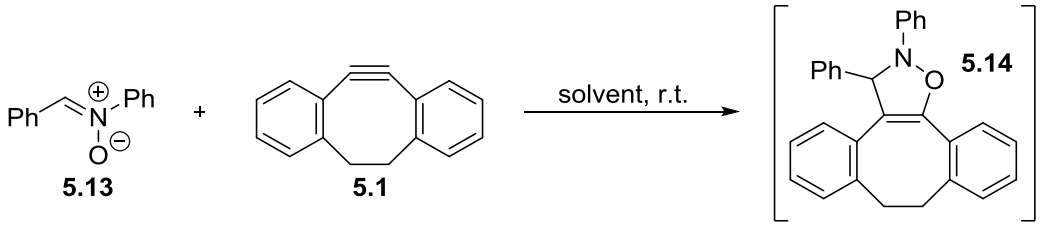

Entry	Solvent	*T* (min)	Yield %
1	toluene	30	96
2	tetrahydrofuran	40	90
3	ethanol	28	88
4	acetonitrile	40	89

Conditions: **5.13** (100 mM), **5.1** (100 mM), r.t., solvent. [a]Isolated yield after column chromatography.

The low solubility of **5.1** and **5.13** in aqueous solution prevented us from conducting these reactions in water. Nevertheless, it was encouraging that the SPANC reaction proceded in high yield and in short reaction times, suggesting that the kinetics of SPANC could be competitive with that of SPAAC.

Careful examination of the ^{1}H NMR of cycloadduct **5.14**, indicated that it had undergone thermal isomerization to the 2-acylaziridine (**5.15**), and rearrangement leading to the azo-methine ylide (**5.16**) (Scheme 5-4). After prolonged storage, hydrolysis of **5.16** to the α-amino-ketone (**5.17**) and benzaldehyde was observed. It well known that Δ^4-isoxazolines are prone to such rearrangements.[49,50] The reactivity of the isoxazoline ring is mainly due the low thermochemical stability of the N-O bond associated with the π system. It was found that this rearrangement could be slowed by storing the cycloadducts at -20 ˚C. Isoxazolines bearing electron withdrawing groups (EWG) at the *N*-position of the nitrone are prone to undergo facile thermal rearrangements.

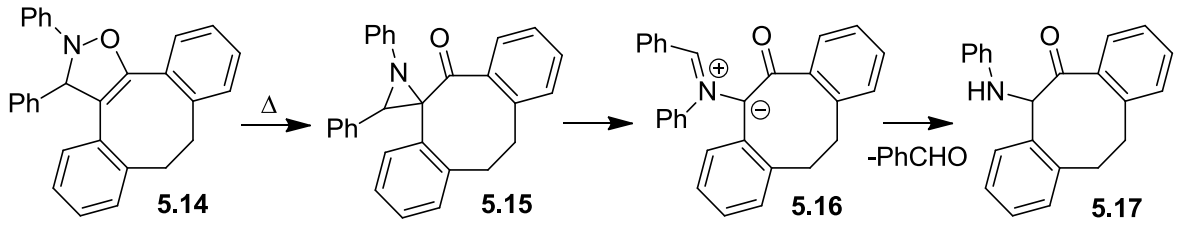

Scheme 5-4. Thermal decomposition of **5.14**.

To improve upon the kinetics of SPANC and increase the stability of the corresponding cycloadducts, we replaced the *N*-phenyl EWG with an electron donating group (EDG), methyl or benzyl (Table 5-2). The acyclic nitrones (**5.18**–**5.27**) were prepared by micelle-promoted condensation of an aryl aldehyde with the appropriate hydroxylamine.[51] As shown in Table 5-2, the α-aryl-*N*-methyl nitrones reacted rapidly with **5.1** and yielded the

isoxazolines in 72-86 % (Table 5-2, Entries 1-3). These corresponding isoxazoline were found to be stable enough for isolation without compromising the kinetics of the reaction. Nitrone **5.18** bearing an α-aryl 4-methyl ester group demonstrated an enhancement in the reaction rate relative to **5.20** bearing an α-aryl 4-methyl ether, suggesting that the EWGs at the α-aryl position increase the reactivity of the nitrone.

Table 5-2. Strain-promoted cycloadditions between acyclic nitrones **5.18**-**5.27** and **5.1**.

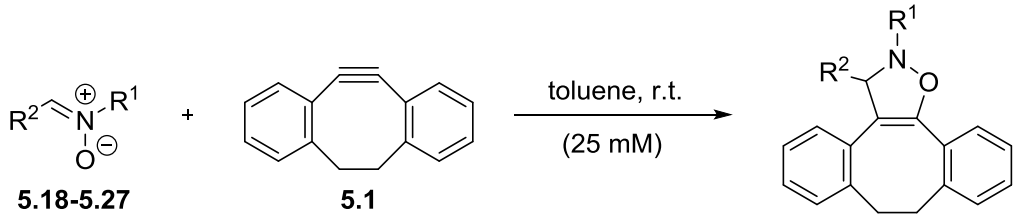

5.18-5.27 + **5.1** → **5.28-5.37**

Entry	Nitrone			T (min)	Product	Yield %[a]
1	**5.18**	R^1 = Me	R^2 = 4-$CO_2MeC_6H_4$	44	**5.28**	84
2	**5.19**	R^1 = Me	R^2 = Ph	90	**5.29**	86
3	**5.20**	R^1 = Me	R^2 = 4-$OMeC_6H_4$	110	**5.30**	72
4	**5.21**	R^1 = Bn	R^2 = 4-$NO_2C_6H_4$	19	**5.31**	97
5	**5.22**	R^1 = Bn	R^2 = 4-$CO_2MeC_6H_4$	20	**5.32**	96
6	**5.23**	R^1 = Bn	R^2 = 4-BrC_6H_4	26	**5.33**	98
7	**5.24**	R^1 = Bn	R^2 = 4-CNC_6H_4	23	**5.34**	99
8	**5.25**	R^1 = Bn	R^2 = 4-MeC_6H_4	30	**5.35**	94
9	**5.26**	R^1 = Bn	R^2 = Ph	30	**5.36**	92
10	**5.27**	R^1 = Bn	R^2 = 4-$OMeC_6H_4$	62	**5.37**	95

Conditions: Nitrone (100 mM), **5.1** (100 mM), 22 ˚C, toluene. [a]Isolated yield after column chromatography.

In another attempt to further optimize the tradeoff between rate and reactant/product stability, we tested α-aryl-*N*-benzyl nitrones (Table 5-2, Entries 4-10) in reactions with **5.1**.

We observed that the cycloaddition proceeded at similar rates as with diphenyl nitrone, and that corresponding products were tolerant to substitution of the nitrone at the α-aryl position. As expected, nitrones bearing EWG's at the *α*-aryl position (Entries 4-7) reacted more rapidly than *α*-phenyl-*N*-benzyl nitrone and those bearing EDG's (Entries 8–10). Further optimization of the nitrone component was viewed as being critical to developing the SPANC reaction as a rapid alternative bioorthogonal reaction.

Next we explored the use of cyclic nitrones since they offered the advantage of locking the nitrone in the more reactive *E*-conformation and the opportunity to introduce strain into the 1,3-dipole component. Endocyclic nitrones **5.38-5.40** were prepared by metal-free oxidation of the corresponding secondary amine following the method of Font.[52] Interestingly, SPANC reactions of cyclic nitrones displayed improved reactivity over their acyclic counterparts in reactions with **5.1** (Table 5-3).

Table 5-3. Strain-promoted cycloadditions of cyclic nitrones with **5.1**.

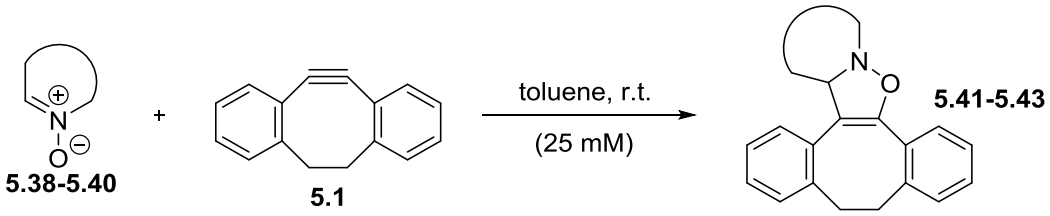

Entr	Nitrone	T (min)	Product	Yield %[a]
1	**5.38**	75	**5.41**	97
2	**5.39**	40	**5.42**	>99[c]
3	**5.40**	2	**5.43**[c]	>99

Conditions: Nitrone (100 mM), **5.1** (100 mM), 22 ˚C, toluene. [a]Isolated yield after column chromatography. [c]Single diastereomer observed.

The SPANC reactions involving cyclic nitrones resulted in quantitative formation of the isoxazolines (**5.41-5.43**). The five membered pyrroline *N*-oxides, **5.38-5.39** (Table 5-3, Entries 1-2) reacted slower than the dihydroisoquinoline *N*-oxide (**5.40**) (Entry 3). Nitrone **5.40**, which features benzylic activation and is contained within a rigid six-membered ring, appeared qualitatively to be the most rapid by TLC analysis and therefore warranted further quantitative study.

Second order rate constants for SPANC reactions were determined by ^{1}H-NMR, by measuring disappearance of the nitrone and **5.1** reactants, and appearance of products, as monitored by integration of peak areas at multiple chemical shifts (Table 5-4). The second order rate constants for acyclic nitrones **5.19** and **5.26** were found to be 0.13 ± 0.01 $M^{-1}s^{-1}$ and 0.088 ± 0.004 $M^{-1}s^{-1}$, respectively, in benzene-d_6 at 25 ˚C (Entries 1 and 2).

Table 5-4. Kinetics of strain-promoted cycloadditions of nitrones or benzyl azide with **5.1**.

Entry	Dipole		k_2 ($M^{-1}s^{-1}$)	k_{rel}
1	**5.19**	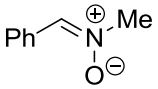	0.13 ± 0.01	2.1
2	**5.26**	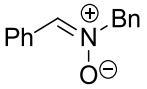	0.088 ± 0.004	1.4
3	**5.40**	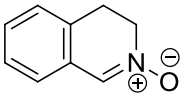	1.5 ± 0.1	24.2
4	**5.44**	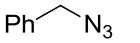	0.062 ± 0.006	1

Kinetic evaluation of nitrones: the appropriate substrate and **5.1** were pre-dissolved in benzene-d_6 and mixed at equimolar concentrations of ~50 mM. Reactions were monitored by ^{1}H NMR at 25 ˚C and were repeated in triplicate.

These rates are comparable with typical values obtained from reactions of benzyl azide (**5.44**) with difluorinated cyclooctyne (DIFO).[19,53] The rate constant for reaction of azide **5.44**

with **5.1** was determined to be 0.062 ± 0.006 $M^{-1}s^{-1}$. Interestingly, the second order rate constant for the reaction of endocyclic nitrone **5.40** with **5.1** in benzene-d_6 at 25 ˚C was determined to be 1.5 ± 0.1 $M^{-1}s^{-1}$. The additional rate acceleration likely arises at least in part due to added strain in the cyclic nitrone, making the reaction doubly strain-promoted. Put in context, this rate is about 20 times faster than the reaction of DIFO with benzyl azide[19] and approximately 24 times faster than the reaction of **5.1** with benzyl azide as determined under our conditions.

Table 5-5. Solvent screen for reaction between **5.40** and **5.1**.

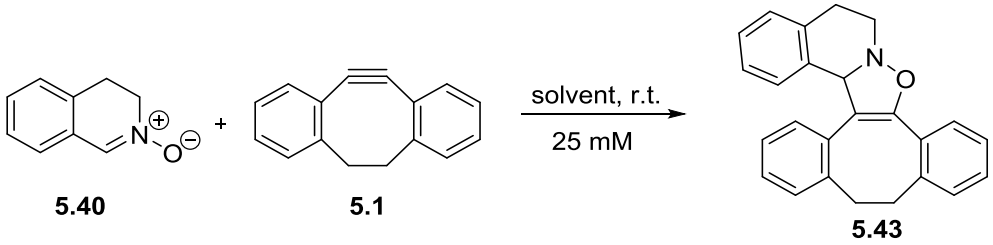

5.40 **5.1** **5.43**

Entry	Solvent	Reaction time for 95% conversion to 5.43 (min)
1	acetonitrile-d_3	8.6
2	benzene-d_6	2.4
3	chloroform-d	33
4	tetrahydrofuran-d_8	2.7
5	acetone-d_6	7.7
6	dimethylsulfoxide-d_6	15

Conditions: A solution of **5.40** was added to a solution of **5.1** (both pre-dissolved, 100 mM, 1 : 1 in appropriate solvent) in an NMR tube and monitored by ^{1}H NMR at 25 ˚C.

To further study the reactive nature of endocyclic nitrone **5.40**, the reaction between **5.40** with **5.1** was tested in a variety of common deuterated solvents at ambient temperature and monitored by ^{1}H NMR (Table 5-5). At starting reaction concentrations of 100 mM, the reaction reached 95 % conversion to isoxazoline **5.43** in less than 33 min for all solvents

employed. It was found that the reaction kinetics were fastest in toluene and slowest in chloroform, suggesting that there may be a pH dependence of the reaction.

Kinetics of Strain-Promoted Alkyne-Diazoalkane Cycloadditions

Inspired by the pioneering work done by Huisgen *et al.*[54] involving 1,3-dipolar cycloadditions of diazoalkanes with linear alkynes,[54-60] we set out to investigate whether a strain-promoted variant could serve as a rapid alternative to reactions of nitrones or azides with cyclooctynes. There are number of ways in which diazoalkanes can be conveniently synthesized.[61] Standard literature procedures were used to prepare diazoalkanes just prior to use. The diazoalkane scope was evaluated with respect to its electronics and conformational rigidity, and kinetics for reaction with **5.1** was measured by ^{1}H NMR (Table 5-6). The reaction of diphenyldiazomethane (**5.45**) with **5.1** in methanol-d_4 yielded the substituted pyrazole **5.49** in > 95 % yield, corresponding to a second-order rate constant of k_2 = 0.07 $M^{-1}s^{-1}$. Substitution with stronger EWG's, such as ethyl 2-diazoacetate (**5.46)**, reduced the reaction rate by 13-fold (k_2 = 0.0053 $M^{-1}s^{-1}$) reaching > 95 % conversion within 18 h (Table 5-6, Entry 2). Diazoalkanes bearing electron-donating methylene groups or those less capable of resonance stabilization displayed dramatic rate enhancements. Trimethylsilyl diazomethane (**5.47**) reacted quite rapidly with **5.1** and reached maximum conversion in less than 1 min. The similar reaction of phenyl diazomethane (**5.48**) reached > 95 % conversion within 1 min. We were unable to determine rate constants for reactions between **5.47-5.48** and **5.1** by ^{1}H NMR, since the reactions were complete upon acquisition of the first data point. The low yield of **5.51** likely resulted from competitive reaction pathways, including carbene reaction pathways of **5.47**. The cycloadducts arising from reactions of diazoalkanes **5.46-5.48** underwent rapid tautomerization to the aromatic pyrazoles (**5.50-5.52**),

respectively. The primary cycloadduct from the reaction of **5.47** with **5.1** suffered loss of the trimethylsilyl group under the aqueous reaction conditions yielding **5.51**.

Table 5-6. Kinetics of strain-promoted cycloadditions between diazo compounds **5.45-5.48** and **5.1**.

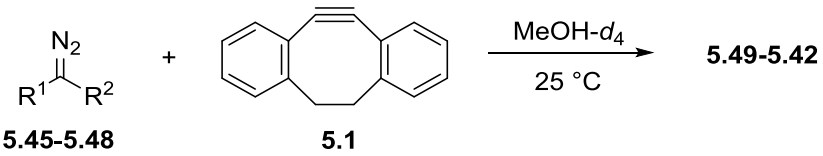

5.45-5.48 **5.1**

Entry	Diazo compound	Product	T (min)	Yield %	k_2 ($M^{-1}s^{-1}$)[a]
1	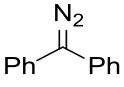 **5.45**	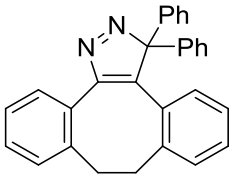 **5.49**	98	>99	0.070
2	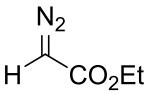 **5.46**	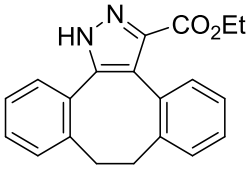 **5.50**[b]	1062	97	0.0053
3	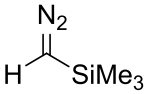 **5.47**	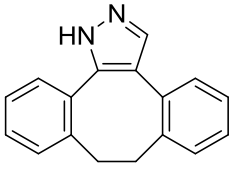 **5.51**[b]	< 1 min	34	n.d.[c]
4	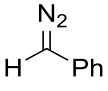 **5.48**	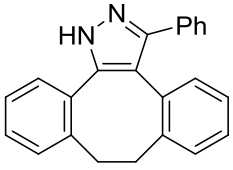 **5.52**[b]	< 1min	93	n.d.[c]

Conditions: diazo compound (50 mM); **5.1** (50 mM); 25 ºC; MeOH-d_4. [a]Kinetic evaluation of diazo compounds: the appropriate substrate and **5.1** were pre-dissolved in MeOH-d_4 and mixed at equimolar concentration of ~25 mM. Reactions were monitored by ^{1}H NMR at 25 ºC. [b]Representative tautomer isolated after column chromatography. [c]n.d. = not determined. Reactions were too fast to be measured by ^{1}H NMR.

Lastly, a screen of various deuterated solvents was used to evaluate the generality of the reaction as well as to determine if there was a solvent effect on the rate of cycloaddition. The reaction of **5.45** with **5.1** reached > 95% conversion within 4 h for all solvents that were tested (Table 5-7). In contrast to the rate of cycloadditions of nitrones being optimal in toluene, it was found that d_4-methanol was an optimal solvent for SPADC, reaching 95 % yield within 98 min as compared to the reaction in toluene (245 min).

Table 5-7. Solvent screen for reaction between **5.45** and **5.1**.

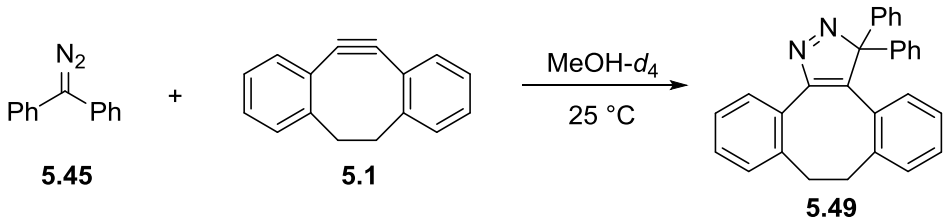

5.45 **5.1** **5.49**

Entry	Solvent	Reaction time for 95% conversion to 5.49 (min)
1	benzene-d_6	245
2	methanol-d_4	98
3	dimethyl sulfoxide-d_6	108
4	acetonitrile-d_3	139

Conditions: **5.1** was added to **5.45** (both pre-dissolved, 100 mM, 1:1) in an NMR tube and monitored by ^{1}H NMR at 25 ºC.

Diazoalkanes can be protonated to form alkane diazonium ions in aqueous solution in biological systems that can alkylate nucleic acids as well as protein side chains, causing cellular stress and carcinogenesis.[62-67] Although the bimolecular rate constants for strain-promoted cycloaddition are slower than those of proton transfer ($k_H^+ \approx 10^2$-10^6 $M^{-1}s^{-1}$)[62-67] under neutral conditions, at physiological pH, where hydronium ion concentration is low (10^{-7} M), cycloaddition rates may be competitive or even dominate over diazonium ion chemistry. Diazoalkanes can give rise to carbene intermediates either through photolytic or

thermolytic processes.[68,69] The generated carbenes can then undergo O–H or C–H insertion reactions, cyclopropanation reactions, as well as intramolecular rearrangements such as 1,2-hydrogen shifts.[68,69] Interestingly, cyclooctynes might also serve as *in vivo* quenchers of diazoalkanes that might be formed through nitrosative stress.

Future Directions

Further optimization of the cyclic nitrone reactivity and stability in SPANC for biological labelling studies will be required. Also, SPANC reactivity in aqueous buffers and pH dependence of the reaction will be explored. The SPANC reaction is well-positioned for development as a novel metal-free bioorthogonal reaction. In chapter 6 we describe applications of SPANC for protein modification and labelling of live cell surface proteins.

Conclusions

We have studied the kinetics of SPANC for reactions of a series of acyclic and cyclic nitrones with dibenzocyclooctyne. Reactions of acyclic nitrones with dibenzocyclooctyne exhibit kinetics on the same order of magnitude as analogous reaction involving benzyl azide. Alternatively, endocyclic nitrones display exceptionally fast reaction kinetics in a variety of solvents. The reaction between cyclic nitrone **5.40** and dibenzocyclooctyne **5.1** corresponded to a second-order rate constant of 1.5 $M^{-1}s^{-1}$. This value is 24 times faster than the analogous reaction involving benzyl azide.

Strain-promoted cycloadditions of diazoalkanes with cyclooctynes represent an alternative rapid conjugation technique for material sciences and a valid method for constructing functionalized pyrazoles. Exceptionally fast kinetics was observed for diazoalkanes containing EDGs adjacent to the diazo moiety. The rate constants observed for resonance stabilized diazoalkane **5.45** are comparable with those of analogous reactions

involving acyclic diaryl nitrones or azides. However, more weakly stabilized diazoalkanes displayed faster kinetics for cycloaddition with **5.1** than cyclic nitrones, benzyl azide, or acyclic nitrones bearing ester or amide groups[70] at the α-position. Optimization of the stability and reactivity of the diazoalkane group may lead to diazoalkanes as reactive and useful alternatives to nitrone and azide dipoles for use in strain-promoted cycloadditions with cyclooctynes.

Acknowledgements

I would like to thank Dr. Joseph Moran for assistance with solvent screens and interpretation of kinetics data for SPANC and SPADC. We also thank Kenneth Chan for assistance with MALDI-MS of the reaction products.

Materials and Methods

General

All chemical reagents were purchased from commercial suppliers and used without further purification. Reactions were monitored by thin layer chromatography (TLC) pre-coated silica gel glass plates (60 F_{254}, layer thickness 250μm), using UV light and potassium permanganate stain to visualize the course of reaction. For flash column chromatography technical grade solvents were used, and chromatographic purification was performed using silica gel (60, particle size 40–63 μm). ^{1}H NMR and ^{13}C NMR spectra were recorded using a Bruker-DRX-400 spectrometer using a frequency of 400.13 MHz for ^{1}H and 100.61 MHz for ^{13}C and processed using Bruker TOPSPIN 2.1 software. Chemical shifts are reported in parts per million (δ) using residual $CHCl_3$ resonance as an internal reference (7.26 and 77.0 ppm for ^{1}H and ^{13}C NMR, respectively). The following abbreviations were used to designate chemical shift multiplicities: s = singlet, d = doublet, t = triplet, m = multiplet or unresolved, br = broad signal and *J* = coupling constants in Hz.

Synthetic Procedures and Characterization Data:

5,6,11,12-tetrahydro-5,11-epoxydibenzo[*a,e*]cyclooctene (5.3):

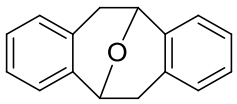

5.3

An oven dried 100 mL Erlenmeyer flask was charged with phenylacetaldehyde (12.5 g, 104 mmol) and freshly distilled dichloromethane (52 mL). The flask was stoppered under an atmosphere of nitrogen and cooled in an ice bath. To this solution was added iodotrimethylsilane (17.5 mL, 125 mmol) and the reaction was allowed to stand at 5 ºC for 7 d. Upon completion, sodium thiosulfate solution (1 M, 100 mL) and dichloromethane (100

mL) were added, and the mixture was stirred until the iodine colour had been discharged. The organic phase was separated, and dried over anhydrous sodium sulfate, filtered and concentrated *in vacuo* yielding a dark brown oil that was purified by silica gel column chromatography eluting 60:40/CH_2Cl_2:hexanes to 100% CH_2Cl_2. The ether (5.78 g, 50 %) was obtained as a brittle brown solid. Spectral data were identical to that previously reported.[33] **R_f** = 0.72 (100 % CH_2Cl_2). **'H NMR (400 MHz, $CDC1_3$)**: δ 7.17-6.99 (m, 8H), 5.32 (d, *J* = 6Hz, 2H), 3.58 (dd, *J* = 16.2, 6.2 Hz, 1H), 2.70 (d, *J* = 16.2 Hz, 2H). **^{13}C NMR (100 MHz, $CDCl_3$)**: δ 137.8, 131.6, 129.0, 126.8, 125.9, 125.1, 69.5, 36.1.

5,6,11,12-tetrahydro-dibenzo[*a,e*]cycloocten-5-ol (5.4):

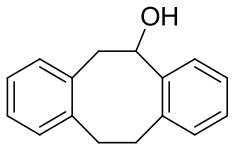

5.4

Li metal (300 mg, ~10 mmol, from a 25% wt./v. dispersion in mineral oil) was placed under Argon in a 15 mL pear shaped flask. The Li metal was washed with THF (3 x 1 mL). The resultant metal was suspended in THF (6 mL) and a catalytic amount of naphthalene (15 mg, 0.1 mmol) was added and the mixture was stirred until it turned a dark green colour. A solution of **5.3** (225 mg, 1 mmol) in THF (0.4 mL) was added drop wise over 5 min. After stirring the reaction mixture for 2 h, a solution of water (23 μL, 1.3 mmol) in THF (1 mL) was carefully added. After stirring for 15 min, the mixture was quenched by slow drop wise addition of H_2O (2 mL) and the resulting mixture extracted with Et_2O (3 x 10 mL). The combined organic phases were washed with brine (10 mL), dried over anhydrous magnesium sulfate, filtered and concentrated. The crude yellow oil was purified by column chromatography eluting 8:2/CH_2Cl_2:hexanes to 100% CH_2Cl_2. The title compound was

obtained as a white crystalline solid (87 mg, 39 %). Spectral data were identical to that previously reported.[33,71] **R_f** = 0.3 (8:2/CH_2Cl_2:hexanes). **^{1}H NMR (400 MHz, $CDCl_3$)**: δ 7.23-6.93 (m, 8H), 5.26 (t, *J* = 8.0 Hz, 1H), 3.54 (dd, *J* = 14.1, 7.7Hz, 1H), 3.43-3.38 (m, 1H), 3.21-3.01 (m, 4H), 2.25 (br, 1H). **^{13}C NMR (100 MHz, $CDCl_3$)**: δ 141.5, 139.3, 138.0, 137.5, 130.1, 130.0, 129.8, 127.5, 126.9, 126.5, 126.4, 126.0, 74.8, 43.7, 35.1, 33.6.

11,12-dihydro-dibenzo[*a,e*]cycloocten-5(*6H*)-one (5.5):

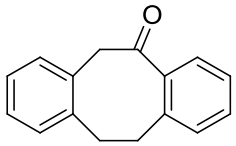

5.5

To a stirring solution of **5.4** (87 mg, 0.39 mmol) in freshly distilled dichloromethane (4 mL), was added crushed 3 Å molecular sieves (150 mg) and the resultant mixture was stirred at room temperature under a stream of nitrogen gas for 5 min. Then pyridinium dichromate (293 mg, 0.78 mmol) was added and the reaction was stirred at room temperature for 8 h until the reaction was complete as evident by thin layer chromatography. The reaction was diluted with dichloromethane (25 mL) and was filtered through a plug of celite. The solvent was removed by rotary evaporation, and the resultant orange residue was purified by flash column chromatography eluting 6:4/CH_2Cl_2:hexanes. This compound was obtained as a white solid (81.2 mg, 94 %). Spectral data corresponds to that previously reported in the literature.[71,72] **R_f** = 0.38 (6:4/CH_2Cl_2:hexanes) **^{1}H NMR (400 MHz, $CDCl_3$)**: δ 7.42-6.99 (m, 8H), 4.16 (s, 2H), 3.40-3.25(m, 4H); **^{13}C NMR (100 MHz, $CDCl_3$)**: δ 204.4, 138.7, 138.4, 137.8, 133.5, 131.5, 130.8, 130.5, 129.6, 128.0, 127.4, 126.7, 126.5, 51.5, 34.7, 33.7.

5,6-didehydro-11,12-dihydro-dibenzo[*a,e*]cyclooctene (5.1):

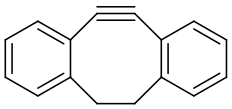

5.1

A stirred solution of **5.5** (991 mg, 4.46 mmol) in freshly distilled THF (44 mL) was cooled to −78 ˚C and *N*-phenyl-trifluoromethanesulfonimide (1.911 g, 5.35 mmol) was added, followed by the slow addition of a potassium bis(trimethylsilyl)amide solution (10.7 mL, 5.35 mmol of a 0.5 M solution in toluene). The resulting mixture was stirred at −78 °C and was allowed to warm to 0 ºC. Potassium bis(trimethylsilyl)amide solution (10.7 mL, 5.35 mmol) was then added drop-wise over 45 minutes at 0 ºC. The reaction was allowed to warm to r.t. for an additional 30 min, then was concentrated *in vacuo*. The crude was purified by flash column chromatography eluting 97:3 to 95:5/Hexanes:CH_2Cl_2. This compound was obtained as an off-white solid (544 mg, 60 %). Spectral data corresponds to that previously reported in the literature.[73] **R_f** = 0.41 (98:2/hexanes:CH_2Cl_2). **^{1}H NMR (400 MHz, $CDCl_3$)**: δ 7.39-7.27 (m, 8H), 3.38-3.29 (m, 2H), 2.51-2.41 (m, 2H). **^{13}C NMR (100 MHz, $CDCl_3$)**: δ 153.5, 129.35, 127.6, 126.5, 126.1, 123.9, 111.5, 36.4.

General Procedure for Micelle-Promoted Nitrone Formation:

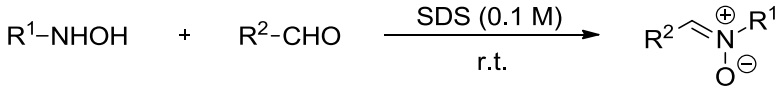

An aldehyde (0.5 mmol), and phenyl hydroxylamine (0.6 mmol, 1.2 equiv.) were added successively to a vigorously stirred solution of SDS (0.2 mmol) dissolved in H_2O (2 mL). The reaction mixture was sonicated for 5 min, and was stirred at r.t. for 2 h. The reaction was monitored by TLC. Upon consumption of the aldehyde, the crude was diluted with brine (5 mL) and extracted with EtOAc (3 x 5 mL). The combined organic phases were dried over

anhydrous $MgSO_4$, filtered, and concentrated *in vacuo*. The crude was purified by flash column chromatography.

***N*-(phenylmethylene)-benzenamine *N*-oxide (5.13):**

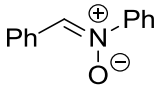

5.13

This compound was obtained in 86 % yield by following the general procedure for micelle promoted nitrone formation. $\mathbf{R_f}$ = 0.30 (7:3/Hexanes:EtOAc). Spectral data corresponded to that previously described in the literature.[74]

4-[(methyloxidoimino)methyl]-benzoic acid methyl ester (5.18):

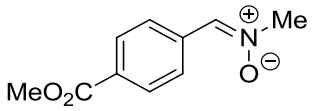

5.18

This compound was obtained in 72 % yield by following the general procedure for micelle promoted nitrone formation. $\mathbf{R_f}$ = 0.25 (7:3/Hexanes:EtOAc). Spectral data corresponded to that previously described in the literature.[75]

***N*-(phenylmethylene)-methanamine *N*-oxide (5.19):**

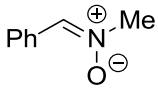

5.19

This compound was obtained in 86 % yield by following the general procedure for micelle promoted nitrone formation. $\mathbf{R_f}$ = 0.39 (95:5/EtOAc:MeOH). Spectral data corresponded to that previously described in the literature.[74]

***N*-[(4-methoxyphenyl)methylene]-methanamine *N*-oxide (5.20):**

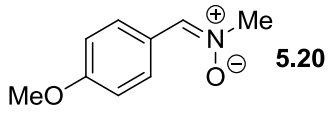

5.20

This compound was obtained in 88 % yield by following the general procedure for micelle promoted nitrone formation. $\mathbf{R_f}$ = 0.27 (96:4/EtOAc:MeOH). Spectral data corresponded to that previously described in the literature.[76]

***N*-[(4-nitrophenyl)methylene]-benzenemethanamine *N*-oxide (5.21):**

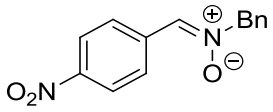

5.21

This compound was obtained in 81 % yield by following the general procedure for micelle promoted nitrone formation. $\mathbf{R_f}$ = 0.38 (1:1/hexanes:EtOAc). Spectral data corresponded to that previously described in the literature.[77]

4-[[oxido(phenylmethyl)imino]methyl]-benzoic acid methyl ester (5.22):

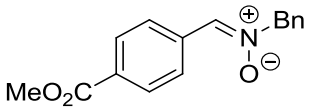

5.22

This compound was obtained in 76 % yield by following the general procedure for micelle promoted nitrone formation. $\mathbf{R_f}$ = 0.41 (6:4/hexanes:EtOAc). Spectral data corresponded to that previously described in the literature.[74]

***N*-[(4-bromophenyl)methylene]-benzenemethanamine *N*-oxide (5.23):**

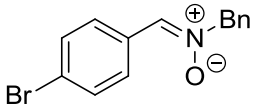

5.23

This compound was obtained in 85 % yield by following the general procedure for micelle promoted nitrone formation. $\mathbf{R_f}$ = 0.70 (1:1/hexanes:EtOAc). Spectral data corresponded to that previously described in the literature.[78]

4-[[oxido(phenylmethyl)imino]methyl]-benzonitrile (5.24):

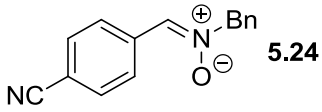

5.24

This compound was obtained in 78 % yield by following the general procedure for micelle promoted nitrone formation. $\mathbf{R_f}$ = 0.42 (1:1/hexanes:EtOAc). Spectral data corresponded to that previously described in the literature.[79]

***N*-[(4-methylphenyl)methylene]-benzenemethanamine *N*-oxide (5.25):**

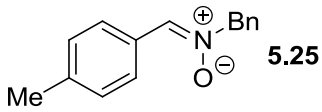

5.25

This compound was obtained in 86 % yield by following the general procedure for micelle promoted nitrone formation. $\mathbf{R_f}$ = 0.42 (1:1/hexanes:EtOAc). Spectral data corresponds to that previously described in the literature.[80]

***N*-(phenylmethylene)-benzenemethanamine *N*-oxide (5.26):**

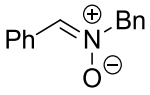

5.26

This compound was obtained in 78 % yield by following the general procedure for micelle promoted nitrone formation. $\mathbf{R_f}$ = 0.46 (1:1/hexanes:EtOAc). Spectral data corresponds to that previously described in the literature.[74]

***N*-[(4-methoxyphenyl)methylene]-benzenemethanamine *N*-oxide (5.27):**

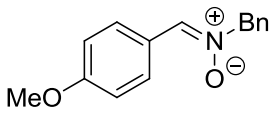

5.27

This compound was obtained in 73 % yield by following the general procedure for micelle promoted nitrone formation. $\mathbf{R_f}$ = 0.27 (1:1/hexanes:EtOAc). Spectral data corresponds to that previously described in the literature.[80]

3,4-dihydro-*2H*-pyrrole 1-oxide (5.38):

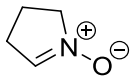

5.38

Synthesis previously reported in the literature.[52]

4-(*tert*-butoxycarbonylamino)-3,4-dihydro-*2H*-pyrrole 1-oxide (5.39) and **3-(*tert*-butoxycarbonylamino)-3,4-dihydro-*2H*-pyrrole 1-oxide (5.53):**

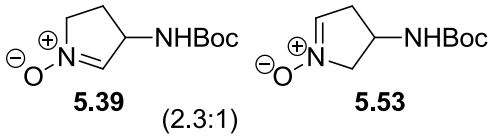

5.39 (2.3:1) **5.53**

mixture of regioisomers

$NaHCO_3$ (1.68 g, 20 mmol) was added to a stirred solution of 3-(Boc-amino)-pyrrolidine (745.2 mg, 4 mmol) in 4:1/acetonitrile:THF (7.4 mL) and Na_2EDTA (0.01 M, 5.6 mL). The resultant mixture was then cooled to 0 ˚C using an ice bath and Oxone® (2.95 g, 4.8 mmol) was added portion wise over 2 h. The mixture was stirred at 5 ºC for 20 min and then diluted with EtOAc (20 mL). The two phases were separated and the aqueous one was extracted with CH_2Cl_2 (3 x 10 mL). The combined organic extracts were dried over anhydrous $MgSO_4$, filtered, and concentrated *in vacuo*. The crude was purified by silica gel column chromatography eluting 15:7:1/CH_2Cl_2:EtOAc:MeOH. The title compounds, **5.39** (400 mg,

2.01 mmol) and **5.53** (174 mmol, 0.87 mmol) were obtained as white solids in a combined yield of 72 %. Spectral data corresponded to that previously reported in the literature.[81] **Compound 5.39: R_f** = 0.13 (15:7:1/CH_2Cl_2:EtOAc:MeOH). **^{1}H NMR ($CDCl_3$, 400 MHz)**: δ 6.84 (q, *J* = 1.7 Hz, 1H), 5.62 (m, 1H), 4.96 (br s, 1H), 4.11-4.03 (m, 1H), 3.92-3.83 (m, 1H), 2.68-2.64 (m, 1H), 2.04-1.98 (m, 1H), 1.41 (s, 9H). **^{13}C NMR ($CDCl_3$, 100 MHz)**: δ 155.0 (C), 134.9 (CH), 80.4 (C), 61.4 (CH2), 52.4 (CH), 28.5 (CH_2), 28.4 (CH3). **LRMS**: Calculated for $C_9H_{17}N_2O_3$ (M^+) 201.1, Found 201.2. **Compound 5.53: R_f** = 0.10 (15:7:1/CH_2Cl_2:EtOAc:MeOH). **^{1}H NMR ($CDCl_3$, 400 MHz)**: δ 6.87 (m, 1H), 5.41 (m, 1H), 4.51 (br s, 1H), 4.26-4.21 (dd, *J* = 14.2, 7.8 Hz, 1H), 3.82 (d, *J* = 14.6 Hz, 1H), 3.13 (dd, *J* = 18.5, 6.5 Hz, 1H), 2.61 (d, *J* = 19.0 Hz, 1H), 1.43 (s, 1H). **^{13}C NMR ($CDCl_3$, 100 MHz)**: δ 155.2 (C), 133.6 (CH), 80.5 (C), 68.3 (CH), 45.8 (CH), 37.0 (CH_2), 28.5 (CH_3). **LRMS** : Calculated for $C_9H_{17}N_2O_3$ (M^+) 201.1, found 201.1.

3,4-dihydroisoquinoline 2-oxide (5.40):

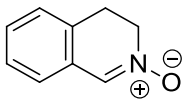

5.40

Synthesis previously reported in the literature.[52]

General Procedure for Strain-Promoted Alkyne-Nitrone Cycloadditions:

To a stirring solution of dibenzocyclooctyne, **5.1** (10.2 mg, 0.05 mmol) in toluene (500 µL) was added nitrone (0.05 mmol). Reactions were stirred open to air and were monitored by thin layer chromatography for disappearance of the nitrone. Upon completion, the solvent was removed under reduced pressure and the crude was purified by silica gel flash column chromatography to afford pure isoxazoline cycloadducts.

4-(2,3,8,9-tetrahydro-2-methyldibenzo[3,4:7,8]cyclooct[1,2-*d*]isoxazol-3-yl)-benzoic acid methyl ester (5.28):

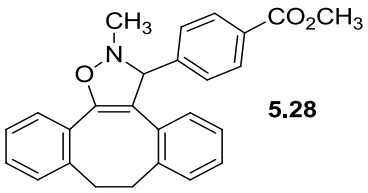

5.28

Purified by eluting 9:1/hexanes:EtOAc. This compound was obtained as a white solid (19.0 mg, 95%). $\mathbf{R_f}$ = 0.34 (9:1/hexanes:EtOAc). **^{1}H NMR ($CDCl_3$, 400 MHz)**: δ 7.96 (d, *J* = 8.3Hz, 2H), 7.52-7.50 (m, 1H), 7.45 (d, *J* = 8.3Hz, 2H), 7.18-7.04 (m, 7H), 5.09 (s, 1H), 3.89 (s, 3H), 3.41-3.33 (m, 1H), 3.15 (s, 3H), 3.19-2.98 (m, 2H), 2.88-2.81 (m, 1H). **^{13}C NMR ($CDCl_3$, 100 MHz)**: δ 167.0, 147.3, 146.2, 141.1, 139.1, 131.9, 131.0, 129.9, 129.8, 129.7, 129.3, 128.8, 127.9, 127.5, 127.2, 126.5, 125.8, 125.5, 109.8, 80.3, 52.0, 47.0, 36.7, 35.7, 32.8. **HRMS**: Calculated for $C_{26}H_{23}NO_3$ (M^+) 398.1756, Found 398.1744.

2,3,8,9-tetrahydro-2-methyl-3-phenyl-dibenzo[3,4:7,8]cyclooct[1,2-*d*]isoxazole (5.29):

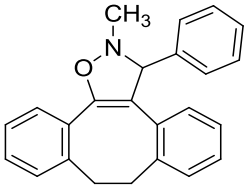

5.29

Purified by eluting 96:4/hexanes:EtOAc. This compound was obtained as a white solid (15.2 mg, 90%). $\mathbf{R_f}$ = 0.41 (96:4/hexanes:EtOAc). **^{1}H NMR ($CDCl_3$, 400 MHz, 298 K, $CHCl_3$)**: δ 7.54-6.98 (m, 13H), 5.03 (m, 1H), 3.45-3.38 (m, 1H), 3.23-3.08 (m, 2H), 3.13 (s, 3H), 3.00-2.93 (m, 1H). **^{13}C NMR ($CDCl_3$, 100 MHz, 298 K, $CHCl_3$)**: δ 147.3, 141.1, 138.9, 132.4, 131.0, 129.8, 129.6, 128.6, 128.6, 127.9, 127.8, 127.6, 127.0, 126.8, 125.7, 125.5, 110.2, 80.9, 47.1, 36.9, 32.9. **HRMS**: Calculated for $C_{24}H_{21}NO$ (M^+) 340.1701, Found 340.1660.

2,3,8,9-tetrahydro-3-(4-methoxyphenyl)-2-methyl-dibenzo[3,4:7,8]cyclooct[1,2-*d*]isoxazole (5.30):

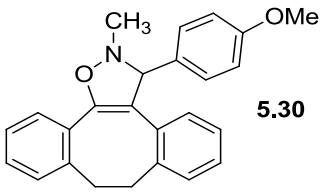

5.30

Purified by eluting 95:5/hexanes:EtOAc. This compound was obtained as a white solid (19.0 mg, 94%). $\mathbf{R_f}$ = 0.43 (95:5/hexanes:EtOAc). **^{1}H NMR ($CDCl_3$, 400 MHz)**: δ 7.53-7.51 (m, 1H), 7.32 (d, *J* = 8.7Hz, 2H), 7.18-6.94 (m, 7H), 6.84 (d, *J* = 8.7Hz, 2H), 4.99 (s, 1H), 3.78 (s, 3H), 3.46-3.39 (m, 1H), 3.26-3.08 (m, 2H), 3.10 (s, 3H), 3.05-2.98 (m, 1H). **^{13}C NMR ($CDCl_3$, 100 MHz, 298 K, $CHCl_3$)** : δ 159.1, 147.3, 141.0, 138.8, 132.5, 131.0, 129.8, 129.6, 128.5, 128.2, 128.0, 127.7, 126.9, 125.7, 125.5, 114.0, 110.3, 80.5, 55.2, 37.0, 32.9. **HRMS**: Calculated for $C_{25}H_{23}NO_2$ (M^+) 370.1807, found 370.1721.

2,3,8,9-tetrahydro-3-(4-nitrophenyl)-2-(phenylmethyl)-dibenzo[3,4:7,8]cyclooct[1,2-*d*]isoxazole (5.31):

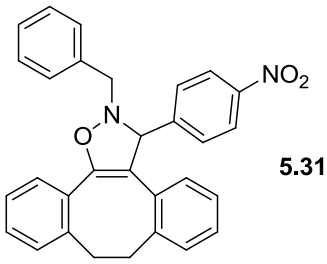

5.31

Purified by eluting 9:1/hexanes:EtOAc. This compound was obtained as a yellow solid (22.3 mg, 97%). $\mathbf{R_f}$ = 0.18 (9:1/hexanes:EtOAc). **^{1}H NMR ($CDCl_3$, 400 MHz)**: δ 8.11 (d, *J* = 8.8 Hz, 2H), 7.55-7.09 (m, 15H), 5.36 (s, 1H), 4.72 (d, *J* = 12.7 Hz, 1H), 4.33 (d, *J* = 12.7 Hz, 1H), 3.39-3.32 (m, 1H), 3.14-2.85 (m, 2H), 2.84-2.78 (m, 1H). **^{13}C NMR ($CDCl_3$, 100**

MHz): δ 148.5, 148.3, 147.2, 141.1, 139.2, 135.7, 131.6, 131.0, 130.0, 129.3, 129.3, 129.1, 128.7, 127.9, 127.4, 127.3, 127.2, 126.0, 125.6, 123.7, 109.5, 76.3, 62.9, 36.5, 33.0. **HRMS**: Calculated for $C_{30}H_{24}N_2O_3$ (M^+) 461.1865, Found 461.1866.

4-[2,3,8,9-tetrahydro-2-(phenylmethyl)dibenzo[3,4:7,8]cyclooct[1,2-*d*]isoxazol-3-yl]-benzoic acid methyl ester (5.32):

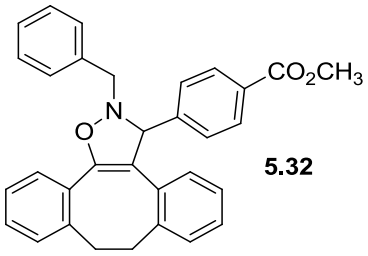

5.32

Purified by eluting 9:1/hexanes:EtOAc. This compound was obtained as a white solid (19.2 mg, 96%). $\mathbf{R_f}$ = 0.31 (9:1/hexanes:EtOAc). **^{1}H NMR ($CDCl_3$, 400 MHz)**: δ 7.93 (d, *J* = 8.3Hz, 2H), 7.53-7.02 (m, 15H), 5.30 (s, 1H), 4.67 (d, *J* = 12.8 Hz, 1H), 4.32 (d, *J* = 12.8 Hz, 1H), 3.89 (s, 3H), 3.39-3.32 (m, 1H), 3.15-2.98 (m, 2H), 2.87-2.80 (m, 1H). **^{13}C NMR ($CDCl_3$, 100 MHz)**: δ 167.0, 148.0, 146.4, 141.1, 139.2, 136.0, 132.0, 131.0, 130.0, 129.8, 129.3, 129.2, 128.8, 128.6, 128.0, 127.8, 127.6, 127.2, 126.6, 125.8, 125.6, 110.0, 76.9, 63.0, 52.0, 36.6, 33.0. **HRMS**: Calculated for $C_{32}H_{27}NO_3$ (M^+) 474.2069, Found 474.2080.

3-(4-bromophenyl)-2,3,8,9-tetrahydro-2-(phenylmethyl)-dibenzo[3,4:7,8]cyclooct[1,2-*d*]isoxazole (5.33):

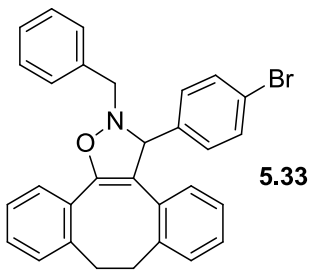

5.33

Purified by eluting 9:1/hexanes:EtOAc. This compound was obtained as an off white solid (24.2 mg, 98%). $\mathbf{R_f}$ = 0.55 (9:1/hexanes:EtOAc). **^{1}H NMR ($CDCl_3$, 400 MHz)**: δ 7.52-7.00 (m, 17H), 5.21 (s, 1H), 4.65 (d, *J* = 12.8 Hz, 1H), 4.30 (d, *J* = 12.8 Hz, 1H), 3.42-3.35 (m, 1H), 3.20-3.04 (m, 2H), 2.95-2.88 (m, 1H). **^{13}C NMR ($CDCl_3$, 100 MHz, 298 K, $CHCl_3$)** : δ 148.0, 141.1, 140.5, 139.1, 136.0, 132.1, 131.6, 131.0, 130.0, 129.8, 129.3, 128.8, 128.6, 128.5, 127.9, 127.8, 127.7, 127.1, 125.8, 125.6, 121.3, 110.0, 63.0, 36.7, 33.0. **HRMS**: Calculated for $C_{30}H_{24}NOBr$ (M^+) 494.1120, Found 494.1098.

4-[2,3,8,9-tetrahydro-2-(phenylmethyl)dibenzo[3,4:7,8]cyclooct[1,2-*d*]isoxazol-3-yl]-Benzonitrile (5.34):

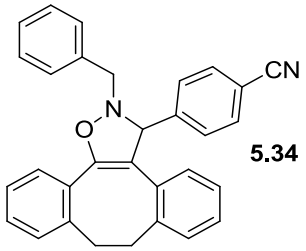

5.34

Purified by eluting 9:1/hexanes:EtOAc. This compound was obtained as an off white solid (21.7 mg, 99%). $\mathbf{R_f}$ = 0.26 (9:1/Hexanes:EtOAc). **^{1}H NMR ($CDCl_3$, 400 MHz)**: δ 7.55-7.05 (m, 17H), 5.30 (s, 1H), 4.70 (d, *J* = 12.7 Hz, 1H), 4.30 (d, *J* = 12.7Hz, 1H), 3.39-3.32 (m, 1H), 3.15-2.96 (m, 2H), 2.87-2.80 (m, 1H). **^{13}C NMR ($CDCl_3$, 100 MHz)**: δ 148.2, 146.5, 141.0, 139.2, 135.7, 132.3, 131.6, 131.0, 129.9, 129.3, 129.0, 128.6, 127.9, 127.9, 127.3, 127.3, 127.1, 125.9, 125.6, 118.9, 111.1, 109.5, 76.5, 62.8, 36.5, 32.9. **LRMS** : Calculated for $C_{31}H_{24}N_2O$ (M^+) 455.4, Found 455.4.

2,3,8,9-tetrahydro-3-(4-methylphenyl)-2-(phenylmethyl)-dibenzo[3,4:7,8]cyclooct[1,2-*d*]isoxazole (5.35):

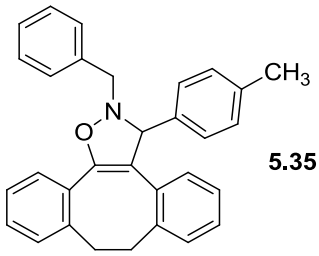

5.35

Purified by eluting 9:1/hexanes:EtOAc. This compound was obtained as a slow crystallizing white solid (23.2 mg, 94%). $\mathbf{R_f}$ = 0.43 (9:1/hexanes:EtOAc). **^{1}H NMR ($CDCl_3$, 400 MHz)**: δ 7.53-6.96 (m, 17H), 5.22 (s, 1H), 4.62 (d, *J* = 12.9Hz, 1H), 4.31 (d, *J* = 12.9Hz, 1H), 3.45-3.38 (m, 1H), 3.25-3.09 (m, 2H), 3.01-2.94 (m, 1H), 2.31 (s, 3H). **^{13}C NMR ($CDCl_3$, 100 MHz)**: δ 147.9, 141.0, 138.9, 138.4, 137.1, 136.3, 132.6, 131.0, 129.9, 129.6, 129.4, 129.2, 128.5, 128.5, 128.1, 127.9, 127.6, 126.9, 126.9, 125.7, 125.5, 110.5, 63.1, 36.9, 33.0, 21.1. **HRMS**: Calculated for $C_{31}H_{27}NO$ (M^+) 430.2171, Found 430.2108.

2,3,8,9-tetrahydro-3-phenyl-2-(phenylmethyl)-dibenzo[3,4:7,8]cyclooct[1,2-*d*]isoxazole (5.36):

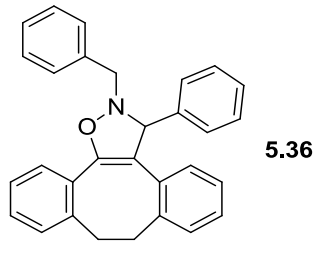

5.36

Purified by eluting 9:1/hexanes:EtOAc. This compound was obtained as a white solid (19.2 mg, 92%). $\mathbf{R_f}$ = 0.33 (9:1/hexanes:EtOAc). **^{1}H NMR ($CDCl_3$, 400 MHz)**: δ 7.53-6.96 (m, 18H), 5.24 (s, 1H), 4.63 (d, *J* = 12.9 Hz, 1H), 4.31 (d, *J* = 12.9 Hz, 1H), 3.43-3.35 (m, 1H), 3.22-3.05 (m, 2H), 2.97-2.90 (m, 1H). **^{13}C NMR ($CDCl_3$, 100 MHz)**: δ 147.9, 141.4, 141.0,

139.0, 136.3, 132.5, 131.0, 130.0, 129.7, 129.4, 128.6, 128.5, 128.5, 127.9, 127.6, 127.4, 127.0, 125.7 ,125.5, 110.4, 63.1, 36.8, 33.0. **HRMS**: Calculated for $C_{30}H_{25}NO$ (M^+) 416.2014, Found 416.1977.

2,3,8,9-tetrahydro-3-(4-methoxyphenyl)-2-(phenylmethyl)-dibenzo[3,4:7,8]cyclooct[1,2-*d*]isoxazole (5.37):

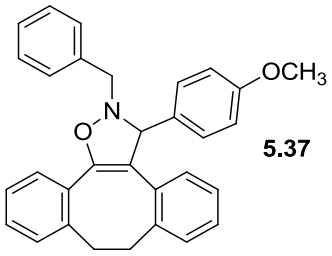

5.37

Purified by eluting 9:1/hexanes:EtOAc. This compound was obtained as a white solid (21.0 mg, 95%). $\mathbf{R_f}$ = 0.44 (9:1/hexanes:EtOAc). **^{1}H NMR ($CDCl_3$, 400 MHz)**: δ 7.52-6.81 (m, 17H), 5.21 (s, 1H), 4.61 (d, *J* = 12.9 Hz, 1H), 4.30 (d, *J* = 12.9 Hz, 1H), 3.78 (s, 3H), 3.45-3.37 (m, 1H), 3.26-3.09 (m, 2H), 3.03-2.96 (m, 1H). **^{13}C NMR ($CDCl_3$, 100 MHz)**: δ 159.0, 147.9, 141.0, 138.9, 136.3, 133.6, 132.6, 131.0, 129.9, 129.6, 129.4, 128.5, 128.5, 128.2, 128.0, 127.8, 127.6, 126.9, 125.7, 125.5, 113.9, 110.4, 63.0, 55.2, 36.9, 33.0. **HRMS**: Calculated for $C_{31}H_{27}NO_2$ (M^+) 446.1946, Found 446.1952.

Compound 5.16:

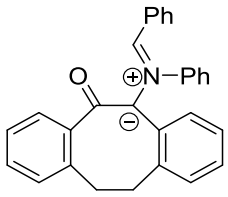

5.16

Purified by eluting 95:5/hexanes:EtOAc. This compound was obtained as an off white solid (19.3 mg, 96%). $\mathbf{R_f}$ = 0.52 (95:5/hexanes:EtOAc). **^{1}H NMR ($CDCl_3$, 400 MHz**): δ 7.86-6.80

(m, 18H), 6.73 (s, 1H), 3.94-3.83 (m, 2H), 3.25-3.13 (m, 2H). **^{13}C NMR ($CDCl_3$, 100 MHz)**: δ 147.3, 141.5, 139.6, 139.5, 138.5, 131.0, 130.8, 130.1,129.7, 129.1, 128.9, 128.8, 128.3, 127.0, 126.3, 126.1, 125.7, 121.0, 119.6, 117.8, 97.9, 35.6, 35.3. **LRMS**: Calculated for $C_{29}H_{23}NO$ (M^+) 402.4, Found 402.4.

1,2,3,3a,8,9-hexahydro-dibenzo[3,4:7,8]cycloocta[1,2-*d*]pyrrolo[1,2-*b*]isoxazole (5.41):

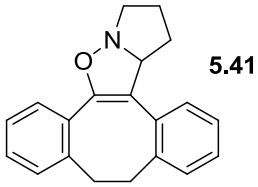

5.41

Purified by eluting 7:3/hexanes:EtOAc. This compound was obtained as a white solid (14.4 mg, 100%). **R_f** = 0.33 (7:3/hexanes:EtOAc). **^{1}H NMR ($CDCl_3$, 400 MHz)**: δ 7.47-7.08 (m, 8H), 5.21 (dd, *J* = 7.3 Hz, 2.2 Hz, 1H), 3.62-3.49 (m, 2H), 3.47-3.40 (m, 1H), 3.32-3.25 (m, 1H), 3.17-3.09 (m, 1H), 2.99-2.92 (m, 1H). 2.07-1.82 (m, 4H). **^{13}C NMR ($CDCl_3$, 100 MHz)**: δ 148.0, 140.8, 138.2, 132.6, 130.9, 129.7, 129.5, 128.4, 128.0, 127.0, 126.0, 125.6, 109.1, 74.9, 59.9, 36.9, 33.3, 31.3, 22.9. **LRMS**: Calculated for $C_{20}H_{19}NO$ (M^+) 290.3, Found 290.3.

(±)-*N*-[-1,2,3,3a,8,9-hexahydrodibenzo[3,4:7,8]cycloocta[1,2-*d*]pyrrolo[1,2-*b*]isoxazol-3-yl]-2,2-dimethyl-propanamide (5.42):

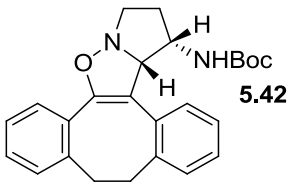

5.42

Purified by eluting 6:4/hexanes:EtOAc. This compound was obtained as a white crystalline solid (20.2 mg, 100%). **R_f** = 0.56 (6:4/hexanes:EtOAc). **^{1}H NMR ($CDCl_3$, 400 MHz)**: δ

7.43-7.08 (m, 8H), 4.94 (s, 1H), 4.76 (d, J = 1.9 Hz, 1H), 4.07 (m, 1H), 3.65-3.56 (m, 1H), 3.55-3.47 (m, 2H), 3.43-3.36 (m, 1H), 3.17-3.09 (m, 1H), 3.00-2.94 (m, 1H), 2.37-2.32 (m, 1H), 1.91-1.88 (m, 1H), 1.37 (s, 9H). **^{13}C NMR ($CDCl_3$, 100 MHz)**: δ 154.8, 149.0, 140.5, 138.4, 131.6, 130.9, 129.9, 129.4, 128.7, 128.1, 127.5, 127.2, 126.1, 125.6, 57.8, 36.7, 33.3, 30.6, 28.3. **LRMS**: Calculated for $C_{25}H_{28}N_2O_3$ (M^+) 405.4, Found 405.4.

4b,10,17,18-tetrahydro-*9H*-dibenzo[3',4':7',8']cyclooct[1',2':4,5]isoxazolo[3,2-*a*]isoquinoline (5.43):

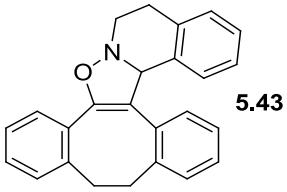

5.43

Purified by eluting 9:1/hexanes:EtOAc. This compound was obtained as a white crystalline solid (17.3 mg, 98%). **R_f** = 0.23 (9:1/hexanes:EtOAc). **^{1}H NMR ($CDCl_3$, 400 MHz)**: δ 7.50-7.48 (m, 1H), 7.17-7.06 (m, 9H), 6.96-6.92 (m, 1H), 6.58 (d, J = 7.7 Hz, 1H), 5.97 (s, 1H), 3.93-3.89 (m, 1H), 3.36-3.22 (m, 3H), 3.10-3.03 (m, 1H), 2.85-2.75 (m, 3H). **^{13}C NMR ($CDCl_3$, 100 MHz)**: δ 148.3, 141.3, 138.9, 135.1, 133.6, 132.1, 131.0, 130.0, 129.4, 129.3, 128.8, 128.3, 127.8, 127.2, 126.6, 126.4, 126.0, 125.6, 125.5, 111.3, 71.1, 50.8, 36.7, 32.7, 24.5. **HRMS**: Calculated for $C_{25}H_{21}NO$ (M^+) 352.1701, Found 352.1683.

Kinetic Measurements of Strain-Promoted Alkyne-Nitrone Cycloadditions:

The appropriate nitrone or benzyl azide and **5.1** were pre-dissolved in C_6D_6 and mixed at equimolar concentrations of ~50 mM. Percent conversion was monitored both by disappearance of starting materials and by appearance of product as determined by integration at multiple chemical shifts in the ^{1}H NMR spectrum. No other products were

detected by ^{1}H NMR and all reactions were performed in triplicate. Second order rate constants in units of $M^{-1}s^{-1}$ were determined by plotting 1/[nitrone] or 1/[azide] versus time and subsequently using analysis by linear regression. The second order rate constant k_2 ($M^{-1}s^{-1}$) corresponded to the determined slope.

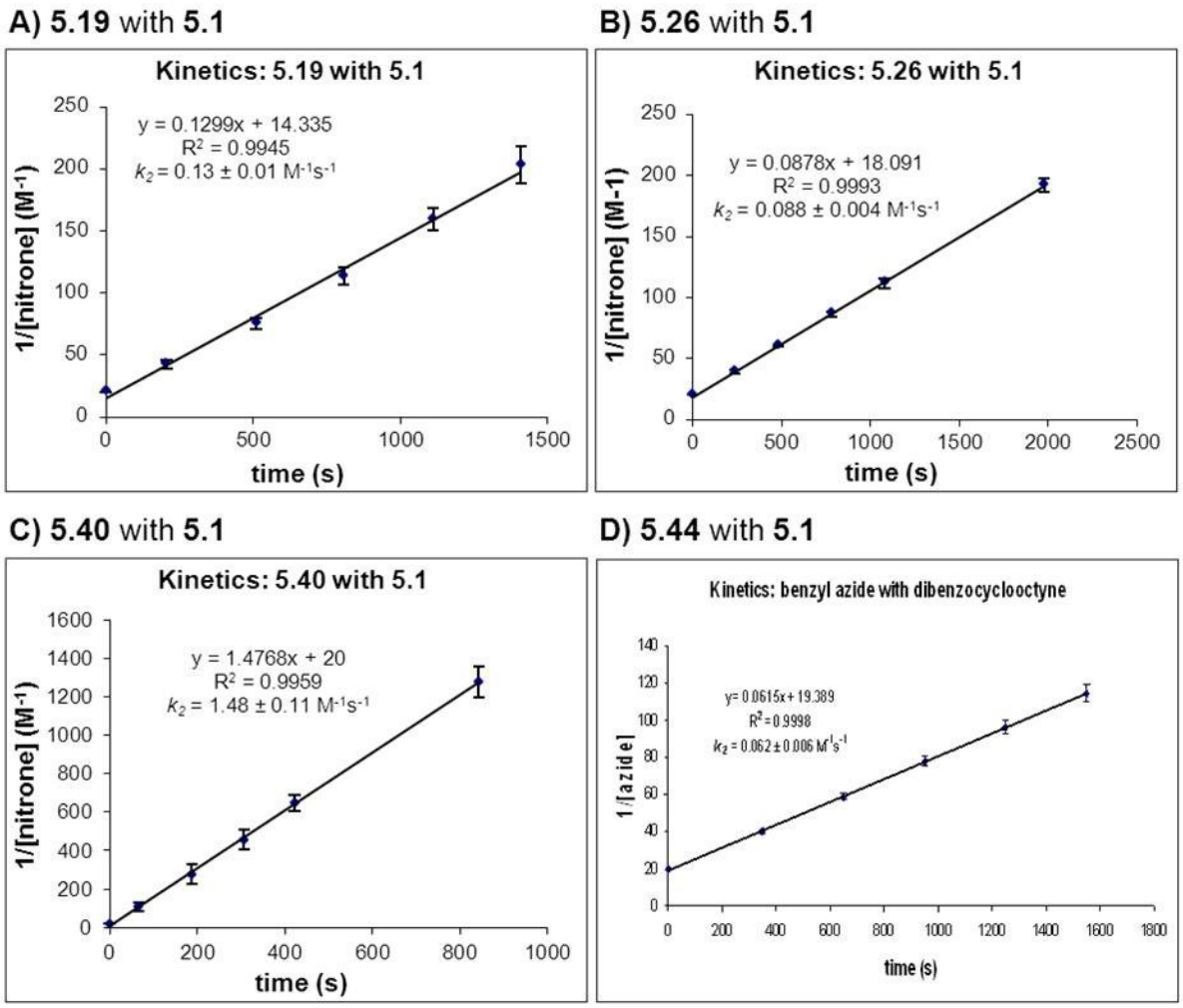

Figure 5-1. Kinetics of SPANC and SPAAC reactions. A) **5.19** with **5.1**, B) **5.26** and **5.1**, C) **5.40** with **5.1**, and D) **5.44** with **5.1**.

General Procedure for Strain-Promoted Alkyne-Diazoalkane Cycloadditions:

A solution of diazoalkane (0.025 mmol) in MeOH (0.5 mL) was combined with a solution of dibenzocyclooctyne (5.1 mg, 0.025 mmol) in MeOH (0.5 mL). Reaction progress was

monitored by thin layer chromatography. Upon completion, the solvent was removed by rotary evaporation and the products (**5.49-5.52**) were purified by flash column chromatography.

diphenyl diazomethane (5.45) and phenyldiazomethane (5.48):

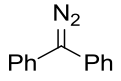

5.45

5.48

Synthesis previously reported in the literature.[82]

Characterization Data for SPADC Cycloadducts:

8,9-dihydro-3,3-diphenyl-*3H*-dibenzo[3,4:7,8]cycloocta[1,2]pyrazole (5.49):

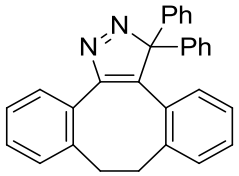

5.49

Compound 5.41: Purified by eluting 95:5/hexanes:CH_2Cl_2. This compound was obtained as a white solid (10.0 mg, 100 %). $\mathbf{R_f}$ = 0.35 (95:5/hexanes:CH_2Cl_2). **^{1}H NMR (*d_6*-DMSO, 400MHz)**: δ 7.71-7.69 (m, 1H), 7.47-7.39 (m, 8H), 7.31-7.24 (m, 5H), 7.10-7.08 (m, 4H), 6.97 (t, 1H), 6.32 (d, 1H), 3.25 (t, *J* = 6.8Hz, 2H), 2.72 (t, *J* = 6.8Hz, 2H). **^{13}C NMR (*d_6*-DMSO, 100MHz)**: δ 154.1, 148.9, 140.8, 138.1, 134.3, 132.0, 131.4, 130.9, 129.8, 129.4, 129.3, 129.2, 129.0, 128.8, 128.6, 127.7, 125.9, 125.9, 125.8, 125.6, 124.8, 107.5, 36.4, 31.0. **HRMS**: Calculated for $C_{29}H_{22}N_2$ (M^+) 399.1861, Found 399.2023.

8,9-dihydro-*1H*-dibenzo[3,4:7,8]cycloocta[1,2]pyrazole-3-carboxylic acid ethyl ester (5.50):

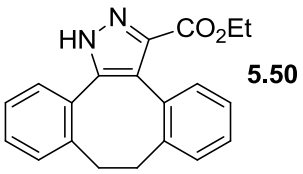

5.50

Purified by eluting 6:4/hexanes:EtOAc. This compound was obtained as a white solid (7.7 mg, 97 %). $\mathbf{R_f}$ = 0.35 (6:4/hexanes:EtOAc). **^{1}H NMR ($CDCl_3$, 400MHz)**: δ 10.98 (br s, 1H), 7.33-7.17 (m, 8H), 4.39-4.28 (m, 2H), 3.43-3.40 (m, 1H), 3.24-3.13 (m, 2H), 2.93-2.91 (m, 1H), 1.30 (t, 3H). **^{13}C NMR ($CDCl_3$, 100MHz)**: δ 160.7, 139.8, 139.1, 131.5, 131.1, 131.0, 130.9, 130.0, 129.0, 128.7, 127.9, 126.0, 125.3, 123.6, 61.1, 36.4, 33.0, 14.1. **HRMS**: Calculated for $C_{20}H_{19}N_2O_2$ (M^+) 319.1447, Found 319.1468.

8,9-dihydro-*1H*-dibenzo[3,4:7,8]cycloocta[1,2]pyrazole (5.51):

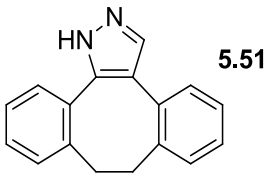

5.51

Purified by eluting 9:1/hexanes:EtOAc. This compound was obtained as a white solid (2.1 mg, 34 %). $\mathbf{R_f}$ = 0.35 (9:1/hexanes:EtOAc). **^{1}H NMR ($CDCl_3$, 400MHz)**: δ 7.64 (br s, 1H), 7.31-7.18 (m, 9H), 3.28-3.16 (m, 4H). **^{13}C NMR ($CDCl_3$, 100MHz)**: 139.6, 139.3, 132.3, 130.8, 130.6, 130.2, 130.1, 128.5, 127.2, 126.1, 126.0, 35.6, 34.3. **HRMS**: Calculated for $C_{17}H_{14}N_2$ ($2M^+$) 494.2392, Found 493.2445.

8,9-dihydro-3-phenyl-*1H*-dibenzo[3,4:7,8]cycloocta[1,2]pyrazole (5.52):

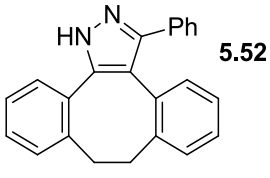

5.52

Purified by eluting 8:2/hexanes:EtOAc. This compound was obtained as a white solid (7.5 mg, 93 %). $\mathbf{R_f}$ = 0.28 (8:2/hexanes:EtOAc). **^{1}H NMR ($CDCl_3$, 400MHz)**: δ 8.01 (br s, 1H), 7.46–6.90 (m, 13H), 3.54-3.27 (m, 2H), 3.18–2.89 (m, 2H). **^{13}C NMR ($CDCl_3$, 100MHz)**: δ 140.1, 139.3, 132.2, 131.2, 131.0, 130.4, 130.0, 129.8, 128.7, 128.5, 128.2, 127.8, 127.4, 126.0, 126.0, 118.4, 36.0, 33.6. **LRMS**: Calculated for $C_{23}H_{18}N_2$ (M^+) 323.1, Found 323.2.

Kinetics Measurements of Strain-Promoted Alkyne-Diazoalkane Cycloadditions:

The diazocompound (50 mM) and **5.1** (50 mM) were pre-dissolved in d_6-methanol and mixed at equimolar concentration of ~25 mM. Percent conversion was monitored both by disappearance of starting materials and by appearance of product as determined by integration at multiple chemical shifts in the ^{1}H NMR spectrum. Second order rate constants in units of $M^{-1}s^{-1}$ were determined by plotting 1/[cyclooctyne] versus time. The second order rate constant k_2 ($M^{-1}s^{-1}$) corresponded to the determined slope.

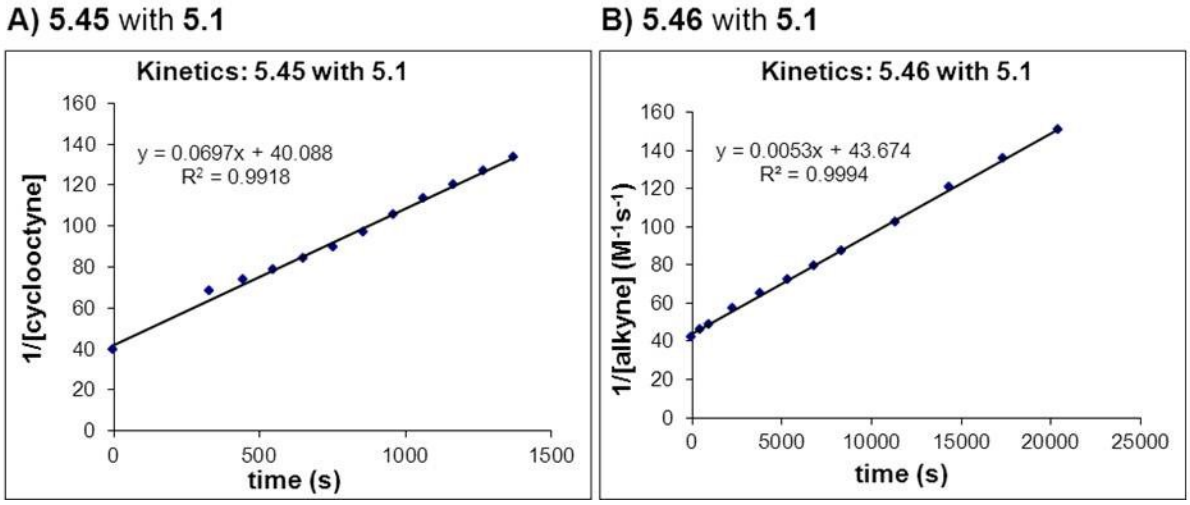

Figure 5-2. Kinetics of SPADC. A) Reaction of **5.45** with **5.1**, B) Reaction of **5.46** with **5.1**.

References

(1) Debets, M. F.; van Berkel, S. S.; Dommerholt, J.; Dirks, A. J.; Rutjes, F. P. J. T.; van Delft, F. L. *Acc. Chem. Res.* **2011**, *44*, 805-815.
(2) Lim, R. K. V.; Lin, Q. *Chem. Commun.* **2010**, *46*, 1589-1600.
(3) Sletten, E. M.; Bertozzi, C. R. *Angew. Chem. Int. Ed.* **2009**, *48*, 6974-6998.
(4) Jewett, J. C.; Bertozzi, C. R. *Chem. Soc. Rev.* **2010**, *39*, 1272-1279.
(5) Wittig, G.; Krebs, A. *Chem. Ber.* **1961**, *94*, 3260-3275.
(6) Agard, N. J.; Baskin, J. M.; Prescher, J. A.; Lo, A.; Bertozzi, C. R. *ACS Chem. Biol.* **2006**, *1*, 644-648.
(7) Link, A. J.; Vink, M. K. S.; Agard, N. J.; Prescher, J. A.; Bertozzi, C. R.; Tirrell, D. A. *Proc. Natl. Acad. Sci. U.S.A.* **2006**, *103*, 10180-10185.
(8) Fernandez-Suarez, M.; Baruah, H.; Martinez-Hernandez, L.; Xie, K. T.; Baskin, J. M.; Bertozzi, C. R.; Ting, A. Y. *Nat. Biotechnol.* **2007**, *25*, 1483-1487.
(9) Nessen, M. A.; Kramer, G.; Back, J.; Baskin, J. M.; Smeenk, L. E. J.; de Koning, L. J.; van Maarseveen, J. H.; de Jong, L.; Bertozzi, C. R.; Hiemstra, H.; de Koster, C. G. *J. Proteome Res.* **2009**, *8*, 3702-3711.
(10) Kele, P.; Mezö, G.; Achatz, D.; Wolfbeis, O. S. *Angew. Chem. Int. Ed.* **2009**, *48*, 344-347.
(11) Jayaprakash, K. N.; Peng, C. G.; Butler, D.; Varghese, J. P.; Maier, M. A.; Rajeev, K. G.; Manoharan, M. *Org. Lett.* **2010**, *12*, 5410-5413.
(12) Wilson, J. T.; Krishnamurthy, V. R.; Cui, W.; Qu, Z.; Chaikof, E. L. *J. Am. Chem. Soc.* **2009**, *131*, 18228-18229.
(13) Sanders, B. C.; Friscourt, F.; Ledin, P. A.; Mbua, N. E.; Arumugam, S.; Guo, J.; Boltje, T. J.; Popik, V. V.; Boons, G.-J. *J. Am. Chem. Soc.* **2011**, *133*, 949–957.
(14) Bach, R. D. *J. Am. Chem. Soc.* **2009**, *131*, 5233-5243.
(15) Chenoweth, K.; Chenoweth, D.; Goddard Iii, W. A. *Org. Biomol. Chem.* **2009**, *7*, 5255-5258.
(16) Ess, D. H.; Houk, K. N. *J. Am. Chem. Soc.* **2008**, *130*, 10187-10198.
(17) Schoenebeck, F.; Ess, D. H.; Jones, G. O.; Houk, K. N. *J. Am. Chem. Soc.* **2009**, *131*, 8121-8133.
(18) Baskin, J. M.; Prescher, J. A.; Laughlin, S. T.; Agard, N. J.; Chang, P. V.; Miller, I. A.; Lo, A.; Codelli, J. A.; Bertozzi, C. R. *Proc. Natl. Acad. Sci. U.S.A.* **2007**, *104*, 16793-16797.
(19) Codelli, J. A.; Baskin, J. M.; Agard, N. J.; Bertozzi, C. R. *J. Am. Chem. Soc.* **2008**, *130*, 11486-11493.
(20) Debets, M. F.; van Berkel, S. S.; Schoffelen, S.; Rutjes, F. P. J. T.; van Hest, J. C. M.; van Delft, F. L. *Chem. Commun.* **2010**, *46*, 97-99.
(21) Jewett, J. C.; Bertozzi, C. R. *Org. Lett.* **2011**, *13*, 5937-5939.
(22) Jewett, J. C.; Sletten, E. M.; Bertozzi, C. R. *J. Am. Chem. Soc.* **2010**, *132*, 3688-3690.
(23) Kuzmin, A.; Poloukhtine, A.; Wolfert, M. A.; Popik, V. V. *Bioconjugate Chem.* **2010**, *21*, 2076-2085.
(24) Ning, X.; Guo, J.; Wolfert, Margreet A.; Boons, G.-J. *Angew. Chem. Int. Ed.* **2008**, *47*, 2253-2255.

(25) Dommerholt, J.; Schmidt, S.; Temming, R.; Hendriks, L. J. A.; Rutjes, F. P. J. T.; van Hest, J. C. M.; Lefeber, D. J.; Friedl, P.; van Delft, F. L. *Angew. Chem. Int. Ed.* **2010**, *49*, 9422-9425.
(26) de Almeida, G.; Sletten, E. M.; Nakamura, H.; Palaniappan, K. K.; Bertozzi, C. R. *Angew. Chem. Int. Ed.* **2012**, *51*, 2443-2447.
(27) Heaney, F. *Eur. J. Org. Chem.* **2012**, *2012*, 3043-3058.
(28) McKay, C. S.; Kennedy, D. C.; Pezacki, J. P. *Tetrahedron Lett.* **2009**, *50*, 1893-1896.
(29) Kennedy, D. C.; Lyn, R. K.; Pezacki, J. P. *J. Am. Chem. Soc.* **2009**, *131*, 2444-2445.
(30) Kennedy, D. C.; McKay, C. S.; Legault, M. C. B.; Danielson, D. C.; Blake, J. A.; Pegoraro, A. F.; Stolow, A.; Mester, Z.; Pezacki, J. P. *J. Am. Chem. Soc.* **2011**, *133*, 17993-18001.
(31) Lallana, E.; Riguera, R.; Fernandez-Megia, E. *Angew. Chem. Int. Ed.* **2011**, *50*, 8794-8804.
(32) Meier, H.; Gugel, H. *Synthesis* **1976**, *1976*, 338-339.
(33) Jung, M. E.; Mossman, A. B.; Lyster, M. A. *J. Org. Chem.* **1978**, *43*, 3698-3701.
(34) Azzena, U.; Demartis, S.; Pilo, L.; Piras, E. *Tetrahedron* **2000**, *56*, 8375-8382.
(35) Torssell, K. B. G. *Nitrile Oxides, Nitrones and Nitronates in Organic Synthesis*; VCH Wiley: Weinheim, Germany, 1988.
(36) Dondoni, A.; Franco, S.; Junquera, F.; Merchán, F. L.; Merino, P.; Tejero, T. *Synth. Commun.* **1994**, *24*, 2537-2550.
(37) Franco, S.; Merchán, F. L.; Merino, P.; Tejero, T. *Synth. Commun.* **1995**, *25*, 2275-2284.
(38) Tsai, P.; Ichikawa, K.; Mailer, C.; Pou, S.; Halpern, H. J.; Robinson, B. H.; Nielsen, R.; Rosen, G. M. *J. Org. Chem.* **2003**, *68*, 7811-7817.
(39) Goti, A.; Nannelli, L. *Tetrahedron Lett.* **1996**, *37*, 6025-6028.
(40) Marcantoni, E.; Petrini, M.; Polimanti, O. *Tetrahedron Lett.* **1995**, *36*, 3561-3562.
(41) Christensen, D.; Joergensen, K. A. *J. Org. Chem.* **1989**, *54*, 126-131.
(42) Cicchi, S.; Cardona, F.; Brandi, A.; Corsi, M.; Goti, A. *Tetrahedron Lett.* **1999**, *40*, 1989-1992.
(43) Cicchi, S.; Goti, A.; Brandi, A. *J. Org. Chem.* **1995**, *60*, 4743-4748.
(44) Goti, A.; Cacciarini, M.; Cardona, F.; Brandi, A. *Tetrahedron Lett.* **1999**, *40*, 2853-2856.
(45) Murahashi, S.; Mitsui, H.; Shiota, T.; Tsuda, T.; Watanabe, S. *J. Org. Chem.* **1990**, *55*, 1736-1744.
(46) Murahashi, S.-I. *Angew. Chem. Int. Ed.* **1995**, *34*, 2443-2465.
(47) Polonski, T.; Chimiak, A. *J. Org. Chem.* **1976**, *41*, 2092-2095.
(48) Gnichtel, H.; Schmitt, B.; Schunk, G. *Chem. Ber.* **1981**, *114*, 2536.
(49) Baldwin, J. E.; Pudussery, R. G.; Qureshi, A. K.; Sklarz, B. *J. Am. Chem. Soc.* **1968**, *90*, 5325-5326.
(50) Pinho e Melo, T. M. V. D. *Eur. J. Org. Chem.* **2010**, *2010*, 3363-3376.
(51) Chatterjee, A.; Maiti, D. K.; Bhattacharya, P. K. *Org. Lett.* **2003**, *5*, 3967-3969.
(52) Gella, C.; Ferrer, È.; Alibés, R.; Busqué, F.; de March, P.; Figueredo, M.; Font, J. *J. Org. Chem.* **2009**, *74*, 6365-6367.
(53) Beatty, K. E.; Fisk, J. D.; Smart, B. P.; Lu, Y. Y.; Szychowski, J.; Hangauer, M. J.; Baskin, J. M.; Bertozzi, C. R.; Tirrell, D. A. *ChemBioChem* **2010**, *11*, 2092-2095.
(54) Huisgen, R.; Stangl, H.; Sturm, H. J.; Wagenhofer, H. *Angew. Chem.* **1961**, *73*, 170-170.

(55) Aggarwal, V. K.; de Vicente, J.; Bonnert, R. V. *J. Org. Chem.* **2003**, *68*, 5381-5383.
(56) Jiang, N.; Li, C.-J. *Chem. Commun.* **2004**, 394-395.
(57) Korobitsyna, I. K.; Bulusheva, V. V.; Rodina, L. L. *Chem. Heterocycl. Compd.* **1978**, *14*, 471-486.
(58) Padwa, A. *1,3-Dipolar Cycloaddition Chemistry*; John Wiley & Sons: New York 1984; Vol. I.
(59) Qi, X.; Ready, J. M. *Angew. Chem. Int. Ed.* **2007**, *46*, 3242-3244.
(60) Vuluga, D.; Legros, J.; Crousse, B.; Bonnet-Delpon, D. *Green Chem.* **2009**, *11*, 156-159.
(61) Zollinger, H. *In Diazo Chemistry*; VCH: New York, 1995; Vol. 1-2.
(62) Kirmse, W. *Angew. Chem. Int. Ed.* **1976**, *15*, 251-261.
(63) Laali, K.; Olah, G. A. *Res. Chem. Intermed.* **1985**, *6*, 237-253.
(64) Lawson, T.; Nagel, D. *Carcinogenesis* **1988**, *9*, 1007-1010.
(65) Liberato, D. J.; Saavedra, J. E.; Farnsworth, D. W.; Lijinsky, W. *Chem. Res. Toxicol.* **1989**, *2*, 307-311.
(66) More O'Ferrall, R. A.; Gold, V. In *Adv. Phys. Org. Chem.*; Academic Press: 1967; Vol. Volume 5, p 331-399.
(67) Whittaker, D. *The Chemistry of Diazonium and Diazo Compounds*; Wiley-Interscience: Chichester, UK, 1978; pp 617-639.
(68) Brinker, U. *Advances in Carbene Chemistry*; Elsevier: New York, 1998; Vol. 1-2.
(69) Moss, R. A.; Platz, M. S.; Jones, M. *Reactive Intemediate Chemistry*; John Wiley & Sons: New York, 2004.
(70) Ning, X.; Temming, R. P.; Dommerholt, J.; Guo, J.; Ania, D. B.; Debets, M. F.; Wolfert, M. A.; Boons, G.-J.; van Delft, F. L. *Angew. Chem. Int. Ed.* **2010**, *49*, 3065-3068.
(71) Moore, J. A.; Mitchell, T. D. *Org. Prep. Proced. Int.* **1984**, *16*, 411-425.
(72) Leeson, P. D.; James, K.; Carling, R. W.; Moore, K. W.; Smith, J. D.; Mahomed, A. A.; Herbert, R. H.; Baker, R. *J. Org. Chem.* **1990**, *55*, 2094-2103.
(73) Bühl, H.; Gugel, H.; Kolshorn, H.; Meier, H. *Synthesis* **1978**, *1978*, 536-537.
(74) Evans, D. A.; Song, H.-J.; Fandrick, K. R. *Org. Lett.* **2006**, *8*, 3351-3354.
(75) Pandya, Shashi U.; Pinet, S.; Chavant, Pierre Y.; Vallée, Y. *Eur. J. Org. Chem.* **2003**, *2003*, 3621-3627.
(76) Tsuge, O.; Sone, K.; Urano, S.; Matsuda, K. *J. Org. Chem.* **1982**, *47*, 5171-5177.
(77) Sapeta, K.; Kerr, M. A. *J. Org. Chem.* **2007**, *72*, 8597-8599.
(78) Yang, Y.-S.; Shen, Z.-L.; Loh, T.-P. *Org. Lett.* **2009**, *11*, 1209-1212.
(79) Yamada, Y. M. A.; Tabata, H.; Ichinohe, M.; Takahashi, H.; Ikegami, S. *Tetrahedron* **2004**, *60*, 4087-4096.
(80) Kano, T.; Hashimoto, T.; Maruoka, K. *J. Am. Chem. Soc.* **2005**, *127*, 11926-11927.
(81) Cicchi, S.; Marradi, M.; Vogel, P.; Goti, A. *J. Org. Chem.* **2006**, *71*, 1614-1619.
(82) Kumar, S.; Murray, R. W. *J. Am. Chem. Soc.* **1984**, *106*, 1040-1045.

Chapter 6 : Strain-Promoted Alkyne-Nitrone Cycloadditions for Functionalizing Cell Surface Proteins

A significant portion of the work presented in this chapter was published in:

McKay, C. S.; Blake, J. A.; Cheng, J.; Danielson, D.C.; Pezacki, J.P. Strain-promoted cycloadditions of cyclic nitrones with cyclooctynes for labeling human cancer cells. *Chem. Commun.* **2011**, *47*, 10040-10042.

Introduction

The incorporation of fluorescent probes into proteins, DNA, RNA, lipids and glycans within their native cellular environments provides opportunities for imaging and understanding their roles *in vivo*.[1-4] Creative metabolic and genetic engineering strategies have made it possible to site-specifically incorporate azides, alkynes, and many other abiotic groups into proteins, glycans, nucleic acids, lipids, metabolites, and various posttranslational modifications in cultured cells and living organisms.[5] The azide group is an extremely versatile bioorthogonal chemical reporter, by virtue of its small size it can be easily introduced into biomolecules or probe molecules without changing their functional properties.[6-10] Most reported applications rely either on copper(I)-catalyzed azide-alkyne cycloaddition (CuAAC), or strain-promoted azide-alkyne cycloadditions (SPAAC).[4,6] Although the former is most suitable for *in vitro* applications resulting from the toxicity of copper, the latter is most suitable for live-cell and *in vivo* applications but is impeded by relatively slow reaction kinetics.[10,11]

New reactions that display fast reaction kinetics and do not require a metal-catalyst are of interest for various molecular imaging applications, enabling labelling at lower reagent concentrations. In the previous chapter we had evaluated the kinetics for reactions of a series of acyclic and cyclic nitrones in strain-promoted alkyne-nitrone cycloadditions (SPANC) (Figure 6-1). It was found that diaryl acyclic nitrones displayed rates that were comparable with azides. Acyclic nitrones predominantly exist in the more stable *Z*-conformation,[12] whereas cyclic nitrones are conformationally locked in the more reactive *E*-conformation. Cyclic nitrones displayed exceptionally fast kinetics in strain-promoted cycloadditions with cyclooctynes, proceeding up to 24 times faster than analogous reactions involving azides.[13]

In addition to the rapid reactivity of cyclic nitrones, the synthetic accessibility and ease of functionalization of cyclic nitrones make them particularly attractive 1,3-dipoles for strain-promoted cycloadditions with cyclooctynes.

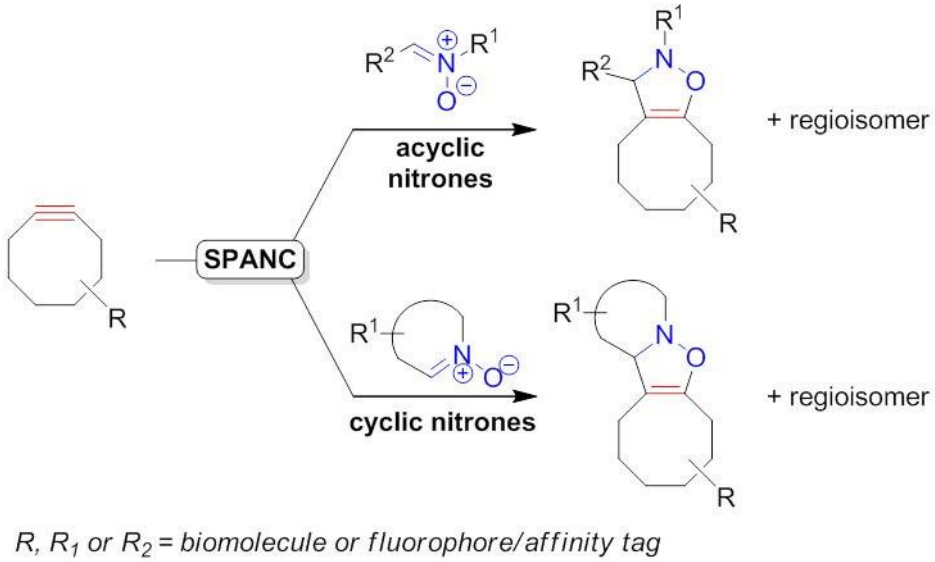

Figure 6-1. Strain-promoted alkyne-nitrone cycloadditions of acyclic and cyclic nitrones.

This chapter describes synthesis and kinetic evaluation of a series of cyclic nitrones in strain-promoted cycloadditions with cyclooctynes to optimize the balance of reactivity and reactant/product stability, and develop SPANC as a tool for bioconjugation. We demonstrate covalent modification of proteins (BSA and EGF) with the nitrone reporter group and perform fluorescence labelling via SPANC *in vitro*. Toward *in vivo* applications, we report pre-targeted labelling of human epidermal growth factor receptors expressed on the surface of breast cancer cells using nitrone modified epidermal growth factor and highly specific fluorescence labelling via SPANC. Lastly, we describe the synthesis of an unnatural nitrone modified oligosaccharide and preliminary attempts to metabolically incorporate the nitrone moiety into cell surface glycans and achieve fluorescence labelling via SPANC.

Hypothesis

Strain-promoted alkyne-nitrone cycloadditions serves as an efficient reaction for the functionalization of proteins and labelling of cell surface proteins.

Results and Discussion

Synthesis of Cyclic Nitrones for SPANC Reactions

To probe the feasibility of SPANC reactions involving cyclic nitrones as a tool for biological labelling, we examined the reaction scope and kinetics for reactions of a series of cyclic nitrones with dibenzocyclooctyne (**6.1**).[13] With the goal of finding optimal cyclic nitrone structures for bioconjugation via SPANC, we synthesized a series of cyclic nitrones differing in ring size, sterics and stereoelectronics to determine their respective contributions to nitrone reactivity in SPANCs.

On the basis of the enhanced rate of SPANC involving 3,4-dihydroisoquinoline 2-oxide from the previous chapter, which featured benzylic activation of the nitrone,[13] we synthesized oxo-piperazine-nitrone (**6.2**) as shown in Scheme 6-1.[14] The oxo-piperazine nitrone is a six membered nitrone, containing an electron withdrawing α-amide group and a pendant ester group that can be further functionalized to biomolecules. Nitrone **6.2** was synthesized in four steps starting from 4-Boc-2-oxo-piperazine (**6.3**). Briefly, alkylation of the amide of **6.3** with bromoacetic acid provided the ester intermediate (**6.4**) in 82 % yield. Following Boc-deprotection using trifluoroacetic acid in anisole, the secondary amine (**6.5**) was oxidized with 30 % aqueous H_2O_2 using $Na_2WO_4{\cdot}2H_2O$ in methanol as catalyst affording nitrone **6.2** in 73 % isolated yield.[15]

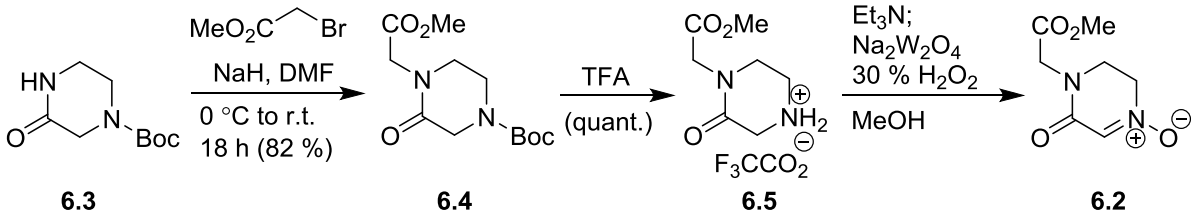

Scheme 6-1. Synthesis of nitrone **6.2**.

We also evaluated the kinetics of various five membered nitrones. Proline based nitrones were tested since they offered a carboxylic acid group that could be further functionalized with biological probes. Despite attempts to regioselectively oxidize the secondary amine of proline (**6.6**) to nitrone (**6.7**), yielded decarboxylated nitrone (**6.8**) as the main product (Scheme 6-2). We had also attempted to perform the oxidation using α-methyl-proline (**6.9**) to facilitate aldonitrone formation, however α-methyl-proline *N*-oxide (**6.10**) was not obtained by this route.

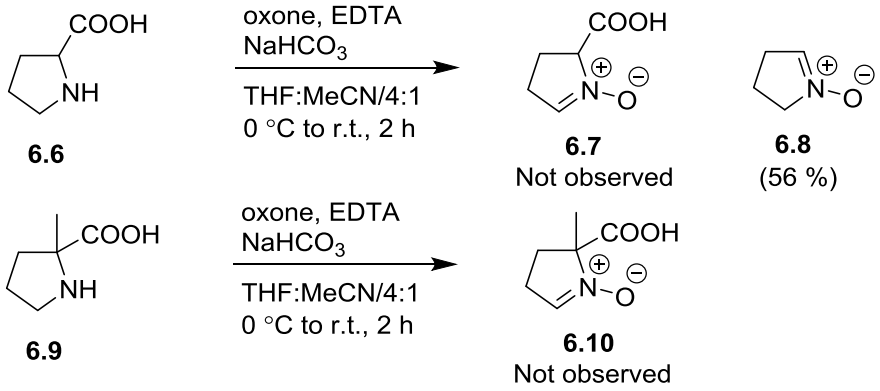

Scheme 6-2. Attempted nitrone formations by oxidation of proline and α-methyl-proline.

It became apparent, that we needed to reduce the carboxylic acid of proline to prolinol in order to avoid decarboxylative nitrone or ketonitrone formation. Scheme 6-3 outlines the synthetic route to prolinol nitrones (**6.11** and **6.12**).[16] Starting from *N*-Boc proline (**6.13**), the carboxylic acid of **6.13** was reduced to the alcohol (**6.14**), the resulting

alcohol was protected as the TBDPS ether (**6.15**) prior to nitrone formation. The bulky TBDPS group was employed in the late stage nitrone oxidation, mainly to facilitate separation of the regioisomeric mixture of ketonitrone **6.11** from aldonitrone **6.12** upon oxidation of the secondary amine (**6.16**). The *N*-Boc group of **6.15** was removed using TFA, and the secondary amine (**6.16**) was oxidized using a biphasic mixture containing oxone® according to the method or Font,[16] affording a 1.3:1 regioisomeric mixture of aldo- and keto-nitrones, **6.11** and **6.12**, respectively.

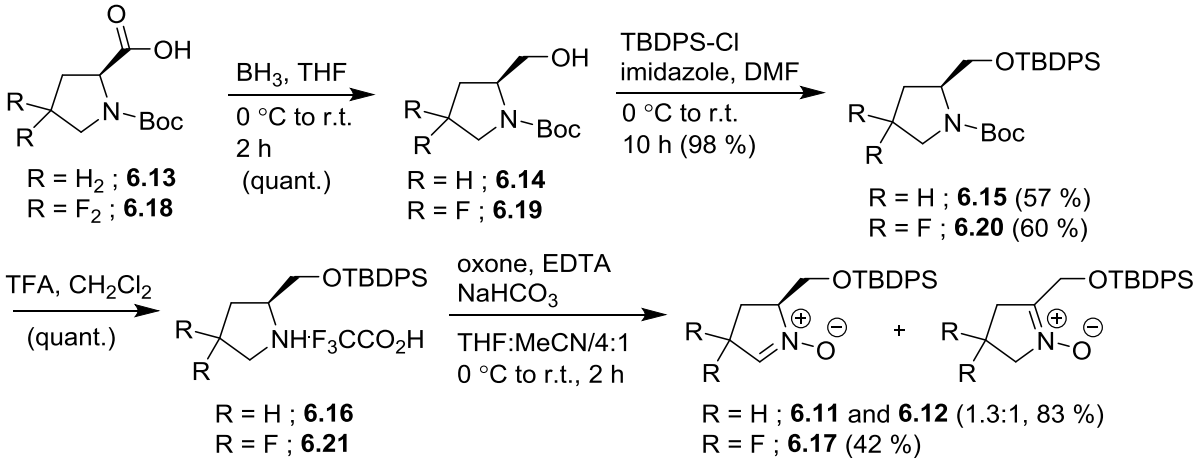

Scheme 6-3. Synthesis of prolinol nitrones **6.11**, **6.12** and **6.17**.

Since there is precedence in the literature that nitrones bearing resonance stabilizing EWGs at the α-position display rate enhancements for SPANC reactions with DIBO and derivatives,[13,17] we installed an inductively withdrawing *gem*-difluoro group at the α-position of the prolinol nitrone in hopes of increasing the reactivity of the nitrone. According to Scheme 6-3, 4,4-difluoro-*L*-prolinol-*N*-oxide (**6.17**) was synthesized analogously to the non-fluorinated prolinol nitrones. Briefly, *N*-Boc-4,4-difluoro-*L*-proline (**6.18**) was reduced to the alcohol (**6.19**), the alcohol was protected as the TBDPS ether (**6.20**). Boc-deprotection of the

secondary amine (**6.20**), and regioselective oxidation of the resultant amine (**6.21**) provided aldonitrone (**6.17**).

Another cyclic nitrone that was pursued was 5-carboxyethyl-5-methyl-pyrroline *N*-oxide (EMPO, **6.22**).[18,19] Rather than pursuing nitrone formation via oxidation of the secondary amine, nitrone **6.22** was synthesized in three steps in 86 % overall through a highly efficient intramolecular cyclization (Scheme 6-4). Briefly, 1,4-addition of ethyl-2-nitro-propionate (**6.23**) with acrolein (**6.24**) provided the aldehyde (**6.25**), that was protected as the dioxolane (**6.26**). Intramolecular condensation of the *in situ* generated hydroxylamine with the deprotected aldehyde yielded **6.22**.

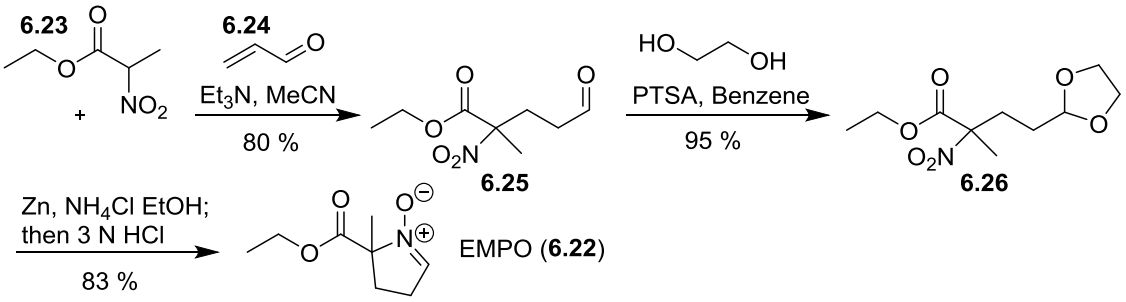

Scheme 6-4. Synthesis of 5-carboxyethyl-5-methyl-pyrroline *N*-oxide **6.22**.

Additionally we synthesized a ketonitrone (**6.27**) following the method of Bode *et al.* that featured a potential activating α-ester group and a carboxylic acid for further functionalization (Scheme 6-5).[20] Nitrone **6.27** was synthesized by annulation of α-ketoglutaric acid (**6.28**) with cyclohexane carboxaldehyde oxime (**6.29**).

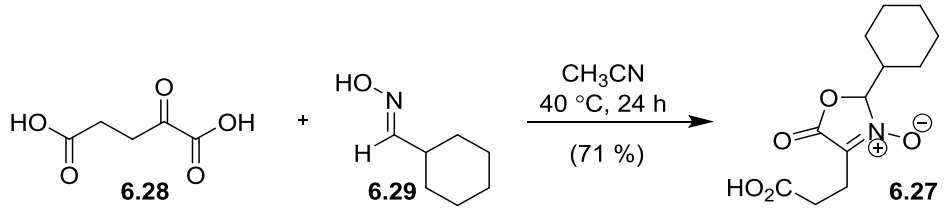

Scheme 6-5. Synthesis of ketonitrone **6.27**.

Kinetics of SPANC Reactions of Cyclic Nitrones with Dibenzocyclooctynes

Having successfully synthesized a series of cyclic nitrones, we measured kinetics of their SPANC reactions with **6.1** (Table 6-1). Aldonitrones (Entries 1-7) reacted significantly faster than the ketonitrones (Entries 8 and 9). All nitrones employed yielded isoxazoline cycloadducts in excellent yields. The five membered pyrroline *N*-oxides, (Entries 1-4) were found to be optimal, blending fast kinetics with enhanced stability under ambient conditions. Reactions of nitrones **6.30** and **6.22** (Entries 1 and 2) resulted in second-order rate constants of 0.63 ± 0.12 $M^{-1}s^{-1}$ and 7.69 ± 0.19 $M^{-1}s^{-1}$, respectively. The rate enhancement of **6.30** may have resulted from electron repulsions of the nitrone oxygen with the pendant ester group, causing less distortion of the nitrone to achieve the transition state geometry. Additionally, prolinol nitrone **6.11** reacted with **6.1** with a rate constant of 1.95 ± 0.60 $M^{-1}s^{-1}$ (Entry 3), suggesting that sterically bulky groups adjacent to the nitrone reduce nitrone reactivity. The presence of an *N*-Boc group adjacent at the α-position in **6.31** resulted in a somewhat slower reaction with **6.1** relative to the analogous reaction of **6.11**.

Attempts to further activate the cyclic nitrone using *gem*-difluoro groups at the α-position in nitrone **6.17** (Table 6-1, Entry 5) resulted in remarkably slower rates for cycloddition than the other 5-membered nitrones. Evidently, nitrones containing resonance stabilized groups at the α-position (ie. amide or aryl groups) reacted faster than those with inductively withdrawing fluoro-groups. We also tested a six membered nitrone, **6.2** containing the electron withdrawing α-amide group. Nitrone **6.2** reacted with **6.1** in 96% yield within 3 min at 25 ˚C; corresponding to a rate constant of 1.41 ± 0.19 $M^{-1}s^{-1}$ (Entry 6). Despite its fast reactivity, nitrone **6.2** was less stable and prone to decomposition at room temperature. Attempts to synthesize additional six membered nitrones that would be

electronically and sterically similar to the five membered nitrones gave similar decomposition products as **6.2**.

Table 6-1. Kinetics of strain-promoted cycloadditions between cyclic nitrones and **6.1**.

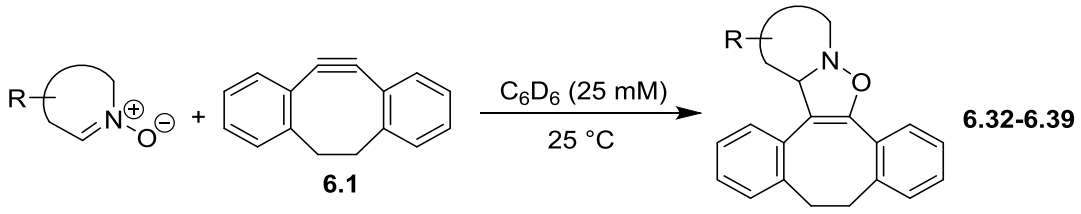

Entry	Nitrone		Product	Yield (%)[a]	T (min.)	k_2 ($M^{-1}s^{-1}$)[b]
1	**6.30**	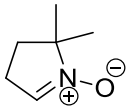	**6.32**	91	15	0.63 ± 0.12
2	**6.22**	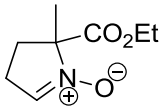	**6.33**	96	<2	7.69 ± 0.19
3	**6.11**	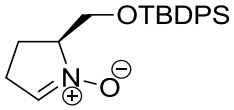	**6.34**	88	5	1.95 ± 0.60
4	**6.31**	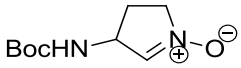	**6.35**	90	18	0.62 ± 0.08
5	**6.17**	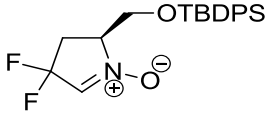	**6.36**	87	180	0.0215 ± 0.00038
6	**6.2**	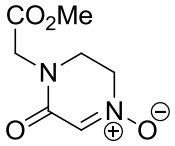	**6.37**	84	3	1.41 ± 0.19
7	**6.12**	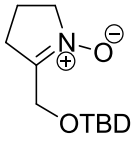	**6.38**	89	1380	n.d.
8	**6.27**	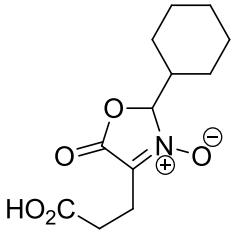	**6.39**	97	1440	n.d.

Conditions: Reagents were mixed 1 : 1 at 25 mM in C_6D_6 at 25 °C. [a]Isolated yield following column chromatography. [b]Rate constant, k_2, was determined by ^{1}H NMR under second-order conditions.

Having established that the five membered cyclic nitrones displayed sufficiently fast reactivity in SPANC reactions with **6.1**, and were stable under ambient conditions, we measured rate constants for reactions of the most reactive cyclic nitrones with dibenzocyclooctynol (DIBO, **6.40**) in acetonitrile (Table 6-2). All cyclic nitrones tested gave excellent yields of isoxazoline products (**6.41-6.44**) with comparable rates upon moving from benzene to acetonitrile.

Table 6-2. Kinetics of strain-promoted cycloadditions between cyclic nitrones and **6.40**.

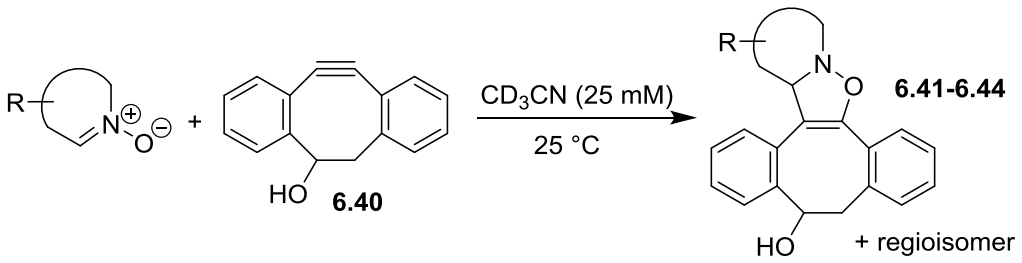

Entry	Nitrone		Product	Yield %[a]	k_2 (M^{-1} s^{-1})[b]
2	**6.30**	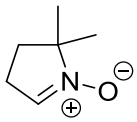	**6.41**	97	0.75 ± 0.04
3	**6.22**	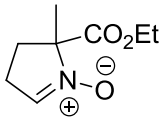	**6.42**	96	3.38 ± 0.31
4	**6.11**	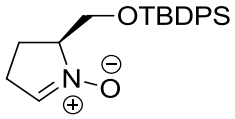	**6.43**	92	1.04 ± 0.17
1	**6.2**	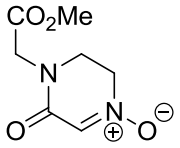	**6.44**	95	0.46 ± 0.01

Conditions: Reagents were mixed 1 : 1 at 25 mM in CD_3CN at 25 ◦C. [a]Yield % was determined by ^1H NMR. [b]Rate constants, k_2, was determined by ^1H NMR under second-order reaction conditions.

The rate constant for reaction of **6.30** with **6.40** was 0.75 ± 0.04 $M^{-1}s^{-1}$ (Table 6-2, Entry 1). Although the value for reactions of **6.30** with DIBO in acetonitrile is within experimental error, with that obtained for its reaction with **6.1** in toluene, it is still 13 times faster than analogous reactions of benzyl azide with DIBO.[21] Cyclic nitrone **6.22** reacted with **6.40** in 96 % yield within 3 min with a rate constant of 3.38 ± 0.31 $M^{-1}s^{-1}$ (Table 6-2, Entry 2). This rate constant corresponds to a 44-fold enhancement relative to the reaction of benzyl azide with DIFO,[7] a 59-fold enhancement relative to reaction with DIBO,[21] and a 3-fold enhancement relative to reaction with BARAC.[22] We also tested the prolinol nitrone, **6.11** in reaction with DIBO and the rate constant was found to be 1.04 ± 0.17 $M^{-1}s^{-1}$, this corresponded to a 18-fold enhancement over analogous reaction of benzyl azide with DIBO. Similar rate enhancements were observed in the reaction of **6.2** with DIBO (0.46 ± 0.01 $M^{-1}s^{-1}$).

Labelling of Cell Surface Proteins via SPANC

To demonstrate direct protein functionalization via SPANC, we labelled bovine serum albumin (BSA) and human epidermal growth factor (EGF) *in vitro* (Figure 6-2). An NHS-activated prolinol nitrone (**6.45**) was prepared by desilylation of **6.11** with TBAF and subsequent reaction of the alcohol (**6.46**) with *N*,*N*'-disuccinimidyl carbonate, yielded NHS-activated nitrone **6.45**. The NHS-activated nitrone was coupled with lysine residues on BSA and EGF. We observed that BSA was modified with an average of four nitrone groups, whereas EGF was modified with an average of two nitrones, as confirmed by MALDI-MS.

Nitrone modified BSA (**6.47**) was treated with DIBO-488 (**6.48**) for time intervals between 0 and 60 min. Highly specific, time-dependent labelling and minimal background labelling in the negative control was detected by in-gel fluorescence scanning (Figure 6-2,

lower left gel). For the SPANC reaction of nitrone modified EGF (**6.49**) with **6.48**, due to co-elution of the DIBO-488 with the EGF-labelled protein on SDS-PAGE, we were unable to separate the unbound DIBO-488 from the fluorescently labelled EGF. Fortunately, through the use of a DIBO-TAMRA probe (**6.50**), we observed highly specific time-dependent labelling of EGF (Figure 6-2, lower right gel) via SPANC. For both proteins that were tested, the negative control (-), is unlabelled BSA or EGF in the presence of appropriate DIBO-fluorophore conjugate.

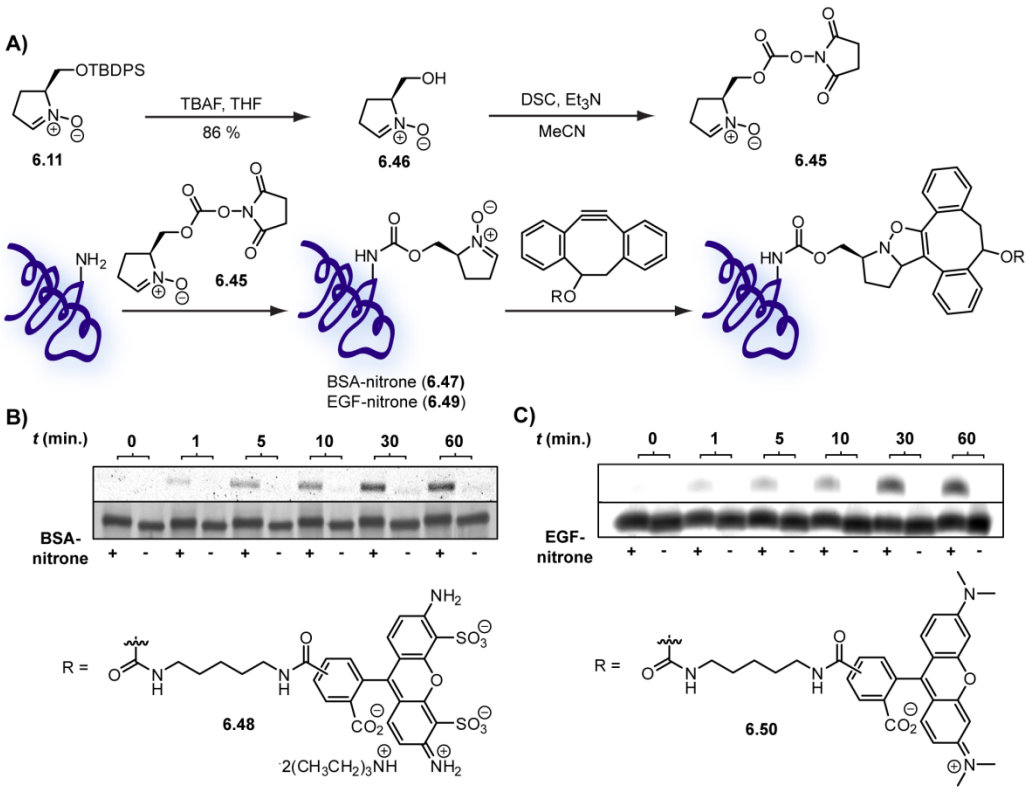

Figure 6-2. Functionalization of BSA and EGF through bioorthogonal SPANC reactions. A) Synthetic scheme for covalent modification of BSA and EGF with a cyclic nitrone by NHS coupling, and subsequent fluorescence labelling via SPANC. B) Time course labelling of BSA by SPANC reaction with **6.48** was detected by SDS-PAGE with fluorescence scan (upper gel) and silver stain as the loading control (lower gel). C) Time course labelling of EGF by SPANC reaction with **6.50** was detected by SDS-PAGE with fluorescence scan (upper gel) and silver stain as the loading control (lower gel).

To illustrate the utility of SPANC for cellular imaging, we labelled epidermal growth factor receptors (EGFRs) that were overexpressed on the surface of human breast cancer cells (MDA-MB-468) (Figure 6-3). Cyclic nitrone modified EGF, **6.49** (10 μM) was targeted to EGFRs on the cell surfaces. Cellular labelling was accomplished by *in situ* SPANC reactions of cyclic nitrone modified EGFRs at the cell surface (**6.51**) with DIBO-biotin[11] (**6.52**) for 30 min prior to staining with a streptavidin-FITC conjugate. For the negative control, cells were pretreated with unmodified EGF (10 μM) followed by treatment with DIBO-biotin (10 μM) and streptavidin-FITC (5 μg/mL). As shown in Figure 6-3, highly specific labelling of EGF-EGFR interactions was achieved, and we observed minimal background fluorescence in the negative control.

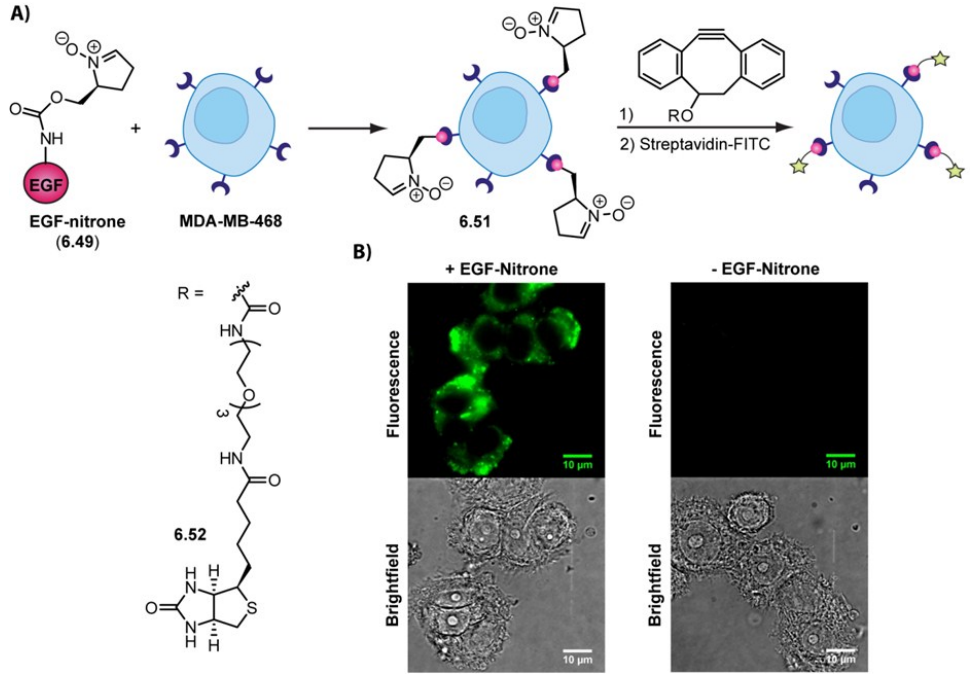

Figure 6-3. *In situ* pre-targeted labelling of EGF–EGFR interactions on the surface of breast cancer cells (MDA-MB-468) via SPANC. A) Cyclic nitrone modified EGF bound to EGFR was labelled by SPANC using DIBO Biotin (**6.52**) for 30 min prior to streptavidin-FITC fluorescent labeling. B) Fluorescence (top) and bright field (bottom) image of *in situ* SPANC. Negative control was cells pre-treated with EGF followed by treatment with **6.52** and streptavidin-FITC. Reagent concentrations: **6.49** (10 μM), EGF (10 μM), **6.52** (10 μM) and streptavidin-FITC (5 μg/mL).

Metabolic Incorporation of Nitrones into Cell Surface Glycans

To validate the SPANC methodology as a viable bioorthogonal reaction, we attempted to incorporate the nitrone moiety into cell surface glycans. Cell surface sialosides are synthesized in a series of biochemical steps (Figure 6-4).[23,24] ManNAc is known as the first committed intermediate, which can be synthesized from N-acetylglucosamine (GlcNAc) or taken up from outside the cell. Upon formation of the CMP-NeuNAc, further processing occurs in the Golgi apparatus prior to being presented on the cell surface. As shown previously, exogenously delivered ManNAc analogs bearing ketone (Lev) or azide (N_3) groups are able to intercept the pathway and produce cell surface sialosides with unique functionality.[25] Toward exploiting the cyclic nitrone group as a bioorthogonal reporter in SPANC reactions, we probed the utility of SPANC for metabolic incorporation of N-acetyl mannosamine (ManNAc) derivatives bearing the cyclic nitrone moiety.

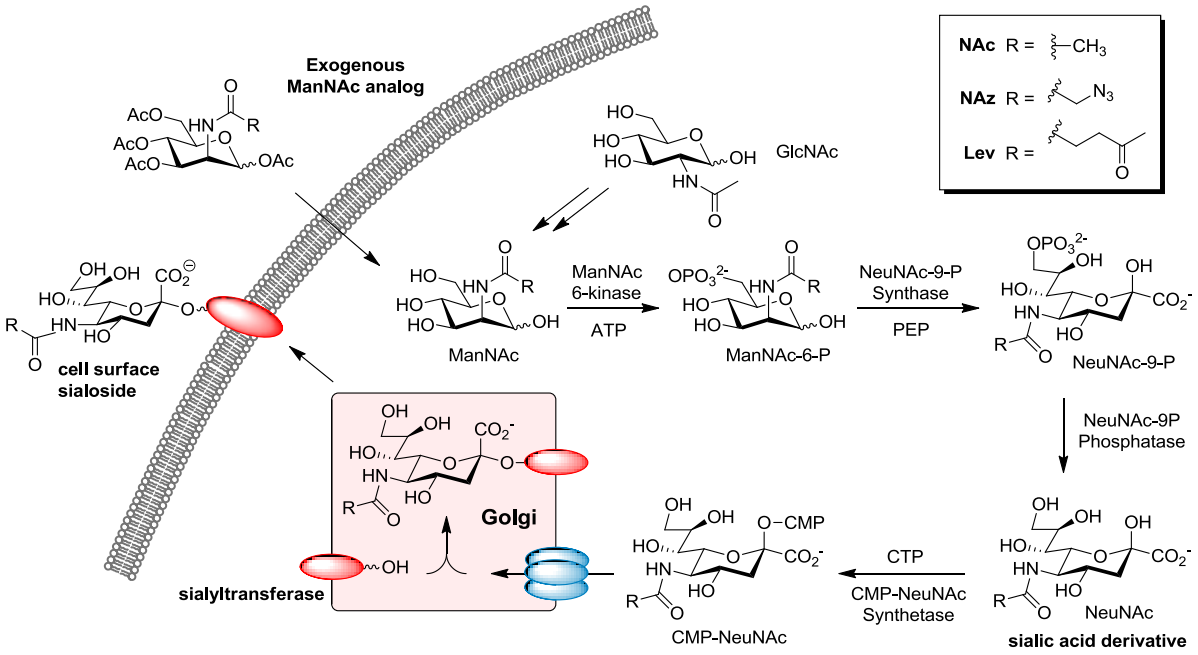

Figure 6-4. Sialic acid biosynthetic pathway. Figure was reprinted from the literature.[25]

Recent attempts to metabolically incorporate monosaccharide derivatives bearing acyclic nitrones into Jurkat cell surfaces, followed by labelling with a DIBO-probe led to no observable fluorescence labelling.[17] Two possible reasons for the lack of metabolic incorporation of the acyclic nitrones could be that either nitones were not tolerated by the cellular machinery or the nitrones underwent intracellular hydrolysis within acidic compartments within the cell. We set out to evaluate the hydrolytic stabilities of cyclic nitrone, **6.30** with acyclic nitrone[17] (**6.53**), under acidic and basic conditions to determine whether the cyclic nitrones would offer improved stability toward hydrolysis (Figure 6-5).

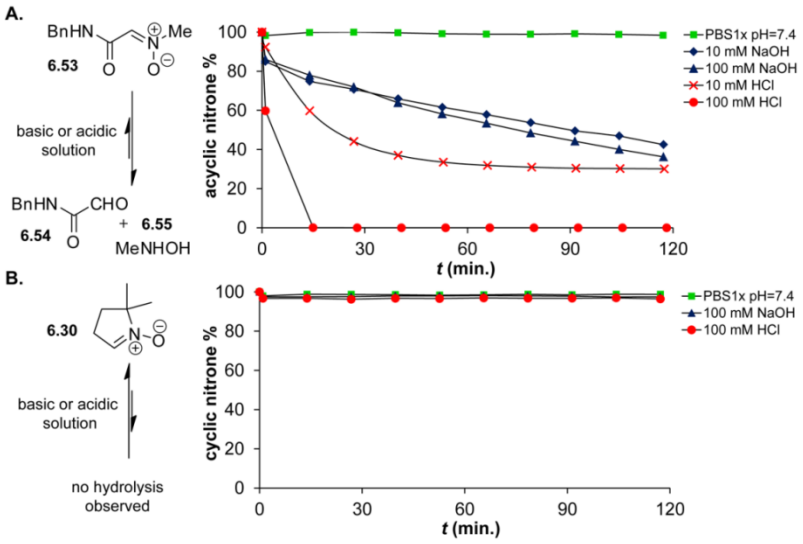

Figure 6-5. Hydrolysis studies of acyclic and cyclic nitrones at variable pH of solution. A) Hydrolysis of acyclic nitrone **6.53** (10 mM) in the presence of PBS 1x, 10 mM NaOH, 100 mM NaOH, 10 mM HCl or 100 mM HCl over 2 h. The exponential decay observed for hydrolysis of **6.53** in the presence of 10 mM HCl is consistent with first order reaction kinetics. For the reaction of **6.53** in the presence of 100 mM HCl, the data was not fit to an exponential equation due to a limited number of HPLC data points acquired during the first 15 min of reaction. B) Hydrolysis of Cyclic nitrone **6.30** (10mM) in the presence of PBS 1x, 100 mM NaOH or 100 mM HCl over 2 hrs.

At neutral pH, both acyclic and cyclic nitrones were stable in aqueous PBS media. However, in the presence of 100 mM HCl solution, the acyclic nitrone **6.53** was rapidly hydrolyzed to the corresponding aldehyde (**6.54**) and *N*-methyl hydroxyl amine (**6.55**) within

15 min (as evidenced by GC-MS). Also, in the presence of 100 mM NaOH, **6.53** was significantly hydrolyzed solution over 2 h. The rapid hydrolysis of the acyclic nitrone at variation of pH, corresponds to only a small fraction of the number of days that are typically required for unnatural carbohydrate metabolites to be taken up by mammalian cells and incorporated into cell surface glycans.[26] Interestingly, the cyclic nitrone **6.30** remained was resilient toward hydrolysis in the presence of acidic or basic solutions.

Encouraged by the superior hydrolytic stability of the cyclic nitrone over the acyclic nitrone, we sought to design a cyclic nitrone modified ManNAc derivative, Ac_4ManNCMPO (**6.56**). Nitrone **6.56** could be efficiently synthesized by an amide coupling between cyclic nitrone 4-carboxy-4methyl-pyrroline-*N*-oxide[19] (CMPO, **6.57**) and 1,3,4,6-Tetra-*O*-acetyl-2-amino-2-deoxy-α-D-mannopyranose[27] (**6.58**) (Scheme 6-6). Following saponification of the ester of nitrone **6.22** according to the conditions of Tsai,[19] carbodiimide-mediated coupling of **6.57** and **6.58** provided Ac_4ManNCMPO in 49 % yield as a mixture of α- and β-anomers in a ratio of 1:1.

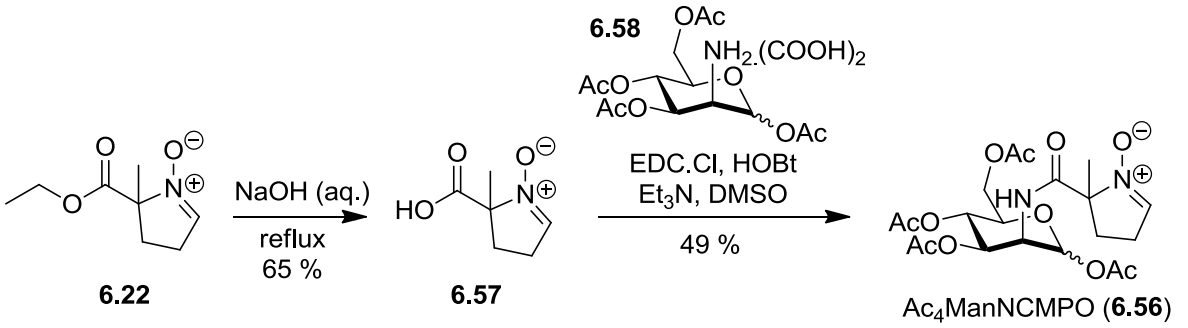

Scheme 6-6. Synthesis of Ac_4ManNCMPO, **6.55**.

To evaluate the efficiency of SPANC, we measured kinetics for SPANC reaction of Ac_4ManNCMPO **6.56** with DIBO in acetonitrile, under pseudo first order reaction conditions by UV-vis absorption spectroscopy, and compared the obtained rate constant with that for

the reaction involving Ac_4ManNAz (**6.59**) (Scheme 6-7). It was found that SPANC displayed a 6-fold rate enhancement over SPAAC, corresponding to rate constants of (3.35 ± 0.07) x 10^{-1} $M^{-1}s^{-1}$ and (5.52 ± 0.18) x 10^{-2} $M^{-1}s^{-1}$, respectively.

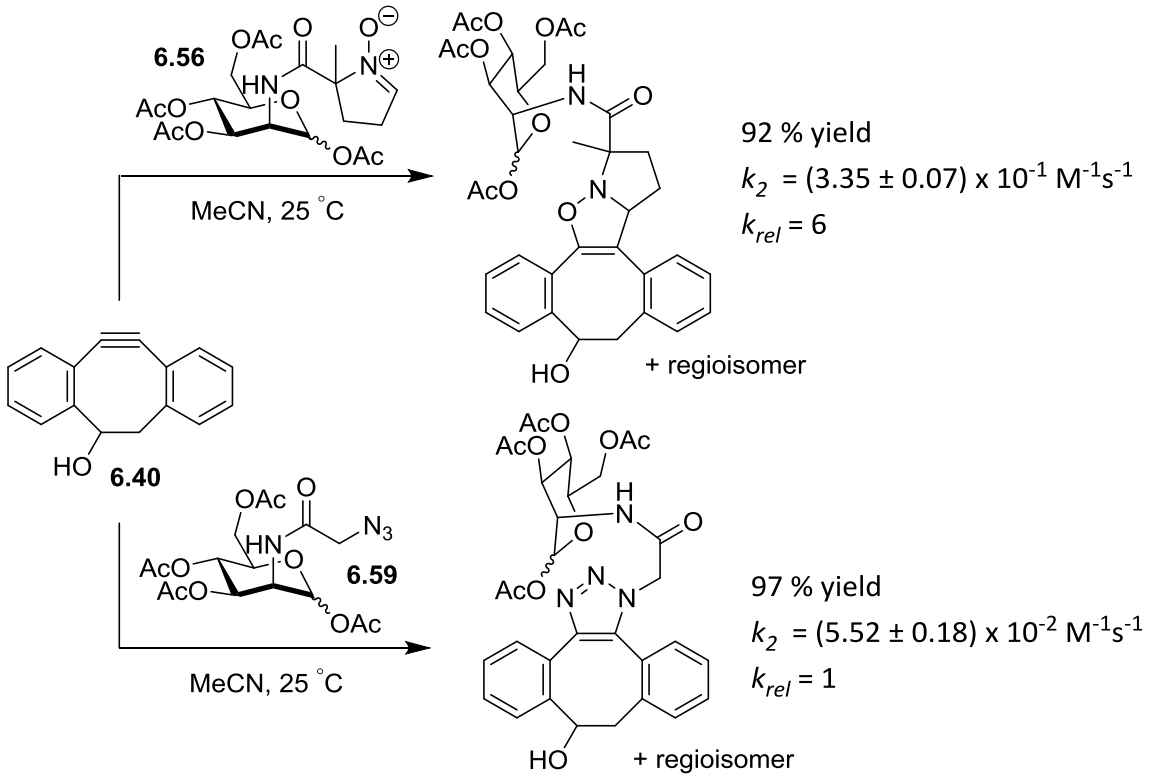

Scheme 6-7. Kinetics of SPANC versus SPAAC with nitrone or azide modified Ac_4ManNAc derivatives. Kinetic were done under pseudo-first order reaction conditions and measured by UV-visible spectroscopy.

Toward metabolic incorporation of the cyclic nitrone into cell surface sialosides (Scheme 6-8), we incubated ManNAc derivatives, Ac_4ManNCMPO and Ac_4ManNAz, with Huh7 liver cells for 3 d. The cells were the fixed and treated with DIBO-Biotin. Following staining with Streptavidin-FITC, we did not observe reproducible fluorescence signal for cells treated with Ac_4ManNCMPO. It has been hypothesized, that incorporation of ManNAc derivatives bearing longer N-acyl chains or branched chains are not tolerated for phosphorylation by ManNAc 6-kinase.[25,28]

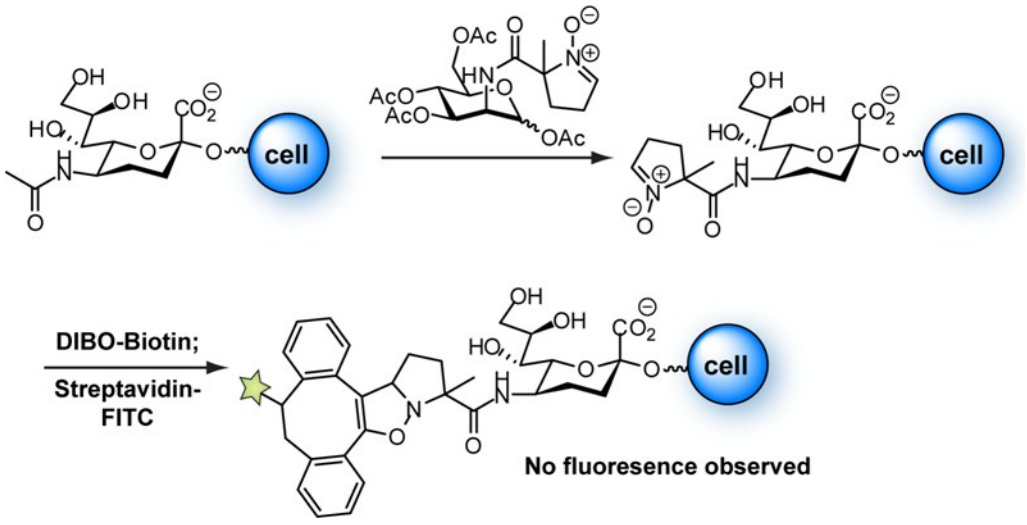

Scheme 6-8. Metabolic incorporation of nitrone modified ManNAc derivative into cell surface glycans and fluorescence labelling by SPANC.

Fortunately, it is possible to bypass the bottle-neck step in the sialic acid biosynthetic pathway, through supplementing cells directly with sialic acid derivatives rather than ManNAc.[28] We are currently exploring the synthesis of unnatural *N*-acetyl neuraminic acid (NeuNAc) derivatives bearing the cyclic nitrone functionality at C-5 (**6.60**) or C-9 (**6.61**) as shown in Scheme 6-9.

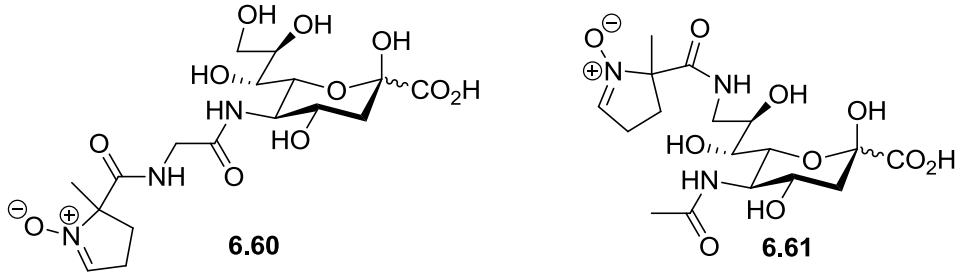

Scheme 6-9. Prospective cyclic nitrone modified NeuNAc derivatives.

We anticipate that through by-passing ManNAc 6-kinase, we will be able incorporate the cyclic nitrone into cell surface sialosides and achieve metabolic incorporation of nitrones and highly specific bioorthogonal labelling via SPANC.

Future Directions

Future directions will involve exploring alternate methods for incorporating the nitrone moiety into biomolecules to demonstrate nitrones as bioorthogonal reporters in strain-promoted cycloadditions with strained alkynes that can be used for imaging biomolecules within living cells. This will involve covalent modification of other metabolic substrates such as unnatural amino acids, nucleotides, or lipids bearing nitrone functionality and their incorporation into biomolecules by either genetic or metabolic routes.

Conclusions

We have established nitrones as versatile alternatives to azides in strain-promoted cycloadditions with cyclooctynes. Advantages of cyclic nitrones includes that they are simple and conveniently prepared, they are fast reacting and stable at variable pH, and perhaps most importantly, their reactivity is tunable. We have shown that five membered cyclic nitrones blend enhanced stability with fast kinetics in SPANC reactions with cyclooctynes. Reactions of cyclic nitrones proceeded with rate constants up to 3.38 ± 0.31 $M^{-1}s^{-1}$ in CD_3CN, corresponding to 59 times faster than the analogous reaction of benzyl azide with DIBO. We have demonstrated highly specific labelling of BSA and EGF *in vitro* and have shown efficient pre-targeted labelling of EGFRs on the surfaces of live cancer cells via SPANC. The SPANC bioconjugation approach presented here is modular and can be extended to other biological imaging applications, since cyclic nitrone functionalities can be easily conjugated to carboxylic acid or amine containing biomolecules. The high selectivity, fast reaction rate, and aqueous compatibility of SPANC makes this reaction ideally suited for a variety of other *in vivo* imaging applications.

Acknowledgements

Jenny Cheng is thanked for technical assistance with protein functionalization via SPANC and Dr. Jessie Blake is thanked for performing confocal microscopy imaging of the SPANC labelled cell surfaces. We also thank Kenneth Chan for MALDI-MS analysis of the reaction products.

Materials and Methods

General

All chemical reagents that were purchased from commercial sources were used without further purification unless otherwise stated. 5,5-dimethyl-1-pyrroline-N-oxide (DMPO, **6.30**) and bovine serum albumin (BSA) were purchased from Sigma-Aldrich. Human recombinant epidermal growth factor (EGF), tetramethyl rhodamine cadaverine (TAMRA), Alexa Fluor® 488 cadaverine sodium salt, and FITC-streptavidin were purchased from Invitrogen. Deuterated solvents were purchased from Cambridge Isotope Laboratories. MDA-MB-468 cell line and culture media were purchased from ATCC. Thin layer chromatography (TLC) was carried out on Analtech Uniplate® silica gel plates (60 Å F254, layer thickness 250μm) using UV light to visualize the course of reaction. Flash column chromatography was performed using silica gel (60 Å, particle size 40–63 μm).

The experimental procedure and spectral data (^{1}H, ^{13}C, ^{19}F, R_f and MS) for any newly reported compounds are included. References for known compounds for which their syntheses were prepared from standard literature procedures are included. ^{1}H and ^{13}C NMR spectra were recorded using a 400 Bruker-DRX-400 spectrometer using a frequency of 400.13 MHz for ^{1}H and 100.61 MHz for ^{13}C and processed using Bruker TOPSPIN 2.1 software. Chemical shifts are reported in parts per million (δ) using residual $CHCl_3$ resonance as an internal reference (7.26 and 77.0 ppm for ^{1}H and ^{13}C NMR, respectively). The following abbreviations were used to designate chemical shift multiplicities: s = singlet, d = doublet, t = triplet, m = multiplet or unresolved, br = broad signal and *J* = coupling constants in Hz. Kinetic experiments were completed either by ^{1}H NMR or by UV-vis

absorption spectroscopy on a Varian system comprising a Cary 3 UV-visible Spectrophotometer and Cary Temperature Controller.

Synthetic Procedures and Characterization Data:

5,6-didehydro-11,12-dihydro-dibenzo[*a,e*]cyclooctene (6.1):

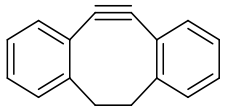

6.1

Synthesis previously reported in the literature.[13]

4-(2-methoxy-2-oxoethyl)-5-oxo-2,3,4,5-tetrahydropyrazine 1-oxide (6.2):

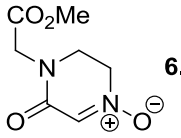

6.2

Synthesis previously reported in the literature.[14]

(S)-2-((tert-butyldiphenylsilyloxy)methyl)-3,4-dihydro-*2H*-pyrrole 1-oxide (6.11):

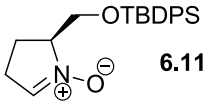

6.11

Synthesis previously reported in the literature.[16]

5-((tert-butyldiphenylsilyloxy)methyl)-3,4-dihydro-*2H*-pyrrole 1-oxide (6.12):

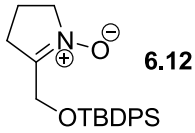

6.12

Synthesis previously reported in the literature.[16]

(S)-*tert*-butyl 4,4-difluoro-2-(hydroxymethyl)pyrrolidine-1-carboxylate (6.19):

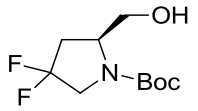

6.19

N-Boc-4,4-difluoro-*L*-proline (500 mg, 1.99 mmol) was dissolved in THF (3.85 mL) and BH_3·THF (3.85 mL, 3.85 mmol from a 1.0 M solution in THF) was added at 0 ˚C. The resultant solution was stirred at 0 ˚C for 2 h. Upon completion, ice water (7 mL) was added and the solution was extracted with EtOAc (3 x 14 mL), the combined organic phases were washed with brine (7 mL), saturated $NaHCO_3$ (7 mL) and H_2O (2 x 7mL). The organic phase was dried over anhydrous Na_2SO_4, filtered and concentrated. The crude was purified by flash column chromatography eluting with 86:6:6/hexanes:EtOAc:EtOH. *N*-Boc-4,4-difluoro-*L*-prolinol was obtained as a colourless oil (467 mg, 1.97 mmol, 99 %). $\mathbf{R_f}$ = 0.17 (88:6:6/Hexanes:EtOAc:EtOH). **^{1}H NMR ($CDCl_3$, 400 MHz)** : δ 4.16 (quintet, *J* = 5.4 Hz, 1H), 3.84 (q, *J* = 11.9 Hz, 1H), 3.72 (t, *J* = 5.2 Hz, 1H), 3.63 (q, *J* = Hz, 1H), 2.54-2.41 (m, 1H), 2.22 (m, 1H), 1.48 (s, 9H). **^{13}C NMR ($CDCl_3$, 100 MHz)**: δ 155.5 (C), 126.4 (t, C), 81.4 (CH_2), 65.3 (CH), 58.4 (CH_2), 54.1 (t, CH_2), 36.9 (t, CH_2), 28.4 (CH_3), 27.5 (C). **^{19}F NMR ($CDCl_3$, 100 MHz)**: δ -99.7. **LRMS**: Calculated for $C_{10}H_{18}F_2NO_3$ (M^+) 238.12, Found 238.1.

(S)-2-((*tert*-butyldiphenylsilyloxy)methyl)-4,4-difluoro-3,4-dihydro-*2H*-pyrrole 1-oxide (6.17):

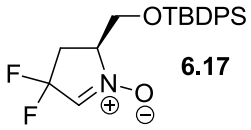

6.17

N-Boc-4,4-difluoro-*L*-prolinol **6.19** (104 mg, 0.44 mmol) was dissolved in dry CH_2Cl_2 (4.4 mL) at 0 ˚C. TBDPS-Cl (236 µL, 0.92 mmol) and imidazole (66 mg, 0.97 mmol) were successively added and the reaction was stirred at 0 ˚C for 15 min, then was warmed to r.t. and stirred overnight. Upon completion, the reaction mixture was filtered through a plug of celite, diluted with a saturated NH_4Cl (10 mL) and extracted with CH_2Cl_2 (3 x 10 mL). The combined organic phases where dried over anhydrous Na_2SO_4, filtered and concentrated. The crude **6.20** was purified by flash column chromatography (85:15/hexanes:EtOAc, $\mathbf{R_f}$ = 0.35). This colourless oil (159 mg, 0.33 mmol) was dissolved in CH_2Cl_2 (4 mL) and TFA (250 µL, 3.3 mmol), stirred for 2 h at r.t. and the solvent was removed under reduced pressure. The crude was used without further purification. The crude oil **6.21** (~0.3 mmol) was dissolved in MeCN:THF/4:1 (1mL) at 5 ˚C. The EDTA (0.5mL from a 0.01 M solution) and $NaHCO_3$ (252 mg, 3 mmol) were added. Subsequently over a 2 h period, oxone® (203 mg, 0.33 mmol) was added portion wise at 5 ˚C. The reaction mixture was allowed to stir for an additional 20 minutes at 5 ˚C. Upon completion, the mixture was extracted into EtOAc (3 x 5 mL) and the combined organic phases were dried over anhydrous Na_2SO_4, filtered and concentrated *in vacuo*. The crude **6.17** was purified by reverse phase preparative HPLC, eluting with 70-80 % MeCN:H_2O during 15 min (column: Sunfire C_{18} 19 x 100 mm, flow rate = 17.0 mL/min). **^{1}H NMR ($CDCl_3$, 400MHz)**: δ 7.70-7.65 (m, 4H), 7.46-7.39 (m, 6H), 7.09 (m, 1H), 4.44 (dd, *J* = 11.3, 1.5 Hz, 1H), 4.20 (m, 1H), 3.63 (dd, *J* = 11.3, 1.9 Hz, 1H),

3.07-2.95 (m, 1H), 2.85-2.73 (m, 1H), 1.05 (s, 9H). **^{13}C NMR ($CDCl_3$, 100MHz)**: δ 135.6, 135.5, 132.8, 132.1, 130.0, 127.8, 73.3, 59.9, 55.6 (t), 26.5, 19.3. **LRMS**: Calculated for $C_{21}H_{26}F_2NO_2Si$ (M^+) 390.17, Found 390.2.

2-(ethoxycarbonyl)-2-methyl-3,4-dihydro-*2H*-pyrrol 1-oxide (6.22):

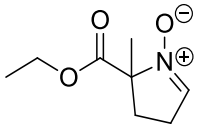

6.22

Synthesis previously reported in the literature.[19]

4-(2-carboxyethyl)-2-cyclohexyl-5-oxo-2,5-dihydrooxazole 3-oxide (6.27):

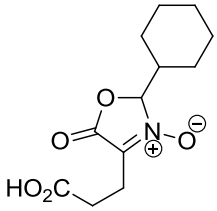

6.27

Synthesis previously reported in the literature.[20]

4-(*tert*-butoxycarbonylamino)-3,4-dihydro-*2H*-pyrrole 1-oxide (6.31):

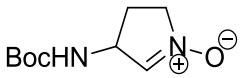

6.31

Synthesis previously reported in the literature.[16]

11,12-didehydro-5,6-dihydro-dibenzo[*a,e*]cycloocten-5-ol, (DIBO, 6.40):

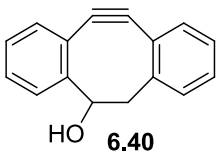

6.40

Synthesis previously reported in the literature.[11]

General Procedure for SPANC Reactions in Model Systems:

The appropriate cyclic nitrone (0.015 mmol) and dibenzocyclooctyne (**6.1**) (0.015 mmol) or dibenzocyclooctynol (**6.31**) (0.015 mmol) were pre-dissolved in either C_6D_6 (0.3 mL) or CD_3CN (0.3 mL) and mixed at equimolar concentrations of ~25 mM (0.6 mL). Percent conversion was monitored both by disappearance of starting materials and by appearance of product as determined by integration at multiple chemical shifts in the ^{1}H NMR spectrum. No other products were detected by ^{1}H NMR and all reactions were performed in triplicate. Upon completion, the triplicate reactions were combined and the solvent was removed by rotary evaporation. The crude reactions were purified by flash column chromatography.

1,2,3,10,11,15c-hexahydro-3,3-dimethyl-dibenzo[3,4:7,8]cycloocta[1,2-*d*]pyrrolo[1,2-*b*]isoxazole (6.32):

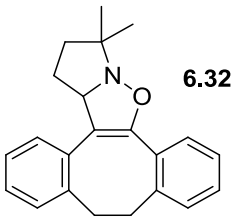

6.32

The crude reaction mixture was concentrated under reduced pressure and **6.32** was purified by flash column chromatography (9:1/hexanes:EtOAc, $\mathbf{R_f}$ = 0.20), affording **6.32** as a white solid (13.0 mg, 0.04 mmol, 91 %). **^{1}H NMR ($CDCl_3$, 400 MHz)**: δ 7.50-7.48 (m, 1H), 7.29-7.08 (m, 7H), 5.18 (dd, *J* = 7.7, 2.8 Hz, 1H), 3.56 – 3.49 (m, 1H), 3.46-3.39 (m, 1H), 2.14-2.04 (m, 1H), 2.01-1.91 (m, 1H), 1.88-1.82 (m, 1H), 1.78-1.73 (m, 1H), 1.47 (s, 3H), 1.20 (s, 3H). **^{13}C NMR ($CDCl_3$, 100 MHz)**: δ 147.5, 140.7, 138.3, 132.7, 130.8, 129.9, 129.7, 128.3, 128.3, 128.1, 126.9, 125.9, 125.5, 110.1, 74.5, 69.5, 36.8, 35.1, 33.3, 31.5, 26.7, 23.7. **HRMS**: Calculated for $C_{22}H_{24}NO_2$ (M^+) 318.1858, Found 318.1832.

1,2,3,3a,8,9-hexahydro-1-methyl-dibenzo[3,4:7,8]cycloocta[1,2-*d*]pyrrolo[1,2-*b*]isoxazole-1-carboxylic acid ethyl ester (6.33 and **6.33'):**

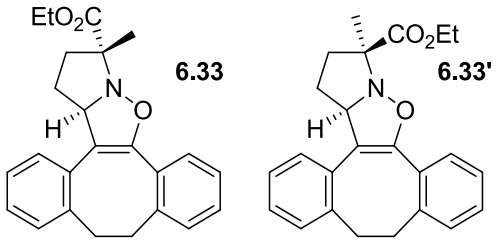

The crude reaction mixture was concentrated under reduced pressure and **6.33** and **6.33'** were separated by flash column chromatography (8:2/ hexanes:EtOAc, $\mathbf{R_f}$ = 0.32 for **6.33** and 0.25 for **6.33'**), affording a 72:28 ratio of **6.33** and **6.33'** as off white solids (16.2 mg, 0.043 mmol, 96 %). **6.33** major**: ^{1}H NMR ($CDCl_3$, 400 MHz)**: δ 7.53-7.52 (m, 1H), 7.24-7.22 (m, 2H), 7.14-7.09 (m, 5H), 5.32 (dd, *J* =7.1, 2.9 Hz, 1H), 4.26 (q, 2H), 3.56-3.49 (m, 1H), 3.44-3.37 (m, 1H), 3.18-3.10 (m, 1H), 3.00-2.94 (m, 1H), 2.43-2.36 (m, 1H), 2.00-1.85 (m, 1H), 1.69 (s, 3H), 1.32 (t, 3H). **^{13}C NMR ($CDCl_3$, 100 MHz)**: δ 173.8, 148.0, 140.7, 138.2, 132.2, 130.8, 129.8, 129.7, 127.0, 126.0, 125.6, 109.8, 76.5, 75.2, 61.4, 36.9, 33.6, 33.3, 30.6, 19.8, 14.2. **6.33'** minor**: ^{1}H NMR ($CDCl_3$, 400 MHz)**: δ 7.42 (d, *J* =7.6 Hz, 1H), 7.26-7.04 (m, 7H), 3.85 (dd, *J* = 8.1, 1.9 Hz, 1H), 4.31-4.21 (m, 2H), 3.56-3.40 (m, 2H), 3.15-3.00 (m, 1H), 2.99-2.94 (m, 1H), 2.68-2.62 (m, 1H), 2.13-2.05 (m, 1H), 1.93 (m, 2H), 1.45 (s, 3H), 1.28 (t, 3H). **^{13}C NMR ($CDCl_3$, 100 MHz)**: δ 171.6, 147.3, 141.0, 138.4, 132.1, 130.8, 129.8, 129.8, 128.4, 138.3, 127.5, 127.2, 126.0, 125.4, 109.8, 74.5, 61.1, 36.8, 33.2, 30.6, 30.4, 22.6, 14.1. **HRMS**: Calculated for $C_{24}H_{26}NO_3$ (M^+) 376.1913, Found 376.1915.

3-[[[(1,1-dimethylethyl)diphenylsilyl]oxy]methyl]-1,2,3,10,11,15*c*-hexahydro-dibenzo-[3,4:7,8]cycloocta[1,2-*d*]pyrrolo[1,2-*b*]isoxazole (6.34 and **6.34'):**

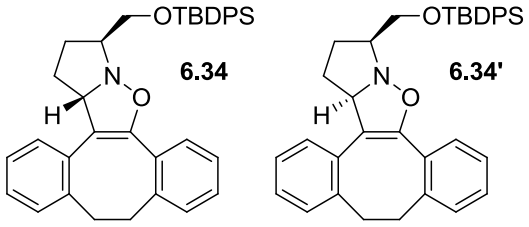

The reaction mixture was concentrated under reduced pressure and **6.34** was purified by flash column chromatography (9:1/ hexanes:EtOAc, $\mathbf{R_f}$ = 0.50 for **6.34** and 0.39 for **6.34'**), affording a 87:13 ratio of **6.34** and **6.34'** as white solids (22.1 mg, 0.040 mmol, 88 %). **6.34** major: **^{1}H NMR ($CDCl_3$, 400 MHz)**: δ 7.70-7.67 (m, 4H), 7.42-7.32 (m, 7H), 7.26-7.23 (m, 1H), 7.17-7.08 (m, 6H), 5.18 (dd, *J* = 6.5, 4.5 Hz, 1H), 4.04 (dd, *J* = 9.6, 4.2 Hz, 1H), 3.75-3.64 (m, 2H), 3.55-3.48 (m, 1H), 3.44-3.37 (m, 1H), 3.19-3.11 (m, 1H), 3.02-2.95 (m, 1H), 2.12-2.04 (m, 2H), 1.86-1.82 (m, 1H), 1.74-1.69 (m, 1H), 1.08 (s, 9H). **^{13}C NMR ($CDCl_3$, 100 MHz)**: δ 147.7, 140.8, 138.1, 135.7, 135.6, 133.7, 133.7, 132.5, 130.8, 129.7, 129.6, 129.4, 128.3, 128.3, 127.6, 126.9, 126.0, 125.5, 109.9, 73.8, 71.4, 66.0, 36.9, 33.3, 29.1, 26.9, 25.5, 19.3. **6.34'** minor: **^{1}H NMR ($CDCl_3$, 400 MHz)**: δ 7.70-7.68 (m, 3H), 7.44-7.08 (m, 15H), 5.20-5.19 (m, 1H), 4.33-4.29 (m, 1H), 3.93-3.89 (m, 1H), 3.51-3.33 (m, 3H), 3.12-3.06 (m, 1H), 2.95-2.88 (m, 1H), 2.08-2.04 (m, 1H), 1.88-1.81 (m, 2H), 1.07 (s, 9H). **^{13}C NMR ($CDCl_3$, 100 MHz)**: δ 148.2, 140.8, 135.6, 133.8, 130.8, 129.9, 129.7, 129.6, 128.4, 128.3, 127.6, 126.0, 125.4, 75.9, 72.8, 50.3, 36.9, 33.2, 32.0, 26.8, 26.6, 19.2. **HRMS**: Calculated for $C_{37}H_{40}NO_2Si$ (M^+) 558.2828, Found 558.2775.

(±)-*N*-[(3R,3aR)-1,2,3,3a,8,9-hexahydrodibenzo[3,4:7,8]cycloocta[1,2-*d*]pyrrolo[1,2-*b*]isoxazol-3-yl]-2,2-dimethyl-propanamide (6.35):

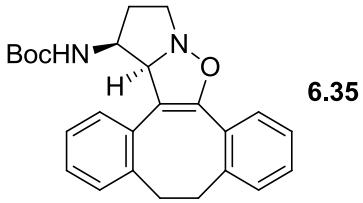

6.35

Synthesis previously reported in the literature.[13]

(1S)- 1-[[[(1,1-dimethylethyl)diphenylsilyl]oxy]methyl]-3,3-difluoro-1,2,3,3a,8,9-hexahydro-dibenzo[3,4:7,8]cycloocta[1,2-*d*]pyrrolo[1,2-b]isoxazole (6.36):

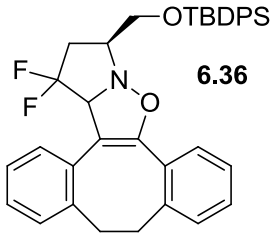

6.36

The reaction mixture was concentrated under reduced pressure and **6.36** was purified by flash column chromatography (85:15/hexanes:EtOAc, $\mathbf{R_f}$ = 0.50), affording **6.36** as a white-solid (22.5 mg, 0.038 mmol 84 %). **^{1}H NMR ($CDCl_3$, 400 MHz)**: δ 7.70-7.66 (m, 4H), 7.44-7.34 (m, 7H), 7.24-7.17 (m, 4H), 7.15-7.19 (m, 3H), 5.31 (dd, *J* = 11.7, 9.5 Hz, 1H), 4.80 (dd, *J* = 10.5, 4.1 Hz, 1H), 3.87 (dd, *J* = 10.5, 6.5 Hz, 1H), 3.78-3.71 (m, 1H), 3.56-3.47 (m, 2H), 3.13-2.94 (m, 2H), 2.51-2.42 (m, 1H), 2.32-2.17 (m, 1H), 1.08 (s, 9H). **^{13}C NMR ($CDCl_3$, 100 MHz)**: δ 149.93, 139.8, 139.2, 135.7, 135.6, 133.3, 133.2, 131.4, 130.6, 130.3, 129.8, 129.2, 129.1, 127.7, 127.4, 127.3, 127.1, 125.9, 125.6, 103.8, 103.7, 79.3, 79.1, 79.0, 78.8, 69.5, 69.4, 64.5, 36.0 (t), 33.7, 26.9, 19.3. **HRMS**: Calculated for $C_{37}H_{38}F_2NO_2Si$ (M^+) 594.2640, Found 594.2665.

1,3,4,11,12,16c-hexahydro-1-oxo-*2H*-dibenzo[3',4':7',8']cyclooct[1',2':4,5]isoxazolo[2,3-*a*]pyrazine-2-acetic acid methyl ester (6.37):

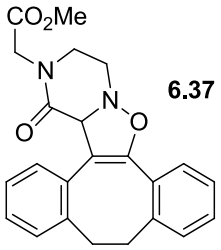

6.37

The reaction mixture was concentrated under reduced pressure and **6.37** was purified by flash column chromatography (8:2/hexanes:EtOAc, $\mathbf{R_f}$ = 0.52), affording **6.37** as an off-white solid (15.2 mg, 0.039 mmol, 87 %). **^{1}H NMR ($CDCl_3$, 400 MHz)**: δ 7.43 (m, 1H), 7.32-7.29 (m, 1H), 7.20-7.11 (m, 6H), 5.46 (s, 1H), 4.35 (d, *J* = 17.4 Hz, 1H), 4.06-4.00 (m, 1H), 3.99 (d, *J* = 17.4 Hz, 1H), 3.80-3.70 (m, 2H), 3.73 (s, 3H), 3.64-3.57 (m, 1H), 3.54-3.47 (m, 1H), 3.41-3.31 (m, 2H), 3.23-3.15 (m, 1H), 3.02-2.96 (m, 1H). **^{13}C NMR ($CDCl_3$, 100 MHz)**: δ 169.0, 165.7, 149.9, 140.3, 139.2, 131.1, 131.0, 129.6, 129.4, 129.3, 129.1, 127.5, 127.2, 125.6, 125.6, 107.8, 71.9, 52.3, 50.5, 48.3, 13.6, 36.7, 33.0. **HRMS**: Calculated for $C_{23}H_{23}N_2O_4$ (M^+) 391.1658, Found 391.1611.

15c-[[[(1,1-dimethylethyl)diphenylsilyl]oxy]methyl]-1,2,3,10,11,15*c*-hexahydro-dibenzo[3,4:7,8]cycloocta[1,2-*d*]pyrrolo[1,2-*b*]isoxazole (6.38):

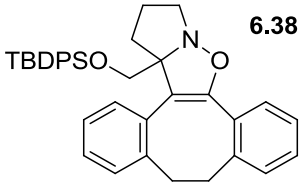

6.38

The reaction mixture was concentrated under reduced pressure and **6.38** was purified by flash column chromatography (95:5/hexanes:EtOAc, $\mathbf{R_f}$ = 0.25), affording **6.38** as an off-white solid (22.2 mg, 0.040 mmol, 89 %). **^{1}H NMR ($CDCl_3$, 400 MHz)**: δ 7.78-7.72 (m,

4H), 7.45-7.36 (m, 7H), 7.28-7.26 (m, 2H), 7.18-7.03 (m, 5H), 3.93 (d, *J* = 10.6 Hz, 1H), 3.73 (d, *J* = 10.6 Hz, 1H), 3.62-3.56 (m, 1H), 3.45-3.32 (m, 2H), 3.29-3.20 (m, 2H), 3.18-3.08 (m, 1H), 2.12-2.02 (m, 1H), 1.93-1.79 (m, 2H), 1.70-1.63 (m, 1H), 1.07 (s, 9H). **^{13}C NMR ($CDCl_3$, 100 MHz)**: δ 150.2, 142.3, 137.6, 136.0, 135.8, 133.8, 133.4, 132.9, 131.3, 130.3, 129.5, 128.9, 128.6, 128.4, 128.2, 127.6, 127.5, 127.2, 125.9, 125.2, 108.3, 85.3, 68.0, 59.4, 37.9, 32.7, 32.1, 26.9, 23.5, 19.4. **HRMS**: Calculated for $C_{37}H_{40}NO_2Si$ (M^+) 558.2828, Found 558.2817.

3-cyclohexyl-10,11-dihydro-1-oxo-*3H*-dibenzo[3,4:7,8]cyclooct[1,2-*d*]oxazolo[3,4-*b*]isoxazole-15*c*(*1H*)-propanoic acid (6.39):

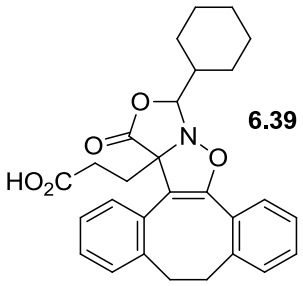

6.39

The reaction mixture was concentrated under reduced pressure and **6.39** was purified by flash column chromatography (7:3/hexanes:EtOAc, $\mathbf{R_f}$ = 0.34), affording **6.39** as a white solid (20.0 mg, 0.044 mmol, 97 %). **^{1}H NMR ($CDCl_3$, 400 MHz)**: δ 7.29-7.10 (m, 8H), 4.98 (d, *J* = 6.3Hz, 1H), 3.44-3.23 (m, 3H), 3.04-2.99 (m, 1H), 2.67-2.59 (m, 1H), 2.55-2.47 (m, 1H), 2.42-2.35 (m, 1H), 2.32-2.24 (m, 2H), 2.01-1.98 (m, 2H), 2.86-1.73 (m, 4H) 1.39-1.22 (m, 1H). **^{13}C NMR ($CDCl_3$, 100 MHz)**: δ 177.6, 170.6, 151.7, 142.1, 138.5, 131.7, 130.2, 129.4, 129.2, 128.8, 128.6, 126.3, 125.9, 125.6, 106.2, 101.4, 78.9, 42.1, 37.6, 32.0, 29.0, 28.7, 27.3, 27.0, 26.2, 25.5, 25.4. **HRMS**: Calculated for $C_{28}H_{30}NO_5$ (M^+) 460.2124, Found 460.2112.

1,2,3,3a,8,9-hexahydro-1,1-dimethyl-dibenzo[3,4:7,8]cycloocta[1,2-*d*]pyrrolo[1,2-*b*]isoxazol-8-ol (6.41):

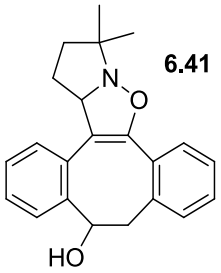

The reaction mixture was concentrated under reduced pressure and **6.42** was purified by flash column chromatography (7:3/hexanes:EtOAc, $\mathbf{R_f}$ = 0.30), affording regio- and diastereomers of **6.42** as an off-white solid (14.7 mg, 0.044 mmol, 97 %). **^{1}H NMR ($CDCl_3$, 400 MHz)**: δ 7.69-7.63 (m, 2.0H), 7.52-7.50 (m, 1.3H), 7.39-7.35 (m, 2.0H), 7.29-7.09 (m, 11H), 5.65-5.61 (m, 1.0H), 5.24-5.20 (m, 1.8H), 5.08-5.03 (m, 0.9H), 3.82-3.77 (dd, *J* = 16.0, 5.2 Hz, 1H), 3.44-3.38 (dd, *J* = 12.6, 11.2 Hz, 0.9H), 3.32-3.27 (dd, J = 12.7, 6.1 Hz, 0.9H), 3.22-3.15 (dd, *J* = 16.0, 10.5 Hz 1.0H), 2.12-1.88 (m, 6.0H), 1.79-1.74 (m, 4.2H), 1.49, 1.46, 1.21, 1.20 (s, 4 x 3H). **^{13}C NMR ($CDCl_3$, 100 MHz)**: δ 149.6, 147.5, 146.8, 143.6, 139.3, 136.7, 135.3, 132.8, 132.6, 131.3, 130.5, 130.4, 130.0, 129.6, 129.0, 128.6, 127.8, 127.7, 127.6, 127.5, 127.2, 127.0, 126.6, 125.9, 125.2, 110.5, 109.1, 74.3, 74.2, 69.6, 69.1, 45.7, 40.5, 35.1, 35.0, 31.1, 30.9, 26.6, 26.5, 23.7. **HRMS**: Calculated for $C_{22}H_{24}NO_2$ (M^+) 334.1807, Found 334.1775.

1,2,3,3a,8,9-hexahydro-8-hydroxy-1-methyl-dibenzo[3,4:7,8]cycloocta[1,2-*d*]pyrrolo[1,2-*b*]isoxazole-1-carboxylic acid ethyl ester (6.42):

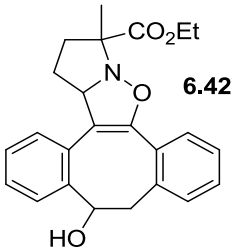

6.42

The reaction mixture was concentrated under reduced pressure and **6.42** was purified by flash column chromatography (65:35/hexanes:EtOAc, $\mathbf{R_f}$ = 0.28), affording a mixture of regio- and diastereomers of **6.42** as an white solid (16.9 mg, 0.043 mmol, 96 %). **^{1}H NMR ($CDCl_3$, 400 MHz)**: δ 7.69-7.66 (m, 1.4H), 7.55-7.50 (m, 0.9 H), 7.46-7.43 (m, 0.4H), 7.37-7.34 (m, 1.6H), 7.30-7.06 (m, 9H), 5.67-5.83 (m, 0.8H), 5.37-5.35 (m, 1H), 5.29-5.25 (m, 0.6H), 5.08-5.04 (m, 0.4H), 5.01-4.96 (m, 0.2H), 4.31-4.09 (m, 3.8H), 3.82-3.75 (m, 0.8H), 3.54-3.13 (m, 2.1H), 2.71-2.59 (m, 0.4H), 2.43-2.33 (m, 1.2H), 2.20-1.77 (m, 8.0H), 1.71, 1.69, 1.48, 1.46 (s, 4 x 3H), 1.3-1.23 (t, 4 x 3H). **^{13}C NMR ($CDCl_3$, 100 MHz)**: δ 173.6, 171.7, 171.4, 171.2, 150.0, 149.3, 148.0, 143.8, 143.6, 139.6, 139.2, 137.1, 136.6, 135.4, 135.2, 132.9, 132.6, 132.4, 132.3, 131.3, 130.2, 130.1, 129.9, 129.9, 129.8, 129.6, 129.6, 129.1, 129.0, 128.7, 128.7, 127.8, 127.7, 127.6, 127.6, 127.5, 127.4, 127.4, 127.2, 127.1, 127.0, 126.6, 126.5, 126.2, 125.9, 125.8, 125.7, 125.3, 125.1, 110.3, 110.1, 108.8, 108.8, 74.9, 74, 9, 74.4, 74.1, 61.5, 61.4, 61.2, 60.4, 45.8, 45.8, 40.8, 40.5, 33.7, 33.6, 31.3, 30.5, 30.4, 30.2, 30.1, 29.7, 29.5, 23.1, 22.6, 21.0, 19.8, 19.8, 14.2, 14.1, 14.0. **HRMS**: Calculated for $C_{24}H_{26}NO_4$ (M^+) 392.1862, Found 392.1799.

1-[[[(1,1-dimethylethyl)diphenylsilyl]oxy]methyl]-1,2,3,3*a*,8,9-hexahydro-dibenzo[3,4:7,8]cycloocta[1,2-*d*]pyrrolo[1,2-*b*]isoxazol-8-ol (6.43):

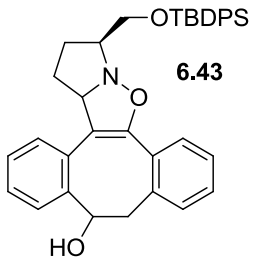

6.43

The reaction mixture was concentrated under reduced pressure and **6.43** was purified by flash column chromatography (8:2/Hx:EtOAc, $\mathbf{R_f}$ = 0.25), affording a mixture of regio- and diastereomers of **6.43** as a white solid (24.0 mg, 0.041 mmol, 92%). **^{1}H NMR ($CDCl_3$, 400 MHz)**: δ 7.71-7.65 (m, 33.2H), 7.63-7.51 (m, 6.2H), 7.43-7.14 (m, 93.5H), 5.65-5.60 (m, 3.5H), 5.53-5.49 (m, 1.4H), 5.39-5.35 (m, 1.0H), 5.30-5.16 (m, 5.5H), 5.09-4.99 (m, 3.1H), 2.13-2.05 (m, 16.8H), 1.96-1.85 (m, 7.2H), 1.80-1.68 (m, 8.6H), 1.08, 1.07, 1.07, 1.06 (s, 4 x 3H). **^{13}C NMR ($CDCl_3$, 100 MHz)**: δ 143.6, 139.1, 136.7, 135.7, 135.7, 135.7, 135.5, 133.7, 133.6, 132.7, 131.6, 131.3, 131.2, 130.4, 130.1, 130.1, 129.8, 129.7, 129.5, 128.9, 128.6, 128.1, 127.6, 127.0, 126.8, 126.6, 125.9, 125.3, 110.3, 109.1, 107.1, 103.5, 73.7, 72.3, 71.5, 69.0, 65.7, 60.4, 45.8, 45.8, 42.1, 40.6, 30.2, 29.6, 29.0, 26.9, 26.8, 26.8, 25.5, 25.4, 21.1, 19.3, 19.2, 14.2. **HRMS**: m/z Calculated for $C_{37}H_{40}NO_3Si$ (M^+) 574.2777, Found 574.2763.

1,3,4,11,12,16c-hexahydro-12-hydroxy-1-oxo-*2H* dibenzo[3',4':7',8']cyclooct[1',2':4,5]-isoxazolo[2,3-*a*]pyrazine-2-acetic acid methyl ester (6.44):

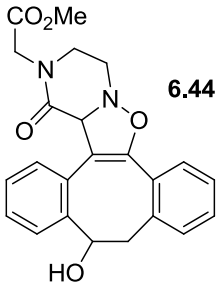

6.44

The reaction mixture was concentrated under reduced pressure and **6.44** was purified by flash column chromatography (6:4/Hx:EtOAc, $\mathbf{R_f}$ = 0.35), affording a mixture of regio- and diastereomers of **6.44** as a white solid (17.4 mg, 0.043 mmol, 95%). **^{1}H NMR ($CDCl_3$, 400 MHz)**: δ 7.67-7.64 (m, 2.1H), 7.58-7.55 (m, 1.1H), 7.48-7.10 (m, 29H), 5.81-5.77 (dd, *J* = 11.6, 5.4 Hz, 1.0H), 5.55-5.23 (m, 2.1H), 5.46-5.43 (m, 3.1H), 5.09-5.04 (dd, *J* = 10.5, 7.3 Hz, 1.0H), 4.99-4.94 (dd, *J* = 10.1, 8.1 Hz, 1.2H), 4.72-4.47 (m, 3.6H), 4.38-4.25 (m, 2.3H), 4.17-4.05 (m, 4.7H), 3.95-3.78 (m, 7.8H), 3.75, 3.74, 3.73, 3.69 (s, 4 x 3H), 3.68-3.43 (m, 8.9H), 3.34-3.10 (m, 8.9H). **^{13}C NMR ($CDCl_3$, 100 MHz)**: δ 169.4, 169.2, 169.1, 169.0, 167.3, 165.8, 165.5, 165.2, 152.2, 149.9, 149.8, 148.7, 144.5, 142.8, 140.4, 140.3, 138.2, 136.5, 136.6, 136.4, 133.8, 132.7, 132.4, 131.7, 131.5, 130.7, 130.4, 130.2, 130.1, 130.0, 130.0, 129.8, 129.7, 129.5, 129.3, 129.2, 129.0, 129.0, 128.8, 128.7, 128.7, 128.6, 128.2, 128.0, 128.0, 127.7, 127.6, 127.5, 127.3, 127.0, 126.8, 126.6, 126.5, 126.4, 126.3, 126.2, 125.9, 125.7, 125.6, 125.4, 125.2, 124.8, 124.5, 110.2, 109.3, 108.5, 105.8, 76.1, 74.2, 72.0, 71.9, 71.8, 71.5, 71.3, 68.1, 65.5, 64.3, 60.4, 57.1, 52.6, 52.5, 52.4, 52.3, 52.0, 51.9, 50.5, 50.2, 50.1, 49.2, 48.8, 48.5, 48.4, 48.3, 45.6, 43.7, 43.6, 43.6, 43.5, 43.1, 42.4, 40.6, 35.1, 30.9, 30.6, 21.0, 19.1, 14.2, 13.7. **HRMS**: Calculated for $C_{23}H_{23}N_2O_5$ (M^+) 407.1617, Found 407.1634.

3,6-diamino-9-[2-carboxy-4(or 5)-[[[5-[[[(11,12-didehydro-5,6-dihydro-dibenzo[*a,e*]-cyclo-octen-5-yl)oxy]carbonyl]amino]pentyl]amino]carbonyl]phenyl]-4,5-disulfo-xanthone (6.48):

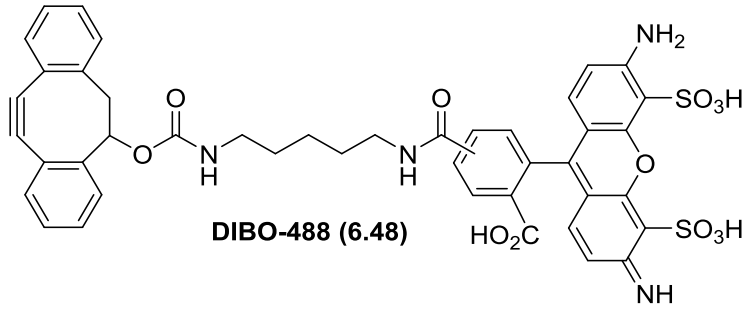

DIBO-488 (6.48)

Alexa Fluor® 488 cadaverine, sodium salt (1mg, 0.00156 mmol) was dissolved in a dry DMF (0.2 mL) solution containing *N*,*N*-diisopropyl amine (1.4 μL, 0.0078 mmol) and 11,12-didehydro-5,6-dihydrodibenzo[*a,e*]cycloocten-5-yl carbonic acid 4-nitrophenyl ester[11] (0.8mg, 0.00312 mmol) at r.t. and the reaction was stirred overnight. The solvent was removed by rotary evaporation and **6.48** was purified by reverse-phase preparative HPLC, eluting with 10-95% MeCN+0.1%TFA:H_2O+0.1%TFA gradient in 10 min. Column: Sunfire C_{18}, 19x100mm, flow rate: 17.0 mL/min. **6.48** was obtained as a dark orange solid (0.8 mg, 0.0009 mmol, 58 %). **LRMS**: Calculated for $C_{43}H_{37}N_4O_{12}S_2$ (M^+) 865.18, Found 865.2.

3,6-bis(dimethylamino)-9-[2-carboxy-4(or 5)-[[[5-[[[(11,12-didehydro-5,6-dihydro-dibenzo-[*a,e*]cycloocten-5-yl)oxy]carbonyl]amino]pentyl]amino]carbonyl]phenyl]-xanthone (6.50):

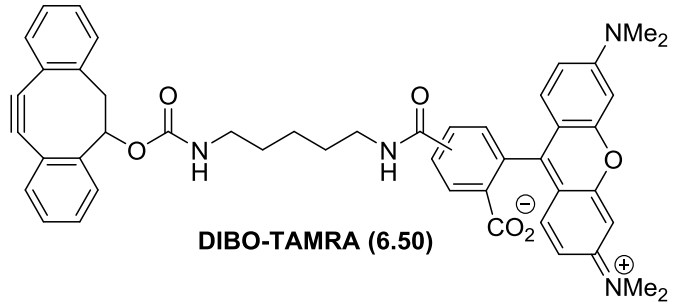

DIBO-TAMRA (6.50)

5-(and-6)-((*N*-(5-aminopentyl)-amino)carbonyl)tetramethylrhodamine (10 mg, 0.019 mmol) was dissolved in DMF (0.5 mL). Then 4-nitrophenyl chloroformate dibenzocyclooctyne[13] (11.2 mg, 0.029 mmol) and Et_3N (8 μL, 0.057 mmol) were added. The reaction was allowed to stir at r.t. in the absence of light for 4 hrs. After the allotted time, the solvent was removed under reduced pressure. **6.50** was purified by reverse-phase preparative HPLC, eluting with 40-65% MeCN+0.1%TFA/H_2O+0.1%TFA gradient in 20 min. Column: Sunfire C_{18} 19x100mm, flow rate: 17.0 mL/min. **6.50** was obtained as a dark purple solid (11.9 mg, 0.015 mmol). **LRMS**: Calculated for $C_{47}H_{45}N_4O_6$ (M^+) 761.33, Found 761.3.

***N*-[5-[[5-[(3aS,4S,6aR)-hexahydro-2-oxo-*1H*-thieno[3,4-d]imidazol-4-yl]-1-oxopentyl]-amino]pentyl]-carbamic acid 11,12-didehydro-5,6-dihydrodibenzo[*a,e*]cycloocten-5-yl ester (6.52):**

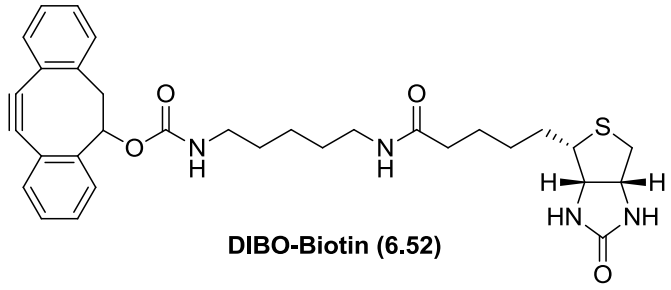

DIBO-Biotin (6.52)

Synthesis previously reported in the literature.[11]

2-(methyloxidoimino)-*N*-(phenylmethyl)-acetamide (6.53):

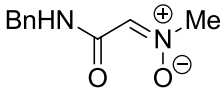

6.53

Synthesis previously reported in the literature.[17]

(2S)-3,4-dihydro-*2H*-pyrrole-2-methanol 1-oxide (6.46):

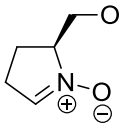

6.46

To a stirring solution of **6.11** (39.2 mg, 0.11 mmol) in dry THF (1.5 mL) was added TBAF (132 μL, 0.13 mmol from a 1.0 M solution in THF). The resultant solution was stirred at r.t. for 3 h. Upon completion, the solvent was removed by rotary evaporation and the crude orange oil was purified by flash column chromatography (85:15/CH_2Cl_2:CH_3OH, $\mathbf{R_f}$ = 0.3), affording **6.46** as an off-white solid (12.0 mg, 0.10 mmol, 95 %). **^{1}H NMR ($CDCl_3$, 400 MHz)**: δ 6.93 (m, 1H), 4.15 (m, 1H), 4.02 (dd, *J* = 12.1, 2.8 Hz, 1H), 3.80 (dd, *J* = 12.1, 6.9 Hz, 1H), 2.70-2.66 (m, 2H), 2.36-2.30 (m, 1H), 2.02-1.97 (m, 1H). **^{13}C NMR ($CDCl_3$, 100**

MHz): δ 135.9, 72.2, 63.8, 27.1, 21.4. **LRMS**: Calculated for $C_5H_{10}NO_2$ (M^+) 116.07, Found 116.1.

[(2S)-3,4-dihydro-1-oxido-*2H*-pyrrol-2-yl]methyl 2,5-dioxo-1-pyrrolidinyl-carbonic acid ester (6.45):

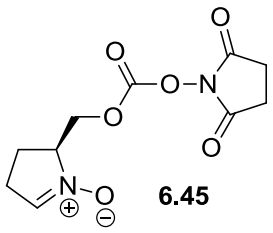

6.45

To a stirring solution of **6.46** (3.3 mg, 0.029 mmol) in dry CH_3CN (0.29 mL), was added DSC (8.7 mg, 0.034 mmol) and Et_3N (5.2 μL, 0.037 mmol). The reaction was stirred overnight under an atmosphere of argon. Upon completion, **6.45** was used directly for coupling with BSA or EGF.

3,4-dihydro-2-methyl-*2H*-pyrrole-2-carboxylic acid 1-oxide (6.57):

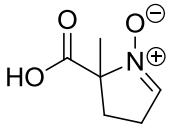

6.57

Synthesis previously reported in the literature.[19]

2-methyl-2-((3R,4R,5S)-2,4,5-triacetoxy-6-(acetoxymethyl)-tetrahydro-*2H*-pyran-3-ylcarbamoyl)-3,4-dihydro-*2H*-pyrrole 1-oxide (Ac_4ManNCMPO, 6.56):

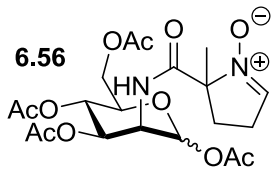

A solution of 6.57 (17 mg, 0.12 mmol) dissolved in DMSO (1.2 mL) was treated wtih EDC·Cl (38.3 mg, 0.2 mmol) and 1-HOBt (16.2 mg, 0.12 mmol) and was allowed to stir at r.t. for 30 min. Then added *D*-Mannopyranose, 2-amino-2-deoxy-, 1,3,4,6-tetraacetate, ethanedioate (1:1)[29] (52.5 mg, 0.12 mmol) and triethyl amine (33 μL, 0.24 mmol). The reaction mixture was allowed to stir at r.t. for 48 hrs. Upon completion, the solvent was evaporated by high vaccuum rotary evaporation and the crude was purified by reverse phase preparative HPLC, eluting with 10 to 50 % MeCN+0.1%FA/H2O+0.1%FA in 20 min. Column: Sunfire C18, 3.5 μm, 19x100mm, flow rate = 17.0 mL/min. A 1:1 mixture of α and β anomers of **6.56** was obtained as an off-white solid (27.6 mg, 0.058 mmol). **^{1}H NMR ($CDCl_3$, 400 MHz)**: δ 8.84 (d, *J* = 9.5 Hz, 1H), 8.70 (d, *J* = 9.4 Hz, 1H), 7.44 (m, 1H), 7.38 (m, 1H), 6.10 (d, *J* = 1.9 Hz, 1H), 6.03 (d, *J* = 1.6 Hz, 1H), 5.32-5.27 (m, 3H), 5.17 (t, *J* = 10.0 Hz, 1H), 4.62-4.56 (m, 2H), 4.25 (dt, *J* = 12.2, 4.0 Hz, 2H), 4.15-4.02 (m, 4H), 3.03-2.95 (m, 2H), 2.76-2.69 (m, 4H), 2.24-2.11 (m, 2H), 2.18 (s, 3H), 2.17 (s, 3H), 2.13 (s, 6H), 2.05 (s, 3H), 2.03 (s, 3H), 1.98 (s, 3H), 1.96 (s, 3H), 1.78 (s, 3H), 1.72 (s, 3H). **^{13}C NMR ($CDCl_3$, 100 MHz)** : δ 171.0 (C), 171.0 (C), 170.5 (C), 170.2 (C), 170.1 (C), 169.9 (C), 169.4 (C), 169.3 (C), 168.2 (C), 168.2 (C), 143.9 (CH), 143.7 (CH), 91.5 (CH), 91.3 (CH), 79.1 (C), 79.0 (C), 70.4 (CH), 70.4 (CH), 69.6 (CH), 69.6 (CH), 65.5 (CH), 65.1 (CH), 61.5 (CH_2), 61.3 (CH_2), 49.5 (CH), 49.2 (CH), 30.1 (CH_2), 29.6 (CH_2), 25.6 (CH_2), 25.4 (CH_2),

24.0 (CH_3), 23.1 (CH_3), 20.8 (CH_3), 20.7 (CH_3), 20.5 (CH_3), 20.5 (CH_3), 20.4 (CH_3). **LRMS**: Calculated for $C_{20}H_{29}N_2O_{11}$ (M+) 473.18, Found 473.2.

(3R,4R,5S)-6-(acetoxymethyl)-3-(2-azidoacetamido)-tetrahydro-*2H*-pyran-2,4,5-triyl triacetate (Ac_4ManNAz, 6.59):

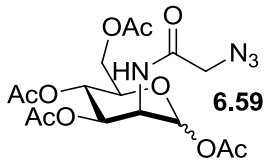

6.59

Synthesis previously reported in the literature.[29]

Kinetics measurements of SPANC by ^{1}H NMR:

The appropriate cyclic nitrone and dibenzocyclooctyne (**6.1**) or 4-dibenzocyclooctynol (**6.40**) were pre-dissolved in either C_6D_6 or CD_3CN and mixed at equimolar concentrations of ~25 mM. Percent conversion was monitored both by disappearance of starting materials and by appearance of product as determined by integration at multiple chemical shifts in the ^{1}H NMR spectrum. No other products were detected by ^{1}H NMR and all reactions were performed in triplicate. Second order rate constants in units of $M^{-1}s^{-1}$ were determined by plotting 1/[nitrone] versus time and subsequently using analysis by linear regression. The second order rate constant k_2 ($M^{-1}s^{-1}$) corresponded to the determined slope. Plots for reactions of cyclic nitrones with dibenzocyclooctyne (**6.1**) in C_6D_6 (25 mM) are shown (Figure 6-6). Plots for reactions of cyclic nitrones with 4-dibenzocyclooctynol (**6.40**) in CD_3CN (25 mM) are shown in Figure 6-7.

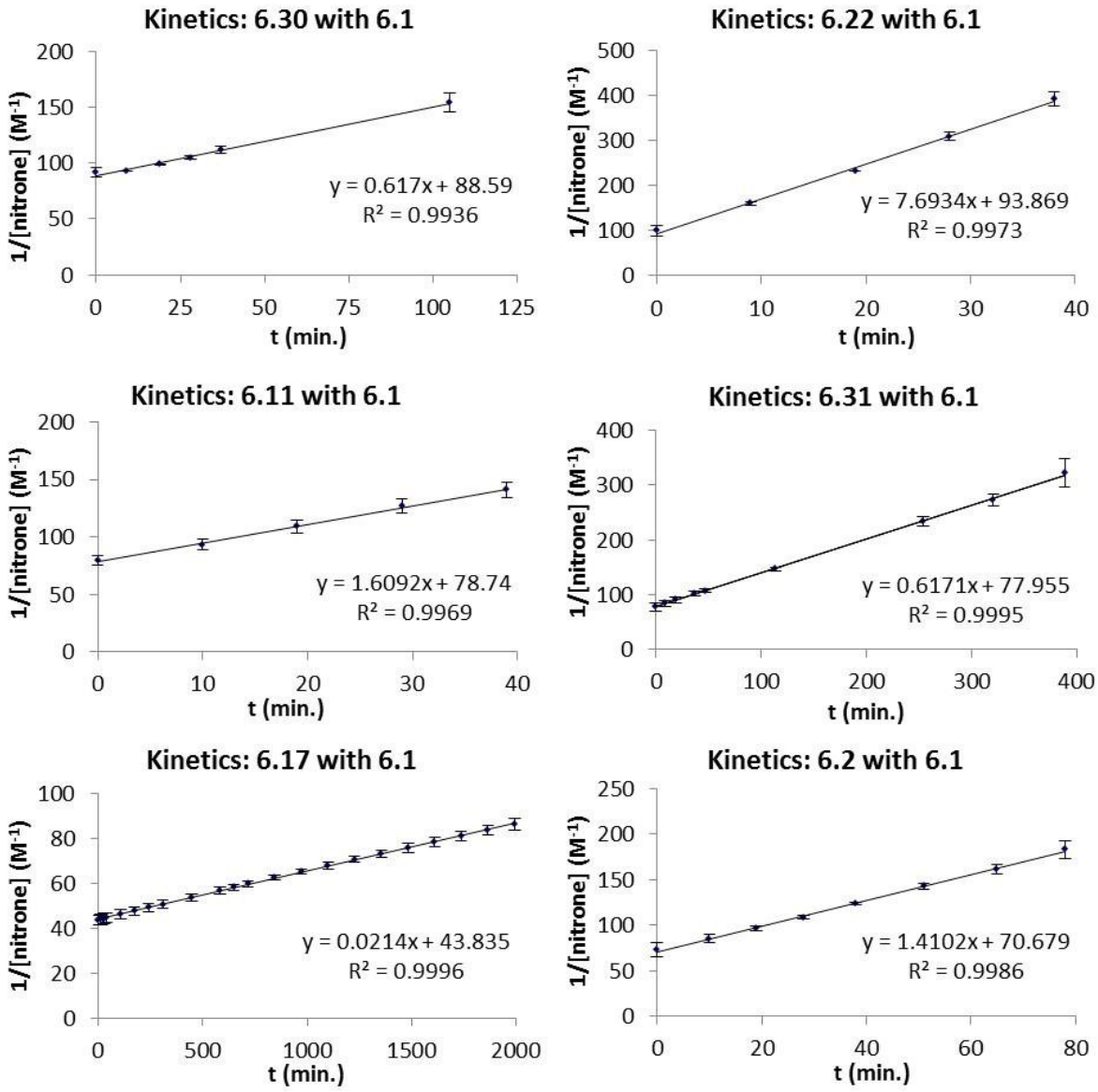

Figure 6-6. Kinetics of SPANC with dibenzocyclooctyne by ^{1}H NMR. Reactions of cyclic nitrones (**6.30**, **6.22**, **6.11**, **6.31**, **6.17** and **6.2**) with dibenzocyclooctyne (**6.1**) in C_6D_6 (25 mM).

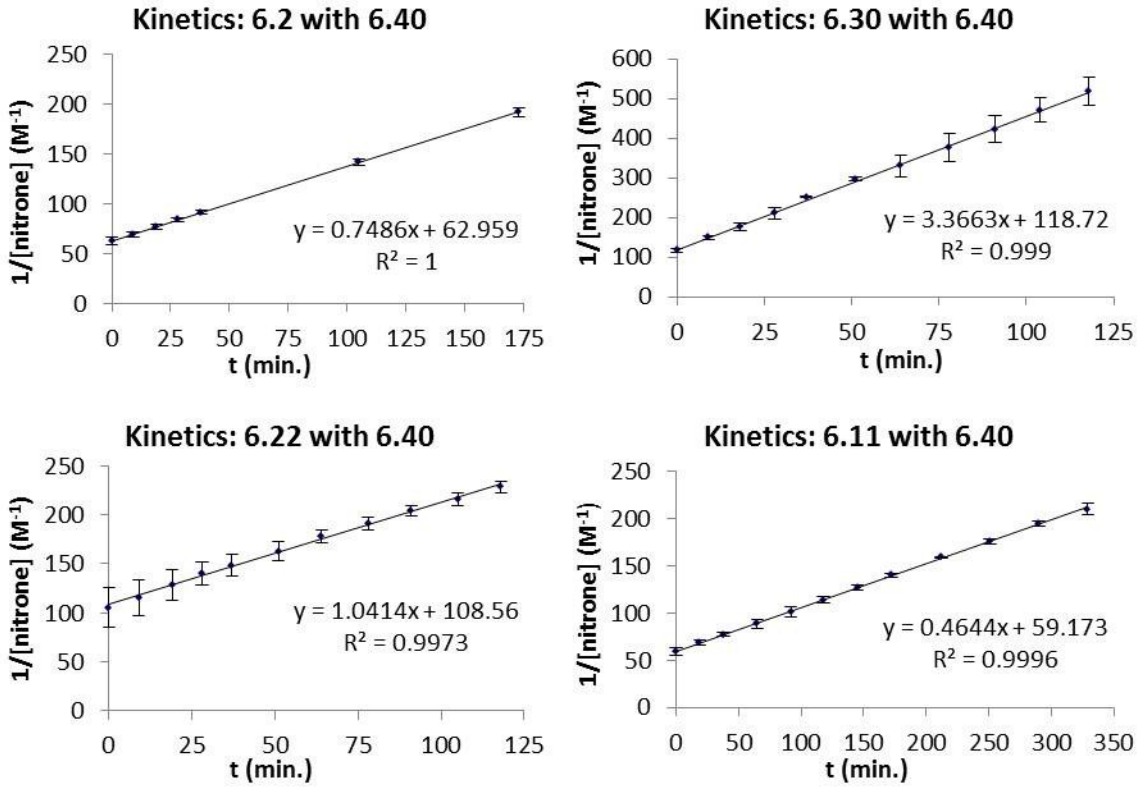

Figure 6-7. Kinetics of SPANC with 4-dibenzocyclooctynol by ^{1}H NMR. Reactions of cyclic nitrones (**6.2**, **6.30**, **6.22** and **6.11**) with DIBO (**6.40**) in CD_3CN (25 mM).

Kinetics Measurements of SPANC Versus SPAAC by Absorption Spectroscopy:

Rate measurements of cycloadditions of Ac_4ManNCMPO (**6.56**) or Ac_4ManNAc (**6.59**) with DIBO (**6.40**) in acetonitrile at 25 ± 0.1 ºC were performed under pseudo-first order conditions by UV-visible spectroscopy with **6.56** and **6.59** in at least 100 fold excess. Reactions were monitored by following the decay of the absorbance at the characteristic wavelengths specified and were repeated in triplicate. For each sample the absorbance (Abs.) at 287 nm (for **6.56**) or 297 nm (for **6.59**) was monitored until reaction was complete as determined by no further change in absorbance. Pseudo first order rate constants (k_{obs}) in units of s^{-1} were determined from the slope obtained by plotting Ln(Abs. – $Abs._{final}$) versus time. The second order rate constant, k_2 ($M^{-1}s^{-1}$), was determined by plotting k_{obs} versus

concentration of **6.56** or **6.59**, respectively (Figure 6-8); the slope of the line corresponded to k_2.

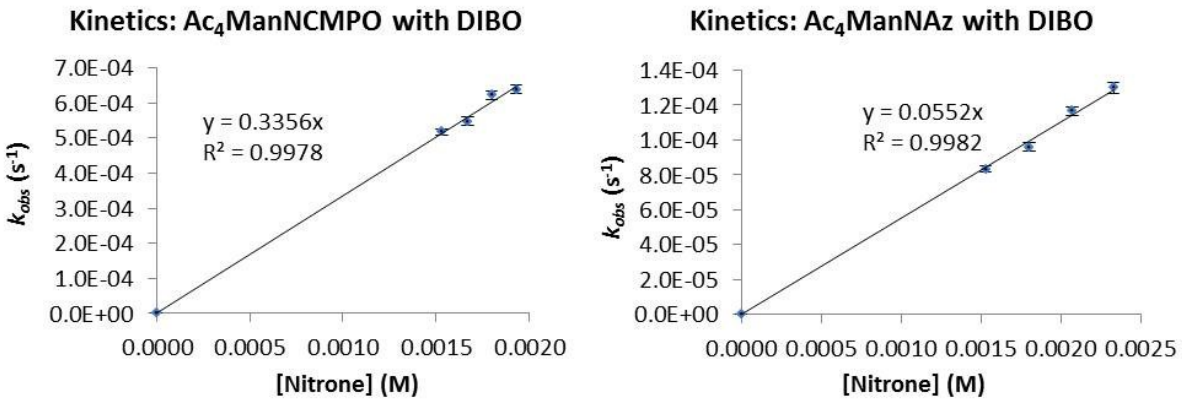

Figure 6-8. Kinetic studies of SPANC versus SPAAC by absorption spectroscopy. A) Reaction of Ac_4ManNCMPO (1.53, 1.67, 1.8, 1.93 mM) with DIBO (0.015 mM) in CH_3CN monitored at λ=287 nm. B) Reaction of Ac_4ManNAz (1.5, 1.8, 2.07, 2.33 mM) with DIBO (0.015 mM) in CH_3CN monitored at λ=297 nm. The second order rate constant k_2 ($M^{-1}s^{-1}$) was determined from multiple pseudo-first order rate constants ($k_2 = k_{obs}$[Ac_4ManNAc]).

Hydrolysis Studies of Acyclic and Cyclic Nitrones at Variable pH of Solution:

The acyclic nitrone[11] (20 µL, 0.01 mmol from a 500 mM stock in DMSO) or cyclic nitrone (20 µL, 0.01 mmol from a 500 mM stock in DMSO) was added to either PBS 1x (980 µL), 10 mM NaOH (980 µL), 100 mM NaOH (980 µL), 10 mM HCl (980 µL) or 100 mM HCl (980 µL). Hydrolysis was monitored by disappearance of the acyclic nitrone as determined by reverse phase analytical HPLC (Figure 6-5). The concentration of nitrone remaining (nitrone %) was determined by substituting the peak area from the HPLC chromatogram into the equations of nitrone calibration curves.[32]

***In vitro* SPANC labeling of BSA and EGF:**

Cyclic Nitrone Modification of BSA or EGF *via* NHS Coupling:

The NHS-activated nitrone, **6.45** (2 μL, 200 nmol from a 100 mM freshly prepared stock in CH_3CN) was added to a solution of BSA (10 nmol) or EGF (8 nmol) in phosphate buffered saline pH =7.4 (100 μL, PBS: 137 mM NaCl, 2.7 mM KCl, 8 mM Na_2HPO_4, and 2 mM KH_2PO_4). The reaction was incubated on a shaking platform over night at r.t. Upon completion, nitrone modified BSA (**6.47**) was first diluted with PBS (15 mL) and then concentrated in an Amicon Ultra-15 centrifugal filter device (Millipore) with a 10-kDa molecular weight cut off (MWCO) by centrifugation at 4000 g. In the second case of nitrone modified EGF (**6.49**), the sample was diluted with PBS (15 mL) in an Amicon Ultra-15 filter device (Millipore) with a 3-kDa MWCO and was concentrated by centrifugation at 4000 g. For both samples, the process was repeated twice more to remove excess **6.45**, excess coupling reagents and byproducts from the NHS activation of **6.46**. The samples were concentrated to final volume of 200-500 μL. The final concentration of **6.47** was determined by a Bio-Rad Bradford Protein Assay (BIO-RAD) against BSA standards. The final concentration of **6.49** was calculated based on the volume remaining in the device. MALDI-MS of **6.47** and unmodified BSA samples indicated that there was on average four cyclic nitrones incorporated (Figure 6-9A and B, respectively). The MALDI-MS of **6.49** and EGF indicated that there were an average of two nitrone groups incorporated (Figure 6-9C and D, respectively).

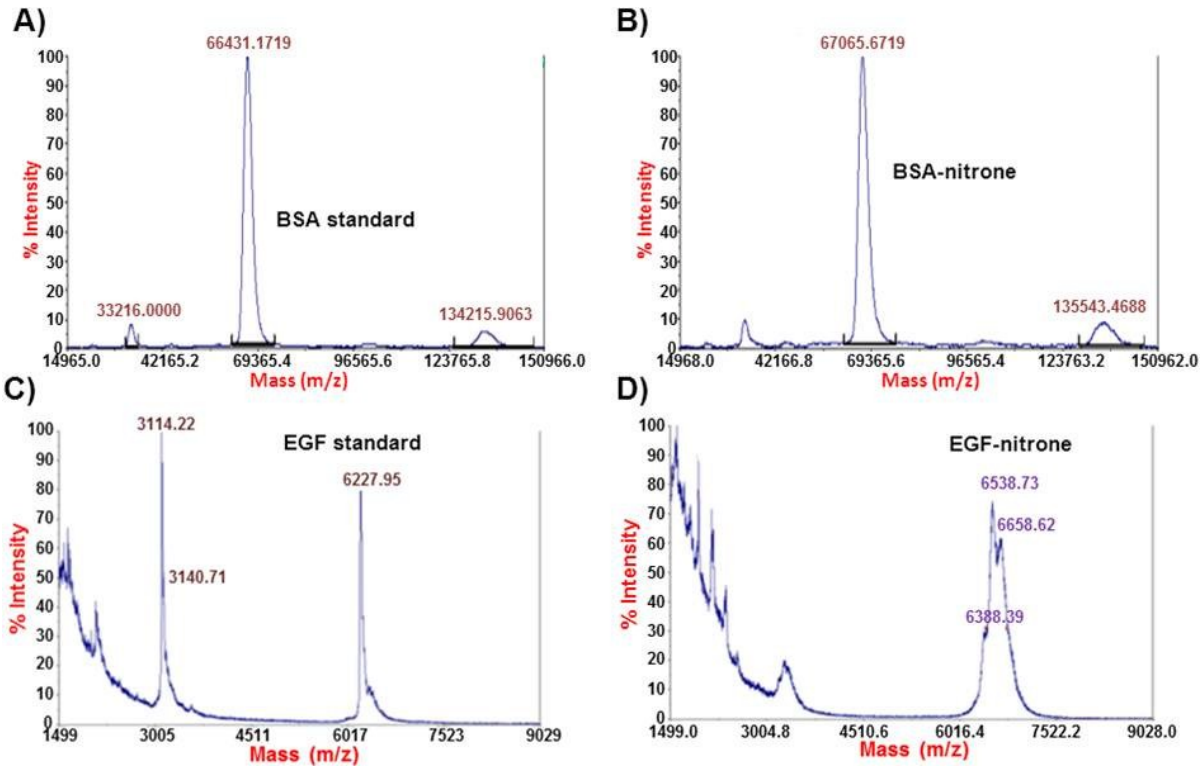

Figure 6-9. MALDI-MS/MS post-modification of BSA and EGF with **6.45**. A) MS of BSA; B) MS of nitrone modified BSA (**6.47**); C) MS of EGF; D) MS of nitrone modified EGF (**6.49**).

***In vitro* SPANC Labelling of Nitrone Modified BSA with DIBO-488:**

The crude nitrone modified BSA, **6.47** (7.36 µL, 0.25 nmol from a 34 µM stock in PBS) was diluted with PBS (993 µL) and was reacted with DIBO-488, **6.48** (1.25 µL, 1.25 µmol from a 100 mM stock solution in PBS). The reaction was incubated on a shaking platform at r.t. in the absence of light for 0-60 min. During this time course experiment, a negative control (-) sample contained unmodified BSA (0.25 nmol) solution in PBS (1 mL) in the presence of DIBO-488 (1.25 µmol). This was used to confirm specific time dependent labelling of BSA via SPANC. At each time point, a 40 µL aliquot from the SPANC reaction and negative control was quenched with cyclic nitrone **6.22** (2 µL, 200 µmol from a 100 mM stock solution in DMSO). Each quenched BSA sample (20 µL) and negative control (20 µL) was

diluted with 4 μL of 6X sodium dodecyl sulphate polyacrylamide gel electrophoresis sample buffer (SDS-PAGE, 300 mM Tris pH 6.8, 12% w/v SDS, 60% glycerol, 600 mM dithiothreitol) and was heated at 95 °C for 10 min. The samples and negative controls were separated by 10 % Tris-glycine SDS-PAGE. After electrophoresis, the gel was imaged using the Fluorescent Method Bio Image Analyzer FMBIO III (Hitachi, Tokyo, Japan). The band intensities corresponding to fluorescently labelled BSA (Figure 6-2B, upper left gel) were quantified with ImageJ software (National Institutes of Health, Bethesda, MD). After the fluorescence measurement, the same gel was silver stained for protein content (Figure 6-2B, lower left gel).

***In vitro* SPANC Labelling of Nitrone Modified EGF with DIBO-TAMRA:**

The crude nitrone modified EGF, **6.49** (64.8 μL, 1.25 nmol from a 19.3 μM stock in PBS) was diluted with PBS (435.2 μL) and was reacted with DIBO-TAMRA, **6.50** (62.5 μL, 6.25 μmol from a 100 μM stock solution in DMSO). The reaction was incubated on a shaking platform at r.t. in the absence of light for 0-60 min. During this time course experiment, a negative control (-) sample contained unmodified EGF (1.25 nmol) solution in PBS 1x (0.5 mL) in the presence of DIBO-TAMRA (6.25 μmol). At each time point, a 40 μL aliquot from the SPANC reaction and negative control was quenched with cyclic nitrone **6.22** (2 μL, 200 μmol from a 100 mM stock solution in DMSO). Each quenched EGF sample (20 μL) and negative control (20 μL) was diluted with 4 μL of 6X sodium dodecyl sulphate polyacrylamide gel electrophoresis sample buffer (SDS-PAGE, 300 mM Tris pH 6.8, 12% w/v SDS, 60% glycerol, 600 mM dithiothreitol) and was heated at 95 °C for 10 min. The samples and negative controls were separated by a 16 % tricine SDS-PAGE gel. After electrophoresis, the gel was imaged using the Fluorescent Method Bio Image Analyzer

FMBIO III (Hitachi, Tokyo, Japan). The band intensities corresponding to fluorescently labeled EGF (Figure 6-2C, upper right gel) were quantified with ImageJ software (National Institutes of Health, Bethesda, MD). After the fluorescence measurement, the same gel was silver stained for protein content (Figure 6-2C, lower right gel).

***In situ* Imaging of Cancer Cells via SPANC:**

Cell culture:

The MDA-MB-468 (breast cancer) cell line was maintained in Leibovitz's L-15 medium supplemented with 10% fetal bovine serum (FBS; CANSERA), 50 U/mL penicillin and 50 μg/mL streptomycin in a humidified incubator at 37 °C with 100 % atmospheric air.

Fixed Cell Labelling of EGFRs by SPANC:

MDA-MB-468 cells were seeded at 20 x 10^4 cells/well in 12 well tissue culture plates in 1 mL of Leibovitz's L-15 medium supplemented with 10 % fetal bovine serum (FBS; CANSERA), 50 U/mL penicillin and 50 μg/mL streptomycin. After 24 h, appropriate samples were treated with BSA (1% in serum free medium) for 30 min at r.t. to block non-specific binding of EGF. The samples were subsequently, treated with cyclic nitrone modified EGF **6.49** (1 μM) and incubated for 5 min at 4˚C. In parallel, the negative control samples were treated with unmodified EGF (1 μM). The cells were washed with media (3X) and PBS (3X) and treated with DIBO-biotin **6.52** (10 μM) for 30 min at r.t. in serum-free media. The cells were washed with media (3X) and PBS (3X), blocked with 1% BSA (in serum free media) for 30 min at r.t., and then stained with FITC-streptavidin (5 μg/mL in PBS) for 30 min at r.t. Cells were then washed with media (2X) and PBS (2X), and then fixed by applying fixing solution (4% paraformaldehyde, 4% sucrose in dH_2O) for 15 min at

4 ˚C. Once the coverslips were mounted on slides, the cells were imaged with an Olympus 1X81 spinning-disk confocal microscope equipped with a FITC filter (Semrock, Excitation: 465-499 nm, Emission: 516-556 nm) and a Photometrics (Coolsnap ES) camera using 100x magnification. Images were taken of samples and controls using both bright-field and the FITC channel (1 s exposure). Image processing was done using ImageJ software, applying pseudocolour to FITC channel images. The same pixel-intensity ranges were applied and displayed for all images taken.

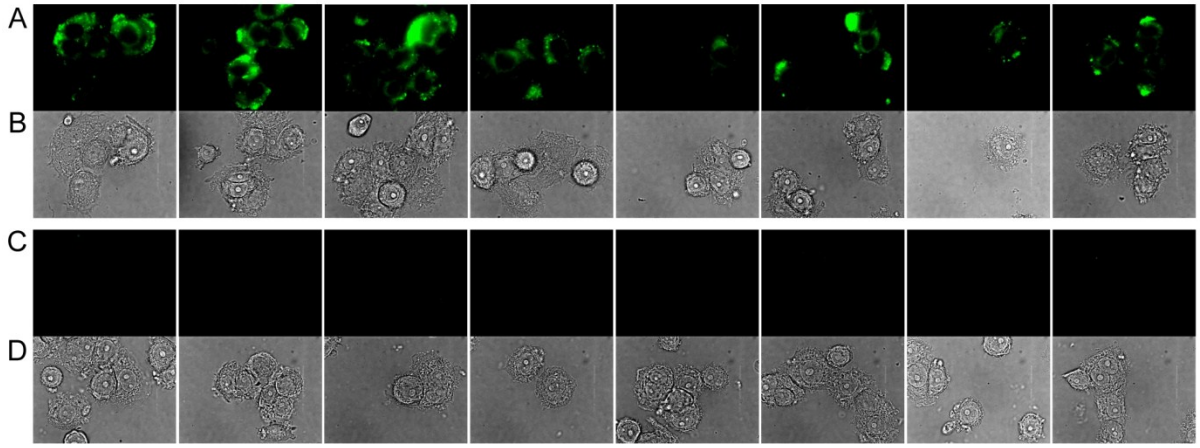

Figure 6-10. Fixed cell imaging of EGFRs via SPANC. Highly specific fluorescent labeling for 8 fields of view (A and B, n = 41) relative to the negative controls (C and D, n = 47). For each image, fluorescence mode is on top and bright field is on the bottom (B and D). The labeling experiment was repeated once with consistent results.

References

(1) Prescher, J. A.; Bertozzi, C. R. *Nat. Chem. Biol.* **2005**, *1*, 13-21.
(2) Best, M. D. *Biochemistry* **2009**, *48*, 6571-6584.
(3) Chen, Y.-X.; Triola, G.; Waldmann, H. *Acc. Chem. Res.* **2011**, *44*, 762-773.
(4) Sletten, E. M.; Bertozzi, C. R. *Angew. Chem. Int. Ed.* **2009**, *48*, 6974-6998.
(5) Bertozzi, C. R. *Acc. Chem. Res.* **2011**, *44*, 651-653.
(6) Sletten, E. M.; Bertozzi, C. R. *Acc. Chem. Res.* **2011**, *44*, 666-676.
(7) Baskin, J. M.; Prescher, J. A.; Laughlin, S. T.; Agard, N. J.; Chang, P. V.; Miller, I. A.; Lo, A.; Codelli, J. A.; Bertozzi, C. R. *Proc. Natl. Acad. Sci. U.S.A.* **2007**, *104*, 16793-16797.
(8) Chang, P. V.; Chen, X.; Smyrniotis, C.; Xenakis, A.; Hu, T.; Bertozzi, C. R.; Wu, P. *Angew. Chem. Int. Ed.* **2009**, *48*, 4030-4033.
(9) Chang, P. V.; Prescher, J. A.; Sletten, E. M.; Baskin, J. M.; Miller, I. A.; Agard, N. J.; Lo, A.; Bertozzi, C. R. *Proc. Natl. Acad. Sci. U.S.A.* **2010**, *107*, 1821-1826.
(10) Agard, N. J.; Prescher, J. A.; Bertozzi, C. R. *J. Am. Chem. Soc.* **2004**, *126*, 15046-15047.
(11) Ning, X.; Guo, J.; Wolfert, Margreet A.; Boons, G.-J. *Angew. Chem. Int. Ed.* **2008**, *47*, 2253-2255.
(12) Thesing, J.; Sirrenberg, V. *Chem. Ber.* **1958**, *91*, 1978.
(13) McKay, C. S.; Moran, J.; Pezacki, J. P. *Chem. Commun.* **2010**, *46*, 931-933.
(14) Wierchem, F.; Rück-Braun, K. *Z. Naturforsch.* **2006**, *61b*, 431-436.
(15) Murahashi, S.; Mitsui, H.; Shiota, T.; Tsuda, T.; Watanabe, S. *J. Org. Chem.* **1990**, *55*, 1736-1744.
(16) Gella, C.; Ferrer, È.; Alibés, R.; Busqué, F.; de March, P.; Figueredo, M.; Font, J. *J. Org. Chem.* **2009**, *74*, 6365-6367.
(17) Ning, X.; Temming, R. P.; Dommerholt, J.; Guo, J.; Ania, D. B.; Debets, M. F.; Wolfert, M. A.; Boons, G.-J.; van Delft, F. L. *Angew. Chem. Int. Ed.* **2010**, *49*, 3065-3068.
(18) Tsai, P.; Elas, M.; Parasca, A. D.; Barth, E. D.; Mailer, C.; Halpern, H. J.; Rosen, G. M. *J. Chem. Soc., Perkin Trans. 2* **2001**, 875-880.
(19) Tsai, P.; Ichikawa, K.; Mailer, C.; Pou, S.; Halpern, H. J.; Robinson, B. H.; Nielsen, R.; Rosen, G. M. *J. Org. Chem.* **2003**, *68*, 7811-7817.
(20) Flores, M. A.; Bode, J. W. *Org. Lett.* **2010**, *12*, 1924-1927.
(21) Poloukhtine, A. A.; Mbua, N. E.; Wolfert, M. A.; Boons, G.-J.; Popik, V. V. *J. Am. Chem. Soc.* **2009**, *131*, 15769-15776.
(22) Jewett, J. C.; Sletten, E. M.; Bertozzi, C. R. *J. Am. Chem. Soc.* **2010**, *132*, 3688-3690.
(23) Saxon, E.; Luchansky, S. J.; Hang, H. C.; Yu, C.; Lee, S. C.; Bertozzi, C. R. *J. Am. Chem. Soc.* **2002**, *124*, 14893-14902.
(24) Tanner, M. E. *Bioorg. Chem.* **2005**, *33*, 216-228.
(25) Dube, D. H.; Bertozzi, C. R. *Curr. Opin. Chem. Biol.* **2003**, *7*, 616-625.
(26) Laughlin, S. T.; Agard, N. J.; Baskin, J. M.; Carrico, I. S.; Chang, P. V.; Ganguli, A. S.; Hangauer, M. J.; Lo, A.; Prescher, J. A.; Bertozzi, C. R.; Minoru, F. *Methods Enzymol.* **2006**, *415*, 230-250.
(27) Angelino, N. J.; Bernacki, R. J.; Sharma, M.; Dodson-Simmons, O.; Korytnyk, W. *Carbohydr. Res.* **1995**, *276*, 99-115.

(28) Oetke, C.; Brossmer, R.; Mantey, L. R.; Hinderlich, S.; Isecke, R.; Reutter, W.; Keppler, O. T.; Pawlita, M. *J. Biol. Chem.* **2002**, *277*, 6688-6695.
(29) Laughlin, S. T.; Bertozzi, C. R. *Nat. Protoc.* **2007**, *2*, 2930-2944.
(30) McKay, C. S.; Blake, J. A.; Cheng, J.; Danielson, D. C.; Pezacki, J. P. *Chem. Commun.* **2011**, *47*, 10040-10042.

Spectral Data

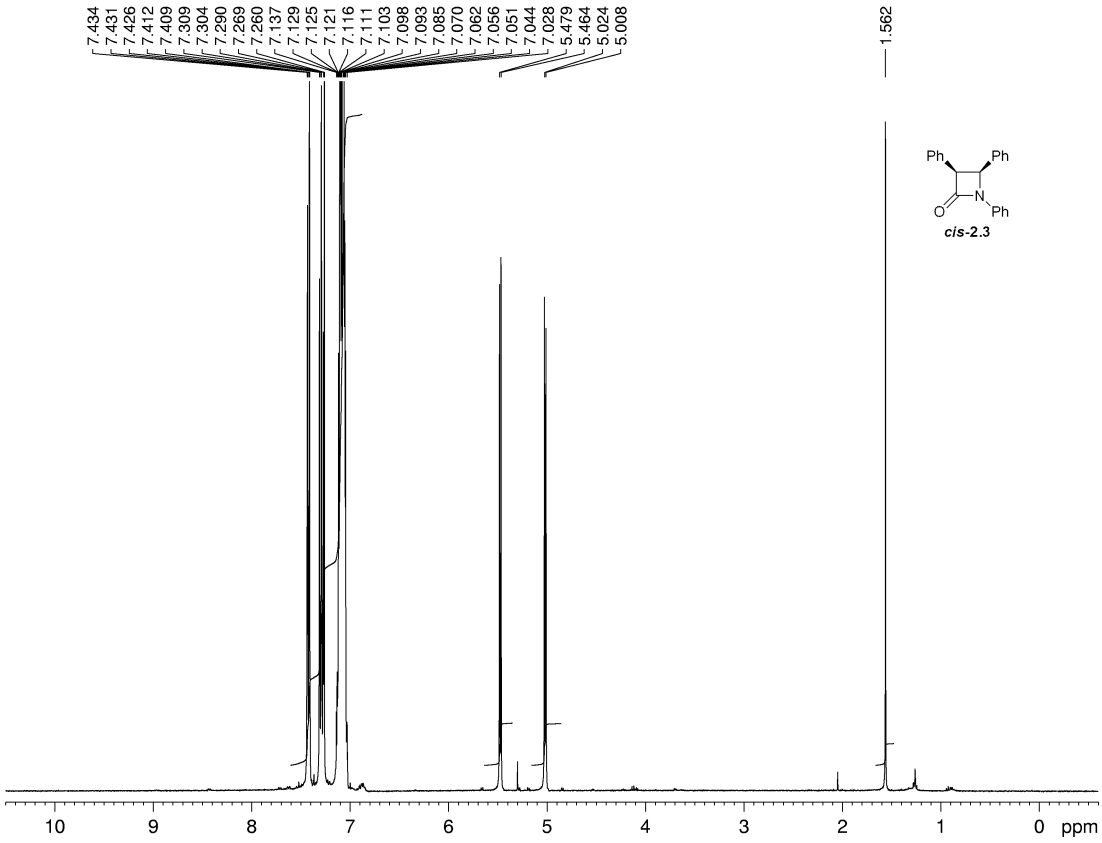
7.434
7.431
7.426
7.412
7.409
7.309
7.304
7.290
7.269
7.260
7.137
7.129
7.125
7.121
7.116
7.111
7.103
7.098
7.093
7.085
7.070
7.062
7.056
7.051
7.044
7.028
5.479
5.464
5.024
5.008
1.562
Ph
Ph
N
O
Ph
cis-2.3
10
9
8
7
6
5
4
3
2
1
0
ppm

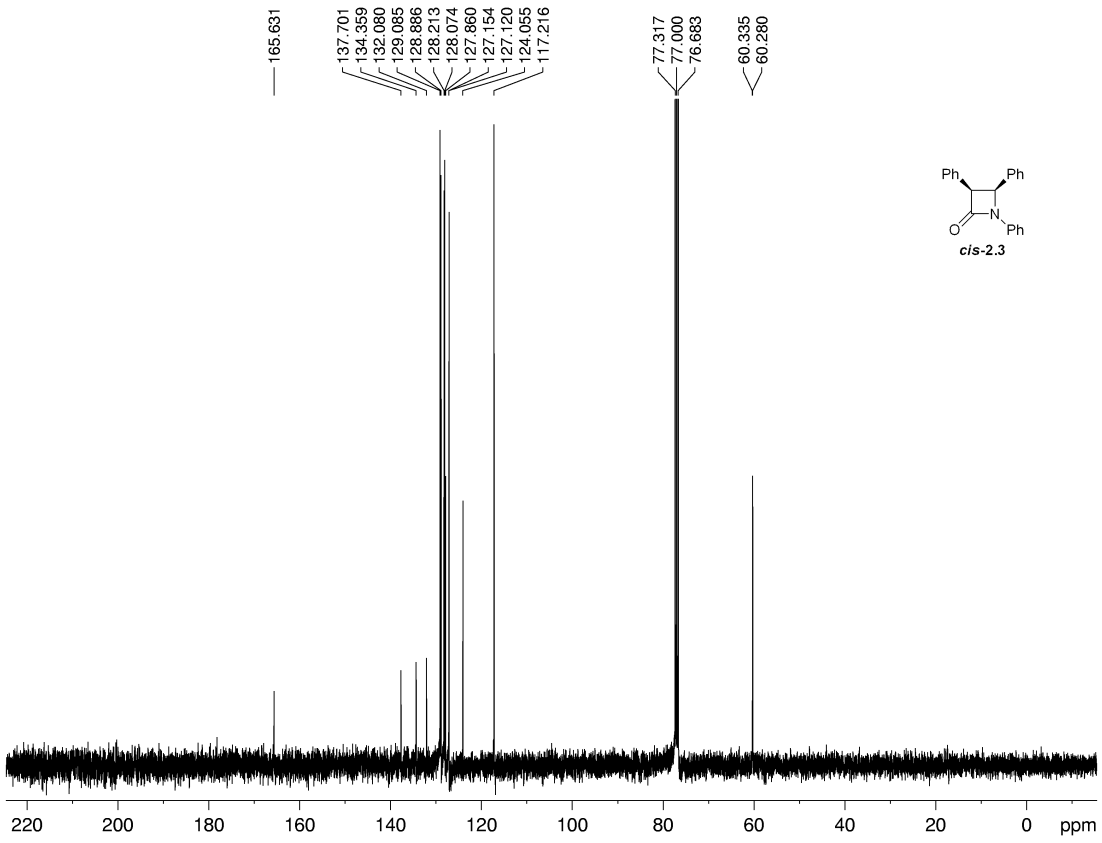
165.631
137.701
134.359
132.080
129.085
128.886
128.213
128.074
127.860
127.154
127.120
124.055
117.216
77.317
77.000
76.683
60.335
60.280
Ph
Ph
N
O
Ph
cis-2.3
220
200
180
160
140
120
100
80
60
40
20
0
ppm

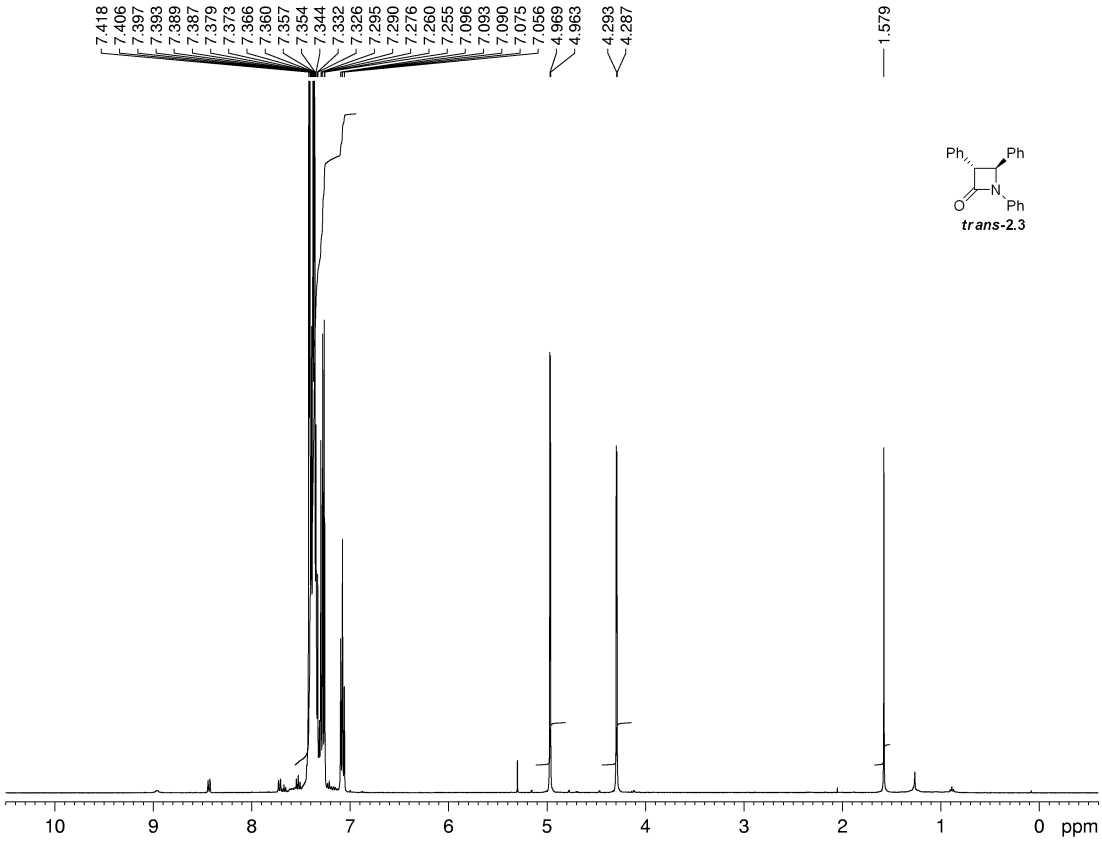
7.418
7.406
7.397
7.393
7.389
7.387
7.379
7.373
7.366
7.360
7.357
7.354
7.344
7.332
7.326
7.295
7.290
7.276
7.260
7.255
7.096
7.093
7.090
7.075
7.056
4.969
4.963
4.293
4.287
1.579
Ph
Ph
N
O
Ph
trans-2.3
10
9
8
7
6
5
4
3
2
1
0
ppm

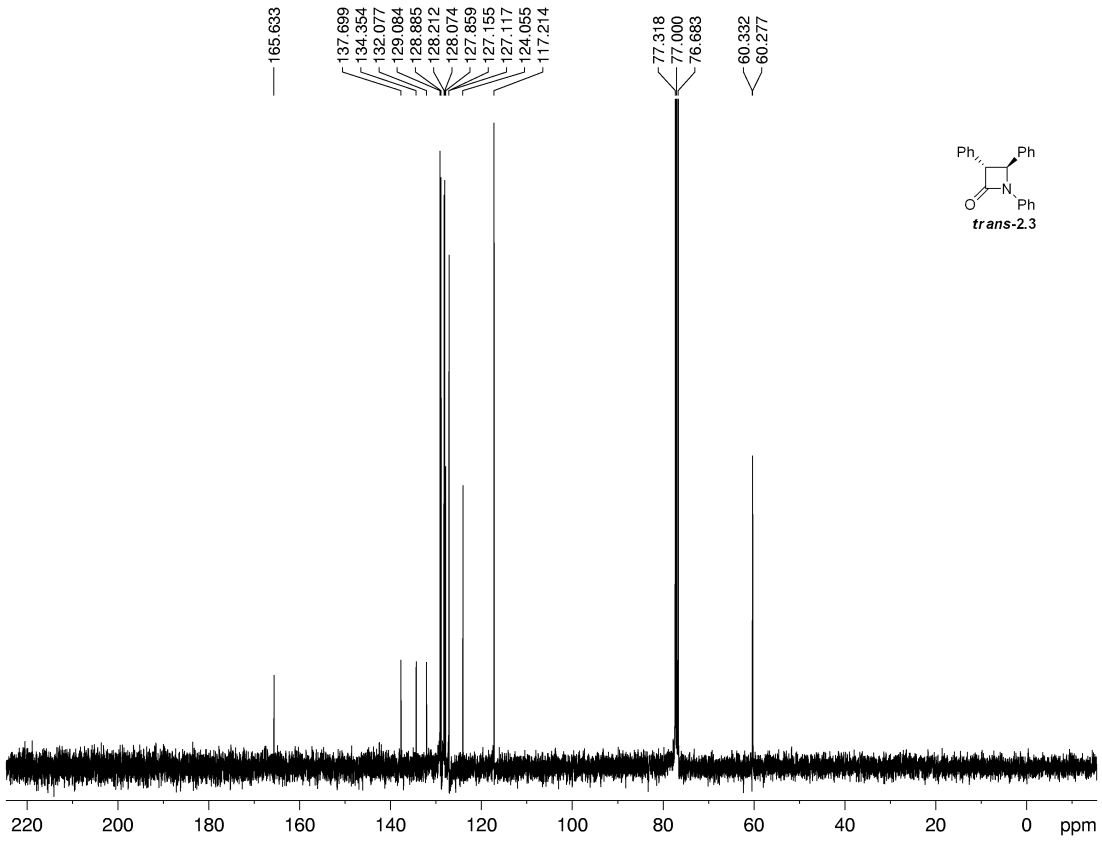
165.633
137.699
134.354
132.077
129.084
128.885
128.212
128.074
127.859
127.155
127.117
124.055
117.214
77.318
77.000
76.683
60.332
60.277
Ph
Ph
N
O
Ph
trans-2.3
220
200
180
160
140
120
100
80
60
40
20
0
ppm

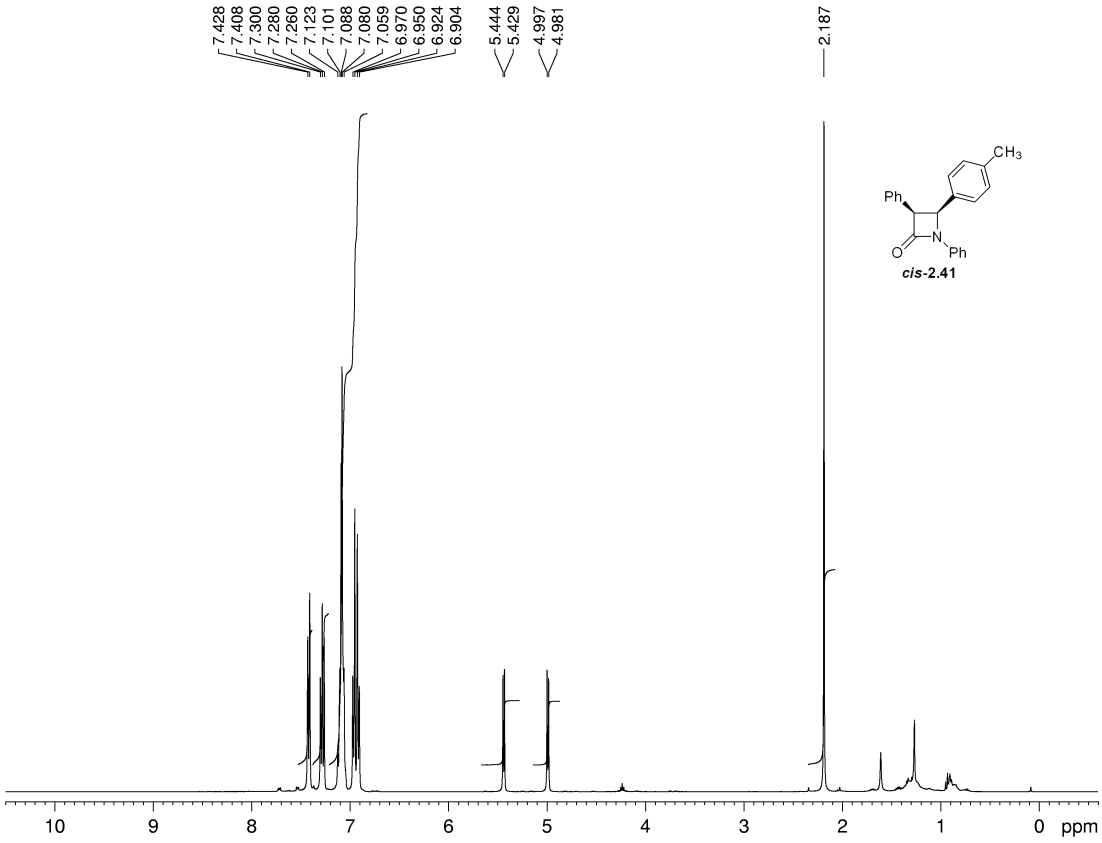
7.428
7.408
7.300
7.280
7.260
7.123
7.101
7.088
7.080
7.059
6.970
6.950
6.924
6.904
5.444
5.429
4.997
4.981
2.187
CH3
Ph
N
Ph
O
cis-2.41
10
9
8
7
6
5
4
3
2
1
0
ppm

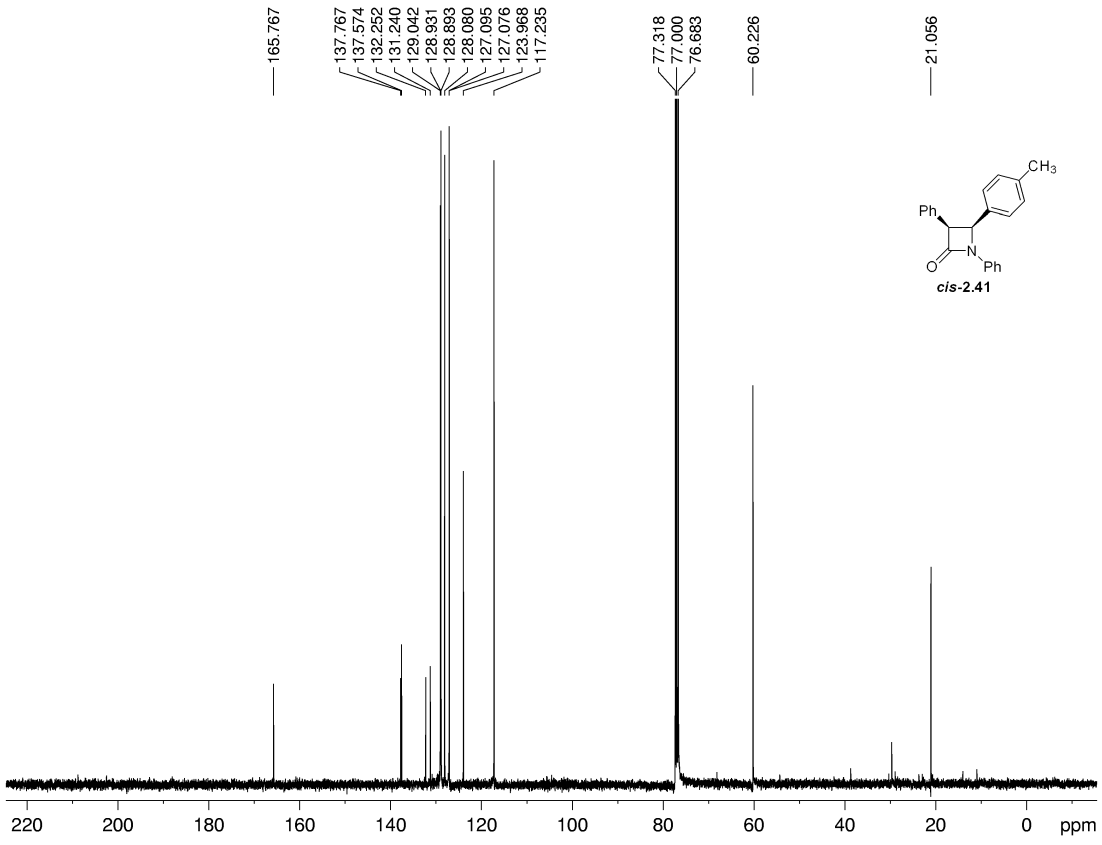
165.767
137.767
137.574
132.252
131.240
129.042
128.931
128.893
128.080
127.095
127.076
123.968
117.235
77.318
77.000
76.683
60.226
21.056
CH3
Ph
N
Ph
O
cis-2.41
220
200
180
160
140
120
100
80
60
40
20
0
ppm

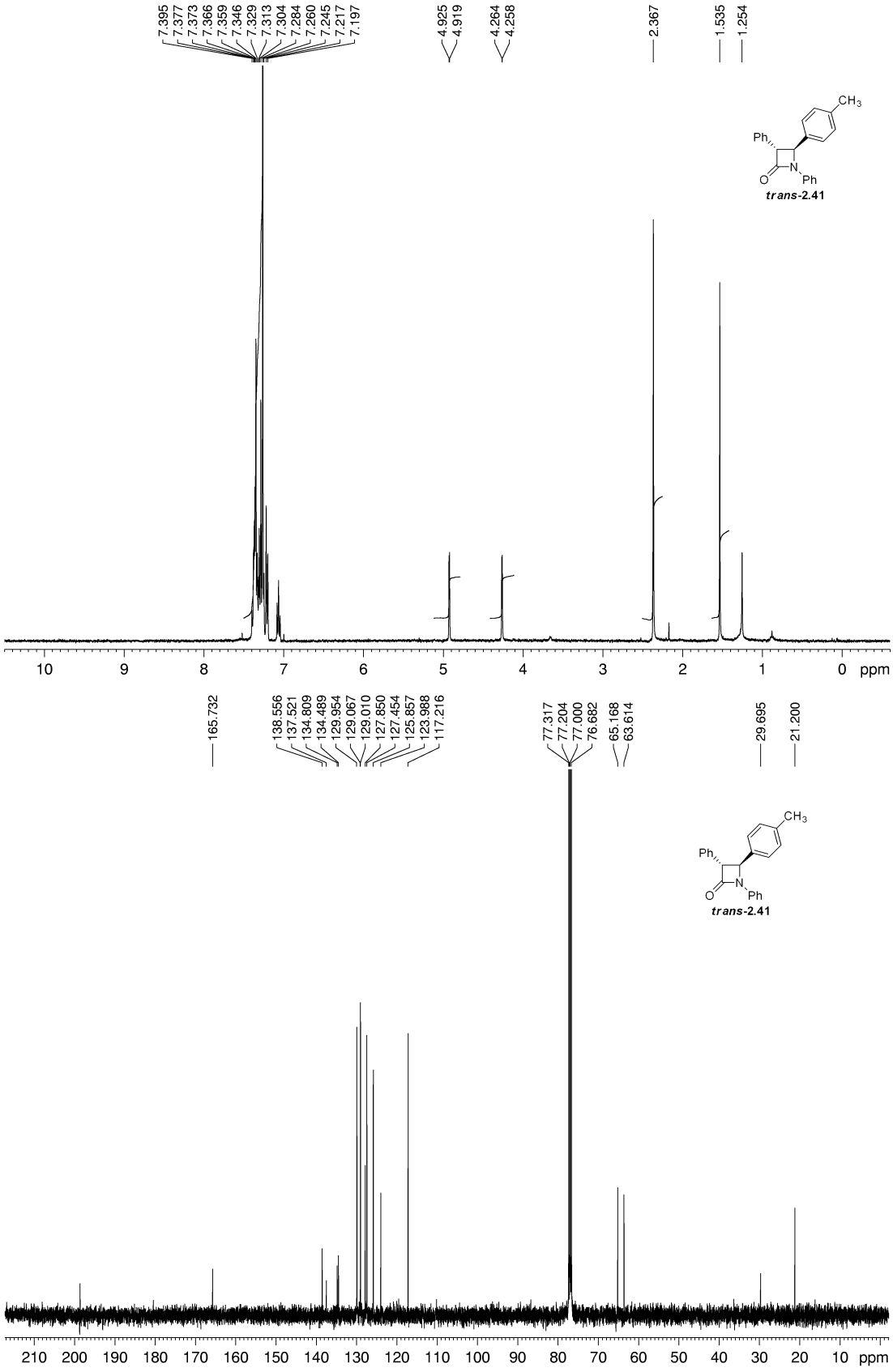
7.395
7.377
7.373
7.366
7.359
7.346
7.329
7.313
7.304
7.284
7.260
7.245
7.217
7.197
4.925
4.919
4.264
4.258
2.367
1.535
1.254
CH3
Ph
N
O
Ph
trans-2.41
10 9 8 7 6 5 4 3 2 1 0 ppm
165.732
138.556
137.521
134.809
134.489
129.954
129.067
129.010
127.850
127.454
125.857
123.988
117.216
77.317
77.204
77.000
76.682
65.168
63.614
29.695
21.200
CH3
Ph
N
O
Ph
trans-2.41
210 200 190 180 170 160 150 140 130 120 110 100 90 80 70 60 50 40 30 20 10 ppm

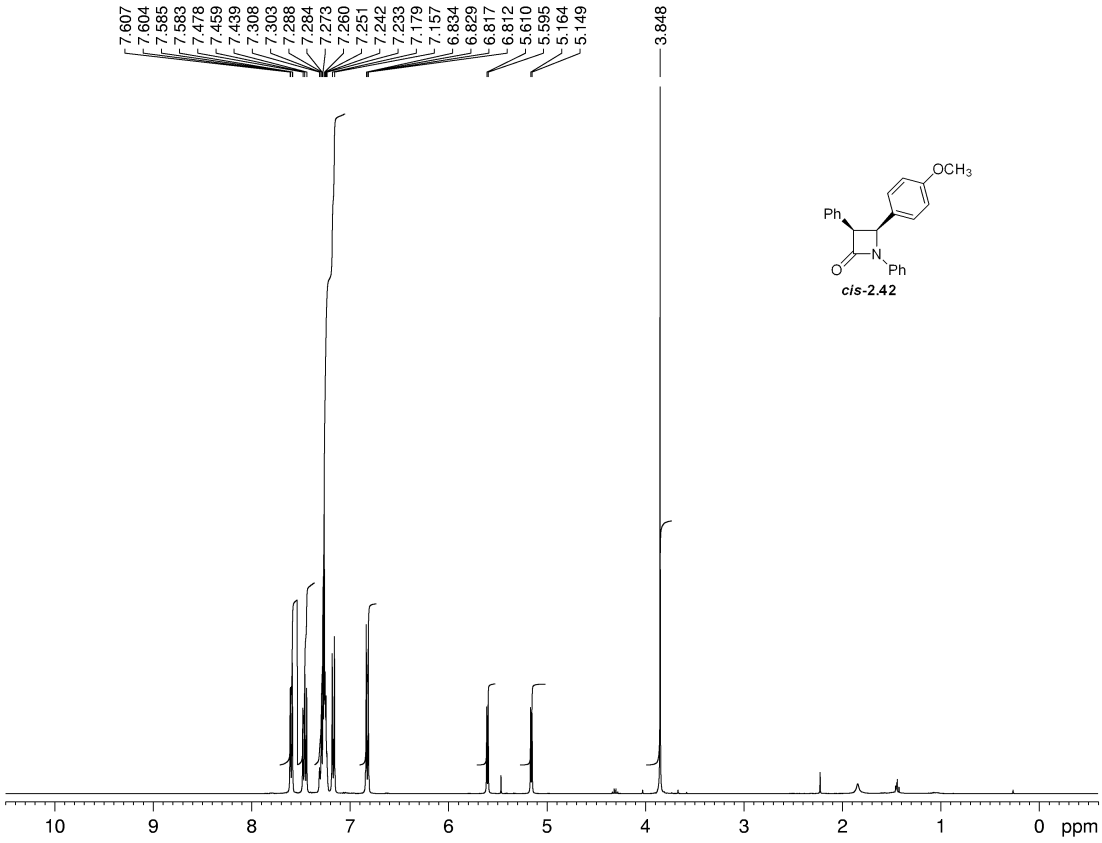
7.607
7.604
7.585
7.583
7.478
7.459
7.439
7.308
7.303
7.288
7.284
7.273
7.260
7.251
7.242
7.233
7.179
7.157
6.834
6.829
6.817
6.812
5.610
5.595
5.164
5.149
3.848
OCH3
Ph
O
N
Ph
cis-2.42
10
9
8
7
6
5
4
3
2
1
0
ppm

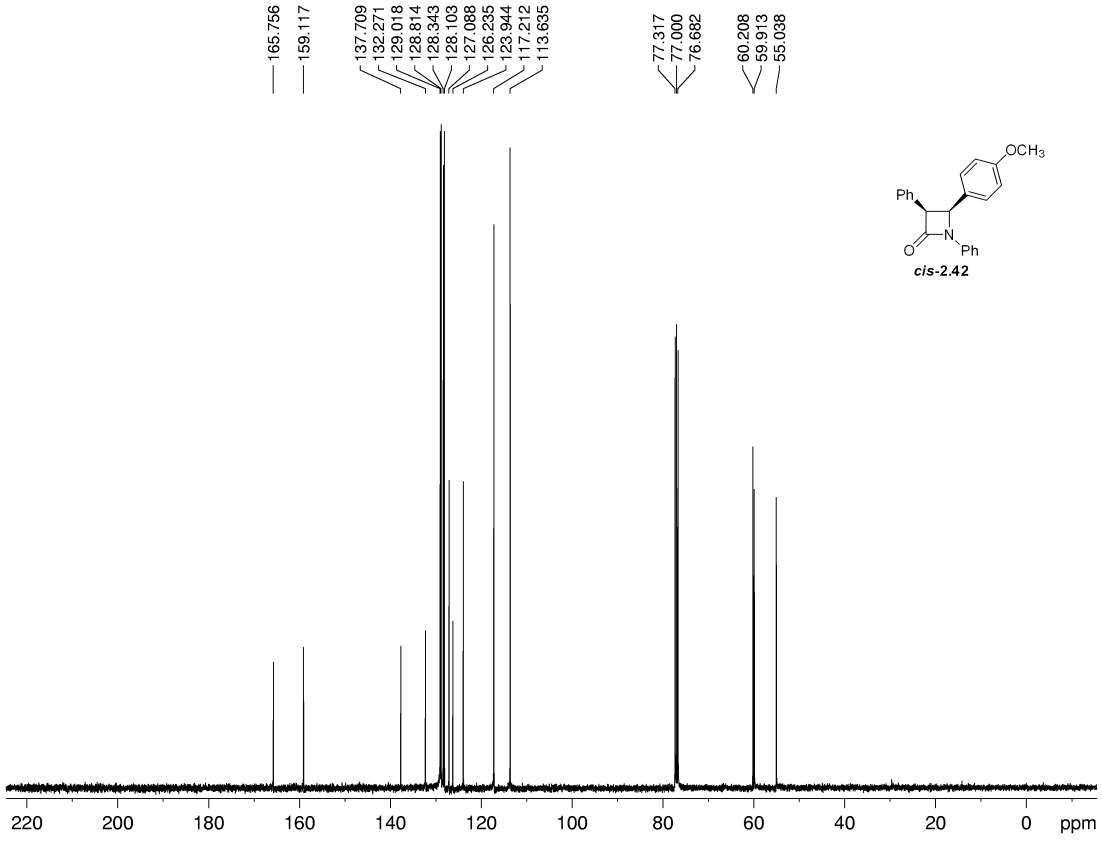
165.756
159.117
137.709
132.271
129.018
128.814
128.343
128.103
127.088
126.235
123.944
117.212
113.635
77.317
77.000
76.682
60.208
59.913
55.038
OCH3
Ph
O
N
Ph
cis-2.42
220
200
180
160
140
120
100
80
60
40
20
0
ppm

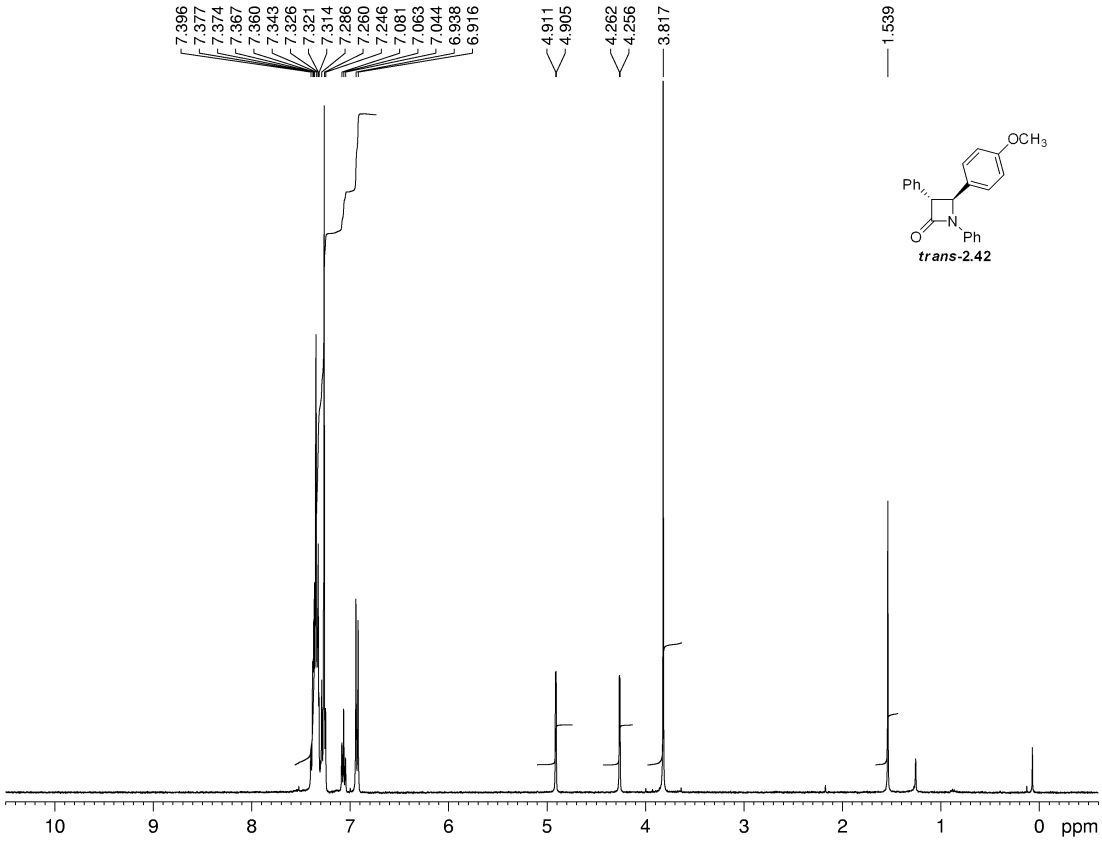
7.396
7.377
7.374
7.367
7.360
7.343
7.326
7.321
7.314
7.286
7.260
7.246
7.081
7.063
7.044
6.938
6.916
4.911
4.905
4.262
4.256
3.817
1.539
OCH3
Ph
N
O
Ph
trans-2.42
10
9
8
7
6
5
4
3
2
1
0
ppm

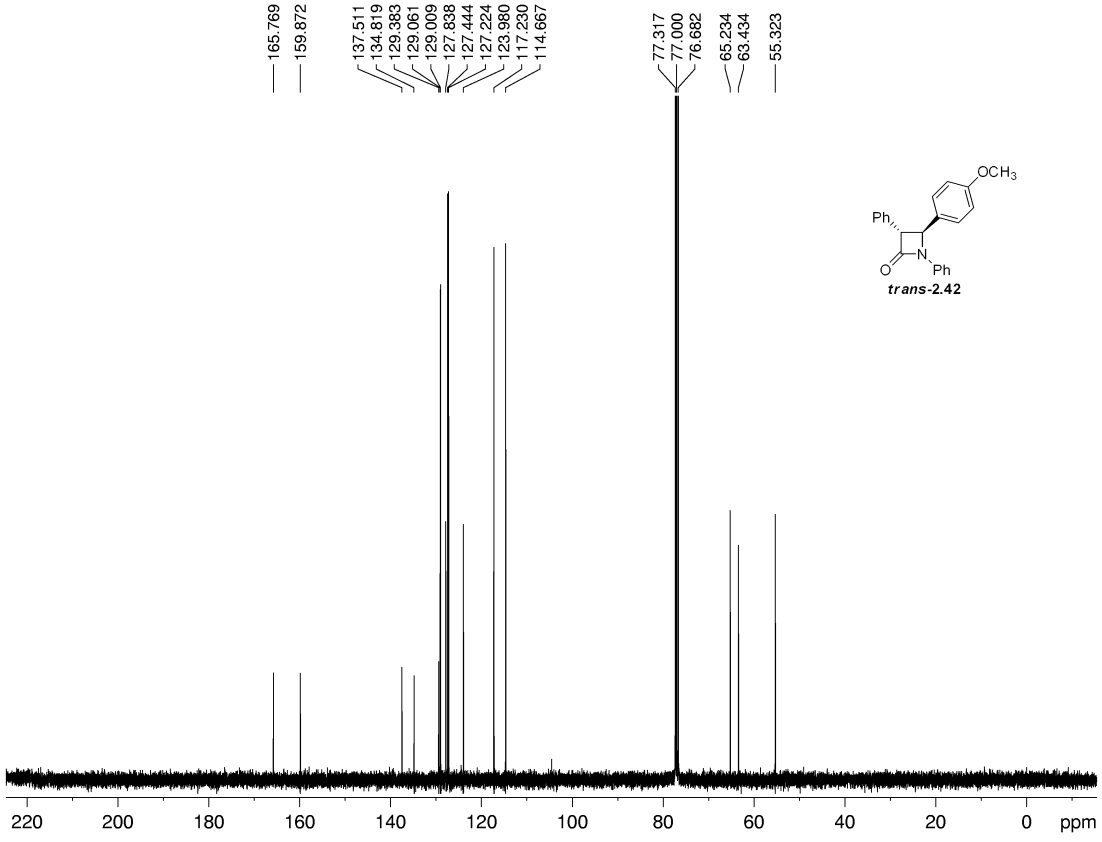
165.769
159.872
137.511
134.819
129.383
129.061
129.009
127.838
127.444
127.224
123.980
117.230
114.667
77.317
77.000
76.682
65.234
63.434
55.323
OCH3
Ph
N
O
Ph
trans-2.42
220
200
180
160
140
120
100
80
60
40
20
0
ppm

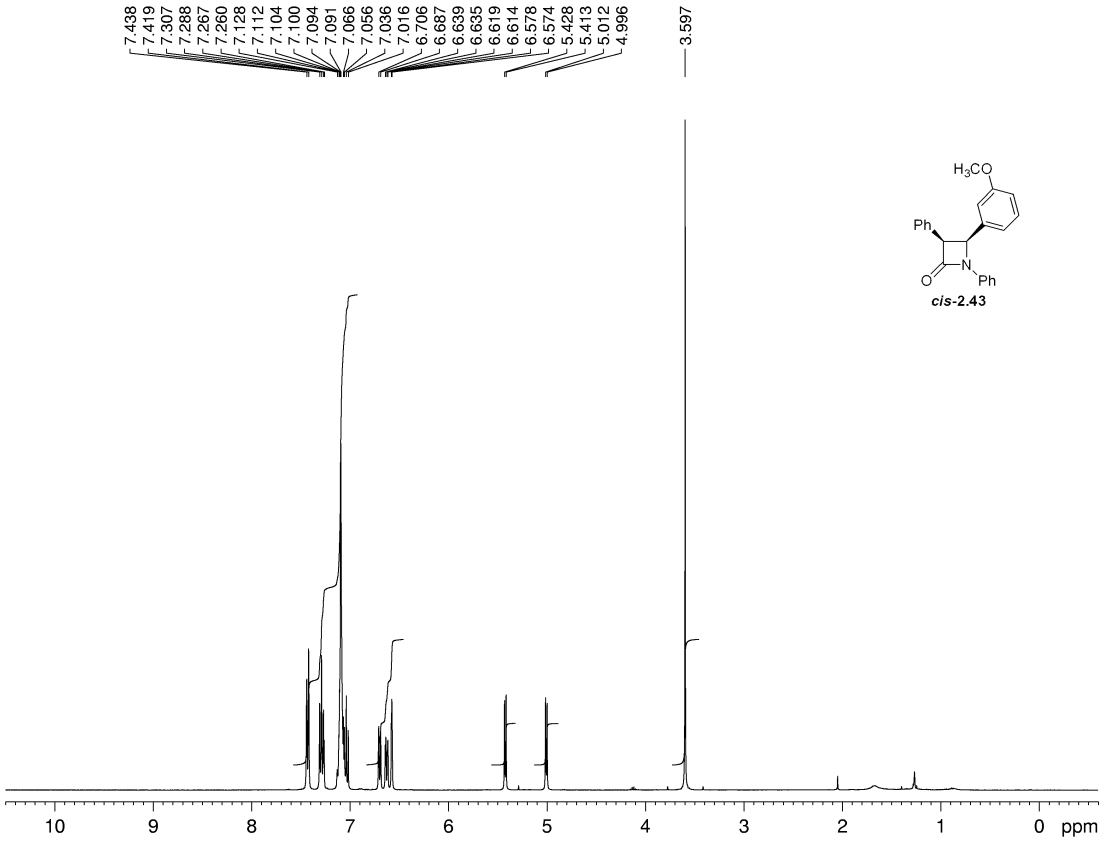
7.438
7.419
7.307
7.288
7.267
7.260
7.128
7.112
7.104
7.100
7.094
7.091
7.066
7.056
7.036
7.016
6.706
6.687
6.639
6.635
6.619
6.614
6.578
6.574
5.428
5.413
5.012
4.996
3.597
H3CO
Ph
O
N
Ph
cis-2.43
10
9
8
7
6
5
4
3
2
1
0
ppm

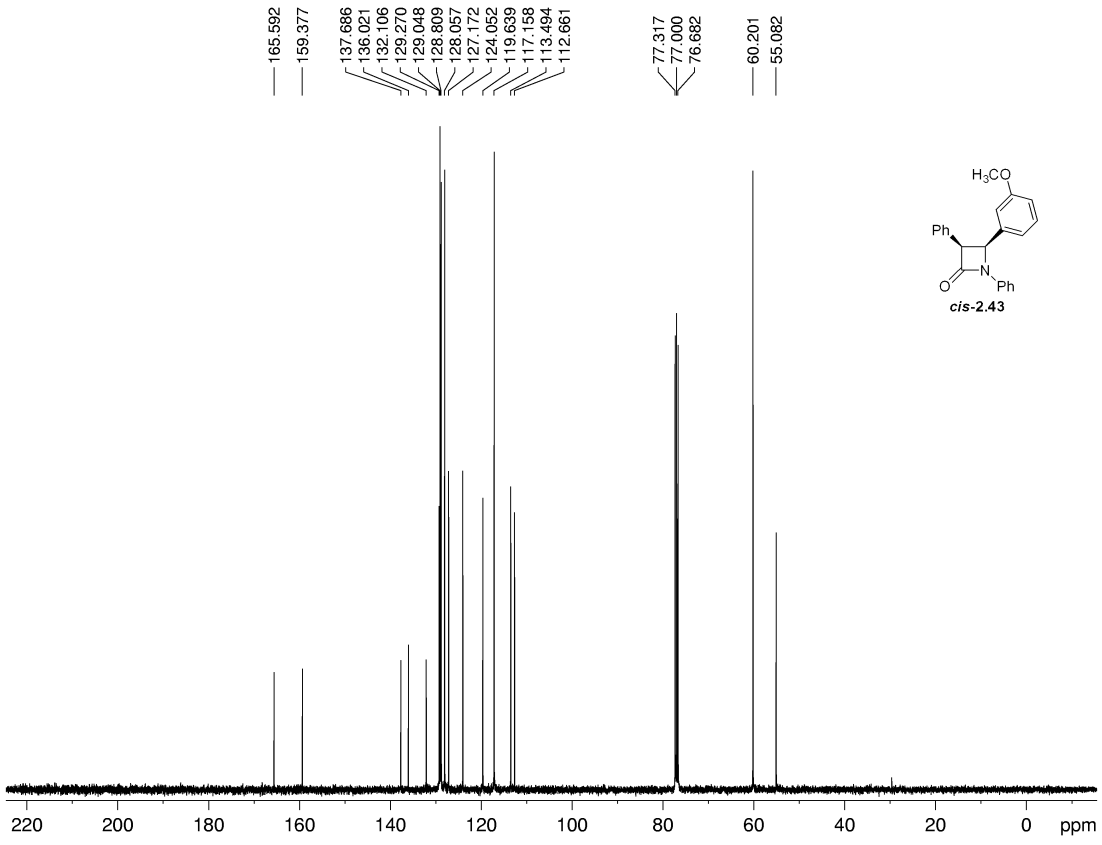
165.592
159.377
137.686
136.021
132.106
129.270
129.048
128.809
128.057
127.172
124.052
119.639
117.158
113.494
112.661
77.317
77.000
76.682
60.201
55.082
H3CO
Ph
O
N
Ph
cis-2.43
220
200
180
160
140
120
100
80
60
40
20
0
ppm

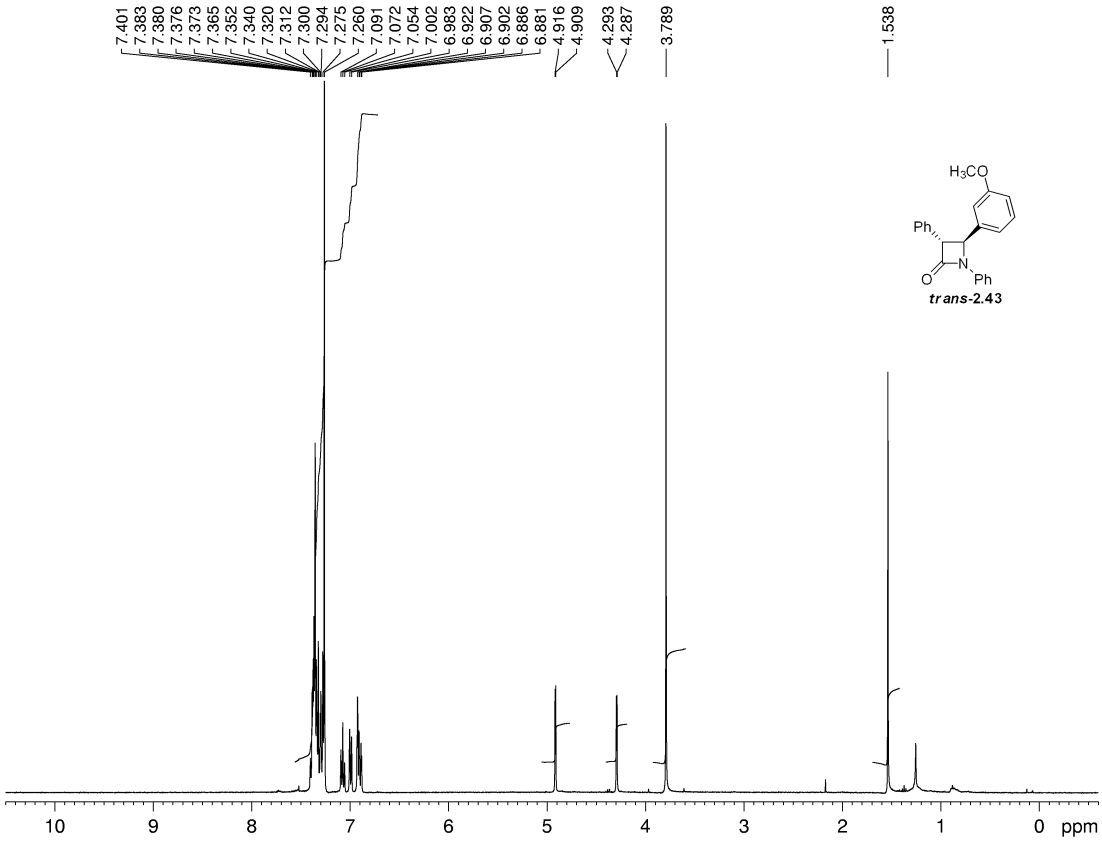
7.401
7.383
7.380
7.376
7.373
7.365
7.352
7.340
7.320
7.312
7.300
7.294
7.275
7.260
7.091
7.072
7.054
7.002
6.983
6.922
6.907
6.902
6.886
6.881
4.916
4.909
4.293
4.287
3.789
1.538
H3CO
Ph
O
N
Ph
trans-2.43
10
9
8
7
6
5
4
3
2
1
0
ppm

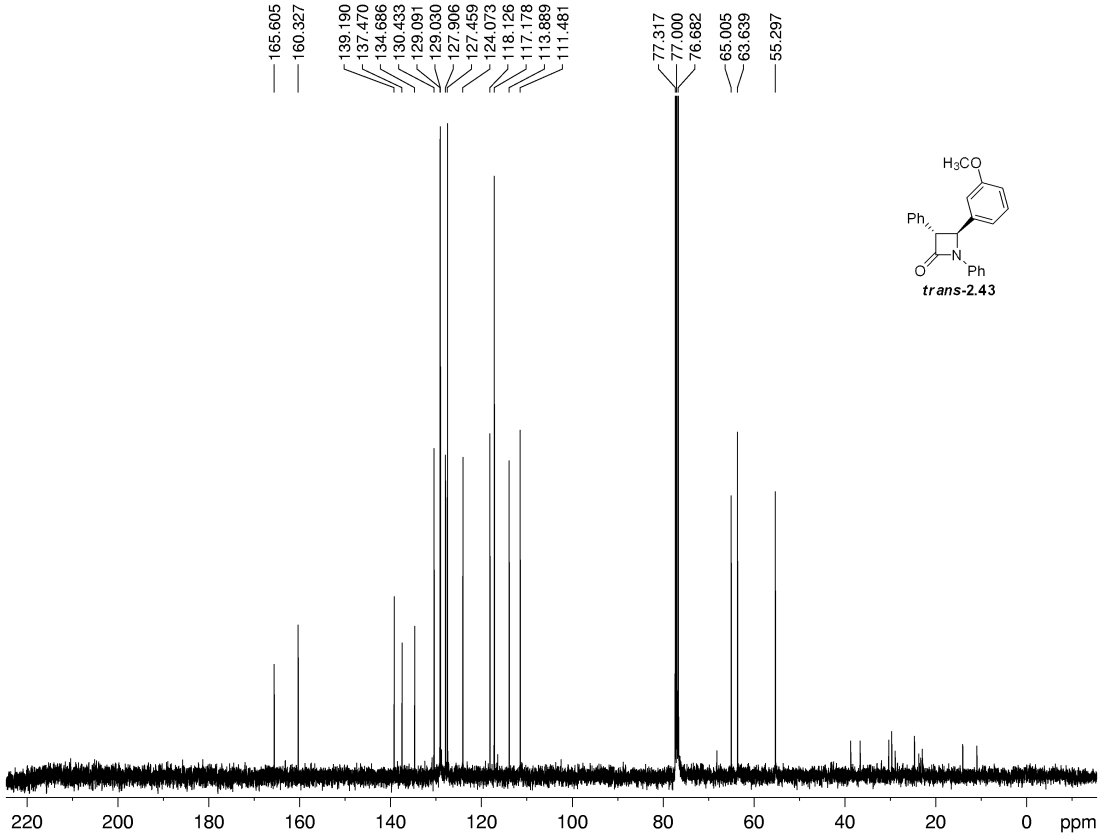
165.605
160.327
139.190
137.470
134.686
130.433
129.091
129.030
127.906
127.459
124.073
118.126
117.178
113.889
111.481
77.317
77.000
76.682
65.005
63.639
55.297
H3CO
Ph
O
N
Ph
trans-2.43
220
200
180
160
140
120
100
80
60
40
20
0
ppm

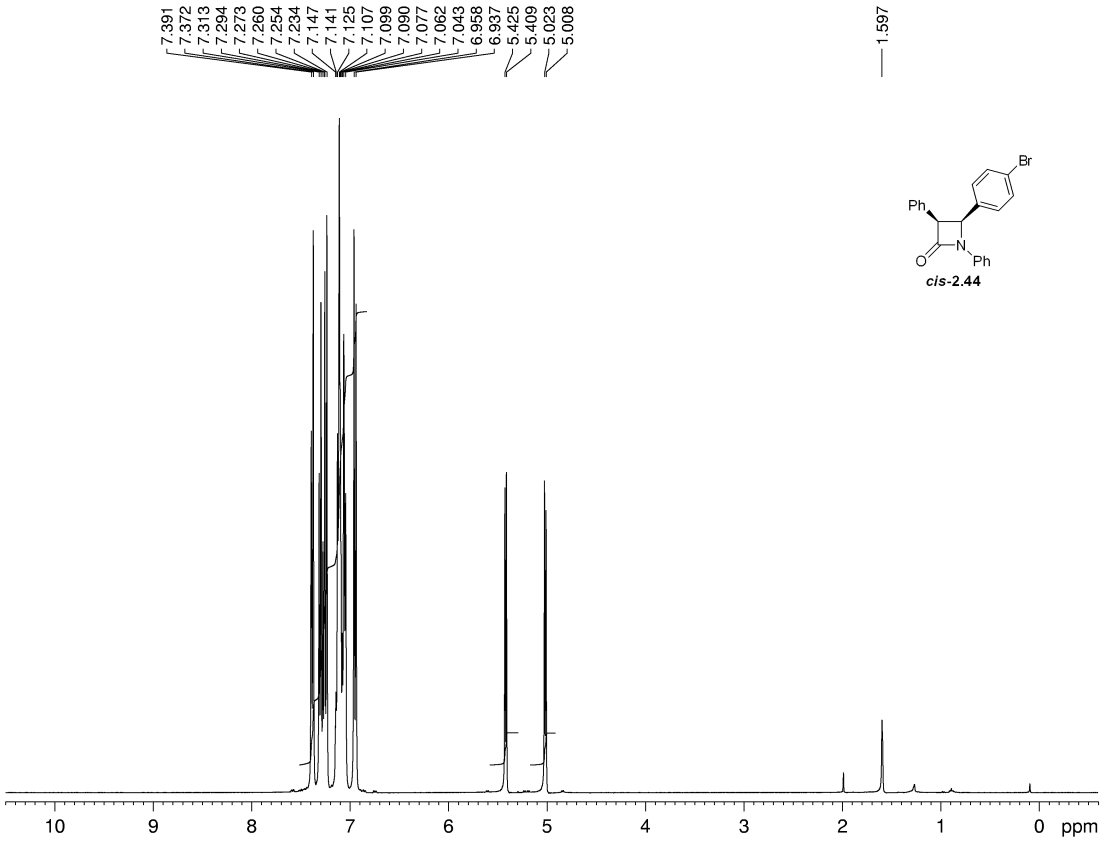
7.391
7.372
7.313
7.294
7.273
7.260
7.254
7.234
7.147
7.141
7.125
7.107
7.099
7.090
7.077
7.062
7.043
6.958
6.937
5.425
5.409
5.023
5.008
1.597
Br
Ph
N
Ph
O
cis-2.44
10
9
8
7
6
5
4
3
2
1
0
ppm

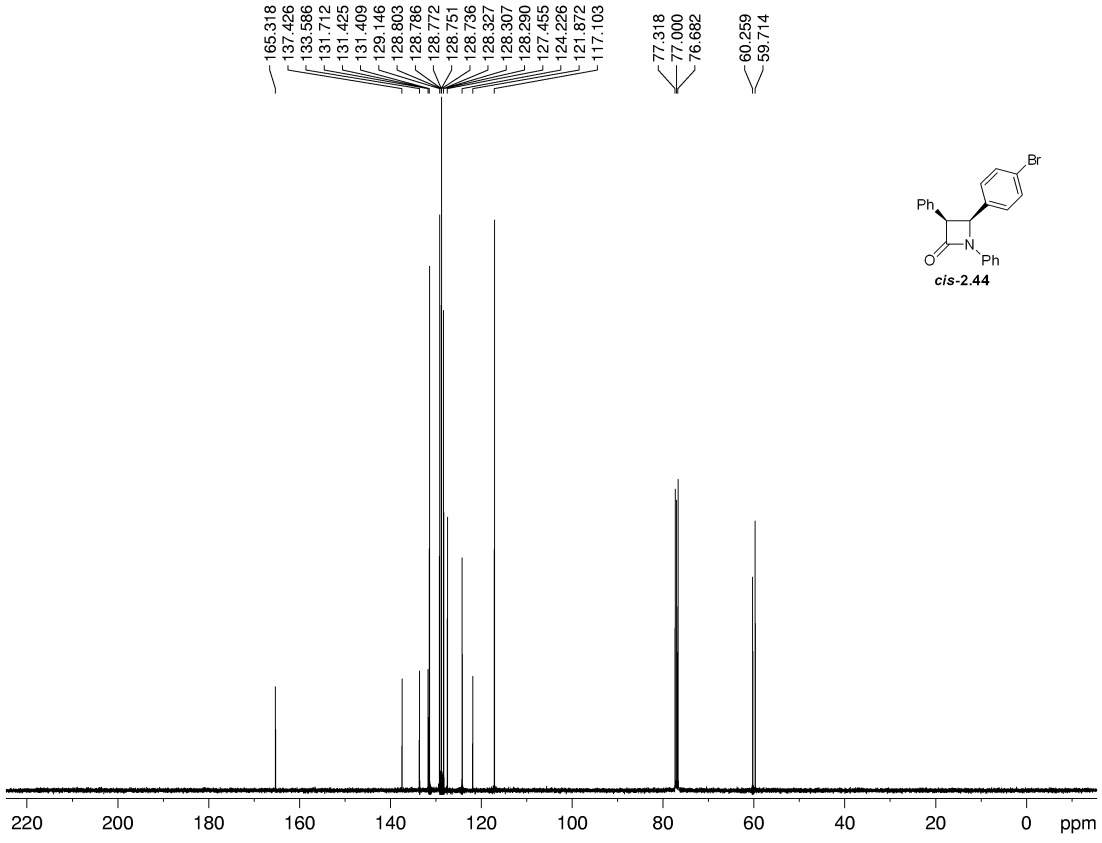
165.318
137.426
133.586
131.712
131.425
131.409
129.146
128.803
128.786
128.772
128.751
128.736
128.327
128.307
128.290
127.455
124.226
121.872
117.103
77.318
77.000
76.682
60.259
59.714
Br
Ph
N
Ph
O
cis-2.44
220
200
180
160
140
120
100
80
60
40
20
0
ppm

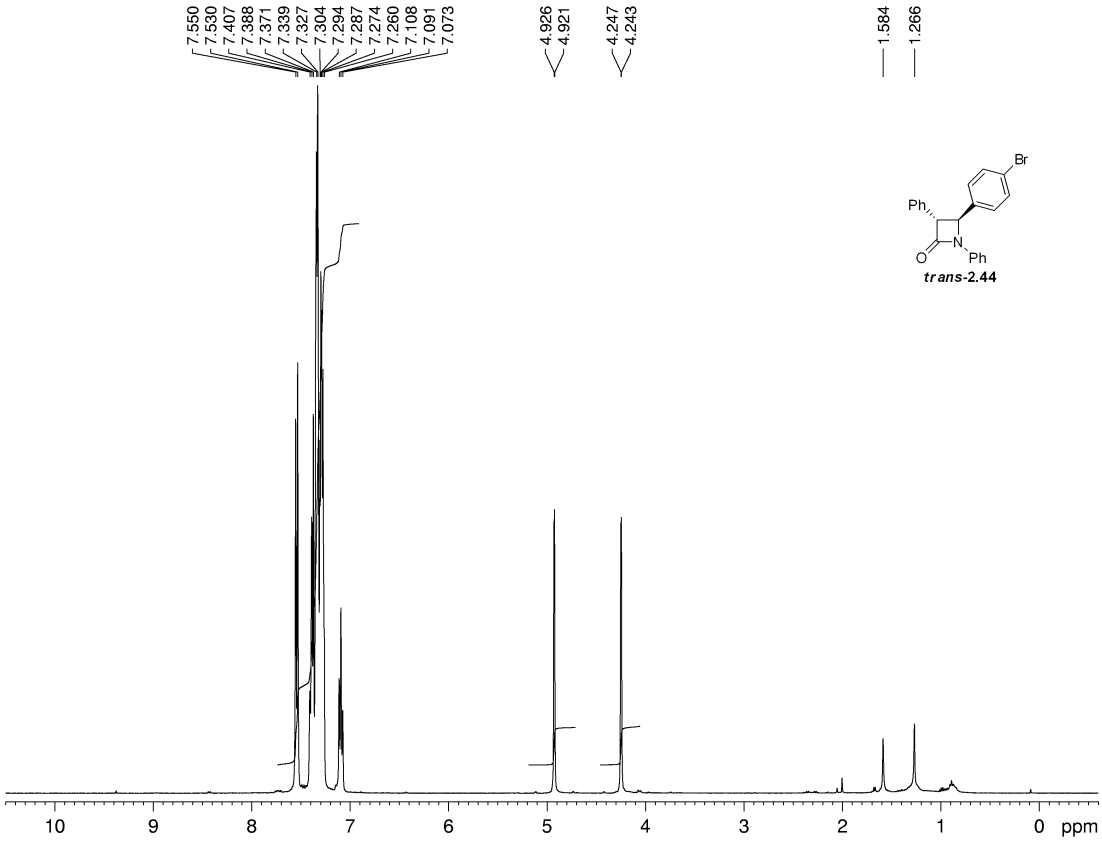
7.550
7.530
7.407
7.388
7.371
7.339
7.327
7.304
7.294
7.287
7.274
7.260
7.108
7.091
7.073
4.926
4.921
4.247
4.243
1.584
1.266
Br
Ph
N
Ph
O
trans-2.44
10
9
8
7
6
5
4
3
2
1
0
ppm

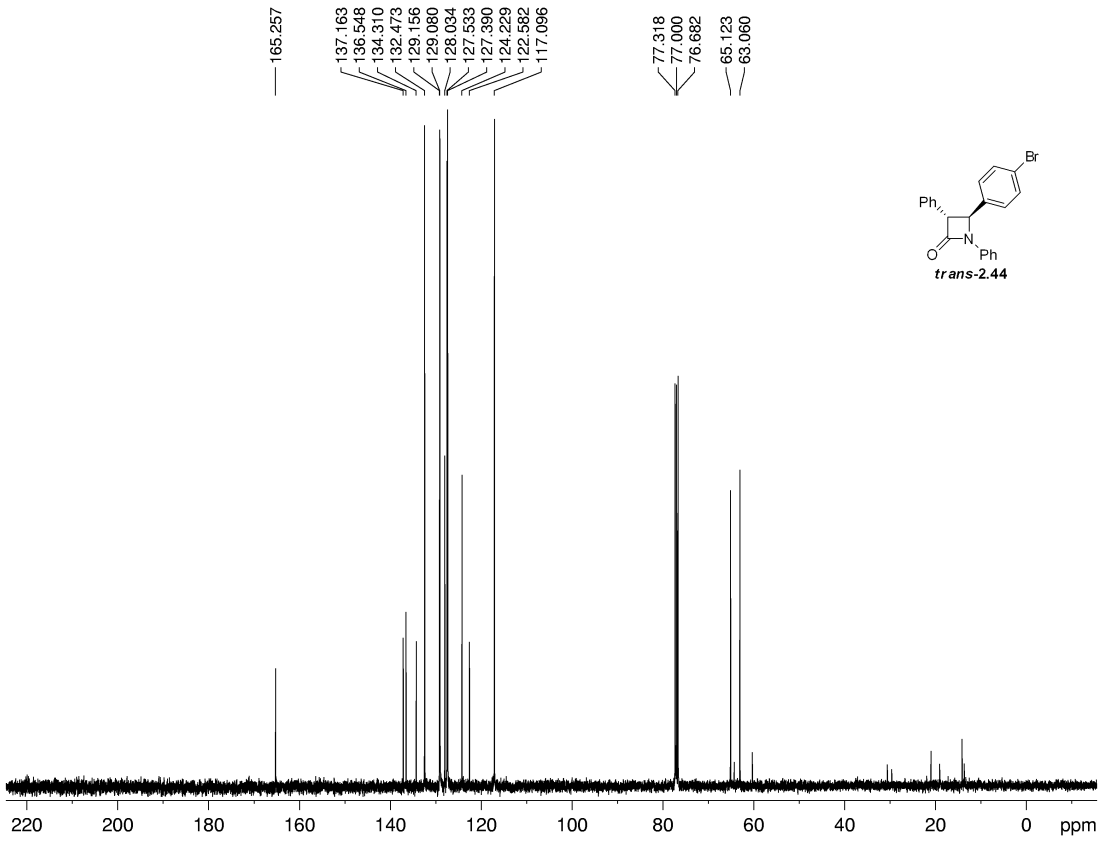
165.257
137.163
136.548
134.310
132.473
129.156
129.080
128.034
127.533
127.390
124.229
122.582
117.096
77.318
77.000
76.682
65.123
63.060
Br
Ph
N
Ph
O
trans-2.44
220
200
180
160
140
120
100
80
60
40
20
0
ppm

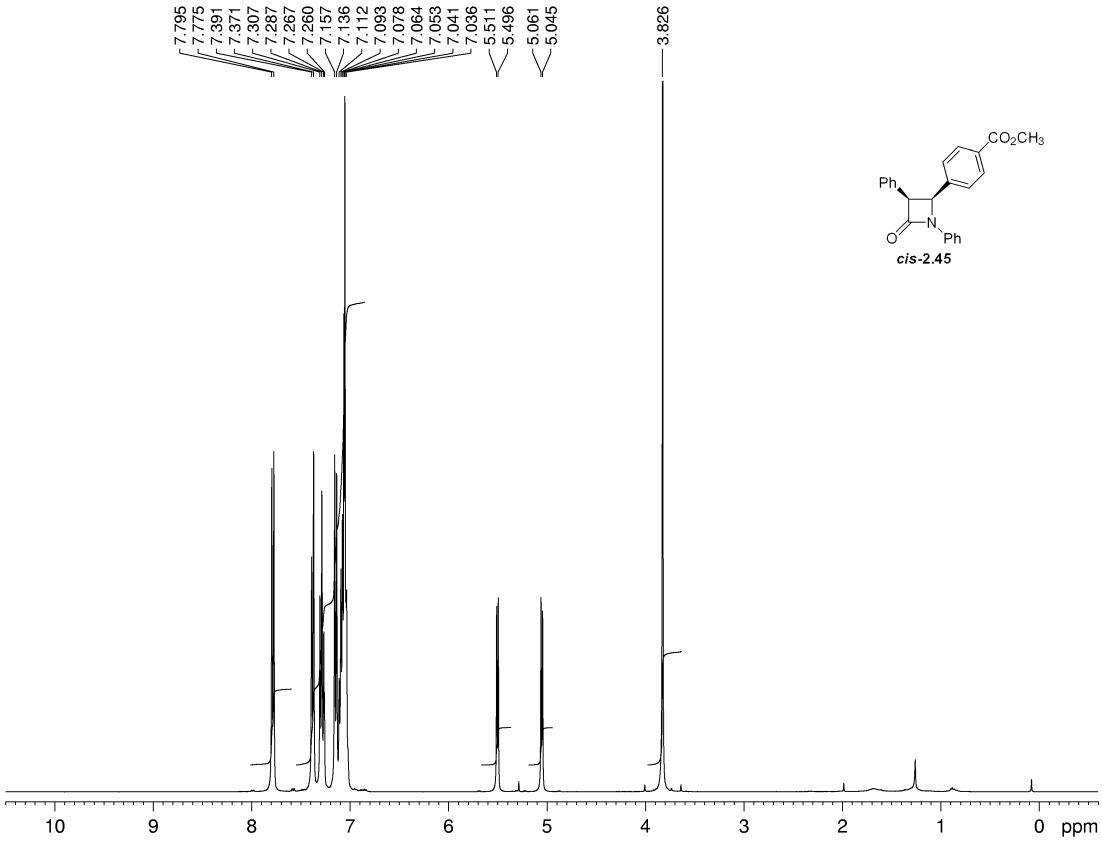
7.795
7.775
7.391
7.371
7.307
7.287
7.267
7.260
7.157
7.136
7.112
7.093
7.078
7.064
7.053
7.041
7.036
5.511
5.496
5.061
5.045
3.826
CO2CH3
Ph
O
N
Ph
cis-2.45
10
9
8
7
6
5
4
3
2
1
0
ppm

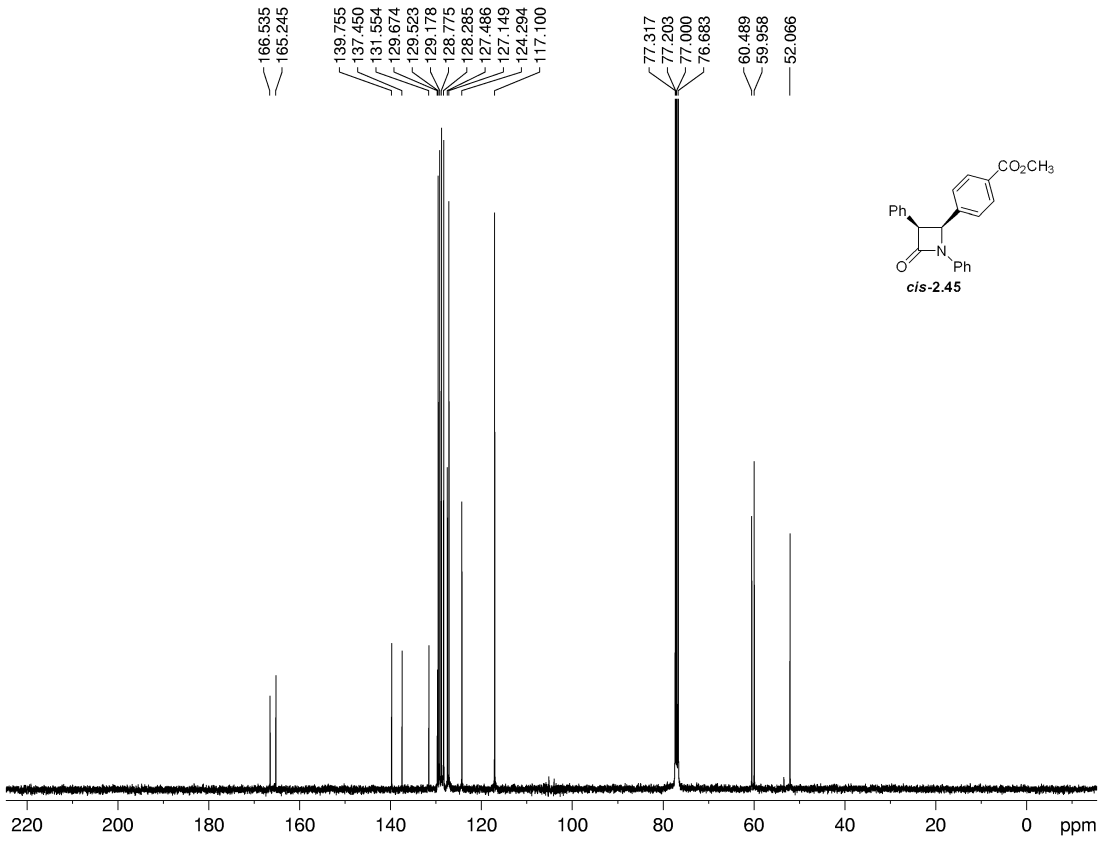
166.535
165.245
139.755
137.450
131.554
129.674
129.523
129.178
128.775
128.285
127.486
127.149
124.294
117.100
77.317
77.203
77.000
76.683
60.489
59.958
52.066
CO2CH3
Ph
O
N
Ph
cis-2.45
220
200
180
160
140
120
100
80
60
40
20
0
ppm

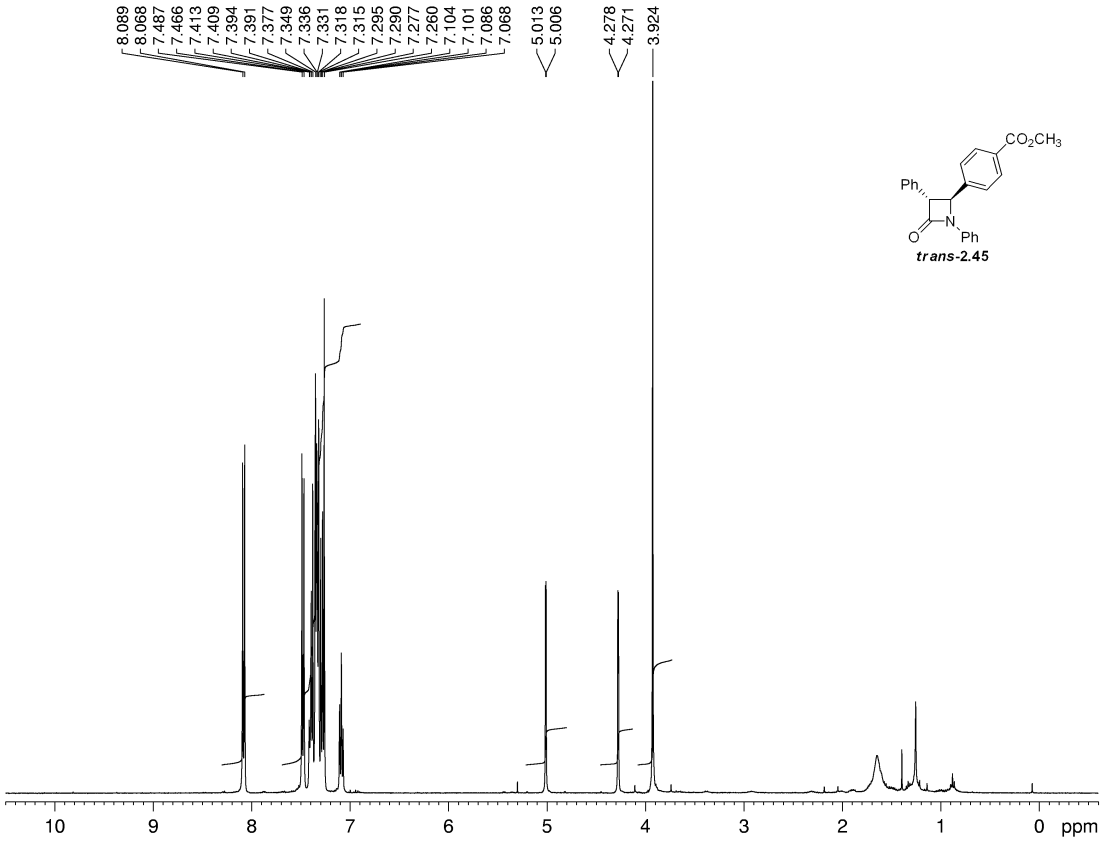
8.089
8.068
7.487
7.466
7.413
7.409
7.394
7.391
7.377
7.349
7.336
7.331
7.318
7.315
7.295
7.290
7.277
7.260
7.104
7.101
7.086
7.068
5.013
5.006
4.278
4.271
3.924
CO2CH3
Ph
O
N
Ph
trans-2.45
10
9
8
7
6
5
4
3
2
1
0
ppm

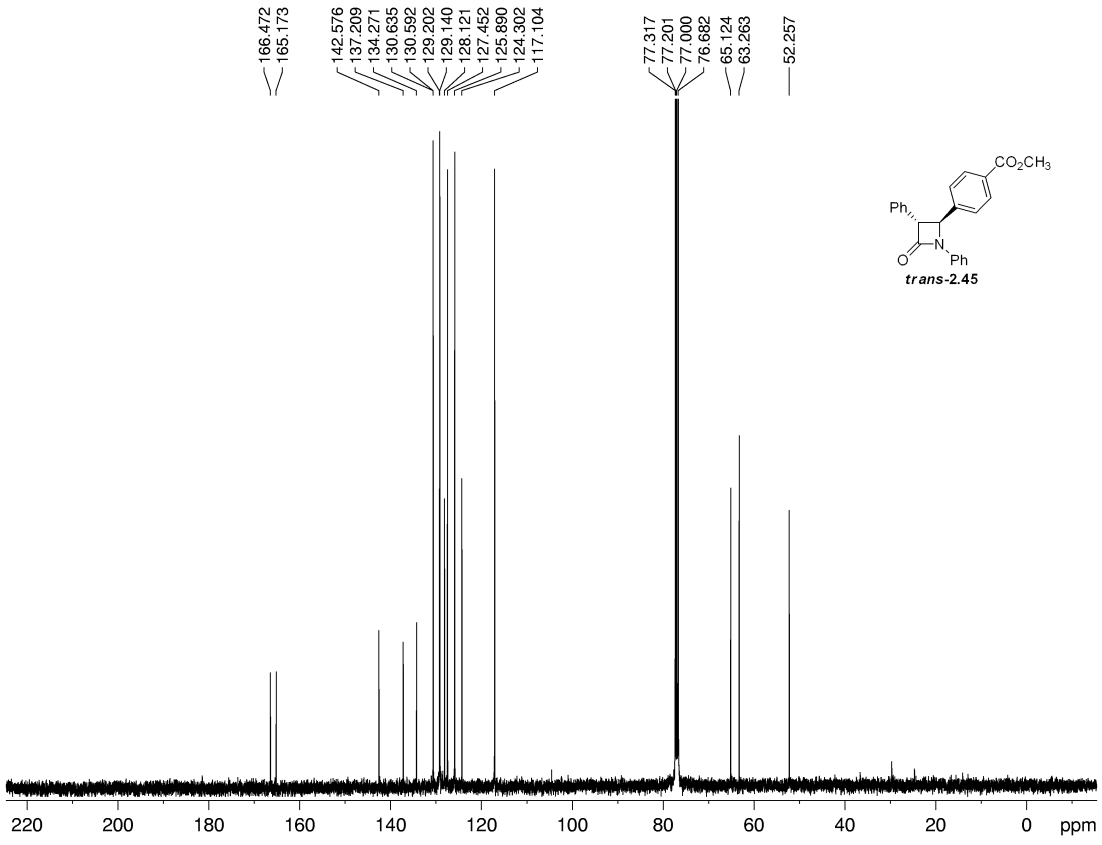
166.472
165.173
142.576
137.209
134.271
130.635
130.592
129.202
129.140
128.121
127.452
125.890
124.302
117.104
77.317
77.201
77.000
76.682
65.124
63.263
52.257
CO2CH3
Ph
O
N
Ph
trans-2.45
220
200
180
160
140
120
100
80
60
40
20
0
ppm

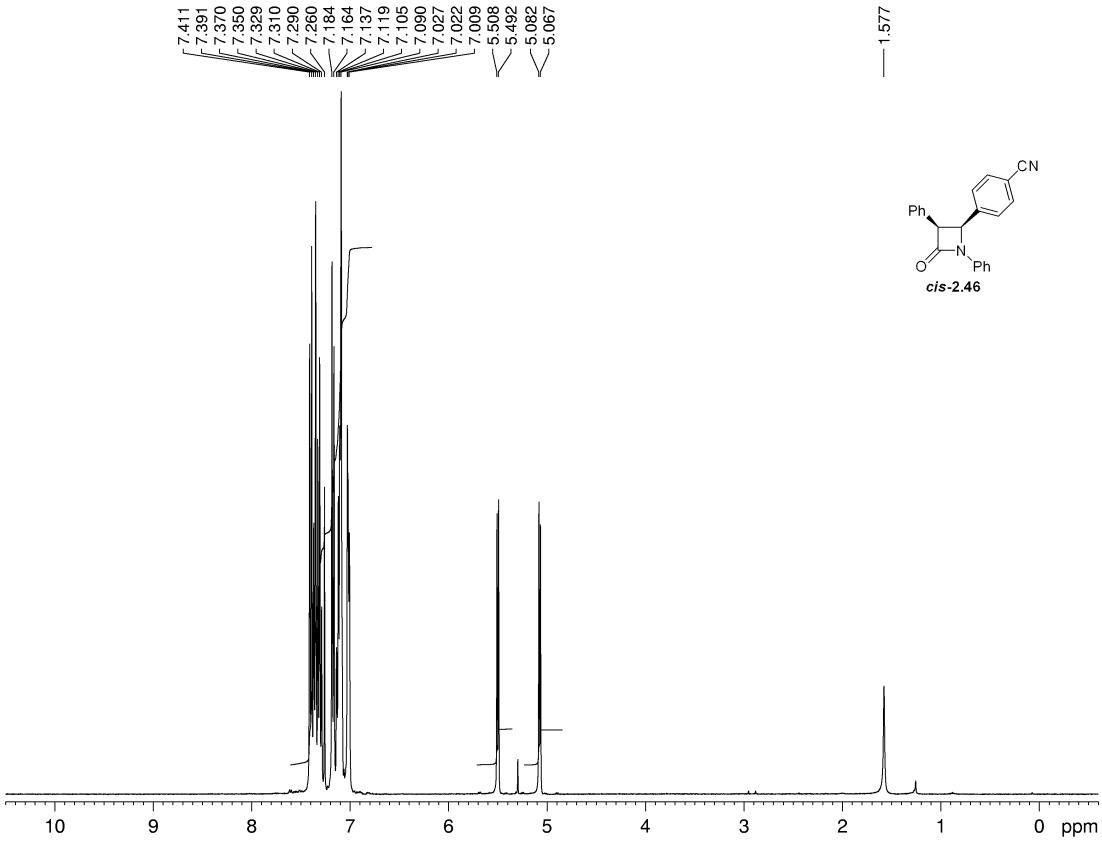
7.411
7.391
7.370
7.350
7.329
7.310
7.290
7.260
7.184
7.164
7.137
7.119
7.105
7.090
7.027
7.022
7.009
5.508
5.492
5.082
5.067
1.577
CN
Ph
N
O
Ph
cis-2.46
10
9
8
7
6
5
4
3
2
1
0
ppm

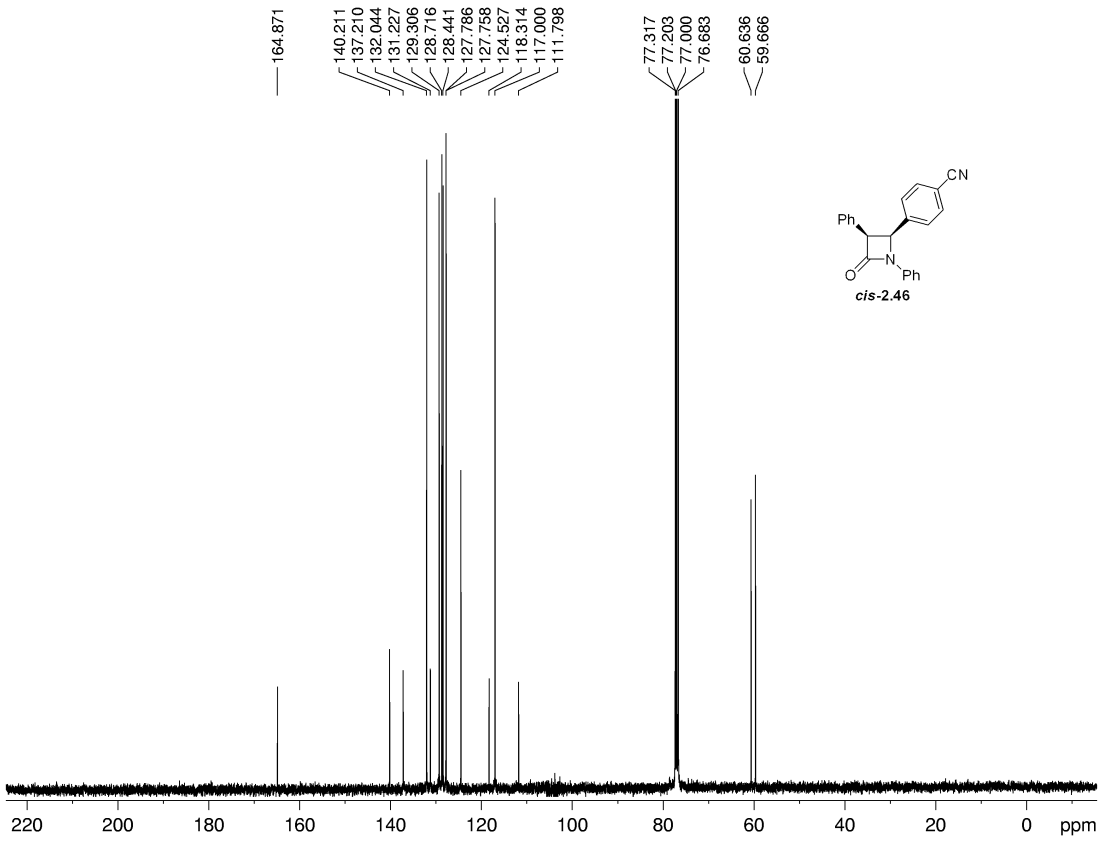
164.871
140.211
137.210
132.044
131.227
129.306
128.716
128.441
127.786
127.758
124.527
118.314
117.000
111.798
77.317
77.203
77.000
76.683
60.636
59.666
CN
Ph
N
O
Ph
cis-2.46
220
200
180
160
140
120
100
80
60
40
20
0
ppm

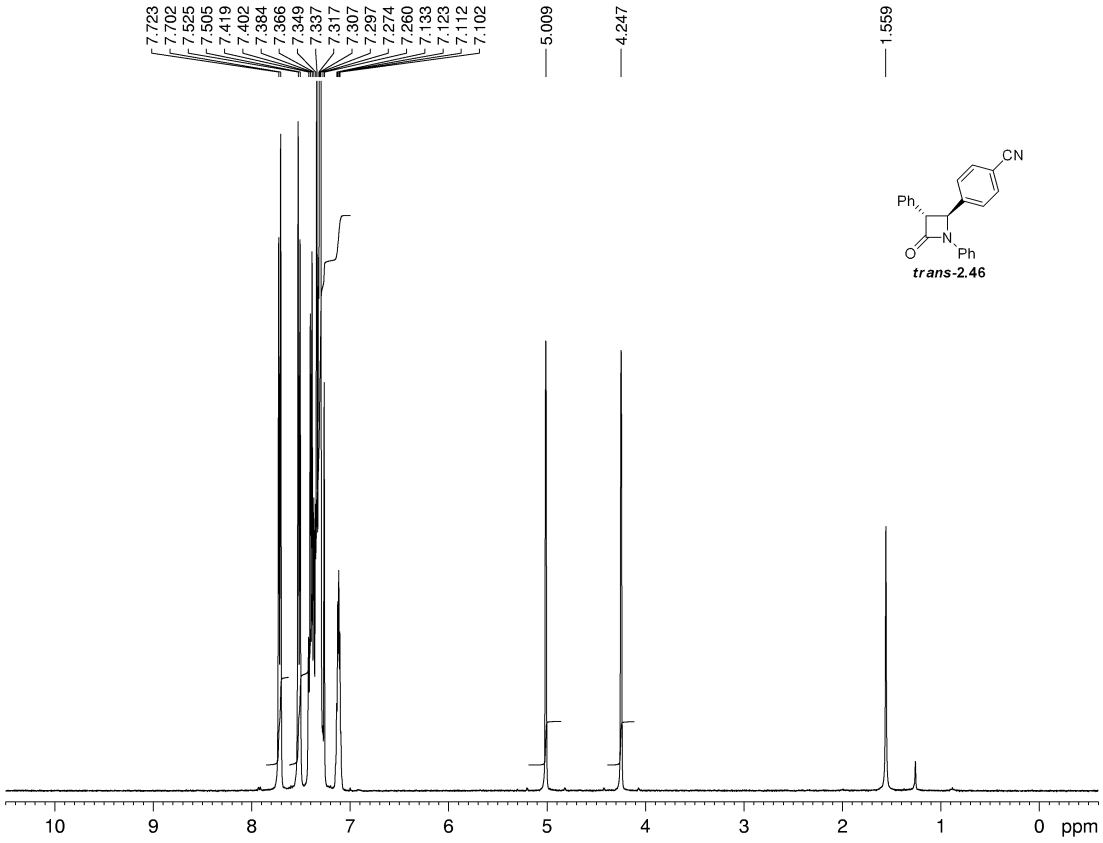
7.723
7.702
7.525
7.505
7.419
7.402
7.384
7.366
7.349
7.337
7.317
7.307
7.297
7.274
7.260
7.133
7.123
7.112
7.102
5.009
4.247
1.559
CN
Ph
N
O
Ph
trans-2.46
10
9
8
7
6
5
4
3
2
1
0
ppm

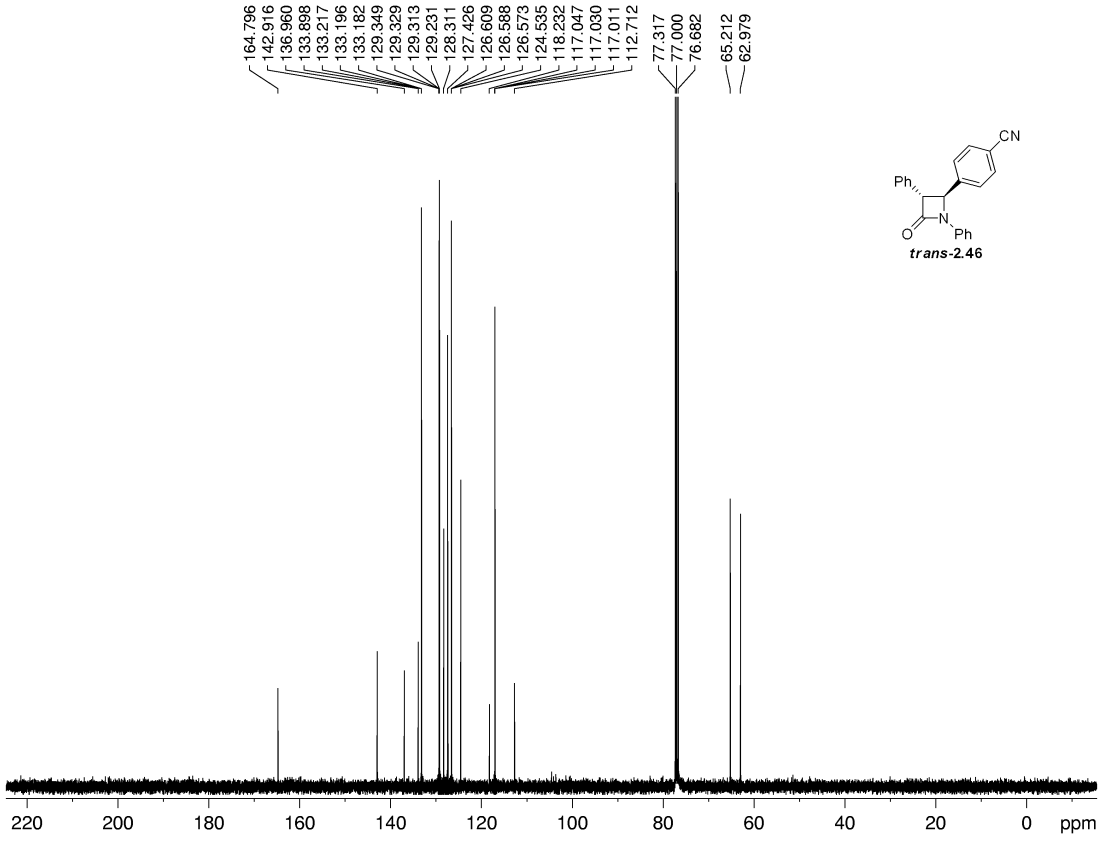
164.796
142.916
136.960
133.898
133.217
133.196
133.182
129.349
129.329
129.313
129.231
128.311
127.426
126.609
126.588
126.573
124.535
118.232
117.047
117.030
117.011
112.712
77.317
77.000
76.682
65.212
62.979
CN
Ph
N
O
Ph
trans-2.46
220
200
180
160
140
120
100
80
60
40
20
0
ppm

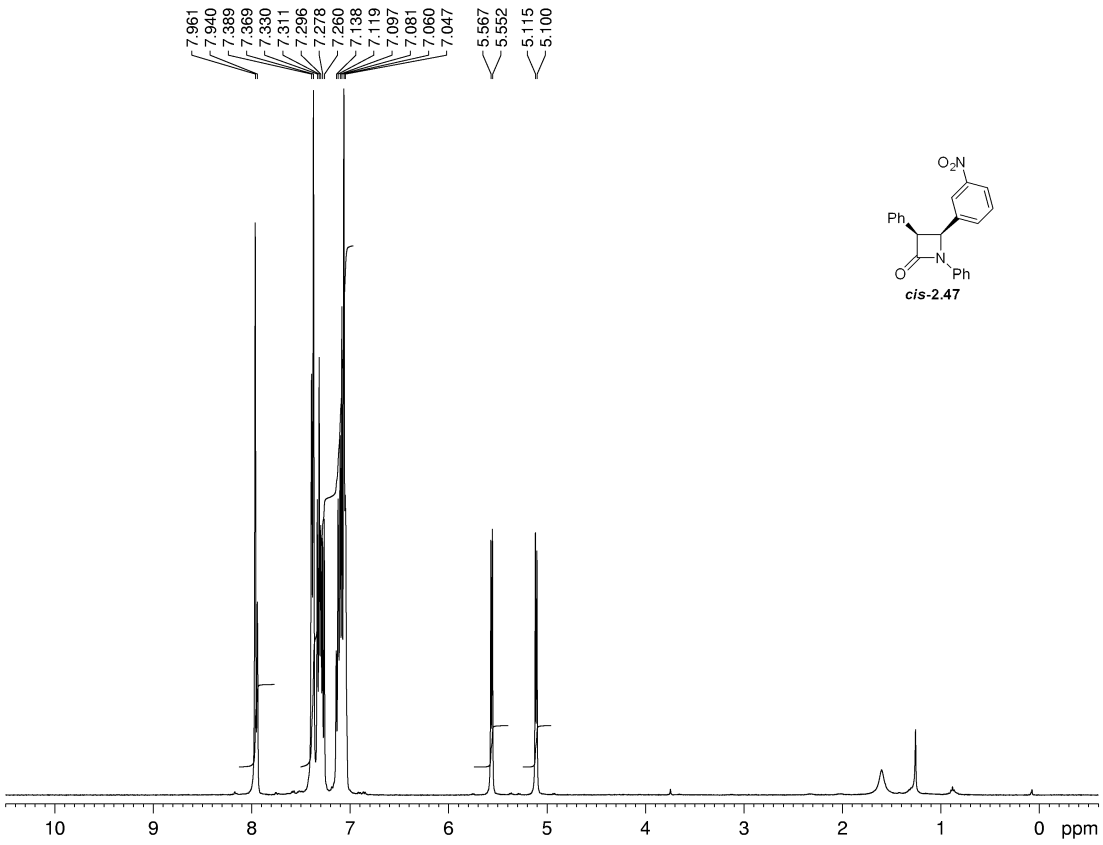

***cis*-2.47**

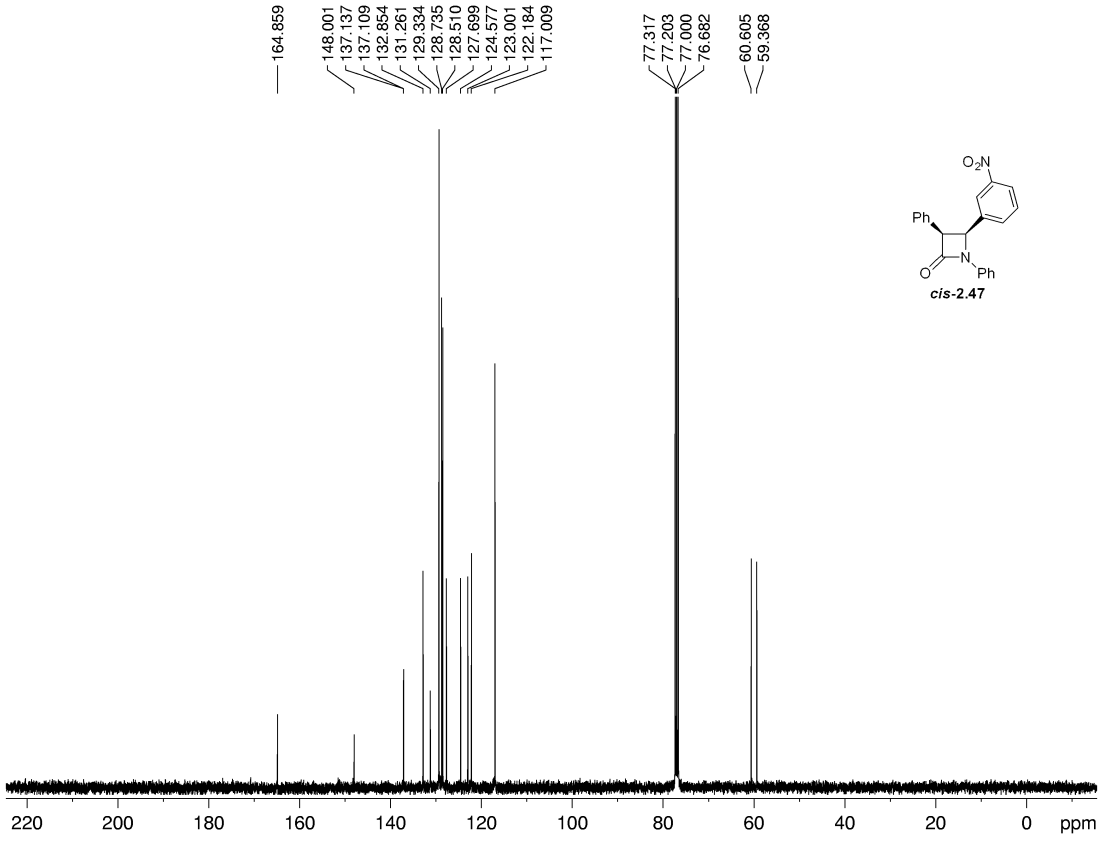

***cis*-2.47**

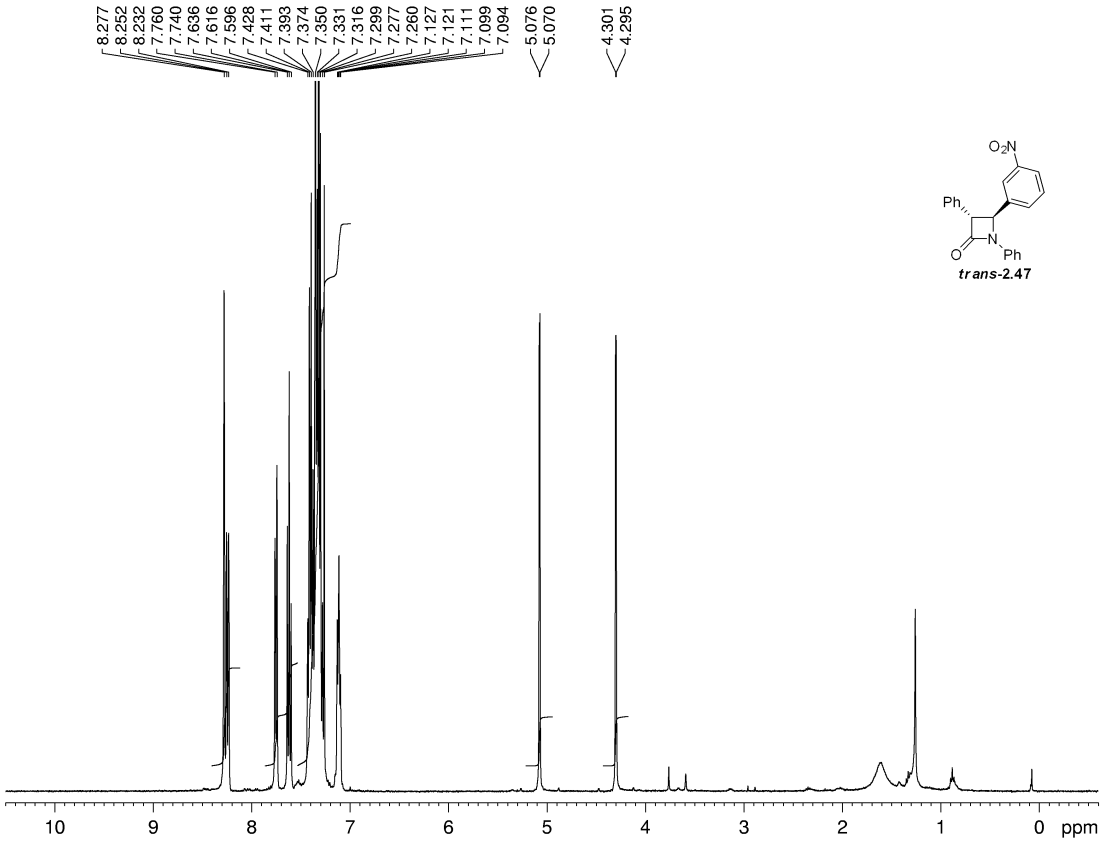
8.277
8.252
8.232
7.760
7.740
7.636
7.616
7.596
7.428
7.411
7.393
7.374
7.350
7.331
7.316
7.299
7.277
7.260
7.127
7.121
7.111
7.099
7.094
5.076
5.070
4.301
4.295
O2N
Ph
N
O
Ph
trans-2.47
10
9
8
7
6
5
4
3
2
1
0
ppm

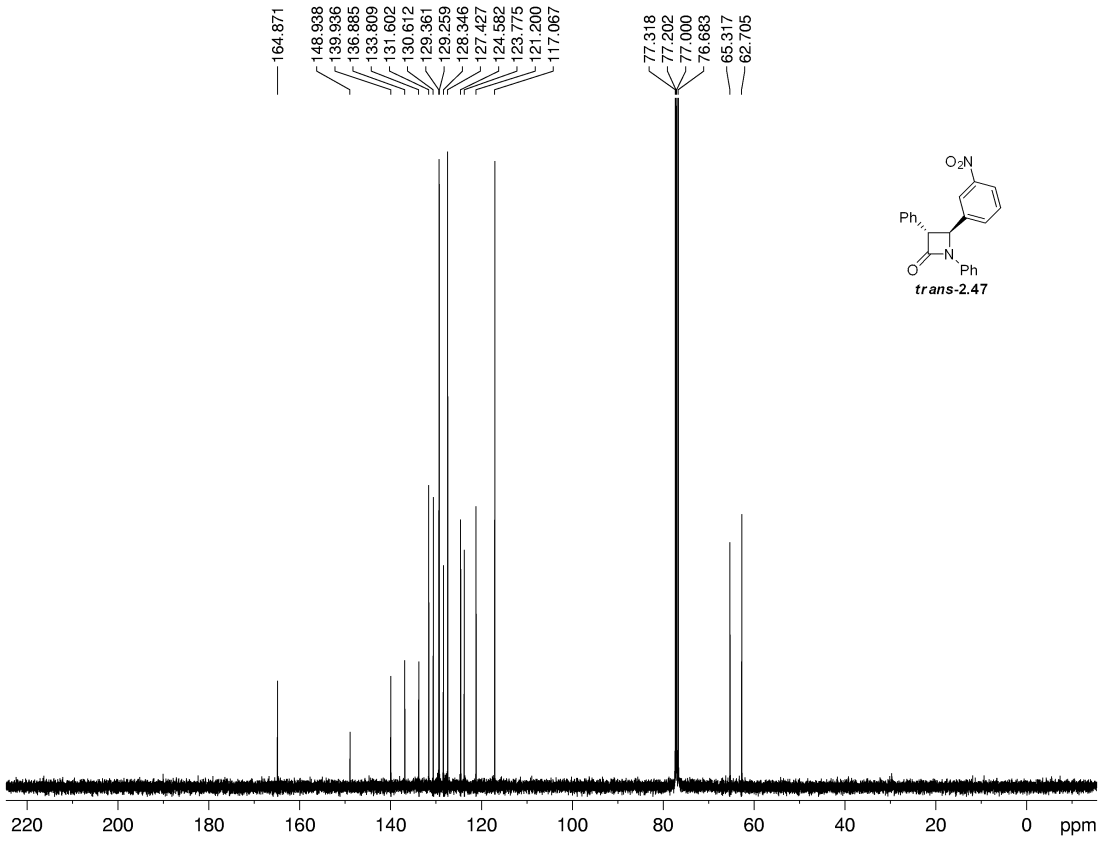
164.871
148.938
139.936
136.885
133.809
131.602
130.612
129.361
129.259
128.346
127.427
124.582
123.775
121.200
117.067
77.318
77.202
77.000
76.683
65.317
62.705
O2N
Ph
N
O
Ph
trans-2.47
220
200
180
160
140
120
100
80
60
40
20
0
ppm

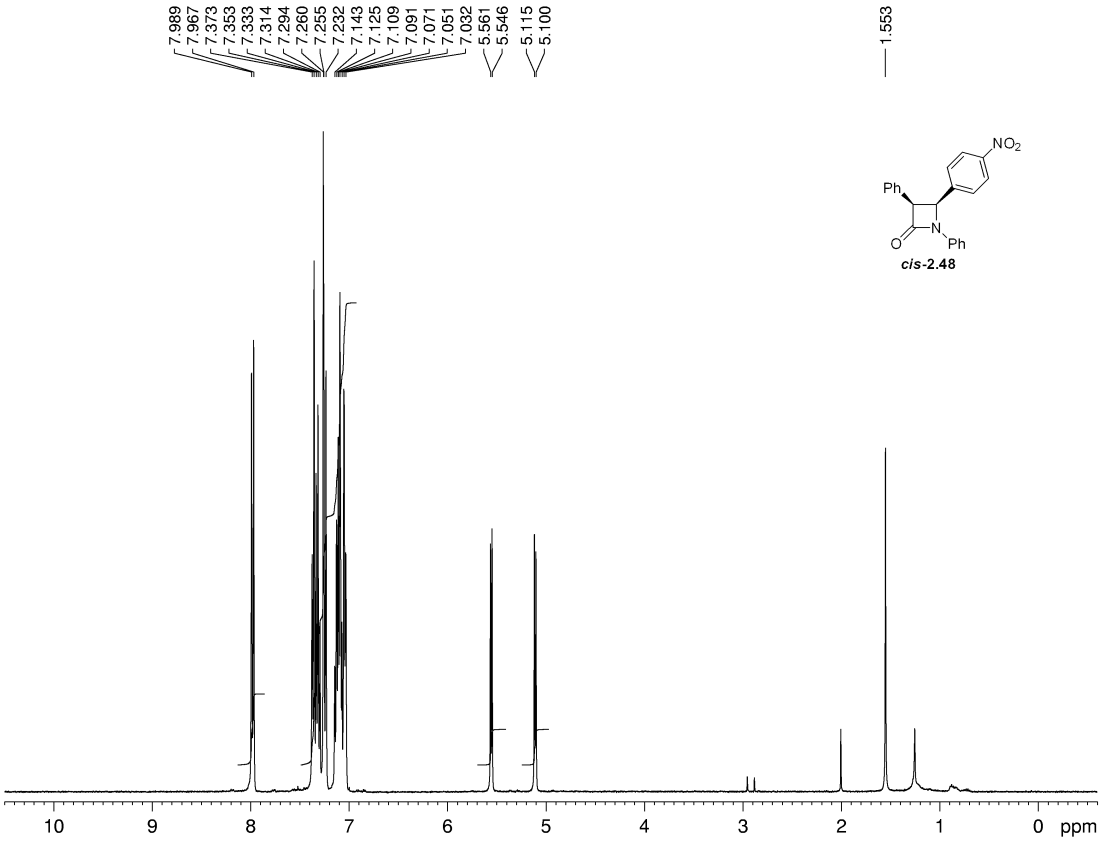
7.989
7.967
7.373
7.353
7.333
7.314
7.294
7.260
7.255
7.232
7.143
7.125
7.109
7.091
7.071
7.051
7.032
5.561
5.546
5.115
5.100
1.553
NO2
Ph
O
N
Ph
cis-2.48
10
9
8
7
6
5
4
3
2
1
0
ppm

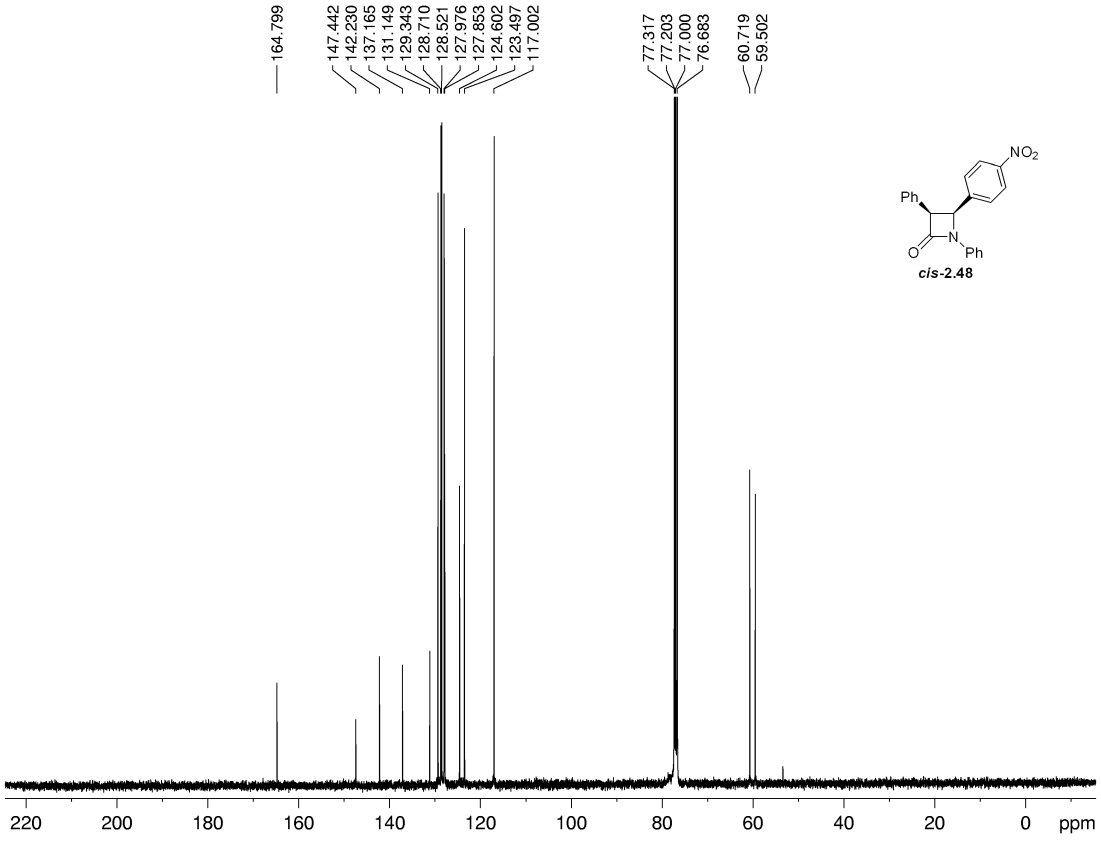
164.799
147.442
142.230
137.165
131.149
129.343
128.710
128.521
127.976
127.853
124.602
123.497
117.002
77.317
77.203
77.000
76.683
60.719
59.502
NO2
Ph
O
N
Ph
cis-2.48
220
200
180
160
140
120
100
80
60
40
20
0
ppm

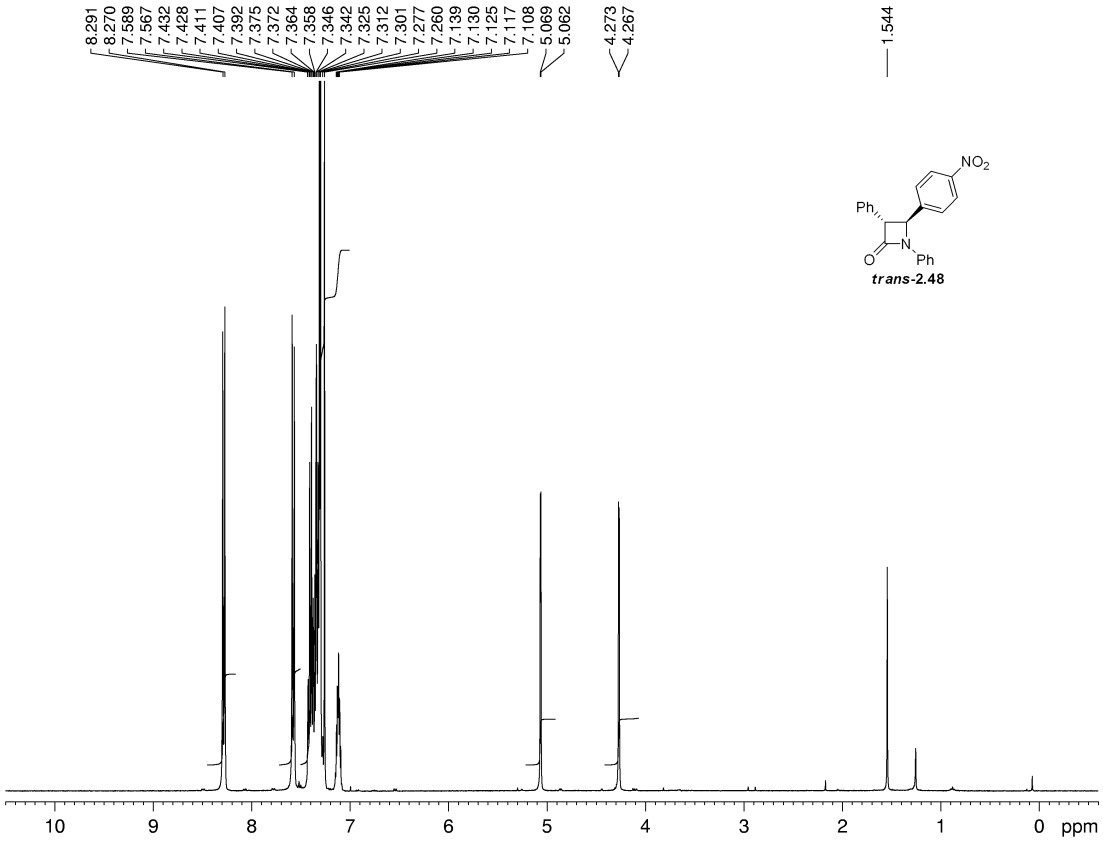
8.291
8.270
7.589
7.567
7.432
7.428
7.411
7.407
7.392
7.375
7.372
7.364
7.358
7.346
7.342
7.325
7.312
7.301
7.277
7.260
7.139
7.130
7.125
7.117
7.108
5.069
5.062
4.273
4.267
1.544
NO2
Ph
N
O
Ph
trans-2.48
10
9
8
7
6
5
4
3
2
1
0
ppm

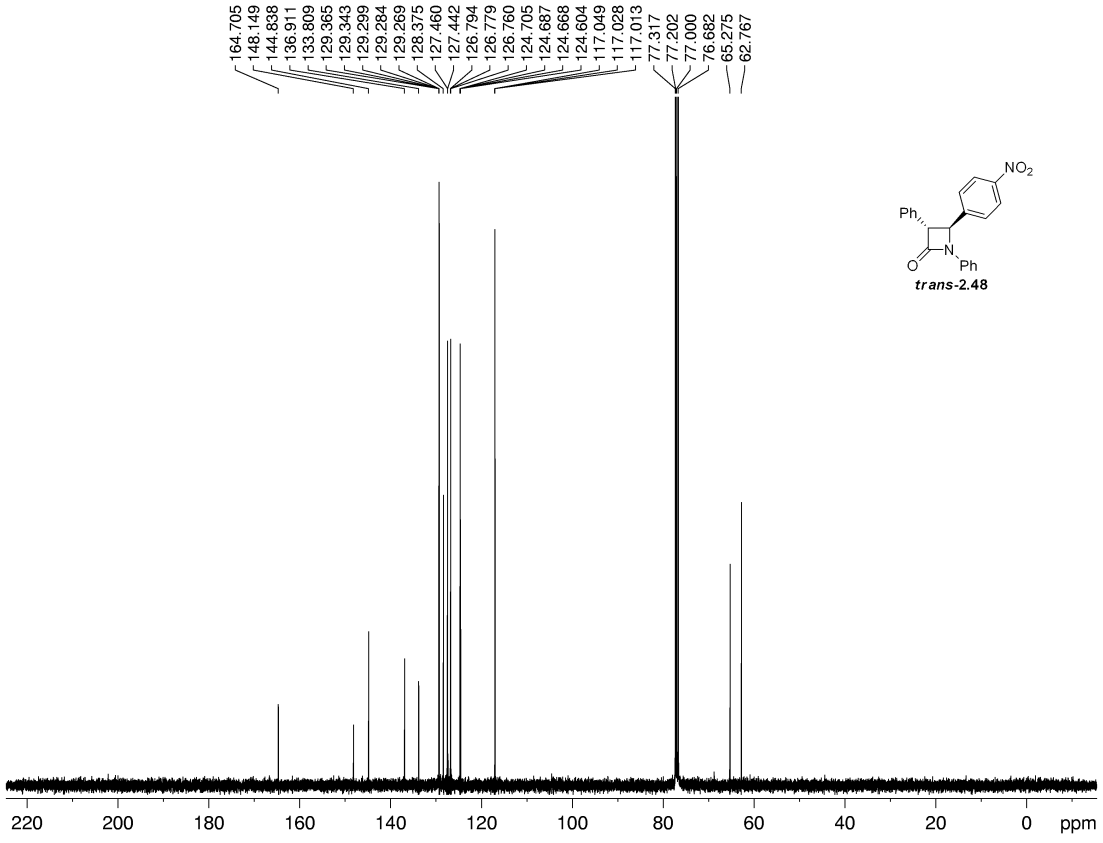
164.705
148.149
144.838
136.911
133.809
129.365
129.343
129.299
129.284
129.269
128.375
127.460
127.442
126.794
126.779
126.760
124.705
124.687
124.668
124.604
117.049
117.028
117.013
77.317
77.202
77.000
76.682
65.275
62.767
NO2
Ph
N
O
Ph
trans-2.48
220
200
180
160
140
120
100
80
60
40
20
0
ppm

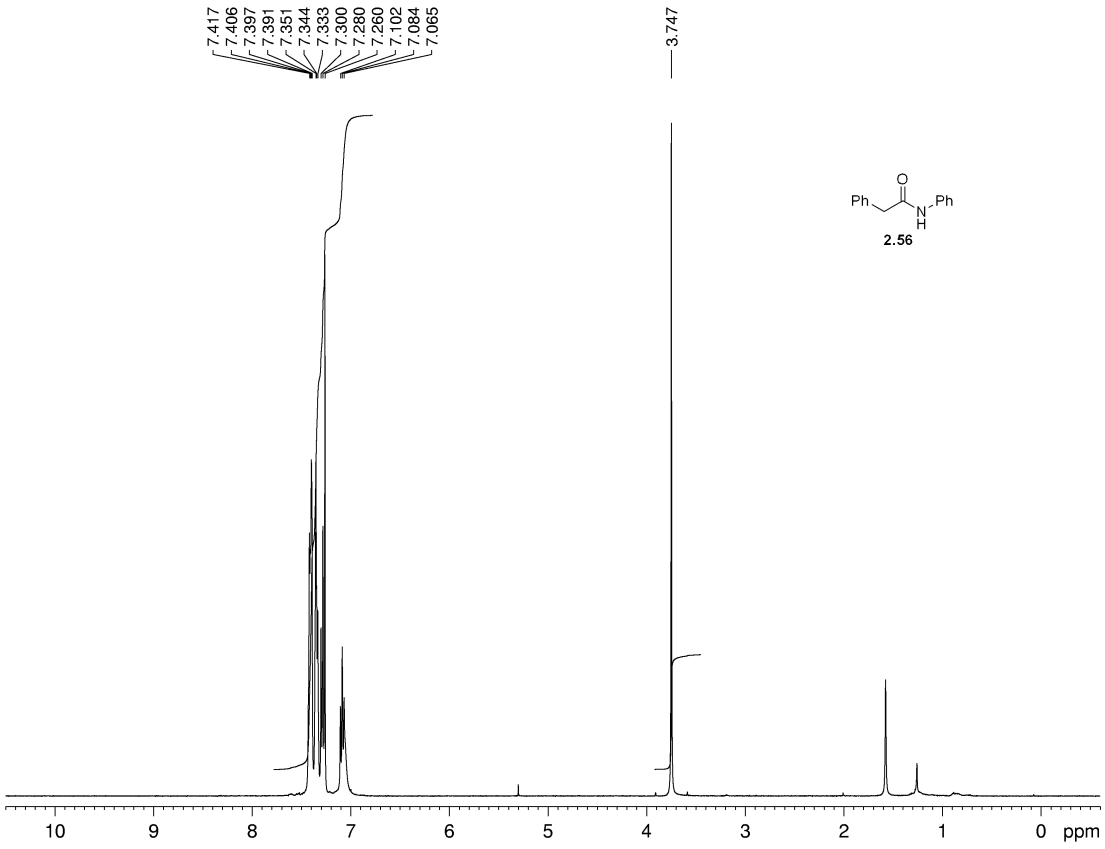
7.417
7.406
7.397
7.391
7.351
7.344
7.333
7.300
7.280
7.260
7.102
7.084
7.065
3.747
Ph
O
N
H
Ph
2.56
10
9
8
7
6
5
4
3
2
1
0
ppm

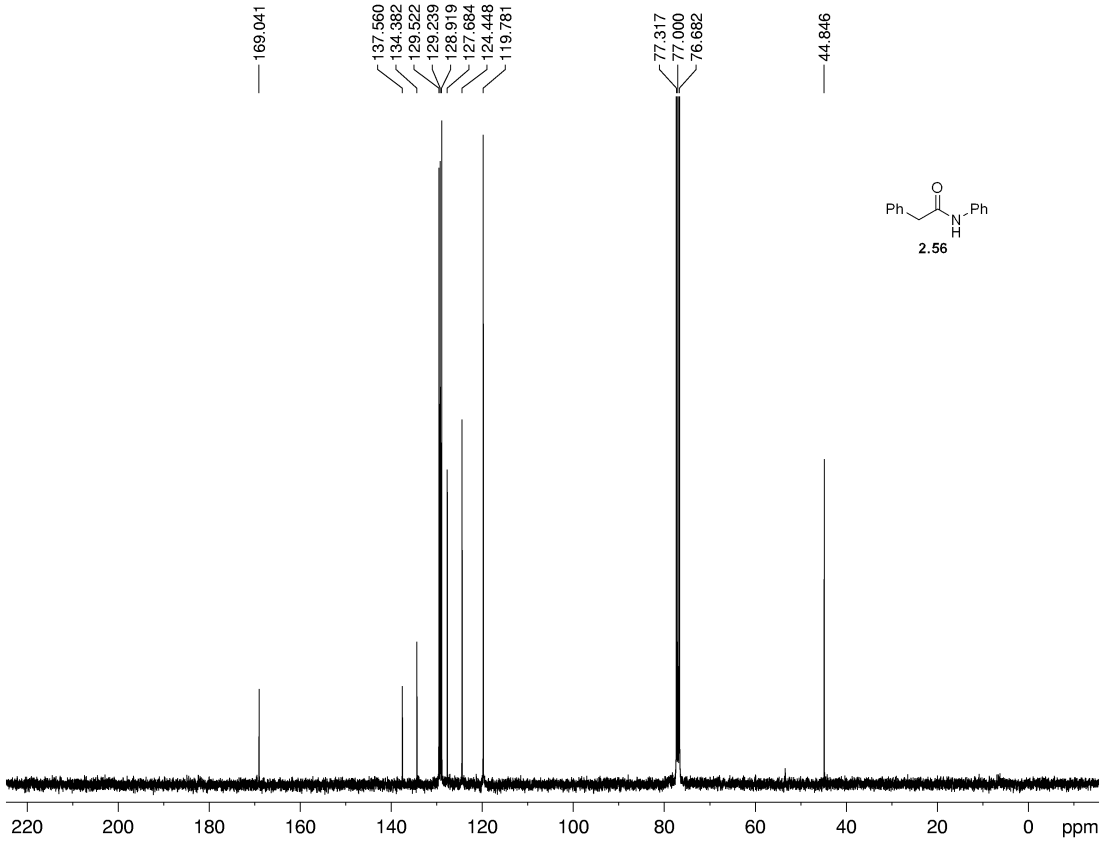
169.041
137.560
134.382
129.522
129.239
128.919
127.684
124.448
119.781
77.317
77.000
76.682
44.846
Ph
O
N
H
Ph
2.56
220
200
180
160
140
120
100
80
60
40
20
0
ppm

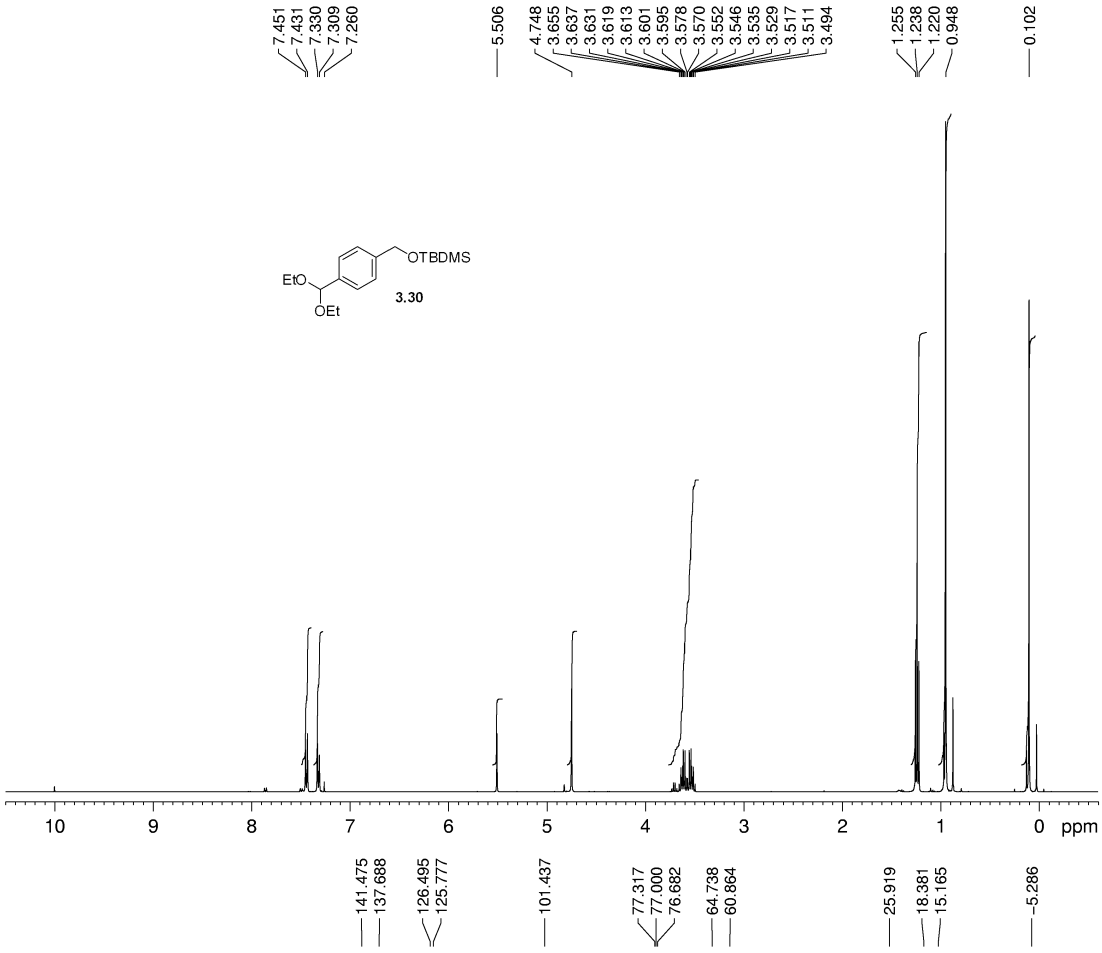
7.451
7.431
7.330
7.309
7.260
5.506
4.748
3.655
3.637
3.631
3.619
3.613
3.601
3.595
3.578
3.570
3.552
3.546
3.535
3.529
3.517
3.511
3.494
1.255
1.238
1.220
0.948
0.102
OTBDMS
EtO
OEt
3.30
10
9
8
7
6
5
4
3
2
1
0
ppm
141.475
137.688
126.495
125.777
101.437
77.317
77.000
76.682
64.738
60.864
25.919
18.381
15.165
-5.286

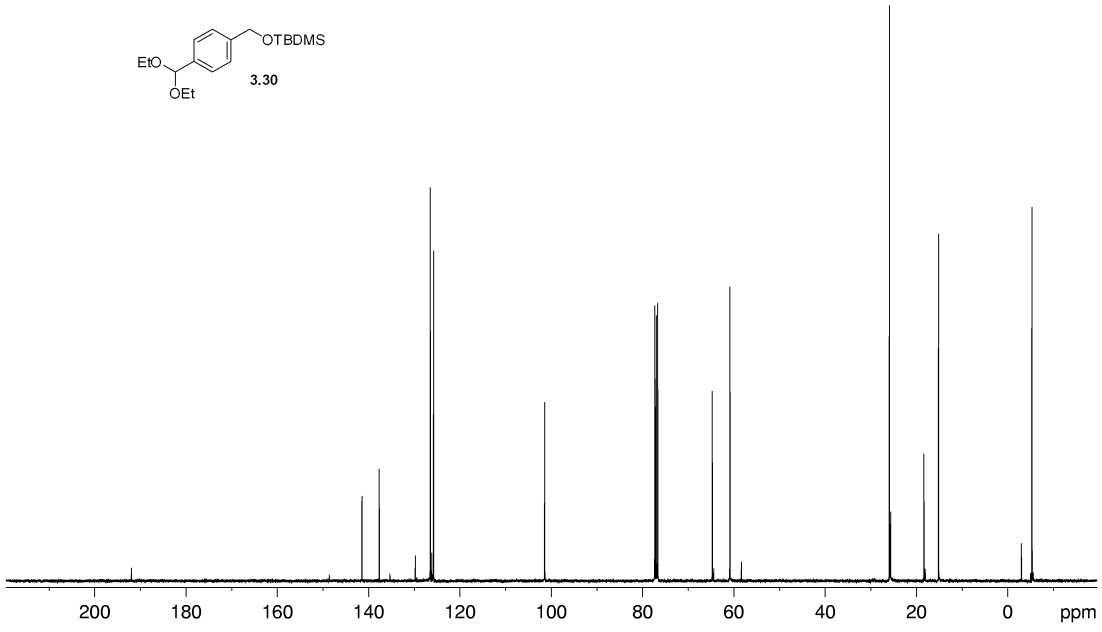
OTBDMS
EtO
OEt
3.30
200
180
160
140
120
100
80
60
40
20
0
ppm

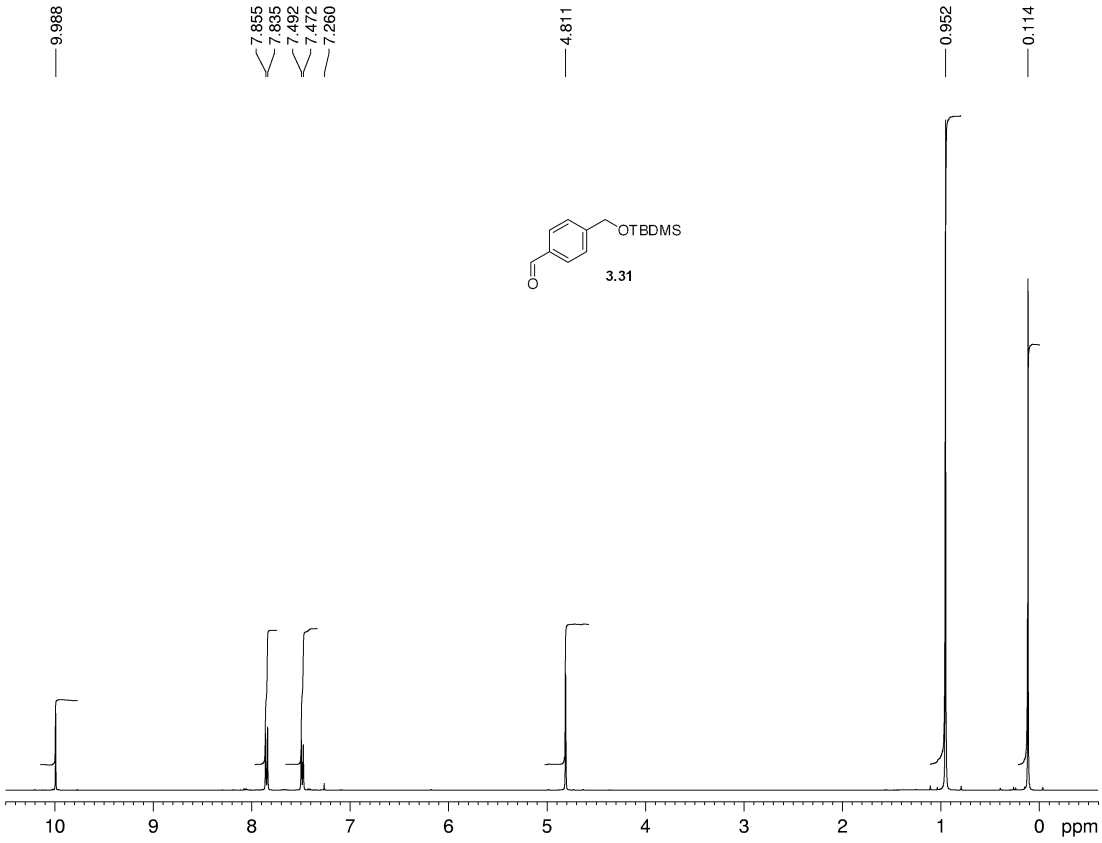
9.988
7.855
7.835
7.492
7.472
7.260
4.811
0.952
0.114
OTBDMS
O
3.31
10
9
8
7
6
5
4
3
2
1
0
ppm

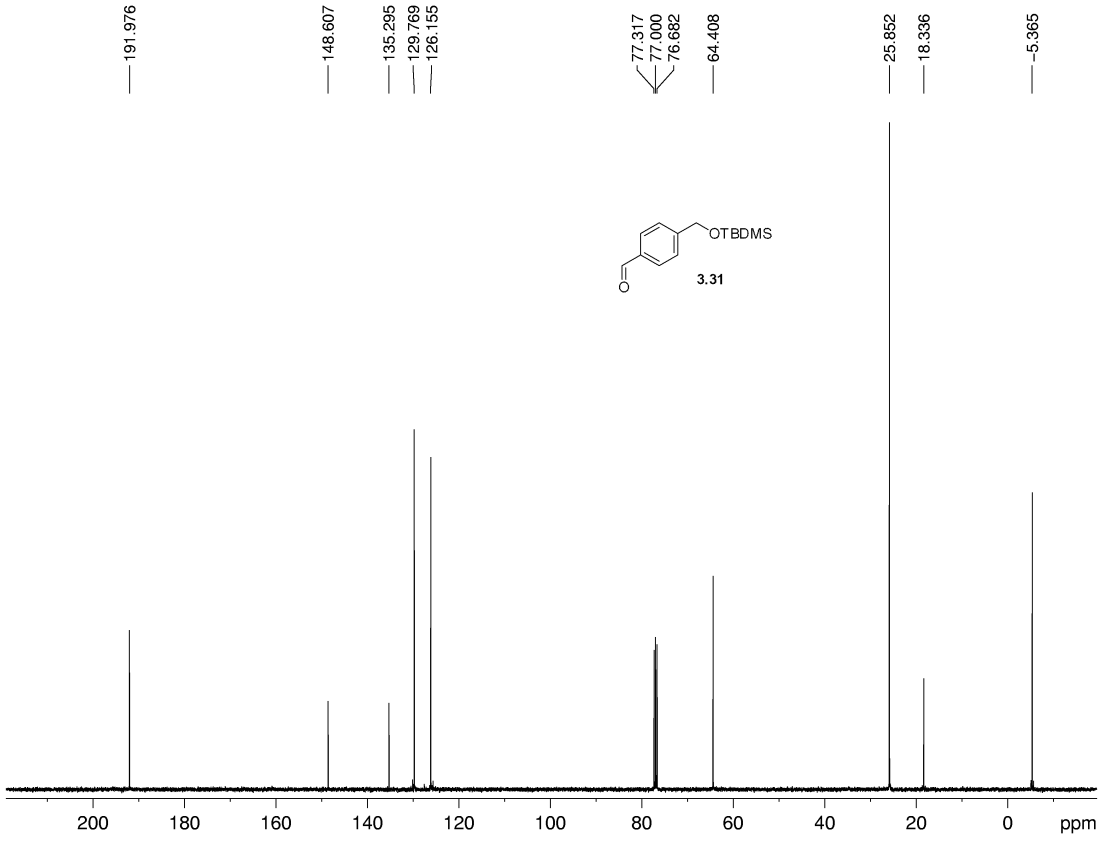
191.976
148.607
135.295
129.769
126.155
77.317
77.000
76.682
64.408
25.852
18.336
-5.365
OTBDMS
O
3.31
200
180
160
140
120
100
80
60
40
20
0
ppm

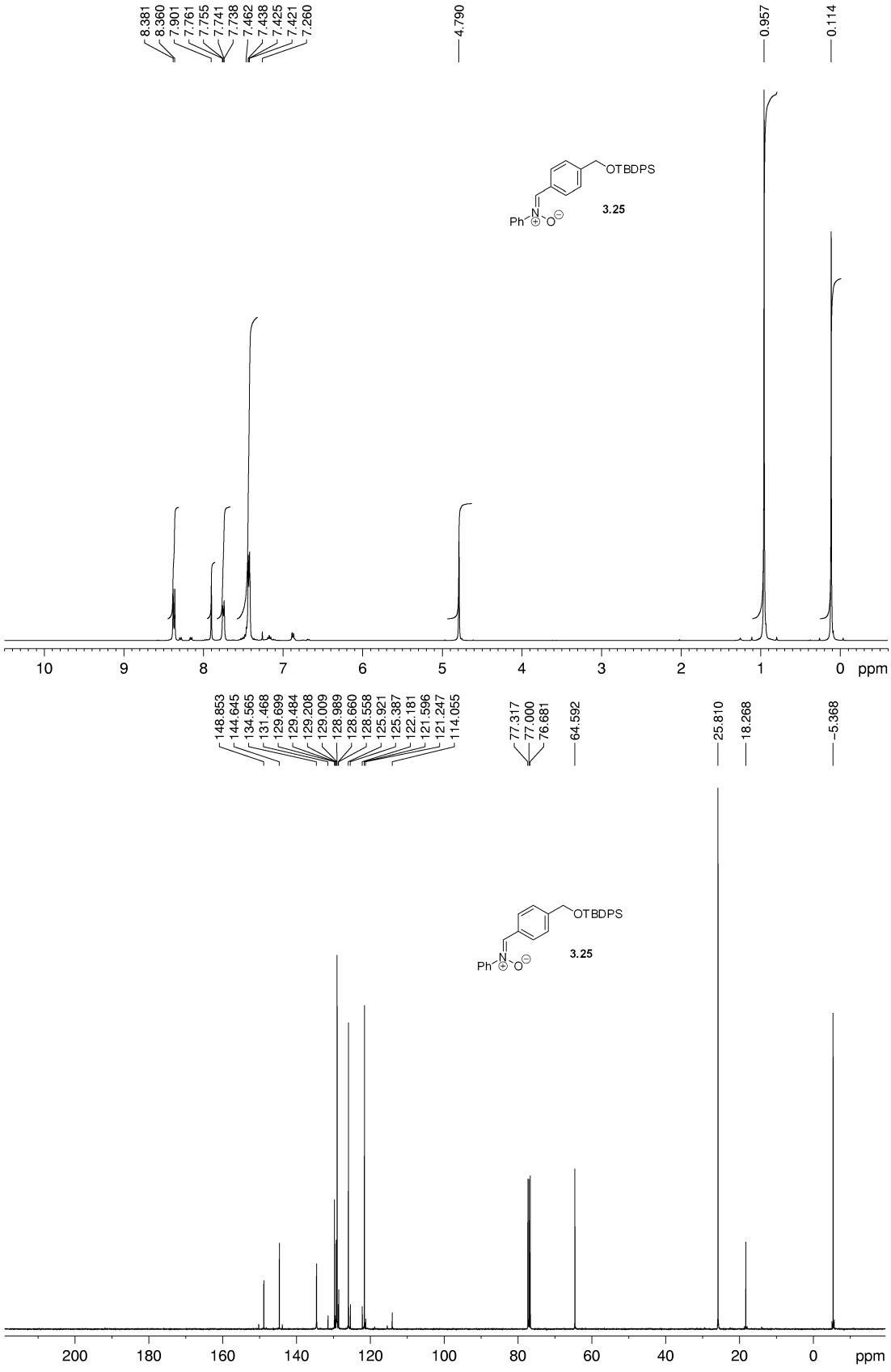
8.381
8.360
7.901
7.761
7.755
7.741
7.738
7.462
7.438
7.425
7.421
7.260
4.790
0.957
0.114
OTBDPS
3.25
Ph
N
O
10
9
8
7
6
5
4
3
2
1
0
ppm
148.853
144.645
134.565
131.468
129.699
129.484
129.208
129.009
128.989
128.660
128.558
125.921
125.387
122.181
121.596
121.247
114.055
77.317
77.000
76.681
64.592
25.810
18.268
-5.368
OTBDPS
3.25
Ph
N
O
200
180
160
140
120
100
80
60
40
20
0
ppm

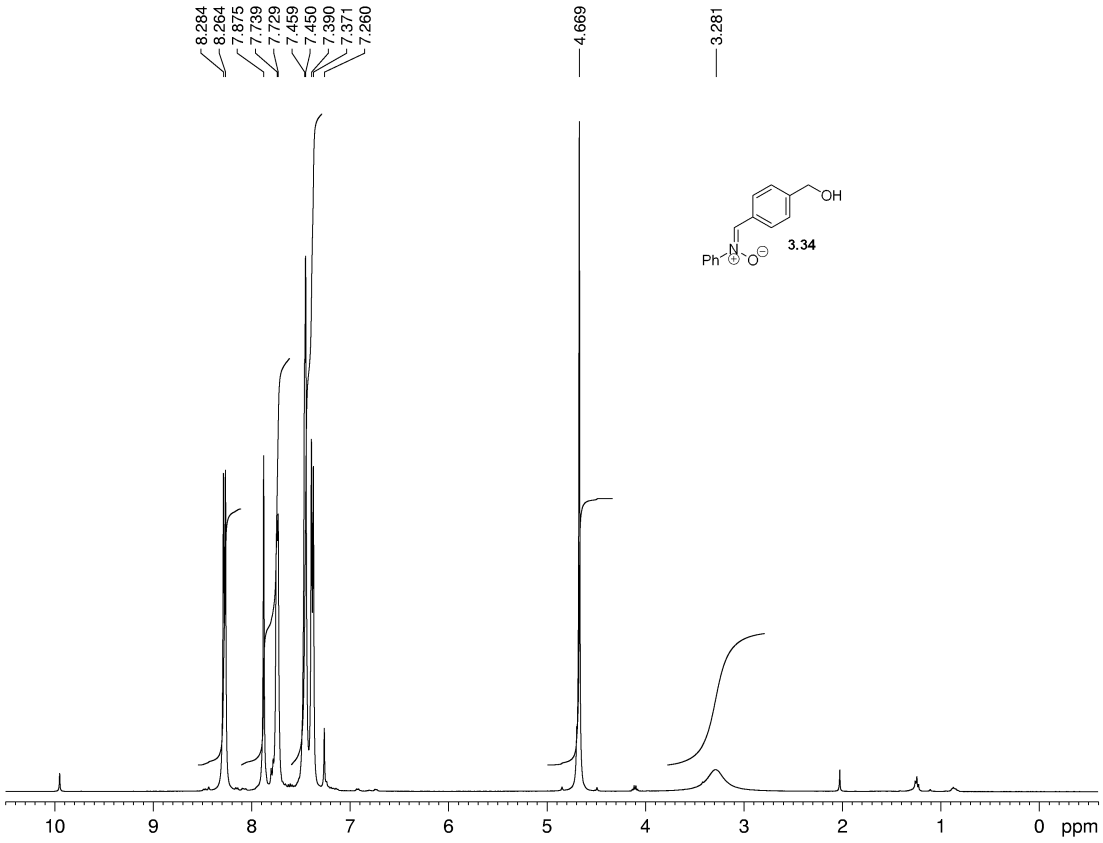
8.284
8.264
7.875
7.739
7.729
7.459
7.450
7.390
7.371
7.260
4.669
3.281
OH
Ph
N
O
3.34
10
9
8
7
6
5
4
3
2
1
0
ppm

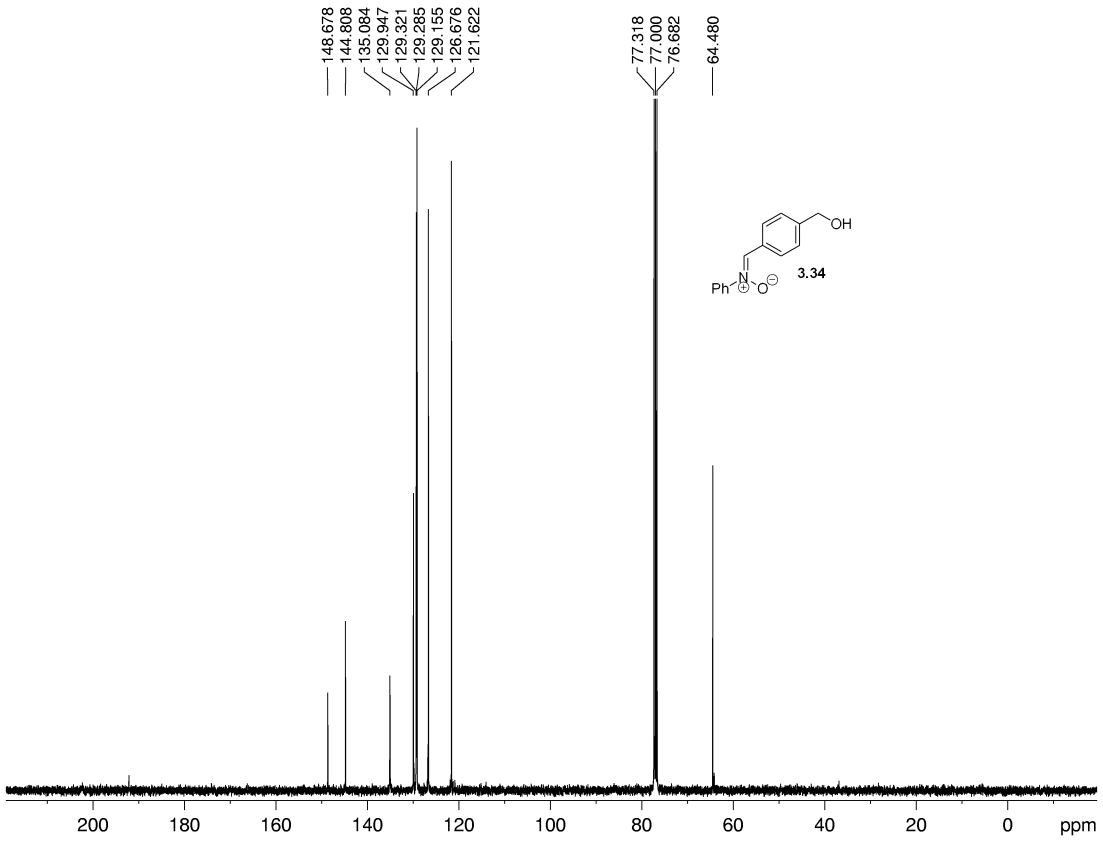
148.678
144.808
135.084
129.947
129.321
129.285
129.155
126.676
121.622
77.318
77.000
76.682
64.480
OH
Ph
N
O
3.34
200
180
160
140
120
100
80
60
40
20
0
ppm

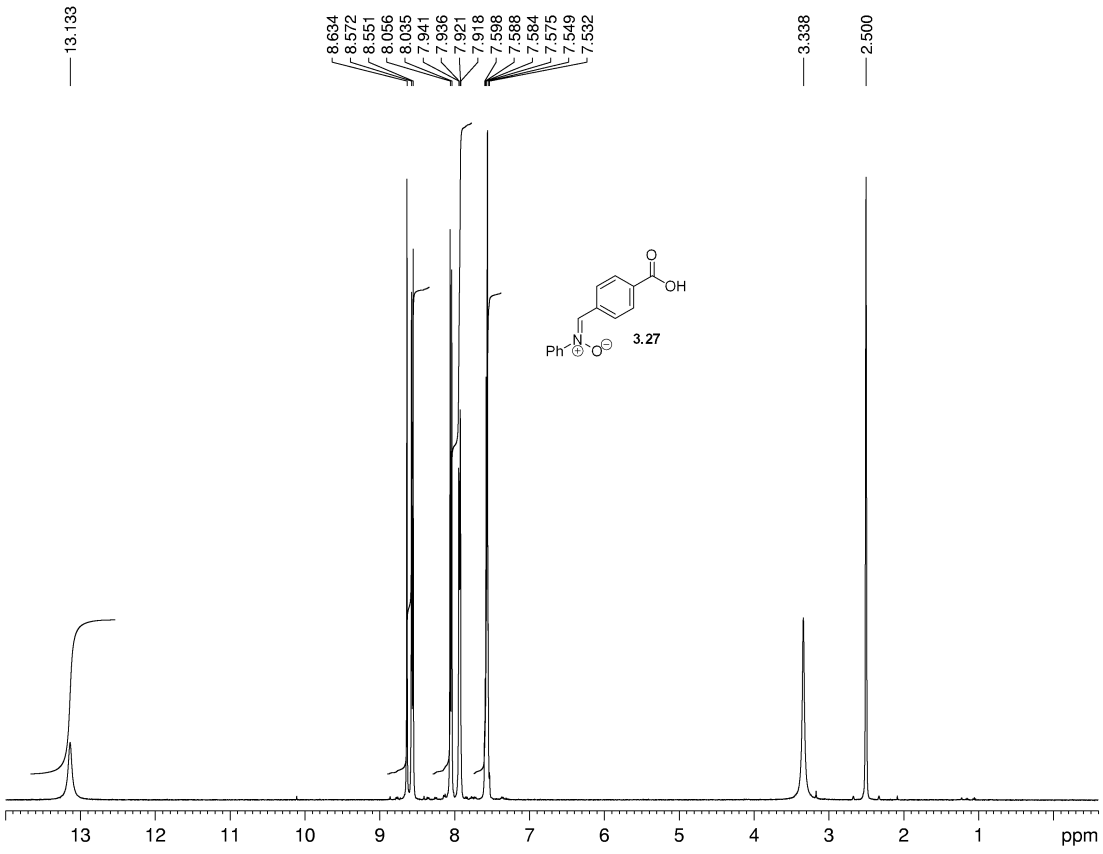
13.133
8.634
8.572
8.551
8.056
8.035
7.941
7.936
7.921
7.918
7.598
7.588
7.584
7.575
7.549
7.532
3.338
2.500
3.27
13
12
11
10
9
8
7
6
5
4
3
2
1
ppm

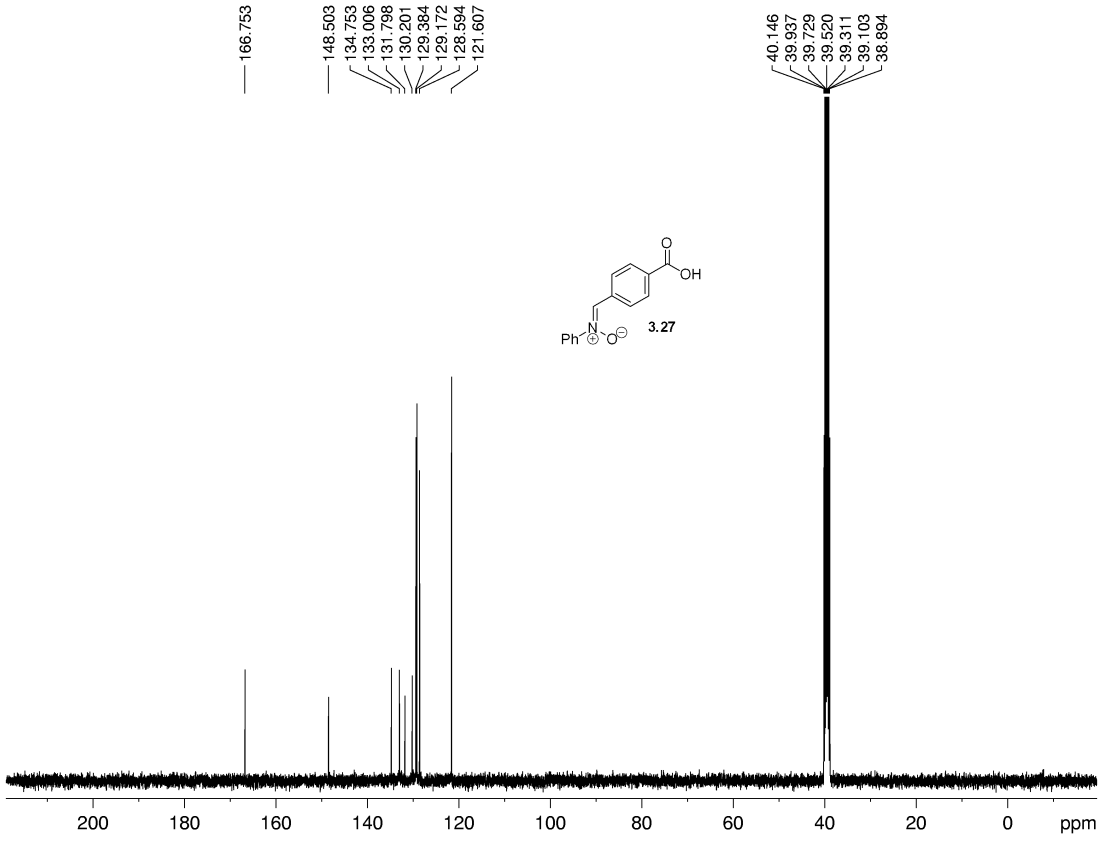
166.753
148.503
134.753
133.006
131.798
130.201
129.384
129.172
128.594
121.607
40.146
39.937
39.729
39.520
39.311
39.103
38.894
3.27
200
180
160
140
120
100
80
60
40
20
0
ppm

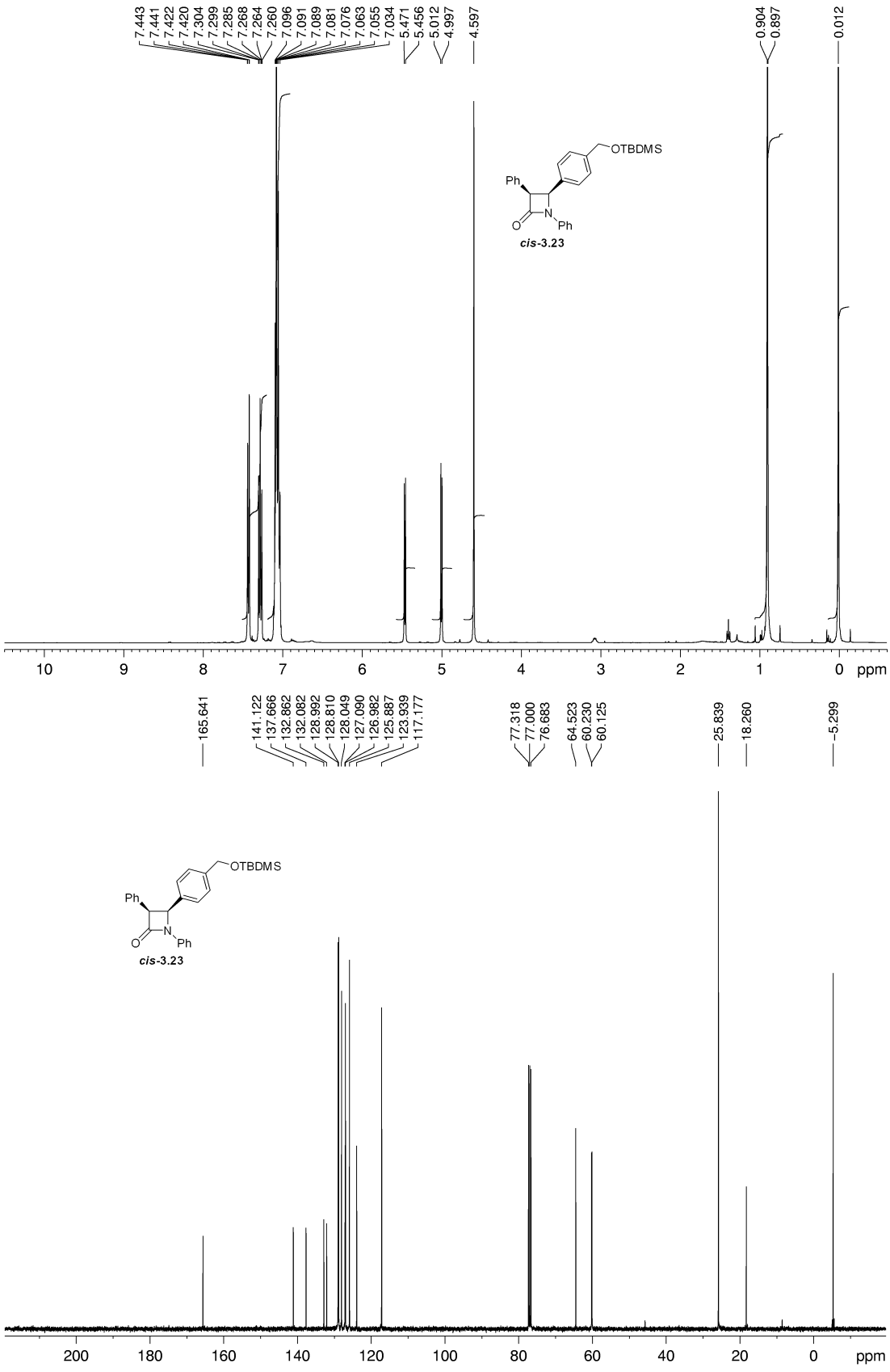
7.443
7.441
7.422
7.420
7.304
7.299
7.285
7.268
7.264
7.260
7.096
7.091
7.089
7.081
7.076
7.063
7.055
7.034
5.471
5.456
5.012
4.997
4.597
0.904
0.897
0.012
OTBDMS
Ph
N
Ph
O
cis-3.23
10
9
8
7
6
5
4
3
2
1
0
ppm
165.641
141.122
137.666
132.862
132.082
128.992
128.810
128.049
127.090
126.982
125.887
123.939
117.177
77.318
77.000
76.683
64.523
60.230
60.125
25.839
18.260
-5.299
OTBDMS
Ph
N
Ph
O
cis-3.23
200
180
160
140
120
100
80
60
40
20
0
ppm

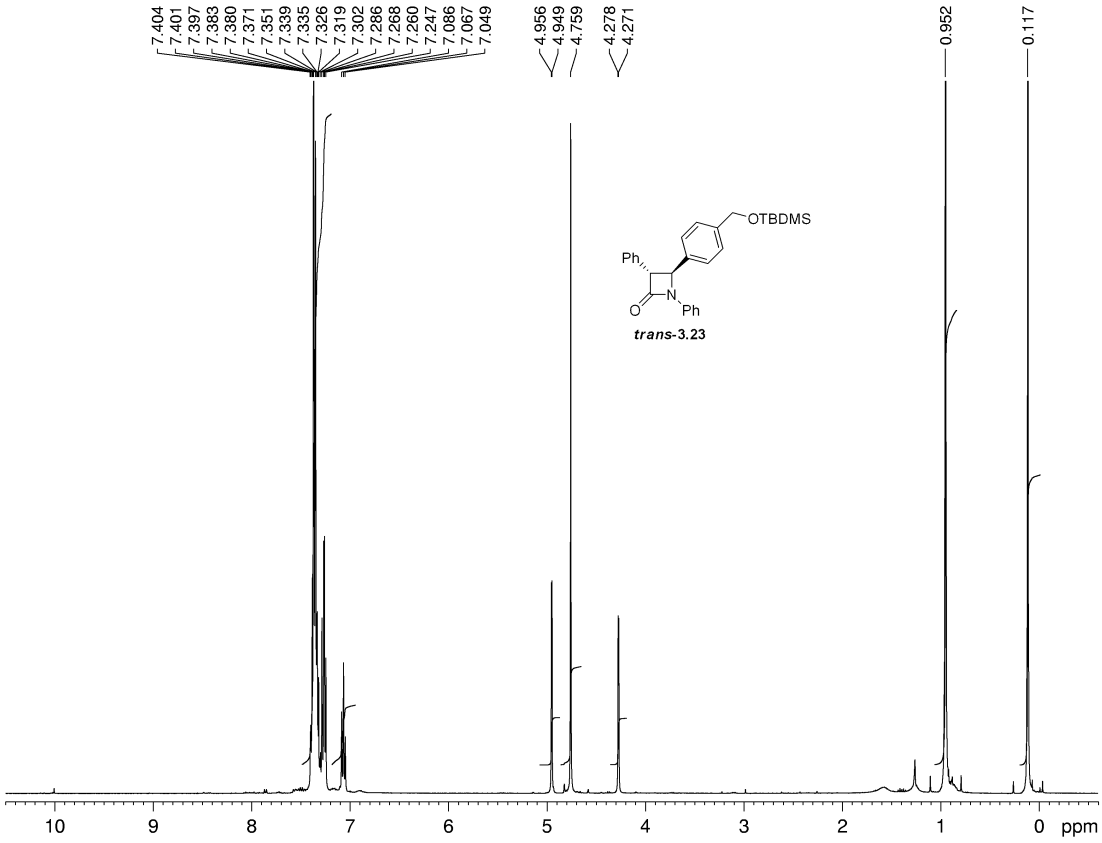
7.404
7.401
7.397
7.383
7.380
7.371
7.351
7.339
7.335
7.326
7.319
7.302
7.286
7.268
7.260
7.247
7.086
7.067
7.049
4.956
4.949
4.759
4.278
4.271
0.952
0.117
OTBDMS
Ph
N
O
Ph
trans-3.23
10
9
8
7
6
5
4
3
2
1
0
ppm

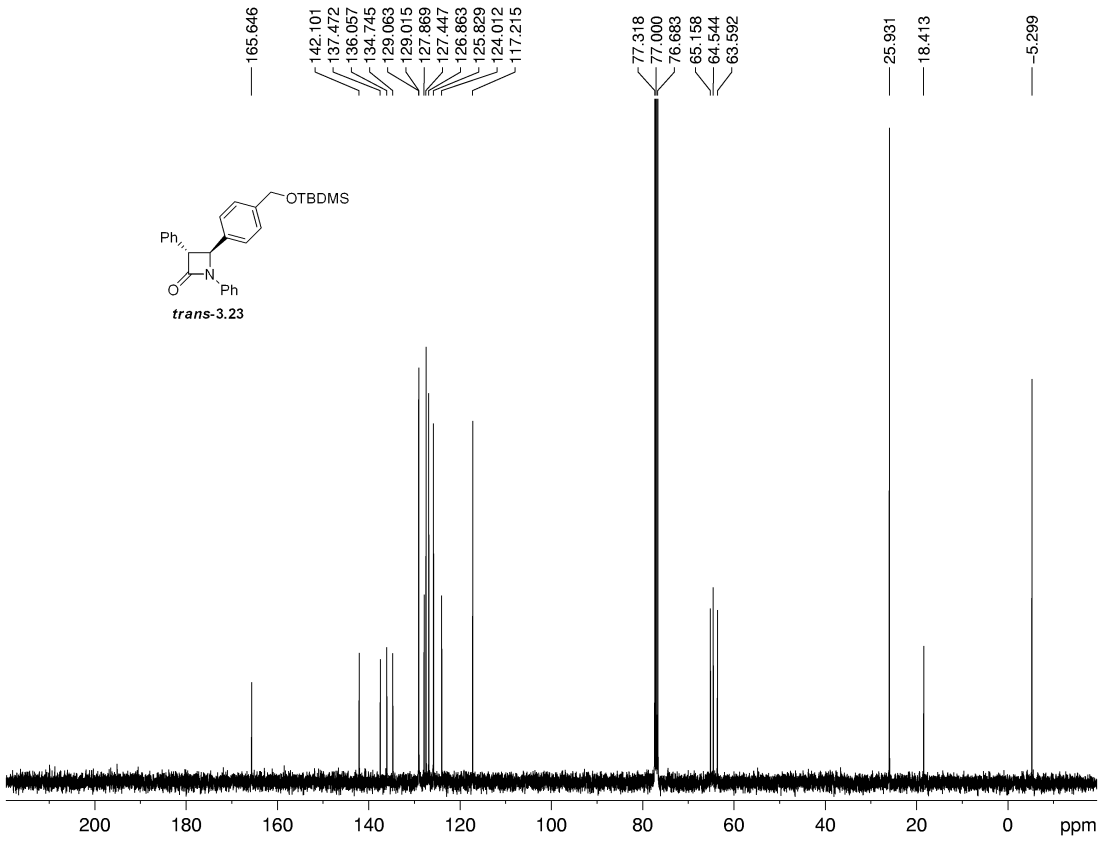
165.646
142.101
137.472
136.057
134.745
129.063
129.015
127.869
127.447
126.863
125.829
124.012
117.215
77.318
77.000
76.683
65.158
64.544
63.592
25.931
18.413
-5.299
OTBDMS
Ph
N
O
Ph
trans-3.23
200
180
160
140
120
100
80
60
40
20
0
ppm

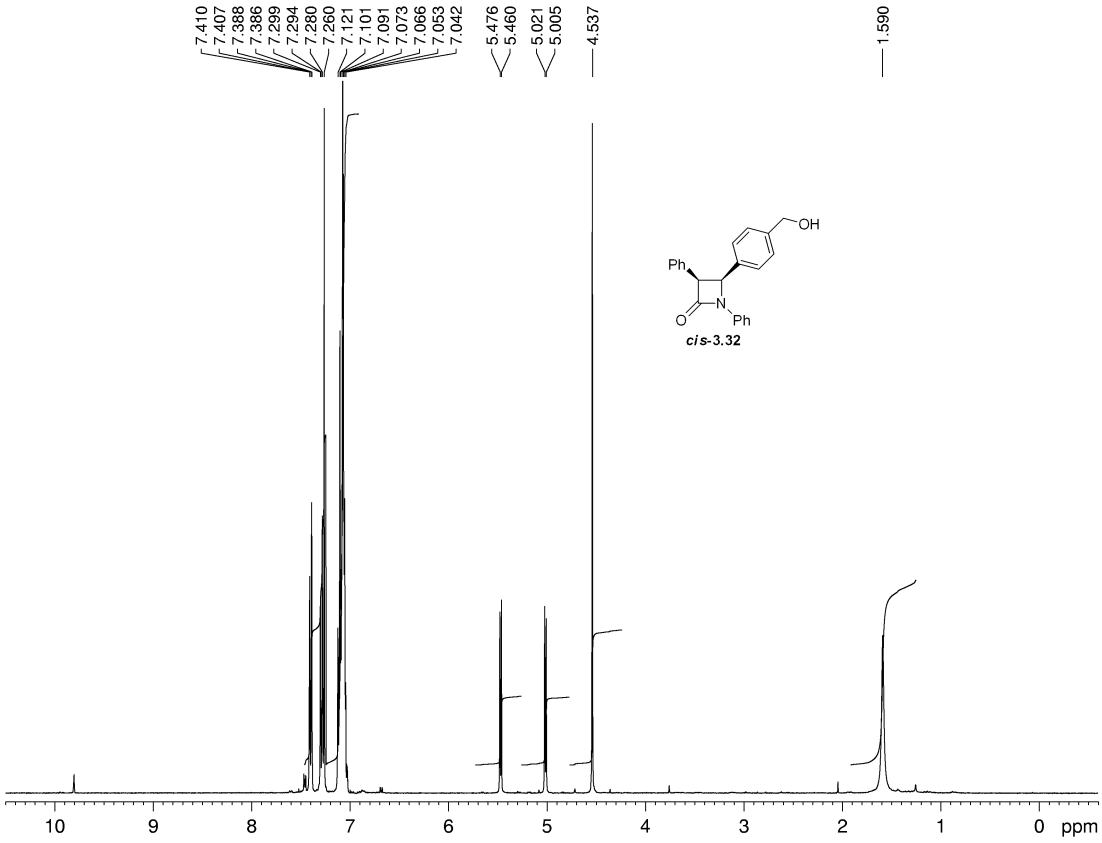
7.410
7.407
7.388
7.386
7.299
7.294
7.280
7.260
7.121
7.101
7.091
7.073
7.066
7.053
7.042
5.476
5.460
5.021
5.005
4.537
1.590
OH
Ph
N
Ph
O
cis-3.32
10
9
8
7
6
5
4
3
2
1
0
ppm

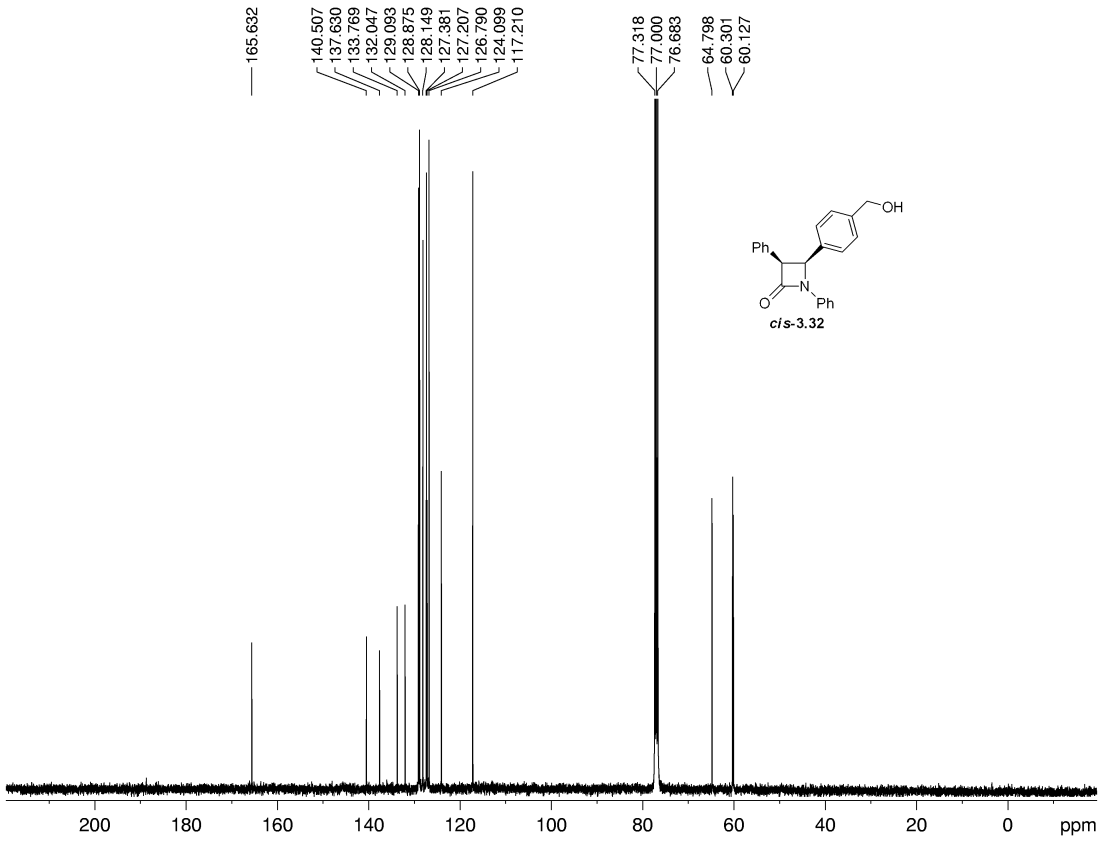
165.632
140.507
137.630
133.769
132.047
129.093
128.875
128.149
127.381
127.207
126.790
124.099
117.210
77.318
77.000
76.683
64.798
60.301
60.127
OH
Ph
N
Ph
O
cis-3.32
200
180
160
140
120
100
80
60
40
20
0
ppm

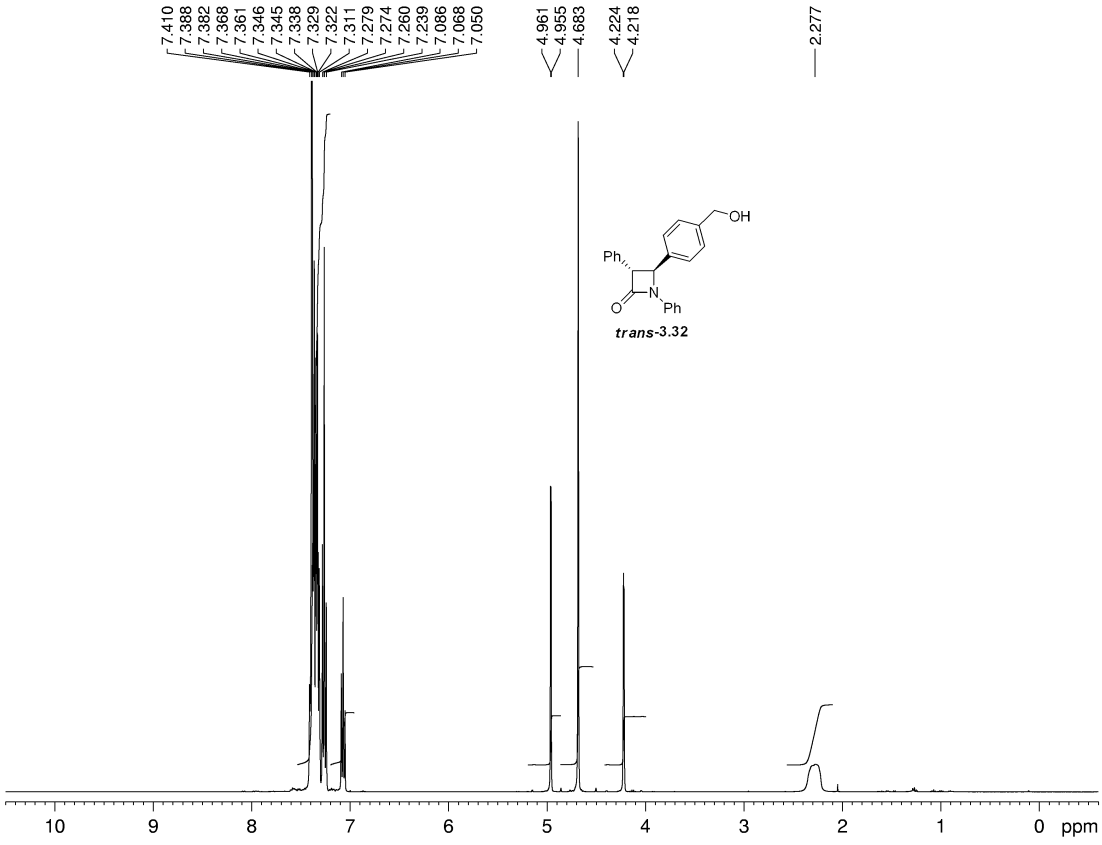
7.410
7.388
7.382
7.368
7.361
7.346
7.345
7.338
7.329
7.322
7.311
7.279
7.274
7.260
7.239
7.086
7.068
7.050
4.961
4.955
4.683
4.224
4.218
2.277
OH
Ph
N
Ph
O
trans-3.32
10
9
8
7
6
5
4
3
2
1
0
ppm

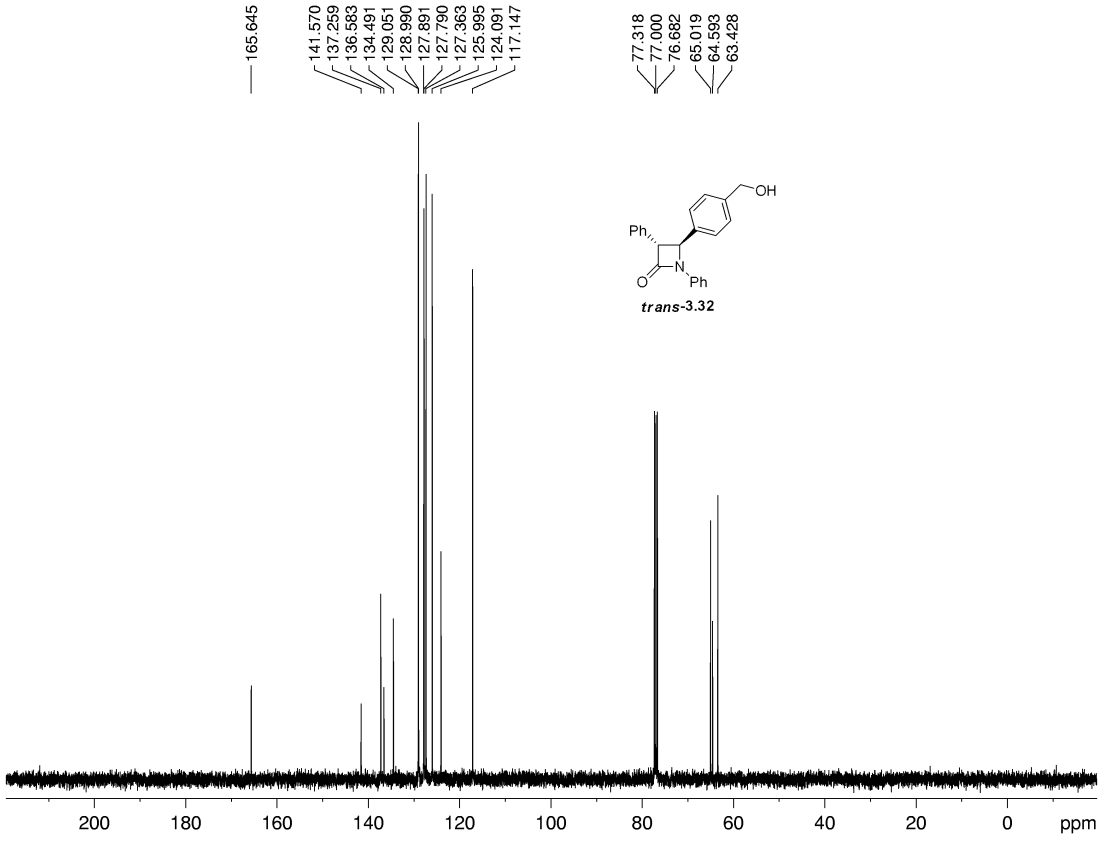
165.645
141.570
137.259
136.583
134.491
129.051
128.990
127.891
127.790
127.363
125.995
124.091
117.147
77.318
77.000
76.682
65.019
64.593
63.428
OH
Ph
N
Ph
O
trans-3.32
200
180
160
140
120
100
80
60
40
20
0
ppm

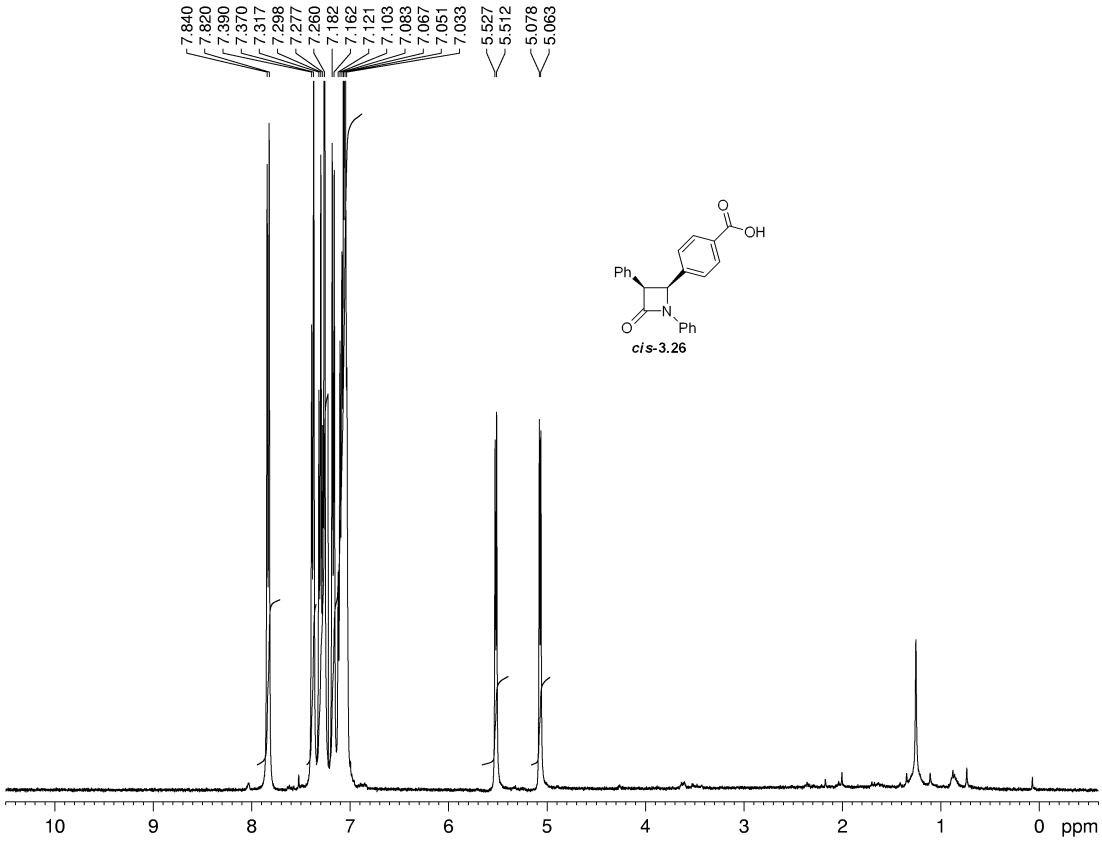
7.840
7.820
7.390
7.370
7.317
7.298
7.277
7.260
7.182
7.162
7.121
7.103
7.083
7.067
7.051
7.033
5.527
5.512
5.078
5.063
O
OH
Ph
O
N
Ph
cis-3.26
10
9
8
7
6
5
4
3
2
1
0
ppm

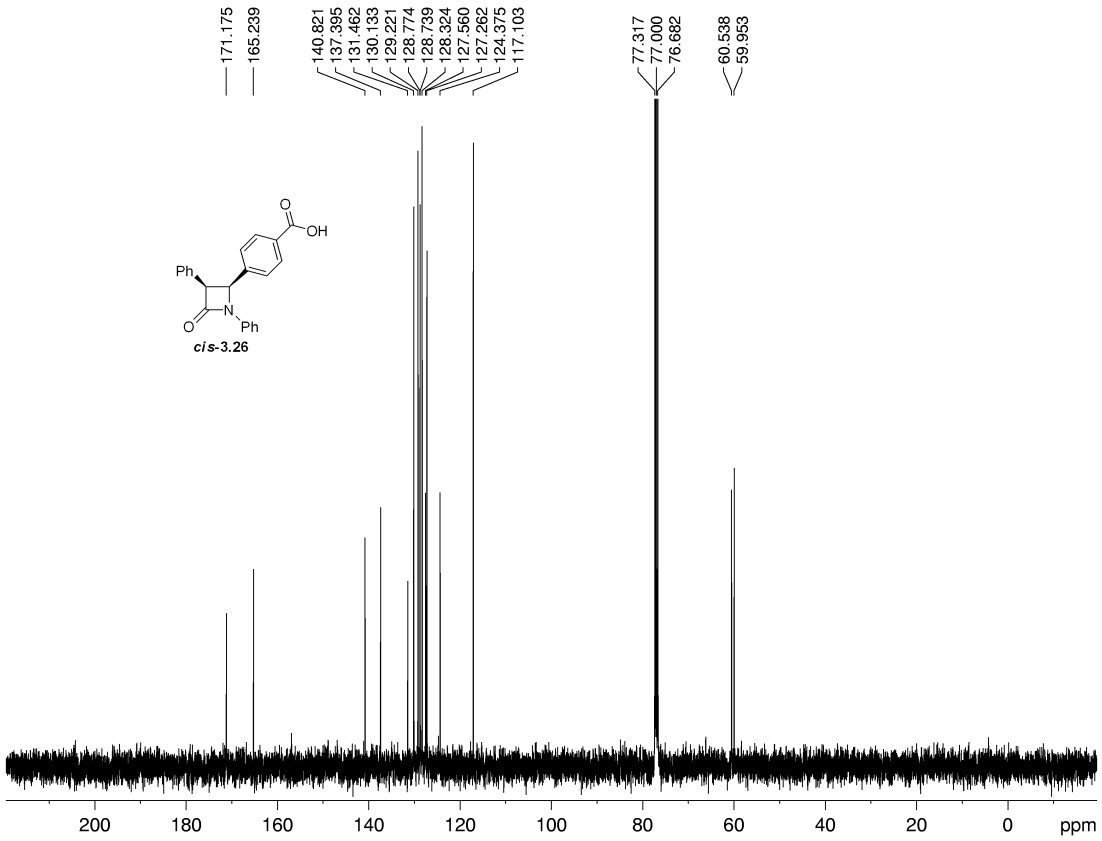
171.175
165.239
140.821
137.395
131.462
130.133
129.221
128.774
128.739
128.324
127.560
127.262
124.375
117.103
77.317
77.000
76.682
60.538
59.953
O
OH
Ph
O
N
Ph
cis-3.26
200
180
160
140
120
100
80
60
40
20
0
ppm

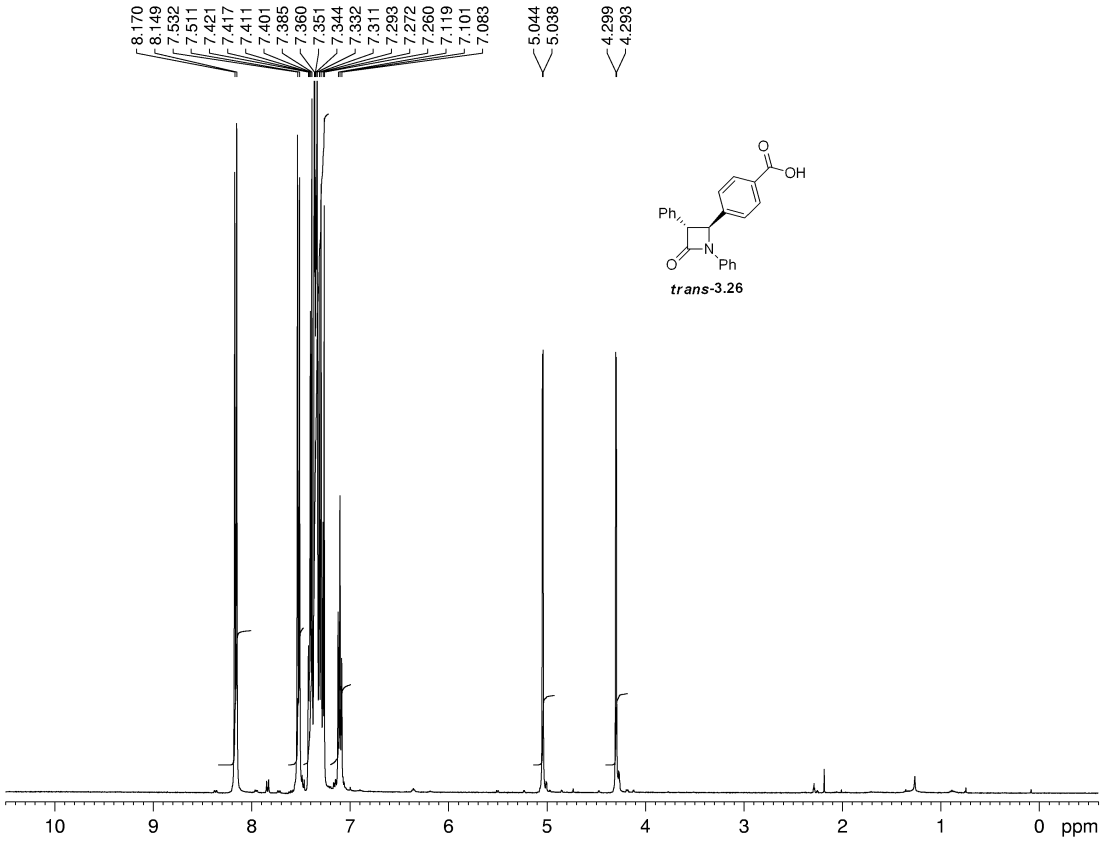

trans-3.26

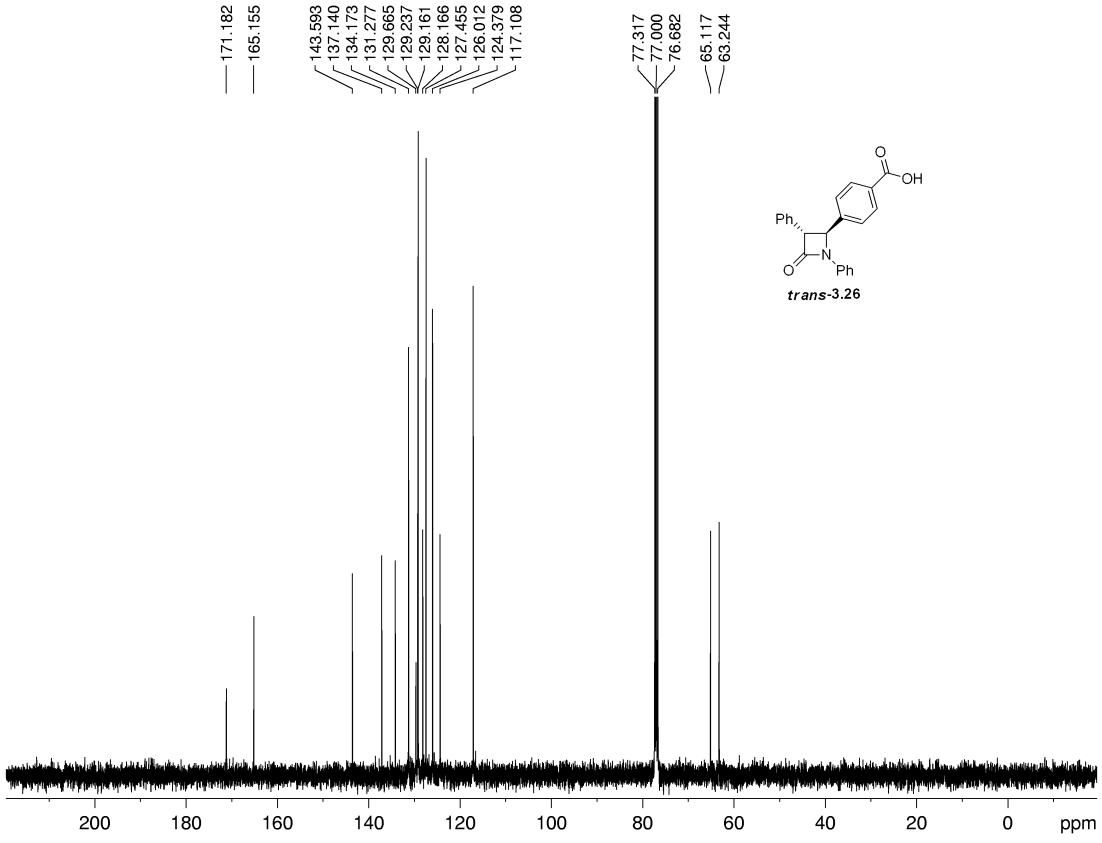

trans-3.26

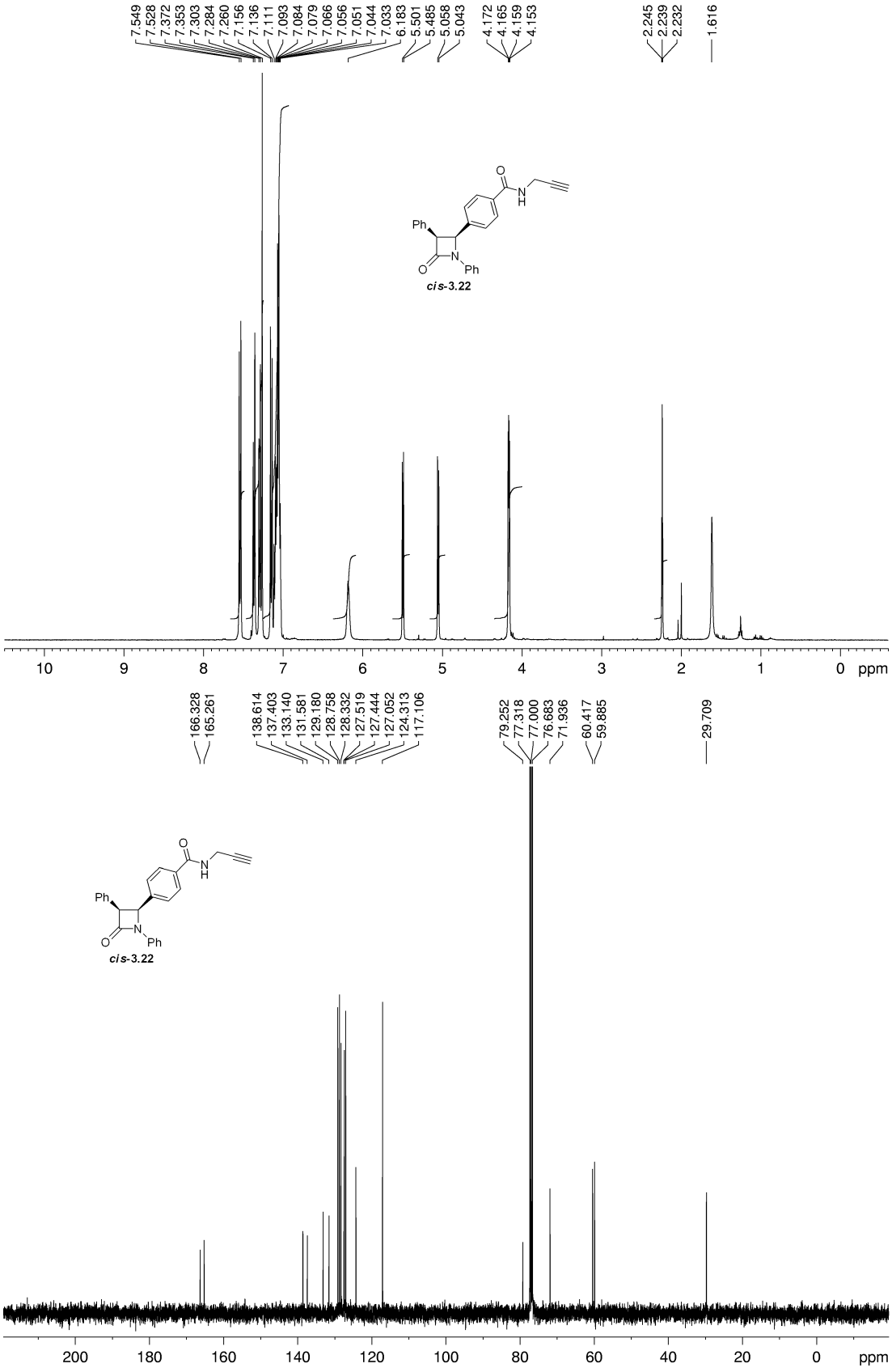
7.549
7.528
7.372
7.353
7.303
7.284
7.260
7.156
7.136
7.111
7.093
7.084
7.079
7.066
7.056
7.051
7.044
7.033
6.183
5.501
5.485
5.058
5.043
4.172
4.165
4.159
4.153
2.245
2.239
2.232
1.616
Ph
N
Ph
O
O
N
H
cis-3.22
10
9
8
7
6
5
4
3
2
1
0
ppm
166.328
165.261
138.614
137.403
133.140
131.581
129.180
128.758
128.332
127.519
127.444
127.052
124.313
117.106
79.252
77.318
77.000
76.683
71.936
60.417
59.885
29.709
200
180
160
140
120
100
80
60
40
20
0
ppm

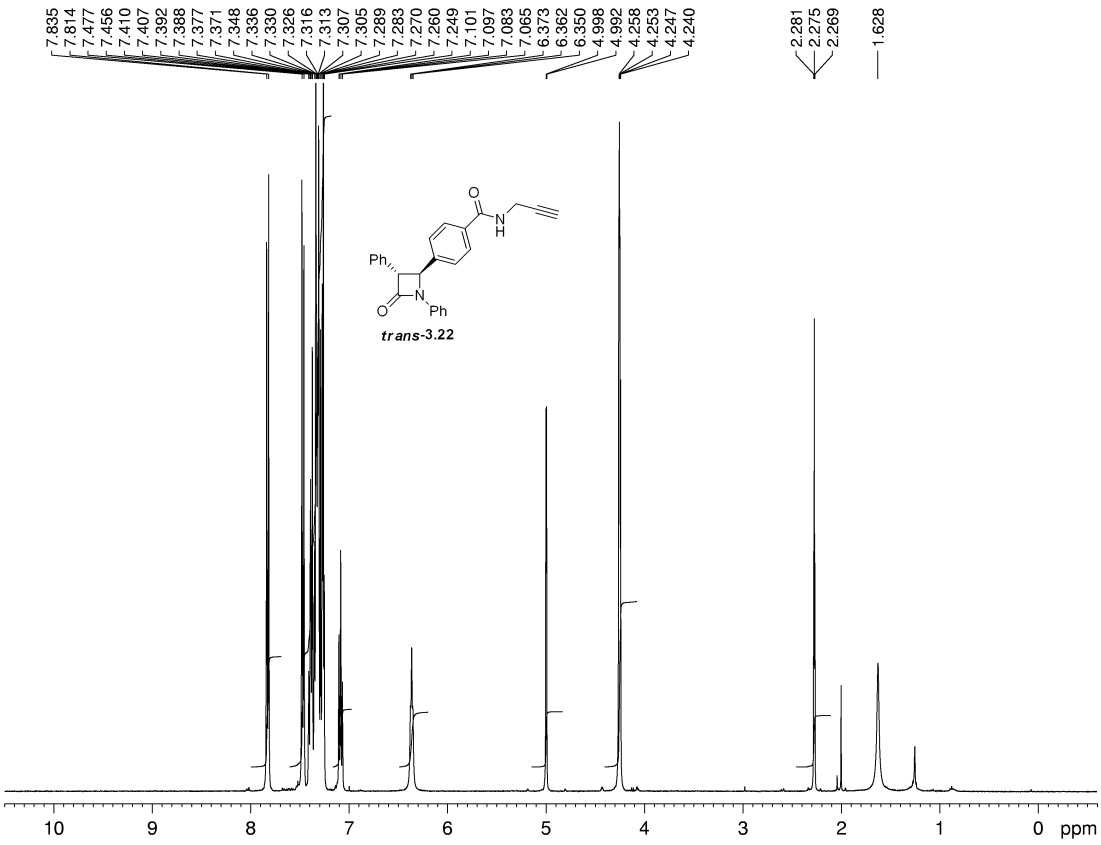
7.835
7.814
7.477
7.456
7.410
7.407
7.392
7.388
7.377
7.371
7.348
7.336
7.330
7.326
7.316
7.313
7.307
7.305
7.289
7.283
7.270
7.260
7.249
7.101
7.097
7.083
7.065
6.373
6.362
6.350
4.998
4.992
4.258
4.253
4.247
4.240
2.281
2.275
2.269
1.628
Ph
N
Ph
O
O
N
H
trans-3.22
10
9
8
7
6
5
4
3
2
1
0
ppm

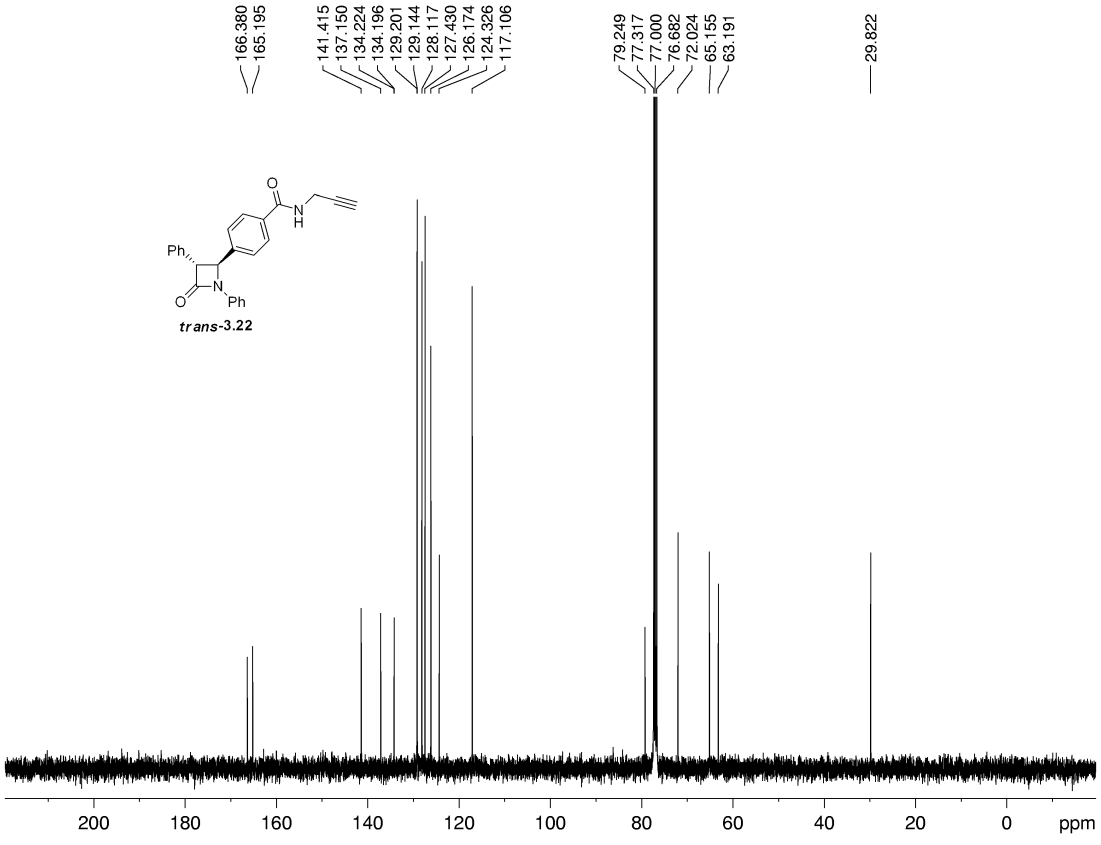
166.380
165.195
141.415
137.150
134.224
134.196
129.201
129.144
128.117
127.430
126.174
124.326
117.106
79.249
77.317
77.000
76.682
72.024
65.155
63.191
29.822
Ph
N
Ph
O
O
N
H
trans-3.22
200
180
160
140
120
100
80
60
40
20
0
ppm

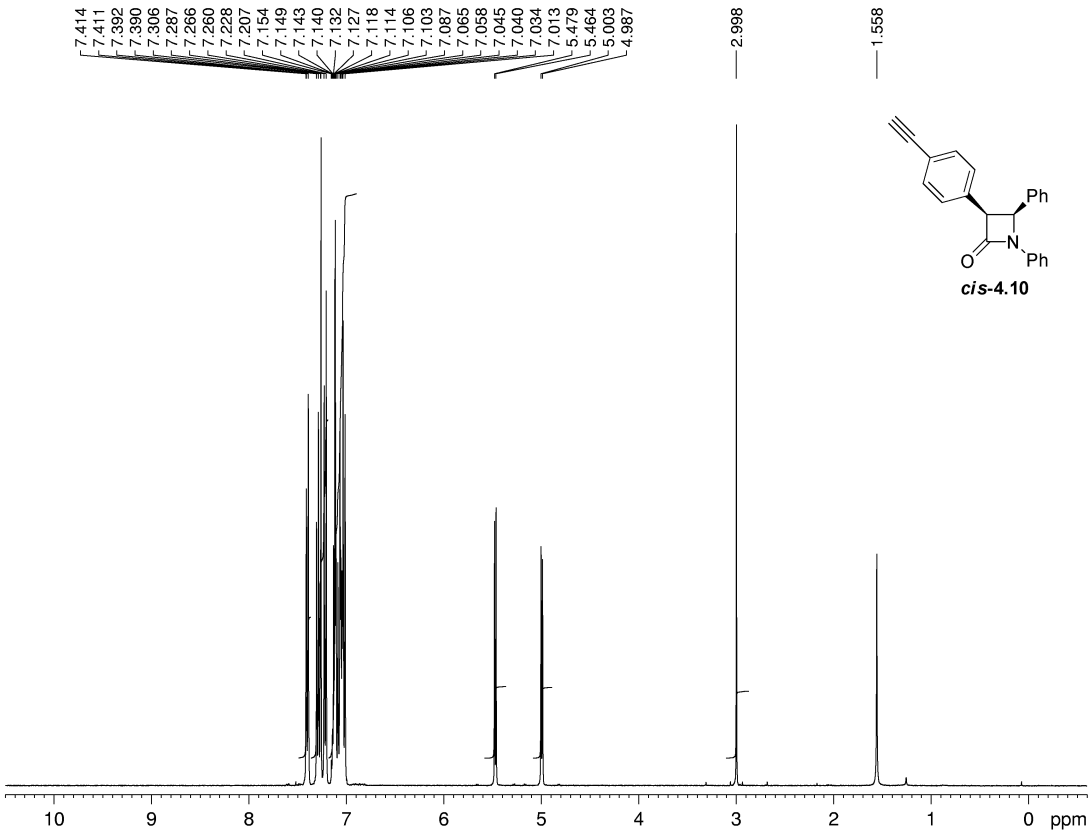
7.414
7.411
7.392
7.390
7.306
7.287
7.266
7.260
7.228
7.207
7.154
7.149
7.143
7.140
7.132
7.127
7.118
7.114
7.106
7.103
7.087
7.065
7.058
7.045
7.040
7.034
7.013
5.479
5.464
5.003
4.987
2.998
1.558
Ph
N
Ph
O
cis-4.10
10
9
8
7
6
5
4
3
2
1
0
ppm

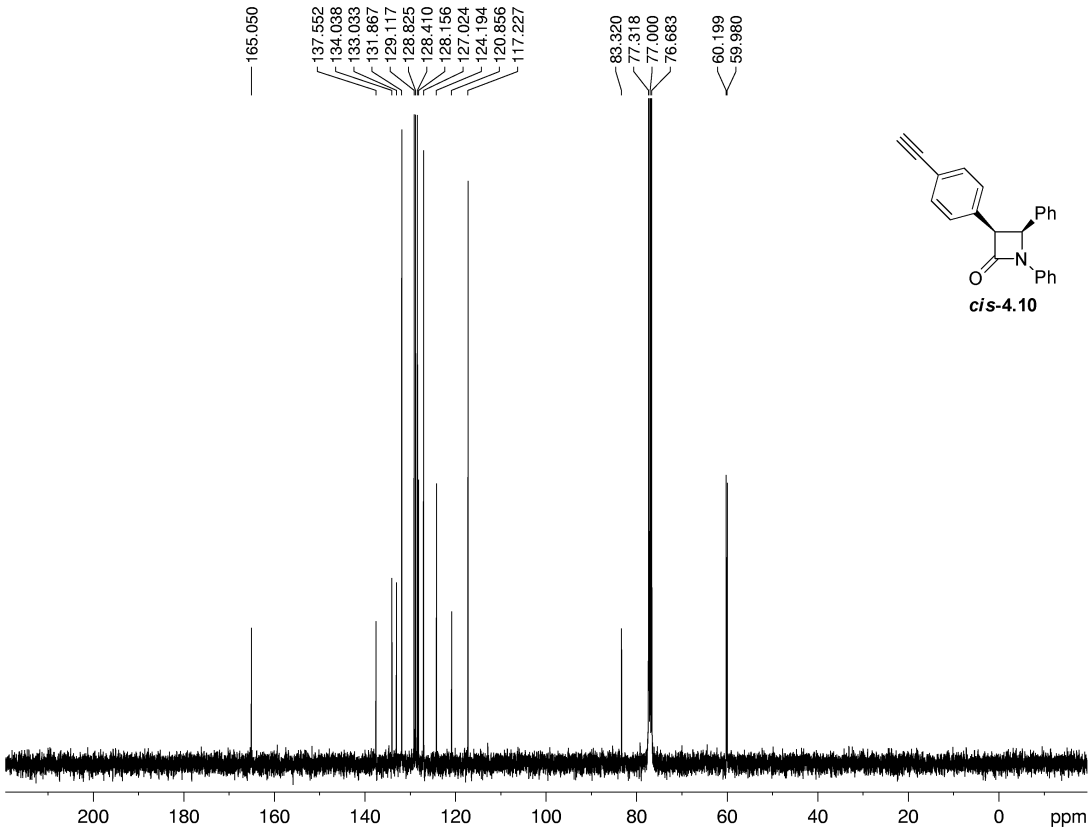
165.050
137.552
134.038
133.033
131.867
129.117
128.825
128.410
128.156
127.024
124.194
120.856
117.227
83.320
77.318
77.000
76.683
60.199
59.980
Ph
N
Ph
O
cis-4.10
200
180
160
140
120
100
80
60
40
20
0
ppm

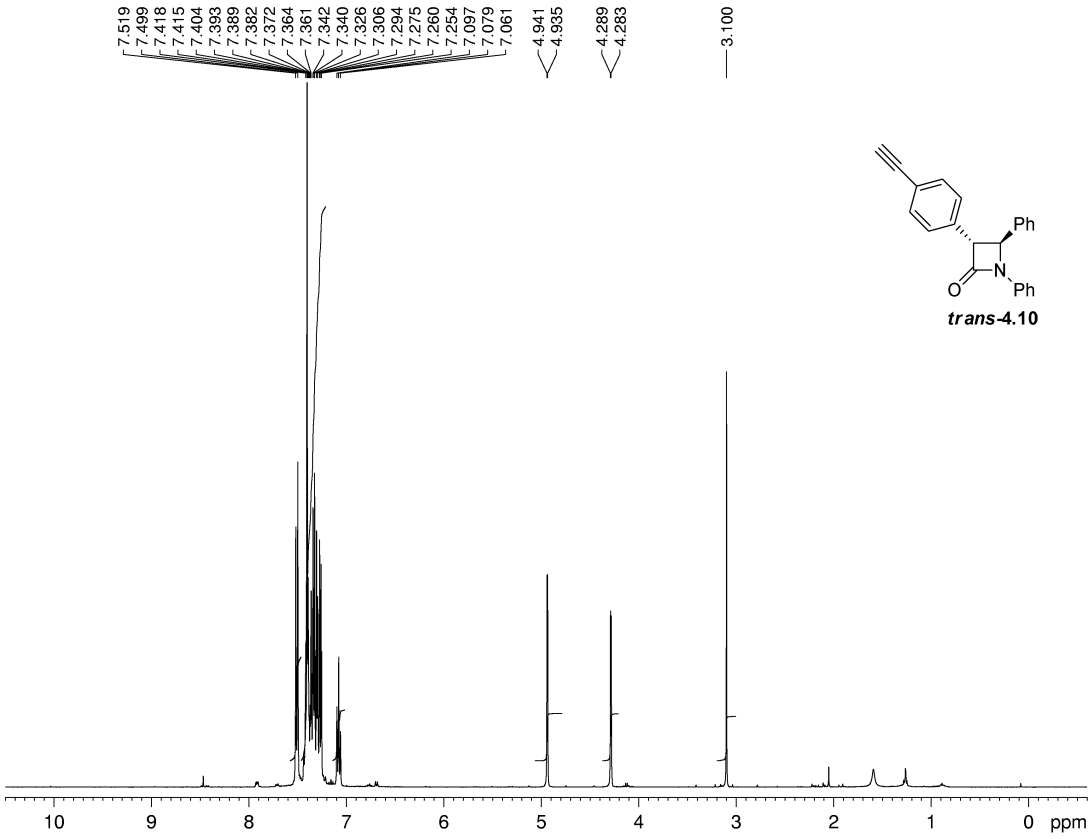

***trans*-4.10**

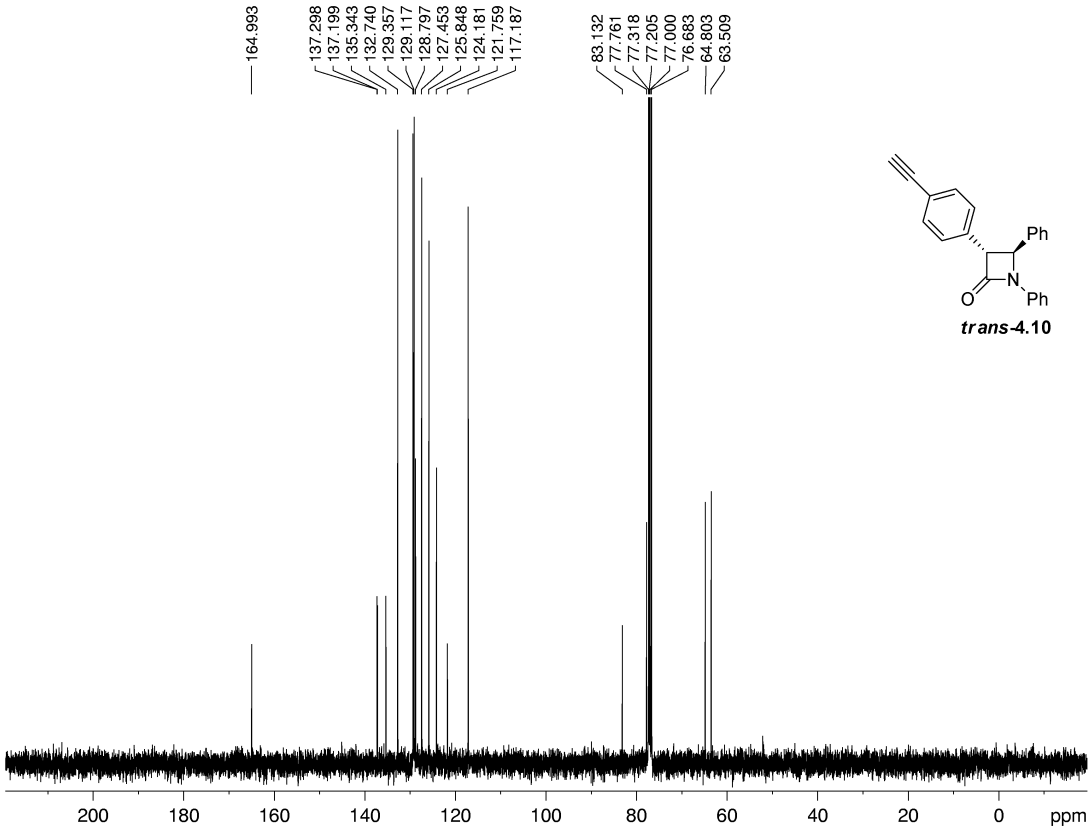

***trans*-4.10**

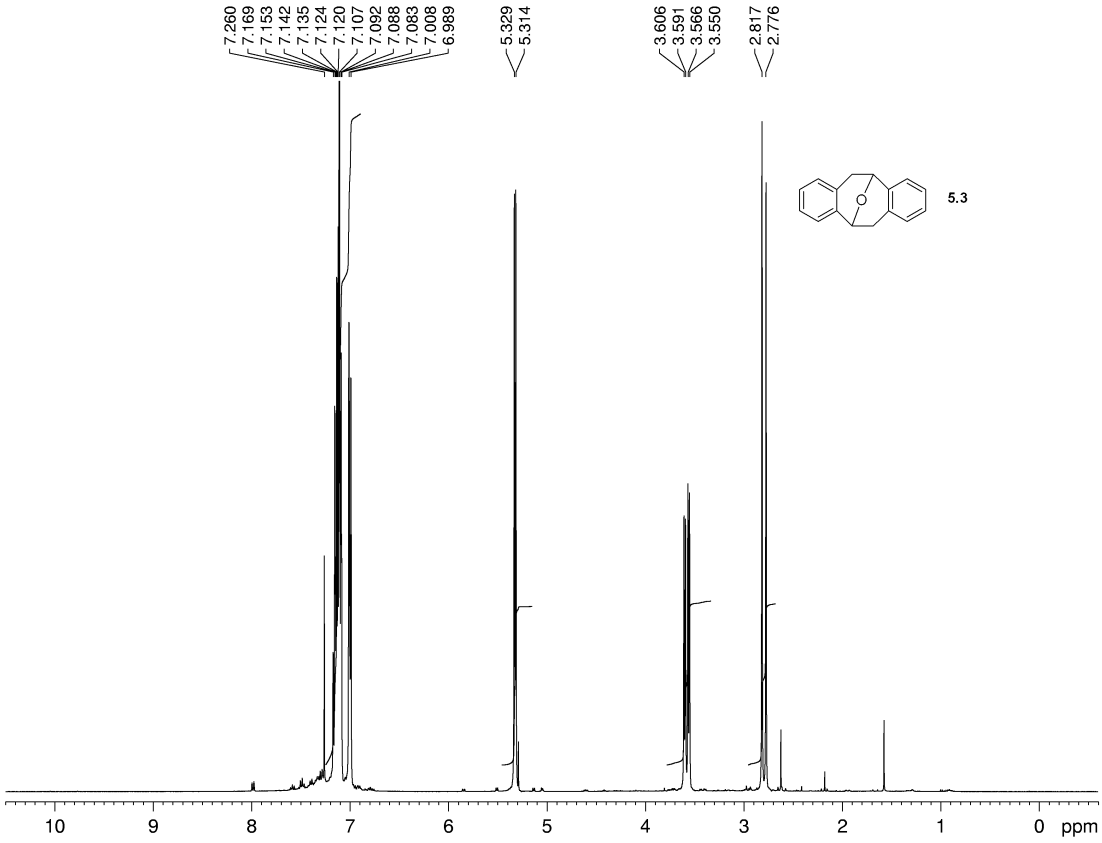
7.260
7.169
7.153
7.142
7.135
7.124
7.120
7.107
7.092
7.088
7.083
7.008
6.989
5.329
5.314
3.606
3.591
3.566
3.550
2.817
2.776
5.3
10
9
8
7
6
5
4
3
2
1
0
ppm

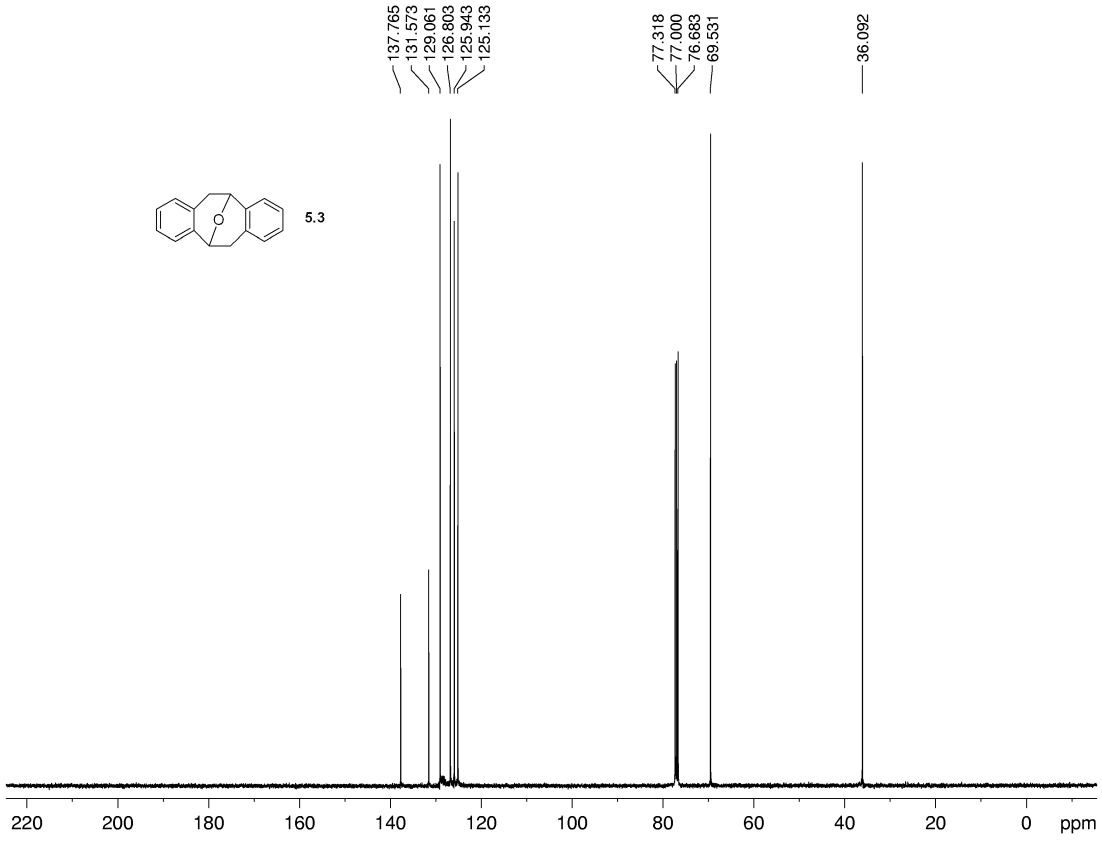
137.765
131.573
129.061
126.803
125.943
125.133
77.318
77.000
76.683
69.531
36.092
5.3
220
200
180
160
140
120
100
80
60
40
20
0
ppm

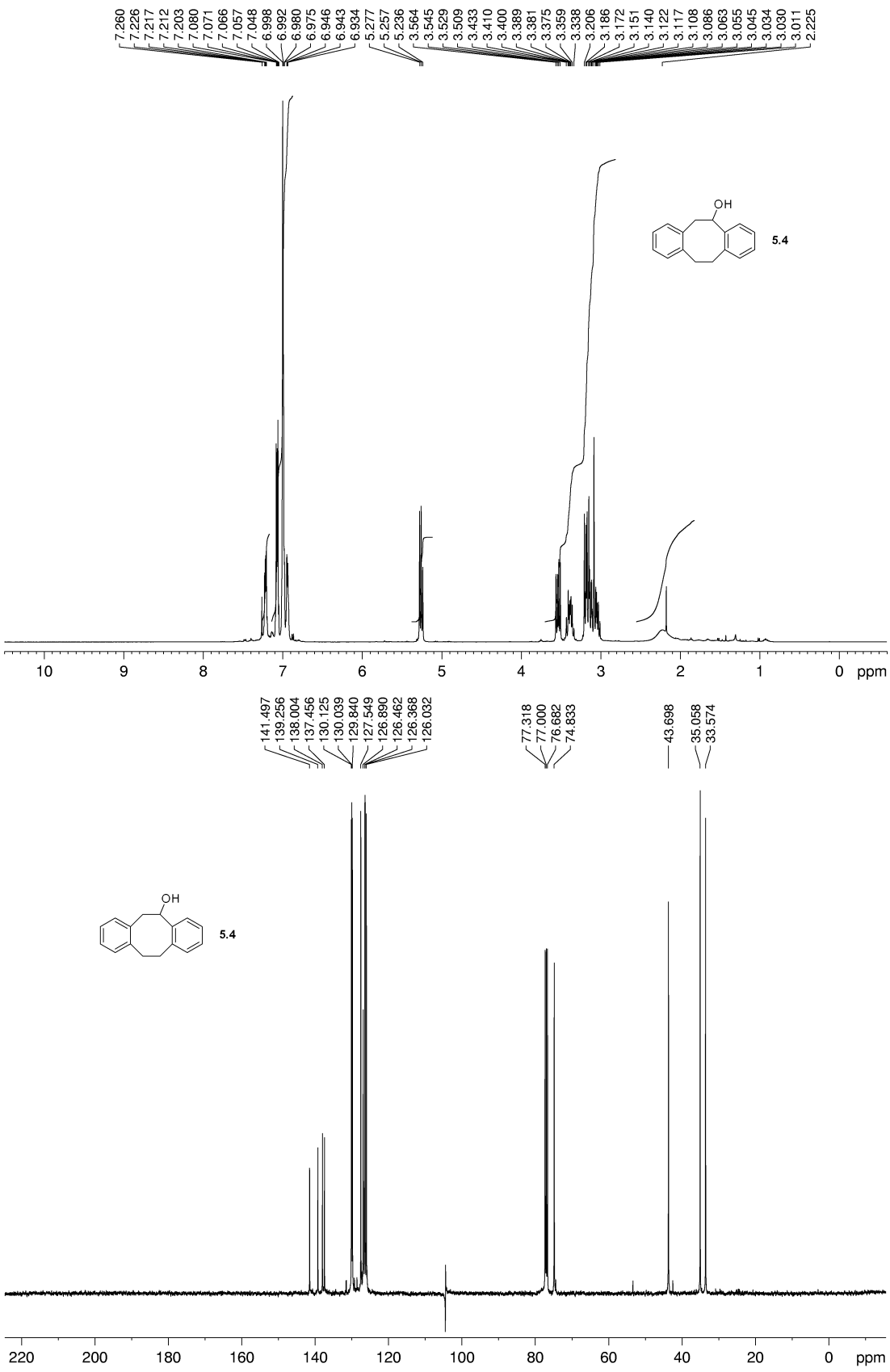
7.260
7.226
7.217
7.212
7.203
7.080
7.071
7.066
7.057
7.048
6.998
6.992
6.980
6.975
6.946
6.943
6.934
5.277
5.257
5.236
3.564
3.545
3.529
3.509
3.433
3.410
3.400
3.389
3.381
3.375
3.359
3.338
3.206
3.186
3.172
3.151
3.140
3.122
3.117
3.108
3.086
3.063
3.055
3.045
3.034
3.030
3.011
2.225
OH
5.4
10
9
8
7
6
5
4
3
2
1
0
ppm
141.497
139.256
138.004
137.456
130.125
130.039
129.840
127.549
126.890
126.462
126.368
126.032
77.318
77.000
76.682
74.833
43.698
35.058
33.574
OH
5.4
220
200
180
160
140
120
100
80
60
40
20
0
ppm

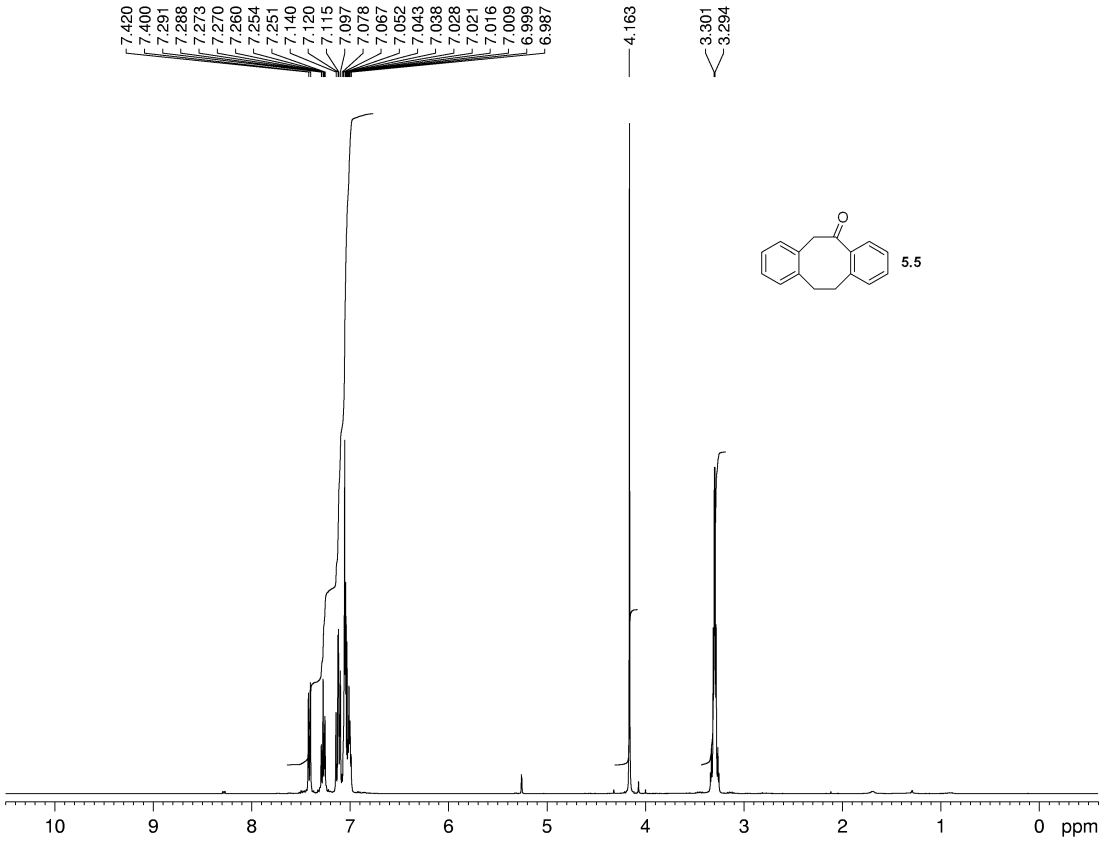
7.420
7.400
7.291
7.288
7.273
7.270
7.260
7.254
7.251
7.140
7.120
7.115
7.097
7.078
7.067
7.052
7.043
7.038
7.028
7.021
7.016
7.009
6.999
6.987
4.163
3.301
3.294
5.5
10
9
8
7
6
5
4
3
2
1
0
ppm

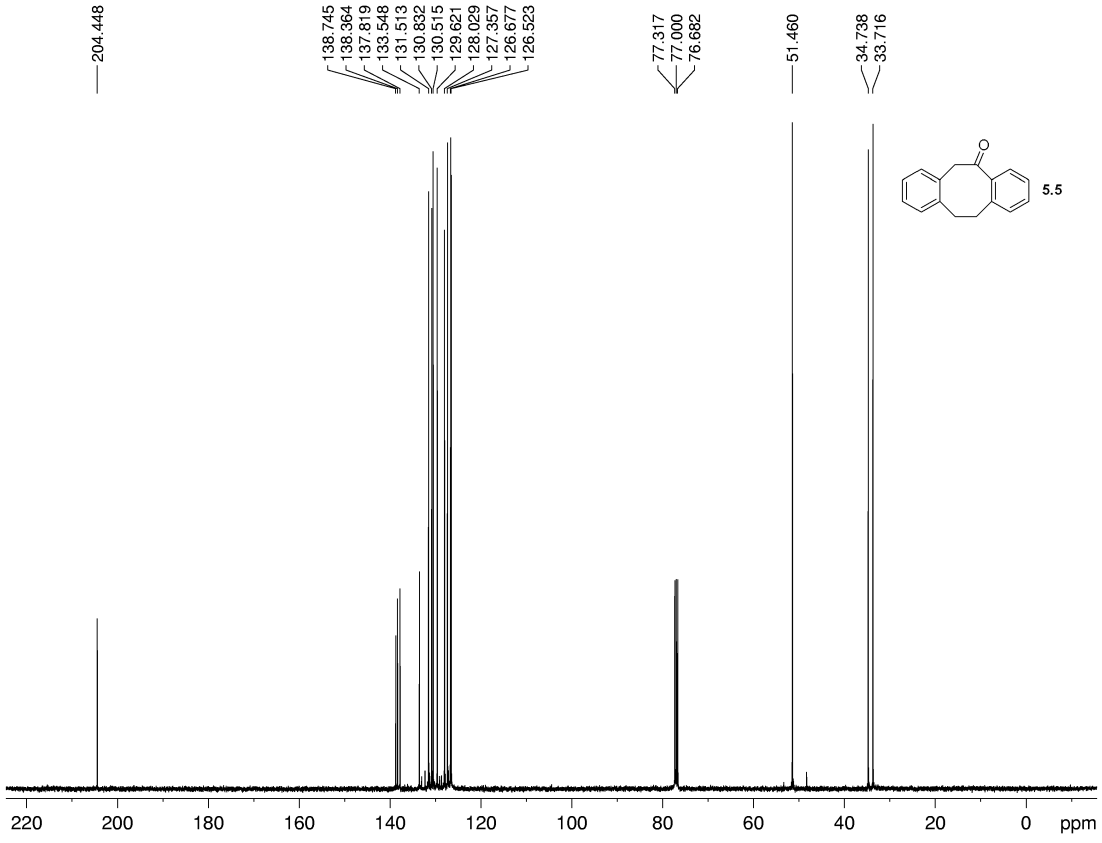
204.448
138.745
138.364
137.819
133.548
131.513
130.832
130.515
129.621
128.029
127.357
126.677
126.523
77.317
77.000
76.682
51.460
34.738
33.716
5.5
220
200
180
160
140
120
100
80
60
40
20
0
ppm

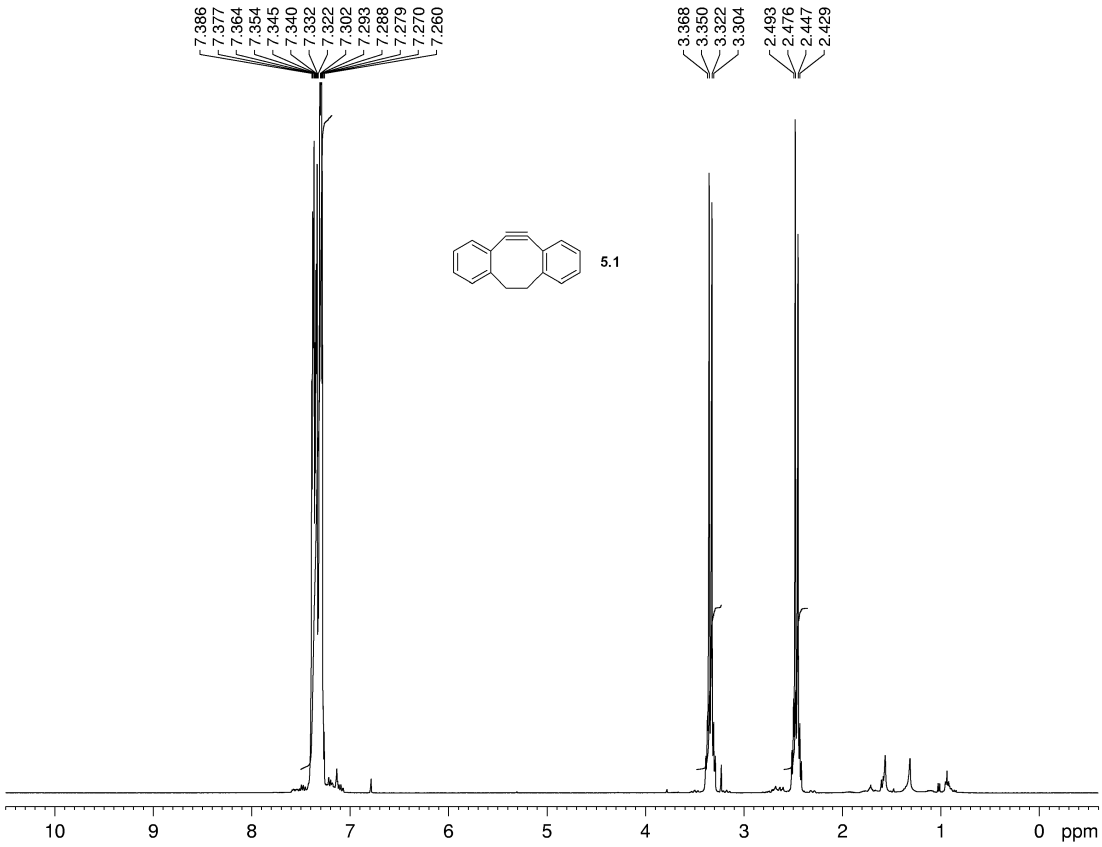
7.386
7.377
7.364
7.354
7.345
7.340
7.332
7.322
7.302
7.293
7.288
7.279
7.270
7.260
3.368
3.350
3.322
3.304
2.493
2.476
2.447
2.429
5.1
10
9
8
7
6
5
4
3
2
1
0
ppm

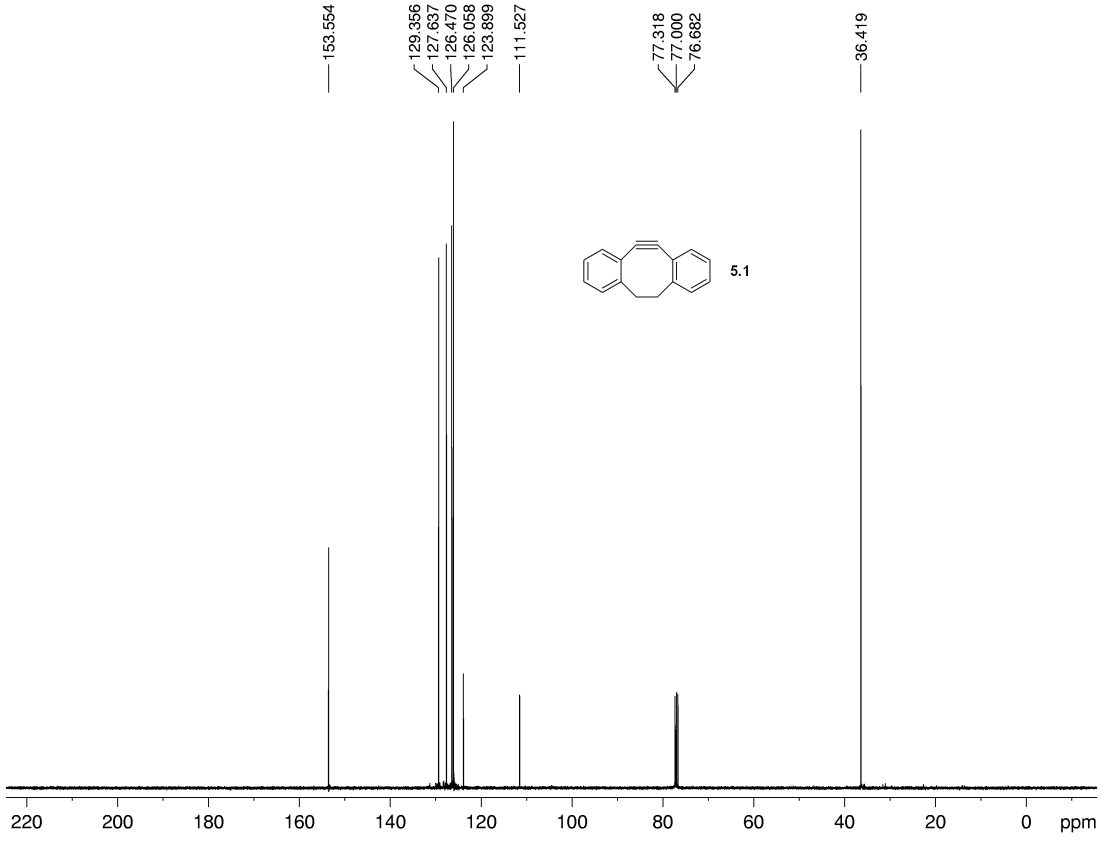
153.554
129.356
127.637
126.470
126.058
123.899
111.527
77.318
77.000
76.682
36.419
5.1
220
200
180
160
140
120
100
80
60
40
20
0
ppm

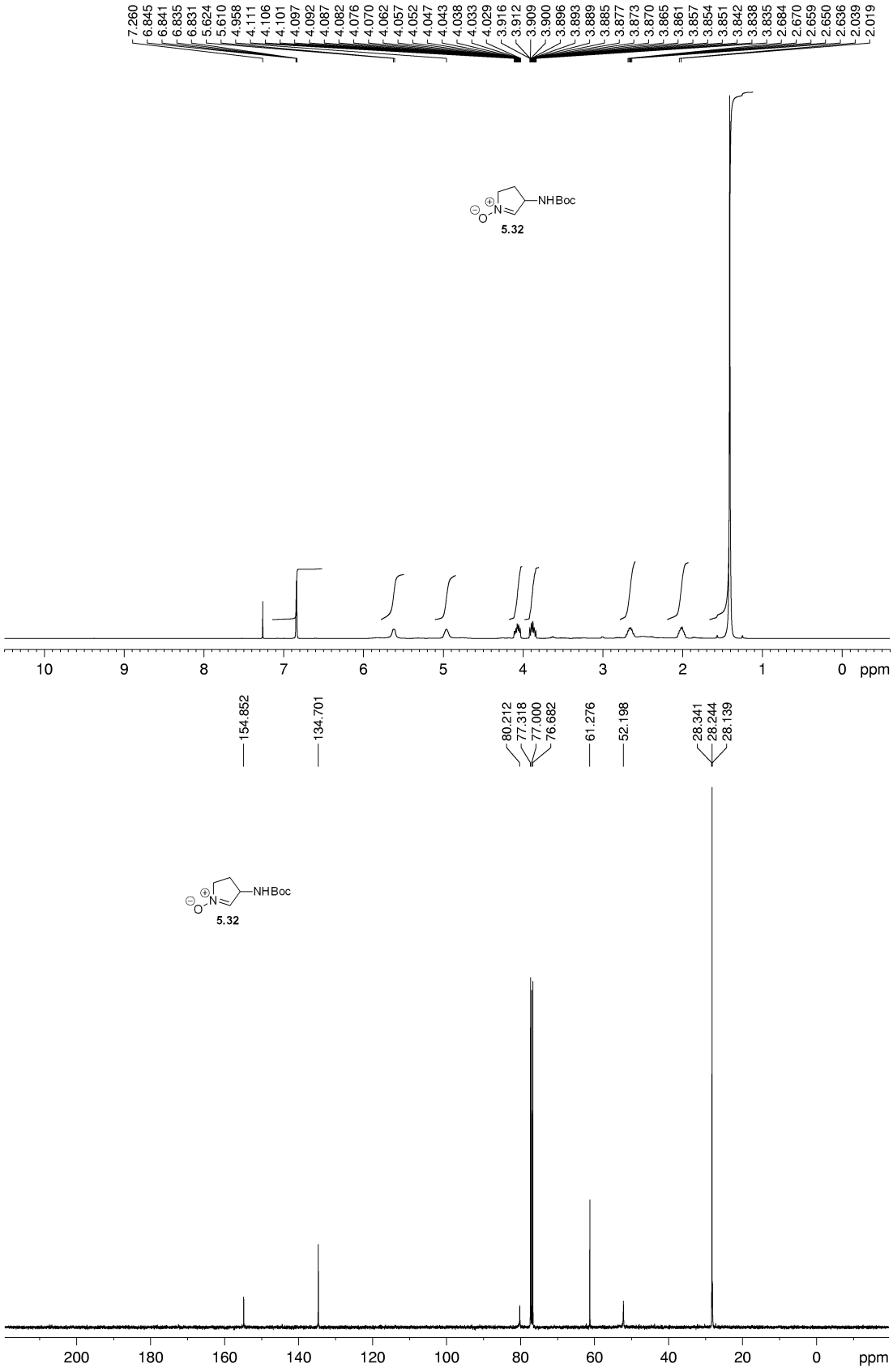
7.260
6.845
6.841
6.835
6.831
6.624
5.610
4.958
4.111
4.106
4.101
4.097
4.092
4.087
4.082
4.076
4.070
4.062
4.057
4.052
4.047
4.043
4.038
4.033
4.029
3.916
3.912
3.909
3.900
3.896
3.893
3.889
3.885
3.877
3.873
3.870
3.865
3.861
3.857
3.854
3.851
3.842
3.838
3.835
2.684
2.670
2.659
2.650
2.636
2.039
2.019
NHBoc
5.32
10
9
8
7
6
5
4
3
2
1
0
ppm
154.852
134.701
80.212
77.318
77.000
76.682
61.276
52.198
28.341
28.244
28.139
NHBoc
5.32
200
180
160
140
120
100
80
60
40
20
0
ppm

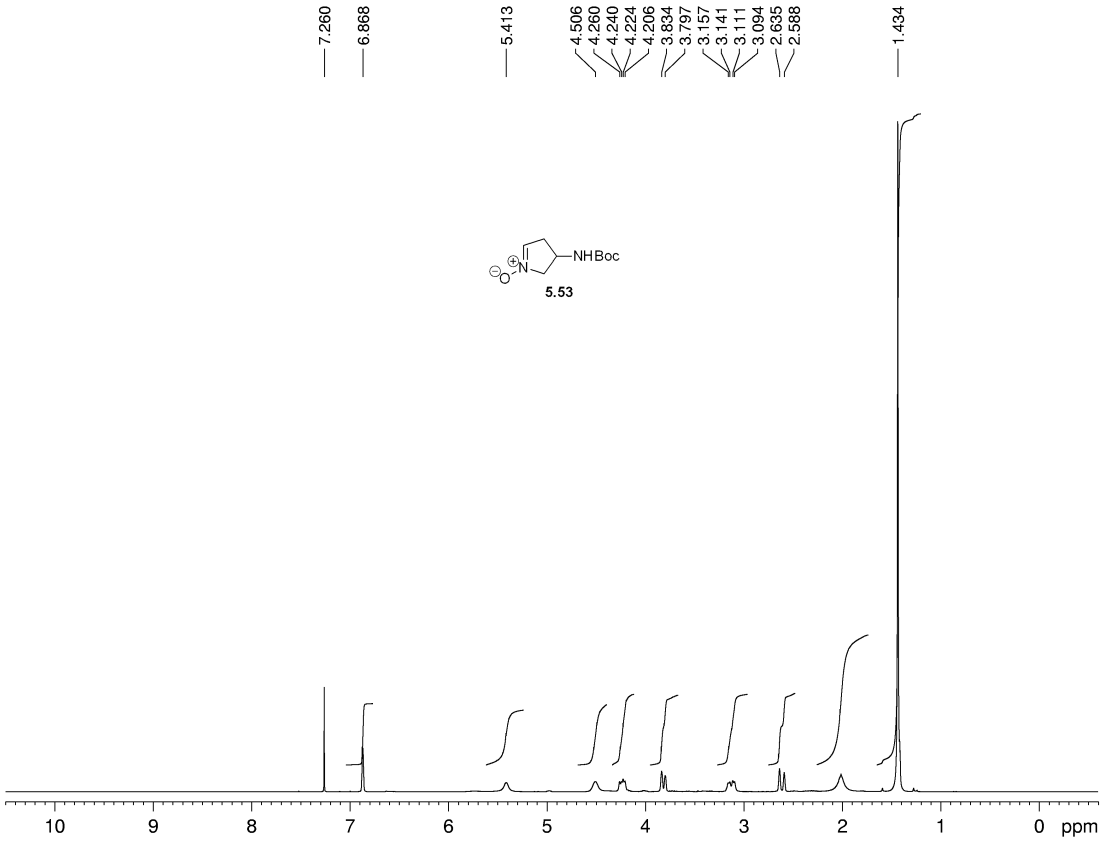
7.260
6.868
5.413
4.506
4.260
4.240
4.224
4.206
3.834
3.797
3.157
3.141
3.111
3.094
2.635
2.588
1.434
NHBoc
5.53
10
9
8
7
6
5
4
3
2
1
0
ppm

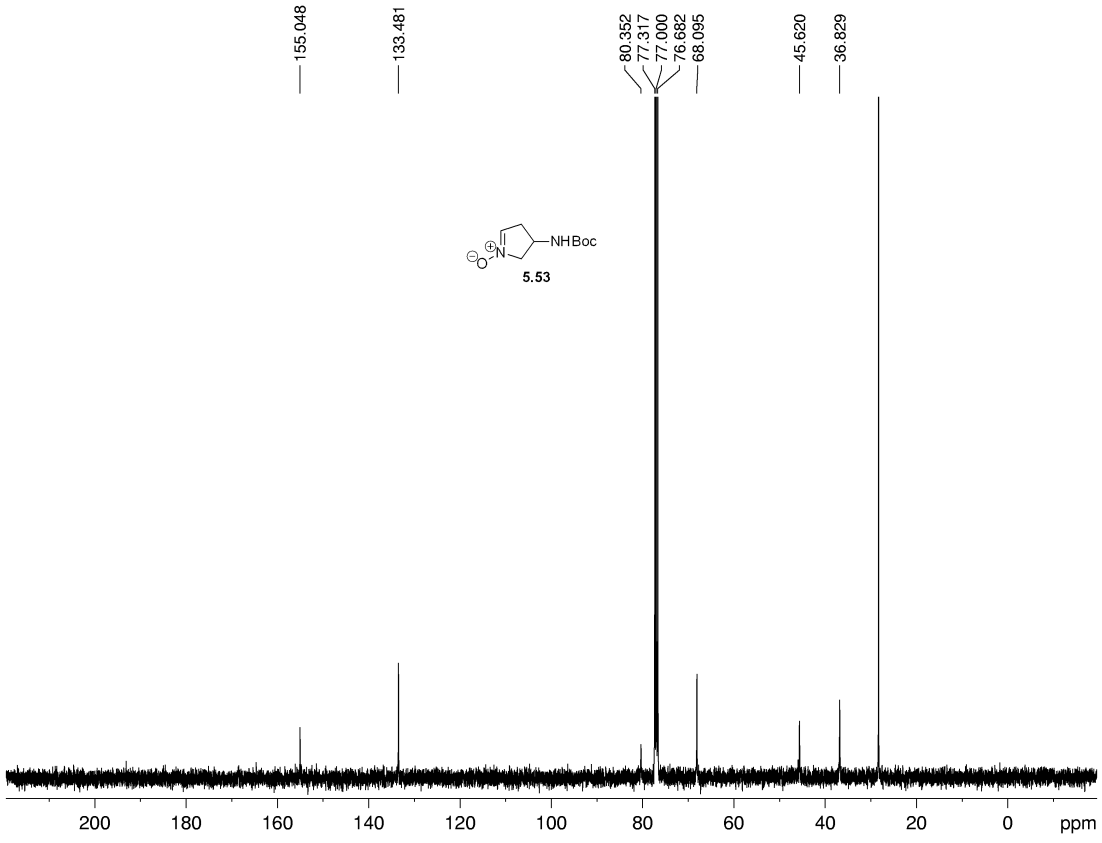
155.048
133.481
80.352
77.317
77.000
76.682
68.095
45.620
36.829
NHBoc
5.53
200
180
160
140
120
100
80
60
40
20
0
ppm

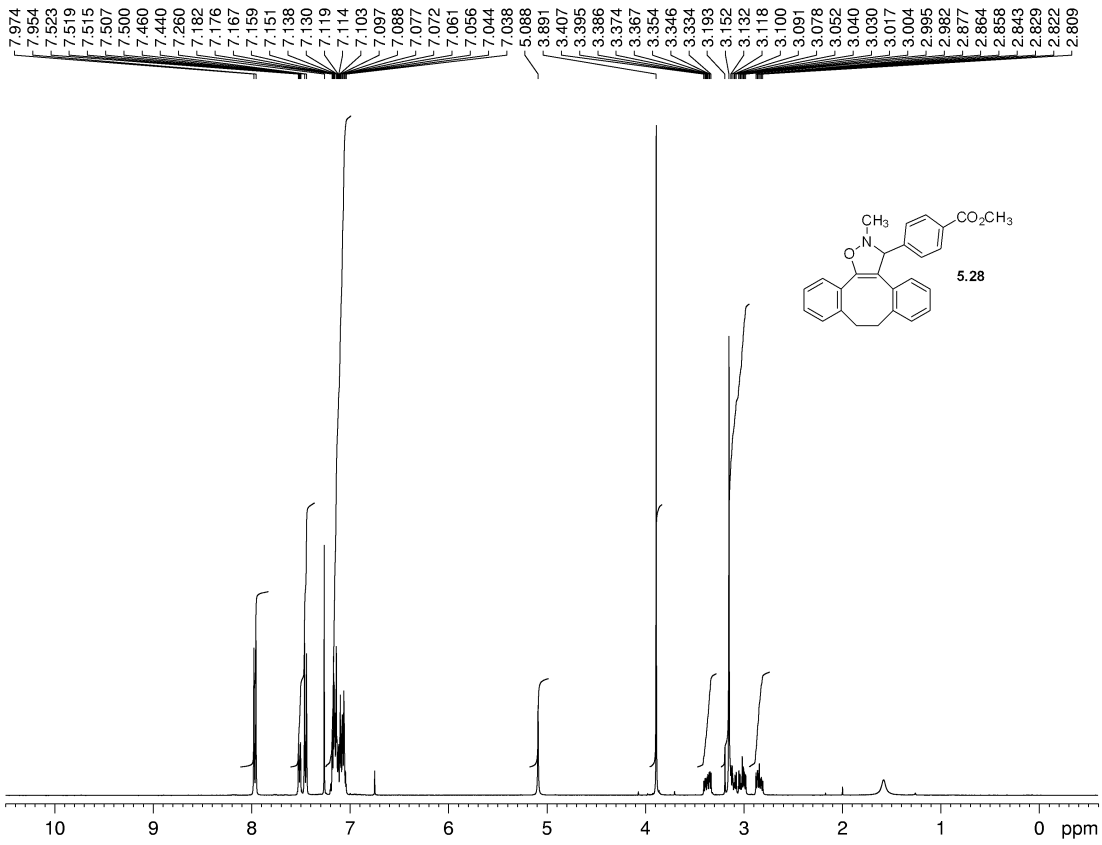
7.974
7.954
7.523
7.519
7.515
7.507
7.500
7.460
7.440
7.260
7.182
7.176
7.167
7.159
7.151
7.138
7.130
7.119
7.114
7.103
7.097
7.088
7.077
7.072
7.061
7.056
7.044
7.038
5.088
3.891
3.407
3.395
3.386
3.374
3.367
3.354
3.346
3.334
3.193
3.152
3.132
3.118
3.100
3.091
3.078
3.052
3.040
3.030
3.017
3.004
2.995
2.982
2.877
2.864
2.858
2.843
2.829
2.822
2.809
CH3
N
O
CO2CH3
5.28
10
9
8
7
6
5
4
3
2
1
0
ppm

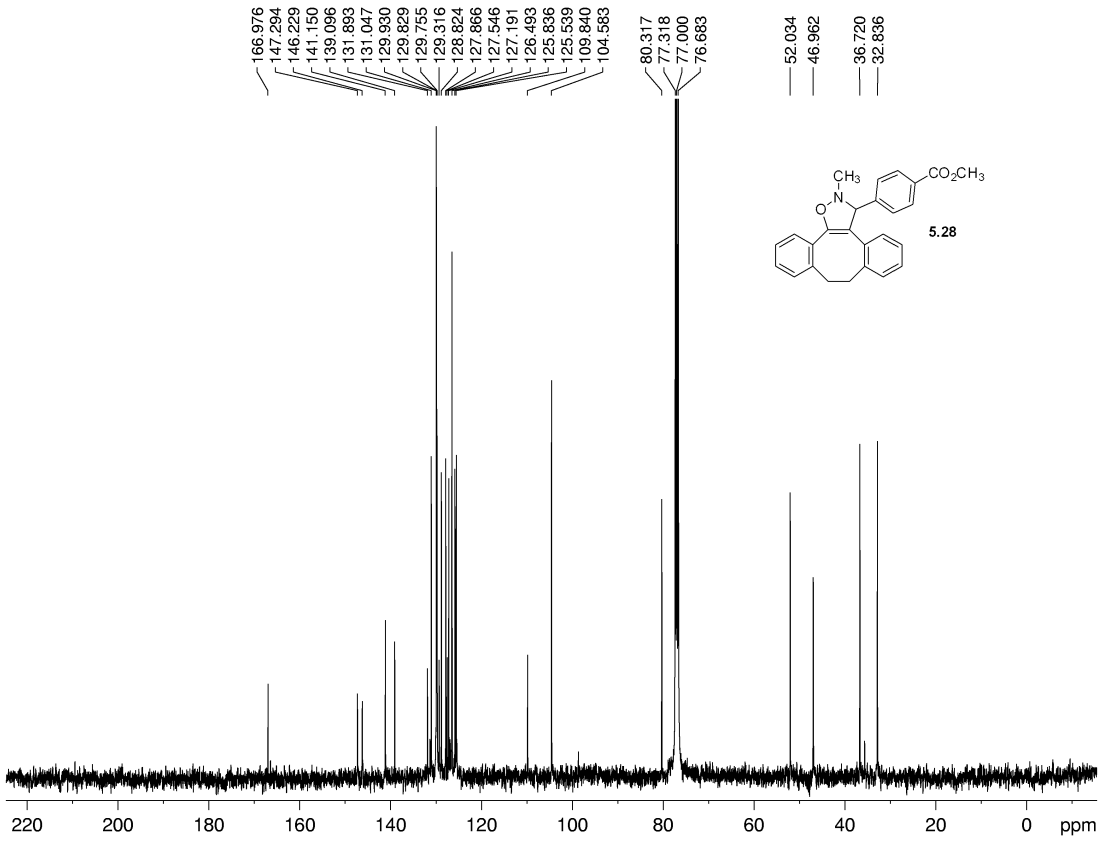
166.976
147.294
146.229
141.150
139.096
131.893
131.047
129.930
129.829
129.755
129.316
128.824
127.866
127.546
127.191
126.493
125.836
125.539
109.840
104.583
80.317
77.318
77.000
76.683
52.034
46.962
36.720
32.836
CH3
N
O
CO2CH3
5.28
220
200
180
160
140
120
100
80
60
40
20
0
ppm

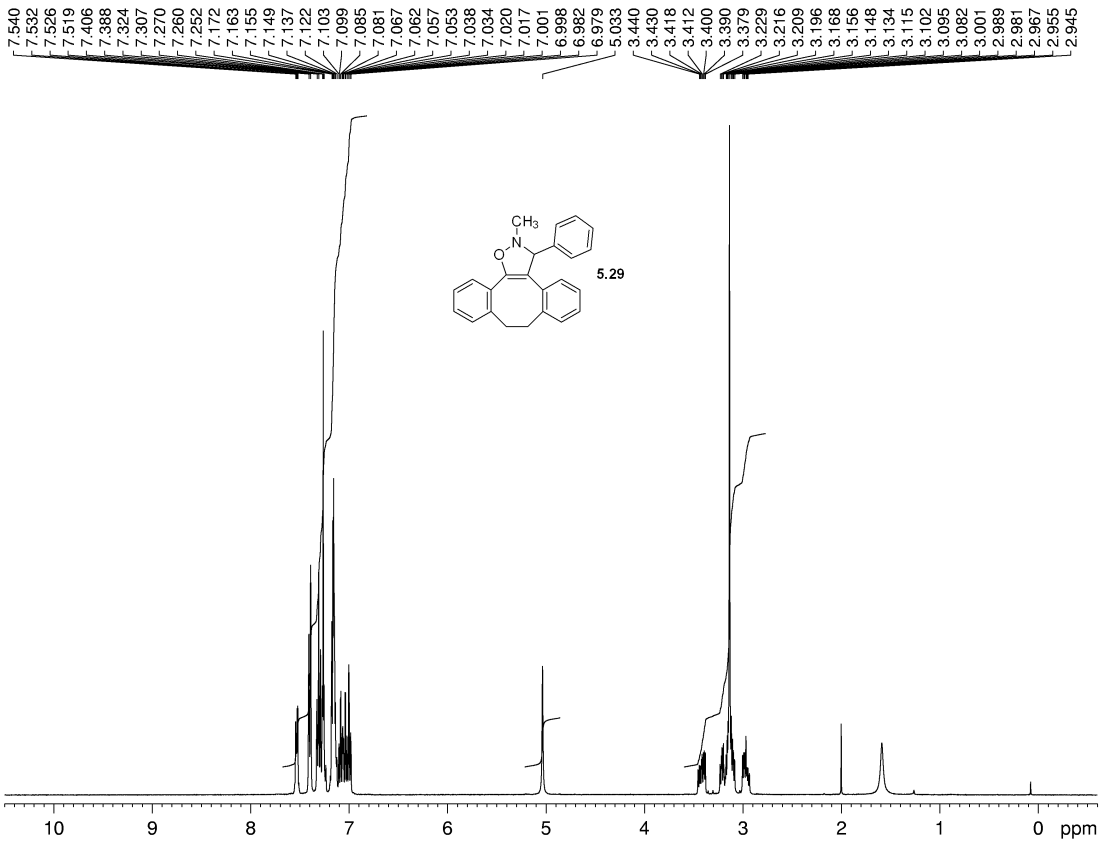
7.540
7.532
7.526
7.519
7.406
7.388
7.324
7.307
7.270
7.260
7.252
7.172
7.163
7.155
7.149
7.137
7.122
7.103
7.099
7.085
7.081
7.067
7.062
7.057
7.053
7.038
7.034
7.020
7.017
7.001
6.998
6.982
6.979
5.033
3.440
3.430
3.418
3.412
3.400
3.390
3.379
3.229
3.216
3.209
3.196
3.168
3.156
3.148
3.134
3.115
3.102
3.095
3.082
3.001
2.989
2.981
2.967
2.955
2.945
CH3
N
O
5.29
10
9
8
7
6
5
4
3
2
1
0
ppm

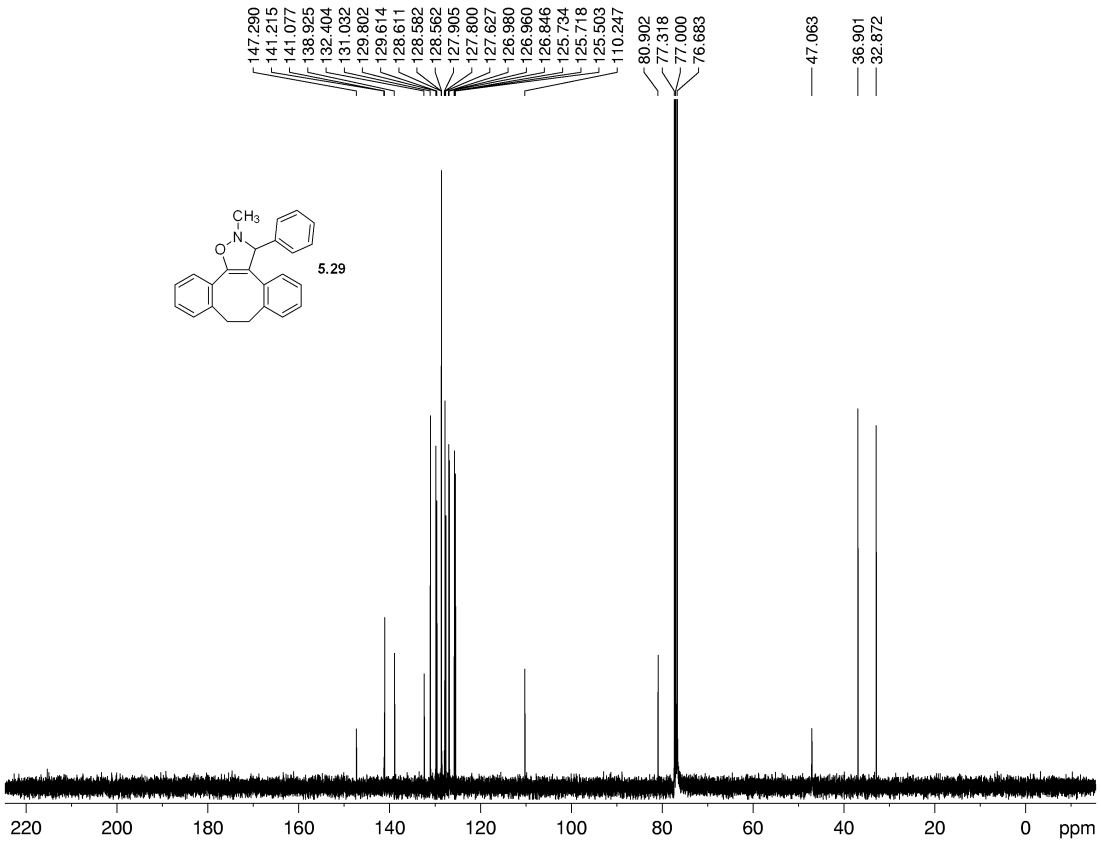
147.290
141.215
141.077
138.925
132.404
131.032
129.802
129.614
128.611
128.582
128.562
127.905
127.800
127.627
126.980
126.960
126.846
125.734
125.718
125.503
110.247
80.902
77.318
77.000
76.683
47.063
36.901
32.872
CH3
N
O
5.29
220
200
180
160
140
120
100
80
60
40
20
0
ppm

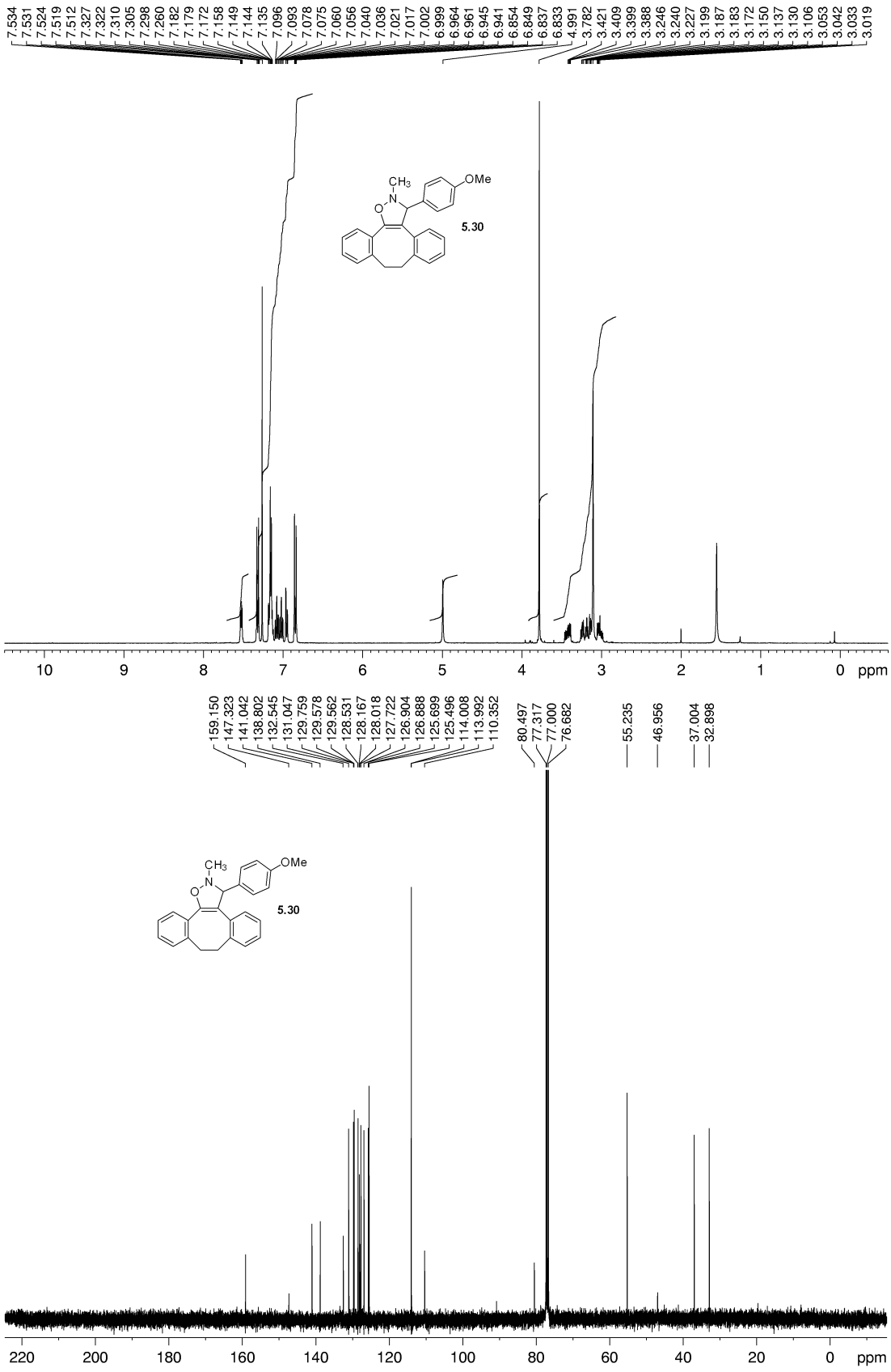
7.534
7.531
7.524
7.519
7.512
7.327
7.322
7.310
7.305
7.298
7.260
7.182
7.179
7.172
7.158
7.149
7.144
7.135
7.096
7.093
7.078
7.075
7.060
7.056
7.040
7.036
7.021
7.017
7.002
6.999
6.964
6.961
6.945
6.941
6.854
6.849
6.837
6.833
4.991
3.782
3.421
3.409
3.399
3.388
3.246
3.240
3.227
3.199
3.187
3.183
3.172
3.150
3.137
3.130
3.106
3.053
3.042
3.033
3.019
CH3
N
O
OMe
5.30
10
9
8
7
6
5
4
3
2
1
0
ppm
159.150
147.323
141.042
138.802
132.545
131.047
129.759
129.578
129.562
128.531
128.167
128.018
127.722
126.904
126.888
125.699
125.496
114.008
113.992
110.352
80.497
77.317
77.000
76.682
55.235
46.956
37.004
32.898
CH3
N
O
OMe
5.30
220
200
180
160
140
120
100
80
60
40
20
0
ppm

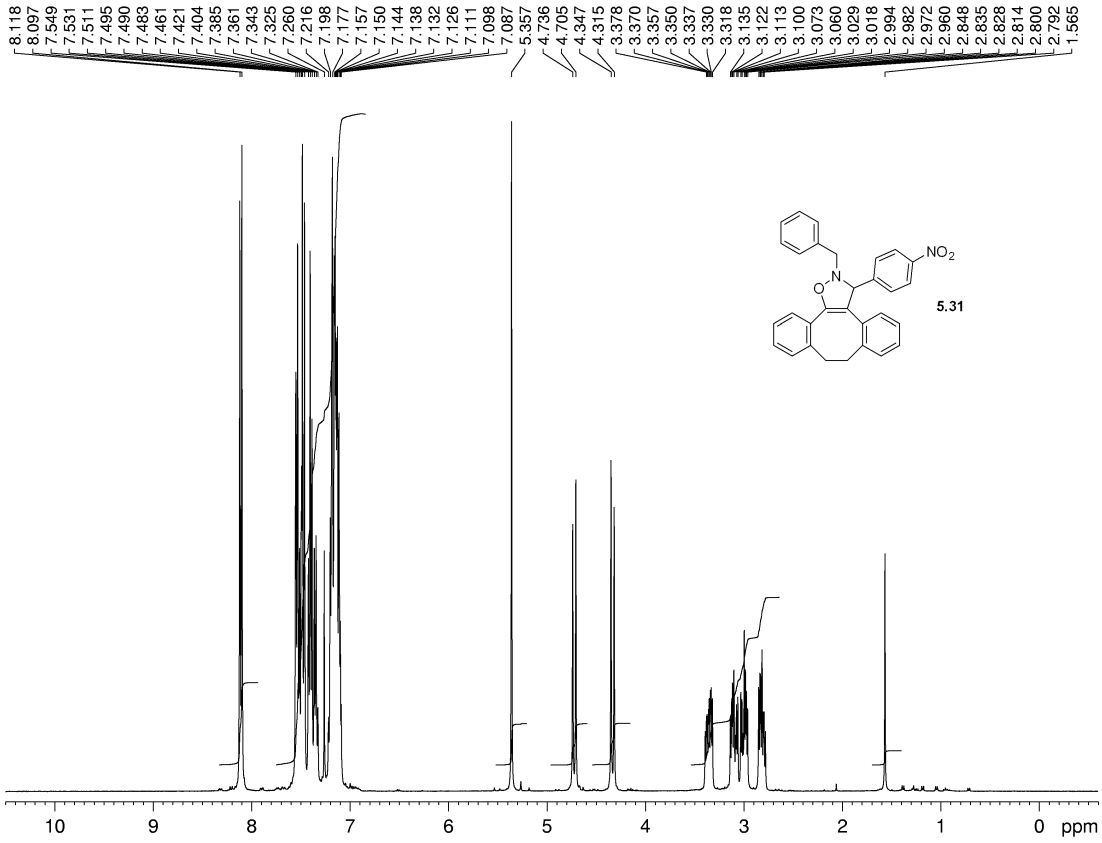
8.118
8.097
7.549
7.531
7.511
7.495
7.490
7.483
7.461
7.421
7.404
7.385
7.361
7.343
7.325
7.260
7.216
7.198
7.177
7.157
7.150
7.144
7.138
7.132
7.126
7.111
7.098
7.087
5.357
4.736
4.705
4.347
4.315
3.378
3.370
3.357
3.350
3.337
3.330
3.318
3.135
3.122
3.113
3.100
3.073
3.060
3.029
3.018
2.994
2.982
2.972
2.960
2.848
2.835
2.828
2.814
2.800
2.792
1.565
NO2
5.31
10
9
8
7
6
5
4
3
2
1
0
ppm

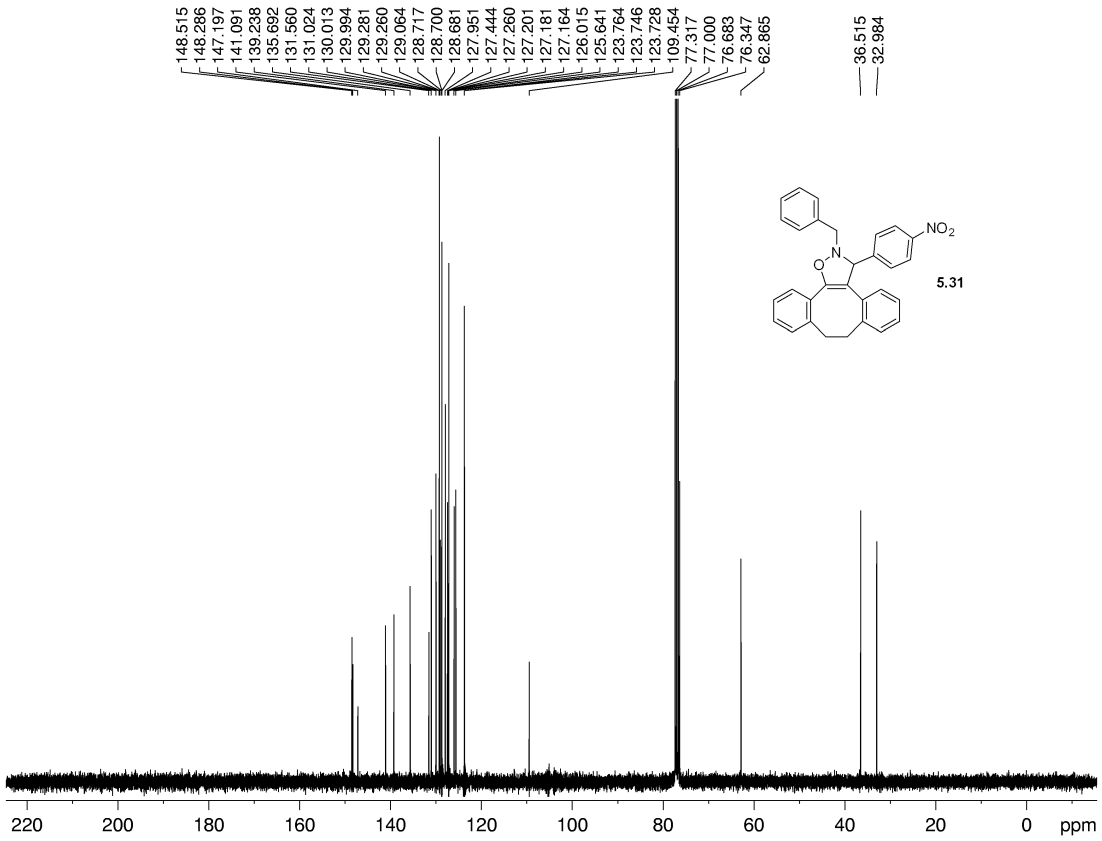
148.515
148.286
147.197
141.091
139.238
135.692
131.560
131.024
130.013
129.994
129.281
129.260
129.064
128.717
128.700
128.681
127.951
127.444
127.260
127.201
127.181
127.164
126.015
125.641
123.764
123.746
123.728
109.454
77.317
77.000
76.683
76.347
62.865
36.515
32.984
NO2
5.31
220
200
180
160
140
120
100
80
60
40
20
0
ppm

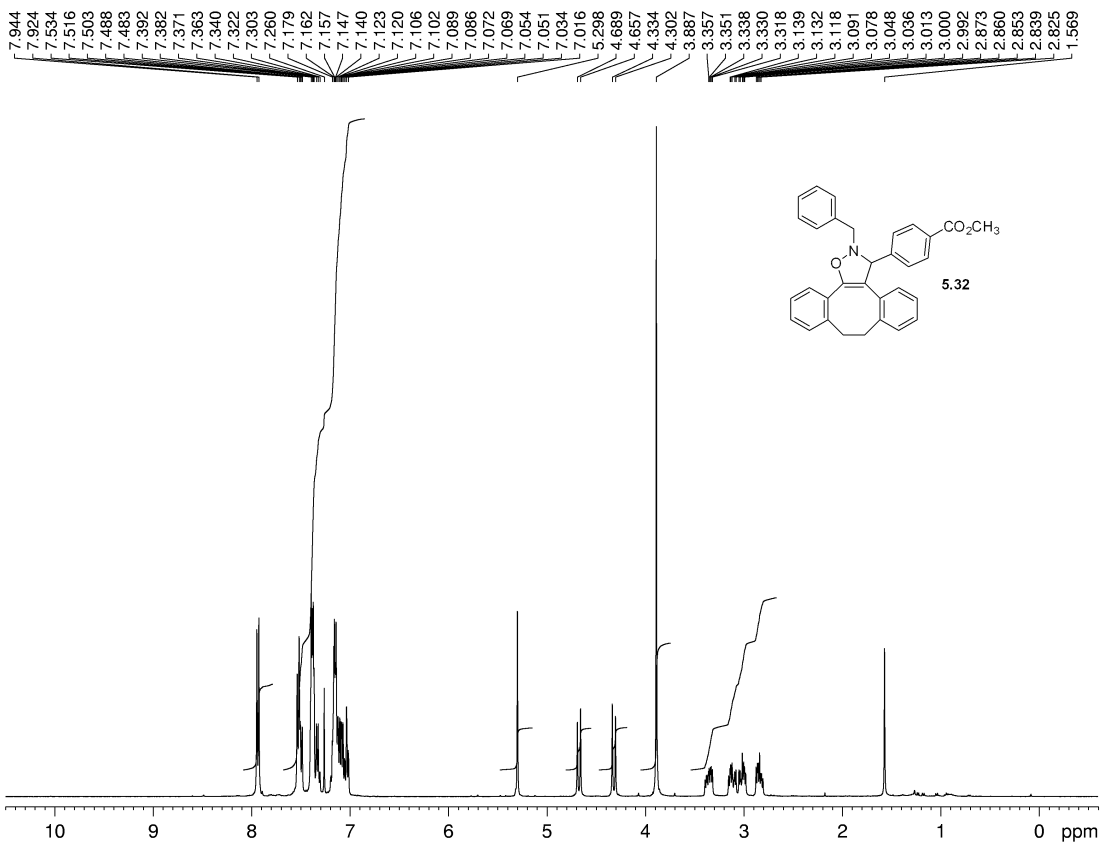
7.944
7.924
7.534
7.516
7.503
7.488
7.483
7.392
7.382
7.371
7.363
7.340
7.322
7.303
7.260
7.179
7.162
7.157
7.147
7.140
7.123
7.120
7.106
7.102
7.089
7.086
7.072
7.069
7.054
7.051
7.034
7.016
5.298
4.689
4.657
4.334
4.302
3.887
3.357
3.351
3.338
3.330
3.318
3.139
3.132
3.118
3.091
3.078
3.048
3.036
3.013
3.000
2.992
2.873
2.860
2.853
2.839
2.825
1.569
CO2CH3
N
O
5.32
10
9
8
7
6
5
4
3
2
1
0
ppm

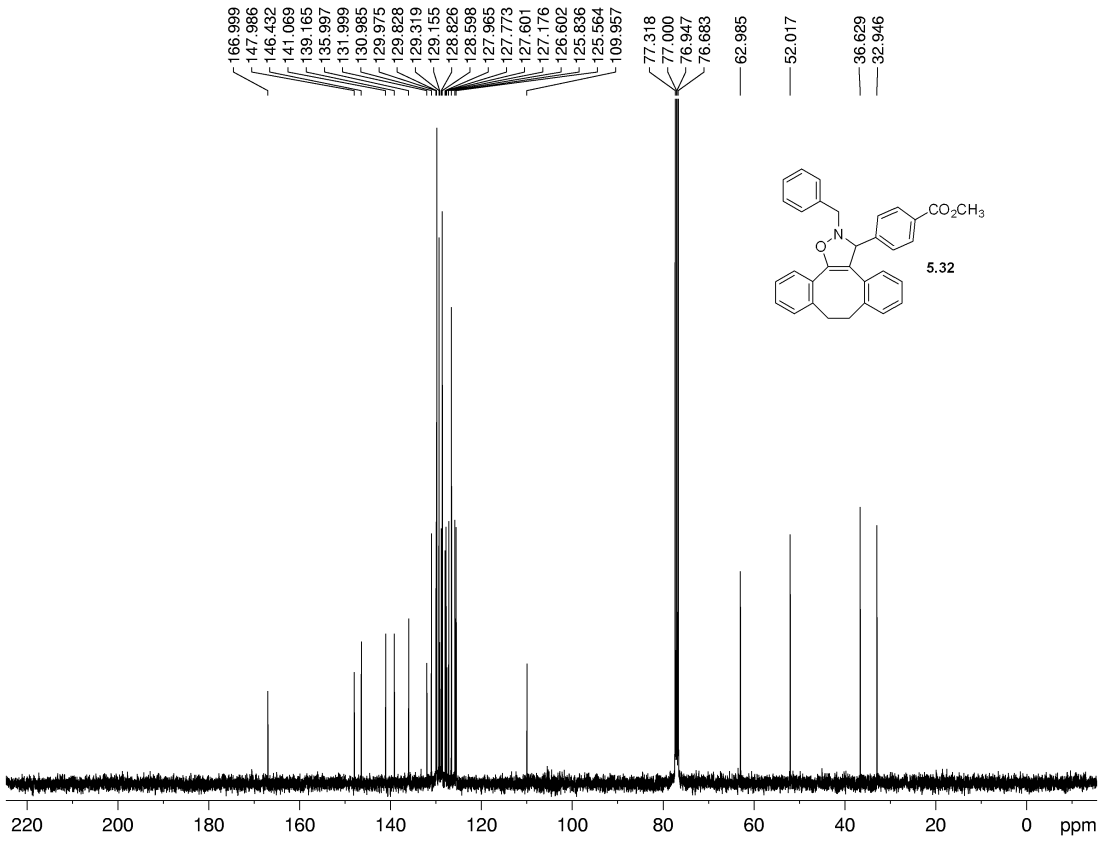
166.999
147.986
146.432
141.069
139.165
135.997
131.999
130.985
129.975
129.828
129.319
129.155
128.826
128.598
127.965
127.773
127.601
127.176
126.602
125.836
125.564
109.957
77.318
77.000
76.947
76.683
62.985
52.017
36.629
32.946
CO2CH3
N
O
5.32
220
200
180
160
140
120
100
80
60
40
20
0
ppm

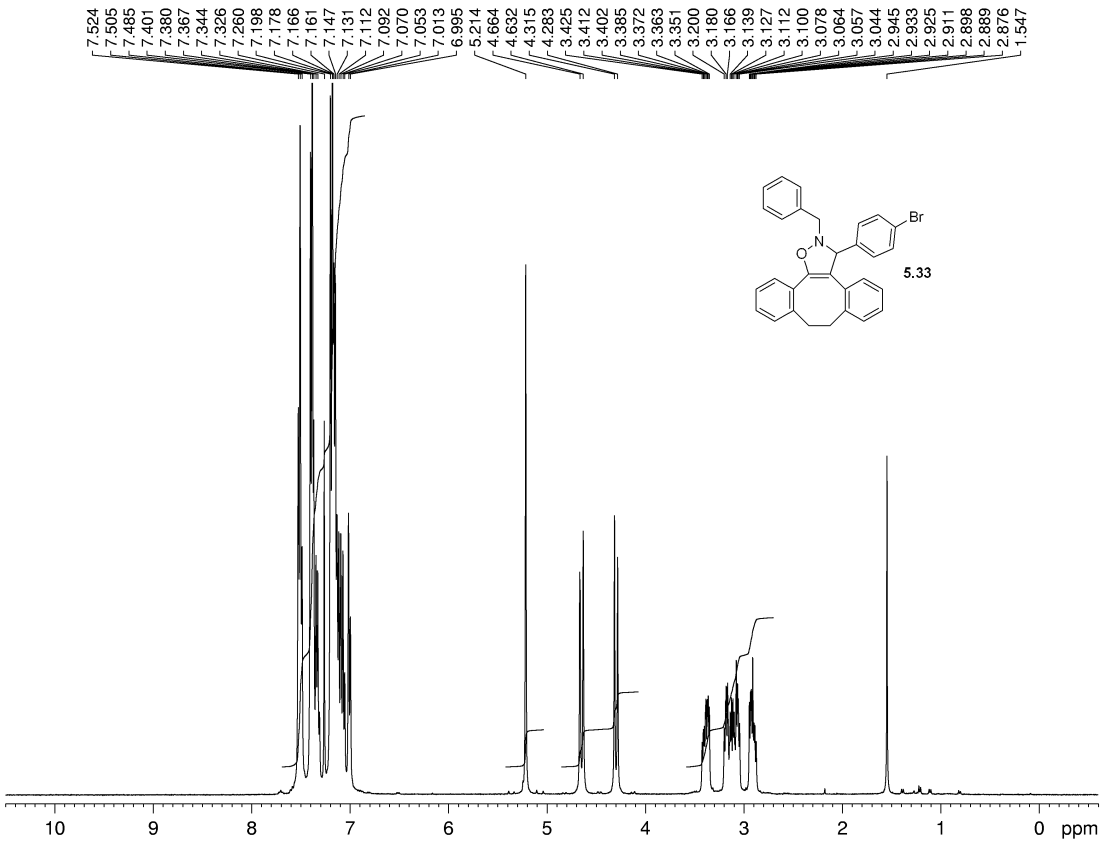
7.524
7.505
7.485
7.401
7.380
7.367
7.344
7.326
7.260
7.198
7.178
7.166
7.161
7.147
7.131
7.112
7.092
7.070
7.053
7.013
6.995
5.214
4.664
4.632
4.315
4.283
3.425
3.412
3.402
3.385
3.372
3.363
3.351
3.200
3.180
3.166
3.139
3.127
3.112
3.100
3.078
3.064
3.057
3.044
2.945
2.933
2.925
2.911
2.898
2.889
2.876
1.547
Br
5.33
10
9
8
7
6
5
4
3
2
1
0
ppm

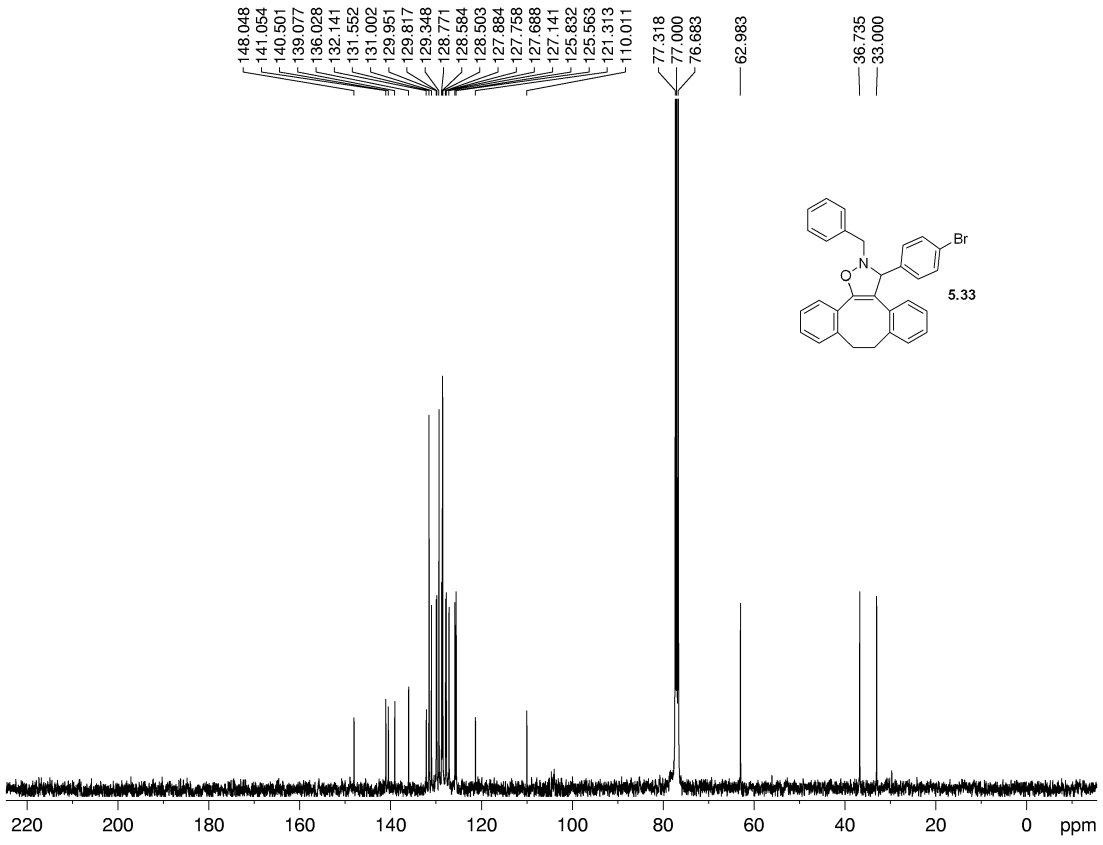
148.048
141.054
140.501
139.077
136.028
132.141
131.552
131.002
129.951
129.817
129.348
128.771
128.584
128.503
127.884
127.758
127.688
127.141
125.832
125.563
121.313
110.011
77.318
77.000
76.683
62.983
36.735
33.000
Br
5.33
220
200
180
160
140
120
100
80
60
40
20
0
ppm

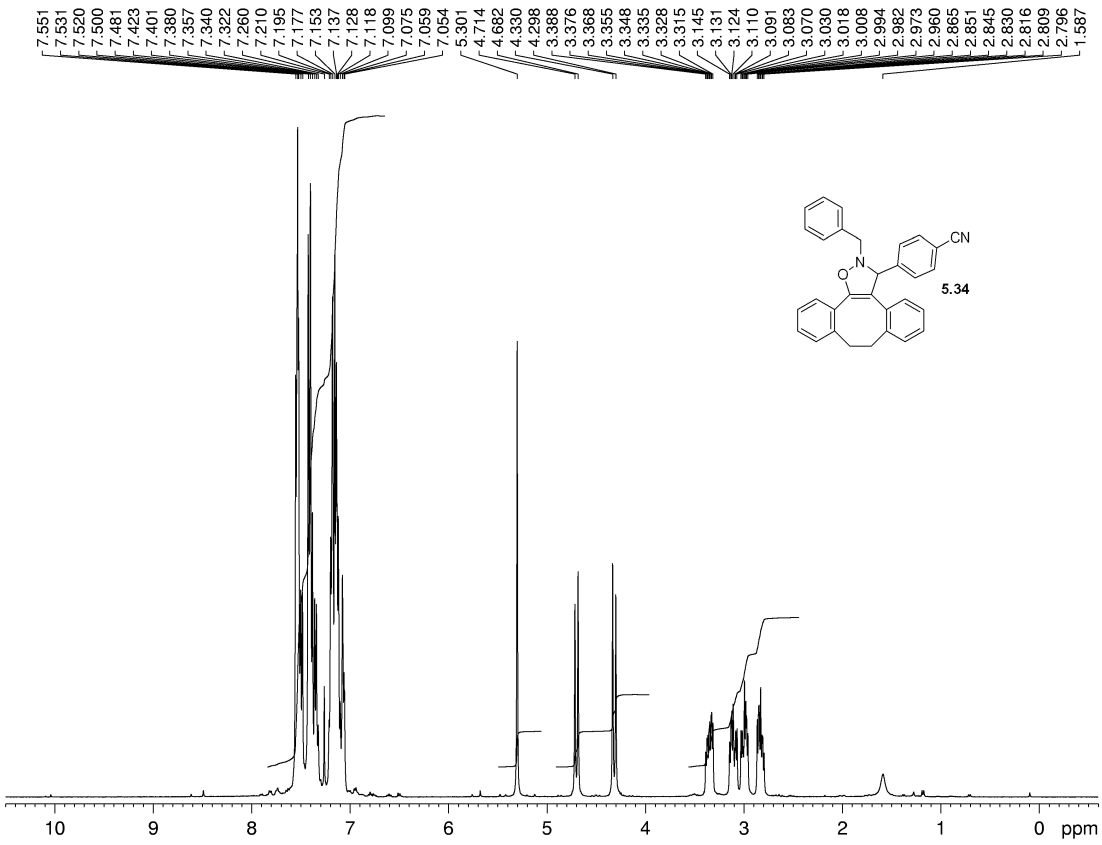
7.551
7.531
7.520
7.500
7.481
7.423
7.401
7.380
7.357
7.340
7.322
7.260
7.210
7.195
7.177
7.153
7.137
7.128
7.118
7.099
7.075
7.059
7.054
5.301
4.714
4.682
4.330
4.298
3.388
3.376
3.368
3.355
3.348
3.335
3.328
3.315
3.145
3.131
3.124
3.110
3.091
3.083
3.070
3.030
3.018
3.008
2.994
2.982
2.973
2.960
2.865
2.851
2.845
2.830
2.816
2.809
2.796
1.587
CN
N
O
5.34
10
9
8
7
6
5
4
3
2
1
0
ppm

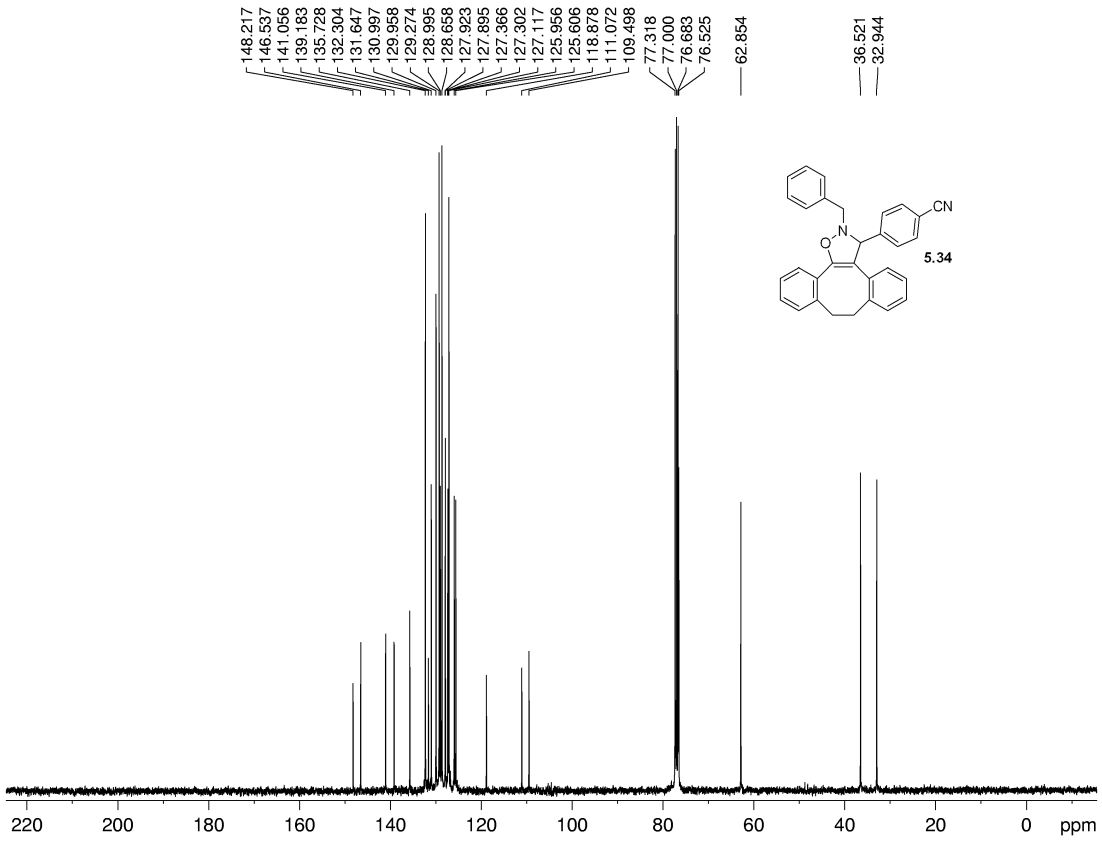
148.217
146.537
141.056
139.183
135.728
132.304
131.647
130.997
129.958
129.274
128.995
128.658
127.923
127.895
127.366
127.302
127.117
125.956
125.606
118.878
111.072
109.498
77.318
77.000
76.683
76.525
62.854
36.521
32.944
CN
N
O
5.34
220
200
180
160
140
120
100
80
60
40
20
0
ppm

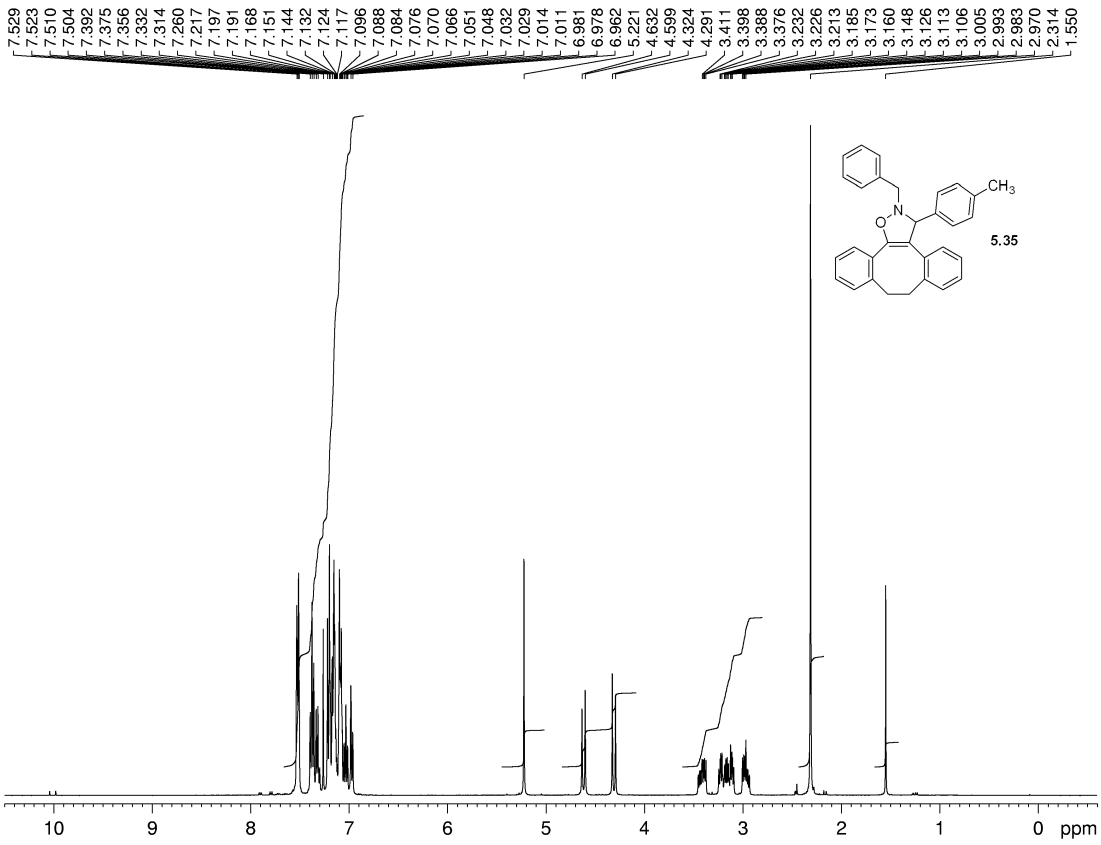
7.529
7.523
7.510
7.504
7.392
7.375
7.356
7.332
7.314
7.260
7.217
7.197
7.191
7.168
7.151
7.144
7.132
7.124
7.117
7.096
7.088
7.084
7.076
7.070
7.066
7.051
7.048
7.032
7.029
7.014
7.011
6.981
6.978
6.962
5.221
4.632
4.599
4.324
4.291
3.411
3.398
3.388
3.376
3.232
3.226
3.213
3.185
3.173
3.160
3.148
3.126
3.113
3.106
3.005
2.993
2.983
2.970
2.314
1.550
CH3
N
O
5.35
10
9
8
7
6
5
4
3
2
1
0
ppm

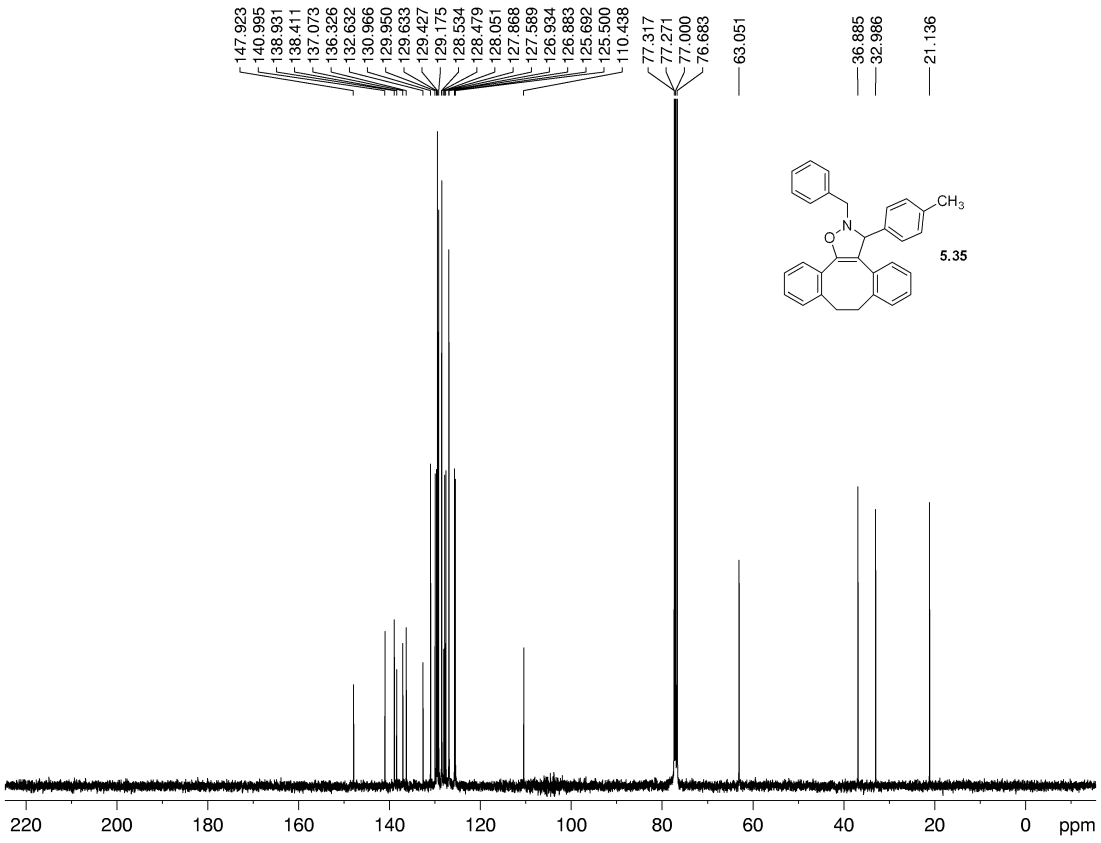
147.923
140.995
138.931
138.411
137.073
136.326
132.632
130.966
129.950
129.633
129.427
129.175
128.534
128.479
128.051
127.868
127.589
126.934
126.883
125.692
125.500
110.438
77.317
77.271
77.000
76.683
63.051
36.885
32.986
21.136
CH3
N
O
5.35
220
200
180
160
140
120
100
80
60
40
20
0
ppm

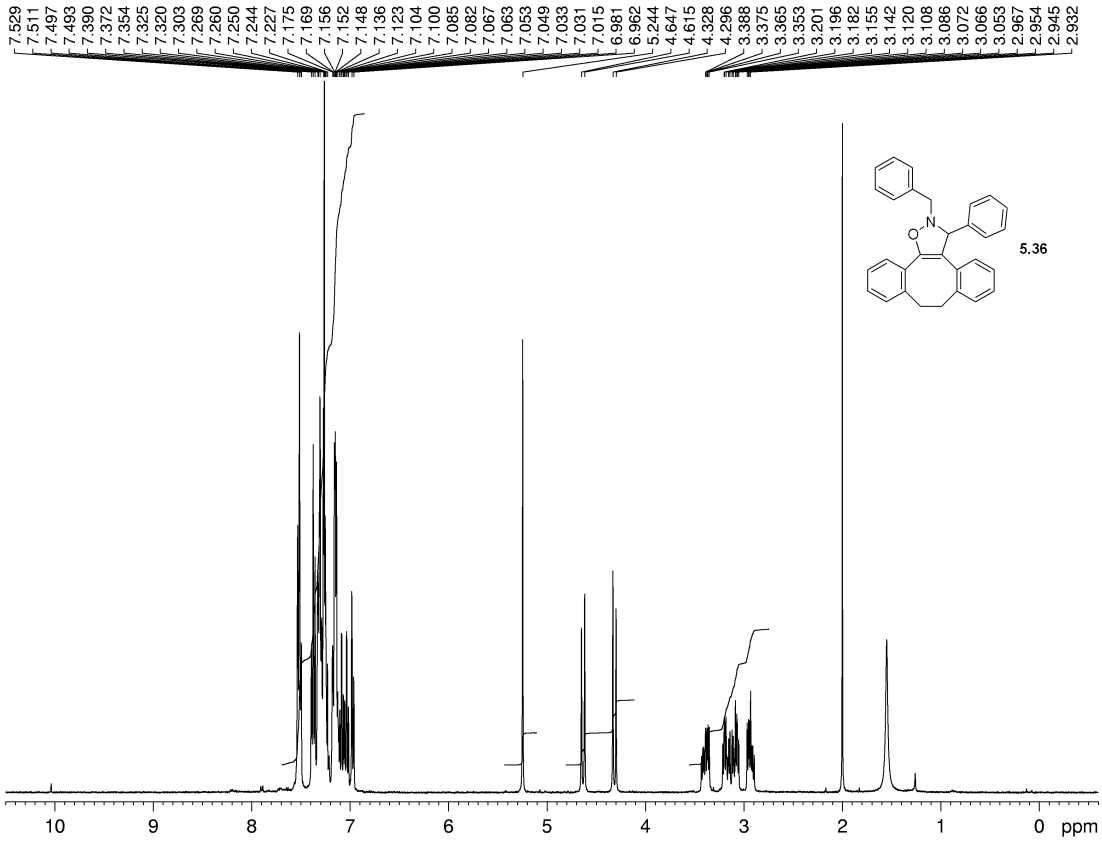
7.529
7.511
7.497
7.493
7.390
7.372
7.354
7.325
7.320
7.303
7.269
7.260
7.250
7.244
7.227
7.175
7.169
7.156
7.152
7.148
7.136
7.123
7.104
7.100
7.085
7.082
7.067
7.063
7.053
7.049
7.033
7.031
7.015
6.981
6.962
5.244
4.647
4.615
4.328
4.296
3.388
3.375
3.365
3.353
3.201
3.196
3.182
3.155
3.142
3.120
3.108
3.086
3.072
3.066
3.053
2.967
2.954
2.945
2.932
5.36
10
9
8
7
6
5
4
3
2
1
0
ppm

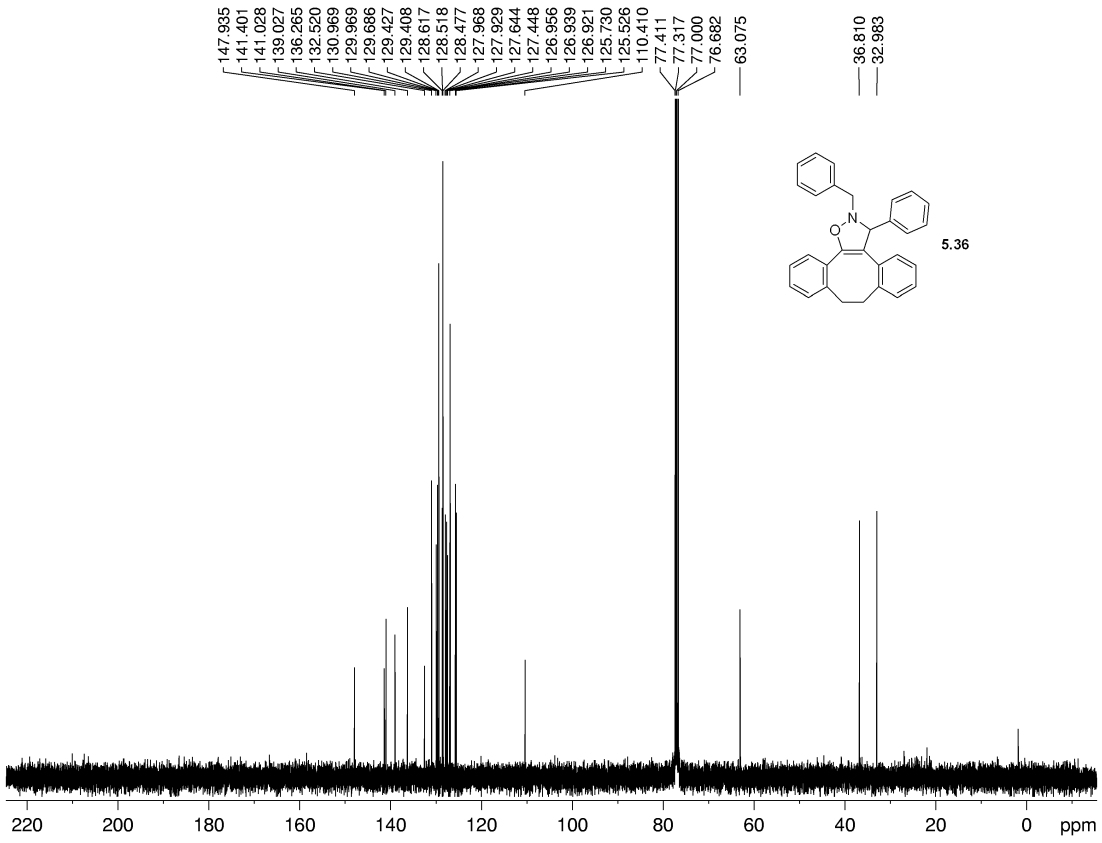
147.935
141.401
141.028
139.027
136.265
132.520
130.969
129.969
129.686
129.427
129.408
128.617
128.518
128.477
127.968
127.929
127.644
127.448
126.956
126.939
126.921
125.730
125.526
110.410
77.411
77.317
77.000
76.682
63.075
36.810
32.983
5.36
220
200
180
160
140
120
100
80
60
40
20
0
ppm

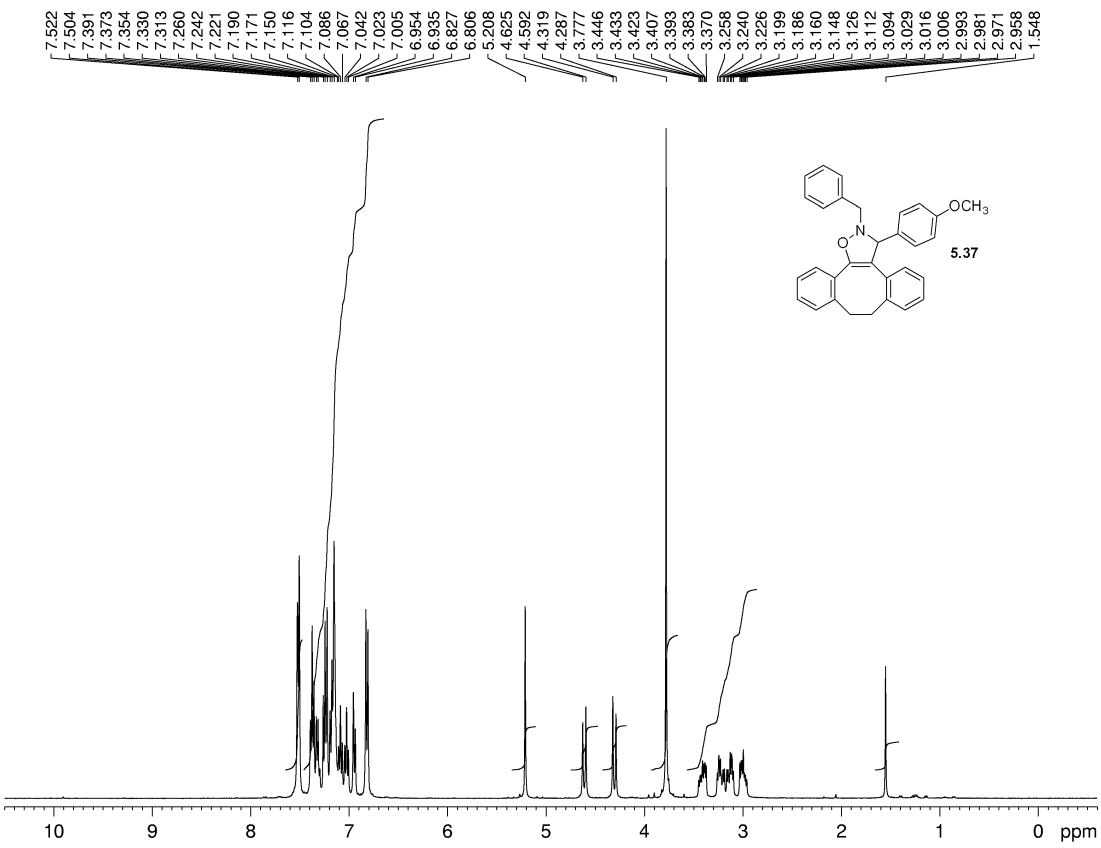
7.522
7.504
7.391
7.373
7.354
7.330
7.313
7.260
7.242
7.221
7.190
7.171
7.150
7.116
7.104
7.086
7.067
7.042
7.023
7.005
6.954
6.935
6.827
6.806
5.208
4.625
4.592
4.319
4.287
3.777
3.446
3.433
3.423
3.407
3.393
3.383
3.370
3.258
3.240
3.226
3.199
3.186
3.160
3.148
3.126
3.112
3.094
3.029
3.016
3.006
2.993
2.981
2.971
2.958
1.548
OCH3
N
O
5.37
10
9
8
7
6
5
4
3
2
1
0
ppm

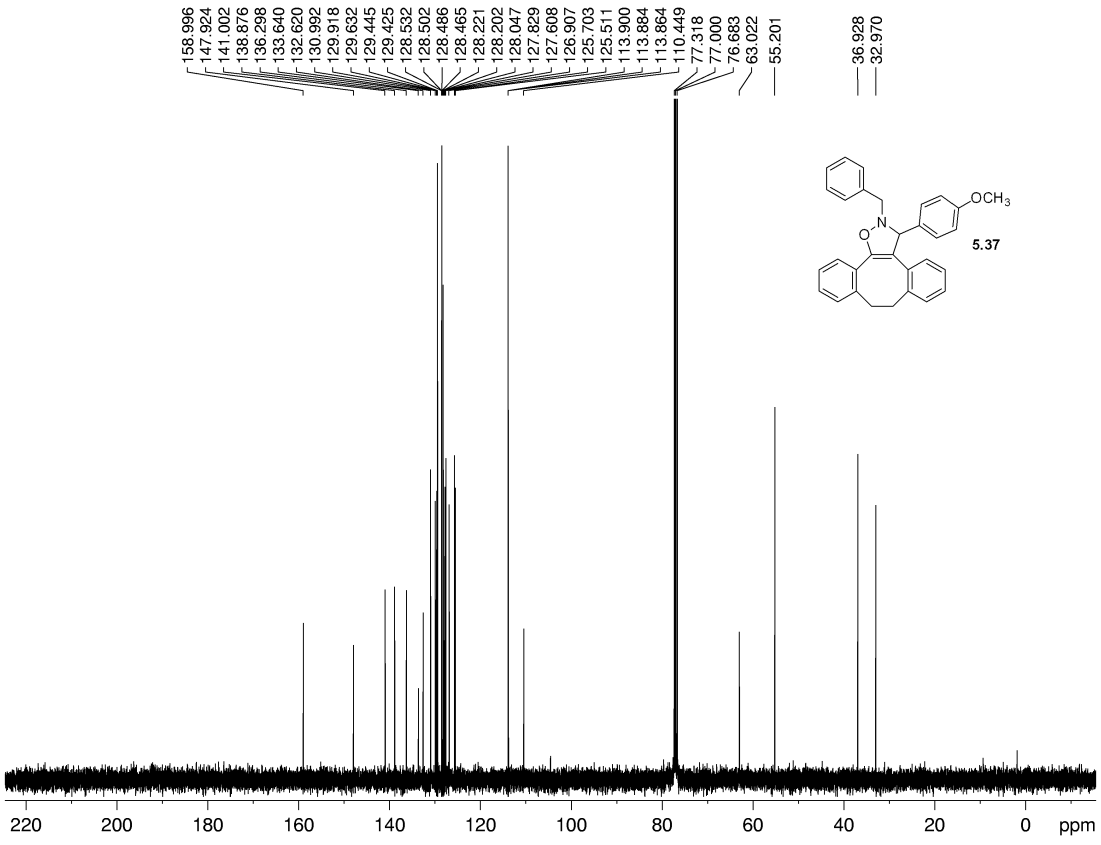
158.996
147.924
141.002
138.876
136.298
133.640
132.620
130.992
129.918
129.632
129.445
129.425
128.532
128.502
128.486
128.465
128.221
128.202
128.047
127.829
127.608
126.907
125.703
125.511
113.900
113.884
113.864
110.449
77.318
77.000
76.683
63.022
55.201
36.928
32.970
OCH3
N
O
5.37
220
200
180
160
140
120
100
80
60
40
20
0
ppm

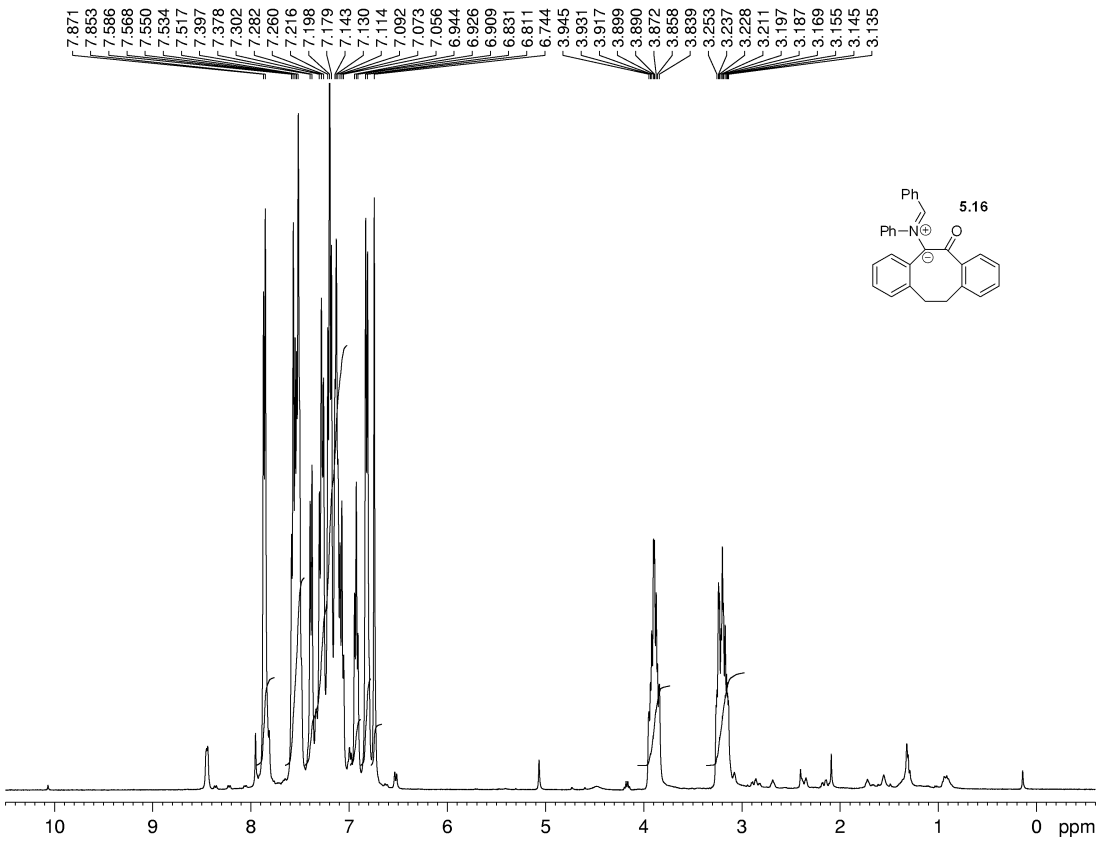
7.871
7.853
7.586
7.568
7.550
7.534
7.517
7.397
7.378
7.302
7.282
7.260
7.216
7.198
7.179
7.143
7.130
7.114
7.092
7.073
7.056
6.944
6.926
6.909
6.831
6.811
6.744
3.945
3.931
3.917
3.899
3.890
3.872
3.858
3.839
3.253
3.237
3.228
3.211
3.197
3.187
3.169
3.155
3.145
3.135
Ph
Ph–N
O
5.16
10
9
8
7
6
5
4
3
2
1
0
ppm

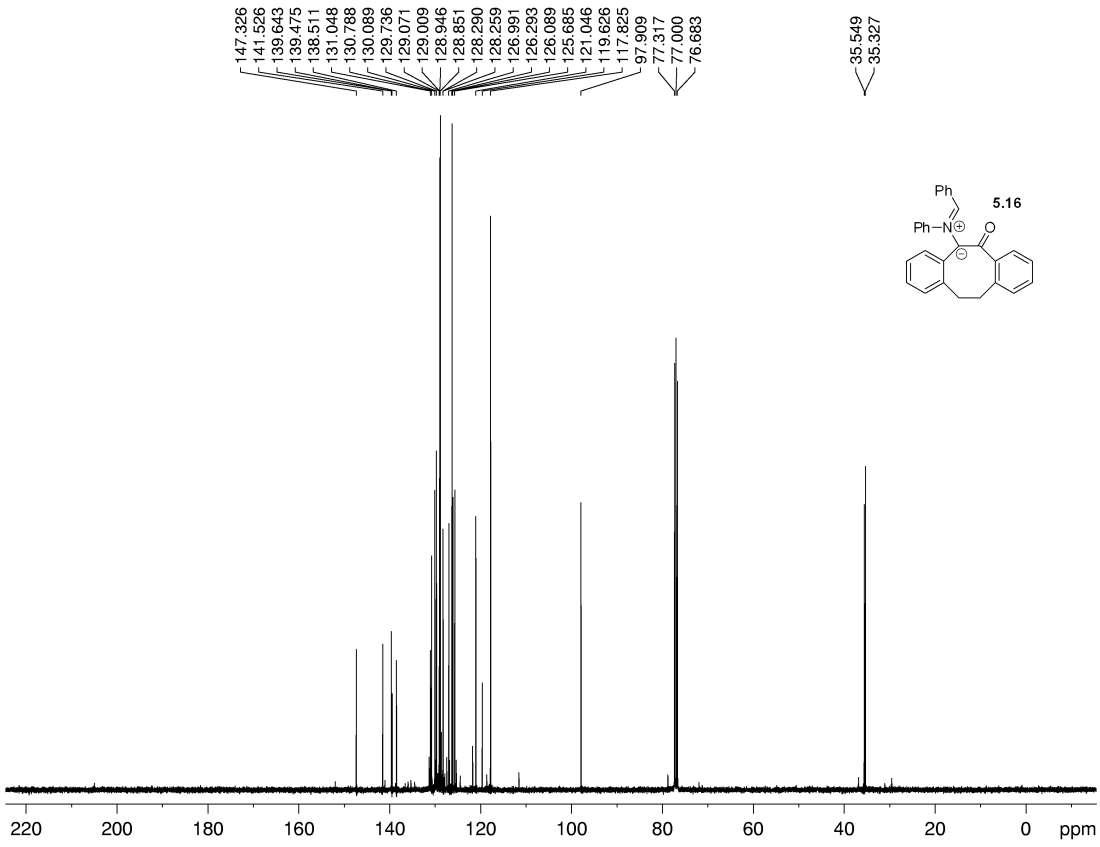
147.326
141.526
139.643
139.475
138.511
131.048
130.788
130.089
129.736
129.071
129.009
128.946
128.851
128.290
128.259
126.991
126.293
126.089
125.685
121.046
119.626
117.825
97.909
77.317
77.000
76.683
35.549
35.327
Ph
Ph–N
O
5.16
220
200
180
160
140
120
100
80
60
40
20
0
ppm

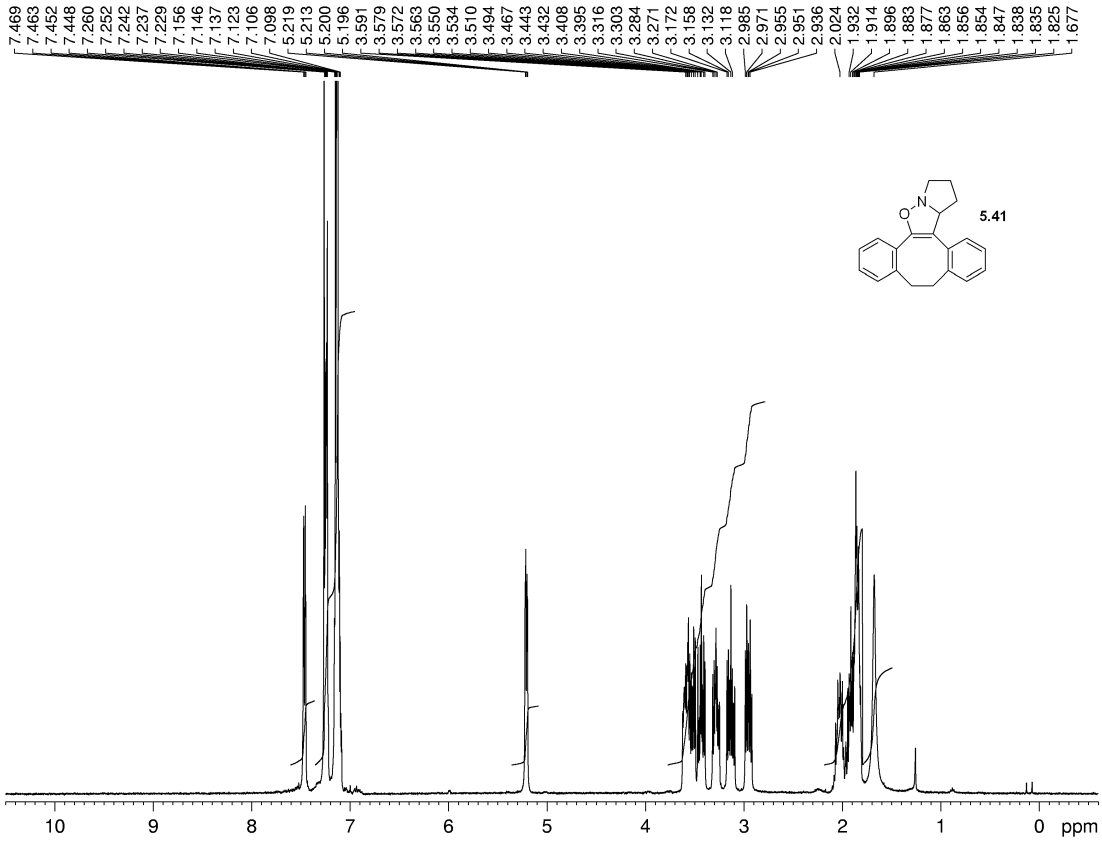
7.469
7.463
7.452
7.448
7.260
7.252
7.242
7.237
7.229
7.156
7.146
7.137
7.123
7.106
7.098
5.219
5.213
5.200
5.196
3.591
3.579
3.572
3.563
3.550
3.534
3.510
3.494
3.467
3.443
3.432
3.408
3.395
3.316
3.303
3.284
3.271
3.172
3.158
3.132
3.118
2.985
2.971
2.955
2.951
2.936
2.024
1.932
1.914
1.896
1.883
1.877
1.863
1.856
1.854
1.847
1.838
1.835
1.825
1.677
5.41
10
9
8
7
6
5
4
3
2
1
0
ppm

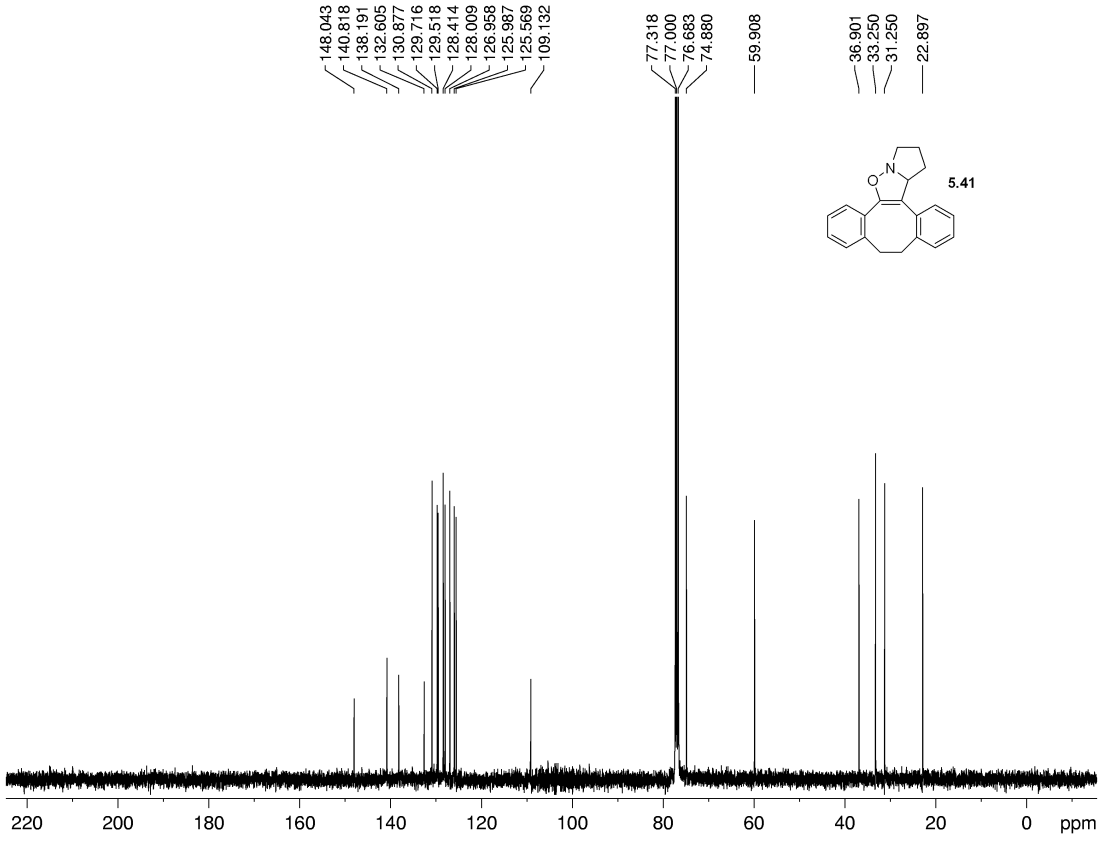
148.043
140.818
138.191
132.605
130.877
129.716
129.518
128.414
128.009
126.958
125.987
125.569
109.132
77.318
77.000
76.683
74.880
59.908
36.901
33.250
31.250
22.897
5.41
220
200
180
160
140
120
100
80
60
40
20
0
ppm

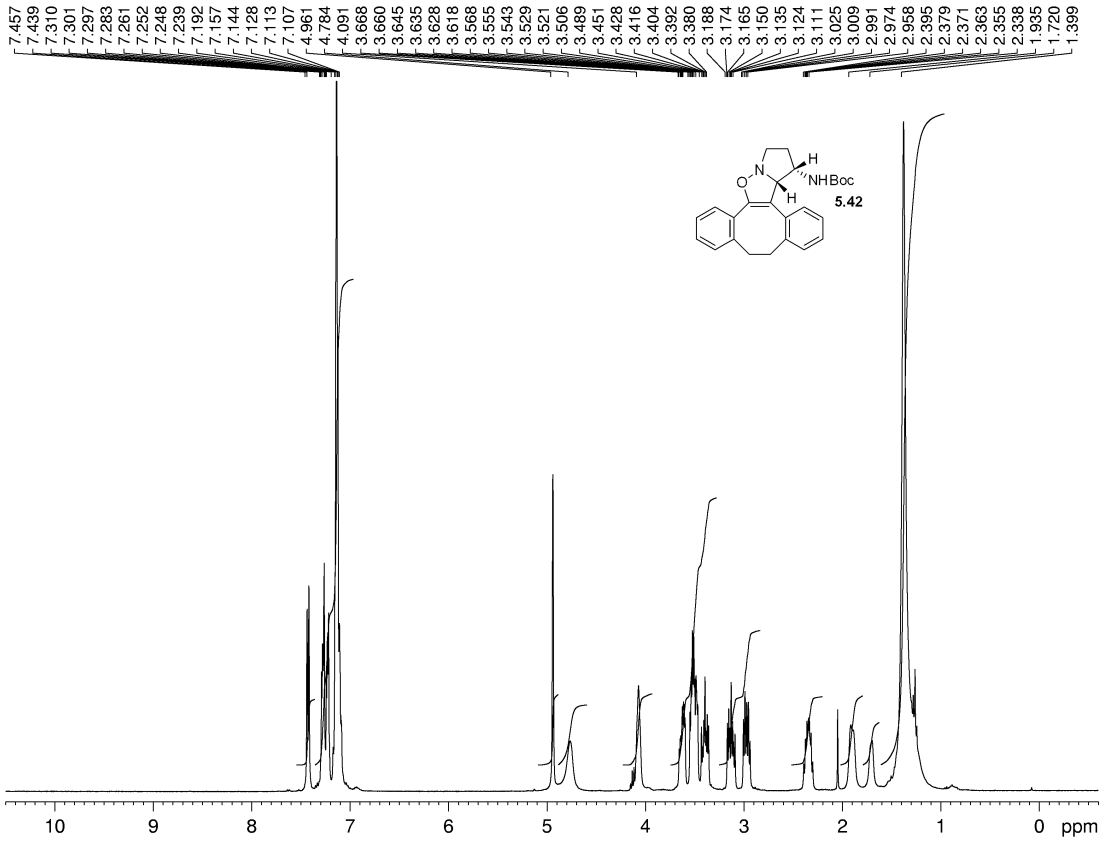
7.457
7.439
7.310
7.301
7.297
7.283
7.261
7.252
7.248
7.239
7.192
7.157
7.144
7.128
7.113
7.107
4.961
4.784
4.091
3.668
3.660
3.645
3.635
3.628
3.618
3.568
3.555
3.543
3.529
3.521
3.506
3.489
3.451
3.428
3.416
3.404
3.392
3.380
3.188
3.174
3.165
3.150
3.135
3.124
3.111
3.025
3.009
2.991
2.974
2.958
2.395
2.379
2.371
2.363
2.355
2.338
1.935
1.720
1.399
NHBoc
5.42
10
9
8
7
6
5
4
3
2
1
0
ppm

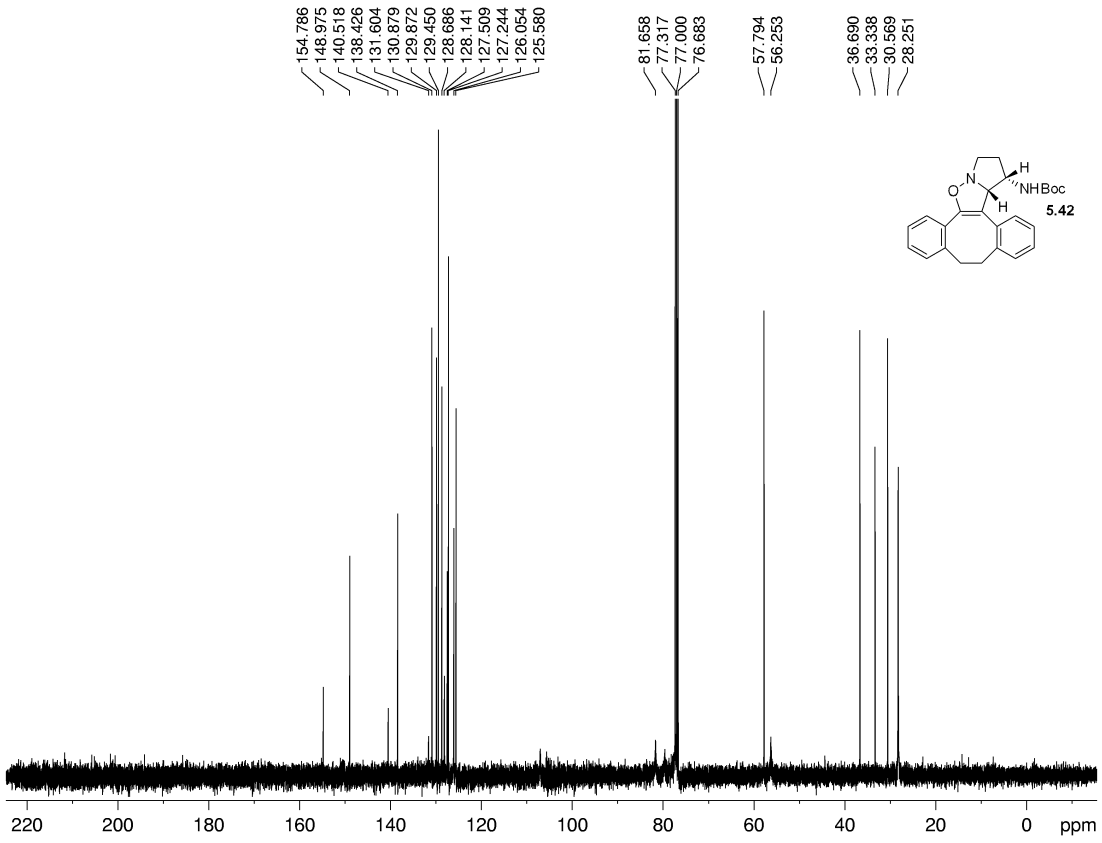
154.786
148.975
140.518
138.426
131.604
130.879
129.872
129.450
128.686
128.141
127.509
127.244
126.054
125.580
81.658
77.317
77.000
76.683
57.794
56.253
36.690
33.338
30.569
28.251
NHBoc
5.42
220
200
180
160
140
120
100
80
60
40
20
0
ppm

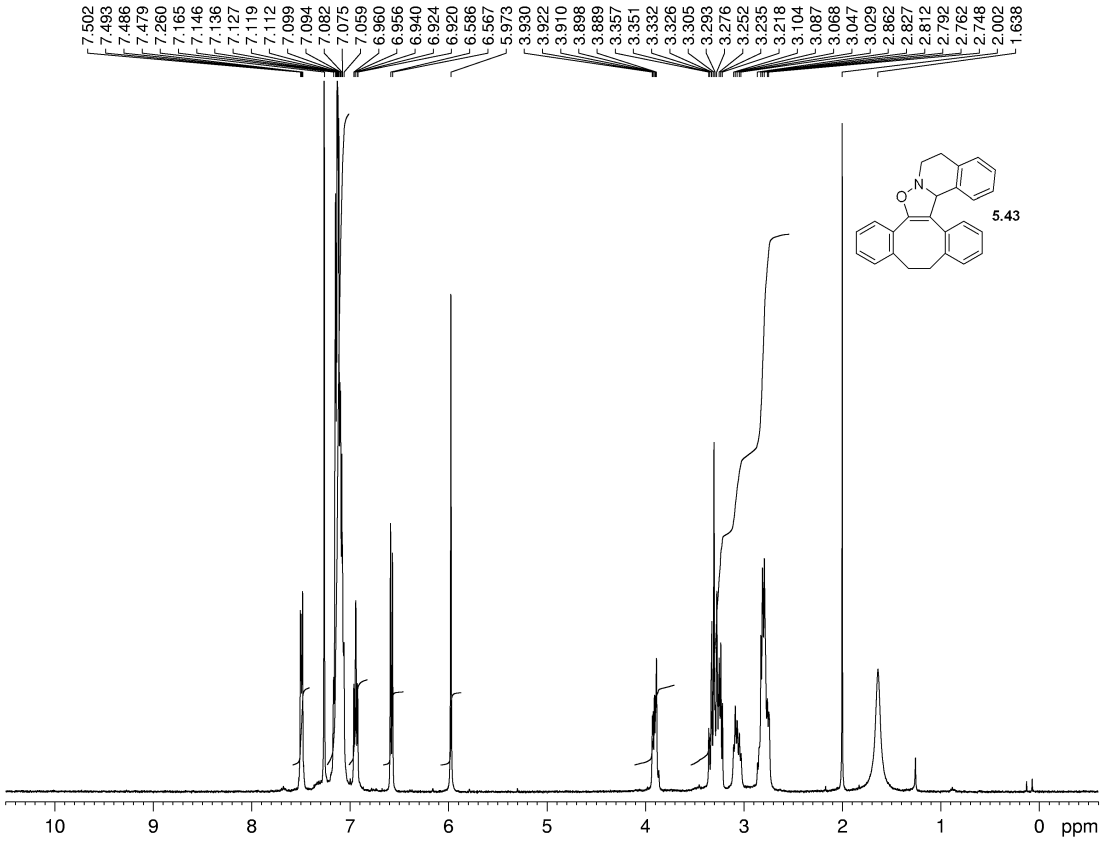
7.502
7.493
7.486
7.479
7.260
7.165
7.146
7.136
7.127
7.119
7.112
7.099
7.094
7.082
7.075
7.059
6.960
6.956
6.940
6.924
6.920
6.586
6.567
5.973
3.930
3.922
3.910
3.898
3.889
3.357
3.351
3.332
3.326
3.305
3.293
3.276
3.252
3.235
3.218
3.104
3.087
3.068
3.047
3.029
2.862
2.827
2.812
2.792
2.762
2.748
2.002
1.638
5.43
10
9
8
7
6
5
4
3
2
1
0
ppm

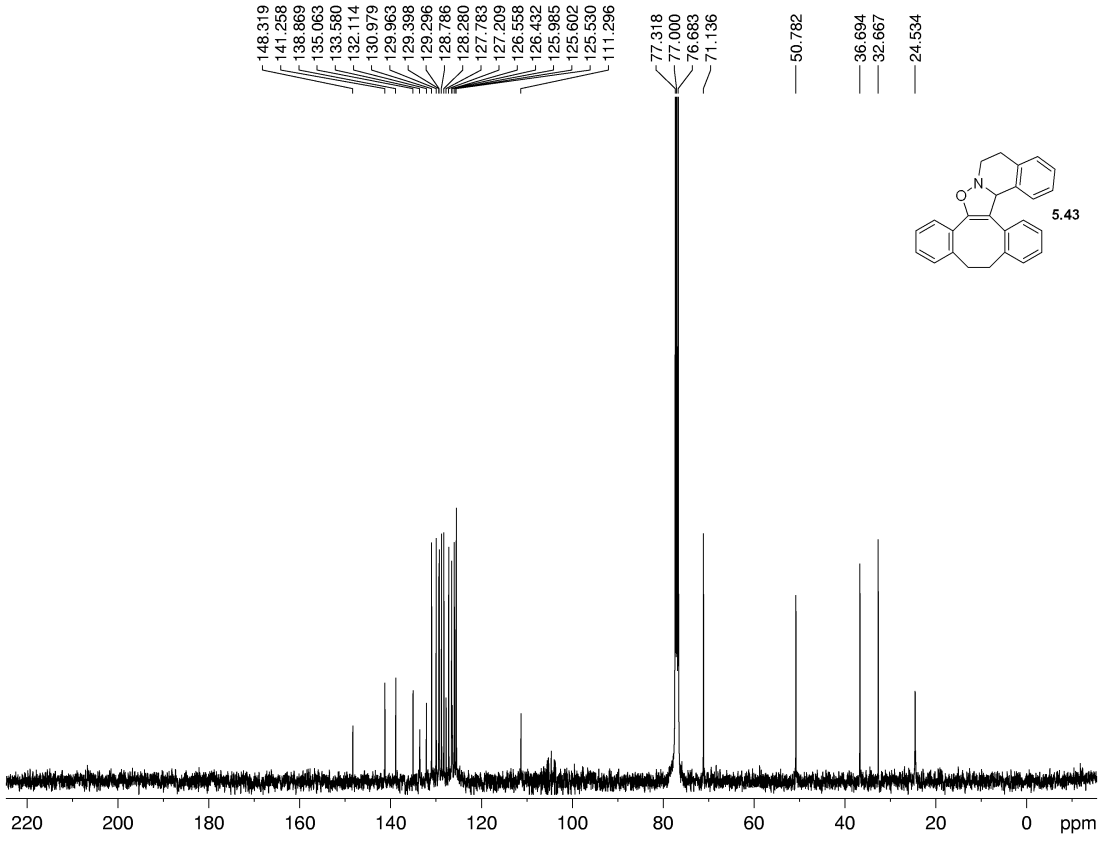
148.319
141.258
138.869
135.063
133.580
132.114
130.979
129.963
129.398
129.296
128.786
128.280
127.783
127.209
126.558
126.432
125.985
125.602
125.530
111.296
77.318
77.000
76.683
71.136
50.782
36.694
32.667
24.534
5.43
220
200
180
160
140
120
100
80
60
40
20
0
ppm

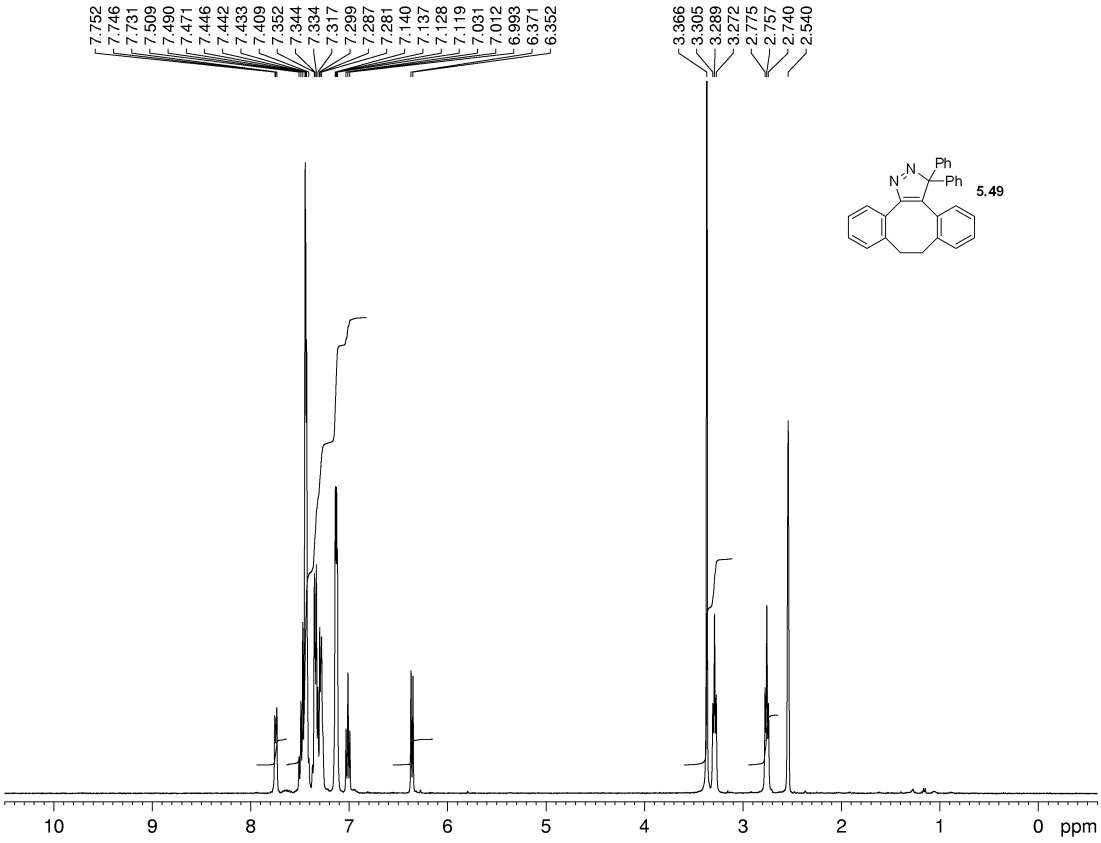
7.752
7.746
7.731
7.509
7.490
7.471
7.446
7.442
7.433
7.409
7.352
7.344
7.334
7.317
7.299
7.287
7.281
7.140
7.137
7.128
7.119
7.031
7.012
6.993
6.371
6.352
3.366
3.305
3.289
3.272
2.775
2.757
2.740
2.540
Ph
Ph
5.49
10
9
8
7
6
5
4
3
2
1
0
ppm

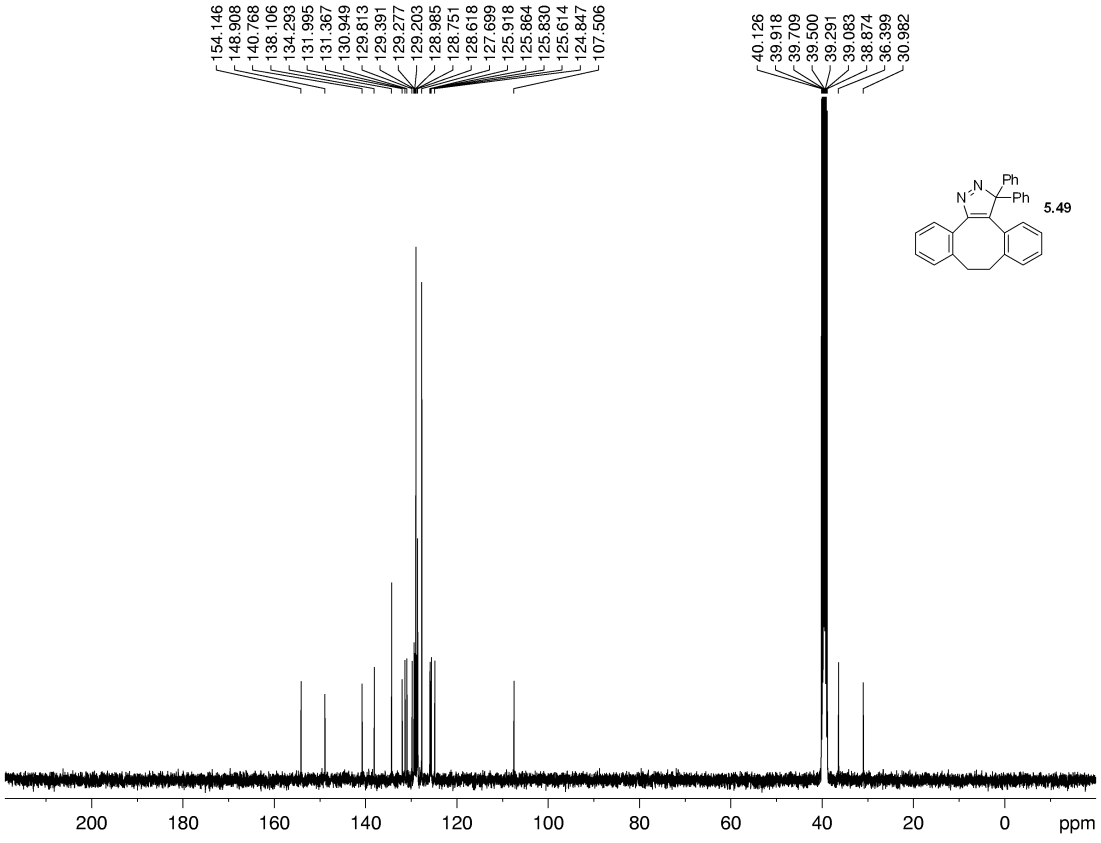
154.146
148.908
140.768
138.106
134.293
131.995
131.367
130.949
129.813
129.391
129.277
129.203
128.985
128.751
128.618
127.699
125.918
125.864
125.830
125.614
124.847
107.506
40.126
39.918
39.709
39.500
39.291
39.083
38.874
36.399
30.982
Ph
Ph
5.49
200
180
160
140
120
100
80
60
40
20
0
ppm

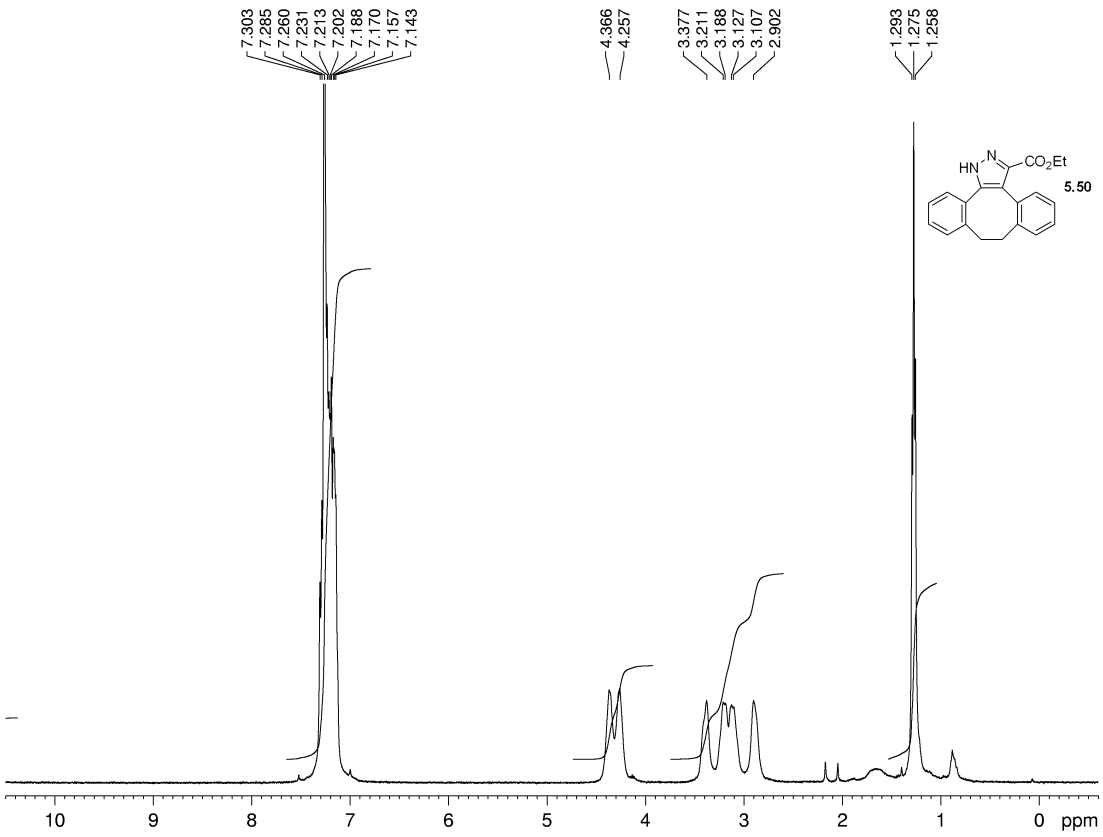
7.303
7.285
7.260
7.231
7.213
7.202
7.188
7.170
7.157
7.143
4.366
4.257
3.377
3.211
3.188
3.127
3.107
2.902
1.293
1.275
1.258
HN
N
CO2Et
5.50
10
9
8
7
6
5
4
3
2
1
0
ppm

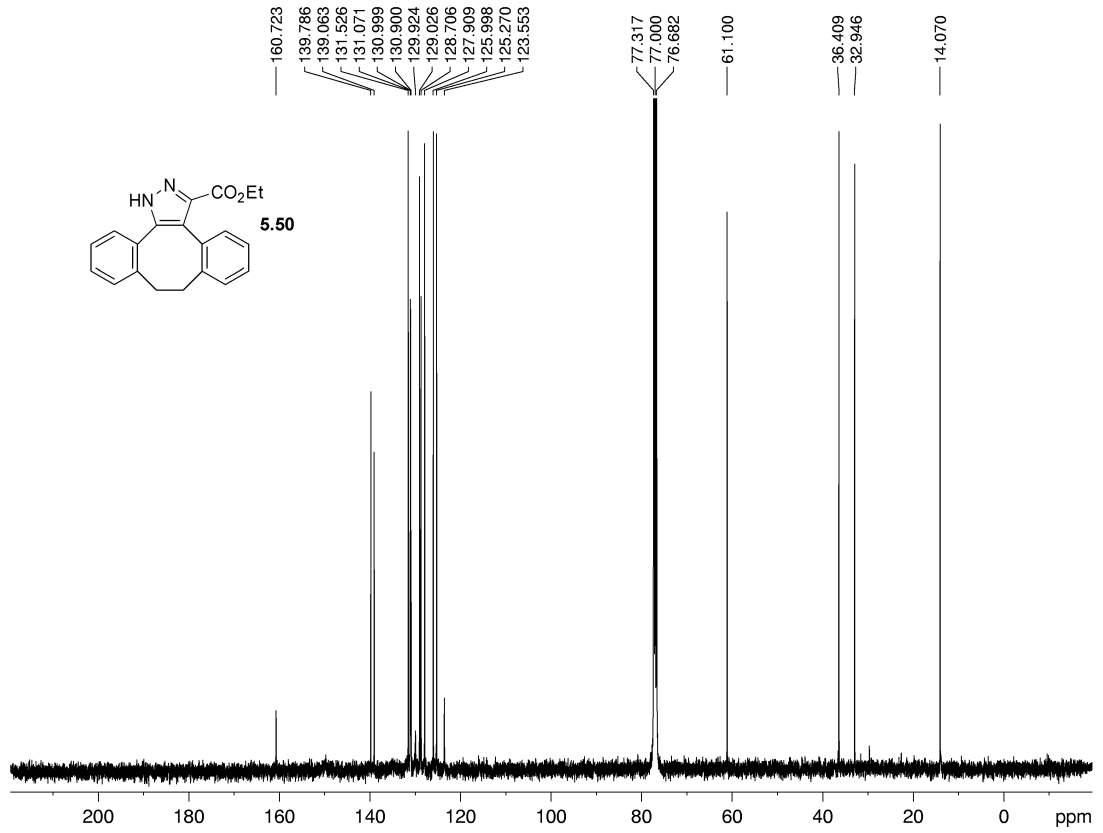
160.723
139.786
139.063
131.526
131.071
130.999
130.900
129.924
129.026
128.706
127.909
125.998
125.270
123.553
77.317
77.000
76.682
61.100
36.409
32.946
14.070
HN
N
CO2Et
5.50
200
180
160
140
120
100
80
60
40
20
0
ppm

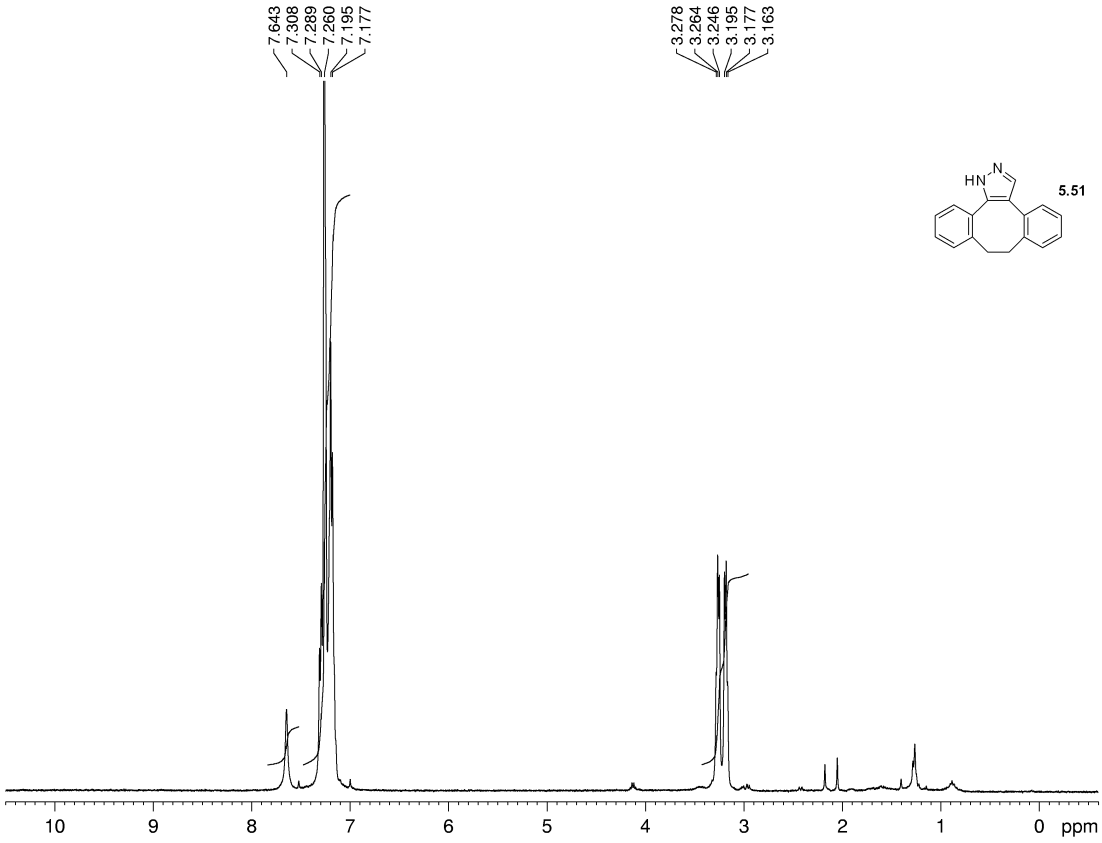
7.643
7.308
7.289
7.260
7.195
7.177
3.278
3.264
3.246
3.195
3.177
3.163
HN
N
5.51
10
9
8
7
6
5
4
3
2
1
0
ppm

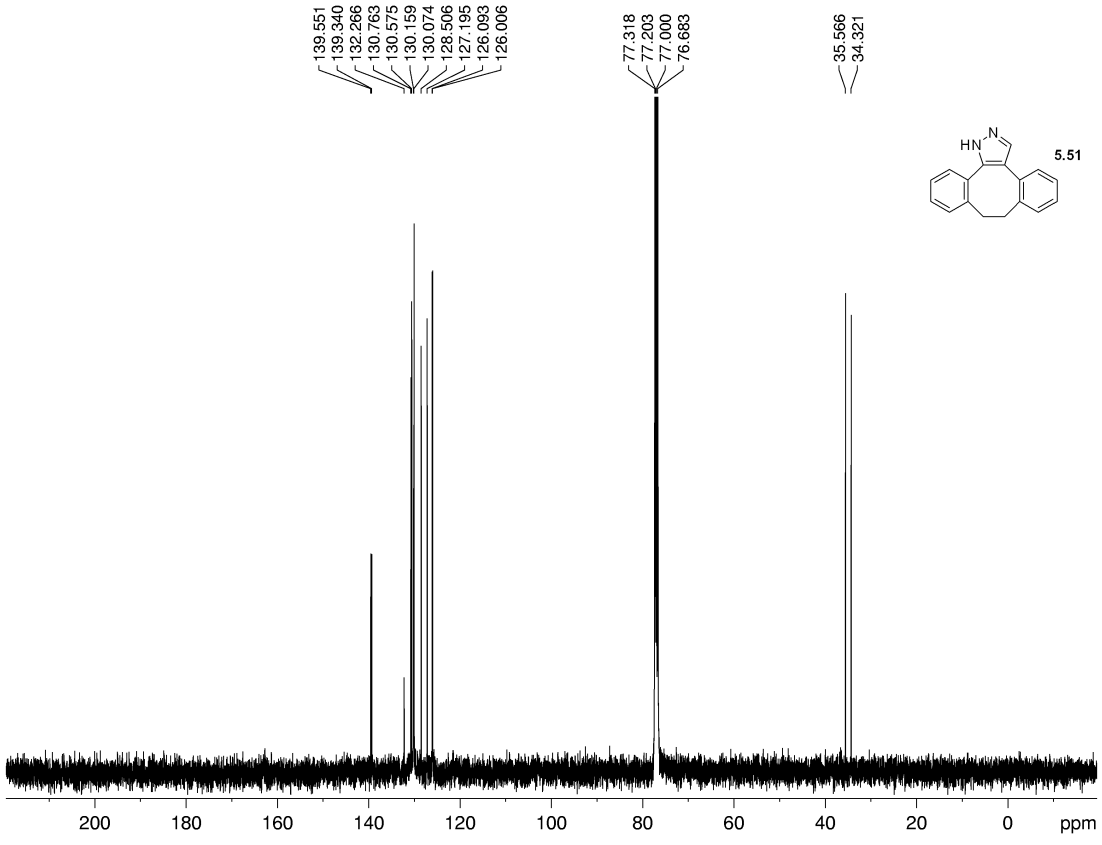
139.551
139.340
132.266
130.763
130.575
130.159
130.074
128.506
127.195
126.093
126.006
77.318
77.203
77.000
76.683
35.566
34.321
HN
N
5.51
200
180
160
140
120
100
80
60
40
20
0
ppm

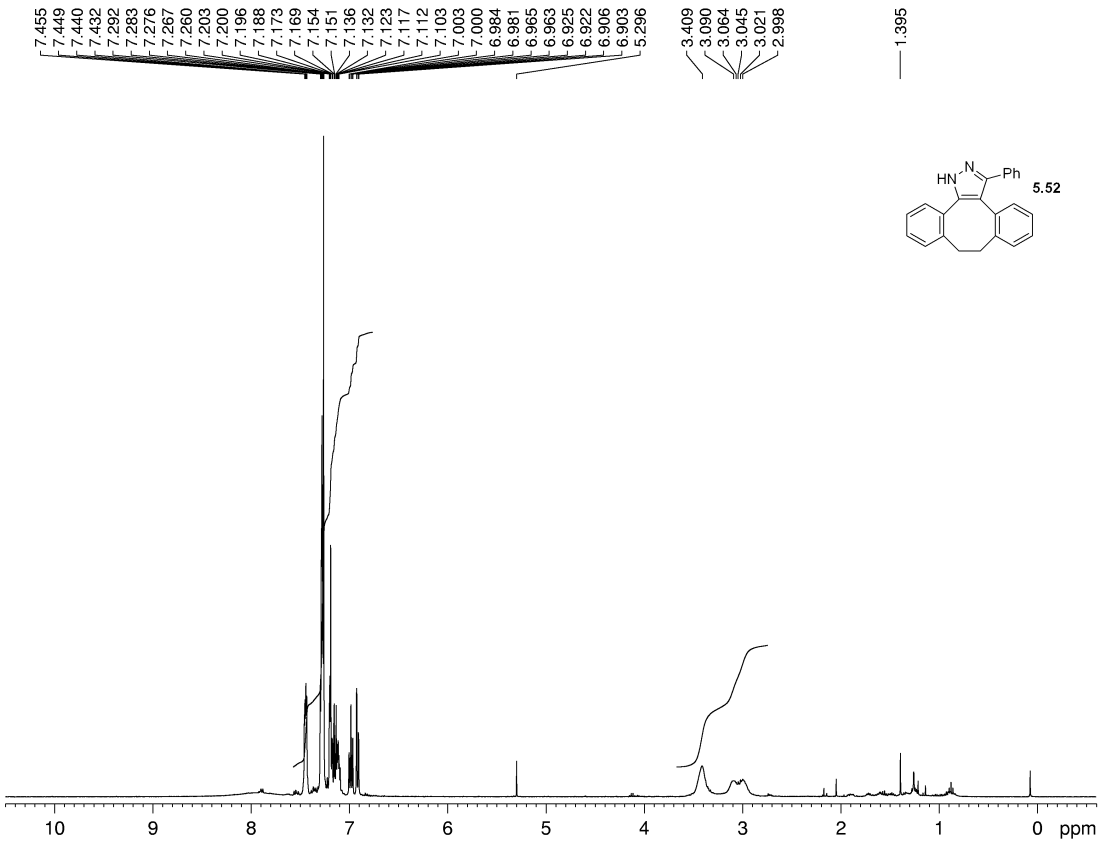
7.455
7.449
7.440
7.432
7.292
7.283
7.276
7.267
7.260
7.203
7.200
7.196
7.188
7.173
7.169
7.154
7.151
7.136
7.132
7.123
7.117
7.112
7.103
7.003
7.000
6.984
6.981
6.965
6.963
6.925
6.922
6.906
6.903
5.296
3.409
3.090
3.064
3.045
3.021
2.998
1.395
HN
N
Ph
5.52
10
9
8
7
6
5
4
3
2
1
0
ppm

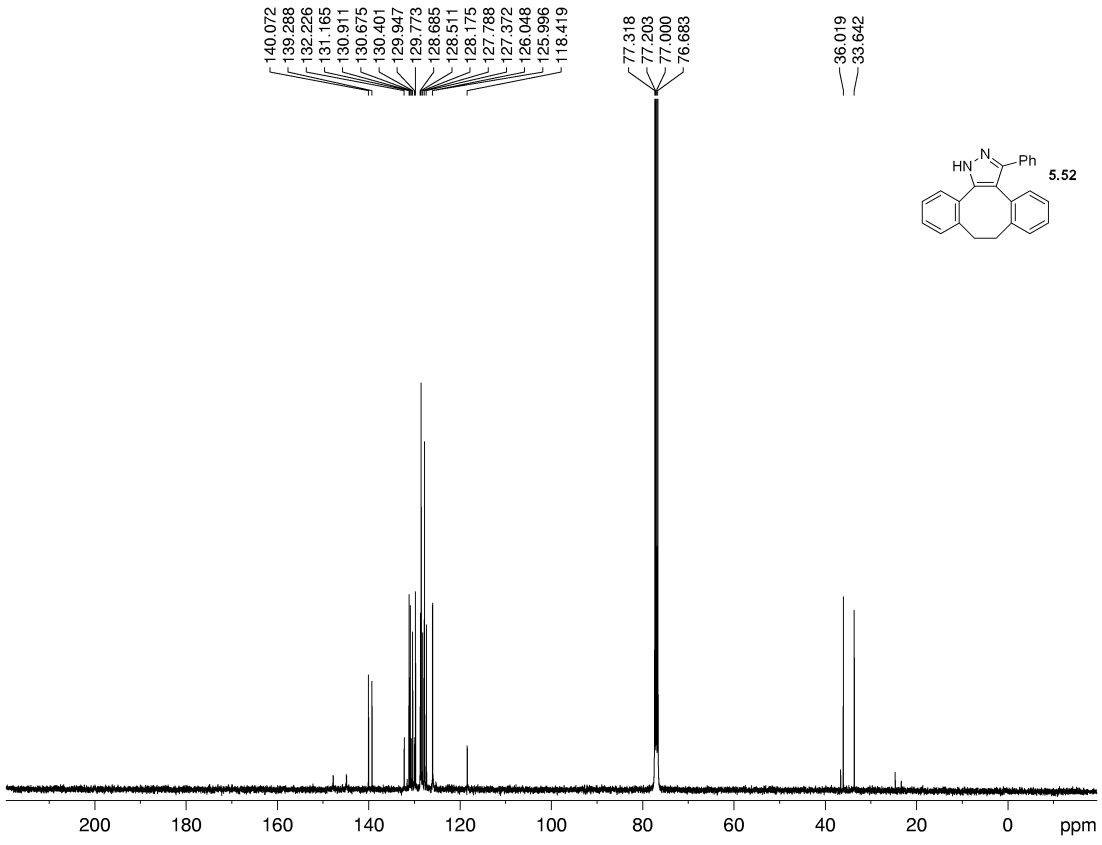
140.072
139.288
132.226
131.165
130.911
130.675
130.401
129.947
129.773
128.685
128.511
128.175
127.788
127.372
126.048
125.996
118.419
77.318
77.203
77.000
76.683
36.019
33.642
HN
N
Ph
5.52
200
180
160
140
120
100
80
60
40
20
0
ppm

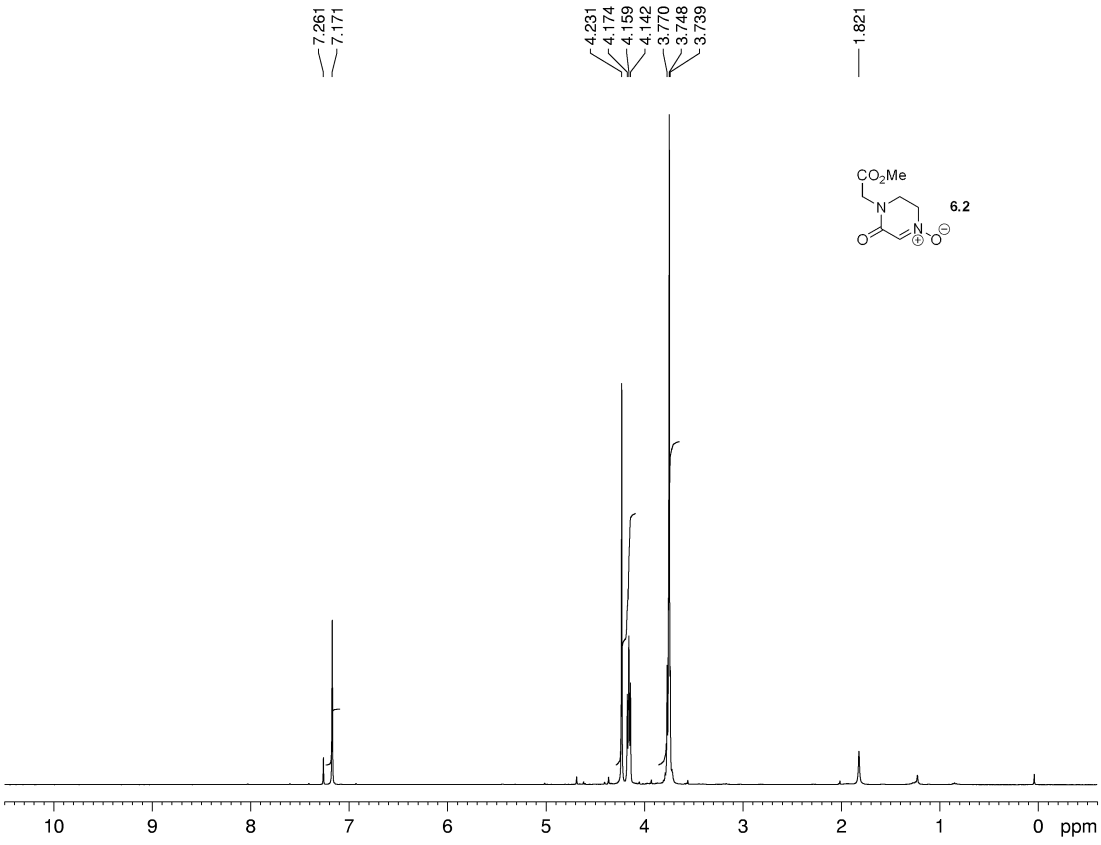
7.261
7.171
4.231
4.174
4.159
4.142
3.770
3.748
3.739
1.821
CO2Me
6.2
10
9
8
7
6
5
4
3
2
1
0
ppm

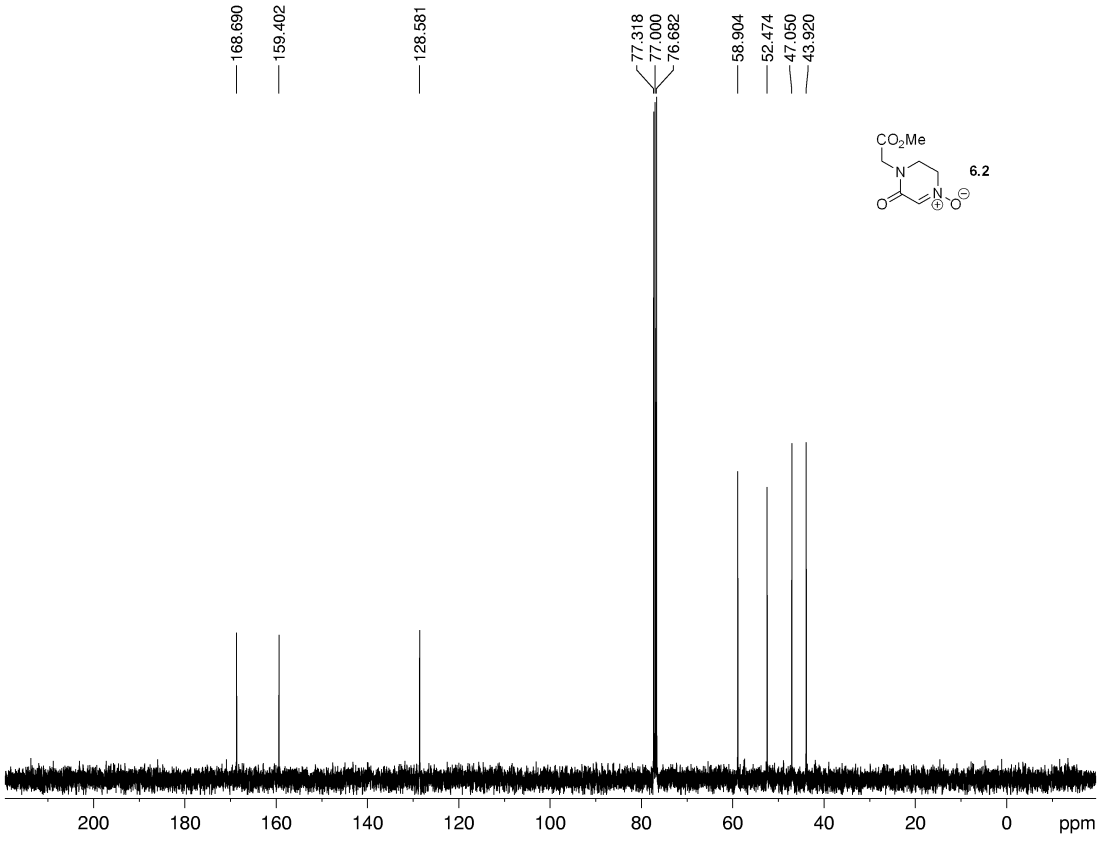
168.690
159.402
128.581
77.318
77.000
76.682
58.904
52.474
47.050
43.920
CO2Me
6.2
200
180
160
140
120
100
80
60
40
20
0
ppm

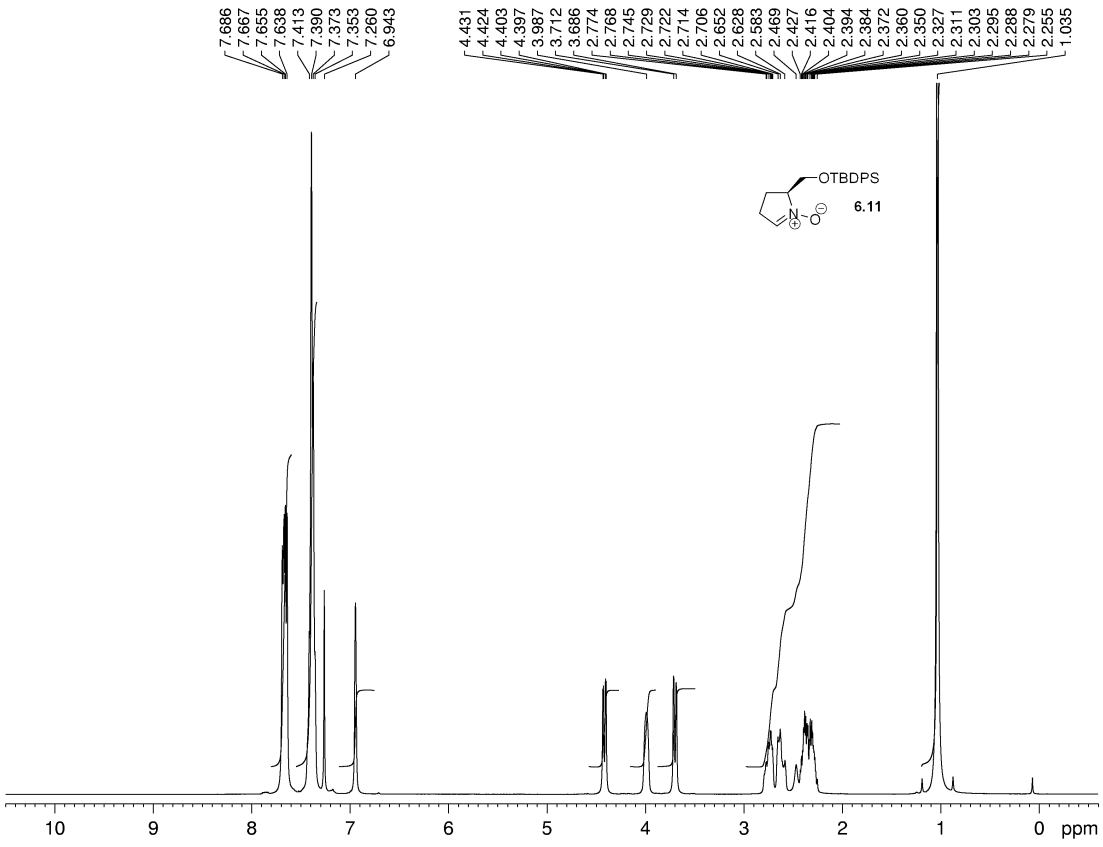
7.686
7.667
7.655
7.638
7.413
7.390
7.373
7.353
7.260
6.943
4.431
4.424
4.403
4.397
3.987
3.712
3.686
2.774
2.768
2.745
2.729
2.722
2.714
2.706
2.652
2.628
2.583
2.469
2.427
2.416
2.404
2.394
2.384
2.372
2.360
2.350
2.327
2.311
2.303
2.295
2.288
2.279
2.255
1.035
OTBDPS
6.11
10
9
8
7
6
5
4
3
2
1
0
ppm

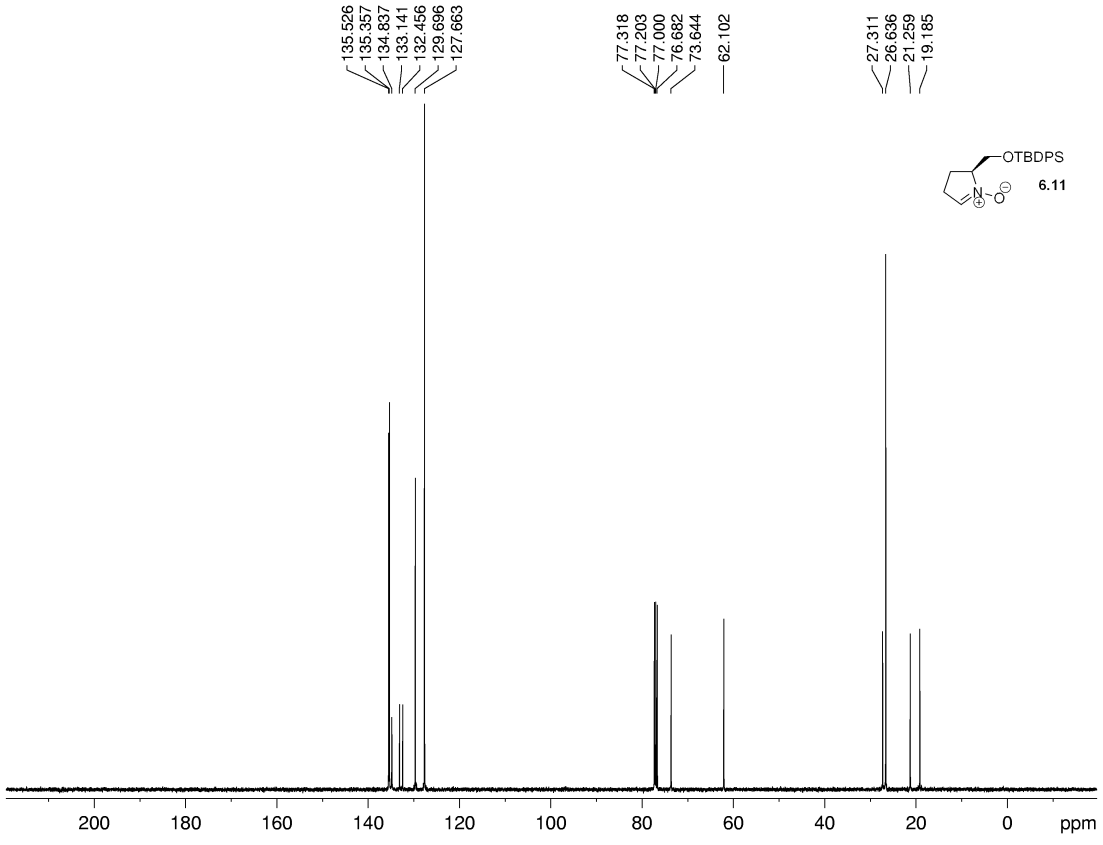
135.526
135.357
134.837
133.141
132.456
129.696
127.663
77.318
77.203
77.000
76.682
73.644
62.102
27.311
26.636
21.259
19.185
OTBDPS
6.11
200
180
160
140
120
100
80
60
40
20
0
ppm

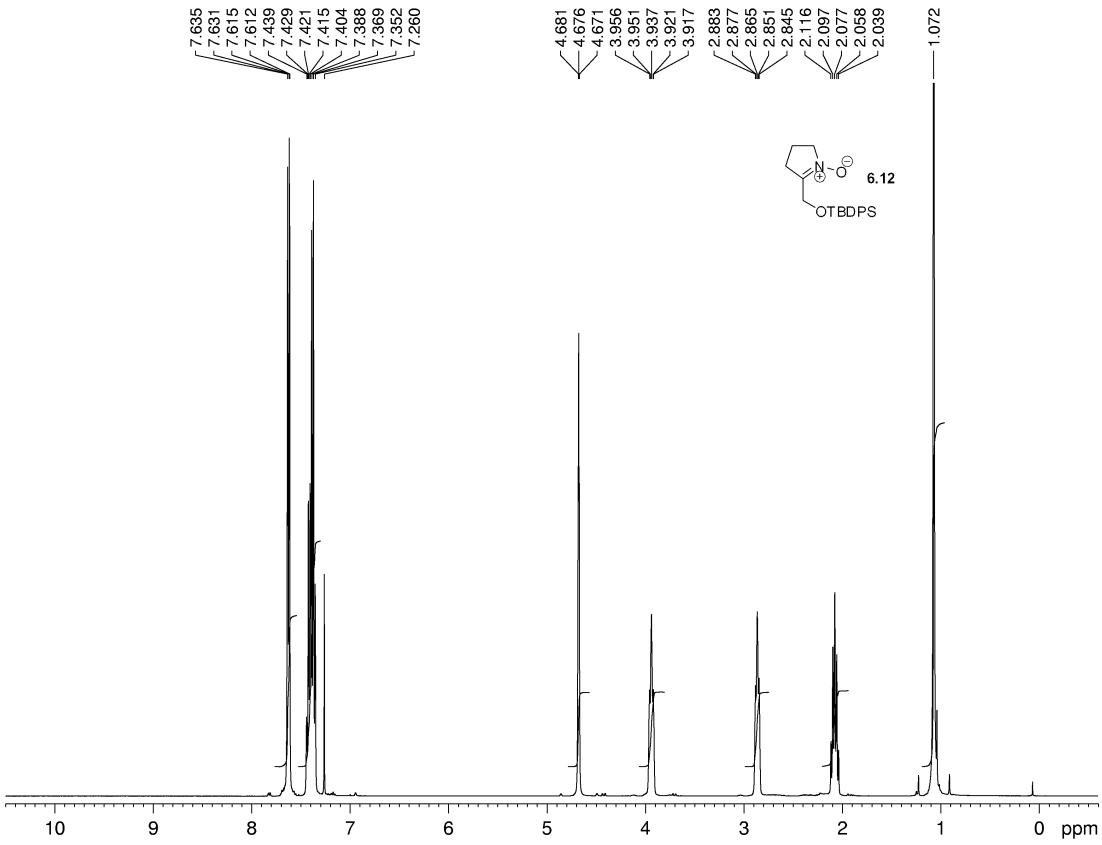
7.635
7.631
7.615
7.612
7.439
7.429
7.421
7.415
7.404
7.388
7.369
7.352
7.260
4.681
4.676
4.671
3.956
3.951
3.937
3.921
3.917
2.883
2.877
2.865
2.851
2.845
2.116
2.097
2.077
2.058
2.039
1.072
6.12
OTBDPS
10
9
8
7
6
5
4
3
2
1
0
ppm

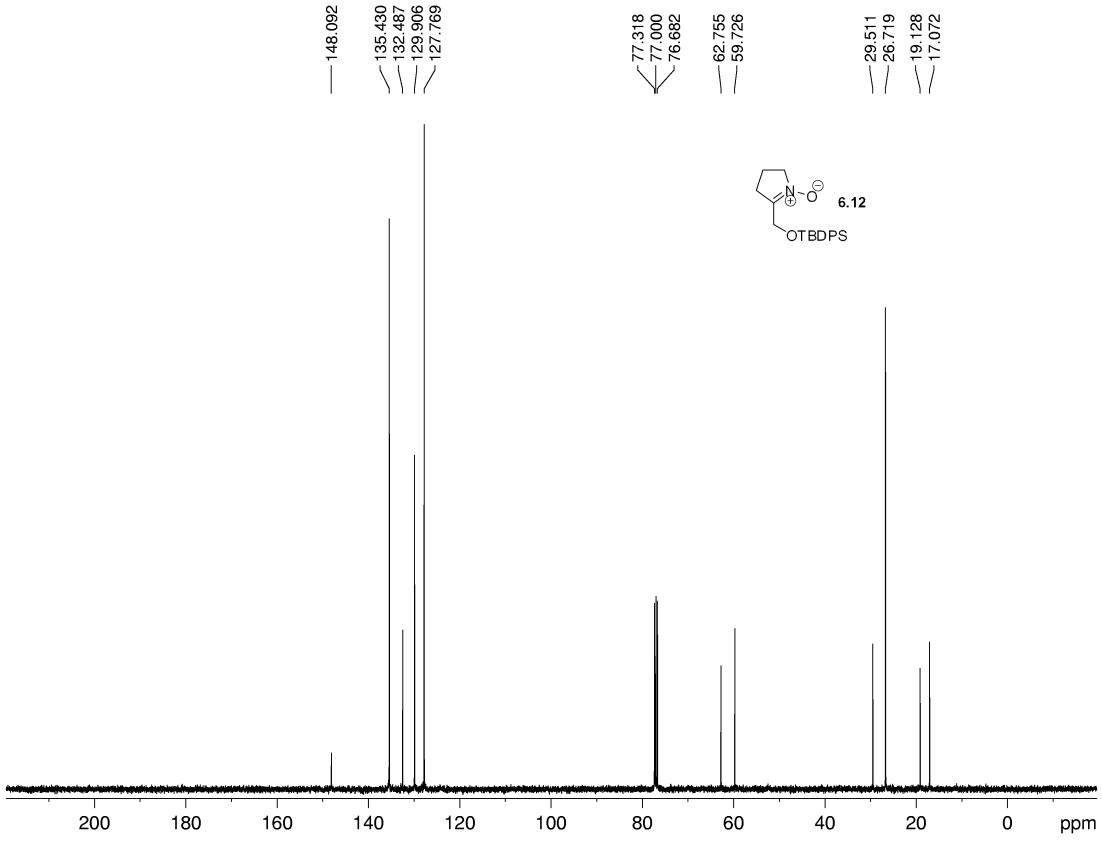
148.092
135.430
132.487
129.906
127.769
77.318
77.000
76.682
62.755
59.726
29.511
26.719
19.128
17.072
6.12
OTBDPS
200
180
160
140
120
100
80
60
40
20
0
ppm

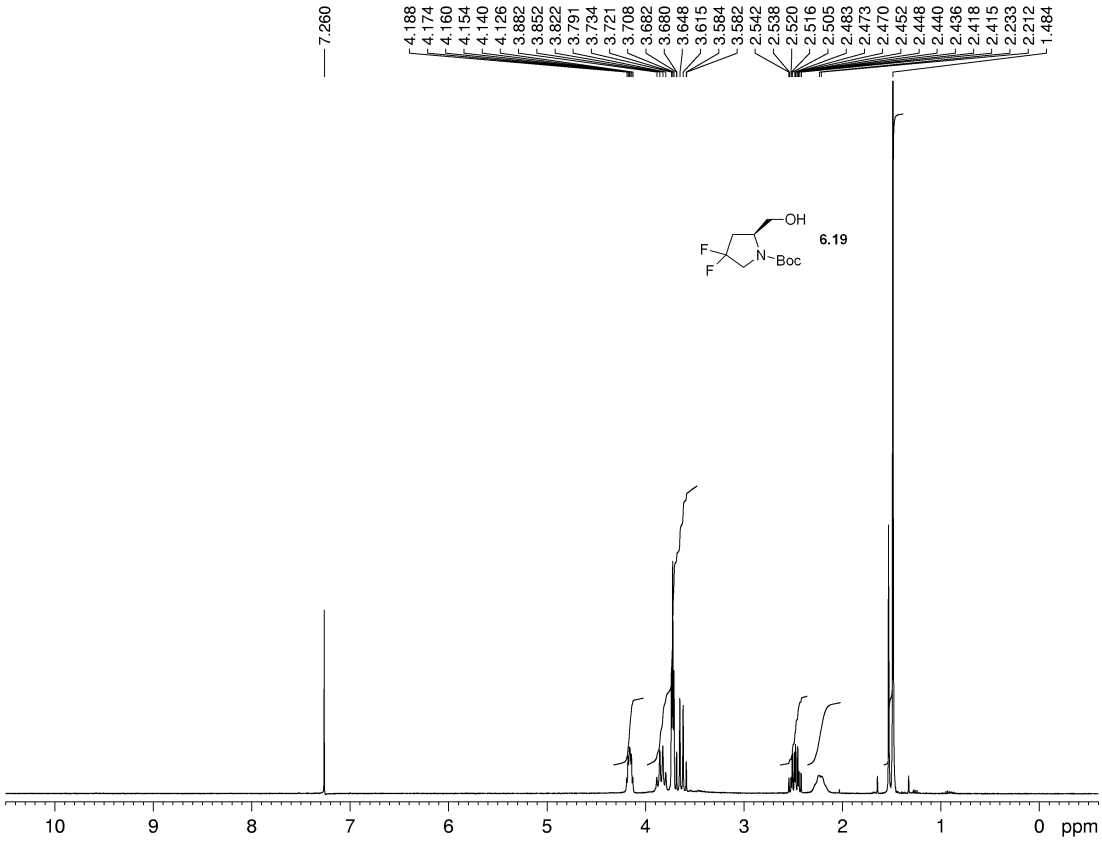
7.260
4.188
4.174
4.160
4.154
4.140
4.126
3.882
3.852
3.822
3.791
3.734
3.721
3.708
3.682
3.680
3.648
3.615
3.584
3.582
2.542
2.538
2.520
2.516
2.505
2.483
2.473
2.470
2.452
2.448
2.440
2.436
2.418
2.415
2.233
2.212
1.484
OH
F
F
N
Boc
6.19
10
9
8
7
6
5
4
3
2
1
0
ppm

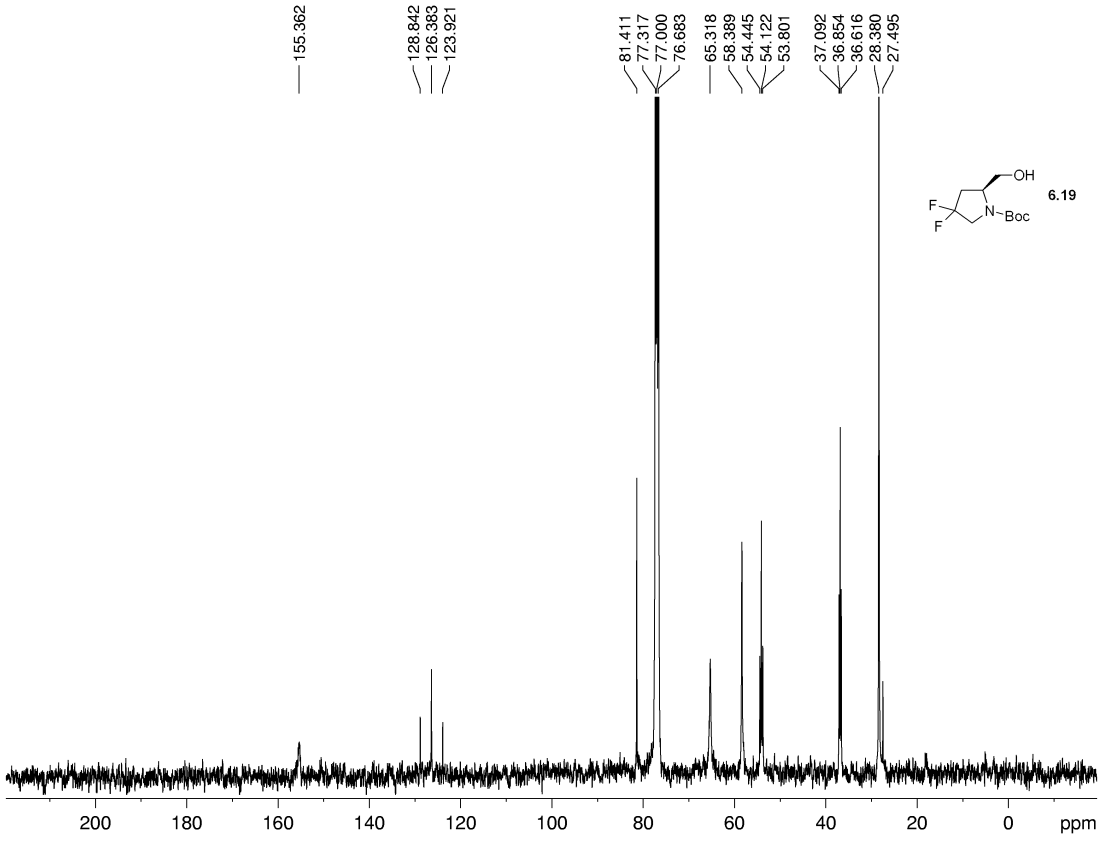
155.362
128.842
126.383
123.921
81.411
77.317
77.000
76.683
65.318
58.389
54.445
54.122
53.801
37.092
36.854
36.616
28.380
27.495
OH
F
F
N
Boc
6.19
200
180
160
140
120
100
80
60
40
20
0
ppm

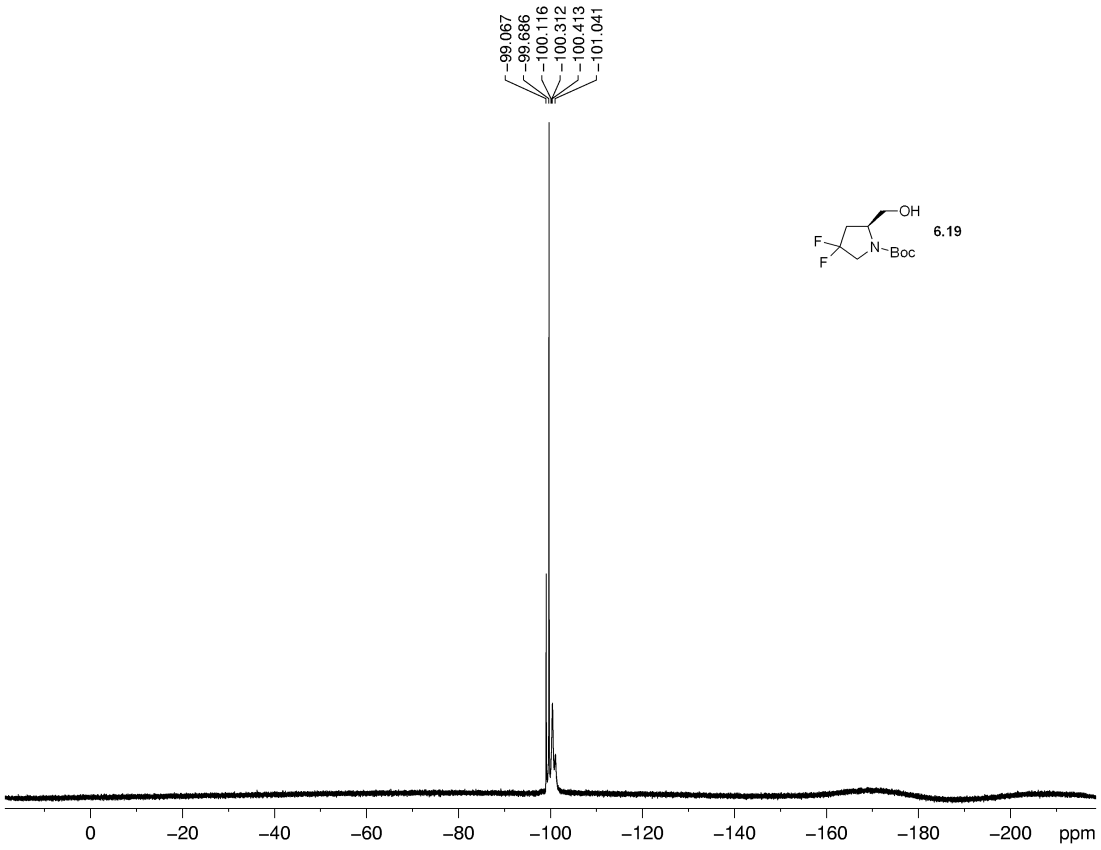
-99.067
-99.686
-100.116
-100.312
-100.413
-101.041
OH
F
F
N
Boc
6.19
0
−20
−40
−60
−80
−100
−120
−140
−160
−180
−200
ppm

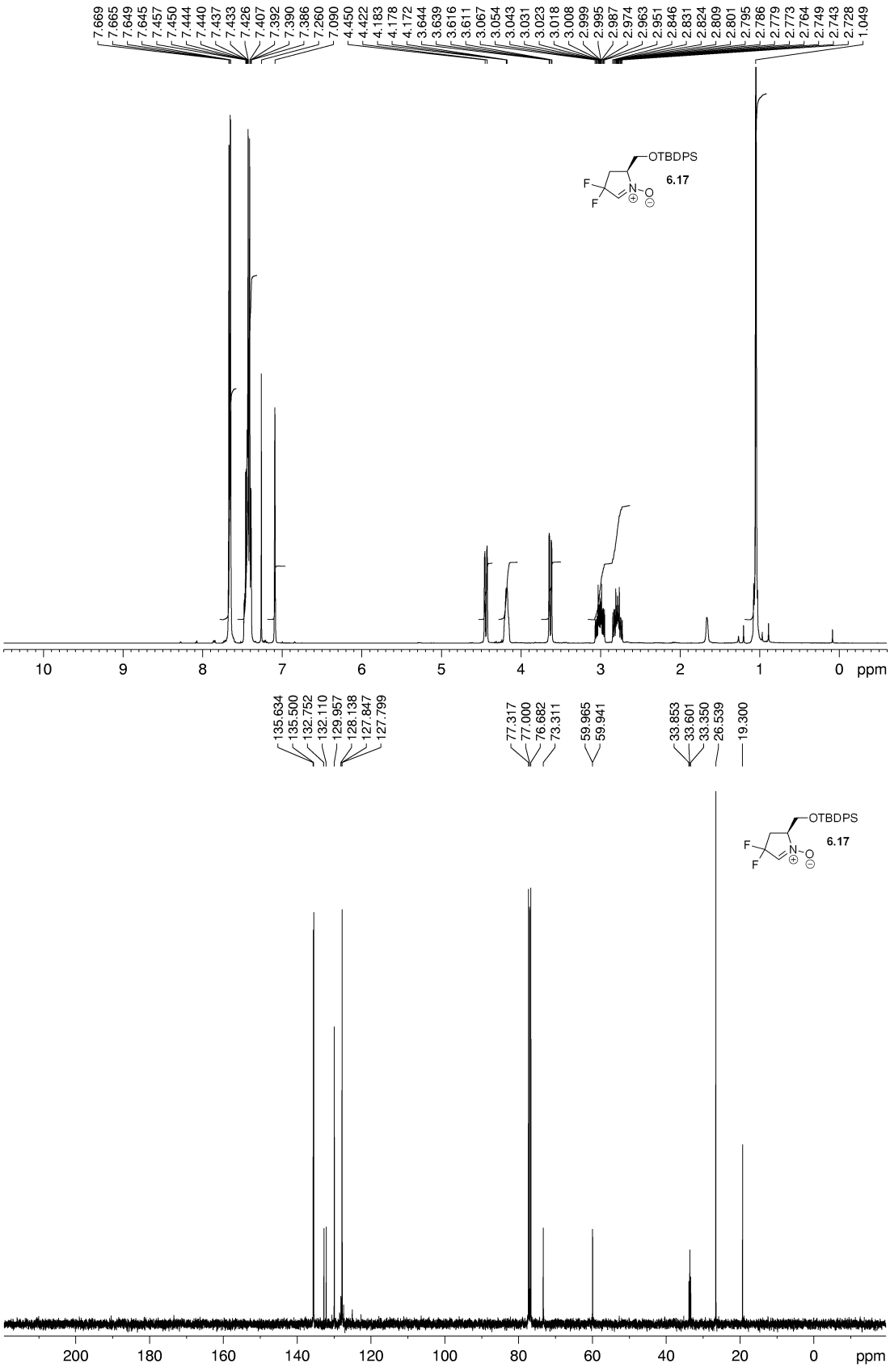
7.669
7.665
7.649
7.645
7.457
7.450
7.444
7.440
7.437
7.433
7.426
7.407
7.392
7.390
7.386
7.260
7.090
4.450
4.422
4.183
4.178
4.172
3.644
3.639
3.616
3.611
3.067
3.054
3.043
3.031
3.023
3.018
3.008
2.999
2.995
2.987
2.974
2.963
2.951
2.846
2.831
2.824
2.809
2.801
2.795
2.786
2.779
2.773
2.764
2.749
2.743
2.728
1.049
OTBDPS
6.17
F
F
N
O
10
9
8
7
6
5
4
3
2
1
0
ppm
135.634
135.500
132.752
132.110
129.957
128.138
127.847
127.799
77.317
77.000
76.682
73.311
59.965
59.941
33.853
33.601
33.350
26.539
19.300
OTBDPS
6.17
F
F
N
O
200
180
160
140
120
100
80
60
40
20
0
ppm

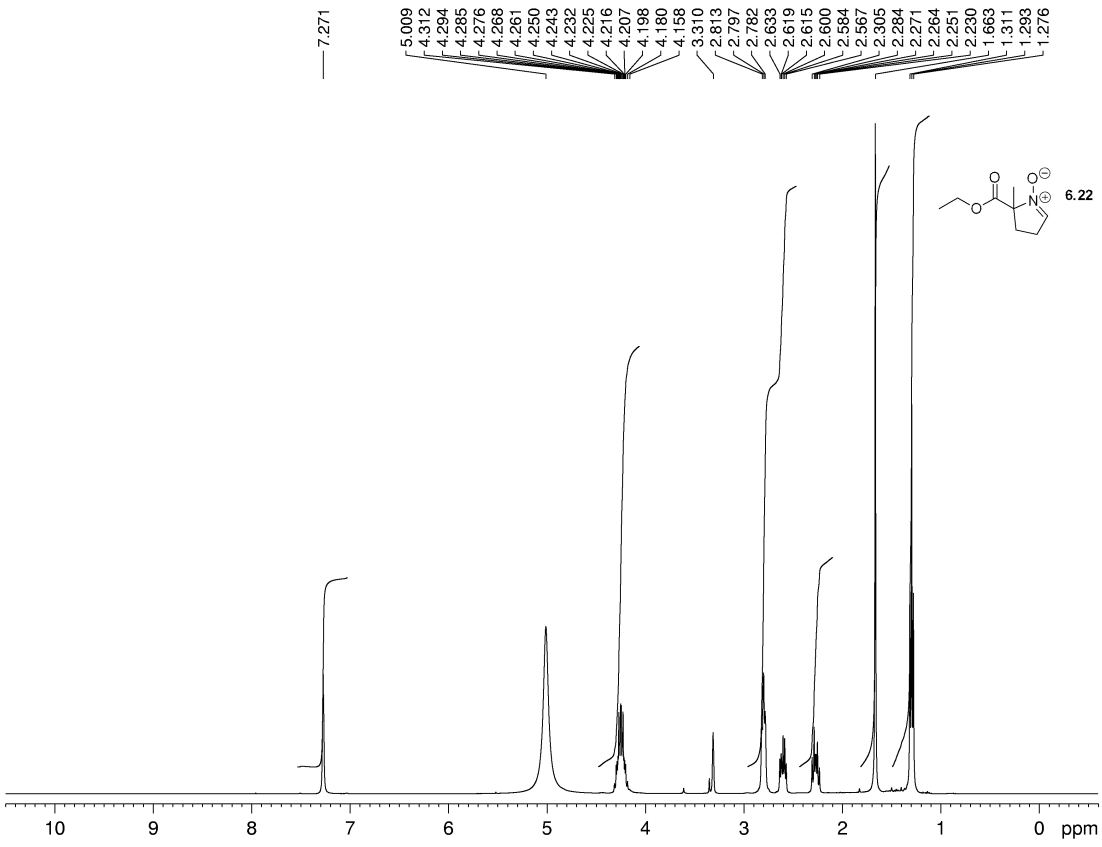
7.271
5.009
4.312
4.294
4.285
4.276
4.268
4.261
4.250
4.243
4.232
4.225
4.216
4.207
4.198
4.180
4.158
3.310
2.813
2.797
2.782
2.633
2.619
2.615
2.600
2.584
2.567
2.305
2.284
2.271
2.264
2.251
2.230
1.663
1.311
1.293
1.276
6.22
10
9
8
7
6
5
4
3
2
1
0
ppm

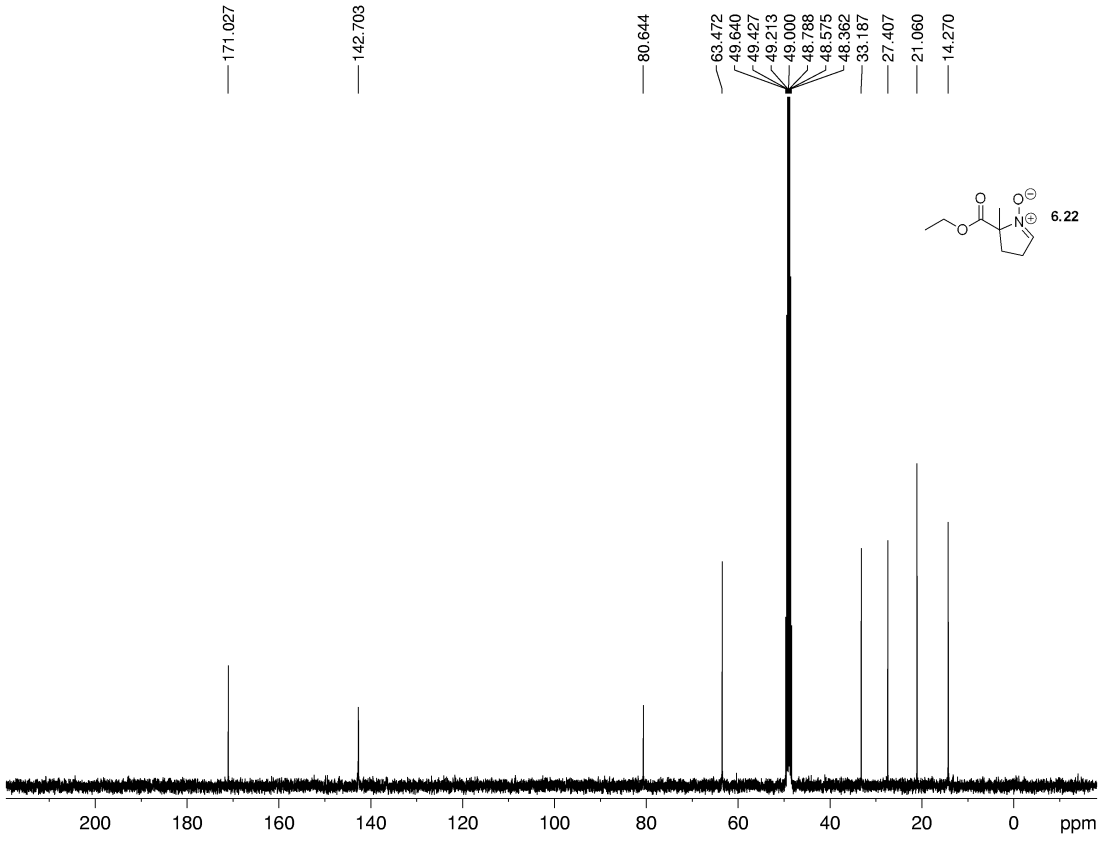
171.027
142.703
80.644
63.472
49.640
49.427
49.213
49.000
48.788
48.575
48.362
33.187
27.407
21.060
14.270
6.22
200
180
160
140
120
100
80
60
40
20
0
ppm

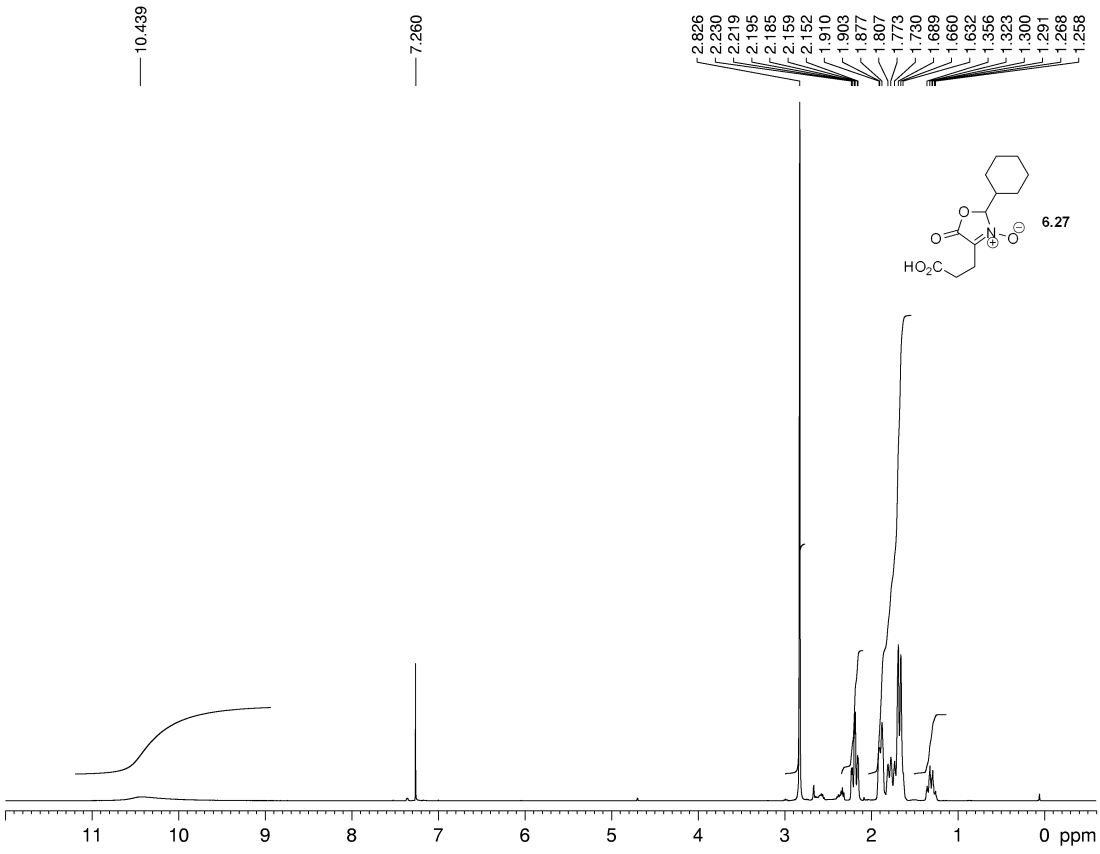
10.439
7.260
2.826
2.230
2.219
2.195
2.185
2.159
2.152
1.910
1.903
1.877
1.807
1.773
1.730
1.689
1.660
1.632
1.356
1.323
1.300
1.291
1.268
1.258
6.27
11
10
9
8
7
6
5
4
3
2
1
0 ppm

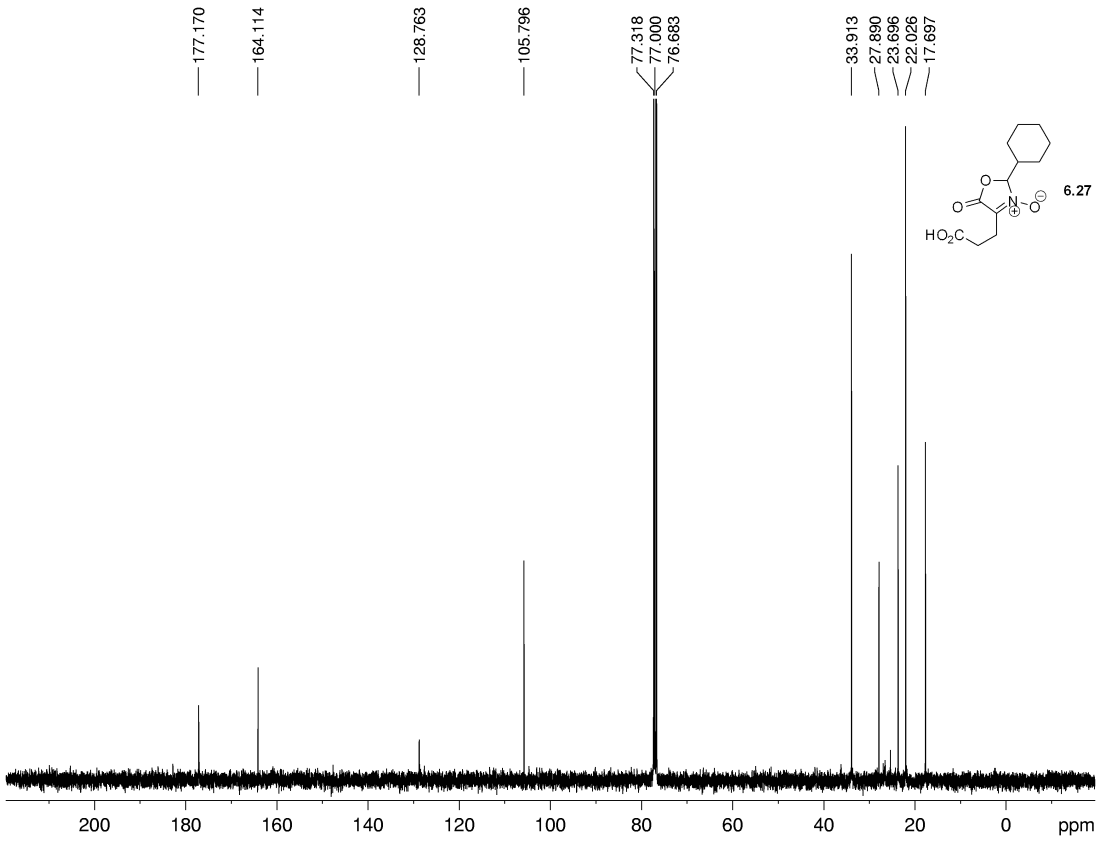
177.170
164.114
128.763
105.796
77.318
77.000
76.683
33.913
27.890
23.696
22.026
17.697
6.27
200
180
160
140
120
100
80
60
40
20
0
ppm

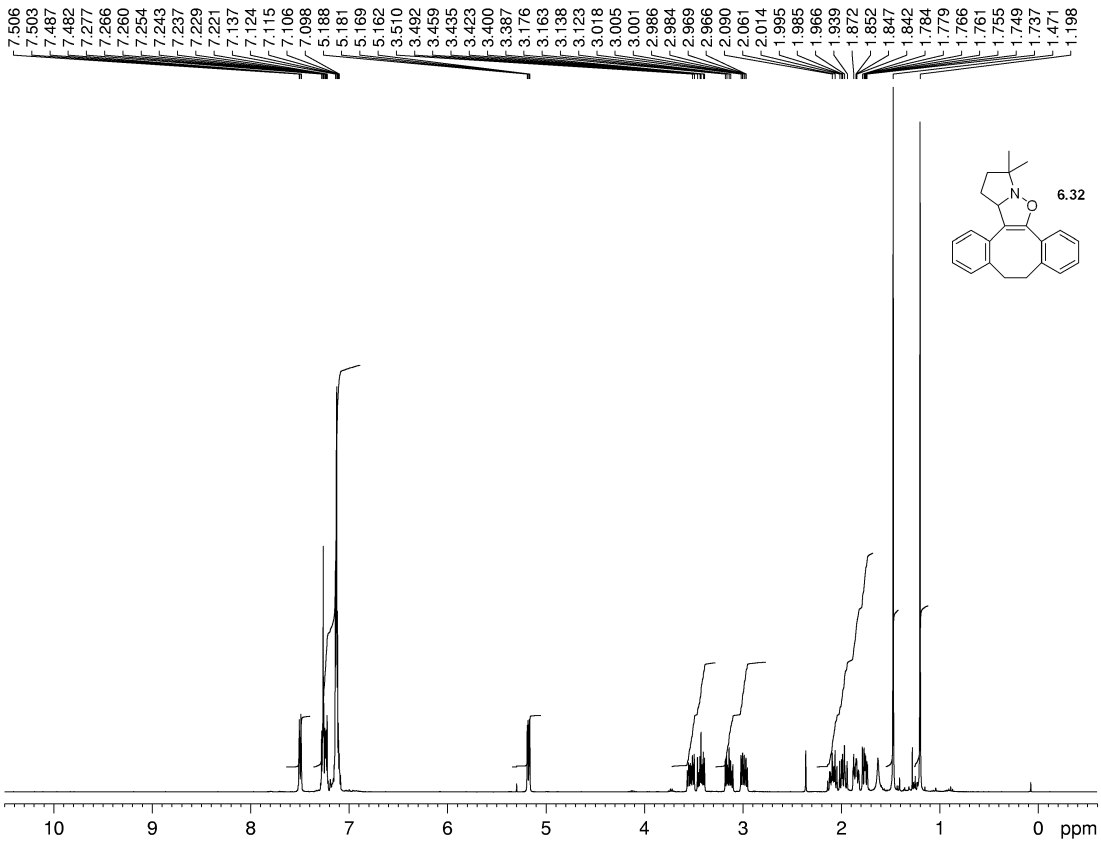
7.506
7.503
7.487
7.482
7.277
7.266
7.260
7.254
7.243
7.237
7.229
7.221
7.137
7.124
7.115
7.106
7.098
5.188
5.181
5.169
5.162
3.510
3.492
3.459
3.435
3.423
3.400
3.387
3.176
3.163
3.138
3.123
3.018
3.005
3.001
2.986
2.984
2.969
2.966
2.090
2.061
2.014
1.995
1.985
1.966
1.939
1.872
1.852
1.847
1.842
1.784
1.779
1.766
1.761
1.755
1.749
1.737
1.471
1.198
6.32
10
9
8
7
6
5
4
3
2
1
0
ppm

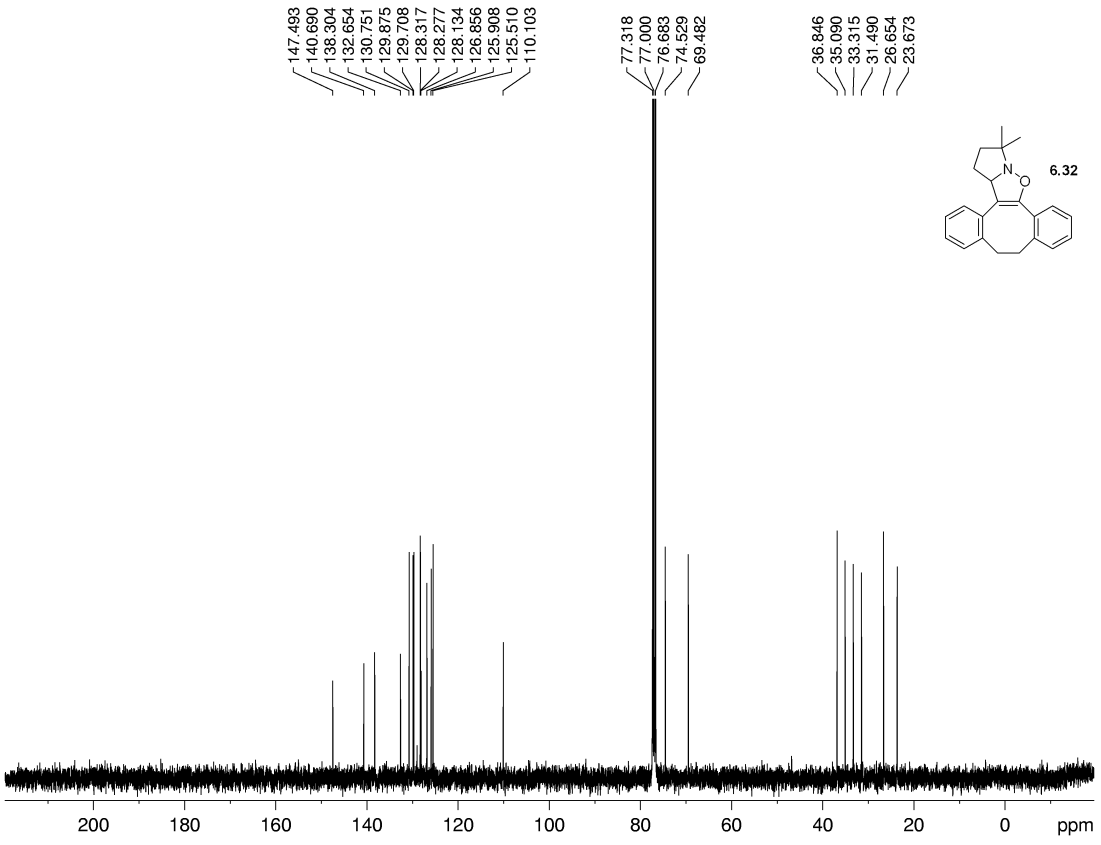
147.493
140.690
138.304
132.654
130.751
129.875
129.708
128.317
128.277
128.134
126.856
125.908
125.510
110.103
77.318
77.000
76.683
74.529
69.482
36.846
35.090
33.315
31.490
26.654
23.673
6.32
200
180
160
140
120
100
80
60
40
20
0
ppm

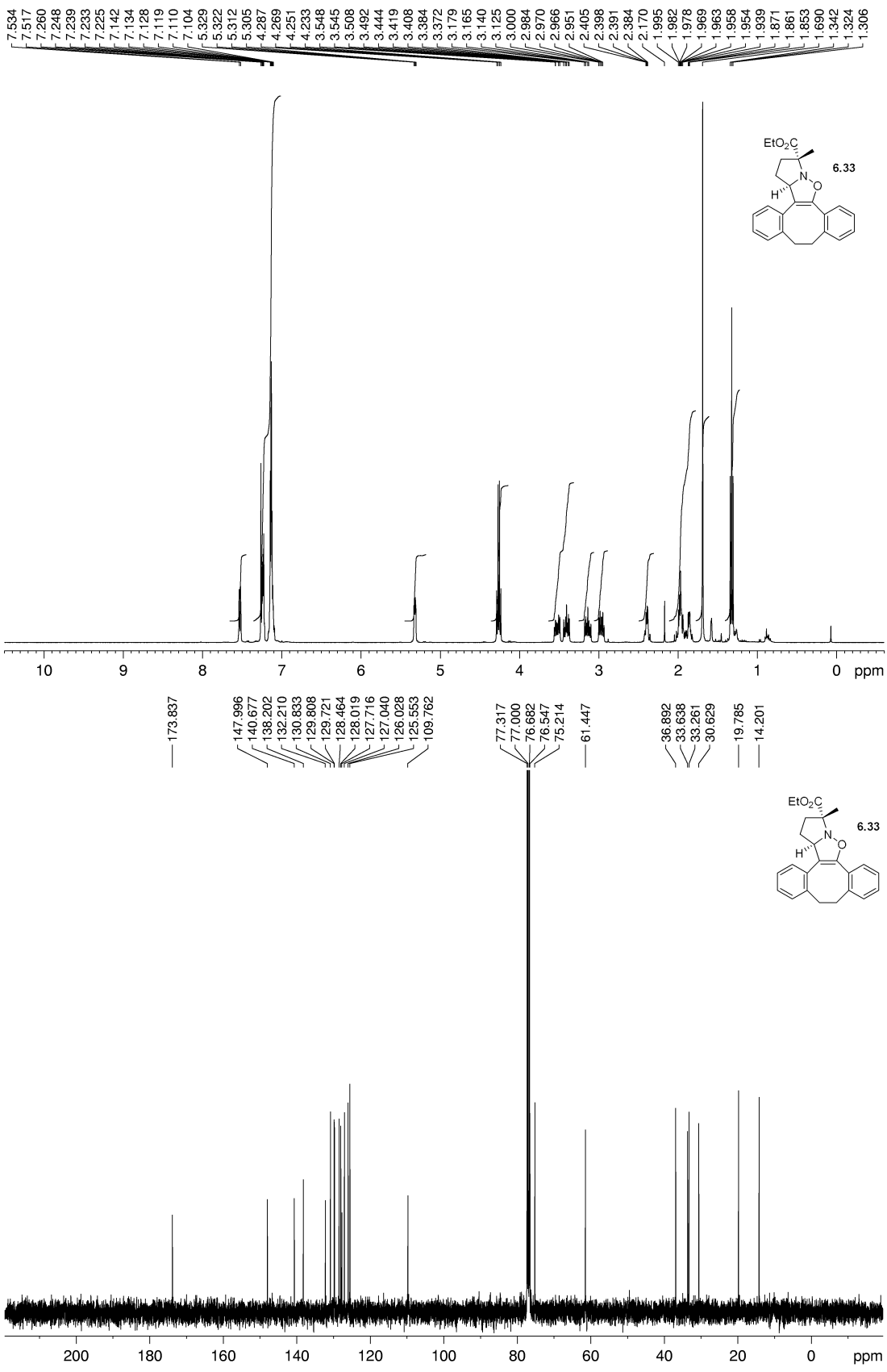
7.534
7.517
7.260
7.248
7.239
7.233
7.225
7.142
7.134
7.128
7.119
7.110
7.104
5.329
5.322
5.312
5.305
4.287
4.269
4.251
4.233
3.548
3.545
3.508
3.492
3.444
3.419
3.408
3.384
3.372
3.179
3.165
3.140
3.125
3.000
2.984
2.970
2.966
2.951
2.405
2.398
2.391
2.384
2.170
1.995
1.982
1.978
1.969
1.963
1.958
1.954
1.939
1.871
1.861
1.853
1.690
1.342
1.324
1.306
EtO2C
6.33
10
9
8
7
6
5
4
3
2
1
0
ppm
173.837
147.996
140.677
138.202
132.210
130.833
129.808
129.721
128.464
128.019
127.716
127.040
126.028
125.553
109.762
77.317
77.000
76.682
76.547
75.214
61.447
36.892
33.638
33.261
30.629
19.785
14.201
EtO2C
6.33
200
180
160
140
120
100
80
60
40
20
0
ppm

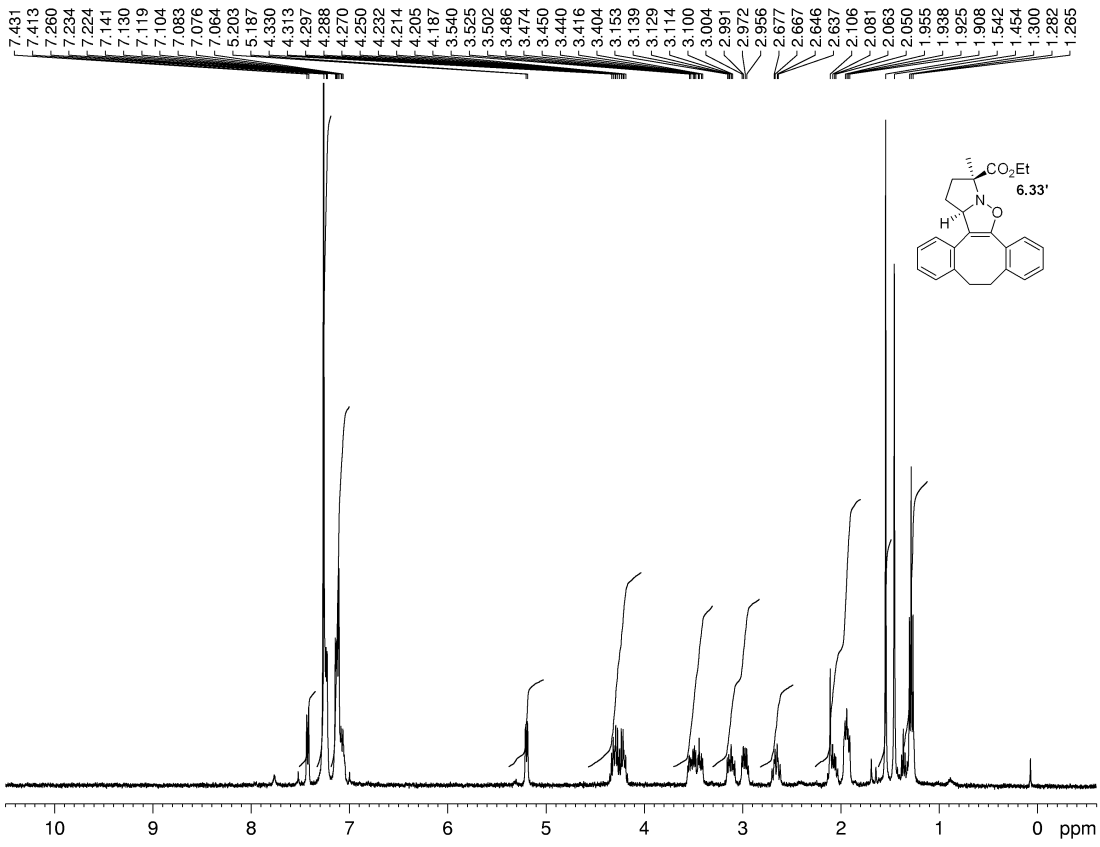
7.431
7.413
7.260
7.234
7.224
7.141
7.130
7.119
7.104
7.083
7.076
7.064
5.203
5.187
4.330
4.313
4.297
4.288
4.270
4.250
4.232
4.214
4.205
4.187
3.540
3.525
3.502
3.486
3.474
3.450
3.440
3.416
3.404
3.153
3.139
3.129
3.114
3.100
3.004
2.991
2.972
2.956
2.677
2.667
2.646
2.637
2.106
2.081
2.063
2.050
1.955
1.938
1.925
1.908
1.542
1.454
1.300
1.282
1.265
CO2Et
6.33'
H
N
O
10
9
8
7
6
5
4
3
2
1
0
ppm

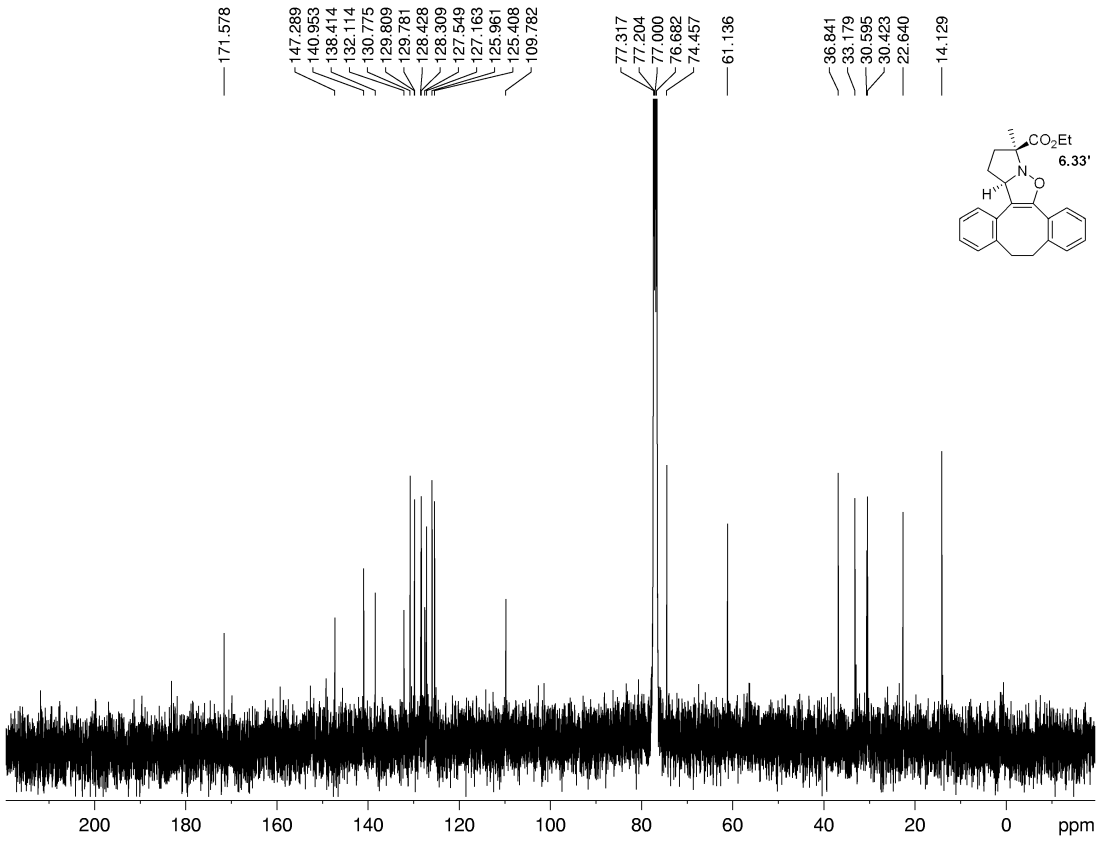
171.578
147.289
140.953
138.414
132.114
130.775
129.809
129.781
128.428
128.309
127.549
127.163
125.961
125.408
109.782
77.317
77.204
77.000
76.682
74.457
61.136
36.841
33.179
30.595
30.423
22.640
14.129
CO2Et
6.33'
H
N
O
200
180
160
140
120
100
80
60
40
20
0
ppm

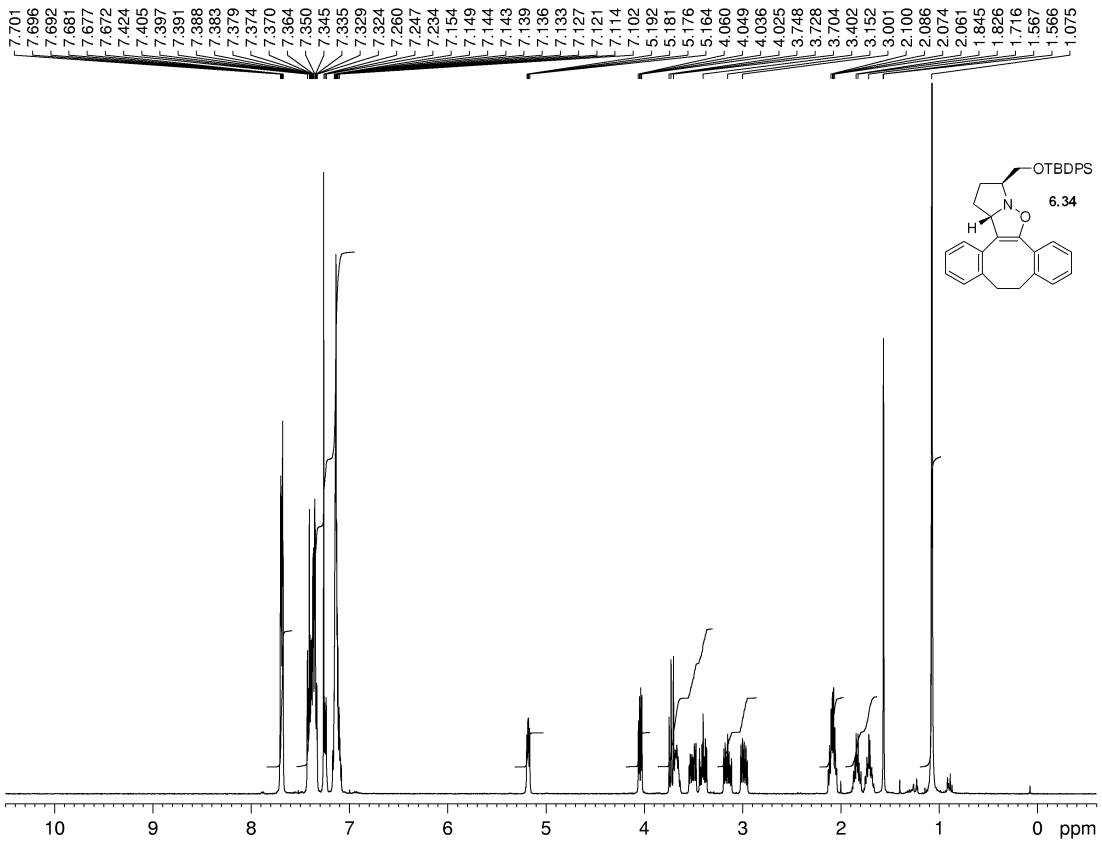
7.701
7.696
7.692
7.681
7.677
7.672
7.424
7.405
7.397
7.391
7.388
7.383
7.379
7.374
7.370
7.364
7.350
7.345
7.335
7.329
7.324
7.260
7.247
7.234
7.154
7.149
7.144
7.143
7.139
7.136
7.133
7.127
7.121
7.114
7.102
5.192
5.181
5.176
5.164
4.060
4.049
4.036
4.025
3.748
3.728
3.704
3.402
3.152
3.001
2.100
2.086
2.074
2.061
1.845
1.826
1.716
1.567
1.566
1.075
OTBDPS
6.34
10
9
8
7
6
5
4
3
2
1
0
ppm

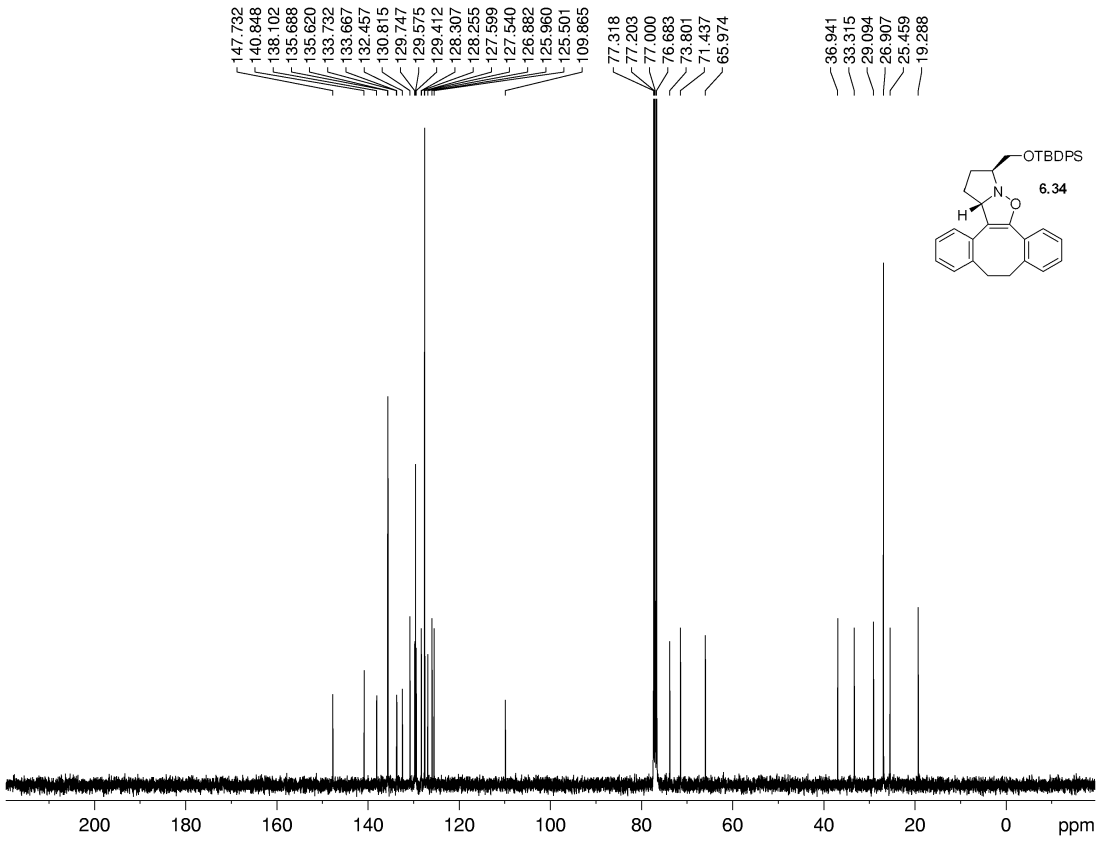
147.732
140.848
138.102
135.688
135.620
133.732
133.667
132.457
130.815
129.747
129.575
129.412
128.307
128.255
127.599
127.540
126.882
125.960
125.501
109.865
77.318
77.203
77.000
76.683
73.801
71.437
65.974
36.941
33.315
29.094
26.907
25.459
19.288
OTBDPS
6.34
200
180
160
140
120
100
80
60
40
20
0
ppm

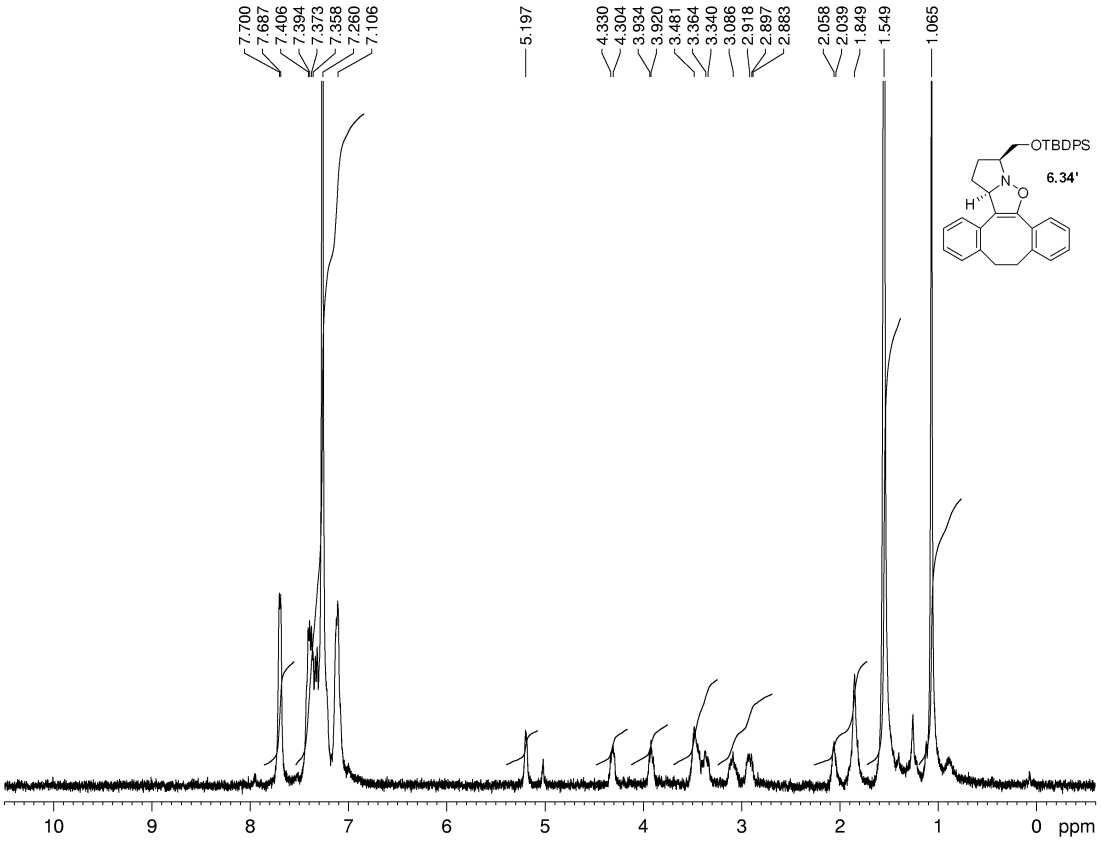
7.700
7.687
7.406
7.394
7.373
7.358
7.260
7.106
5.197
4.330
4.304
3.934
3.920
3.481
3.364
3.340
3.086
2.918
2.897
2.883
2.058
2.039
1.849
1.549
1.065
OTBDPS
6.34'
10
9
8
7
6
5
4
3
2
1
0
ppm

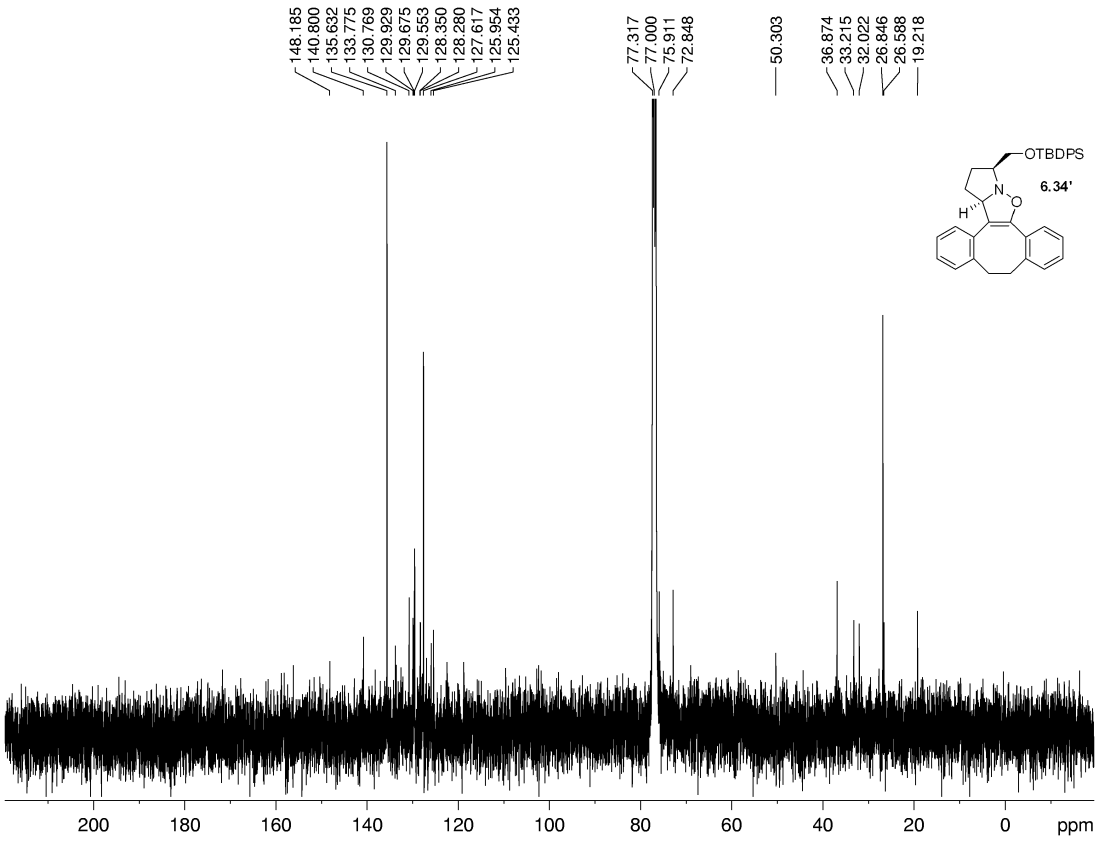
148.185
140.800
135.632
133.775
130.769
129.929
129.675
129.553
128.350
128.280
127.617
125.954
125.433
77.317
77.000
75.911
72.848
50.303
36.874
33.215
32.022
26.846
26.588
19.218
OTBDPS
6.34'
200
180
160
140
120
100
80
60
40
20
0
ppm

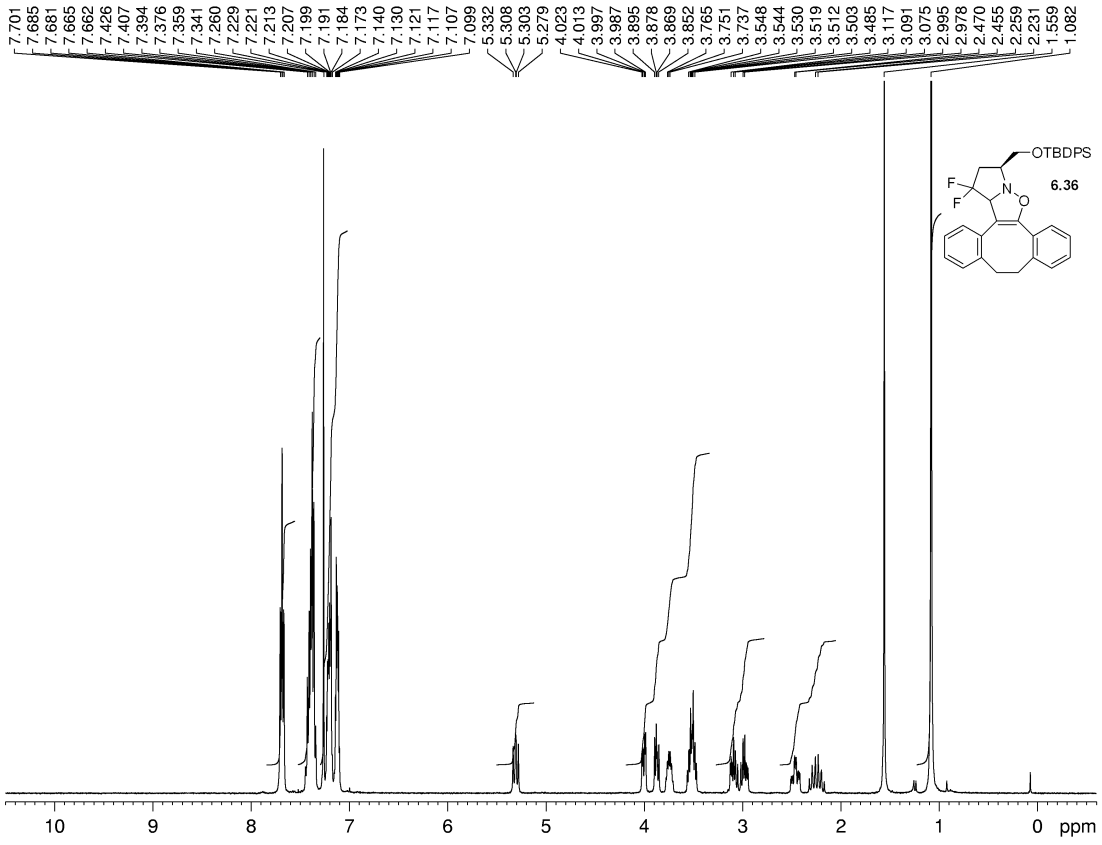
7.701
7.685
7.681
7.665
7.662
7.426
7.407
7.394
7.376
7.359
7.341
7.260
7.229
7.221
7.213
7.207
7.199
7.191
7.184
7.173
7.140
7.130
7.121
7.117
7.107
7.099
5.332
5.308
5.303
5.279
4.023
4.013
3.997
3.987
3.895
3.878
3.869
3.852
3.765
3.751
3.737
3.548
3.544
3.530
3.519
3.512
3.503
3.485
3.117
3.091
3.075
2.995
2.978
2.470
2.455
2.259
2.231
1.559
1.082
OTBDPS
F
F
N
O
6.36
10
9
8
7
6
5
4
3
2
1
0
ppm

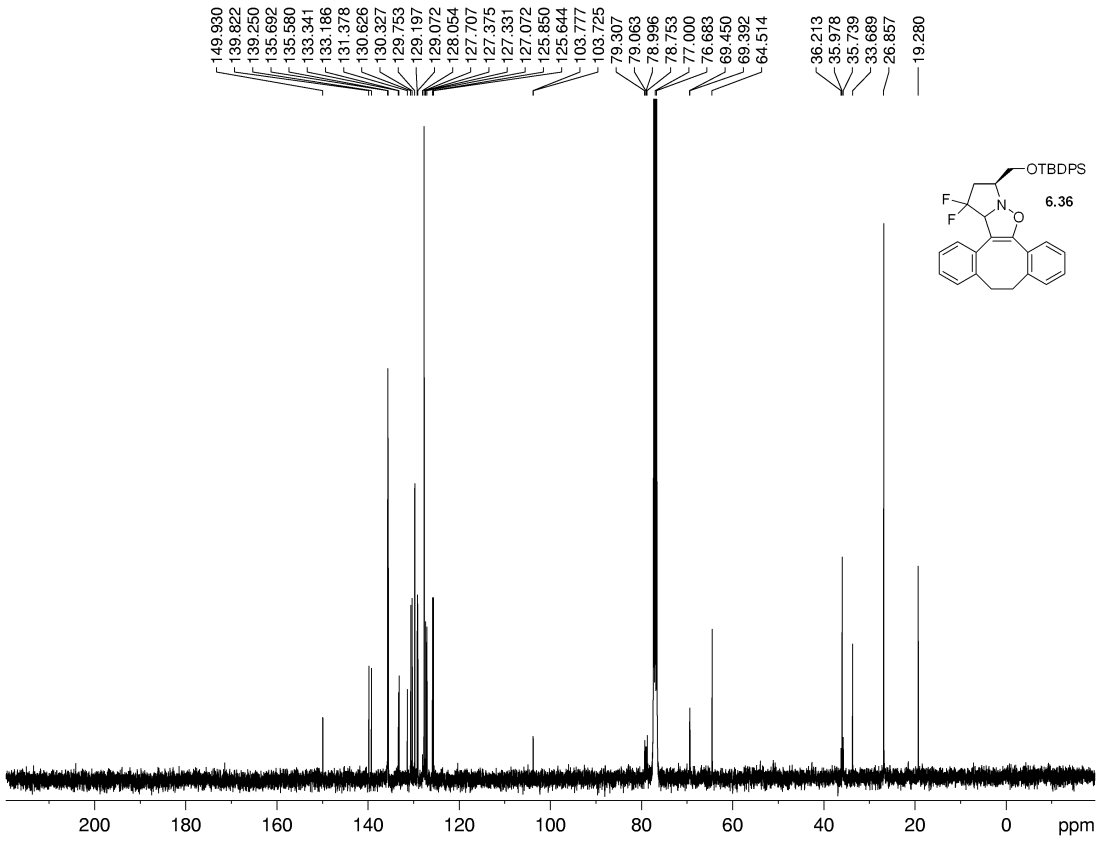
149.930
139.822
139.250
135.692
135.580
133.341
133.186
131.378
130.626
130.327
129.753
129.197
129.072
128.054
127.707
127.375
127.331
127.072
125.850
125.644
103.777
103.725
79.307
79.063
78.996
78.753
77.000
76.683
69.450
69.392
64.514
36.213
35.978
35.739
33.689
26.857
19.280
OTBDPS
F
F
N
O
6.36
200
180
160
140
120
100
80
60
40
20
0
ppm

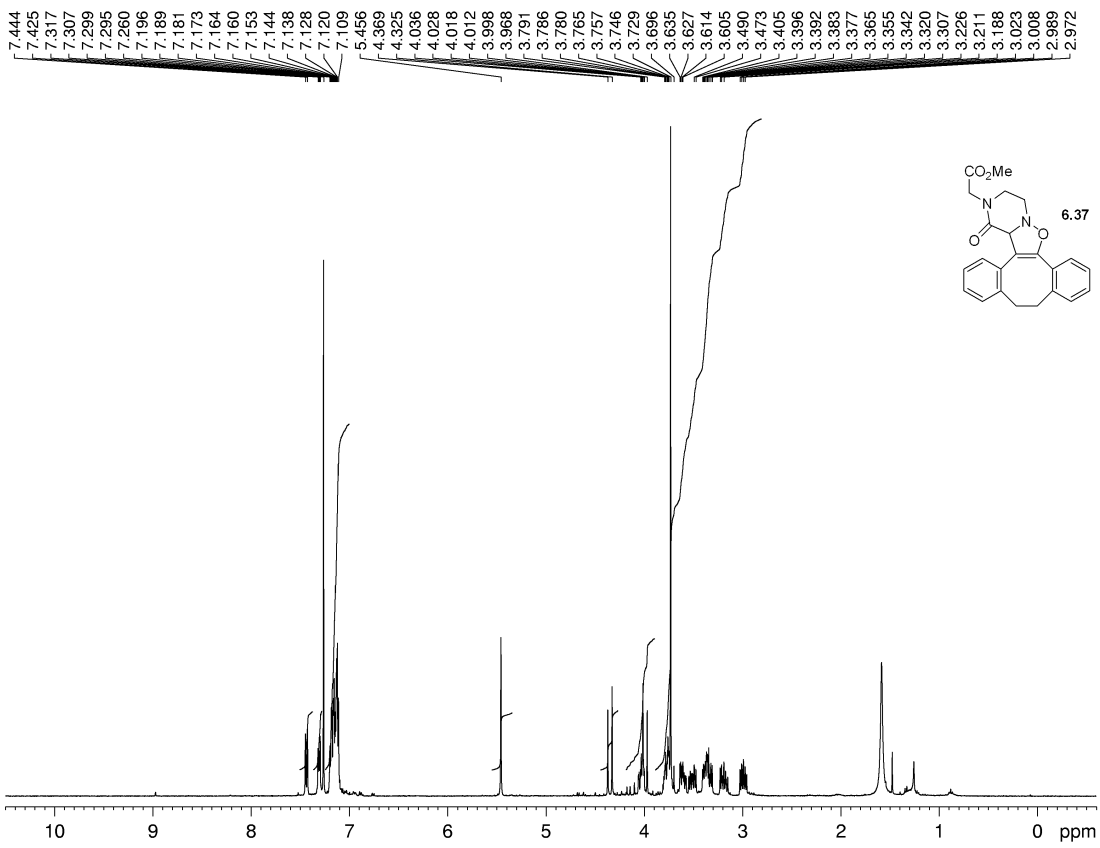
7.444
7.425
7.317
7.307
7.299
7.295
7.260
7.196
7.189
7.181
7.173
7.164
7.160
7.153
7.144
7.138
7.128
7.120
7.109
5.456
4.369
4.325
4.036
4.028
4.018
4.012
3.998
3.968
3.791
3.786
3.780
3.765
3.757
3.746
3.729
3.696
3.635
3.627
3.614
3.605
3.490
3.473
3.405
3.396
3.392
3.383
3.377
3.365
3.355
3.342
3.320
3.307
3.226
3.211
3.188
3.023
3.008
2.989
2.972
CO2Me
6.37
10
9
8
7
6
5
4
3
2
1
0
ppm

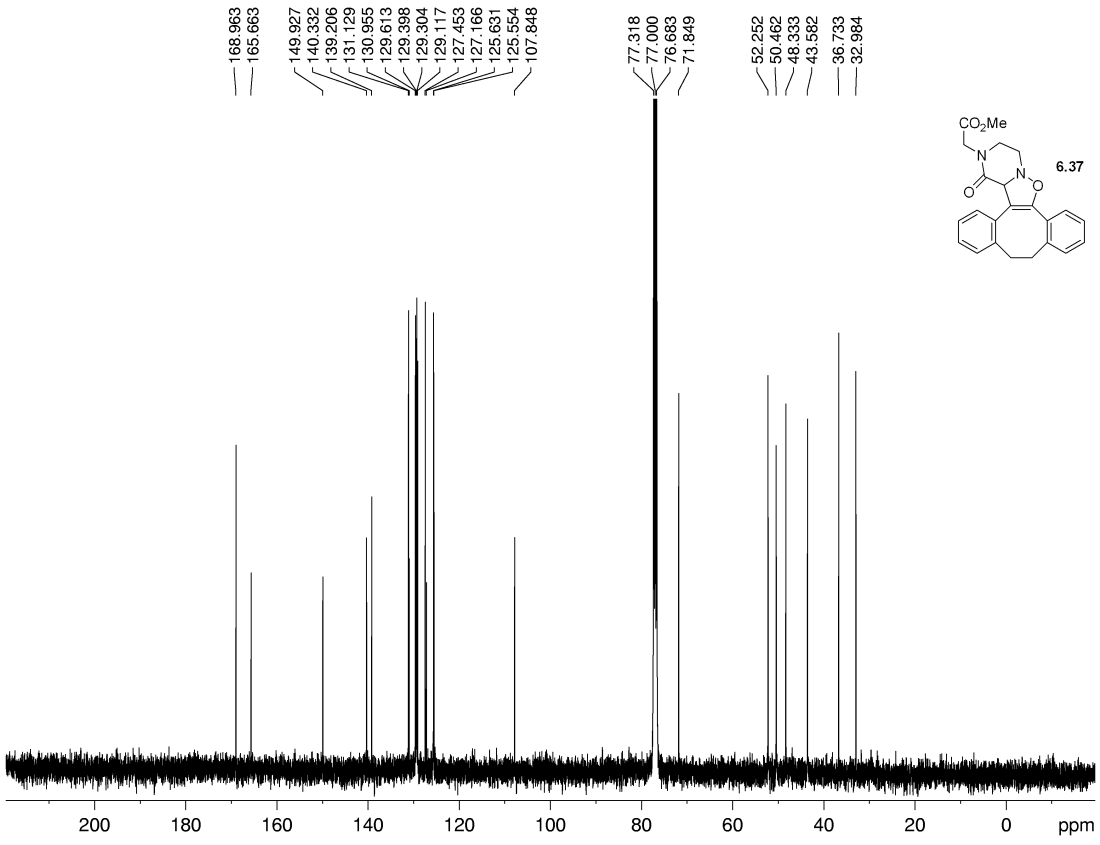
168.963
165.663
149.927
140.332
139.206
131.129
130.955
129.613
129.398
129.304
129.117
127.453
127.166
125.631
125.554
107.848
77.318
77.000
76.683
71.849
52.252
50.462
48.333
43.582
36.733
32.984
CO2Me
6.37
200
180
160
140
120
100
80
60
40
20
0
ppm

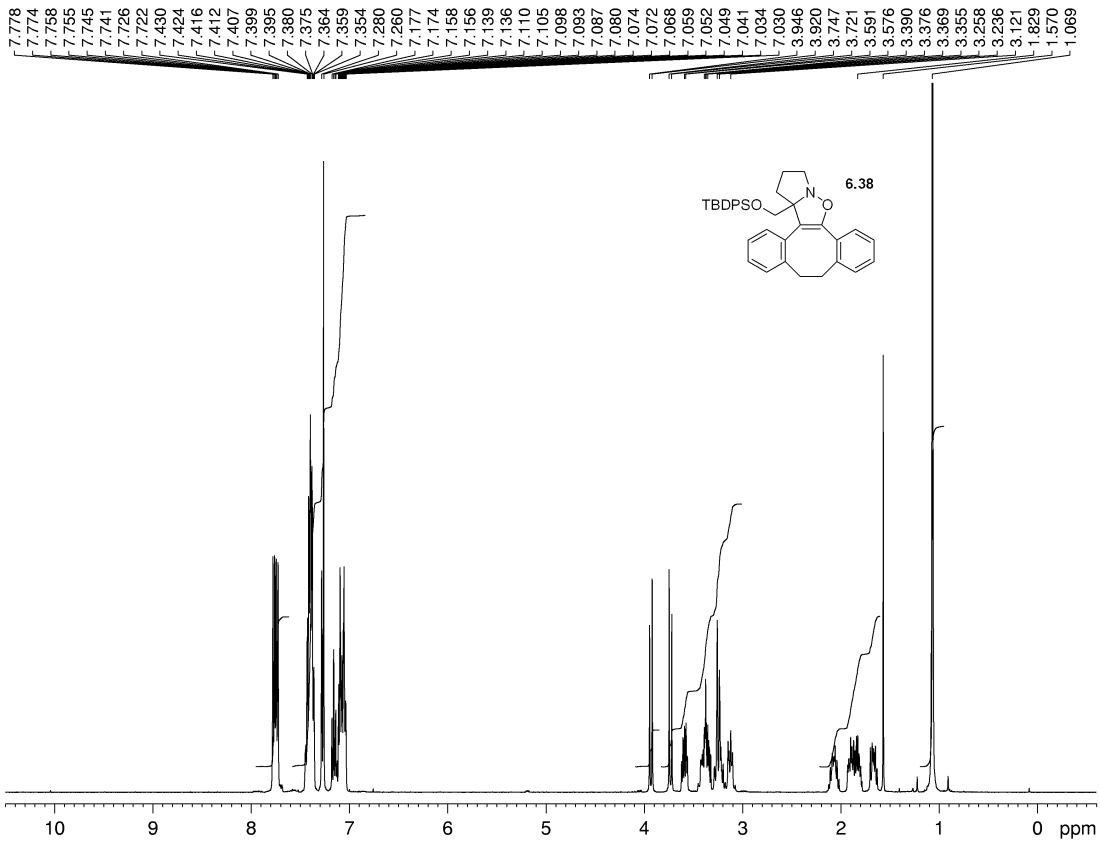
7.778
7.774
7.758
7.755
7.745
7.741
7.726
7.722
7.430
7.424
7.416
7.412
7.407
7.399
7.395
7.380
7.375
7.364
7.359
7.354
7.280
7.260
7.177
7.174
7.158
7.156
7.139
7.136
7.110
7.105
7.098
7.093
7.087
7.080
7.074
7.072
7.068
7.059
7.052
7.049
7.041
7.034
7.030
3.946
3.920
3.747
3.721
3.591
3.576
3.390
3.376
3.369
3.355
3.258
3.236
3.121
1.829
1.570
1.069
TBDPSO
N
O
6.38
10
9
8
7
6
5
4
3
2
1
0
ppm

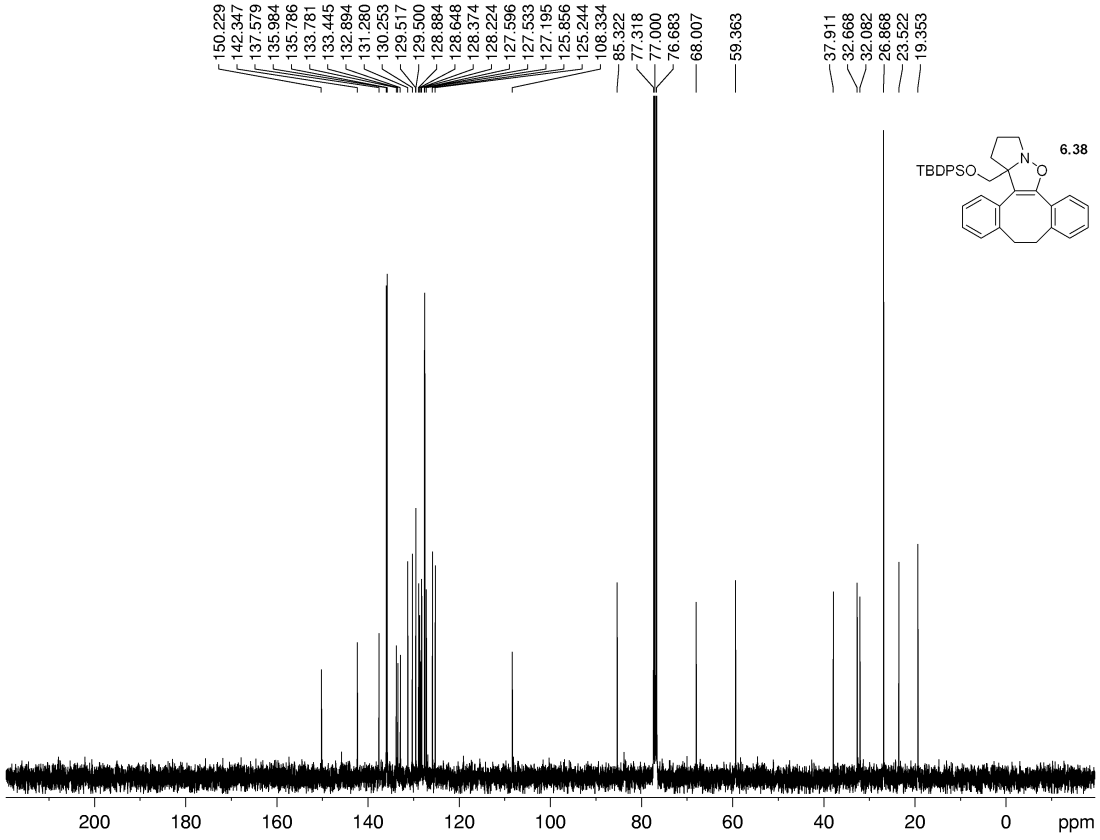
150.229
142.347
137.579
135.984
135.786
133.781
133.445
132.894
131.280
130.253
129.517
129.500
128.884
128.648
128.374
128.224
127.596
127.533
127.195
125.856
125.244
108.334
85.322
77.318
77.000
76.683
68.007
59.363
37.911
32.668
32.082
26.868
23.522
19.353
TBDPSO
N
O
6.38
200
180
160
140
120
100
80
60
40
20
0
ppm

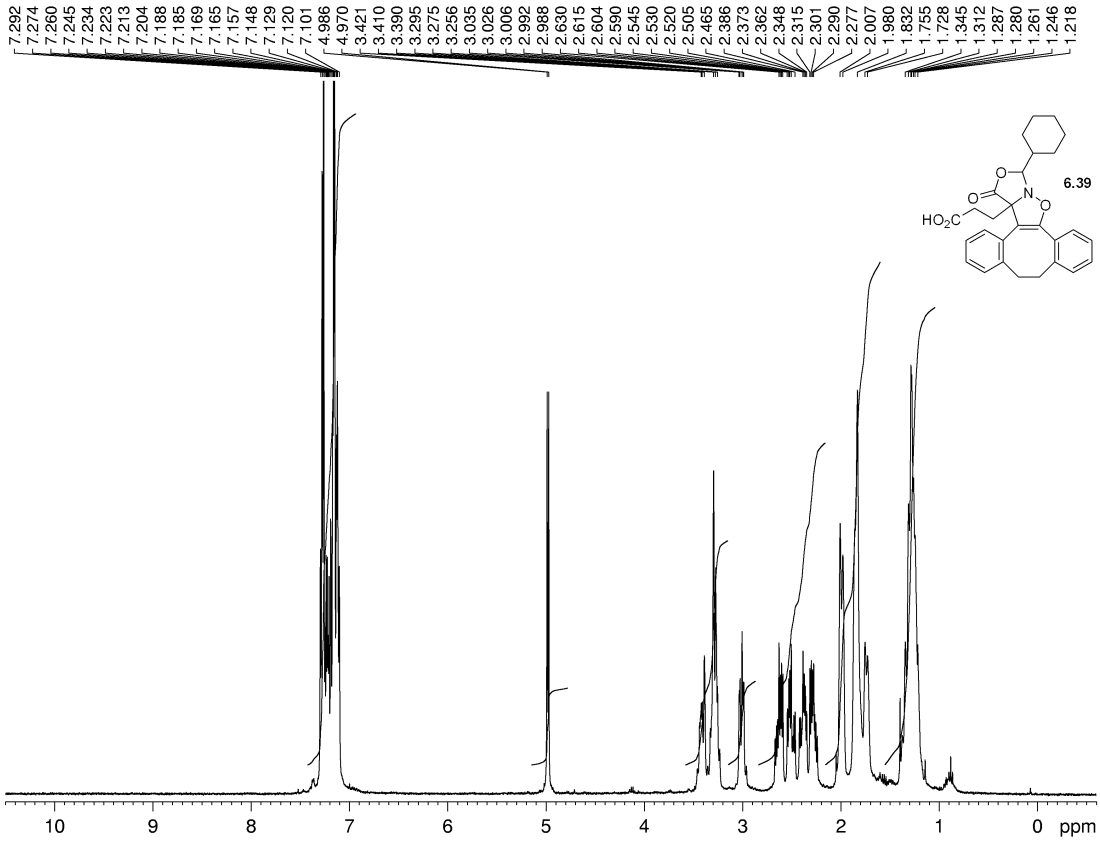
7.292
7.274
7.260
7.245
7.234
7.223
7.213
7.204
7.188
7.185
7.169
7.165
7.157
7.148
7.129
7.120
7.101
4.986
4.970
3.421
3.410
3.390
3.295
3.275
3.256
3.035
3.026
3.006
2.992
2.988
2.630
2.615
2.604
2.590
2.545
2.530
2.520
2.505
2.465
2.386
2.373
2.362
2.348
2.315
2.301
2.290
2.277
2.007
1.980
1.832
1.755
1.728
1.345
1.312
1.287
1.280
1.261
1.246
1.218
6.39
HO2C
10
9
8
7
6
5
4
3
2
1
0
ppm

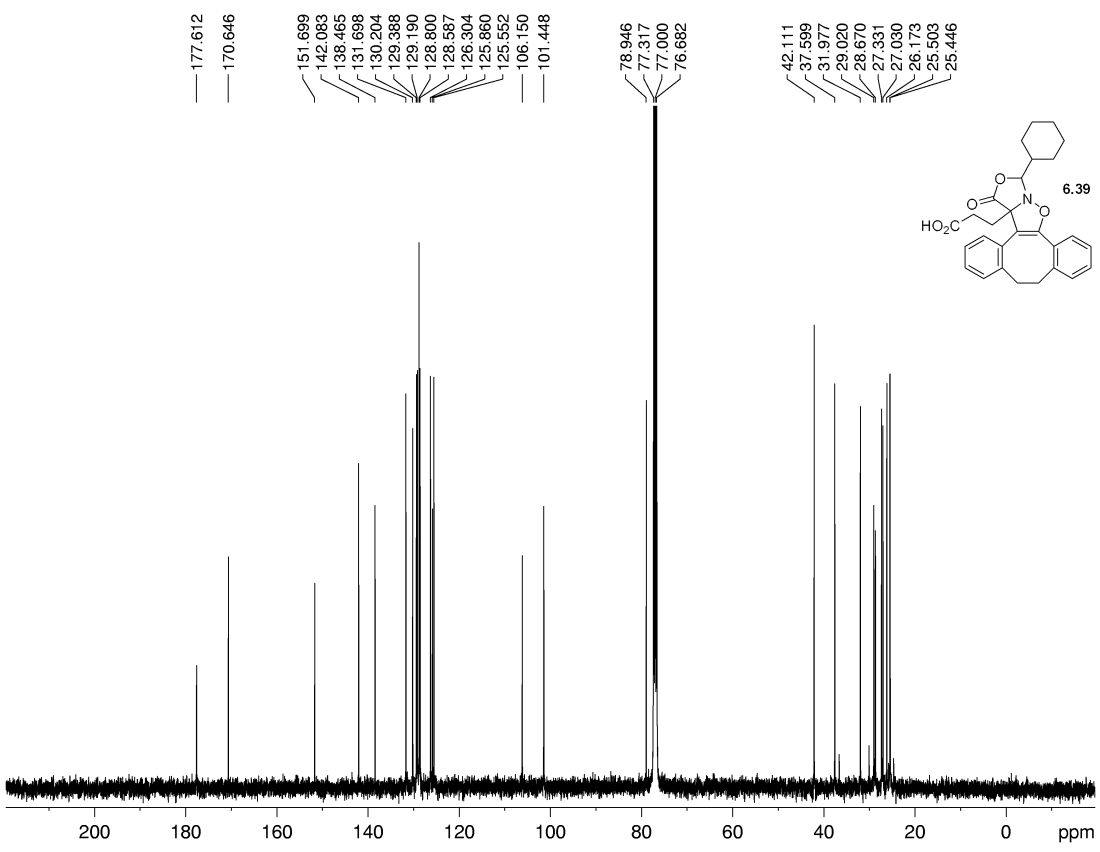
177.612
170.646
151.699
142.083
138.465
131.698
130.204
129.388
129.190
128.800
128.587
126.304
125.860
125.552
106.150
101.448
78.946
77.317
77.000
76.682
42.111
37.599
31.977
29.020
28.670
27.331
27.030
26.173
25.503
25.446
6.39
HO2C
200
180
160
140
120
100
80
60
40
20
0
ppm

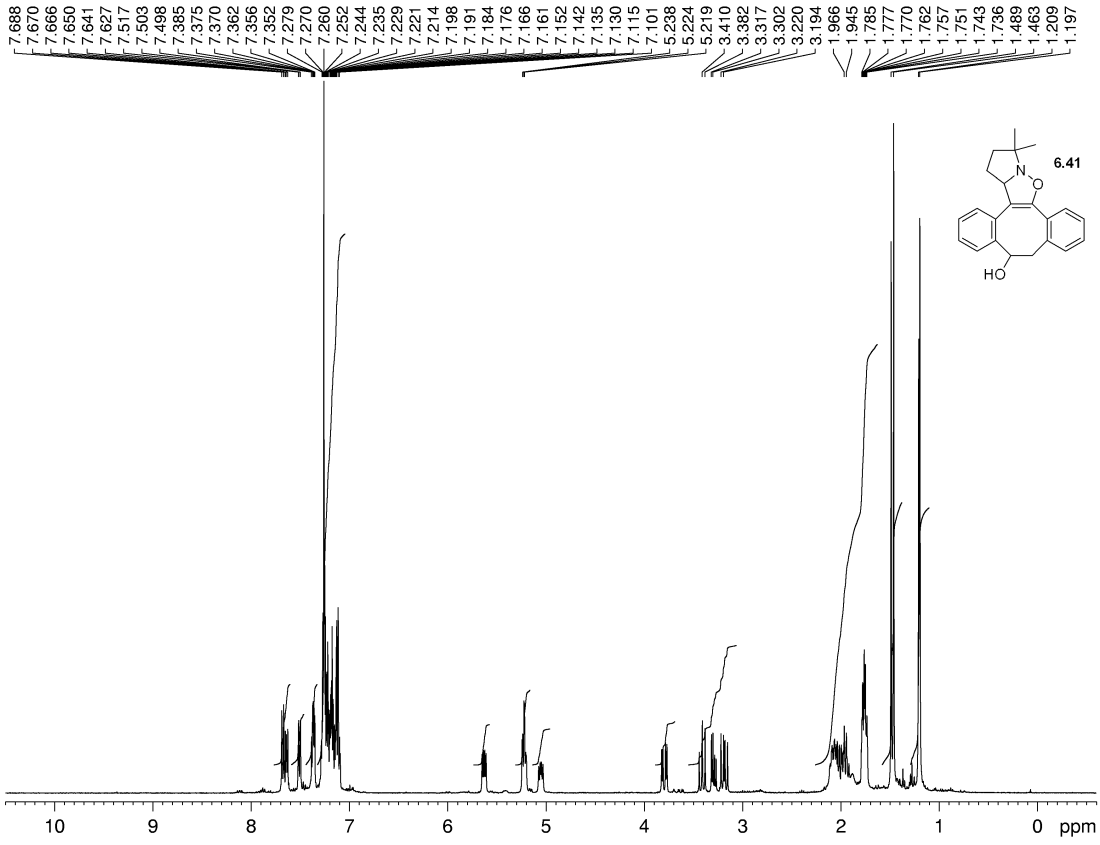
7.688
7.670
7.666
7.650
7.641
7.627
7.517
7.503
7.498
7.385
7.375
7.370
7.362
7.356
7.352
7.279
7.270
7.260
7.252
7.244
7.235
7.229
7.221
7.214
7.198
7.191
7.184
7.176
7.166
7.161
7.152
7.142
7.135
7.130
7.115
7.101
5.238
5.224
5.219
3.410
3.382
3.317
3.302
3.220
3.194
1.966
1.945
1.785
1.777
1.770
1.762
1.757
1.751
1.743
1.736
1.489
1.463
1.209
1.197
6.41
HO
10
9
8
7
6
5
4
3
2
1
0
ppm

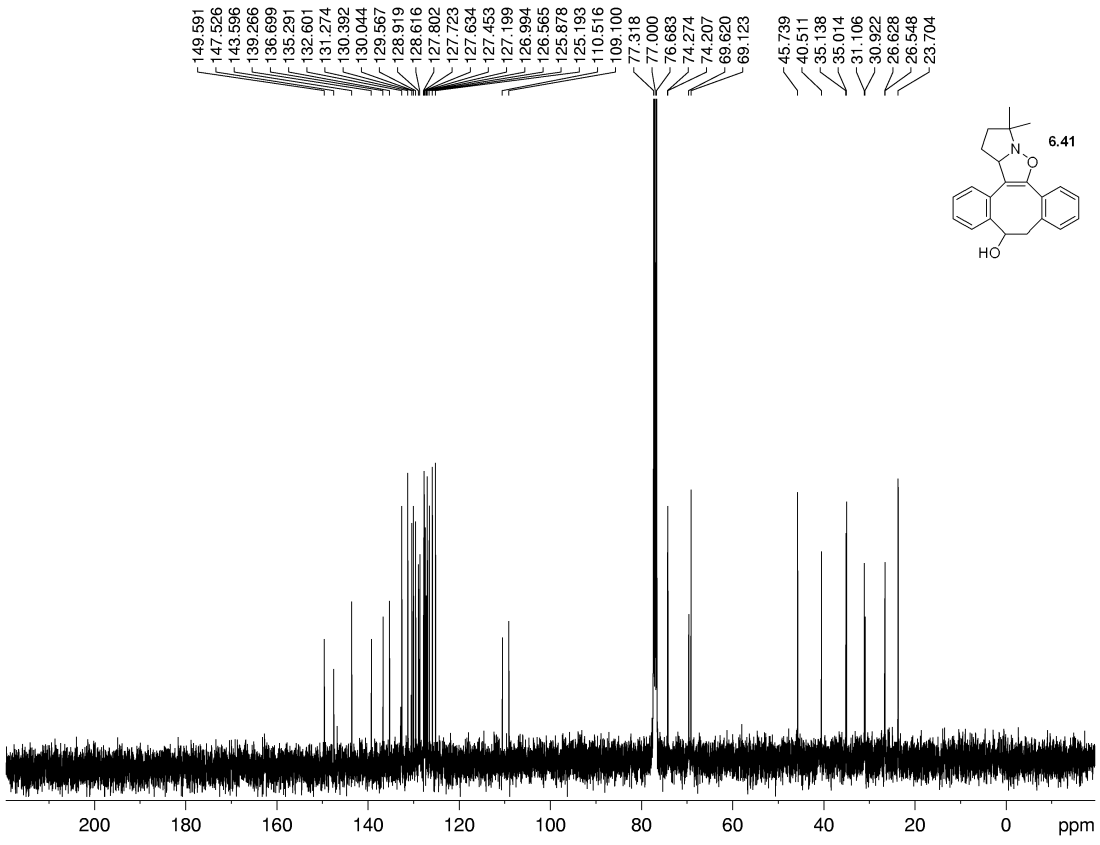
149.591
147.526
143.596
139.266
136.699
135.291
132.601
131.274
130.392
130.044
129.567
128.919
128.616
127.802
127.723
127.634
127.453
127.199
126.994
126.565
125.878
125.193
110.516
109.100
77.318
77.000
76.683
74.274
74.207
69.620
69.123
45.739
40.511
35.138
35.014
31.106
30.922
26.628
26.548
23.704
6.41
HO
200
180
160
140
120
100
80
60
40
20
0
ppm

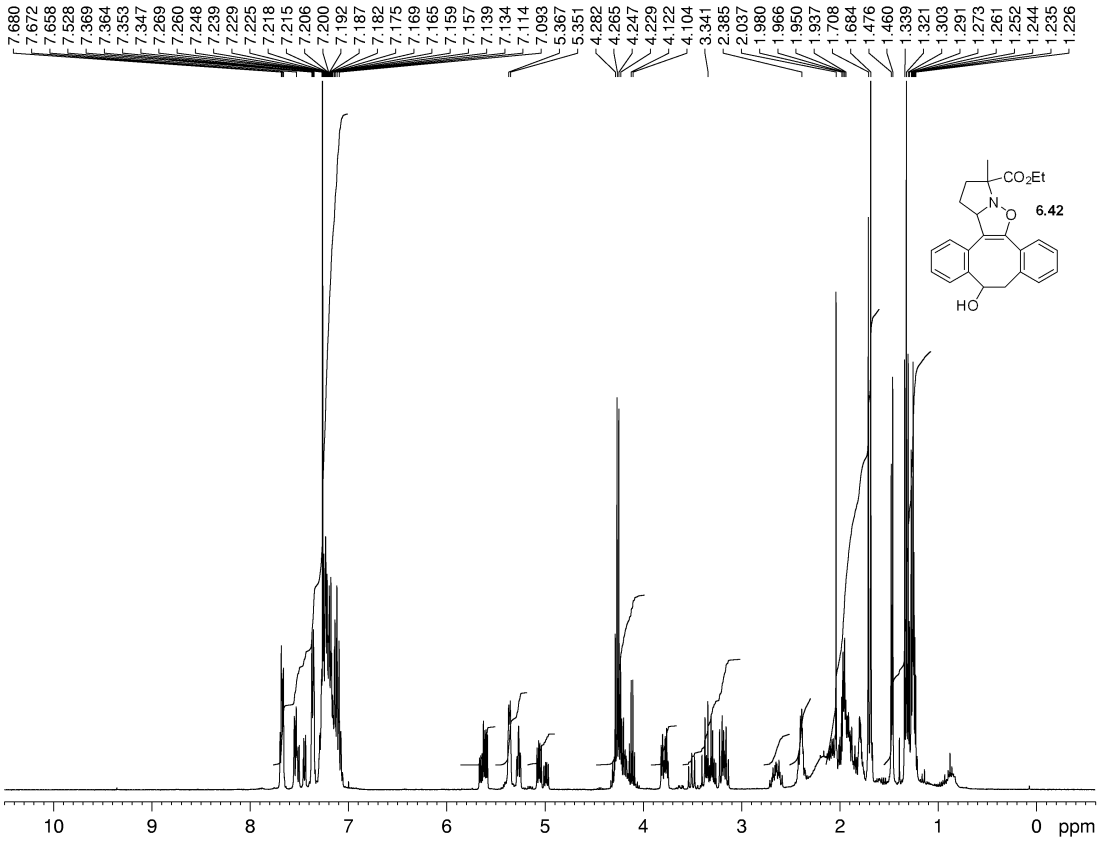
7.680
7.672
7.658
7.528
7.369
7.364
7.353
7.347
7.269
7.260
7.248
7.239
7.229
7.225
7.218
7.215
7.206
7.200
7.192
7.187
7.182
7.175
7.169
7.165
7.159
7.157
7.139
7.134
7.114
7.093
5.367
5.351
4.282
4.265
4.247
4.229
4.122
4.104
3.341
2.385
2.037
1.980
1.966
1.950
1.937
1.708
1.684
1.476
1.460
1.339
1.321
1.303
1.291
1.273
1.261
1.252
1.244
1.235
1.226
CO2Et
N
O
6.42
HO
10
9
8
7
6
5
4
3
2
1
0
ppm

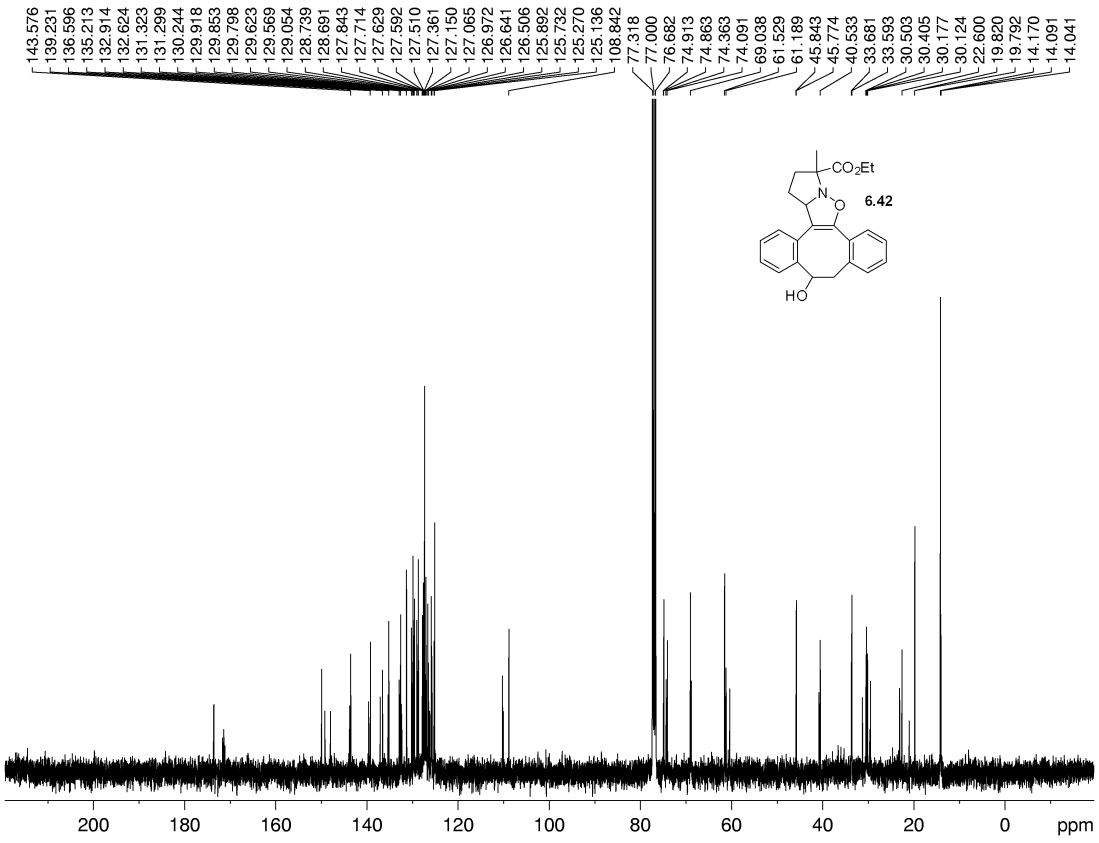
143.576
139.231
136.596
135.213
132.914
132.624
131.323
131.299
130.244
129.918
129.853
129.798
129.623
129.569
129.054
128.739
128.691
127.843
127.714
127.629
127.592
127.510
127.361
127.150
127.065
126.972
126.641
126.506
125.892
125.732
125.270
125.136
108.842
77.318
77.000
76.682
74.913
74.863
74.363
74.091
69.038
61.529
61.189
45.843
45.774
40.533
33.681
33.593
30.503
30.405
30.177
30.124
22.600
19.820
19.792
14.170
14.091
14.041
CO2Et
N
O
6.42
HO
200
180
160
140
120
100
80
60
40
20
0
ppm

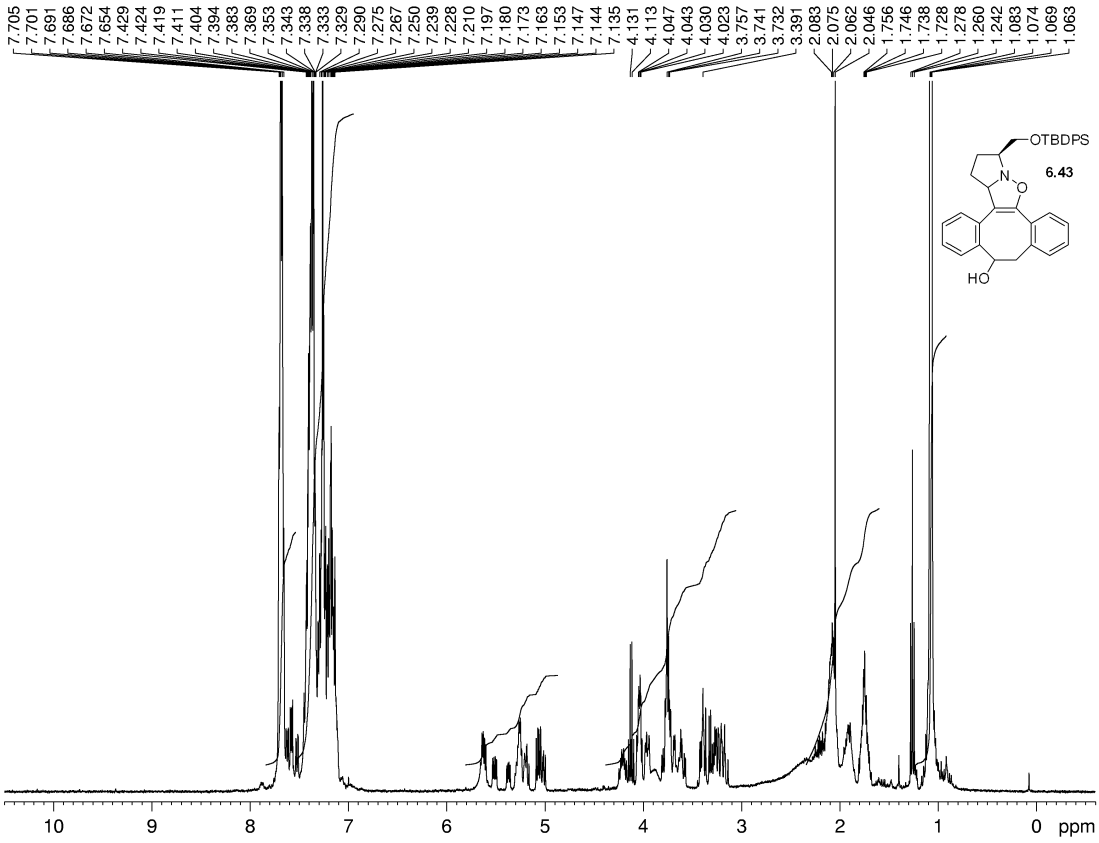
7.705
7.701
7.691
7.686
7.672
7.654
7.429
7.424
7.419
7.411
7.404
7.394
7.383
7.369
7.353
7.343
7.338
7.333
7.329
7.290
7.275
7.267
7.250
7.239
7.228
7.210
7.197
7.180
7.173
7.163
7.153
7.147
7.144
7.135
4.131
4.113
4.047
4.043
4.030
4.023
3.757
3.741
3.732
3.391
2.083
2.075
2.062
2.046
1.756
1.746
1.738
1.728
1.278
1.260
1.242
1.083
1.074
1.069
1.063
OTBDPS
6.43
HO
10
9
8
7
6
5
4
3
2
1
0
ppm

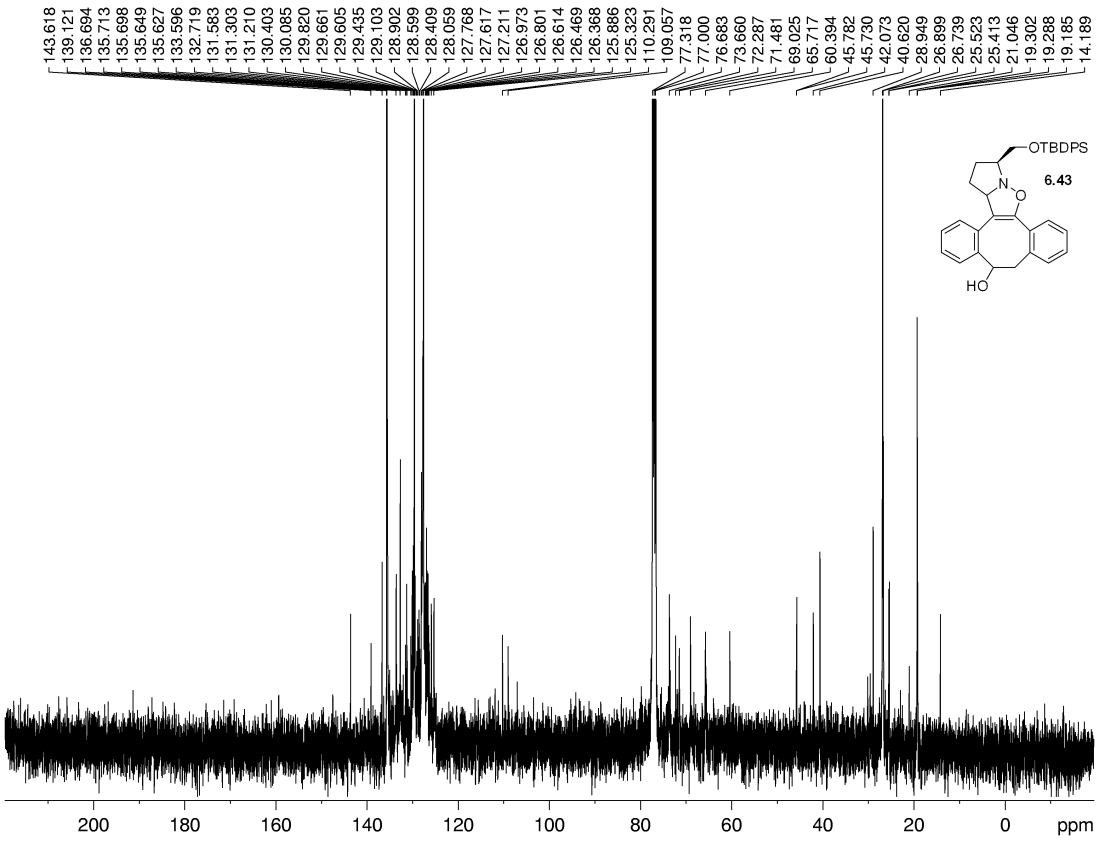
143.618
139.121
136.694
135.713
135.698
135.649
135.627
133.596
132.719
131.583
131.303
131.210
130.403
130.085
129.820
129.661
129.605
129.435
129.103
128.902
128.599
128.409
128.059
127.768
127.617
127.211
126.973
126.801
126.614
126.469
126.368
125.886
125.323
110.291
109.057
77.318
77.000
76.683
73.660
72.287
71.481
69.025
65.717
60.394
45.782
45.730
42.073
40.620
28.949
26.899
26.739
25.523
25.413
21.046
19.302
19.288
19.185
14.189
OTBDPS
6.43
HO
200
180
160
140
120
100
80
60
40
20
0
ppm

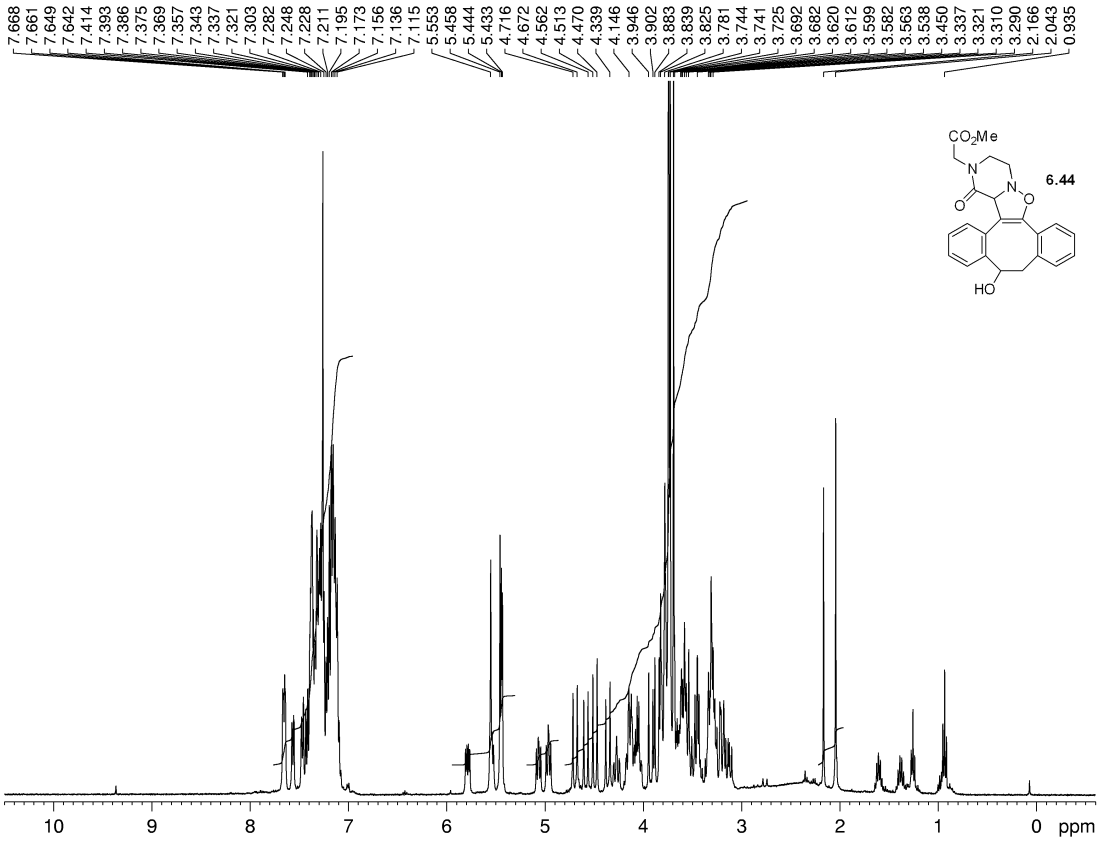
7.668
7.661
7.649
7.642
7.414
7.393
7.386
7.375
7.369
7.357
7.343
7.337
7.321
7.303
7.282
7.248
7.228
7.211
7.195
7.173
7.156
7.136
7.115
5.553
5.458
5.444
5.433
4.716
4.672
4.562
4.513
4.470
4.339
4.146
3.946
3.902
3.883
3.839
3.825
3.781
3.744
3.741
3.725
3.692
3.682
3.620
3.612
3.599
3.582
3.563
3.538
3.450
3.337
3.321
3.310
3.290
2.166
2.043
0.935
CO2Me
N
O
N
O
HO
6.44
10
9
8
7
6
5
4
3
2
1
0
ppm

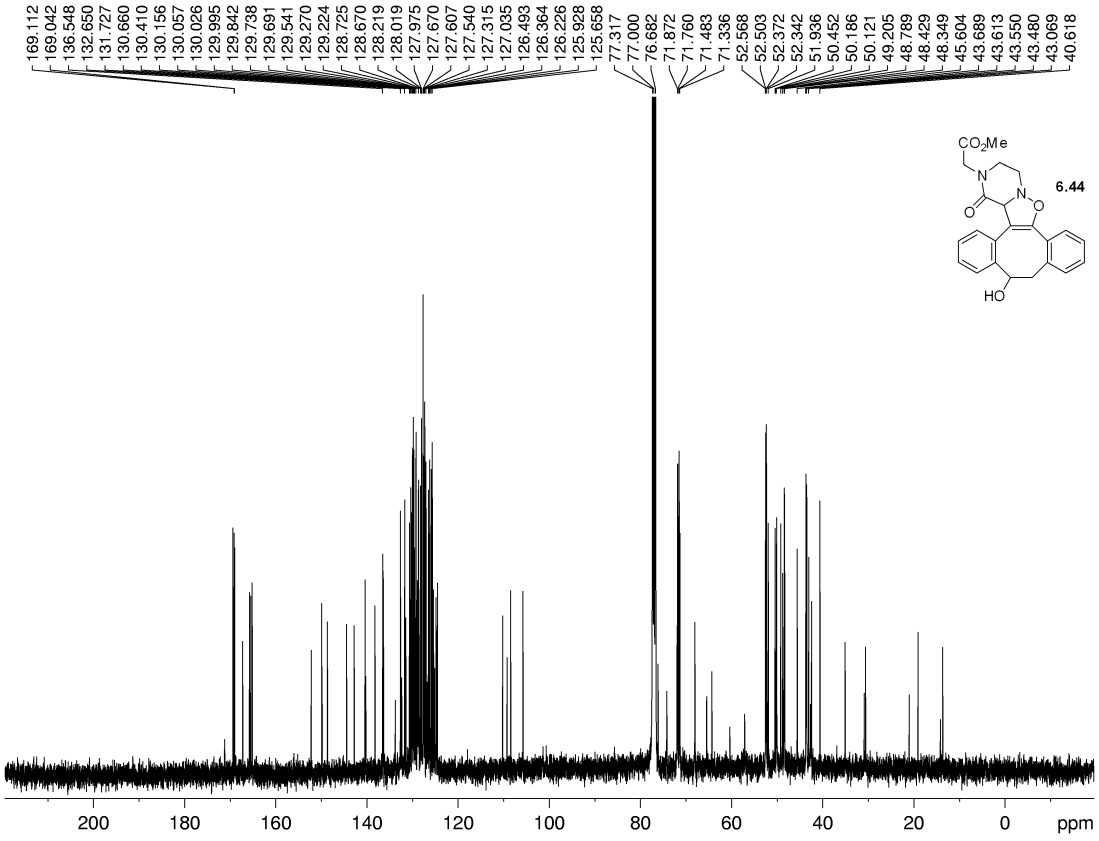
169.112
169.042
136.548
132.650
131.727
130.660
130.410
130.156
130.057
130.026
129.995
129.842
129.738
129.691
129.541
129.270
129.224
128.725
128.670
128.219
128.019
127.975
127.670
127.607
127.540
127.315
127.035
126.493
126.364
126.226
125.928
125.658
77.317
77.000
76.682
71.872
71.760
71.483
71.336
52.568
52.503
52.372
52.342
51.936
50.452
50.186
50.121
49.205
48.789
48.429
48.349
45.604
43.689
43.613
43.550
43.480
43.069
40.618
CO2Me
N
O
N
O
HO
6.44
200
180
160
140
120
100
80
60
40
20
0
ppm

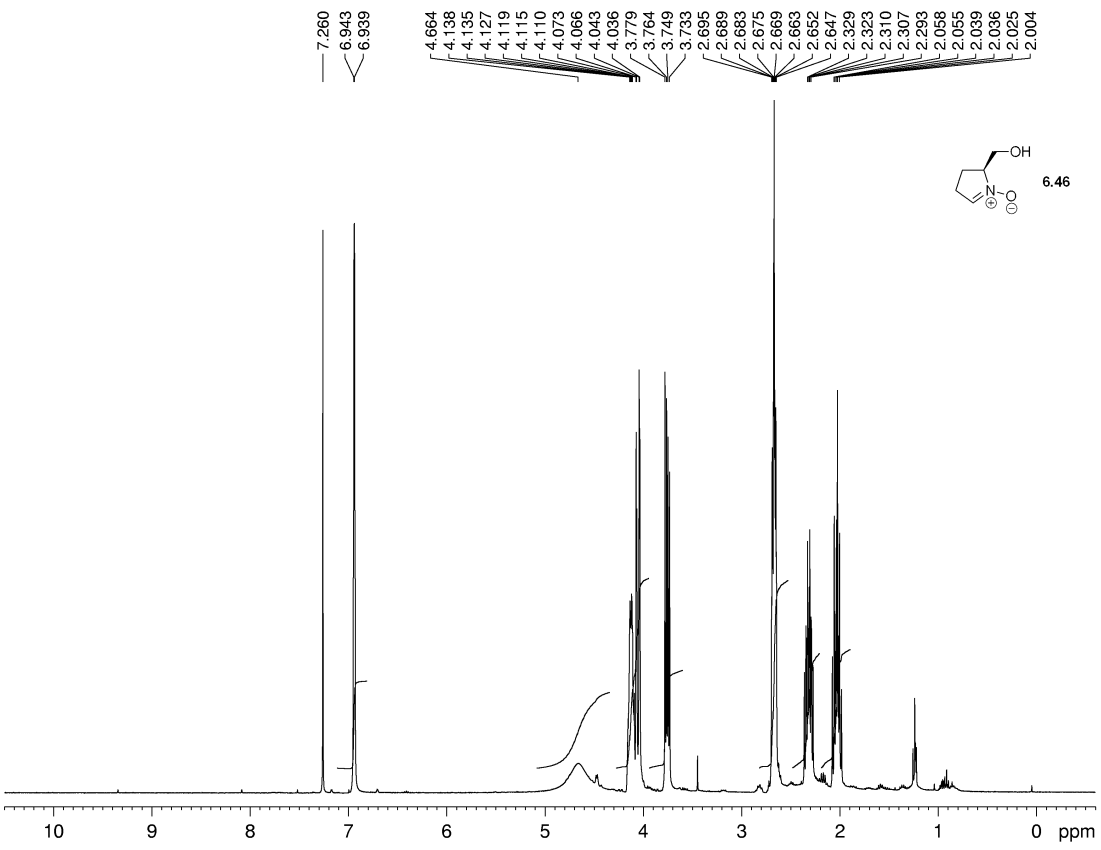
7.260
6.943
6.939
4.664
4.138
4.135
4.127
4.119
4.115
4.110
4.073
4.066
4.043
4.036
3.779
3.764
3.749
3.733
2.695
2.689
2.683
2.675
2.669
2.663
2.652
2.647
2.329
2.323
2.310
2.307
2.293
2.058
2.055
2.039
2.036
2.025
2.004
OH
6.46
10
9
8
7
6
5
4
3
2
1
0
ppm

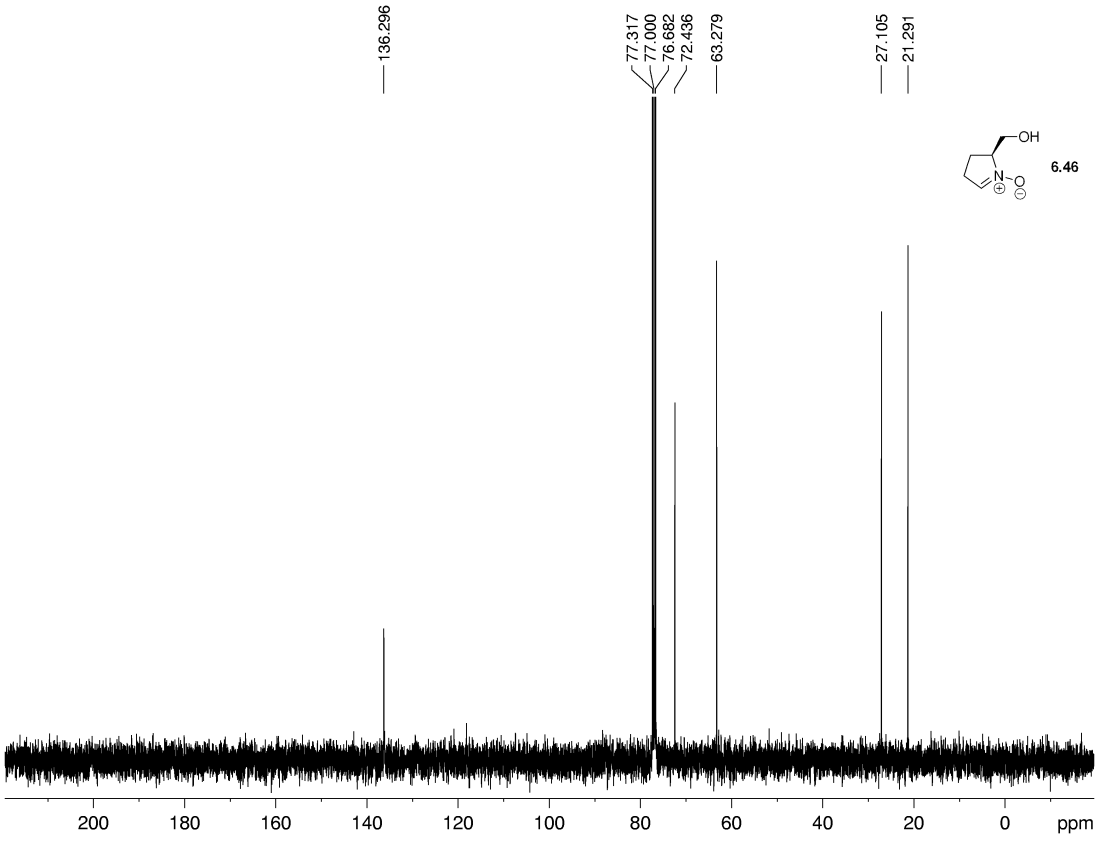
136.296
77.317
77.000
76.682
72.436
63.279
27.105
21.291
OH
6.46
200
180
160
140
120
100
80
60
40
20
0
ppm

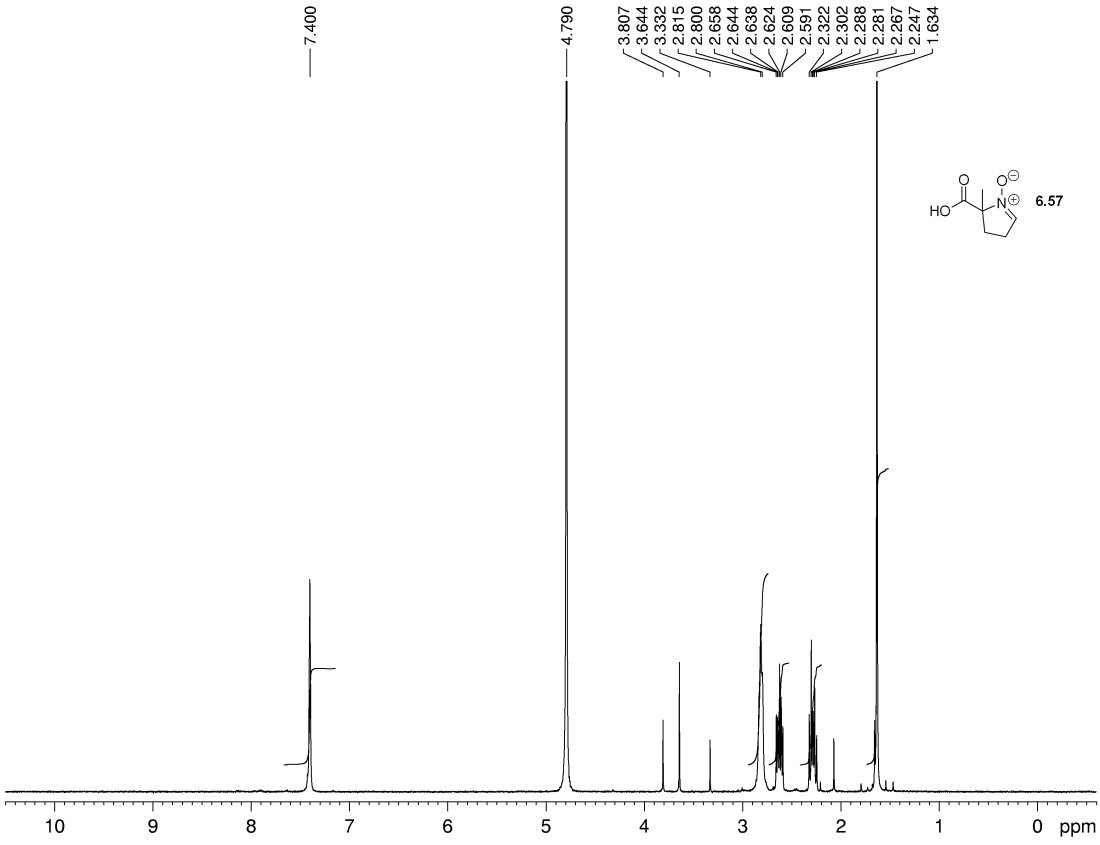
7.400
4.790
3.807
3.644
3.332
2.815
2.800
2.658
2.644
2.638
2.624
2.609
2.591
2.322
2.302
2.288
2.281
2.267
2.247
1.634
HO
O
N
6.57
10
9
8
7
6
5
4
3
2
1
0
ppm

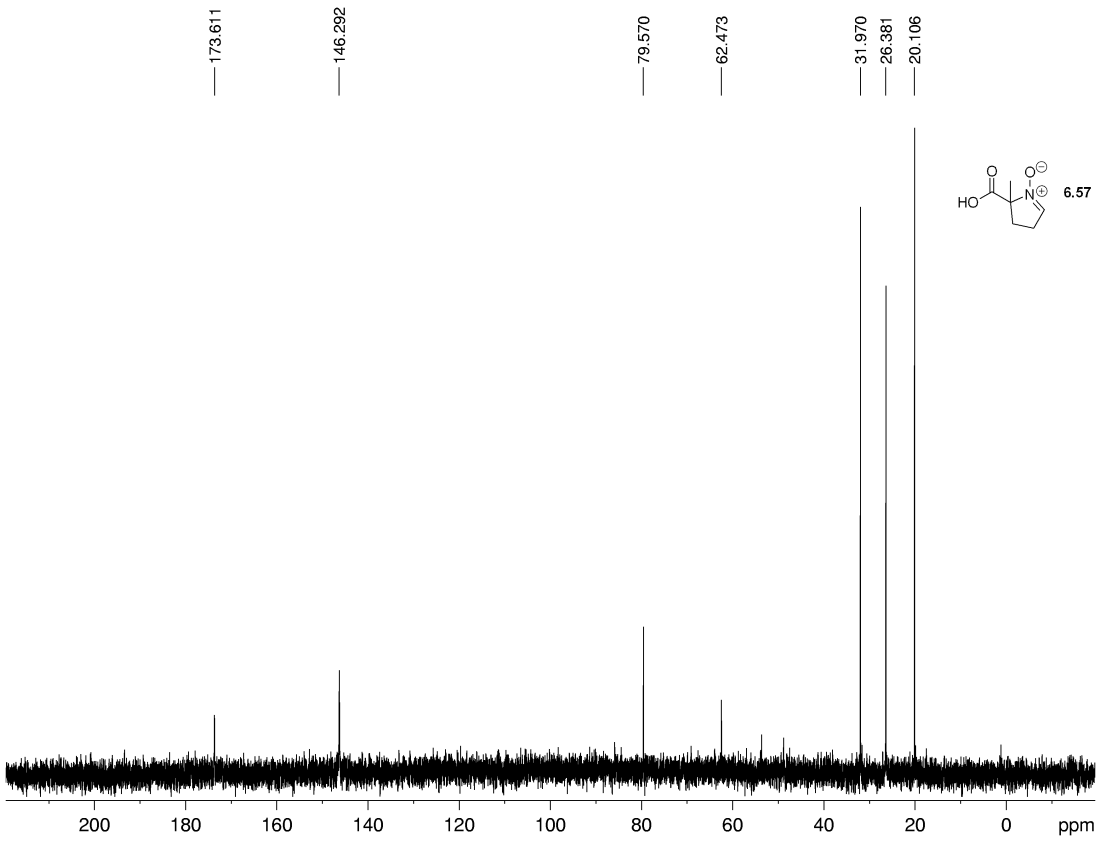
173.611
146.292
79.570
62.473
31.970
26.381
20.106
HO
O
N
6.57
200
180
160
140
120
100
80
60
40
20
0
ppm

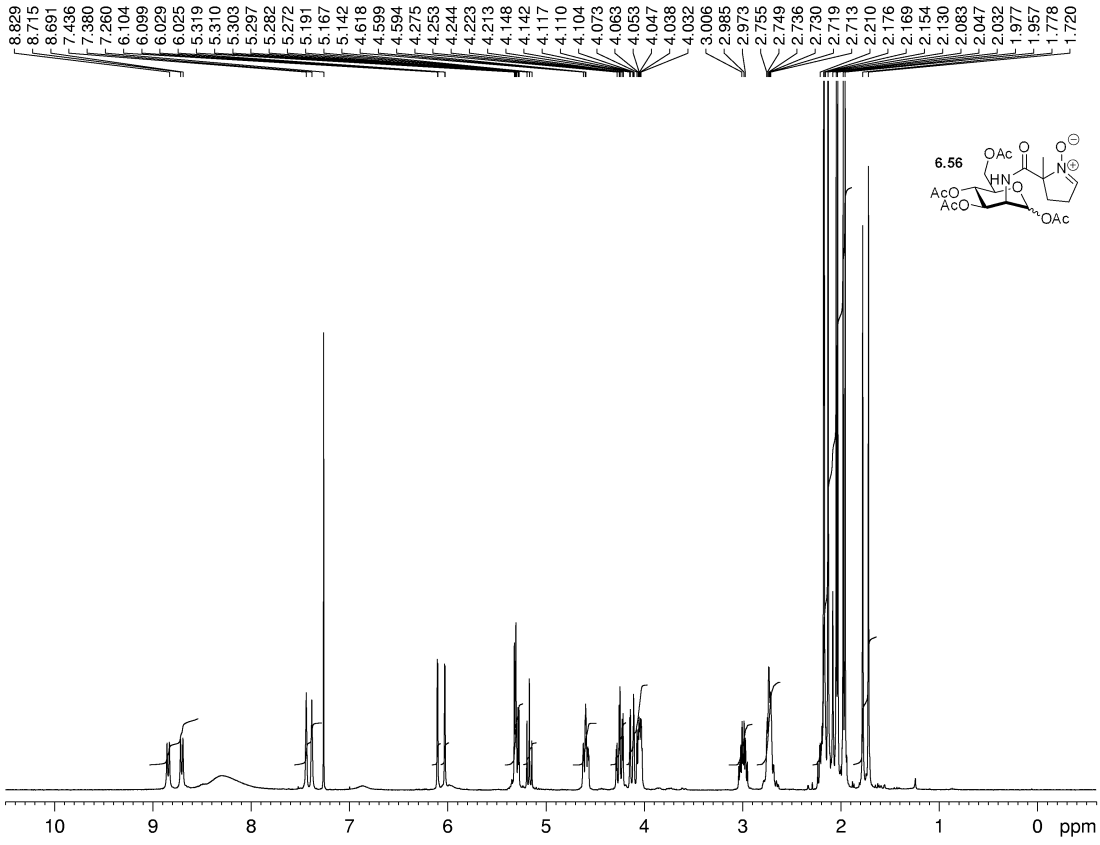
8.829
8.715
8.691
7.436
7.380
7.260
6.104
6.099
6.029
6.025
5.319
5.310
5.303
5.297
5.282
5.272
5.191
5.167
5.142
4.618
4.599
4.594
4.275
4.253
4.244
4.223
4.213
4.148
4.142
4.117
4.110
4.104
4.073
4.063
4.053
4.047
4.038
4.032
3.006
2.985
2.973
2.755
2.749
2.736
2.730
2.719
2.713
2.210
2.176
2.169
2.154
2.130
2.083
2.047
2.032
1.977
1.957
1.778
1.720
6.56
OAc
O
O
N
HN
O
AcO
AcO
OAc
10
9
8
7
6
5
4
3
2
1
0
ppm

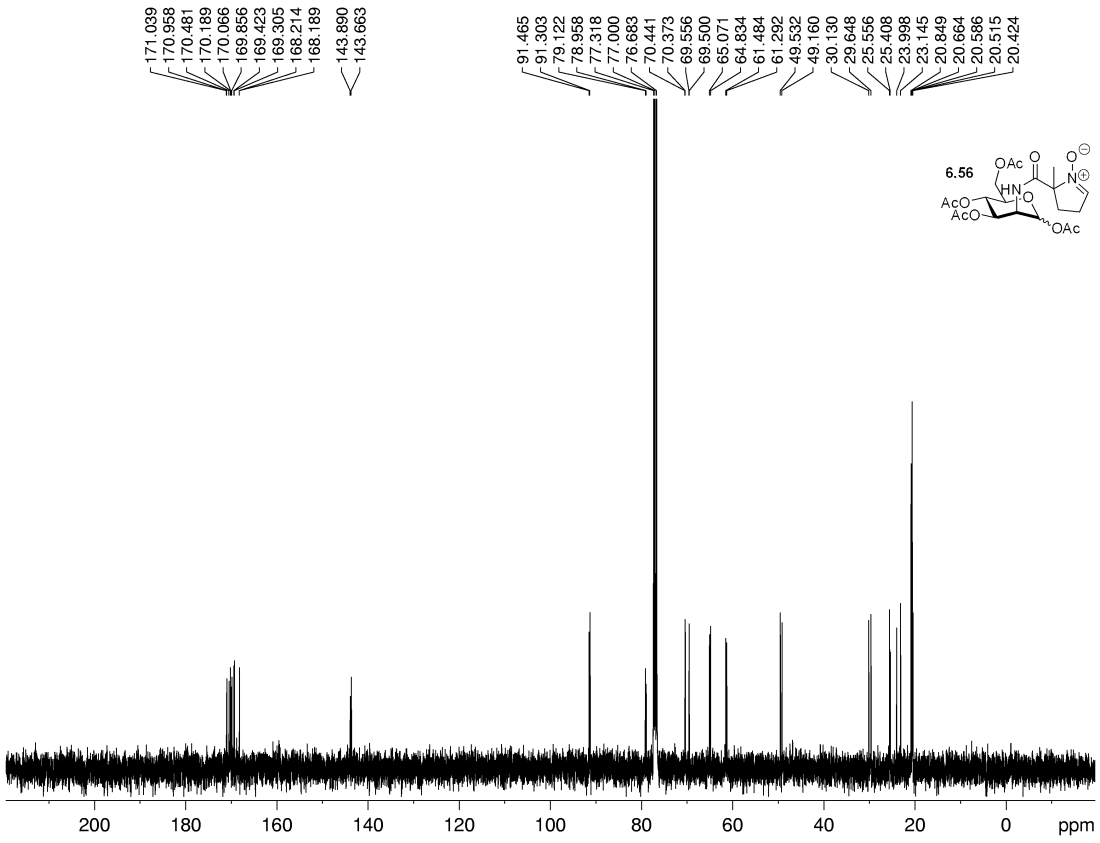
171.039
170.958
170.481
170.189
170.066
169.856
169.423
169.305
168.214
168.189
143.890
143.663
91.465
91.303
79.122
78.958
77.318
77.000
76.683
70.441
70.373
69.556
69.500
65.071
64.834
61.484
61.292
49.532
49.160
30.130
29.648
25.556
25.408
23.998
23.145
20.849
20.664
20.586
20.515
20.424
6.56
OAc
O
O
N
HN
O
AcO
AcO
OAc
200
180
160
140
120
100
80
60
40
20
0
ppm

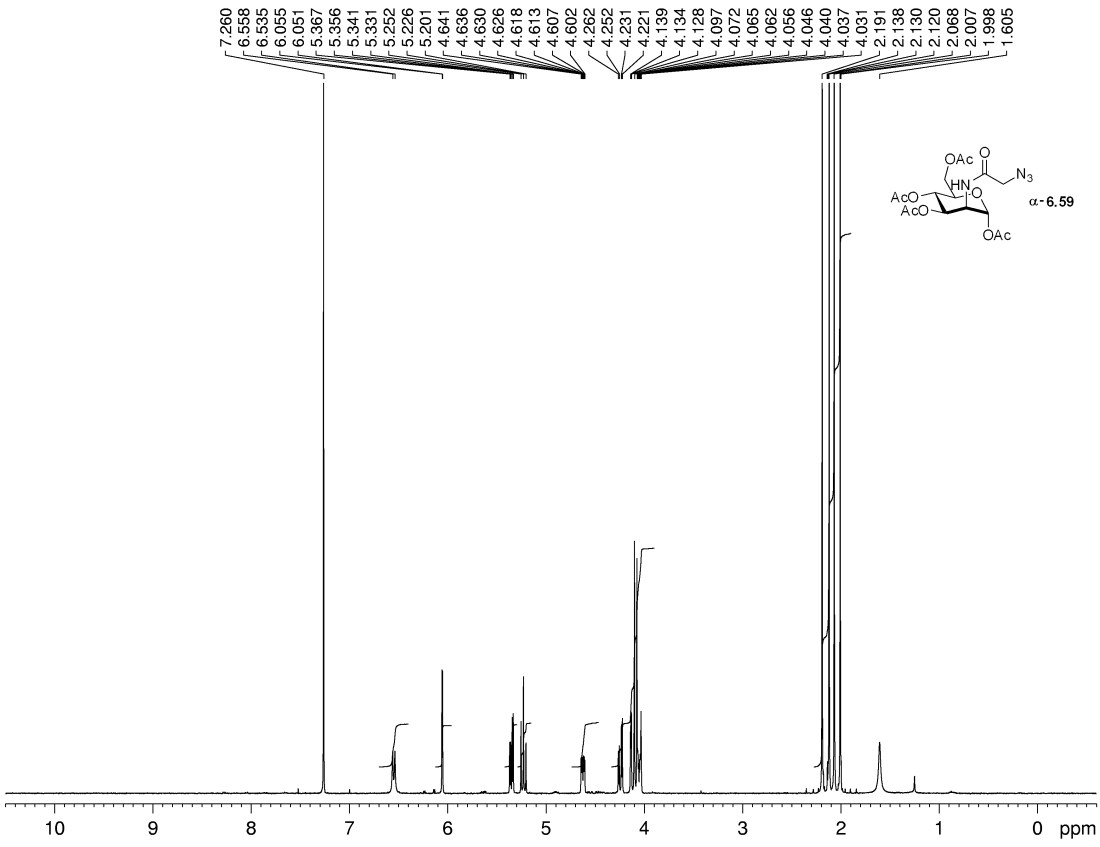
7.260
6.558
6.535
6.055
6.051
5.367
5.356
5.341
5.331
5.252
5.226
5.201
4.641
4.636
4.630
4.626
4.618
4.613
4.607
4.602
4.262
4.252
4.231
4.221
4.139
4.134
4.128
4.097
4.072
4.065
4.062
4.056
4.046
4.040
4.037
4.031
2.191
2.138
2.130
2.120
2.068
2.007
1.998
1.605
OAc
O
N3
HN
O
AcO
AcO
OAc
α-6.59
10
9
8
7
6
5
4
3
2
1
0
ppm

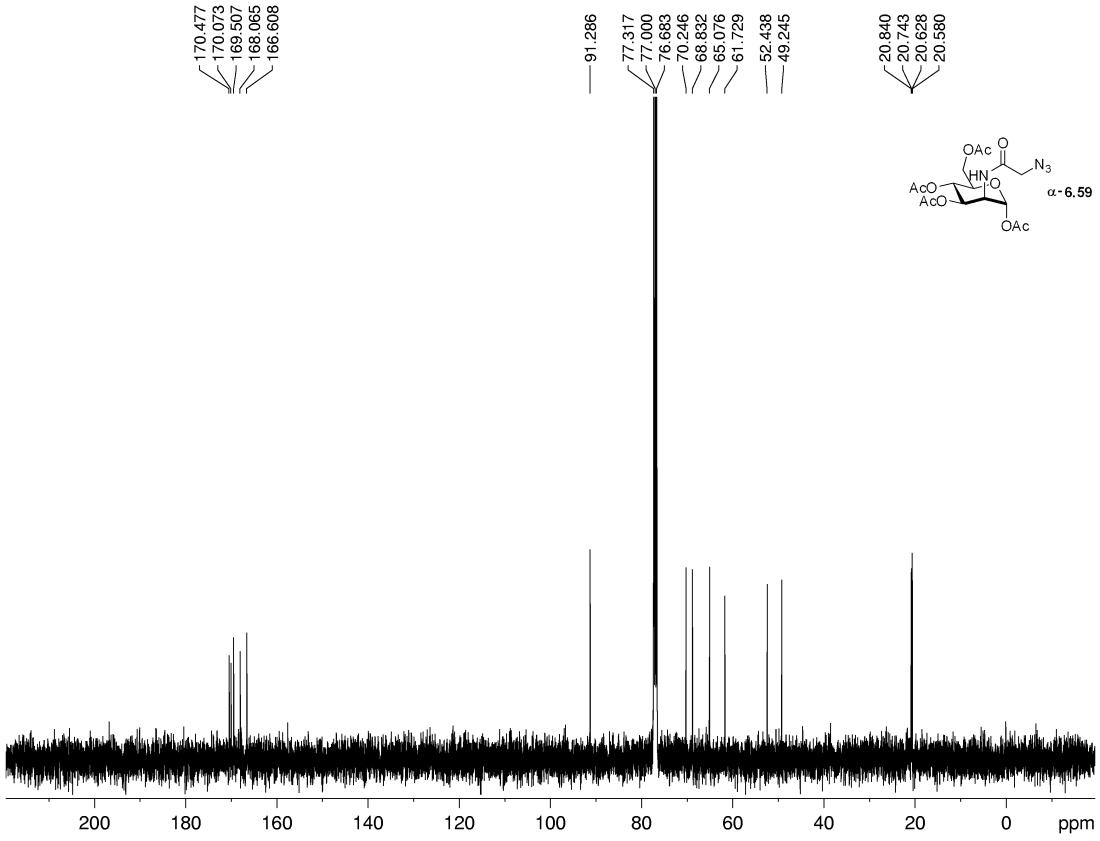
170.477
170.073
169.507
168.065
166.608
91.286
77.317
77.000
76.683
70.246
68.832
65.076
61.729
52.438
49.245
20.840
20.743
20.628
20.580
OAc
O
N3
HN
O
AcO
AcO
OAc
α-6.59
200
180
160
140
120
100
80
60
40
20
0
ppm

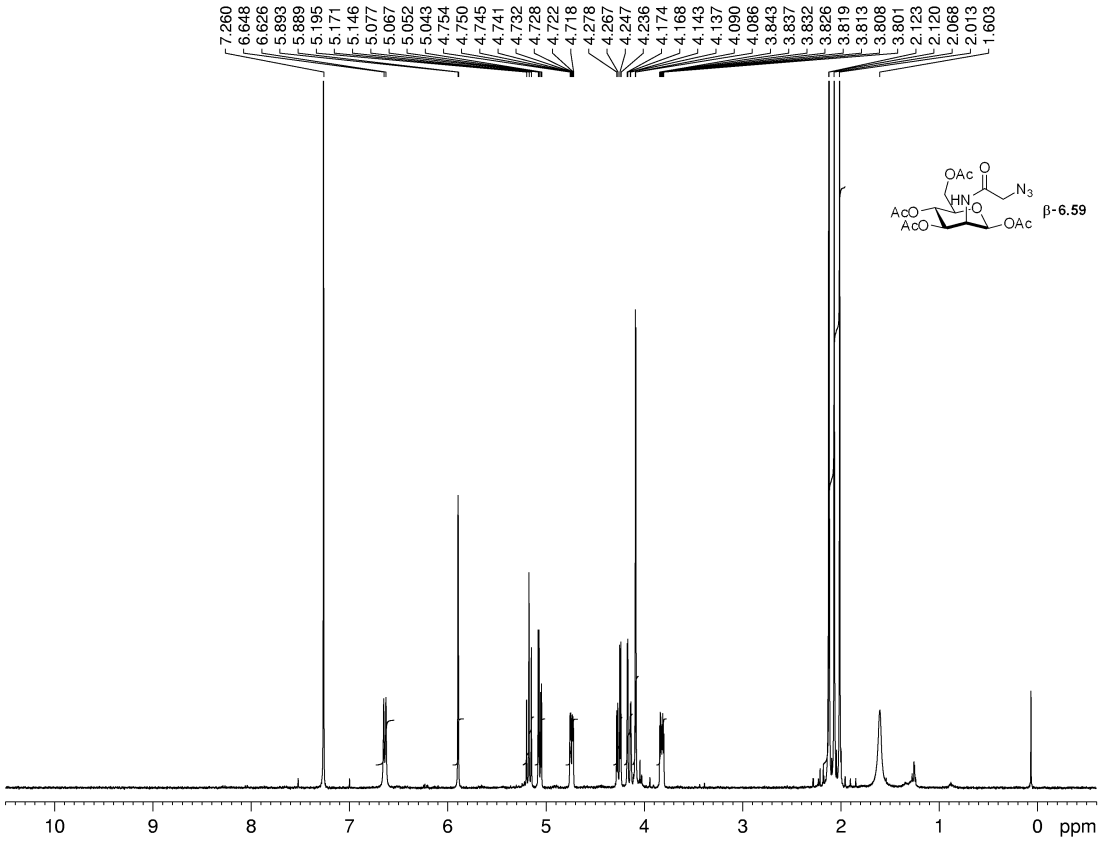
7.260
6.648
6.626
5.893
5.889
5.195
5.171
5.146
5.077
5.067
5.052
5.043
4.754
4.750
4.745
4.741
4.732
4.728
4.722
4.718
4.278
4.267
4.247
4.236
4.174
4.168
4.143
4.137
4.090
4.086
3.843
3.837
3.832
3.826
3.819
3.813
3.808
3.801
2.123
2.120
2.068
2.013
1.603
OAc
O
N3
HN
O
AcO
AcO
OAc
β-6.59
10
9
8
7
6
5
4
3
2
1
0
ppm

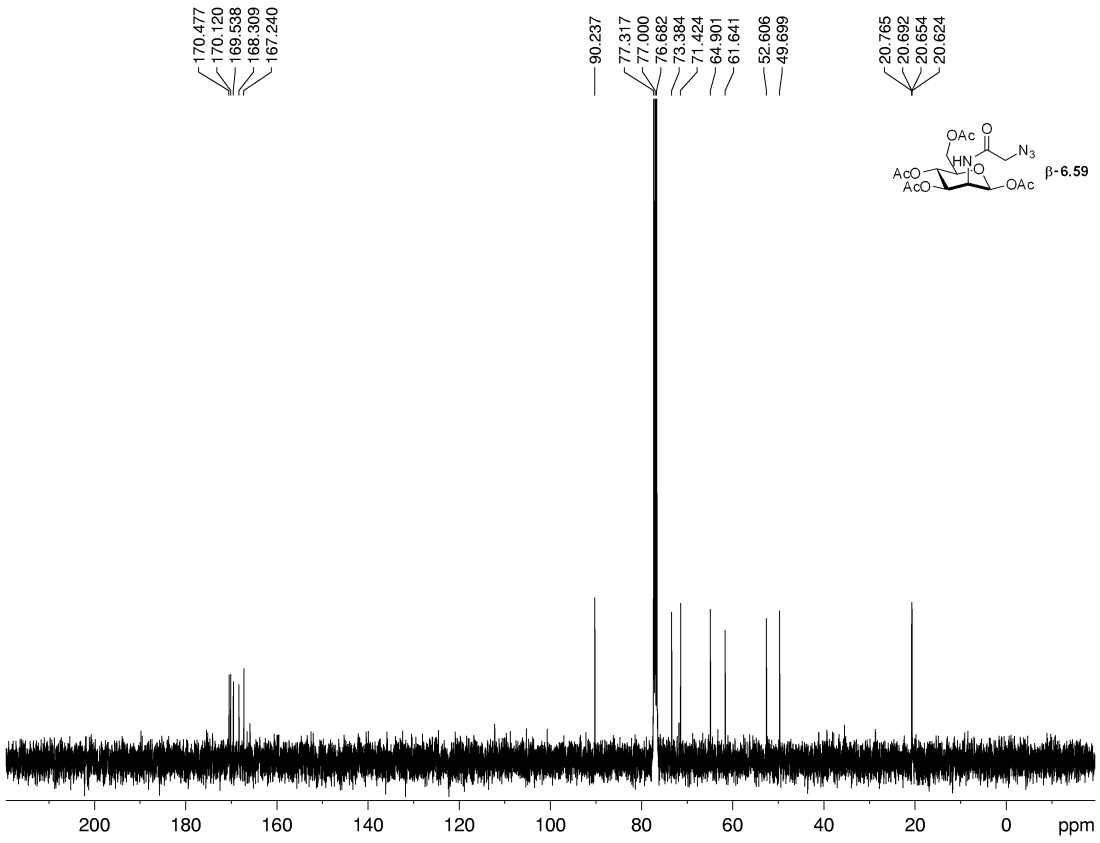
170.477
170.120
169.538
168.309
167.240
90.237
77.317
77.000
76.682
73.384
71.424
64.901
61.641
52.606
49.699
20.765
20.692
20.654
20.624
OAc
O
N3
HN
O
AcO
AcO
OAc
β-6.59
200
180
160
140
120
100
80
60
40
20
0
ppm